MycoKeys 106: 1–21 (2024)
DOI: 10.3897/mycokeys.106.121840

Research Article

Morphological and molecular data reveal *Cerrena caulinicystidiata* sp. nov. and *Polyporus minutissimus* sp. nov. in Polyporales from Asia

Zi-Wei Zheng[1*], Qiu-Yue Zhang[1*], Li-Rong Zhang[2], Hai-Sheng Yuan[3], Fang Wu[1]

1 *State Key Laboratory of Efficient Production of Forest Resources, School of Ecology and Nature Conservation, Beijing Forestry University, Beijing 100083, China*
2 *Center for Biodiversity and Nature Reserve, Chinese Academy of Environmental Planning, Beijing 100043, China*
3 *Institute of Applied Ecology, Chinese Academy of Sciences, Shenyang 110016, Liaoning, China*
Corresponding author: Fang Wu (fangwubjfu2014@bjfu.edu.cn)

Abstract

Two new species of Polyporales, *Cerrena caulinicystidiata* and *Polyporus minutissimus*, are illustrated and described on the basis of morphological studies and phylogenetic analyses from southern China and Vietnam. *C. caulinicystidiata* is characterized by annual, resupinate, sometimes effused-reflexed basidiocarps, greyish orange to brownish orange pore surface, irregular pores (3–8 per mm), a trimitic hyphal system, pyriform to ventricose cystidia, and subglobose basidiospores 3.2–4.5 × 2.8–3.5 µm in size. *P. minutissimus* is characterized by annual, solitary, fan-shaped with a depressed center or infundibuliform basidiocarps, obvious black stipe, cream to buff yellow pileal surface with glabrous, occasionally zonate and radially aligned stripes, angular pores (6–9 per mm), a dimitic hyphal system, and cylindrical basidiospores, 5–9.2 × 2.2–4 µm. Detailed descriptions and illustrations of the two new species are provided. The differences between the two new species and their morphologically similar and phylogenetically related species are discussed.

Key words: Cerrenaceae, phylogeny, Polyporaceae, taxonomy, wood-decaying fungi

Academic editor: María P. Martín
Received: 28 February 2024
Accepted: 6 May 2024
Published: 13 June 2024

Citation: Zheng Z-W, Zhang Q-Y, Zhang L-R, Yuan H-S, Wu F (2024) Morphological and molecular data reveal *Cerrena caulinicystidiata* sp. nov. and *Polyporus minutissimus* sp. nov. in Polyporales from Asia. MycoKeys 106: 1–21. https://doi.org/10.3897/mycokeys.106.121840

Introduction

The order Polyporales presents a great diversity of basidiocarp types and hymenophore configurations (Binder et al. 2013). It is an important group of fungi, as Polyporales species can cause wood-decay and thus play an essential role in the carbon cycle. In addition, some species of Polyporales may have medicinal properties (Dai 1996, 1999, 2012; Dai et al. 2009). The order has long been the subject of research on taxonomic diversity, distribution patterns, and ecological functions (Hibbett et al. 2014). As of early 2024, more than 1,800 species are recognized in the order (Martinez et al. 2004; Martinez et al. 2009; Kirk et al. 2008; Grigoriev et al. 2013; Zhao et al. 2015; Justo et al. 2017). Due to its great diversity, the order is intensively studied worldwide (Justo et al. 2017).

* These authors contributed equally to this paper.

Cerrena Gray is the type genus of Cerrenaceae within the Polyporales (Ryvarden and Gilbertson 1993; Justo et al. 2017), and it is typified by *C. unicolor* (Bull.) Murrill. It is widely distributed throughout the world. The genus is characterized by resupinate, effused-reflexed or pileate basidiocarps, irregular hymenophore, dimitic or trimitic hyphal systems, cylindric to ellipsoid basidiospores, and white rot (Ryvarden and Gilbertson 1993; Ryvarden et al. 2022). The genus *Cerrena* published in 1821 has priority above *Trametes* Fr., published in 1838, and the two genera were considered as a single taxon in several studies. Thus, a huge number of new combinations in *Cerrena*. (Cunningham and Cunningham1965; Gilbertson and Ryvarden 1987; Corner 1989; Ryvarden and Melo 2022). However, Ryvarden (1991) recommended to keep *Cerrena* as a separate genus based on their anatomical characters. According to Index Fungorum (http://www.indexfungorum.org) and Yuan (2014), *Cerrena* currently comprises around 10 species.

Polyporus P. Micheli ex Adans., the type genus of the Polyporaceae, is a well-known polypore genus (Gilbertson and Ryvarden 1987). Given that Micheli (1729) did not originally select a type species for *Polyporus*, there is no consensus on the selection of the type. Since Donk (1933) selected *P. tuberaster* (Jacq. ex Pers.) Fr. as the type species, this lectotype was accepted by most subsequent mycologists (Cunningham and Cunningham 1965; Singer 1986; Niemelä and Kotiranta 1991; Ryvarden 1991; Sotome et al. 2008; Ji et al. 2022). Morphologically, *Polyporus* is a heterogeneous genus including many species belonging to six morphological groups described by Núñez and Ryvarden (1995), viz, the *Polyporus* group, the *Favolus* group (= *Favolus* Fr.), the *Melanopus* group (= *Melanopus* Pat.), the *Polyporellus* group (= *Polyporellus* Karst.), the *Admirabilis* group, and the *Dendropolyporus* group (= *Dendropolyporus* (Pouz.) Jülich). Phylogenetically, *Polyporus* s. str. is known as a polyphyletic genus (Krüger et al. 2006; Sotome et al. 2008, 2011; Ji et al. 2022). Phylogenetic analyses of *Polyporus* did not conform to the six morphological groups, for which further in-depth study of the group is needed (Sotome et al. 2008; Zhou et al. 2016).

During investigations on wood-decaying polypores from South China and Vietnam, specimens that morphologically fit the definitions of *Cerrena* and *Polyporus* were collected. Phylogenetically, these samples formed two distinct lineages within *Cerrena* and *Polyporus*, respectively, and they are different from their morphologically similar and phylogenetically related species. Therefore, we describe and illustrate two new species, *Cerrena caulinicystidiata* sp. nov. and *Polyporus minutissimus* sp. nov. within the Polyporales on the basis of morphological studies and phylogenetic analyses.

Materials and methods

Morphological studies

The studied specimens are deposited in the Fungarium of Beijing Forestry University (BJFC) and the Institute of Applied Ecology of the Chinese Academy of Sciences (IFP). Macro-morphological descriptions were based on field notes and voucher herbarium specimens. Microscopic measurements and drawings were made from slides prepared from voucher tissues and stained with Cotton Blue and Melzer's reagent. The following abbreviations were used: KOH = 5%

potassium hydroxide; CB = Cotton Blue; CB+ = cyanophilous in Cotton Blue; CB– = acyanophilous in Cotton Blue; IKI = Melzer's; IKI– = neither amyloid nor dextrinoid in Melzer's reagent; L = mean basidiospore length (arithmetic average of basidiospores); W = mean basidiospore width (arithmetic average of basidiospores); Q = variation in the L/W ratios between specimens studied; n (a/b) = number of basidiospores (a) measured from the given number of specimens (b). When we present basidiospore size variation, 5% of measurements were excluded from each end of the range. These excluded values are given in parentheses. Special color terms follow Anonymous (1969) and Petersen (1996).

DNA extraction and sequencing

A CTAB rapid plant genome extraction kit (Aidlab Biotechnologies, Co., Ltd., Beijing, China) was used to obtain DNA products from voucher specimens following the manufacturer's instructions with some modifications (Wu et al. 2020, 2022). The following primer pairs were used to amplify the DNA: ITS5 and ITS4 for the internal transcribed spacer (ITS) region (White et al. 1990) and LR0R and LR7 for the nuclear large subunit (nLSU) rDNA gene (Vilgalys and Hester 1990).

The procedures for DNA extraction and polymerase chain reaction (PCR) used in this study were the same as described by Wu et al. (2022). The PCR products were purified and sequenced by Beijing Genomics Institute (BGI), China. All newly generated sequences in this study were deposited in GenBank (Sayers et al.2024; http://www.ncbi.nlm.nih.gov/genbank/) and listed in Table 1.

Phylogenetic analysis

Phylogenetic trees of *Cerrena* and *Polyporus* were constructed using the two concatenated ITS1-5.8S-ITS2-nLSU sequences dataset, respectively, and phylogenetic analyses were performed with Maximum Likelihood (ML) and Bayesian Inference (BI) methods. New sequences generated in this study and reference sequences retrieved from GenBank (Table 1) were partitioned to ITS1, 5.8S, ITS2, nLSU and then aligned separately using MAFFT v.74 (Katoh et al. 2019; http://mafft.cbrc.jp/alignment/server/) with the G-INS-I iterative refinement algorithm and optimised manually in BioEdit v.7.0.5.3 (Hall 1999). The separate alignments were then concatenated using PhyloSuite v.1.2.2 (Zhang et al. 2020). Unreliably aligned sections were removed before the analyses, and efforts were made to manually inspect and improve the alignment. The data matrix was edited in Mesquite v3.70. *Irpex latemarginatus* (Durieu & Mont.) C.C. Chen & Sheng H. Wu was used as an outgroup in the phylogenetic analysis of *Cerrena* (Parmasto and Hallenberg 2000). *Trametes conchifer* (Schwein.) Pilát, *T. elegans* (Spreng.) Fr. and *T. polyzona* (Pers.) Justo were selected as outgroups in the phylogenetic analysis of *Polyporus* (Ji et al. 2022). The final alignments and the retrieved topologies were deposited in TreeBASE (http://www.treebase.org) under accessions 31102, 31103.

RAxML 7.2.8 was used to infer ML trees for both datasets with the GTR+I+G model of site substitution, including estimation of Gamma-distributed rate heterogeneity and a proportion of invariant sites (Stamatakis 2006). The branch support was evaluated with a bootstrapping method of 1,000 replicates (Hillis and Bull 1993).

Table 1. Taxa information and GenBank accession numbers of the sequences used in this study.

Species	Specimen No.	Country	ITS	LSU
Cerrena albocinnamomea	Miettinen 10511	China	OR262168	OR262168
Cerrena albocinnamomea	NIBRFG0000102423	South Korea	FJ821532	–
Cerrena albocinnamomea	Dai 12892	China	KC485522	KC485539
Cerrena albocinnamomea	KUC20121102-06	South Korea	KJ668561	–
Cerrena caulinicystidiata	**Yuan 12664**	**Vietnam**	**MT269762**	**MT259328**
Cerrena caulinicystidiata	**Yuan 12666**	**Vietnam**	**MT269763**	**MT259329**
Cerrena caulinicystidiata (*Cerrena* sp. 1)	BJ2-11	China	KX527879	–
Cerrena caulinicystidiata (*Cerrena* sp. 1)	G1669	China	MK247953	–
Cerrena caulinicystidiata (*Cerrena* sp. 1)	Otu0185	China	MT908560	–
Cerrena caulinicystidiata*	**Wu 661**	**China**	**PP035831**	**PP035828**
Cerrena cystidiata	548/17	Brazil	MZ649034	MZ649034
Cerrena gilbertsonii	JV 1609/29	Guadeloupe	OR262202	–
Cerrena gilbertsonii	Vandevender 94-144	Mexico	OR262171	OR262171
Cerrena multipileata	JV 1407/63	Costa Rica	OR262201	OR262201
Cerrena multipileata	Ryvarden 43881	Costa Rica	OR262155	OR262155
Cerrena multipileata	Kout A36	Guatemala	OR262203	–
Cerrena sp. 2	F12	China	OP022000	–
Cerrena sp. 2	7-SU-3-B-77(M)-B	Indonesia	KJ654531	–
Cerrena sp. 2	NTOU5117	Taiwan	MN592928	–
Cerrena unicolor	B2	Antarctica	HM589361	–
Cerrena unicolor	D.T6.5_2	Argentina	MH019790	–
Cerrena unicolor	CBS 154.29	Canada	MH855029	–
Cerrena unicolor	He6082	China	OM100740	OM083972
Cerrena unicolor	GSM-10	China	JQ798288	–
Cerrena unicolor	Han 849	China	MW467890	–
Cerrena unicolor	CU2	Czech	FJ821536	–
Cerrena unicolor	H:Otto Miettinen 9443	Finland	FN907915	FN907915
Cerrena unicolor	MUT<ITA_:5063	Italy	MK581063	–
Cerrena unicolor	FCG-1937	Japan	LC415531	–
Cerrena unicolor	Pertti Uotila 47558 (H)	Kyrgyzstan	OR262167	–
Cerrena unicolor	Feketic	Serbia	MW485440	–
Cerrena unicolor	KA17-0024	South Korea	MN294859	–
Cerrena unicolor	3115	Sweden	JN710525	JN710525
Cerrena unicolor	CUZFVG179	Turkey	MK120293	–
Cerrena unicolor	K(M):249944	UK	MZ159683	–
Cerrena unicolor	FD-299	USA	KP135304	KP135209
Cerrena unicolor	TASM: YG/PS79	Uzbekistan	MT526291	–
Cerrena zonata	Gates 2008-4-17 (H)	Australia	OR262160	OR262160
Cerrena zonata	Otto Miettinen 9773 (H)	China	OR262157	OR262157
Cerrena zonata	Otto Miettinen 9889 (H)	China	OR262158	OR262158
Cerrena zonata	Otto Miettinen 13798 (H)	Indonesia	OR262166	OR262166
Cerrena zonata	WS36_1_2_B_As	Japan	LC631683	–
Cerrena zonata	PDD:95790	New Zealand	HQ533016	–

Species	Specimen No.	Country	ITS	LSU
Cerrena zonata	KA17-0224	South Korea	MN294861	–
Cerrena zonata	LE-BIN 4492	Vietnam	OP985107	–
Datroniella scutellata	RLG9584T	USA	JN165004	JN164792
Datroniella tropica	Dai 13147	China	KC415181	KC415189
Echinochaete brachypora	TFM:F 24996	Japan	AB462321	AB462309
Echinochaete russiceps	TFM:F 15716	Japan	AB462310	AB368065
Echinochaete russiceps	TFM:F 24250	Japan	AB462313	AB462301
Favolus acervatus	Cui 11053	China	KU189774	KU189805
Favolus acervatus	Dai 10749b	China	KX548953	KX548979
Favolus gracilisporus	Cui 4292	China	KX548970	KX548992
Favolus gracilisporus	Li 1938	China	KX548971	KX548993
Hexagonia glabra	Dai 10691	China	JX569733	JX569750
Hexagonia tenuis	Cui 8468	China	JX559277	JX559302
Irpex latemarginatus	Dai 8289	China	KY131835	–
Lentinus longiporus	DAOM:229479	Canada	AB478880	LC052217
Lentinus longiporus	WD2579	Japan	AB478879	LC052218
Lentinus substrictus	Wei 1582	China	KU189767	KU189798
Lentinus substrictus	Wei 1600	China	KC572022	KC572059
Microporus affinis	Cui 7714	China	JX569739	JX569746
Microporus flabelliformis	Dai 11574	China	JX569740	JX569747
Mycobonia flava	CulTENN10256	Costa Rica	AY513570	AJ487934
Mycobonia flava	TENN59088	Argentina	AY513571	AJ487933
*Neodatronia gaoligongensis**	Cui 8055	China	JX559269	JX559286
*Neodatronia sinensis**	Dai 11921	China	JX559272	JX559283
Neofavolus cremeoalbidus	Cui 12412	China	KX899982	KX900109
*Neofavolus cremeoalbidus**	TUMH:50009	Japan	AB735980	AB735957
Neofavolus mikawai	Cui 11152	China	KU189773	KU189804
Neofavolus mikawai	Dai 12361	China	KX548975	KX548997
Physisporinus lineatus	JV_1008_18	Costa Rica	OM669902	–
Physisporinus lineatus	JV_1407_37	Costa Rica	OM669903	–
Physisporinus vinctus	JV0610_A31B-1	Mexico	JQ409460	–
Physisporinus vinctus	JV0610_A31B-2	Mexico	JQ409461	–
Picipes ailaoshanensis	Cui 12585	China	KX900068	KX900183
*Picipes ailaoshanensis**	Cui 12578	China	KX900067	KX900182
Picipes americanus	JV 0809-104	USA	KC572003	KC572042
*Picipes americanus**	JV 0509-149	USA	KC572002	KC572041
*Picipes annularius**	Cui 10123	China	KX900060	KX900176
Picipes atratus	Dai 13375	China	KX900042	KX900158
*Picipes atratus**	Cui 11289	China	KX900043	KX900159
Picipes auriculatus	Yuan 4221	China	KX900064	KX900180
*Picipes auriculatus**	Cui 13616	China	KX900063	KX900179
Picipes badius	Cui 10853	China	KU189780	KU189811
Picipes badius	Cui 11136	China	KU189781	KU189812
Picipes baishanzuensis	Cui 11395	China	KU189763	KU189794
*Picipes baishanzuensis**	Dai 13418	China	KU189762	KU189793

Species	Specimen No.	Country	ITS	LSU
Picipes brevistipitatus	Cui 11345	China	KX900074	KX900188
*Picipes brevistipitatus**	Cui 13652	China	KX900075	KX900189
Picipes cf. dictyopus	Cui 11109	China	KX900025	KX900145
Picipes cf. dictyopus	Cui 11092	China	KX900026	KX900146
Picipes conifericola	Cui 9950	China	KU189783	KU189814
*Picipes conifericola**	Dai 11114	China	JX473244	KC572061
Picipes dictyopus	TENN 59385	Belize	AF516561	AJ487945
Picipes fraxinicola	Dai 2494	China	KC572023	KC572062
Picipes fraxinicola	Wei 6025	China	KC572024	KC572063
Picipes melanopus	H 6003449	Finland	JQ964422	KC572064
Picipes melanopus	MJ 372-93	Czech	KC572026	KC572065
*Picipes nigromarginatus**	Cui 8113	China	KX900062	KX900178
Picipes pumilus	Cui 5464	China	KX851628	KX851682
Picipes pumilus	Dai 6705	China	KX851630	KX851684
Picipes rhizophilus	Dai 11599	China	KC572028	KC572067
Picipes rhizophilus	Dai 16082	China	KX851634	KX851687
Picipes subdictyopus	Cui 11220	China	KX900057	KX900173
Picipes subdictyopus	Cui 12539	China	KX900058	KX900174
Picipes submelanopus	Dai 13294	China	KU189770	KU189801
Picipes submelanopus	Dai 13296	China	KU189771	KU189802
Picipes subtropicus	Li 1928	China	KU189758	KU189790
*Picipes subtropicus**	Cui 2662	China	KU189759	KU189791
Picipes subtubaeformis	Cui 10793	China	KU189753	KU189785
*Picipes subtubaeformis**	Dai 11870	China	KU189752	KU189784
Picipes taibaiensis	Dai 5741	China	JX489169	KC572071
*Picipes taibaiensis**	Dai 5746	China	KX196783	KX196784
Picipes tibeticus	Cui 12225	China	KU189756	KU189788
*Picipes tibeticus**	Cui 12215	China	KU189755	KU189787
Picipes tubaeformis	Niemela 6855	Finland	KC572036	KC572073
Picipes tubaeformis	JV 0309-1	USA	KC572034	KC572072
Picipes ulleungus	Cui 12410	China	KX900022	KX900142
Picipes virgatus	CulTENN11219	Argentina	AF516581	AJ488122
Picipes virgatus	CulTENN11406	Argentina	AF516582	AJ488122
*Picipes wuyishanensis**	Dai 7409	China	KX900061	KX900177
Podofomes mollis	RLG6304sp	USA	JN165002	JN164791
Podofomes stereoides	Holonen	Finland	KC415179	KC415196
*Polyporus auratus**	Dai 13665	China	KX900056	KX900172
Polyporus austrosinensis	Cui 11140	China	KX900046	KX900162
*Polyporus austrosinensis**	Cui 11126	China	KX900045	KX900161
Polyporus cuticulatus	Cui 8637	China	KX851614	KX851668
Polyporus cuticulatus	Dai 13141	China	KX851613	KX851667
Polyporus guianensis	TENN 58404	Venezuela	AF516566	AJ487948
Polyporus guianensis	TENN 59093	Argentina	AF516564	AJ487947
*Polyporus hapalopus**	Yuan 5809	China	KC297219	KC297220

Species	Specimen No.	Country	ITS	LSU
Polyporus hemicapnodes	Cui 11259	China	KX851625	KX851679
Polyporus hemicapnodes	Dai 13403	China	KX851627	KX851681
Polyporus lamelliporus	Dai 12327	China	KX851622	KX851676
*Polyporus lamelliporus**	Dai 15106	China	KX851623	KX851677
Polyporus leprieurii	TENN 58579	Costa Rica	AF516567	AJ487949
*Polyporus mangshanensis**	Dai 15151	China	KX851796	KX851797
Polyporus minutissimus	**Wu 970**	**China**	**PP035829**	**PP035826**
Polyporus minutissimus*	**Wu 971**	**China**	**PP035830**	**PP035827**
Polyporus parvovarius	Yuan 6639	China	KX900049	KX900165
Polyporus parvovarius	Dai 13948	China	KX900050	KX900166
Polyporus radicatus	DAOM198916	Canada	AF516584	AJ487955
Polyporus radicatus	TENN 58831	USA	AF516585	AJ487956
Polyporus sp.*1*	Cui 11071	China	KX851642	KX851695
Polyporus sp.*1*	Cui 11045	China	KX851643	KX851696
Polyporus sp.*2*	Dai 13585A	China	KX900055	KX900171
Polyporus squamosus	Cui 10394	China	KX851635	KX851688
Polyporus squamosus	Cui 10595	China	KU189778	KU189809
Polyporus subvarius	WD2368	Japan	AB587643	AB587638
*Polyporus subvarius**	Yu 2	China	AB587632	AB587621
Polyporus tuberaster	Dai 11271	China	KU189769	KU189800
Polyporus tuberaster	Dai 12462	China	KU507580	KU507582
Polyporus umbellatus	Pen 13513	China	KU189772	KU189803
Polyporus varius	Cui 12249	China	KU507581	KU507583
Polyporus varius	Dai 13874	China	KU189777	KU189808
Pseudofavolus cucullatus	Dai 13584A	China	KX900071	KX900185
Pseudofavolus cucullatus	WD2157	Japan	AB587637	AB368114
Trametes conchifer	FP106793sp	USA	JN164924	JN164797
Trametes elegans	FP105679sp	USA	JN164944	JN164799
Trametes polyzona	Cui 11040	China	KR605824	KR605767

Notes: New sequences are in bold; "–" represents missing data; * represents type specimens

For BI, the best-fit partitioning scheme and substitution model were determined by using ModelFinder (Kalyaanamoorthy et al. 2017) via the "greedy" algorithm, branch lengths estimated as "linked" and AICc. The BI was conducted with MrBayes 3.2.6 in two independent runs, each of which had four chains for 20 million generations and started from random trees (Ronquist et al. 2012). Trees were sampled every 1,000 generations. The first 25% of the sampled trees were discarded as burn-in and the remaining ones were used to reconstruct a majority rule consensus and calculate Bayesian Posterior Probabilities (BPP) of the clades.

Phylogenetic trees were visualized using FigTree version 1.4.4 (Rambaut 2018). Branches that received bootstrap support (BS) for ML and BPPs greater than or equal to 75% (ML) and 0.95 (BPP) were considered significantly supported, respectively.

Results

Phylogenetic analyses

In the phylogenetic analysis of *Cerrena* (Fig. 1), the combined ITS1-5.8S-ITS2-nLSU dataset included sequences from 50 fungal collections representing 11 taxa, and one sample of *Irpex latemarginatus* was used as an outgroup. ModelFinder proposed models were HKY+F+G4 for ITS1, GTR+F+I+G4 for 5.8s, HKY+F+G4 for ITS2 and GTR+F+I for nLSU, for Bayesian analysis. The BI analysis resulted in an average standard deviation of split frequencies = 0.008865. As both ML and BI trees resulted in similar topologies, only the topology of the ML analysis is presented together with the statistical values of the ML (≥75%) and BPP (≥0.90) algorithms (Fig. 1). The phylogeny inferred from ITS1-5.8S-ITS2-nLSU sequences (Fig. 1) showed that our three newly sequenced samples together with three samples defined as *Cerrena* sp. 1 by Miettinen et al. (2023) formed an independent lineage with strong support (97/0.98, Fig. 1). The lineage is defined as the new species *Cerrena caulinicystidiata*.

In the phylogenetic analysis of *Polyporus* (Fig. 2), the combined ITS1-5.8S-ITS2-nLSU dataset included sequences from 113 fungal collections representing 71 species, and three samples of *Trametes* were used as outgroups. ModelFinder suggested models were GTR+F+I+G4 for ITS1, K2P+I+G4 for 5.8s, K2P+I+G4 for ITS2 and GTR+F+I+G4 for nLSU, for Bayesian analysis. The BI analysis resulted in an average standard deviation of split frequencies = 0.009675. The ML and BI trees were similar in topology, and only the topology of the ML analysis is presented along with the statistical values of the ML (≥75%) and BPP (≥0.90) algorithms (Fig. 2). The phylogeny inferred from the combined ITS1-5.8S-ITS2-nLSU sequences (Fig. 2) revealed that a new lineage with high support (100/1.00,) nests in the squamosus clade in Polyporus, namely *Polyporus minutissimus*. The new species is closely related to *P. hemicapnodes* Berk. & Broome and *P. parvovarius* H. Lee, N.K. Kim & Y.W. Lim.

Taxonomy

***Cerrena caulinicystidiata* T. Cao, F. Wu & H.S. Yuan, sp. nov.**
MycoBank No: 853719
Figs 3, 4

Holotype. China • Zhejiang Province, Hangzhou, Xiaoshan District, Yangjingwu Forest Park; 30°4'1"N, 120°19'35"E; 134 m a.s.l.; 27 Mar. 2023; on fallen angiosperm branch; F. Wu leg., Wu 661 (BJFC040654).

Etymology. *Caulinicystidiata* (Lat.): Refers to the cystidia with a tapering base.

Description. *Basidiocarps*. Annual, resupinate, sometimes effused-reflexed, continuous, easily separable, without special odor or taste when fresh, corky when dry, up to 10 cm long, 3 cm wide and 0.5 mm thick. Pore surface greyish orange to brownish orange; pores irregular, 3–8 per mm, partly split up to 2 mm long; dissepiments thin. Sterile margin finely fimbriated. Subiculum very thin, yellowish white, ca. 0.5 mm thick, a very thin brownish red crust present in the bottom next to wood. Tubes concolorous with pore surface, corky, 0.5–1 mm long.

***Hyphal structure*.** Hyphal system trimitic, generative hyphae with clamp connections; skeletal and binding hyphae CB+, IKI–; tissues unchanged in KOH.

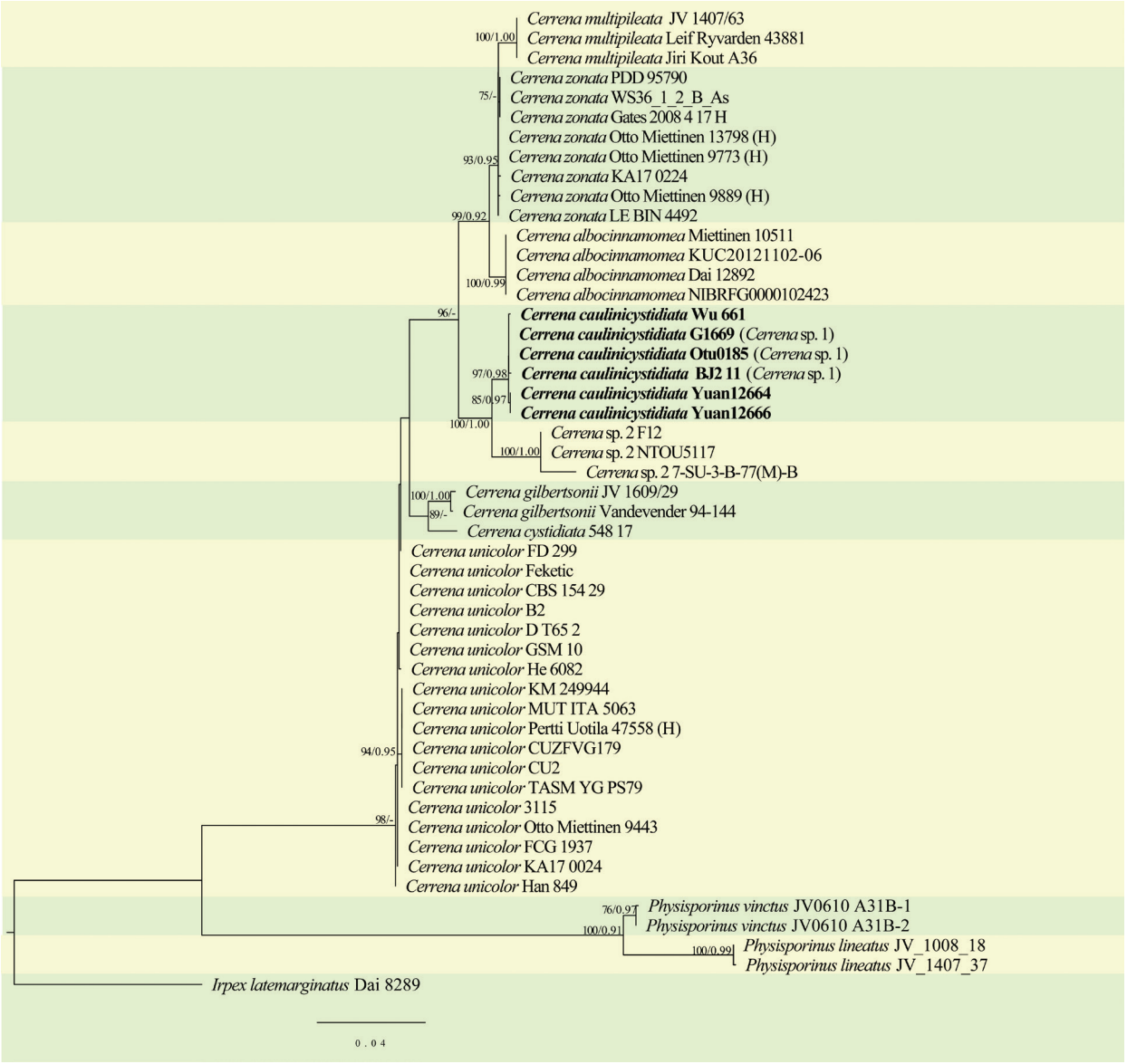

Figure 1. Maximum Likelihood (ML) phylogenetic tree illustrating the phylogeny of *Cerrena* and related genera in five families based on the combined ITS1-5.8S-ITS2-nLSU dataset. Branches are labeled with maximum likelihood bootstrap values (ML) higher than 75% and Bayesian posterior probabilities above 0.90. The new species is given in bold.

***Subiculum*.** Generative hyphae thin- to slightly thick-walled, hyaline, clamped, frequently branched, 2–5 µm in diam; skeletal hyphae dominant, thick-walled to subsolid, unbranched, interwoven, 2.5–6 µm in diam; binding hyphae hyaline, thick-walled to subsolid, tortuose, moderately branched, 1.5–2.5 µm diam. The thin crust made up of subsolid, brownish and strongly agglutinated hyphae.

***Tubes*.** Generative hyphae infrequent, hyaline, thin- to slightly thick-walled, clamped, rarely branched, 2–3 µm diam; skeletal hyphae dominant, hyaline, thick-walled to subsolid, rarely branched, sometimes with septate, interwoven, 2–4 µm in diam; binding hyphae rare. Cystidia clavate to pyriform to ventricose, mostly thin-walled, occasionally thick-walled, smooth, 13–20 × 6–12 µm; encrusted cystidia numerous, clavate, originated from and tightly embedded in trama, 10–25 × 7–15 µm (with encrustation). Basidia short clavate, with four sterigmata and a basal clamp, 8–11 × 4–5 µm, basidioles in shape similar to basidia, but slightly smaller.

Figure 2. Maximum Likelihood (ML) phylogenetic tree illustrating the phylogeny of *Polyporus* and related genera based on the combined ITS1-5.8S-ITS2-nLSU dataset. Branches are labeled with maximum likelihood bootstrap values (ML) higher than 75% and Bayesian posterior probabilities (BPPs) more than 0.90. The new species is given in bold.

Figure 3. Basidiocarps of *Cerrena caulinicystidiata* (Holotype, Wu 661).

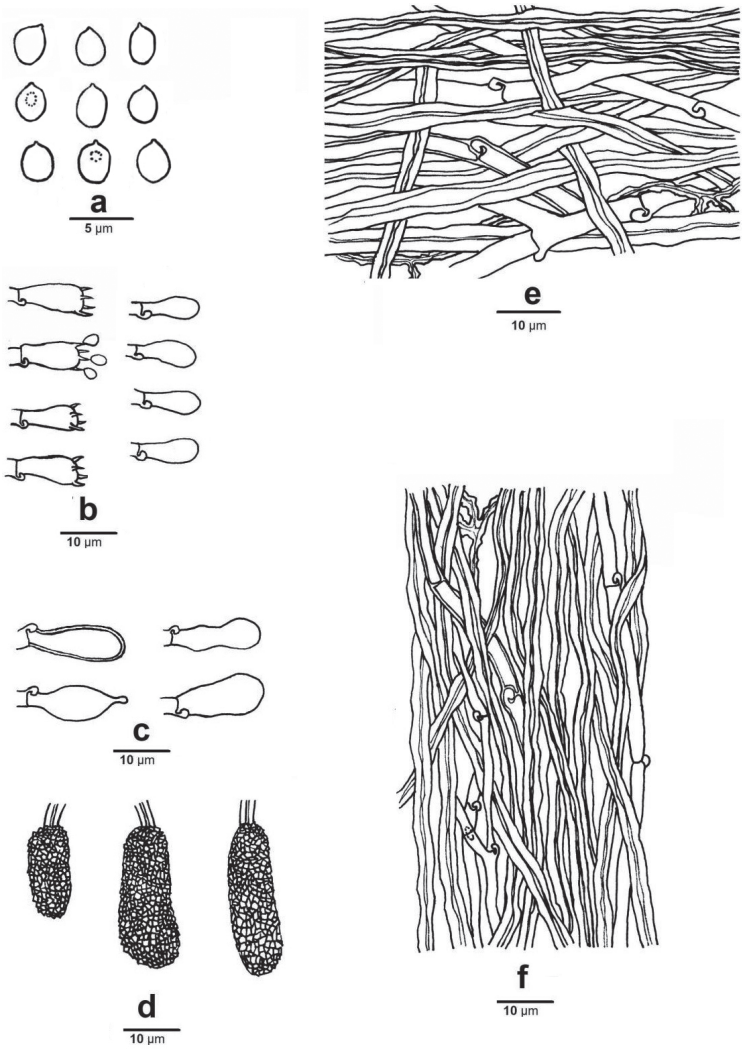

Figure 4. Microscopic structures of *Cerrena caulinicystidiata* (Wu 661) **a** basidiospores **b** basidia and basidioles **c** cystidia **d** encrusted cystidia **e** hyphae from subiculum **f** hyphae from trama.

***Basidiospores*.** Basidiospores broadly-ellipsoid to ovoid, hyaline, thin-walled, smooth, CB–, IKI–, (3–)3.2–4.5(–4.8) × (2.5–)2.8–3.5(–3.9) µm, L = 3.94 µm, W = 2.84 µm, Q = 1.38–1.44 (n = 60/2).

Additional specimens examined (paratypes). Vietnam • Lam dong Province (Lat.), Lac Duong District, Bidoup Nui Ba National Park; 12°11'8"N, 108°40'41"E; 1495 m a.s.l.; 15 Oct. 2017; on fallen angiosperm branch; H.S. Yuan leg., Yuan 12666 (IFP 019379), Yuan 12664 (IFP 019378).

***Polyporus minutissimus* Q.Y. Zhang, Z.W. Zheng & F. Wu, sp. nov.**
MycoBank No: 853720
Figs 5, 6

Holotype. China • Zhejiang Province, Hangzhou, Yuhang District, Luniao Town; 30°25'50"N, 119°42'38"E; 158.47 m a.s.l.; 9 Jun. 2023; on ground of Bamboo forest; F. Wu leg., Wu 971 (BJFC040963, holotype).

Etymology. *Minutissimus* (Lat.): Referring to the species having tiny basidiocarps.

Description. *Basidiocarps*. Annual, centrally stipitate, solitary, fleshy to soft leathery when fresh, becoming fragile when dry. Pilei flat with a depressed center or infundibuliform, up to 1.5 cm in diam and 0.5–1 mm thick. Pileal surface cream to buff yellow when dry, glabrous, occasionally zonate and with radially aligned stripes; margin sharp, incurved upon drying. Pore surface cream when dry; pores angular, 6–9 per mm; dissepiments thin, entire. Context buff cream to pale neutral when dry, fragile upon drying, up to 0.5 mm thick. Tubes white to cream when dry, decurrent, up to 0.5 mm thick. Stipe dark violet, glabrous, 0.3–0.5 cm long and 1–2 mm in diam.

***Hyphal structure*.** Hyphal system dimitic; generative hyphae bearing clamp connections, thin-walled, hyaline; skeleton-binding hyphae thick-walled with a wide lumen, with arboriform branches, IKI–, CB+; tissue unchanged in KOH.

***Context*.** Generative hyphae frequent, colorless, thin-walled, 2.5–4 µm in diam; skeleto-binding hyphae dominant, colorless, thick-walled with a wide lumen, moderately branched, strongly interwoven, 2–4.5 µm diam.

Figure 5. Basidiocarps of *Polyporus minutissimus* (Holotype, Wu 971).

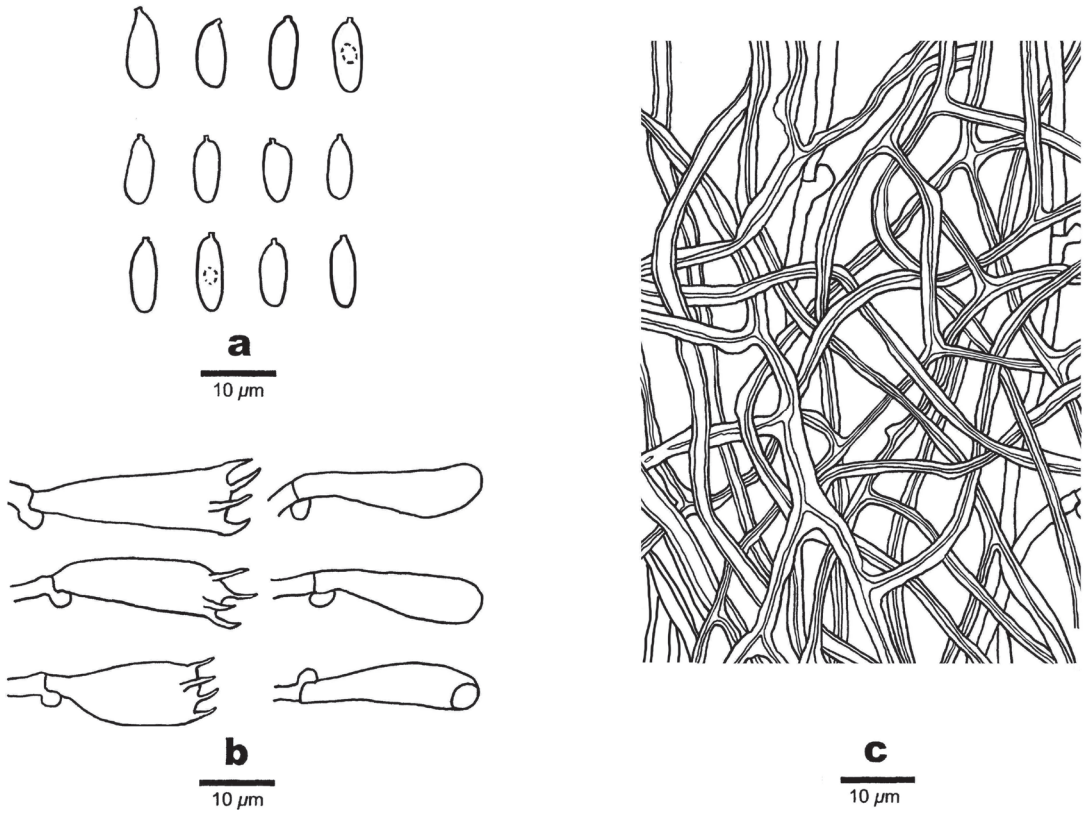

Figure 6. Microscopic structures of *Polyporus minutissimus* (Wu970/Wu 971) **a** basidiospores **b** basidia and basidioles **c** hyphae from trama.

***Tubes*.** Generative hyphae frequent, colorless, thin-walled, 2–3 μm in diam; skeleto-binding hyphae dominant, colorless, thick-walled with a wide lumen, moderately branched, interwoven, 1–3 μm in diam. Cystidia and cystidioles absent. Basidia clavate, with four sterigmata and a basal clamp connection, 22–28 × 7–9 μm; basidioles in shape similar to basidia, but slightly smaller.

***Stipe*.** Generative hyphae frequent, colorless, thin-walled, rarely branched, 3–4 μm in diam; skeleto-binding hyphae dominant, colorless, thick-walled with a wide lumen, moderately branched, interwoven, 1.5–4 μm in diam.

***Basidiospores*.** Basidiospores cylindrical to oblong, colorless, thin-walled, smooth, IKI–, CB–, 5–9.2(–10) × (2–)2.2–4(–4.2) μm, L = 7.30 μm, W = 3.23 μm, Q = 2.25–2.27 (n = 60/2).

Additional specimen examined (paratype). China • Zhejiang Province, Hangzhou, Yuhang District, Luniao Town; 30°25'50"N, 119°42'38"E; 155.11 m a.s.l; on ground of bamboo forest, 9 Jun. 2023; F. Wu leg., Wu 970 (BJFC040962).

Discussion

In this study, two new species of the Polyporales - *Cerrena caulinicystidiata* and *Polyporus minutissimus* - are proposed based on morphological and phylogenetic evidence. Our three newly sequenced *Cerrena* samples together with three samples which were defined as *Cerrena* sp. 1 by Miettinen et al. (2023) formed an independent well-supported lineage in our phylogeny (Fig. 1). The lineage is proposed as the new species *C. caulinicystidiata*. Another lineage which is defined as *Cerrena* sp. 2 in our phylogeny is closely related to

C. caulinicystidiata, but we didn't collect one specimen within the lineage, so the lineage is considered to be *Cerrena* sp.

Cerrena caulinicystidiata is characterized by its resupinate, sometimes effused-reflexed basidiocarps, greyish orange to brownish orange pore surface, 3–8 per mm pores, and subglobose basidiospores, 3.2–4.5 × 2.8–3.5 µm in size. *C. albocinnamomea* (Y.C. Dai & Niemelä) H.S. Yuan originally described from Northeast China resembles *C. caulinicystidiata* by sharing resupinate and easily separable basidiocarps. However, *C. albocinnamomea* differs from *C. caulinicystidiata* by its clavate to pyriform cystidia, slightly smaller ellipsoid basidiospores (2.8–3.5 × 2–3 µm vs. 3.2–4.5 × 2.8–3.5 µm), and a dimitic hyphal system (Yuan 2014).

In addition, *Rigidoporus vinctus* (Berk.) Ryvarden [≡ *Physisporinus vinctus* (Berk.) Murrill, Wu et al. 2017] resembles *C. caulinicystidiata* by having resupinate basidiocarps, ochraceous pore surface, ventricose cystidia with a subcylindric appendage, encrusted cystidia, and subglobose basidiospores, but it can be distinguished from the latter species by its smaller pores (6–12 per mm vs. 3–8 per mm) and generative hyphae with simple septa (Ryvarden and Johansen 1980).

The genus *Cerrena* is widely distributed and has diverse morphological characteristics. Currently, there are 13 records according to Index Fungorum (http://www.indexfungorum.org). However, *C.* '*gilbertsonii*' Ryvarden cannot be distinguished from *C. cystidiata* Rajchenb. & De Meijer by morphological characteristics, and *C.* '*multipileata*' (C.L. Leite & J.E. Wright) Miettinen cannot be distinguished from *C. zonata* (Berk.) H.S. Yuan (Miettinen et al. 2023). *Cerrena aurantiopora* J.S. Lee & Y.W. Lim is a synonym of *C. albocinnamomea* (Lee and Lim 2010; Miettinen et al. 2023). Therefore, we provide a Key to 11 undisputed *Cerrena* species including the new species.

Key to species of the *Cerrena*

1	Paleotropical or temperate-boreal species	**2**
–	Neotropical (South American) species	**9**
2	Basidiocarp poroid, occasionally lacerate	**3**
–	Basidiocarp irpicoid	**8**
3	Pore surface umbrinous to bay or blackish	***C. subglabrescens***
–	Pore surface white, light orange to brown	**4**
4	Pores umber, round, 1–2 per mm	***C. drummondii***
–	Pores round to angular, > 3 per mm	**5**
5	Basidiospores narrowly ellipsoid, 7.5–10 × 2.5–3.5 µm	***C. caperata***
–	Basidiospores ellipsoid to broadly-ellipsoid, < 6 µm in length	**6**
6	Pores angular, dissepiments even or lacerate	***C. albocinnamomea***
–	Pores rounded to irregular	**7**
7	Basidiocarps coriaceous, imbricate	***C. fulvocinerea***
–	Basidiocarps resupinate, sometimes effused-reflexed	***C. caulinicystidiata***
8	Pore surface white to cream	***C. unicolor***
–	Pore surface first white to pale ochraceous	***C. zonata***
9	Cystidia present	***C. cystidiata***
–	Cystidia absent	**10**
10	Pore surface pale cinnamon to brown	***C. sclerodepsis***
–	Pore surface dark brown to almost black	***C. hydnoides***

In the phylogenetic analysis of *Polyporus*, *P. minutissimus* was assigned to the squamosus clade with strong support (100/1.00, Fig. 2). The squamosus clade has always been supported by phylogenetic analysis based on the ITS+nLSU or eight-gene datasets, but the species within this clade cannot be combined into a monophyletic genus because they manifest greatly diverse morphology (Ji et al. 2022). Phylogenetically, *P. minutissimus* is closely related to *P. hemicapnodes* and *P. parvovarius* (Fig. 2). *P. hemicapnodes* was described from Dolosbagey (Sri Lanka). For some time, it was treated as a synonymy of *P. leprieurii* (Núñez and Ryvarden 1995), which differs from *P. minutissimus* by its larger basidiocarps (up to 10 cm vs. up to 1.5 cm), cream to tan pore surface, and longer stipe (up to 5 cm vs. up to 0.5 cm, Berkeley and Broome 1873). *Polyporus parvovarius* has microscopic features similar to *P. minutissimus*. However, *P. parvovarius* differs by its smaller basidiocarps (up to 0.35 cm vs. up to 1.5 cm) and light buff to brown pileal surface (Tibpromma et al. 2017).

Macro-morphologically, *Polyporus minutissimus* has a depressed center or infundibuliform basidiocarps and black stipe, cream to buff yellow pileal surface, and 6–9 per mm pores. Microscopically, it has a dimitic hyphal system, strongly branched skeleton-binding hyphae in both trama and context, and cylindrical basidiospores. Morphologically, *P. lamelliporus* B.K. Cui, Xing Ji & J.L. Zhou is similar to *P. minutissimus* by sharing depressed center or infundibuliform basidiocarps, cream to buff yellow pileal surface, and similar-sized basidiospores, but the former differs through its larger basidiocarps (up to 5.2 cm vs. up to 1.5 cm), longer stipe (1–3.5 cm vs. 0.3–0.5 cm), and larger pores (0.5–1 per mm vs. 6–9 per mm, Ji et al. 2022). In addition, *Picipes baishanzuensis* J.L. Zhou & B.K. Cui, which is similar to *P. minutissimus* and shares infundibuliform basidiocarps and a black stipe, has also been reported from Baishanzu nature reserve, which is the type producing area of our new species. However, *P. baishanzuensis* differs from *P. minutissimus* by its larger basidiocarps (up to 5.5 cm vs. up to 1.5 cm) and smaller basidiospores (6.6–7.9 × 2.5–3.1 µm vs. 5–9.2 × 2.2–4 µm; Zhou et al. 2016).

Polyporus is a very complicated genus with more than 3000 records according to the Index Fungorum. However, studies on *Polyporus* species in China are gradually being carried out, with some Chinese species having been described in Cui et al. (2019) and Ji et al. (2022). Therefore, we provide a Key to Chinese *Polyporus* species including the new species.

Key to species of *Polyporus* in China

1 Stipe absent ..... ***P. megasporoporus***
– Stipe present **2**
2 Stipe bearing black cuticle **3**
– Stipe white to ochraceous **7**
3 Pileal surface covered with dark-brown to reddish-brown squamules ..... ***P. squamosus***
– Pileal surface glabrous **4**
4 Pores more than 5 per mm **5**
– Pores less than 5 per mm **6**
5 Pileal surface concentrically zonate; basidiospores 5.4–7.6 × 2.9–3.8 µm ..... ***P. hemicapnodes***
– Pileal surface azonate; basidiospores 7.5–9 × 2.5–3.3 µm ..... ***P. varius***

6 Pores 3–5 per mm ..... ***P. mangshanensis***
– Pores 1–2 per mm ..... ***P. subvarius***
7 Stipes numerous and branched ..... ***P. umbellatus***
– Stipes usually single and not branched **8**
8 Basidiospores < 8 µm in length **9**
– Basidiospores > 8 µm in length **11**
9 Basidiocarps imbricate ..... ***P. hapalopus***
– Basidiocarps solitary **10**
10 Pores angular, 2–3 per mm ..... ***P. brumalis***
– Pores round, 4–5 per mm ..... ***P. ciliatus***
11 Pileal surface with radial stripes **12**
– Pileal surface without radial stripes **13**
12 Pores 2–5 per mm ..... ***P. cuticulatus***
– Pores 6–9 per mm ..... ***P. minutissimus***
13 Basidiospores usually < 10 µm in length **14**
– Basidiospores usually > 10 µm in length ..... ***P. tuberaster***
14 Cystidioles absent **15**
– Cystidioles infrequent ..... ***P. austrosinensis***
15 Basidia < 27 µm in length **16**
– Basidia > 27 µm in length ..... ***P. lamelliporus***
16 Basidiospores smaller, 6–8.3 × 2.2–3 µm ..... ***P. arcularius***
– Basidiospores larger, 7.7–10 × 3–3.9 µm ..... ***P. auratus***

Polyporales is a large group of Basidiomycota with diverse morphology and phylogeny. There have been over 577 taxonomic proposals in the Polyporales and 2,183 publications with the keyword 'Polyporales' over the past decade (Binder et al. 2013; Justo et al. 2017). However, the species in the order are still not sufficiently investigated in Asia, especially in the subtropics and tropics (Li et al. 2016; Hyde 2022). New DNA sequencing techniques have revolutionized fungal taxonomy and diversity, with multi-marker datasets. In the present study, two new polypore species, *C. caulinicystidiata* and *P. minutissimus* were found in subtropical regions, which enriches our understanding of the fungal diversity of the Polyporales in Asia.

Additional information

Conflict of interest

The authors have declared that no competing interests exist.

Ethical statement

No ethical statement was reported.

Funding

This study was financed by the National Natural Science Foundation of China (Project Nos. 32070006, 32270011, 31701978), the Tibet Autonomous Region Science and Technology Project (XZ202201ZY0006N), and the Fundamental Research Funds for the Central Universities (No. QNTD202307).

Author contributions

Data curation: LRZ. Investigation: HSY, QYZ, FW, ZWZ. Methodology: QYZ, ZWZ. Resources: HSY. Supervision: LRZ, FW. Validation: QYZ, ZWZ. Writing - original draft: ZWZ, QYZ. Writing - review and editing: FW.

Author ORCIDs

Zi-Wei Zheng https://orcid.org/0009-0006-8442-408X
Qiu-Yue Zhang https://orcid.org/0000-0001-9458-3566
Hai-Sheng Yuan https://orcid.org/0000-0001-7056-140X
Fang Wu https://orcid.org/0000-0002-1455-6486

Data availability

All of the data that support the findings of this study are available in the main text or Supplementary Information.

References

Anonymous (1969) Flora of British fungi. Colour identification chart. Her Majesty's Stationery Office, London, 1–3.

Berkeley MJ, Broome CE (1873) Enumeration of the Fungi of Ceylon. Part II., containing the remainder of the Hymenomycetes, with the remaining established tribes of Fungi. (Continued.). Journal of the Linnean Society of London, Botany 14(74): 65–140. https://doi.org/10.1111/j.1095-8339.1873.tb00302.x

Binder M, Justo A, Riley R, Salamov A, Riley R, Salamov A, Lopez-Giraldez F, Sjökvist E, Copeland A, Foster B, Sun H, Larsson E, Larsson KH, Townsend J, Grigoriev IV, Hibbett DS (2013) Phylogenetic and phylogenomic overview of the Polyporales. Mycologia 105(6): 1350–1373. https://doi.org/10.3852/13-003

Corner EJH (1989) Ad Polyporaceae VI. The genus *Trametes*. Beihefte zur Nova Hedwigia, 97 pp.

Cui BK, Li HJ, Ji X, Zhou JL, Song J, Si J, Yang ZL, Dai YC (2019) Species diversity, taxonomy and phylogeny of Polyporaceae (Basidiomycota) in China. Fungal Diversity 97(1): 137–392. https://doi.org/10.1007/s13225-019-00427-4

Cunningham GH, Cunningham GH (1965) Polyporaceae of New Zealand. New Zealand Department of Scientific and Industrial Research, Bulletin, 304 pp.

Dai YC (1996) Changbai wood-rotting fungi 5. Study on *Polyporus mongolicus* and *P. tubaeformis*. Annales Botanici Fennici 33: 153–163.

Dai YC (1999) Changbai wood-rotting fungi 11. Species of *Polyporus* sensu stricto. Fungal Science 14: 67–77.

Dai YC (2012) Polypore diversity in China with an annotated checklist of Chinese polypores. Mycoscience 53(1): 49–80. https://doi.org/10.1007/s10267-011-0134-3

Dai YC, Yuan HS, Wang HC, Yang F, Wei YL (2009) *Polypores* (Basidiomycota) from Qin Mts. in Shaanxi Province, Central China. Annales Botanici Fennici 46(1): 54–61. https://doi.org/10.5735/085.046.0105

Donk MA (1933) Revision der Niederländischen Homobasidiomycetes. Aphyllophoraceae II. Mededelingen van het Botanisch Museum en Herbarium van de Rijksuniversiteit te Utrecht 9: 1–278.

Gilbertson RL, Ryvarden L (1987) North American polypores. Vol. I. *Abortiporus-Lindtneria*. Fungiflora, Oslo, 433 pp.

Grigoriev IV, Nikitin R, Haridas S, Kuo A, Ohm R, Otillar R, Riley R, Salamov A, Zhao X, Korzeniewski F, Smirnova T, Nordberg H, Dubchak I, Shabalov I (2013) Myco-Cosm portal: Gearing up for 1000 fungal genomes. Nucleic Acids Research 42(1): 699–704. https://doi.org/10.1093/nar/gkt1183

Hall TA (1999) BioEdit: A user-friendly biological sequence alignment editor and analysis program for Windows 95/98/NT. Nucleic Acids Symposium Series 41: 95–98.

Hibbett D, Bauer R, Binder M, Giachini AJ, Hosaka K, Justo A, Larsson E, Larsson KH, Lawrey JD, Miettinen O, Nagy L, Nilsson RH, Weiss M, Thorn RG (2014) Agaricomycetes. In: McLaughlin DJ, Spatafora JW (eds), TheMycota. Part A. Springer, Berlin, 373–429. https://doi.org/10.1007/978-3-642-55318-9_14

Hillis DM, Bull JJ (1993) An empirical test of bootstrapping as a method for assessing confidence in phylogenetic analysis. Systematic Biology 42(2): 182–192. https://doi.org/10.1093/sysbio/42.2.182

Hyde KD (2022) The numbers of fungi. Fungal Diversity 114(1): 1. https://doi.org/10.1007/s13225-022-00507-y

Ji X, Zhou JL, Song CG, Xu TM, Wu DM, Cui BK (2022) Taxonomy, phylogeny and divergence times of *Polyporus* (Basidiomycota) and related genera. Mycosphere 13(1): 1–52. https://doi.org/10.5943/mycosphere/13/1/1

Justo A, Miettinen O, Floudas D, Ortiz-Santana B, Sjökvist E, Lindner D, Nakasone K, Niemelä T, Larsson KH, Ryvarden L, Hibbet DS (2017) A revised family-level classification of the Polyporales (Basidiomycota). Fungal Biology 121(9): 798–824. https://doi.org/10.1016/j.funbio.2017.05.010

Kalyaanamoorthy S, Minh BQ, Wong TKF, von Haeseler A, Jermiin LS (2017) ModelFinder: Fast model selection for accurate phylogenetic estimates. Nature Methods 14(6): 587–589. https://doi.org/10.1038/nmeth.4285

Katoh K, Rozewicki J, Yamada KD (2019) MAFFT online service: Multiple sequence alignment, interactive sequence choice and visualization. Briefings in Bioinformatics 20(4): 1160–1166. https://doi.org/10.1093/bib/bbx108

Kirk PM, Cannon PF, Minter DW, Stalpers JA (2008) Dictionary of the Fungi. CABI, Wallingford.

Krüger D, Petersen RH, Hughes KW (2006) Molecular phylogenies and mating study data in *Polyporus* with special emphasis on group "*Melanopus*" (Basidiomycota). Mycological Progress 5(4): 185–206. https://doi.org/10.1007/s11557-006-0512-y

Lee JS, Lim YW (2010) *Cerrena aurantiopora* sp. nov. (Polyporaceae) from eastern Asia. Mycologia 102(1): 211–216. https://doi.org/10.3852/09-048

Li GJ, Hyde KD, Zhao RL, Hongsanan S, Abdel-Aziz FA, Abdel-Wahab MA, Alvarado P, Alves-Silva G, Ammirati JF, Ariyawansa HA, Baghela A, Bahkali AH, Beug M, Bhat DJ, Bojantchev D, Boonpratuang T, Bulgakov TS, Camporesi E, Boro MC, Ceska O, Chakraborty D, Chen JJ, Chethana KWT, Chomnunti P, Consiglio C, Cui BK, Dai DQ, Dai YC, Daranagama DA, Das K, Dayarathne MC, Crop ED, De Oliveira RJV, de Souza CAF, de Souza JI, Dentinger BTM, Dissanayake AJ, Doilom M, Drechsler-Santos ER, Ghobad-Nejhad M, Gilmore SP, Góes-Neto A, Gorczak M, Haitjema CH, Hapuarachchi KK, Hashimoto A, He MQ, Henske JK, Hirayama K, Iribarren MJ, Jayasiri SC, Jayawardena RS, Jeon SJ, Jerônimo GH, Jesus AL, Jones EBG, Kang JC, Karunarathna SC, Kirk PM, Konta S, Kuhnert E, Langer E, Lee HS, Lee HB, Li WJ, Li XH, Liimatainen K, Lima DX, Lin CG, Liu JK, Liu XZ, Liu ZY, Luangsa-ard JJ, Lücking R, Lumbsch HT, Lumyong S, Leaño EM, Marano AV, Matsumura M, McKenzie EHC, Mongkolsamrit S, Mortimer PE,

Nguyen TTT, Niskanen T, Norphanphoun C, O'Malley MA, Parnmen S, Pawłowska J, Perera RH, Phookamsak R, Phukhamsakda C, Pires-Zottarelli CLA, Raspé O, Reck MA, Rocha SCO, de Santiago ALCMA, Senanayake IC, Setti L, Shang QJ, Singh SK, Sir EB, Solomon KV, Song J, Srikitikulchai P, Stadler M, Suetrong S, Takahashi H, Takahashi T, Tanaka K, Tang LP, Thambugala KM, Thanakitpipattana D, Theodorou MK, Thongbai B, Thummarukcharoen T, Tian Q, Tibpromma S, Verbeken A, Vizzini A, Vlasák J, Voigt K, Wanasinghe DN, Wang Y, Weerakoon G, Wen HA, Wen TC, Wijayawardene NN, Wongkanoun S, Wrzosek M, Xiao YP, Xu JC, Yan JY, Yang J, Yang SD, Hu Y, Zhang JF, Zhao J, Zhou LW, Peršoh D, Phillips AJL, Maharachchikumbura SSN (2016) Fungal diversity notes 253–366: Taxonomic and phylogenetic contributions to fungal taxa. Fungal Diversity 78(1): 1–237. https://doi.org/10.1007/s13225-016-0366-9

Martinez D, Larrondo LF, Putnam N, Gelpke MD, Huang K, Chapman J, Helfenbein KG, Ramaiya P, Detter JC, Larimer F, Coutinho PM, Henrissat B, Berka R, Cullen D, Rokhsar D (2004) Genome sequence of the lignocellulose degrading fungus *Phanerochaete chrysosporium* strain RP78. Nature Biotechnology 22(6): 695–700. https://doi.org/10.1038/nbt967

Martinez D, Challacombe J, Morgenstern I, Hibbett D, Schmoll M, Kubicek CP, Ferreira P, Ruiz-Duenas FJ, Martinez AT, Kersten P, Hammel KE, Vanden Wymelenberg A, Gaskell J, Lindquist E, Sabat G, Splinter BonDurant S, Larrondo LF, Canessa P, Vicuna R, Yadav J, Doddapaneni H, Subramanian V, Pisabarro AG, Lavín JL, Oguiza JA, Master E, Henrissat B, Coutinho PM, Harris P, Magnuson JK, Baker SE, Bruno K, Kenealy W, Hoegger PJ, Kües U, Ramaiya P, Lucas S, Salamov A, Shapiro H, Tu H, Chee CL, Misra M, Xie G, Teter S, Yaver D, James T, Mokrejs M, Pospisek M, Grigoriev IV, Brettin T, Rokhsar D, Berka R, Cullen D (2009) Genome, transcriptome, and secretome analysis of wood decay fungus *Postia* placenta supports unique mechanisms of lignocellulose conversion. Proceedings of the National Academy of Sciences of the United States of America 106(6): 1954–1959. https://doi.org/10.1073/pnas.0809575106

Micheli PA (1729) Nova Plantarum Genera. B. Paperninii, Florence.

Miettinen O, Vlasák J, Larsson E, Vlasák JJ, Seelan JSS, Levicky Q, Larsson K, Spirin V (2023) A revised genus-level classification for Cerrenaceae (Polyporales, Agaricomycetes). Fungal Systematics and Evolution 12(1): 271–322. https://doi.org/10.3114/fuse.2023.12.14

Niemelä T, Kotiranta H (1991) Polypore survey of Finland 5. The genus *Polyporus*. Karstenia 31(2): 55–68. https://doi.org/10.29203/ka.1991.285

Núñez M, Ryvarden L (1995) *Polyporus* (Basidiomycotina) and related genera. Synopsis Fungorum 10: 1–85.

Parmasto E, Hallenberg N (2000) A taxonomic study of phlebioid fungi (Basidiomycota). Nordic Journal of Botany 20(1): 105–118. https://doi.org/10.1111/j.1756-1051.2000.tb00740.x

Petersen JH (1996) The Danish mycological society's colour-chart. Foreningen til Svampekundskabens Fremme, Greve, 1–6.

Rambaut A (2018) Molecular evolution, phylogenetics and epidemiology. FigTree ver.4.4 software. [Accessed October 2022]

Ronquist M, Teslenko M, Mark P, Ayres DL, Darling A, Höhna S, Larget B, Liu L, Suchard MA, Huelsenbeck JP (2012) MrBayes 3.2: Efficient Bayesian Phylogenetic Inference and Model Choice Across a Large Model Space. Systematic Biology 61(3): 539–542. https://doi.org/10.1093/sysbio/sys029

Ryvarden L (1991) Genera of polypores. Nomenclature and taxonomy. Synopsis Fungorum 5: 1–363.

Ryvarden L, Gilbertson RL (1993) *European polypores*: Part 1: *Abortiporus-Lindtneria*. Fungiflora A/S, Oslo, 387 pp.

Ryvarden L, Johansen I (1980) A preliminary polypore flora of East Africa. Fungiflora, Oslo, 636 pp.

Ryvarden L, Melo I (2022) Poroid fungi of Europe, 3rd edn. Synopsis Fungorum 37: 1–431.

Ryvarden L, Decock C, Mossebo D, Masuka A (2022) Poroid fungi of Africa. Synopsis Fungorum 45: 1–271.

Sayers EW, Cavanaugh M, Clark K, Pruitt KD, Sherry ST, Yankie L, Karsch-Mizrachi I (2024) GenBank 2024 Update. Nucleic Acids Research 52(1): 134–137. https://doi.org/10.1093/nar/gkad903

Singer R (1986) The Agaricales in modern taxonomy, 4th edn. Koeltz Scientific Book, Koenigstein, 981 pp.

Sotome K, Hattori T, Ota Y, To-anun C, Salleh B, Kakishima M (2008) Phylogenetic relationships of *Polyporus* and morphologically allied genera. Mycologia 100(4): 603–615. https://doi.org/10.3852/07-191R

Sotome K, Hattori T, Ota Y (2011) Taxonomic study on a threatened polypore, *Polyporus pseudobetulinus*, and a morphologically similar species, *P. subvarius*. Mycoscience 52(5): 319–326. https://doi.org/10.1007/S10267-011-0111-X

Stamatakis A (2006) RAxML-VI-HPC: Maximum Likelihood-based phylogenetic analyses with thousands of taxa and mixed models. Bioinformatics (Oxford, England) 22(21): 2688–2690. https://doi.org/10.1093/bioinformatics/btl446

Tibpromma S, Hyde KD, Jeewon R, Maharachchikumbura SSN, Liu JK, Bhat DJ, Jones EBG, McKenzie EHC, Camporesi E, Bulgakov TS, Doilom M, Santiago ALCMA, Das K, Manimohan P, Gibertoni TB, Lim YW, Ekanayaka AH, Thongbai B, Lee HB, Yang JB, Kirk PM, Sysouphanthong P, Singh SK, Boonmee S (2017) Fungal diversity notes 491–602: Taxonomic and phylogenetic contributions to fungal taxa. Fungal Diversity 83(1): 1–261. https://doi.org/10.1007/s13225-017-0378-0

Vilgalys R, Hester M (1990) Rapid genetic identification and mapping of enzymatically amplified ribosomal DNA from several *Cryptococcus* species. Journal of Bacteriology 172(8): 4238–4246. https://doi.org/10.1128/jb.172.8.4238-4246.1990

White TJ, Bruns T, Lee S, Taylor J (1990) "Amplification and direct sequencing of fungal ribosomal RNA genes for phylogenetics," in PCR Protocols: A Guide to Methods and Applications. Academic Press, New York, 315–322. https://doi.org/10.1016/B978-0-12-372180-8.50042-1

Wu F, Chen JJ, Ji XH, Vlasák J, Dai YC (2017) Phylogeny and diversity of the morphologically similar polypore genera *Rigidoporus*, *Physisporinus*, *Oxyporus*, and *Leucophellinus*. Mycologia 109: 749–765. https://doi.org/10.1080/00275514.2017.1405215

Wu F, Li SJ, Dong CH, Dai YC, Papp V (2020) The genus *Pachyma* (Syn. *Wolfiporia*) reinstated and species clarification of the cultivated medicinal mushroom "Fuling" in China. Frontiers in Microbiology 11: 590788. https://doi.org/10.3389/fmicb.2020.590788

Wu F, Zhou LW, Vlasák J, Dai YC (2022) Global diversity and systematics of Hymenochaetaceae with poroid hymenophore. Fungal Diversity 113(1): 1–192. https://doi.org/10.1007/s13225-021-004 96-4

Yuan HS (2014) Molecular phylogenetic evaluation of *Antrodiella* and morphologically allied genera in China. Mycological Progress 13(2): 353–364. https://doi.org/10.1007/s11557-013-0921-7

Zhang D, Gao F, Jakovlić I, Zou H, Zhang J, Li WX, Wang GT (2020) PhyloSuite: An integrated and scalable desktop platform for streamlined molecular sequence data

management and evolutionary phylogenetics studies. Molecular Ecology Resources 20(1): 348–355. https://doi.org/10.1111/1755-0998.13096

Zhao CL, Cui BK, Song J, Dai YC (2015) Fragiliporiaceae, a new family of Polyporales (Basidiomycota). Fungal Diversity 70(1): 115–126. https://doi.org/10.1007/s13225-014-0299-0

Zhou JL, Zhu L, Chen H, Cui BK (2016) Taxonomy and phylogeny of *Polyporus* group *Melanopus* (Polyporales, Basidiomycota) from China. PLoS ONE 11(8): e0159495. https://doi.org/10.1371/journal.pone.0159495

Supplementary material 1

31102 Treebase

Authors: Zi-Wei Zheng, Qiu-Yue Zhang, Li-Rong Zhang, Hai-Sheng Yuan, Fang Wu

Data type: nxs

Link: https://doi.org/10.3897/mycokeys.106.121840.suppl1

Supplementary material 2

31103 Treebase

Authors: Zi-Wei Zheng, Qiu-Yue Zhang, Li-Rong Zhang, Hai-Sheng Yuan, Fang Wu

Data type: nxs

Link: https://doi.org/10.3897/mycokeys.106.121840.suppl2

MycoKeys 106: 23–41 (2024)
DOI: 10.3897/mycokeys.106.124944

Research Article

Multi-gene phylogenetic and taxonomic contributions to *Xylaria* (Ascomycota) associated with fallen fruits from China

An-Hong Zhu[1,2,3,4], Zi-Kun Song[1,2], Jun-Fang Wang[1,2,5], Hao-Wen Guan[1,2,6], Zhi Qu[1,2], Hai-Xia Ma[1,2,7]

1 *Hainan Key Laboratory of Tropical Microbe Resources, Institute of Tropical Bioscience and Biotechnology, Chinese Academy of Tropical Agricultural Sciences, Haikou 571101, China*
2 *Haikou Key Laboratory for Protection and Utilization of Edible and Medicinal Fungi, Hainan Institute for Tropical Agricultural Resources, Haikou 571101, China*
3 *School of Ecology and Nature Conservation, Beijing Forestry University, Beijing 100083, China*
4 *Coconut Research Institute, Chinese Academy of Tropical Agricultural Sciences, Wenchang 571339, China*
5 *College of Plant Protection, Jilin Agricultural University, Changchun 130118, China*
6 *School of Life Science, Liaoning University, Shenyang 110036, China*
7 *Chongzuo Key Laboratory for Protection and Utilization of Edible and Medicinal Fungi, Fusui 532100, China*

Corresponding author: Hai-Xia Ma (mahaixia@itbb.org.cn)

Abstract

Morphological and phylogenetic analyses on samples of *Xylaria* species associated with fallen fruits from China were carried out, and two new species were described, namely *X. aleuriticola* and *X. microcarpa*. *Xylaria aleuriticola* is found on fallen fruits of *Aleurites moluccana*, and characterized by stromata dichotomously branched several times with long acute sterile apices, fertile parts roughened with perithecia and tomentose, and ellipsoid to fusiform ascospores. *Xylaria microcarpa* differs in its very small stromata with dark brown tomentum, light brown ascospores with an inconspicuous straight germ slit, and grows on leguminous pods. The differences between the new species and morphologically similar species are discussed. Phylogenetic analyses on ITS-RPB2-TUB sequences confirmed that the two species are clearly separated from other species of the genus *Xylaria*. *Xylaria liquidambaris* is reported as a new record from China. A key to the *Xylaria* species associated with fallen fruits and seeds reported from China is provided to facilitate future studies of the genus.

Key words: Ascomycota, fructicolous fungi, new species, seminicolous fungi, Xylariaceae

This article is part of:
Diversity, taxonomy, and systematics of macrofungi from tropical Asia
Edited by Olivier Raspé, Rui-Lin Zhao, Jennifer Luangsa-ard

Academic editor: Jennifer Luangsa-ard
Received: 8 April 2024
Accepted: 19 May 2024
Published: 13 June 2024

Citation: Zhu A-H, Song Z-K, Wang J-F, Guan H-W, Qu Z, Ma H-X (2024) Multi-gene phylogenetic and taxonomic contributions to *Xylaria* (Ascomycota) associated with fallen fruits from China. MycoKeys 106: 23–41. https://doi.org/10.3897/mycokeys.106.124944

Introduction

Xylaria Hill ex Schrank, with more than 878 epithets listed in Index Fungorum (http://www.indexfungorum.org/Names/Names.asp, accessed on 22 November 2023), was currently the largest genus in the family Xylariaceae (Hsieh et al. 2010; Fournier et al. 2018a). The members of *Xylaria* have a worldwide distribution, but they are highly diverse in the tropics and subtropics (Dennis 1956; Ju and Rogers 1999; Ju and Hsieh 2007; Lodge et al. 2008; Fournier et al. 2011; Wangsawat et al. 2021). Species of *Xylaria* are saprobic, pathogenic, or endophytic and associated with a wide range of host (Rogers 1979a; Vannini et al. 1996; Whalley 1996; Crozier et al. 2006; Thomas et al. 2008; U'Ren et al. 2009; de Vega et al. 2010). According to the substrate in which these fungi grow,

the taxa of the genus can be divided into four different ecological types, viz., wood-inhabiting type, termite nests inhabiting type, foliicolous type, and fructicolous/seminicolous type. The *Xylaria* species associated with fallen fruits and seeds preferred to somewhat substrate-specific (Rogers 1979b; Læssøe and Lodge 1994; Ju et al. 2018; Perera et al. 2020).

The generic concept of *Xylaria* was traditionally based on morphological studies (Dennis 1957, 1958; Rogers et al. 1987, 1988; San Martín and Rogers 1989; Fournier 2014; Fournier et al. 2020). In the past two to three decades, molecular phylogenetic analysis was carried out on the family Xylariaceae by using a single-gene to multi-gene (Lee et al. 2000; Bahl et al. 2005; Ju et al. 2004, 2007; Peláez et al. 2008; Hsieh et al. 2010; Læssøe et al. 2013; Wangsawat et al. 2021). Nuclear ribosomal DNA, ITS-5.8S, and protein-coding gene are commonly used for inferring phylogenetic relationships (Tang et al. 2009; Visser et al. 2009). The new genus *Neoxylaria* was segregated from *Xylaria* based on morphological and phylogenetic evidence (Konta et al. 2020). The genus *Xylaria* is quite common in China, however, molecular studies on the *Xylaria* are still poorly used (Teng 1963; Tai 1979; Li and Li 1994; Xu 1999; Zhu and Guo 2011; Ma et al. 2011, 2013). Especially, the phylogenetic relationships inferring from multi-gene between *Xylaria* species associated with fruits and other *Xylaria* species as well as other genera in the Xylariaceae remain unsolved, and the species diversity and geographical distribution in China are unclear.

During the investigation of xylariaceous taxa from China, 18 samples belonging to 3 species of *Xylaria* associated with fruits were collected. Based on morphological and multi-gene phylogenetic evidences, two new species and one new Chinese record are introduced in this study.

Materials and methods

Sample collection and morphological studies

The studied samples were collected from south China during 2013–2020. The fallen fruits bearing xylariaceous stromata were dried with a SX-770 portable drier of Foshan Taomeihui Electric Appliance Co., Ltd (Guangdong, China), and deposited in the Fungarium of Institute of Tropical Bioscience and Biotechnology, Chinese Academy of Tropical Agricultural Sciences (FCATAS). Macro- and micro-morphological studies were carried out in this study and followed Ma et al. (2022). Stromatal surface and perithecia were observed and measured by using a VHX-600E 3D microscope of the Keyence Corporation (Osaka, Japan). Microscopic observations and examinations were performed by using an Olympus IX73 inverted fluorescence microscope (Tokyo, Japan) and the CellSens Dimensions Software (Olympus, Tokyo, Japan). In presenting ascospore size variation, 5% of measurements were excluded from each end of the range and given in parentheses. The following abbreviations were used: KOH = 5% potassium hydroxide, SDS = 1% sodium dodecyl sulfate, M = mean ascospore length × mean ascospore width, Q = the ration of mean ascospore length / mean ascospore width, n (a/b) = number of ascospores (a) measured from number of specimens (b). Colour terms followed Rayner (1970).

DNA extraction, amplification, and sequencing

Total genomic DNA was extracted from dried specimens using a cetyltrimethylammonium bromide (CTAB) rapid extraction kit (Aidlab Biotechnologies, Beijing) following its instruction with some modifications as in Song et al. (2022). Three DNA gene fragments, the internal transcribed spacer (ITS) region, RNA polymerase II subunit (RPB2) gene, and β-tubulin (TUB) were amplified using the primer pairs ITS5/ITS4 (White et al. 1990), fRPB2-5F/fRPB2-7cR (Liu et al. 1999), and T1/T22 (O' Donnell et al. 1997), respectively. The PCR procedures for the three sequences followed Pan et al. (2022). Newly generated sequences were uploaded on GenBank and listed in Table 1.

Table 1. List of taxa used for the phylogenetic reconstruction. GenBank accession numbers, specimen numbers, origin and host are given. Holotype specimens are labelled with HT. Species highlighted in bold were derived from this study. N/A: not available.

Species	Specimen No.	Origin	Host	GenBank Accession Number		
				ITS	RPB2	ß-tubulin
Amphirosellinia fushanensis	HAST91111209(HT)	China	dead twigs	GU339496	GQ848339	GQ495950
A. nigrospora	HAST91092308(HT)	China	dead twigs	GU322457	GQ848340	GQ49595
Astrocystis bambusae	HAST89021904	China	bamboo culms	GU322449	GQ844836	GQ495942
As. mirabilis	HAST94070803	China	bamboo culms	GU322448	GQ844835	GQ49594
Kretzschmaria clavus	JDR114	French Guiana	wood	EF026126	GQ844789	EF025611
K. guyanensis	HAST89062903	China	bark	GU300079	GQ844792	GQ478214
K. neocaledonica	HAST94031003	China	bark	GU300078	GQ844788	GQ478213
Nemania abortiva	BiSH467(HT)	USA	–	GU292816	GQ844768	GQ470219
N. diffusa	HAST91020401	China	bark	GU292817	GQ844769	GQ470220
N. sphaeriostomum	JDR261	USA	wood	GU292821	GQ844774	GQ470224
Podosordaria mexicana	WSP176	Mexico	horse dung	GU324762	GQ853039	GQ844840
P. muli	WSP167(HT)	Mexico	mule dung	GU324761	GQ853038	GQ844839
Poronia pileiformis	WSP88113001(ET)	China	cow dung	GU324760	GQ853037	GQ502720
Rosellinia merrillii	HAST89112601	China	bark	GU300071	GQ844781	GQ470229
R. sanctacruciana	HAST90072903	China	fronds of *Arenga engleri*	GU292824	GQ844777	GQ470227
Xylaria adscendens	HAST570	Guadeloupe	wood	GU300101	GQ844817	GQ487708
X. aethiopica	YMJ1136	Ethiopia	pods of *Millettia ferruginea*	MH790445	MH785222	MH785221
X. aleuriticola	**FCATAS858(HT)**	**China**	**fruits of *Aleurites moluccana***	**MZ648856**	**MZ707101**	**MZ695778**
X. aleuriticola	**FCATAS859**	**China**	**fruits of *Aleurites moluccana***	**MZ648857**	**MZ707102**	**MZ695779**
X. aleuriticola	**FCATAS862**	**China**	**fruits of *Aleurites moluccana***	**MZ648858**	**N/A**	**MZ695780**
X. aleuriticola	**FCATAS863**	**China**	**fruits of *Aleurites moluccana***	**MZ648859**	**N/A**	**MZ695781**
X. aleuriticola	**FCATAS864**	**China**	**fruits of *Aleurites moluccana***	**MZ648860**	**MZ707103**	**N/A**
X. allantoidea	HAST94042903	China	trunk	GU324743	GQ848356	GQ502692

Species	Specimen No.	Origin	Host	GenBank Accession Number		
				ITS	RPB2	ß-tubulin
X. amphithele	HAST529	Guadeloupe	dead leaves	GU300083	GQ844796	GQ478218
X. apoda	HAST90080804	China	bark	GU322437	GQ844823	GQ495930
X. arbuscula	HAST89041211	China	bark	GU300090	GQ844805	GQ478226
X. atrosphaerica	HAST91111214	China	bark	GU322459	GQ848342	GQ495953
X. berteri	HAST90112623	China	wood	GU324749	GQ848362	AY951763
X. brunneovinosa	HAST720(HT)	China	ground of bamboo plantation	EU179862	GQ853023	GQ502706
X. cirrata	HAST664(ET)	China	ground of vegetable farm	EU179863	GQ853024	GQ502707
X. cranioides	HAST226	China	wood	GU300075	GQ844785	GQ478210
X. cubensis	JDR860	USA	wood	GU991523	GQ848365	GQ502700
X. culleniae	JDR189	Thailand	pod	GU322442	GQ844829	GQ495935
X. curta	HAST92092022	China	bark	GU322443	GQ844830	GQ495936
X. digitata	HAST919	Ukraine	wood	GU322456	GQ848338	GQ495949
X. enterogena	HAST785	French Guiana	wood	GU324736	GQ848349	GQ502685
X. escharoidea	HAST658(ET)	China	ground of mango orchard	EU179864	GQ853026	GQ502709
X. fabacearum	MFLU16-1061(HT)	Thailand	seed pods of Fabaceae	NR171104	MT212202	MT212220
X. fabaceicola	MFLU16-1072(HT)	Thailand	seed pods of Fabaceae	NR171103	MT212201	MT212219
***Xylaria* sp.**	**FCATAS917**	**China**	**pericarps of *Fagus longipetiolata***	**MZ621171**	**MZ707122**	**MZ695801**
X. feejeensis	HAST92092013	China	bark	GU322454	GQ848336	GQ495947
X. fimbriata	HAST491	Martinique	termite nest	GU324753	GQ853022	GQ502705
X. fissilis	HAST367	Martinique	bark	GU300073	GQ844783	GQ470231
X. frustulosa	HAST92092010	China	bark	GU322451	GQ844838	GQ495944
X. cf. *glebulosa*	HAST431	Martinique	Fruits of *Swietenia macrophylla*	GU322462	GQ848345	GQ495956
X. globosa	HAST775	Guadeloupe	bark	GU324735	GQ848348	GQ502684
X. grammica	HAST479	China	wood	GU300097	GQ844813	GQ487704
X. griseosepiacea	HAST641(HT)	China	ground of mango orchard	EU179865	GQ853031	GQ502714
X. haemorrhoidalis	HAST89041207	China	bark	GU322464	GQ848347	GQ502683
X. hedyosmicola	FCATAS856(HT)	China	leaves of *Hedyosmum orientale*	MZ227121	MZ221183	MZ683407
X. hypoxylon	HAST95082001	China	wood	GU300095	GQ844811	GQ487703
X. intracolorata	HAST90080402	China	bark	GU324741	GQ848354	GQ502690
X. ianthinovelutina	HAST553	Martinique	fruit of *Swietenia macrophylla*	GU322441	GQ844828	GQ495934
X. intraflava	HAST725(HT)	China	ground of bamboo plantation	EU179866	GQ853035	GQ502718
X. juruensis	HAST92042501	China	*Arenga engleri*	GU322439	GQ844825	GQ495932
X. laevis	HAST95072910	China	bark	GU324747	GQ848360	GQ502696
X. lindericola	FCATAS852	China	leaves of *Lindera robusta*	MZ005635	MZ031982	MZ031978
X. liquidambaris	HAST93090701	China	fruits of *Liquidambar formosana*	GU300094	GQ844810	GQ487702
X. liquidambaris	**FCATAS872**	**China**	**fruits of *Liquidambar formosana***	**MZ620273**	**MZ707106**	**N/A**

Species	Specimen No.	Origin	Host	GenBank Accession Number		
				ITS	RPB2	ß-tubulin
X. liquidambaris	**FCATAS874**	**China**	**fruits of *Liquidambar formosana***	**MZ620275**	**MZ707107**	**MZ695775**
X. liquidambaris	**FCATAS877**	**China**	**fruits of *Liquidambar formosana***	**MZ620276**	**MZ707109**	**N/A**
X. liquidambaris	**FCATAS879**	**China**	**fruits of *Liquidambar formosana***	**MZ620278**	**MZ707110**	**N/A**
X. meliacearum	JDR148	Puerto Rico	petioles and infructescence of *Guarea guidonia*	GU300084	GQ844797	GQ478219
X. microcarpa	**FCATAS883(HT)**	**China**	**pods of legume**	**MZ648823**	**MZ707111**	**MZ695776**
X. microcarpa	**FCATAS885**	**China**	**pods of legume**	**MZ648824**	**N/A**	**MZ695777**
X. microceras	HAST414	Guadeloupe	wood	GU300086	GQ844799	GQ478221
X. montagnei	HAST495	Martinique	wood	GU322455	GQ848337	GQ495948
X. multiplex	JDR259	USA	wood	GU300099	GQ844815	GQ487706
X. muscula	HAST520	Guadeloupe	dead branch	GU300087	GQ844800	GQ478222
X. nigripes	HAST653	China	ground of mango orchard	GU324755	GQ853027	GQ502710
X. ochraceostroma	HAST401(HT)	China	ground of mango orchard	EU179869	GQ853034	GQ502717
X. oligotoma	HAST784	French Guiana	wood	GU300092	GQ844808	GQ487700
X. ophiopoda	HAST93082805	China	bark	GU322461	GQ848344	GQ495955
X. oxyacanthae	JDR859	USA	seeds of *Crataegus monogyna*	GU322434	GQ844820	GQ495927
X. palmicola	PDD604	New Zealand	fruits of palm	GU322436	GQ844822	GQ495929
X. papulis	HAST89021903	China	wood	GU300100	GQ844816	GQ487707
X. phyllocharis	HAST528	Guadeloupe	dead leaves	GU322445	GQ844832	GQ495938
X. plebeja	HAST91122401	China	trunk of *Machilus zuihoensis*	GU324740	GQ848353	GQ502689
X. polymorpha	JDR1012	USA	wood	GU322460	GQ848343	GQ495954
X. polysporicola	FCATAS848(HT)	China	leaves of *Polyspora hainanensis*	MZ005592	MZ031980	MZ031976
X. reevesiae	HAST90071609(HT)	China	fruits of *Reevesia formosana*	GU322435	GQ844821	GQ495928
X. regalis	HAST920	India	log of *Ficus racemosa*	GU324745	GQ848358	GQ502694
X. rogersii	FCATAS915(HT)	China	fruits of *Magnolia* sp.	MZ648827	MZ707121	MZ695800
X. schimicola	FCATAS896(HT)	China	fruits of *Schima noronhae*	MZ648850	MZ707114	MZ695787
X. schweinitzii	HAST92092023	China	bark	GU322463	GQ848346	GQ495957
X. scruposa	HAST497	Martinique	wood	GU322458	GQ848341	GQ495952
X. sicula	HAST90071613	China	fallen leaves	GU300081	GQ844794	GQ478216
Xylaria sp. 6	JDR258	USA	leaves of *Tibouchina semidecandra*	GU300082	GQ844795	GQ478217
X. striata	HAST304	China	branch of *Punica granatum*	GU300089	GQ844803	GQ478224
X. telfairii	HAST90081901	China	bark	GU324738	GQ848351	GQ502687
X. theaceicola	FCATAS903(HT)	China	fruits of *Schima villosa*	MZ648848	MZ707115	MZ695788
X. tuberoides	HAST475	Martinique	wood	GU300074	GQ844784	GQ478209
X. venustula	HAST 88113002	China	bark	GU300091	GQ844807	GQ487699
X. vivantii	HAST519(HT)	Martinique	fruits of *Magnolia* sp.	GU322438	GQ844824	GQ495931
X. wallichii	FCATAS923(HT)	China	fruits of *Schima wallichii*	MZ648861	MZ707118	MZ695793

Phylogenetic analyses

Xylaria species associated with fallen fruits and seeds were subjected to phylogenetic analyses in other various species of *Xylaria* and closely related genera including *Amphirosellinia*, *Astrocystis*, *Kretzschmaria*, *Nemania*, *Podosordaria*, and *Rosellinia* (Table 1). *Poronia pileiformis* (Berk.) Fr. was selected as an outgroup (Wangsawat et al. 2021; Ma et al. 2022).

The sequences of ITS, RPB2 and TUB2 were aligned individually using the online MAFFT tool (http://mafft.cbrc.jp/alignment/server/index.html), and improved manually using BioEdit 7.0.5.3 (Hall 1999) and ClustalX 1.83 (Thompson et al. 1997). The individual gene data sets were concatenated using the MEGA 6.0 (Tamura et al. 2011). The concatenated data set of ITS, RPB2 and TUB (ITS-RPB2-TUB) data set of studied species were carried out using Bayesian inference (BI) and maximum likelihood (ML) analyses. Maximum likelihood (ML) analysis was conducted by raxmlGUI 2.0 using rapid bootstrapping with 1000 replicates, and GTRGAMMA+G as a substitution model (Felsenstein 1981). Bayesian inference (BI) analysis was performed in MrBayes 3.2.6 with jModelTest 2 conducting model discrimination (Huelsenbeck and Ronquist 2001). Six simultaneous Markov chains were run from random starting trees for 1 million generations, and trees were sampled every 1000th generations. The first 25% of sampled trees were discarded as burn-in, and the remaining were used to calculate the posterior probability (PP) of each branch (Larget and Simon 1999). The combined alignment and phylogenetic tree were deposited in Figshare (https://figshare.com/s/e1c181f1e3a56164ecc3).

Results

Molecular phylogeny

Eighteen *Xylaria* species associated with fallen fruits and seeds were subjected to phylogenetic analyses based on ITS-RPB2-TUB dataset in Xylariaceae. The BI and ML analyses generated highly similar topologies, the ML tree is presented with bootstrap values ≥ 75% and Bayesian posterior probabilities ≥ 0.90 respectively (Fig. 1).

In the phylogenetic tree (Fig. 1), the genus *Podosordaria* separated from other genera, *Amphirosellinia*, *Astrocystis*, *Kretzschmaria*, *Nemania*, and *Rosellinia* were nested within *Xylaria* clade. All *Xylaria* species associated with fallen fruits and seeds were distributed within clade HY or clade PO as shown in Hsieh et al. (2010) and Ma et al. (2022). In HY clade, a *Xylaria* species on fruits of *Fagus longipetiolata* and four known *Xylaria* species associated with pericarps of fruits, including *X. schimicola* Hai X. Ma & Yu Li, *X. theaceicola* Hai X. Ma & Yu Li, *X. wallichii* Hai X. Ma & Yu Li and *X. liquidambaris* J.D. Rogers, Y.M. Ju & F. San Martín, formed a subclade with high support values (BS = 88, PP = 1.00). In the PO clade, the new species *X. aleuriticola* on fruits of *Aleurites moluccana* and *X. microcarpa* on pods grouped with six fructicolous *Xylaria* species including *X. aethiopica* J. Fourn., Y.M. Ju, H.M. Hsieh & U. Lindem., *X. ianthinovelutina* (Mont.) Fr., *X. culleniae* Berk. & Broome, *X. fabaceicola* R.H. Perera, E.B.G. Jones & K.D. Hyde, *X. vivantii* Y.M. Ju, J.D. Rogers, J. Fourn. & H.M. Hsieh, *X. rogersii* Hai X. Ma & Yu Li, and *X. juruensis* Henn. on *Arenga engleri* in a subclade with high support values (BS = 100, PP = 1.00).

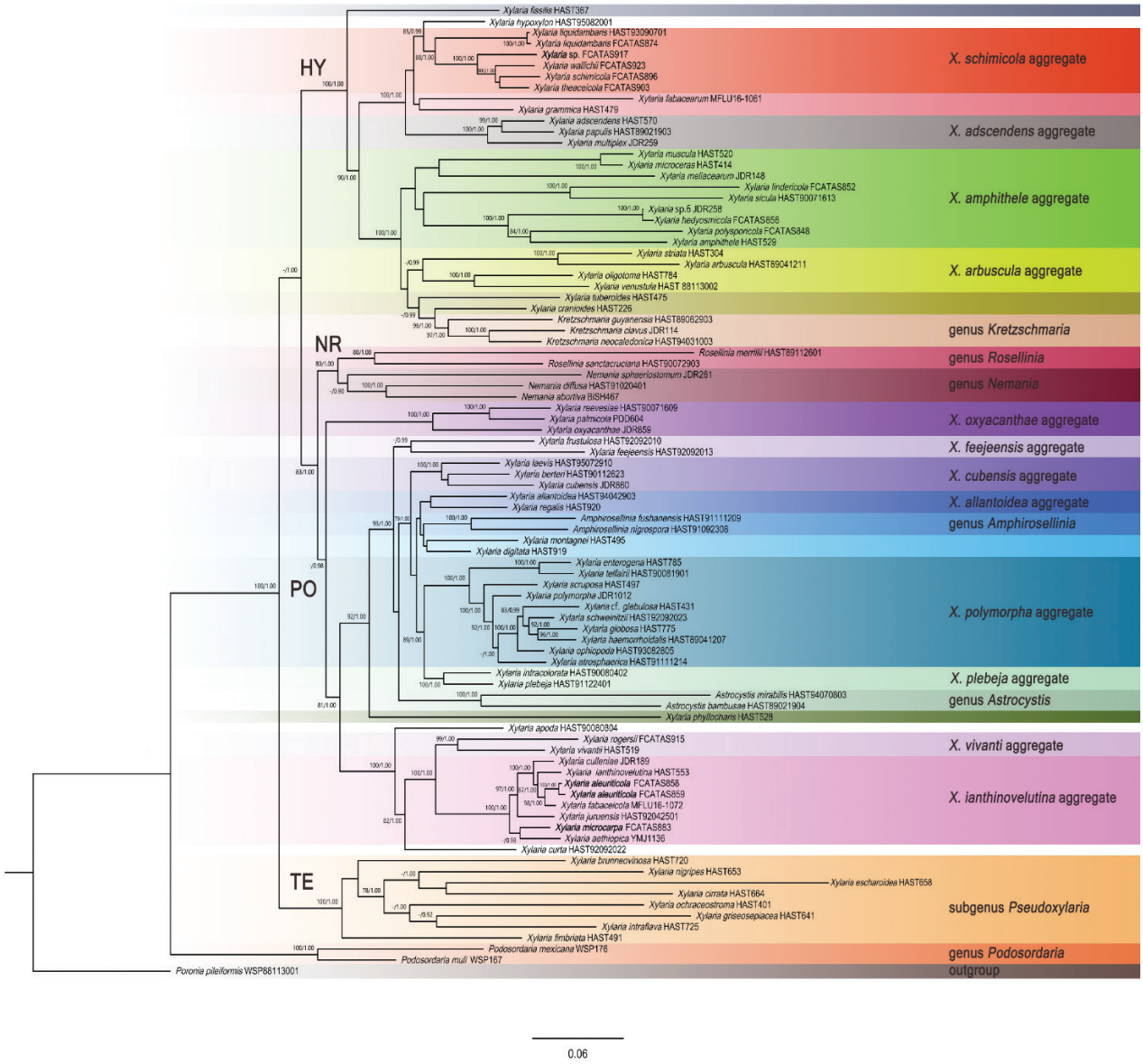

Figure 1. Phylogenetic tree of *Xylaria* based on the multigene alignment of ITS-RPB2-TUB2 in the ML tree. ML bootstrap support (BS) ≥ 75% and Bayesian posterior probabilities (PP) ≥ 0.90 are given at the nodes in this order. New species in this study are indicated in bold.

Taxonomy

***Xylaria aleuriticola* Hai X. Ma, A.H. Zhu & Yu Li, sp. nov.**
MycoBank No: 840908
Fig. 2

Type. China. Yunnan Province, Jinghong City, Xishuangbanna Primeval Forest Park, on buried fruits of *Aleurites moluccana* (L.) Willd (Euphorbiaceae), 22 October 2013, Ma HaiXia, FCATAS 858 (Col. 11).

Etymology. *Aleuriticola* (Lat.): referring to the host which the fungus inhabits.

Teleomorph. Stromata upright or prostrate, solitary to often densely clustered, dichotomously branched several times, or unbranched infrequently, 2–11 cm

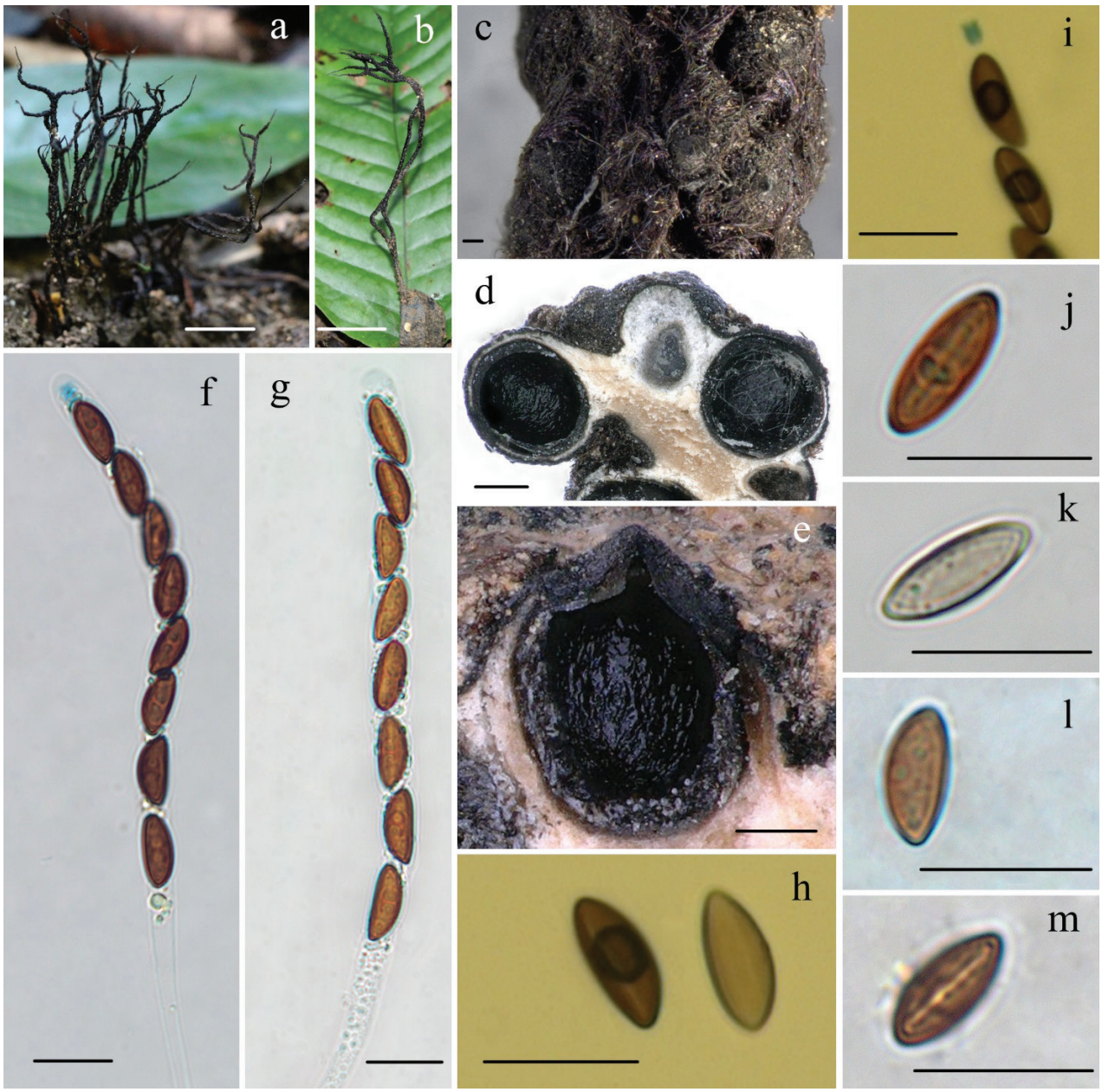

Figure 2. *Xylaria aleuriticola* (FCATAS858, holotype) **a, b** stromata on fallen fruits **c** stromatal surface **d, e** section through stroma, showing perithecia **f** asci in Melzer's reagent **g** asci in water **h** ascospores in Melzer's reagent **i** ascal apical ring in Melzer's reagent **j, k** ascospore in 1% SDS **l** ascospore in India ink **m** ascospore with germ slit in India ink. Scale bars: 2 cm (**a, b**); 100 µm (**c, e**); 200 µm (**d**); 10 µm (**f–m**).

total height, long-stipitate; fertile parts 7–30 mm high × 1.0–2.5 mm broad, narrowly fusiform to cylindrical, often flattened, with acute sterile apices up to 8 mm long, strongly nodulose, particularly tomentose; stipes 12–90 mm high × 0.7–2.6 mm broad, terete to rarely flattened, most often contorted, usually ill-defined, with conspicuously tomentose, arising from a slightly enlarged pannose base; surface roughened with perithecial mounds and tomentose except for stromatal apices, black brown to black; interior white to cream, tan at center, solid, woody. Perithecia subglobose, 300–500 µm. Ostioles conic-papillate. Asci eight-spored arranged in uniseriate manner, cylindrical, long-stipitate, (90–)110–135(–150) µm total length, the spore-bearing parts (55–)60–70(–75) µm long ×

(5.5–)6.0–7.0(–7.5) µm broad, the stipes 30–70 µm long, with apical ring bluing in Melzer's reagent, urn-shaped, 2.0–2.8 µm high × 1.0–1.8 µm diam. Ascospores brown to dark brown, unicellular, ellipsoid to fusiform, inequilateral, with narrowly rounded ends, occasionally one end slightly pinched, smooth, (7.1–)7.5–9.5(–10.5) × (3–)3.5–4(–4.5) µm (M = 8.1 × 3.6 µm, Q = 2.3, n = 60/2), with a conspicuous straight germ slit spore-length or slightly less than spore-length, lacking a hyaline sheath or appendages visible in india ink or 1% SDS.

Additional specimen examined. China. Yunnan Province, Jinghong City, Xishuangbanna Primeval Forest Park, on buried fruits of *Aleurites moluccana* (Euphorbiaceae), 22 October 2013, Ma HaiXia, FCATAS 859 (Col. 23); 22 January 2015, Ma Haixia, FCATAS 862 (Col. 231), FCATAS 863 (Col. 232), FCATAS 864 (Col. 238), FCATAS 865 (COL. 270).

Notes. *Xylaria aleuriticola*, associated with the pericarps of *A. moluccana* (Euphorbiaceae), is characterized by stromata dichotomously branched several times with long acute sterile apices, fertile parts roughened with perithecia and tomentose, and tomentose stipes. It is similar to *X. culleniae* Berk. & Broome by having dichotomously branched stromata and ascospores dimensions, but the latter species branches dichotomously only once in fertile parts, ascospores surrounded with a hyaline sheath and non-cellular appendages, and grows on capsules of *Cullenia excelsa* (Malvaceae) (Rogers et al. 1988; Ju et al. 2018). *Xylaria euphorbiicola* Rehm was described on fruits of *Euphorbia* (Euphorbiaceae) from Brazil, but it has unbranched stromata, lacking perithecial mounds, overlain with a brown striped outermost layer, and smaller discoid apical ring 1µm high × 1.5–2 µm broad (Ju et al. 2018). *Xylaria ianthinovelutina* somewhat resembles *X. aleuriticola* in stromatal morphology, but it has stronger stromata, larger ascospores (9–)9.5–11(–12) × (3.5–)4–4.5(–5) µm (M = 10.3 × 4.0 µm), and often associated with leguminous pods (Dennis 1956, 1957; Ju et al. 2018), while stromata of the new speices has sharper and longer sterile apices, more forked. *Xylaria luzonensis* Henn. differs from *X. aleuriticola* by its smaller stromata (1.5–3 cm long × 0.5–1 mm diam), smaller perithecia (200–300 µm diam), slightly smaller apical ring (1–1.5 µm high × 1.5 µm broad), light brown ascospores, and grows on pod of *Bauhinia cumingiana* (Fabaceae) (Ju et al. 2018). *Xylaria apeibae* Mont. is close to *X. aleuriticola* in stromatal morphology, from which it differs mainly by having smaller stromata 4 cm long × 0.8–1.5 mm diam, light brown and larger ascospores (9.5–)10–12(–13) × (3–)3.5–4(–4.5) µm (M = 11.0 × 3.7 µm), and grows on fruits of *Apeiba* species (Tiliaceae) (Ju et al. 2018). In the phylogenetic analysis (Fig. 1), *X. aleuriticola* clustered together with high support values (BS = 98, PP = 1.00) with *X. fabaceicola*, but the latter species is distinguished by its smaller stromata 13–25 mm long, pale brown to brown ascospores with a hyaline sheath and appendages, and the fact that it grows on decaying pods of Fabaceae (Perera et al. 2020).

Xylaria microcarpa **Hai X. Ma & Yu Li, sp. nov.**
MycoBank No: 840911
Fig. 3

Type. China. Yunnan Province, Xishuangbanna Prefecture, Dadugang Town, Guanping Village, on legume pods, 21 January 2015, Haixia Ma, FCATAS 883 (Col. 233).

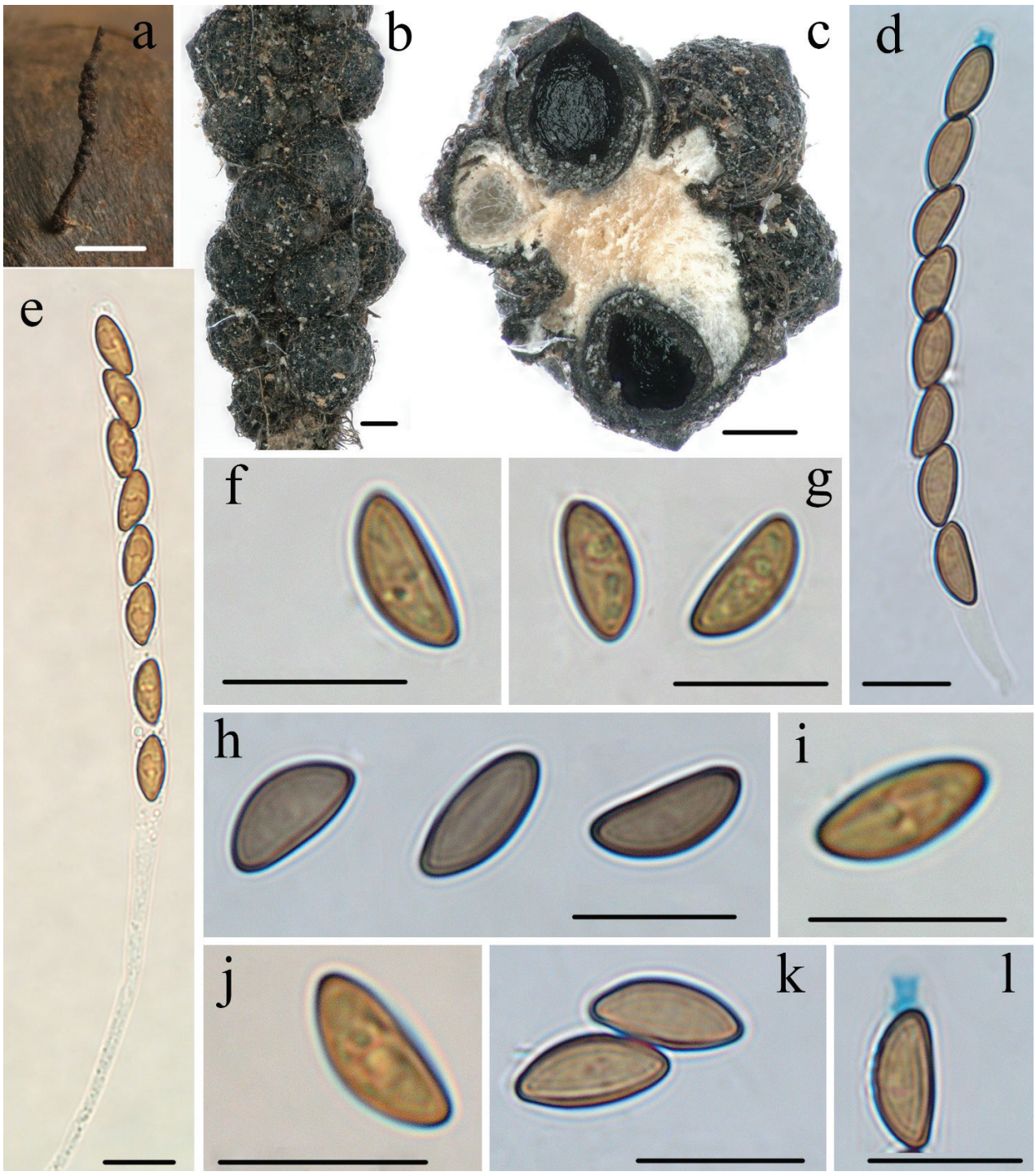

Figure 3. *Xylaria microcarpa* (FCATAS883, holotype) **a** stroma on fallen pod **b** stromatal surface **c** section through stroma, showing perithecia **d** asci with ascal apical ring in Melzer's reagent **e** asci in India ink **f, g** ascospores in water **h** ascospores in Melzer's reagent **i** ascospore with germ slit in India ink **j** ascospore in India ink **k** ascospores in Melzer's reagent **l** ascal apical ring in Melzer's reagent. Scale bars: 0.3 mm (**a**); 200 µm (**b, c**); 10 µm (**d–l**).

Etymology. *Microcarpa* (Lat.): referring to its stroma that it is very small.

Teleomorph. Stromata upright or prostrate, often densely gregarious in large groups, unbranched, cylindrical to filiform, with acute sterile apices, on tomentose stipes, 3.5–9 mm total height; fertile parts 2–6 mm high × 0.6–1.5 mm broad, filiform to cylindrical, brown tomentose dense or sparse, nodulose with

perithecial contours exposed; stipes 1.5–4 mm high × 0.3–0.5 mm broad, terete, with conspicuously dark brown tomentose, arising from slighly enlarged base; surface black, interior light yellow, solid, woody. Perithecia subglobose, 300–500 µm. Ostioles conic-papillate. Asci eight-spored arranged in uniseriate manner, cylindrical, long-stipitate, (96–)105–125(–140) µm total length, the spore-bearing parts (56–)60–70(–75) µm long ×(6.0–)6.4–7.1(–7.6) µm broad, the stipes 30–56 µm long, with apical ring bluing in Melzer's reagent, tubular or urn-shaped, 1.5–2.5 (–2.9) µm high × 1.4–1.8 µm diam. Ascospores light brown, unicellular, ellipsoid-inequilateral, with narrowly rounded ends, sometimes with pinched on one end, smooth, (9.5–)10–11(–11.5) ×(4.5–)5–6(–6.2) µm (M = 10.5 × 5.5 µm, Q = 1.9, n = 60/2), with a inconspicuous straight germ slit almost spore-length, lacking a sheath or appendages visible in india ink or 1% SDS.

Additional specimen examined. China. Yunnan Province, Xishuangbanna Prefecture, Xishuangbanna Tropical Botanical Garden, on legume pods, 20 January 2015, Haixia Ma, FCATAS 885 (Col. 239).

Notes. *Xylaria microcarpa* is characterized by very small stromata growing in groups, overlain with a dark brown tomentum, ascospores light brown with an inconspicuous straight germ slit, lacking a sheath or appendages, and grows on leguminous pods. The new species resembles *X. fabacearum* R.H. Perera, E.B.G. Jones & K.D. Hyde by sharing small stromata and ascospores length dimensions, but differs from the latter species in having stromata branched sometimes, stromatal surface without tomentose, brown to dark brown ascospores with conspicuous straight germ slit (Perera et al. 2020). *Xylaria luzonensis* on *Bauhinia cumingiana* (Fabaceae) differs from *X. microcarpa* by having branched and larger stromata, smaller perithecia, and smaller ascospores (8–)8.5–9.5(–10) × 3–3.5(–4) µm (M = 8.9 × 3.4 µm) (Ju et al. 2018). *Xylaria microcarpa* is somewhat similar to *X. ianthinovelutina* and *X. culleniae* in stromatal surface with tomentum and grow on leguminous pods, but the later two taxa differ in larger stromata, ascospores with a straight germ slit slightly less than spore-length, surrounded with a hyaline sheath and non-cellular appendages (Ju et al. 2018). The phylogenetic tree showed that *Xylaria microcarpa* and *X. aethiopica* J. Fourn., Y.M. Ju, H.M. Hsieh & U. Lindem are sister taxa with a strong supported branch in BI tree (BS=0.98), but *X. aethiopica* is distinct morphologically with larger stromata 15–30 mm total height, brown to dark brown and slightly larger ascospores (9.7–)11–13(–13.5) × (3.5–)3.8–4.5(–4.9) µm (M = 11.9 × 4.1 µm) with a conspicuous straight germ and appendages, and grows on fallen woody pods of *Millettia ferruginea* (Fabaceae) (Fournier et al. 2018b).

Xylaria liquidambaris J.D. Rogers, Y.M. Ju & F. San Martín, Sydowia 54(1): 92. 2002

Fig. 4

Teleomorph. Stromata upright, solitary or sometimes clustered, unbranched or occasionally branched, 1.2–8.0 cm total height; fertile parts 6–25 mm high × 1.5–5.0 mm broad, cylindrical with acute sterile apices, at times longitudinally furrowed, with wrinkles isolating somewhat prominent perithecia; stipes 6–55 mm high × 1.0–2.5 mm broad, glabrous to pubescent arising from a pan-

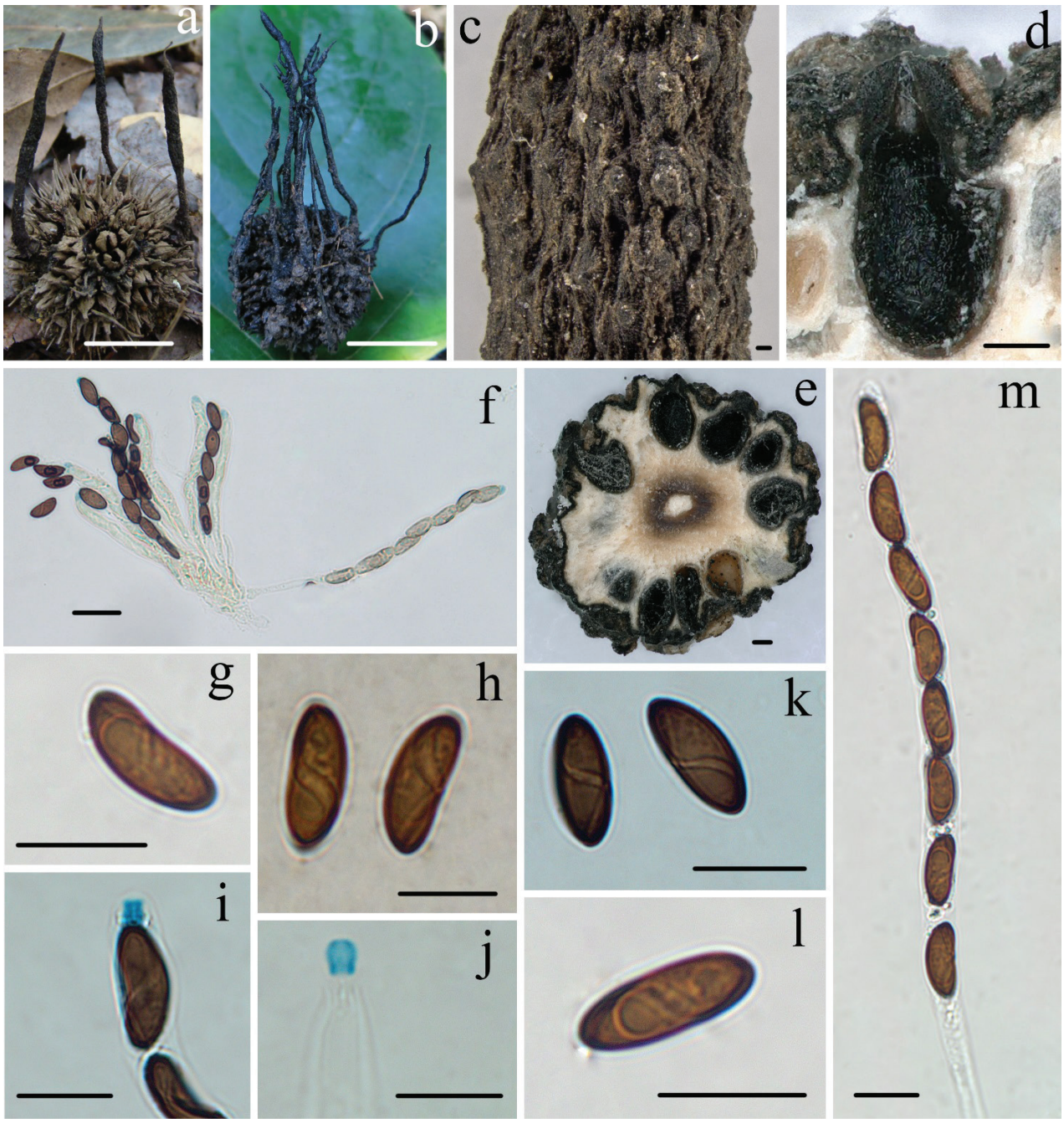

Figure 4. *Xylaria liquidambaris* (**a** from Col.10062607 **b–m** from FCATAS874) **a, b** stromata on fallen fruits **c** stromatal surface **d, e** section through stroma, showing perithecia **f** asci in Melzer's reagent **g, l** ascospore in water **h** ascospores with germ slit in India ink **i, j** ascal apical ring in Melzer's reagent **k** ascospores with germ slit in Melzer's reagent **m** asci in water. Scale bars: 1.5 cm (**a, b**); 100 µm (**c, d, e**); 20 µm (**f**); 10 µm (**g–m**).

nose base; surface dark brown to black, interior white, with dark brown to black a circle, and white at center. Texture solid, soft, woody. Perithecia subglobose, 250–400 µm. Ostioles conic-papillate. Asci eight-spored arranged in uniseriate manner, cylindrical, long-stipitate, (110–)125–145(–165) µm total length, the spore-bearing parts (80–)90–105(–115) µm long × (6–)7–8(–8.5) µm broad, the stipes 30–60 µm long, with apical ring bluing in Melzer's reagent, inverted hap-shaped to more or less rectangular, 2.5–3.5 µm high × 2.0–2.5 µm diam. Ascospores brown, unicellular, ellipsoid-inequilateral with narrowly to broadly

rounded ends, smooth, (12.5–)13–14(–15) × (4.8–)5.5–6.5(–6.8) µm (M = 13.5 × 6.1 µm, Q = 2.2, n = 90/3), with spiraling germ slit, lacking a sheath or appendages in india ink or 1% SDS.

Specimens examined. **China**. Guangdong Province, Chebaling Nature Reserve, on fruits of *Liquidambar formosana*, 26 June 2010, Ma Haixia, Col. 10062607; Fengkai County, Heishiding Nature Reserve, on fruits of *L. formosana*, 2 July 2010, Ma Haixia, Col. 10070206; Jiangxi Province, Guanshan Nature Reserve, on fruits of *L. formosana*, 21 June 2013, Ma Haixia, FCATAS 873 (Col. 16); Fuzhou City, Tang Xianzu Museum, on fruits of *L. formosana*, 17 June 2013, Ma Haixia, FCATAS 877 (Col. 36); Anyuan County, Sanbai Mountain Nature Reserve, on fruits of *L. formosana*, 15 August 2016, Ma Haixia, FCATAS 878 (Col. O37); Zhejiang Province, Tianmu Mountain Nature Reserve, on fruits of *L. formosana*, 6 August 2013, Ma Haixia, FCATAS 872 (Col. 10); Gutian Mountain Nature Reserve, on fruits of *L. formosana*, 13 August 2013, Ma Haixia, FCATAS 496 (Col. 29); Anhui Province, Huangshan City, Qiman County, Guniujiang Nature Reserve, on fruits of *L. formosana*, 8 August 2013, Ma Haixia, FCATAS 874 (Col. 19); Huangshan Nature Reserve, on fruits of *L. formosana*, 27 June 2019, Ma Haixia, FCATAS 879 (Col. P6); Hainan Province, Diaoluoshan Nature Reserve, on fruits of *L. formosana*, 31 December 2020, Ma Haixia, FCATAS 880 (Col. Z211).

Notes. *Xylaria liquidambaris* was originally described by Rogers et al. (2002) from USA, and has high specificity to fruits of *Liquidambar* (Altingiaceae). It is characterized by unbranched stromata with acute sterile apex, embedded to slightly prominent perithecia with longitudinal striations, brown ascospores with long spiraling germ slit (Rogers et al. 2002). These Chinese materials well fit the descriptions and illustrations of *X. liquidambaris* by Rogers et al. (2002).

Discussion

In the present study, two new *Xylaria* species associated with fallen fruits were described and compared with closely related species based on morphological and molecular data. In addition, *X. liquidambaris* has been reported from China for the first time. We included eighteen *Xylaria* species on fallen fruits and seeds in the phylogenetic trees based on a combined ITS-RPB2-TUB2 dataset. The phylogenetic analyses showed that seventeen species are mainly distributed in three different subclades, while *Xylaria* cf. *gleculosa* clustered with *Xylaria* species on wood, which is consistent with the previous studies (Hsieh et al. 2010; Perera et al. 2020; Ma et al. 2022).

By inclusion of the two new species we described here, thirty-seven species on fallen fruits and seeds are now recognized in the genus *Xylaria* (Rogers 1979b; Stowell and Rogers 1983; Rogers et al. 2002; Pande and Waingankar 2004; Rönsch et al. 2010; Hsieh et al. 2010; Dillon et al. 2018; Ju et al. 2018; Fournier et al. 2018b; Perera et al. 2020; Ma et al. 2022). Compared to the number of *Xylaria* species on fruits and seeds, the available sequences of these species in NCBI are relatively fewer. Most species in this group are lacking DNA sequences, and some species only have one or two sequences, for *X. carpophila* just has ITS sequences, and *X. karyophthora* from Guyana with ITS and RPB2 sequences available (Dillon et al. 2018; Vu et al. 2019). Moreover, almost half the taxa, e.g., *X. apeibae* Mont., *X. clusiae* K.F. Rodrigues, *X. duranii* San

Martín & Vanoye, *X. euphorbiicola* Rehm, *X. guazumae* San Martín & J.D. Rogers, *X. heloidea* Penz. & Sacc., *X. himalayensis* Narula & Rawla, *X. jaliscoensis* San Martín, J.D. Rogers & Y.M. Ju, *X. luzonensis* Henn., *X. magnolia* J.D. Rogers, *X. magnolia* var. *microspora* J.D. Rogers, Y.M. Ju & Whalley, *X. patrisiae* Henn., *X. psidii* J.D. Rogers & Hemmes, *X. rhizocola* (Mont.) Fr., *X. rossmanae* Y.M. Ju, J.D. Rogers, *X. terminaliae-bellericae* Pande & Waingankar, *X. terminaliae-crenulatae* Pande & Waingankar, and *X. warburgii* Henn., still have no available sequences. The current molecular study of *Xylaria* usually uses ITS, RPB2, TUB, and α-ACT (Hsieh et al. 2010; Fournier et al. 2018b; Perera et al. 2020; Ma et al. 2022), which is not so sufficient. In recent years, genome sequencing, sanger sequencing and next-generation sequencing have been used in some macrofungi groups for inferring phylogenetic relationships (Wibberg et al. 2021; Wang et al. 2023). To further understand the taxonomy and phylogeny of *Xylaria* associated with fruits and seeds, newly collected specimens from their original regions, more taxa and more DNA sequences need to be included in future study.

Dichotomous key to species of *Xylaria* associated with fruits and seeds in China

1 Ascospores pale or subhyaline **2**
– Ascospores brown to dark brown **5**
2 Ascospores with a conspicuous straight germ slit ..... ***X. theaceicola***
– Ascospores without a germ slit or inconspicuous germ slit **3**
3 Stromata with half- to fully exposed perithecial mounds, frequently dichotomously branched ..... ***X. wallichii***
– Stromata with inconspicuous perithecial mounds, unbranched in most cases **4**
4 Stromata associated with fruits of *Magnolia* (Magnoliaceae); ascospores (13.0–)13.8–15.0(–15.6) × (3.3–) 3.6–4.0(–4.4) µm ..... ***X. rogersii***
– Stromata associated with fruits of *Schima noronhae* (Theaceae); ascospores (9.5–)10.5–12.0(–13.0) × (1.6–)1.9–2.5(–3.0) µm ..... ***X. schimicola***
5 Stromata glabrous on the fertile part **6**
– Stromata tomentose on the fertile part **10**
6 Ascospores with a spiral germ slit, (12.5–)13–14(–15) × (4.8–)5.5–6.5(–6.8) µm ..... ***X. liquidambaris***
– Ascospores with a straight germ slit **7**
7 Stromata associated with pericarps of fruits **8**
– Stromata associated with endocarps of fruits **9**
8 Stromata associated with fruits of *Fagus longipetiolata* (Fagaceae); ascospores (11.0–)11.8–13.5(–15) × (6–)6.5–7.5(–8) µm ..... ***Xylaria* sp.**
– Stromata associated with fruits of *Sloanea* (Elaeocarpaceae); ascospores (9.5–)10–11.5(–12.5) × (3.5–)4–4.5(–5) µm ..... ***X. warburgii***
9 Stromata on fallen fruits of *Reevesia formosana* (Sterculiaceae); ascospores (8.5–)9–10.5(–11) × (4–)4.5–5.5(–6) µm ..... ***X. reevesiae***
– Stromata on seeds of *Crataegus oxyacantha* (Rosaceae); ascospores (10–)11–12(–12.5) × (4.5–)5.0–5.5(–6) µm ..... ***X. oxyacanthae***
10 Stromata unbranched; ascospores (9.5–)10–11(–11.5) × (4.5–) 5–6(–6.2) µm, with an inconspicuous straight germ slit ..... ***X. microcarpa***
– Stromata branched **11**

11 Stromata on buried fruits of *Aleurites moluccana* (Euphorbiaceae); ascospores (7.1–)7.5–9.5(–10.5) × (3–)3.5–4(–4.5) µm.....***X. aleuriticola***
– Stromata on fruits of legume pods (Fabaceae); ascospores (9.6–)10.5–13(–14) × (3.9–)4.3–5.0(–5.5) µm .....***X. ianthinovelutina***

Acknowledgments

We wish to thank Dr. Wan-Jin Liao (Beijing Normal University) who helped us to identify the host.

Additional information

Conflict of interest

The authors have declared that no competing interests exist.

Ethical statement

No ethical statement was reported.

Funding

National Natural Science Foundation of China (Project Nos. 31972848); Central Public-interest Scientific Institution Basal Research Fund for Chinese Academy of Tropical Agricultural Sciences (No. 1630032022003); Yazhou Bay Scientific and Technological Project for Trained Talents of Sanya City (SCKJ-JYRC-2023-74).

Author contributions

Conceptualization and supervision, H.-X. M.; Resources, H.-X. M., Z. Q., and A.-H.Z.; Investigation, methodology and data curation, A.-H. Z., and S.-Z. K.; Software, J.-F. W. and H.-W. G.; Writing – original draft preparation, A.-H. Z.; Writing – review and editing, H.-X. M.; Project administration, H.-X. M.; Funding acquisition, H.-X. M. All authors have read and agreed to the published version of the manuscript.

Author ORCIDs

An-Hong Zhu https://orcid.org/0000-0002-2812-8108
Zi-Kun Song https://orcid.org/0000-0001-9532-2536
Jun-Fang Wang https://orcid.org/0009-0007-1197-6008
Hao-Wen Guan https://orcid.org/0009-0000-2714-4061
Hai-Xia Ma https://orcid.org/0000-0001-6699-7454

Data availability

Publicly available datasets were analyzed in this study. All newly generated sequences were deposited in GenBank (https://www.ncbi.nlm.nih.gov/genbank/; accessed on 26 July 2021; Table 1). All new taxa were deposited in MycoBank (https:www.mycobank.org/; accessed on 19 January 2024; MycoBank identifiers follow new taxa).

References

Bahl J, Jeewon R, Hyde KD (2005) Phylogeny of *Rosellinia capetribulensis* sp. nov. and its allies (Xylariaceae). Mycologia 97(5): 1102–1110. https://doi.org/10.1080/15572536.2006.11832758

Crozier J, Thomas SE, Aime MC, Evans HC, Holmes KA (2006) Molecular characterization of fungal endophytic morphospecies isolated from stems and pods of *Theobroma cacao*. Plant Pathology 55(6): 783–791. https://doi.org/10.1111/j.1365-3059.2006.01446.x

de Vega C, Arista M, Ortiz PL, Talavera S (2010) Anatomical relations among endophytic holoparasitic angiosperms, autotrophic host plants and mycorrhizal fungi: A novel tripartite interaction. American Journal of Botany 97(5): 730–737. https://doi.org/10.3732/ajb.0900147

Dennis RWG (1956) Some Xylarias of tropical America. Kew Bulletin 11(3): 401–444. https://doi.org/10.2307/4109126

Dennis RWG (1957) Further notes on tropical American Xylariaceae. Kew Bulletin 12(2): 297–332. https://doi.org/10.2307/4114428

Dennis RWG (1958) Some Xylosphaeras of tropical Africa. Revista de Biologia (Lisboa) 1: 175–208.

Dillon RH, Hector U, Susy MLM, Catherine A (2018) *Xylaria karyophthora*: A new seed-inhabiting fungus of Greenheart from Guyana. Mycologia 110(2): 434–447. https://doi.org/10.1080/00275514.2018.1457349

Felsenstein J (1981) Evolutionary trees from DNA sequences: A maximum likelihood approach. Journal of Molecular Evolution 17(6): 368–376. https://doi.org/10.1007/BF01734359

Fournier J (2014) Update on European species of *Xylaria*.

Fournier J, Flessa F, Peršoh D, Stadler M (2011) Three new *Xylaria* species from southwestern Europe. Mycological Progress 10(1): 33–52. https://doi.org/10.1007/s11557-010-0671-8

Fournier J, Lechat C, Courtecuisse R (2018a) The genus *Xylaria* sensu lato (Xylariaceae) in Guadeloupe and Martinique (French West Indies) I. Taxa with penzigioid stromata. Ascomycete.Org 10(4): 131–176. https://doi.org/10.25664/ART-0239

Fournier J, Ju YM, Hsieh HM, Lindermann U (2018b) *Xylaria aethiopica* sp. nov. – a new pod-inhabiting species of *Xylaria* (Xylariaceae) from Ethiopia. Ascomycete.Org 10(5): 209–215.

Fournier J, Lechat C, Courtecuisse R (2020) The genus *Xylaria* sensu lato (Xylariaceae) in Guadeloupe and Martinique (French West Indies) III. Taxa with slender upright stromata. Ascomycete.Org 12(3): 81–164. https://doi.org/10.1128/jb.172.8.4238-4246.1990

Hall TA (1999) Bioedit: A user-friendly biological sequence alignment editor and analysis program for windows 95/98/NT. Nucleic Acids Symposium Series 41: 95–98. https://doi.org/10.1021/bk-1999-0734.ch008

Hsieh HM, Lin CR, Fang MJ, Rogers JD, Fournier J, Lechat C, Ju YM (2010) Phylogenetic status of *Xylaria* subgenus *Pseudoxylaria* among taxa of the subfamily Xylarioideae (Xylariaceae) and phylogeny of the taxa involved in the subfamily. Molecular Phylogenetics and Evolution 54(3): 957–969. https://doi.org/10.1016/j.ympev.2009.12.015

Huelsenbeck JP, Ronquist F (2001) MRBAYES: Bayesian inference of phylogenetic trees. Bioinformatics (Oxford, England) 17(8): 754–755. https://doi.org/10.1093/bioinformatics/17.8.754

Ju YM, Hsieh HM (2007) *Xylaria* species associated with nests of *Odontotermes formosanus* in Taiwan. Mycologia 99(6): 936–957. https://doi.org/10.1080/15572536.2007.11832525

Ju YM, Rogers JD (1999) The Xylariaceae of Taiwan (excluding *Anthostomella*). Mycotaxon 73: 343–440.

Ju YM, Rogers JD, Hsieh HM, Vasilyeva L (2004) *Amphirosellinia* gen. nov. and a new species of *Entoleuca*. Mycologia 96(6): 1393–1402. https://doi.org/10.1080/15572536.2005.11832889

Ju YM, Hsieh HM, Ho MC, Szu DH, Fang MJ (2007) *Theissenia rogersii* sp. nov. and phylogenetic position of *Theissenia*. Mycologia 99(4): 612–621. https://doi.org/10.1080/15572536.2007.11832555

Ju YM, Rogers JD, Hsieh HM (2018) *Xylaria* species associated with fallen fruits and seeds. Mycologia 110(4): 726–749. https://doi.org/10.1080/00275514.2018.1469879

Konta S, Hyde KD, Phookamsak R, Xu JC, Maharachchikumbura SSN, Daranagama DA, McKenzie EHC, Boonmee S, Tibpromma S, Eungwanichayapant PD, Samarakoon MC, Lu YZ (2020) Polyphyletic genera in Xylariaceae (Xylariales): *Neoxylaria* gen. nov. and *Stilbohypoxylon*. Mycosphere 11(1): 2629–2651. https://doi.org/10.5943/mycosphere/11/1/17

Læssøe T, Lodge DJ (1994) Three host-specific *Xylaria* species. Mycologia 86(3): 436–446. https://doi.org/10.1080/00275514.1994.12026431

Læssøe T, Srikitikulchai P, Luangsa-ard JJD, Stadler M (2013) *Theissenia* reconsidered, including molecular phylogeny of the type species *T. pyrenocrata* and a new genus *Durotheca* (Xylariaceae, Ascomycota). IMA Fungus 4(1): 57–69. https://doi.org/10.5598/imafungus.2013.04.01.07

Larget B, Simon DL (1999) Markov chain Monte Carlo algorithms for the Bayesian analysis of phylogenetic trees. Molecular Biology and Evolution 16(6): 750–759. https://doi.org/10.1093/oxfordjournals.molbev.a026160

Lee JS, Ko KS, Jung HS (2000) Phylogenetic analysis of *Xylaria* based on nuclear ribosomal ITS1-5.8S-ITS2 sequences. FEMS Microbiology Letters 187(1): 89–93. https://doi.org/10.1111/j.1574-6968.2000.tb09142.x

Li YL, Li HJ (1994) A novel species of *Xylaria*. Journal of Nanjing Agricultural University 17(3): 145–147.

Liu YJ, Whelen S, Hall BD (1999) Phylogenetic relationships among ascomycetes: Evidence from an RNA polymerse II subunit. Molecular Biology and Evolution 16(12): 1799–1808. https://doi.org/10.1093/oxfordjournals.molbev.a026092

Lodge D, Læssøe T, Aime M, Henkel T (2008) Montane and cloud forest specialists among neotropical *Xylaria* species. North American Fungi 3: 193–213. https://doi.org/10.2509/naf2008.003.00713

Ma HX, Vasilyeva L, Li Y (2011) A new species of *Xylaria* from China. Mycotaxon 116(1): 151–155. https://doi.org/10.5248/116.151

Ma HX, Vasilyeva L, Li Y (2013) The genus *Xylaria* in the south of China – 7. Two penzigioid *Xylaria* species. Sydowia 65(2): 329–335.

Ma HX, Song ZK, Pan XY, Qu Z, Yang ZE, Li Y, Zhu AH (2022) Four new pale-spored species of *Xylaria* (Xylariaceae, Xylariales) with a key to worldwide species on fallen fruits and seeds. Biology 11(6): 885. https://doi.org/10.3390/biology11060885

O' Donnell K, Cigelnik E (1997) Two Divergent Intragenomic rDNA ITS2 Types within a Monophyletic Lineage of the Fungus. Molecular Phylogenetics and Evolution 7(1): 103–116. https://doi.org/10.1006/mpev.1996.0376

Pan XY, Song ZK, Qu Z, Liu TD, Ma HX (2022) Three new *Xylaria* species (Xylariaceae, Xylariales) on fallen leaves from Hainan Tropical Rainforest National Park. MycoKeys 86: 47–63. https://doi.org/10.3897/mycokeys.86.71623

Pande A, Waingankar V (2004) Four new taxa in *Xylaria* from Western India. Journal of Economic and Taxonomic Botany 28: 610–613. https://doi.org/10.54207/bsmps1000-2005-Y46383

Peláez F, González V, Platas G, Sánchez-Ballesteros J, Rubio V (2008) Molecular phylogenetic studies within the Xylariaceae based on ribosomal DNA sequences. Fungal Diversity 31: 111–134.

Perera RH, Hyde KD, Maharachchikumbura SSN, Jones EBG, McKenzie EHC, Stadler M, Lee HB, Samarakoon MC, Ekanayaka AH, Camporesi E, et al. (2020) Fungi on wild seeds and fruits. Mycosphere 11(1): 2108–2480. https://doi.org/10.5943/mycosphere/11/1/14

Rayner RW (1970) A mycological color chart. Cmi. & British Mycological Society Kew, London, UK.

Rogers JD (1979a) The Xylariaceae: Systematic, biological and evolutionary aspects. Mycologia 71(1): 1–42. https://doi.org/10.1080/00275514.1979.12020984

Rogers JD (1979b) *Xylaria magnoliae* sp. nov. and comments on several other fruit-inhabiting species. Canadian Journal of Botany 57(8): 941–945. https://doi.org/10.1139/b79-115

Rogers JD, Callan BE, Samuels GJ (1987) The Xylariaceae of the rain forests of North Sulawesi (Indonesia). Mycotaxon 29: 113–172.

Rogers JD, Callan BE, Rossman AY, Samuels GJ (1988) *Xylaria* (Sphaeriales, Xylariaceae) from Cerro de la Neblina, Venezuela. Mycotaxon 31: 103–153.

Rogers JD, San Martín F, Ju YM (2002) A reassessment of the *Xylaria* on *Liquidambar* fruits and two new taxa on *Magnolia* fruits. Sydowia 54: 91–97.

Rönsch P, Rönsch S, Reiher A, Otto P (2010) Investigations on the fructicolous *Xylaria delitschii* and *Xylaria oxyacanthae*. Boletus 32: 106–122.

San Martín F, Rogers JD (1989) A preliminary account of *Xylaria* of Mexico. Mycotaxon 34: 283–373.

Song ZK, Zhu AH, Liu ZD, Qu Z, Li Y, Ma HX (2022) Three new species of *Hypoxylon* (Xylariales, Ascomycota) on a multigene phylogeny from Medog in southwest China. Journal of Fungi 8(5): 500. https://doi.org/10.3390/jof8050500

Stowell EA, Rogers JD (1983) Studies on *Xylaria oxyacanthae*. Mycotaxon 17: 433–444.

Tai FL (1979) Sylloge fungorum Sinicorum. Science Press, Peking.

Tamura K, Peterson D, Peterson N, Stecher G, Nei M, Kumar S (2011) MEGA5: Molecular evolutionary genetics analysis using maximum likelihood, evolutionary distance, and maximum parsimony methods. Molecular Biology and Evolution 28(10): 2731–2739. https://doi.org/10.1093/molbev/msr121

Tang AMC, Jeewon R, Hyde KD (2009) A re-evaluation of the evolutionary relationships within the Xylariaceae based on ribosomal and protein-coding gene sequences. Fungal Diversity 34: 127–155.

Teng SQ (1963) Fungi of China. Science Press, Peking.

Thomas SE, Crozier J, Aime MC, Evans HC, Holmes KA (2008) Molecular characterisation of fungal endophytic morphospecies associated with the indigenous forest tree, *Theobroma gileri*, in Ecuador. Mycological Research 112(7): 852–860. https://doi.org/10.1016/j.mycres.2008.01.008

Thompson JD, Gibson TJ, Plewniak F, Franois J, Higgins DG (1997) The CLUSTAL X windows interface: Flexible strategies for multiple sequence alignment aided by quality analysis tools. Nucleic Acids Research 25(24): 4876–4882. https://doi.org/10.1093/nar/25.24.4876

U'Ren JM, Dalling JW, Gallery RE, Maddison DR, Davis EC, Gibson CM, Arnold AE, U'Ren JM (2009) Diversity and evolutionary origins of fungi associated with seeds of a neotropical pioneer tree: A case study for analysing fungal environmental samples. Mycological Research 113(4): 432–449. https://doi.org/10.1016/j.mycres.2008.11.015

Vannini A, Valentini R, Luisi N (1996) Impact of drought and *Hypoxylon mediterraneum* on oak decline in the Mediterranean region. Annales des Sciences Forestieres 53(2–3): 753–760. https://doi.org/10.1051/forest:19960251

Visser AA, Ros VID, de Beer ZW, Debets AJM, Hartog E, Kuyper TW, Læssøe T, Slippers B, Aanen DK (2009) Levels of specificity of *Xylaria* species associated with fungus-growing termites: A phylogenetic approach. Molecular Ecology 18(3): 553–567. https://doi.org/10.1111/j.1365-294X.2008.04036.x

Vu D, Groenewald M, de Vries M, Gehrmann T, Stielow B, Eberhardt U, Al-Hatmi A, Groenewald JZ, Cardinali G, Houbraken J, Boekhout T, Crous PW, Robert V, Verkley GJM (2019) Large-scale generation and analysis of filamentous fungal DNA barcodes boosts coverage for kingdon fungi and reveals thresholds for fungal species and higher taxon delimitation. Studies in Mycology 92(1): 135–154. https://doi.org/10.1016/j.simyco.2018.05.001

Wang GS, Cai Q, Hao YJ, Bau T, Chen ZH, Li MX, Kraisitudomsook N, Yang ZL (2023) Phylogenetic and taxonomic updates of Agaicales, with an emphasis on *Tricholomopsis*. Mycology 14: 1–30. https://doi.org/10.1080/21501203.2023.2263031

Wangsawat N, Ju YM, Phosri C, Whalley AJS, Suwannasai N (2021) Twelve new taxa of *Xylaria* associated with termite nests and soil from Northeast Thailand. Biology 10(7): 575. https://doi.org/10.3390/biology10070575

Whalley AJS (1996) The xylariaceous way of life. Mycological Research 100(8): 897–922. https://doi.org/10.1016/S0953-7562(96)80042-6

White TJ, Burns T, Lee S, Taylor J (1990) Amplification and direct sequencing of fungal ribosomal RNA genes for phylogenetics. In: Innis MA, Gelfand DH, Sninsky JJ, White TJ (Eds) PCR protocols, a guide to methods and applications. Academic Press, San Diego, 315–322. https://doi.org/10.1016/B978-0-12-372180-8.50042-1

Wibberg D, Stadler M, Lambert C, Bunk B, Spröer C, Rückert C, Kalinowski J, Cox RJ, Kuhnert E (2021) High quality genome sequences of thirteen Hypoxylaceae (Ascomycota) strengthen the phylogenetic family backbone and enable the discovery of new taxa. Fungal Diversity 106(1): 7–28. https://doi.org/10.1007/s13225-020-00447-5

Xu AS (1999) A new species of *Xylaria*. Mycosystema 18(2): 137–140.

Zhu YF, Guo L (2011) *Xylaria hainanensis* sp. nov. (Xylariaceae) from China. Mycosystema 30(4): 526–528.

MycoKeys 106: 43–96 (2024)
DOI: 10.3897/mycokeys.106.125044

Research Article

An overview of Melanommataceae (Pleosporales, Dothideomycetes): Current insight into the host associations and geographical distribution with some interesting novel additions from plant litter

Danushka S. Tennakoon[1,2,3], Kasun M. Thambugala[4,5,6], Nimali I. de Silva[7,8], Hai-Yan Song[1,2], Nakarin Suwannarach[7,8], Fu-Sheng Chen[3], Dian-Ming Hu[1,2]

1 *Bioengineering and Technological Research Centre for Edible and Medicinal Fungi, Jiangxi Agricultural University, Nanchang 330045, China*
2 *Nanchang Key Laboratory of Edible and Medicinal Fungi, Jiangxi Agricultural University, Nanchang 330045, China*
3 *Jiangxi Provincial Key Laboratory of Subtropical Forest Resource Cultivation, Jiangxi Agricultural University, Nanchang 330045, China*
4 *Genetics and Molecular Biology Unit, Faculty of Applied Sciences, University of Sri Jayewardenepura, Gangodawila, Nugegoda 10250, Sri Lanka*
5 *Center for Biotechnology, Department of Zoology, University of Sri Jayewardenepura, Nugegoda 10250, Sri Lanka*
6 *Center for Plant Materials and Herbal Product Research, Department of Botany, Faculty of Applied Sciences, University of Sri Jayewardenepura, Nugegoda 10250, Sri Lanka*
7 *Center of Excellence in Microbial Diversity and Sustainable Utilization, Chiang Mai University, Chiang Mai 50200, Thailand*
8 *Department of Biology, Faculty of Science, Chiang Mai University, Chiang Mai, 50200, Thailand*
Corresponding author: Dian-Ming Hu (hudianming1@163.com)

Abstract

Melanommataceous species exhibit high diversity with a cosmopolitan distribution worldwide and show a prominent saprobic lifestyle. In this study, we explored five saprobic species collected from plant litter substrates from terrestrial habitats in China and Thailand. A combination of morphological characteristics and multi-locus phylogenetic analyses was used to determine their taxonomic classifications. Maximum Likelihood and Bayesian Inference analyses of combined LSU, SSU, ITS and *tef1-α* sequence data were used to clarify the phylogenetic affinities of the species. *Byssosphaeria poaceicola* and *Herpotrichia zingiberacearum* are introduced as new species, while three new host records, *Bertiella fici*, *By. siamensis* and *Melanomma populicola* are also reported from litter of *Cinnamomum verum*, *Citrus trifoliata* and *Fagus sylvatica*, respectively. Yet, despite the rising interest in the melanommataceous species, there is a considerable gap in knowledge on their host associations and geographical distributions. Consequently, we compiled the host-species associations and geographical distributions of all the so far known melanommataceous species.

Key words: Biodiversity, multi-gene phylogeny, new host records, Pleosporales, saprobes, systematics

Academic editor: Nalin Wijayawardene
Received: 9 April 2024
Accepted: 19 May 2024
Published: 17 June 2024

Citation: Tennakoon DS, Thambugala KM, de Silva NI, Song H-Y, Suwannarach N, Chen F-S, Hu D-M (2024) An overview of Melanommataceae (Pleosporales, Dothideomycetes): Current insight into the host associations and geographical distribution with some interesting novel additions from plant litter. MycoKeys 106: 43–96. https://doi.org/10.3897/mycokeys.106.125044

Introduction

Fungi occur in a wide range of ecosystems (Hawksworth 2001; De Silva et al. 2016; Hernández-Restrepo et al. 2017). With over 98,334 extant species, Ascomycota is the largest phylum of fungi and is widely distributed in terrestrial, freshwater and marine environments (Hill et al. 2021; Senanayake et

al. 2022; Bánki et al. 2023). The class Dothideomycetes is estimated to have 32,365 species and is one of the most ecologically diverse group of ascomycetes (Hongsanan et al. 2020; Bánki et al. 2023). Pleosporales is considered the largest and most diverse order in the class Dothideomycetes (Zhang et al. 2012; Hongsanan et al. 2020). They exhibit a wide range of lifestyles (e.g. biotrophs, endophytes, epiphytes, hemibiotrophs, pathogens, saprobes) and can be found worldwide, including terrestrial, marine and freshwater environments (Jones et al. 2019; Hongsanan et al. 2020; Calabon et al. 2022; Gao et al. 2023). In addition, they are extremely adaptable to various ecological niches and can exist in anaerobic, aquatic, mutualistic, terrestrial and even in severe habitats, such as deserts (Zhang et al. 2012; Hyde et al. 2013; Hongsanan et al. 2020). Pleosporales species play significant functional roles from an agricultural, ecological and economic perspectives (Zhang et al. 2012; Raja et al. 2017; Wen et al. 2020; Pimenta et al. 2021). According to the recent outline of Wijayawardene et al. (2022), Pleosporales consists of 91 families.

Melanommataceae is one of the species-rich families in Pleosporales, Dothideomycetes. It was introduced by Winter (1885) to include *Melanomma* as the type genus and species have globose or depressed ascomata, fissitunicate asci, pigmented and phragmosporous ascospores (Tian et al. 2015; Hongsanan et al. 2020). The ordinal level placement of Melanommataceae was controversial for a long time and Barr (1983) introduced Melanommatales to accommodate all taxa which have trabeculate pseudoparaphyses. The nature of trabeculate pseudoparaphyses was broadly discussed by Liew et al. (2000) and illustrated that they are generally 1 µm or thinner, clearly anastomose between the asci and are embedded in a gelatinous matrix. Subsequently, Barr (1990) introduced five genera in Melanommataceae (*Byssosphaeria*, *Keissleriella*, *Melanomma*, *Ostropella* and *Strickeria*) based on erumpent to superficial ascomata and thick-walled peridium. Over time, Melanommataceae has been transferred from Melanommatales to Pleosporales with the revolution of DNA-based molecular phylogenetic studies (Eriksson 2006; Wang et al. 2007; Zhang et al. 2012; Hyde et al. 2013; Tian et al. 2015; Hongsanan et al. 2020).

The species of Melanommataceae have cosmopolitan distribution worldwide in temperate, subtropical and tropical regions (Hyde et al. 2013; Tian et al. 2015; Jaklitsch and Voglmayr 2017; Kularathnage et al. 2022). They can play a vital role as saprobes, endophytes or hyperparasites and occur on twigs or bark of various woody plants in terrestrial, marine or freshwater habitats (Tian et al. 2015; Hashimoto et al. 2017; Tennakoon et al. 2018; Hongsanan et al. 2020; Gao et al. 2023). In addition, some species (e.g. *Seifertia alpina*) have been recorded as plant pathogens and cause bud blight or bud blast disease of *Rhododendron* species (Glawe and Hummel 2006; Li et al. 2016a). Interestingly, several species have also been reported from soil (e.g. *Herpotrichia gelasinosporoides*, *H. striatispora* and *Pleotrichocladium opacum*), on lichen species (e.g. *Aposphaeria ramalinae*) and on mushroom species (e.g. *Exosporiella fungorum* on *Thelephora* sp.) (Karsten 1892; Pitard and Harmand 1911).

The cosmopolitan nature of Melanommataceae is further supported by the numerous novel genera and species that have been introduced in the past years. Based on the year of introduction, we compiled the data and revealed that nine genera were introduced between 1800 and 1899 and nine more genera between 1900 and 1999. In addition, 18 genera were introduced between 2000 and 2024

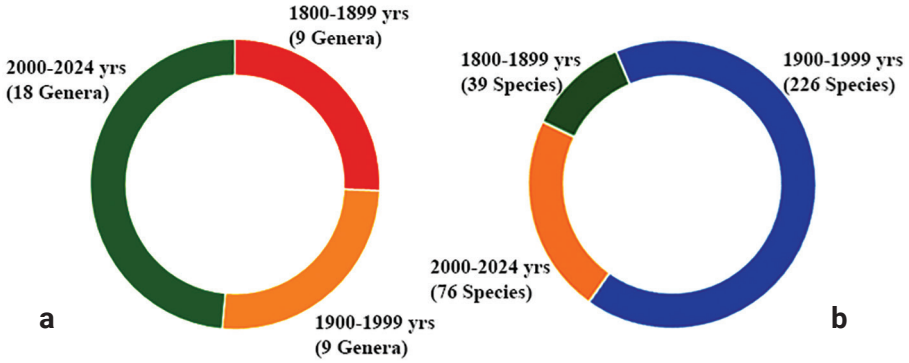

Figure 1. a The number of melanommataceous genera introduced in different time periods **b** the number of melanommataceous species introduced in different time periods (Source – MycoBank Database).

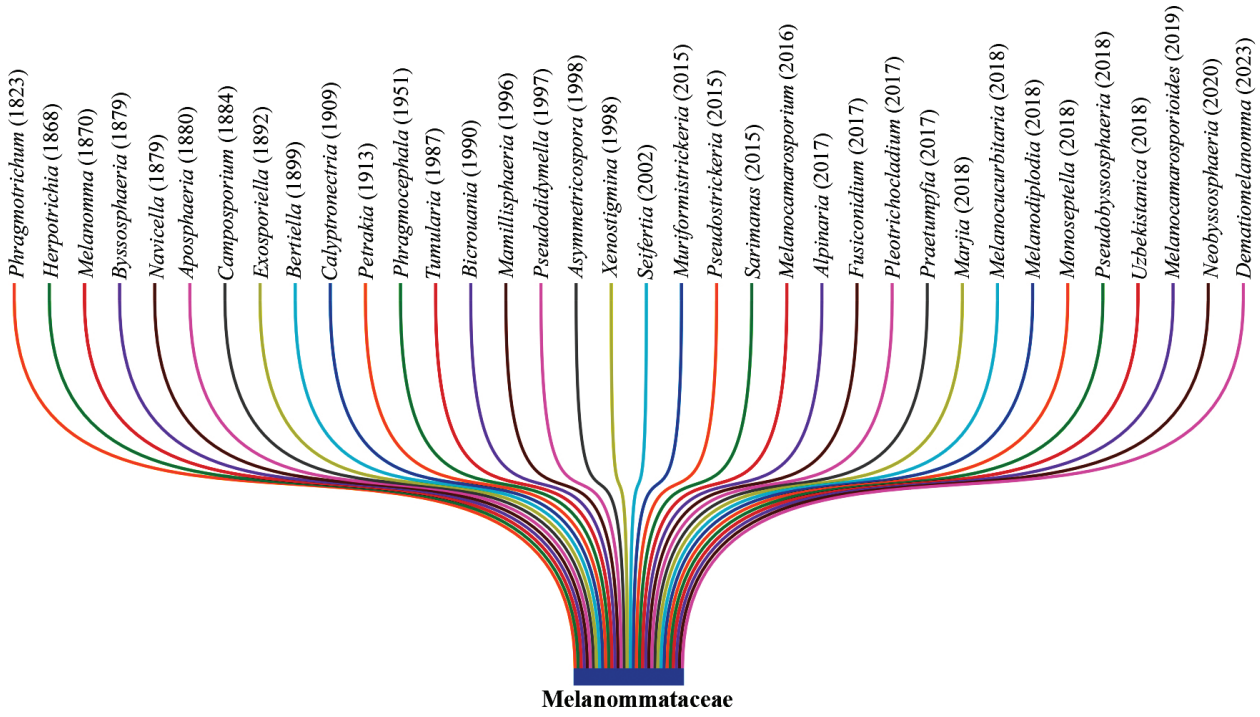

Figure 2. The melanommataceous genera introduced in different time periods (Source – MycoBank Database).

(Fig. 1). This rapid increase may be primarily due to the revolution in fungal taxonomical studies with DNA sequence-based molecular phylogenies in the last two decades. Interestingly, six genera were introduced in the year 2018, such as *Marjia*, *Melanocucurbitaria*, *Melanodiplodia*, *Monoseptella*, *Pseudobyssosphaeria* and *Uzbekistanica* (Fig. 2). Consequently, 36 genera are currently accepted in Melanommataceae, viz. *Alpinaria*, *Aposphaeria*, *Asymmetricospora*, *Bertiella*, *Bicrouania*, *Byssosphaeria*, *Calyptronectria*, *Camposporium*, *Dematiomelanomma*, *Exosporiella*, *Fusiconidium*, *Herpotrichia*, *Mamillisphaeria*, *Marjia*, *Melanocamarosporioides*, *Melanocamarosporium*, *Melanocucurbitaria*, *Melanodiplodia*, *Melanomma*, *Monoseptella*, *Muriformistrickeria*, *Navicella*, *Neobyssosphaeria*, *Petrakia*, *Phragmocephala*, *Phragmotrichum*, *Pleotrichocladium*, *Praetumpfia*, *Pseudobyssosphaeria*, *Pseudodidymella*, *Pseudostrickeria*, *Sarimanas*, *Seifertia*,

Tumularia, *Uzbekistanica* and *Xenostigmina* (Hongsanan et al. 2020; Gao et al. 2023). Conversely, the species discoveries are much higher during the 1900 and 1999 period (226 species) and thirty-nine species have been introduced between 1800 and 1899. However, despite having introduced 18 genera during the 2000–2024 period, only 76 species have been introduced (Fig. 1). Nevertheless, it could be much more in future with the extensive taxon samplings, particularly in poorly studied countries/regions, substrates and hosts.

We are exploring the fungal diversity of plant litter substrates with the aim of clarifying their taxonomy, based on morphology coupled with multi-gene phylogeny (Thambugala et al. 2017; Tennakoon et al. 2018, 2021, 2023; Wanasinghe et al. 2018). Thus, we have collected five taxa from China and Thailand which belong to the family Melanommataceae. The objectives of this study are to identify the melanommataceous taxa associated with plant litter using both morphological and phylogenetic approaches and to provide an updated checklist of species in Melanommataceae. This study provides a database on melanommataceous species for future studies, increases knowledge of fungal diversity and helps to understand their global distribution and host associations.

Materials and methods

Sample collection and examination

Fresh fungal specimens were collected from plant litter (dead wood and leaves) from Chiang Mai, Thailand and Kunming, China. The collected specimens were taken back to the laboratory in zip lock bags and paper envelopes. All the samples were subjected for an incubation period (one day) in plastic boxes lined with wet tissue paper. The micro- and macro-morphological characteristics were observed as described by Tennakoon et al. (2023). Sections of ascomata were taken manually and were mounted in distilled water. A stereomicroscope (AXIOSKOP 2 PLUS Series, Göttingen, Germany) was used to examine the surface morphological characteristics of fungal fruiting bodies. Micro-morphological characteristics, such as asci, ascospores and pseudoparaphyses were examined using Axioskop 2 Plus (Göttingen, Germany) compound microscope. Images were taken using Canon Axiocam 506 color digital camera (Hanover, Germany) fitted to a Axioskop 2 Plus (Göttingen, Germany) compound microscope. The micro morphological characteristics, such as colour, shape, height and diameter of ascomata, asci, ascospores, peridium and pseudoparaphyses were recorded. Indian ink was used to inspect the existence of the mucilaginous sheath in ascospores. The prepared slides were permanently preserved using lactoglycerol and sealed by applying nail-polish around the margins of cover slips. All measurements were obtained using Tarosoft (R) Image Framework application. Adobe Photoshop CS3 Extended version 10.0 software (Adobe Systems, USA) was used to construct the photo plates. Specimens were deposited in the Herbarium of Department of Biology (CMUB) and Sustainable Development of Biological Resources Laboratory (SDBR), Faculty of Science, Chiang Mai University and Herbarium of Fungi, Jiangxi Agricultural University (HFJAU), Nanchang, China. The Faces of Fungi (FOF) and Index Fungorum (IF) numbers were obtained for new species (*Byssosphaeria poaceicola* and *Herpotrichia zingiberacearum*) as mentioned in Jayasiri et al. (2015) and Index Fungorum (2024).

DNA extraction, PCR amplification and sequencing

Genomic DNA was extracted from fungal fruiting bodies on the natural substrate by using a DNA extraction kit (E.Z.N.A. ® Forensic DNA Kit, D3591-01, Omega BIO-TEK) following the manufacturer's protocol. DNA products were intended for use as a template for PCR and stored at 4 °C and the duplicates were kept at -20 °C for long-term storage. Four genomic regions were amplified, the internal transcribed spacer (ITS) region (ITS1-5.8S-ITS2), the 28S large subunit rDNA (LSU), 18S small subunit rDNA (SSU) and the translation elongation factor 1-alpha gene (*tef1-α*). The primers ITS4 and ITS5 were used to amplify the ITS (White et al. 1990), LR0R and LR5 primers for LSU (Vilgalys and Hester 1990), NS1 and NS4 for SSU (White et al. 1990) and EF1-983F and EF1-2218R primers for *tef1-α* (Rehner 2001). The amplification reactions were performed in a total reaction volume of 25 µl, which contained 9.5 µl of sterilised distilled water, 12.5 µl of 2 × Power Taq PCR MasterMix (a premix and ready to use solution, including 0.1 Units/µl Taq DNA Polymerase, 500 µM dNTP Mixture each (dATP, dCTP, dGTP, dTTP) (Bioteke Co., China), 1 µl of each forward and reverse primers (stock concentration 10 pM) and 1 µl of DNA template. The polymerase chain reaction (PCR) thermal cycle programmes for ITS, LSU, SSU and *tef1-α* genes amplification were adjusted as described in Tennakoon et al. (2022). To check the quality of PCR products, agarose gel electrophoresis (1%) was conducted. The purified PCR products were subjected for sequencing at Sangon Biotech (Shanghai) Co., Ltd, China. Generated sequences were deposited in GenBank and accession numbers were listed (Table 1).

Phylogenetic analyses

The obtained sequences were initially assembled (forward and reverse sequences) using SeqMan v. 7.0.0 (DNASTAR, Madison, WI). Assembled sequences were subjected to BLAST search in GenBank to obtain strains which have high similarities (https://blast.ncbi.nlm.nih.gov/). In addition, some other sequences for taxa in Melanommataceae were obtained using recent publications (Kularathnage et al. 2022; Gao et al. 2023). In total, 85 isolates were used for phylogenetic analyses including *Hysterium angustatum* (MFLU 16-1179) as the outgroup taxon. The combined dataset comprised four genes, ITS, LSU, SSU and *tef1-α*. Single gene sequences were aligned with MAFFT v.7.490 online application (Katoh and Standley 2013) (https://mafft.cbrc.jp/alignment/software/) and manually improved in necessary places. Aligned sequences were combined using BioEdit v.7.2.5 (Hall 1999).

The concatenated aligned dataset was analysed separately using Maximum Likelihood (ML) and Bayesian Inference (BI). Maximum Likelihood analysis was performed using the online portal CIPRES Science Gateway v. 3.3 (Miller et al. 2010), with RAxML-HPC v.8 on XSEDE (8.2.12) tool (Stamatakis et al. 2008; Stamatakis 2014) using the GTR+I+G model of nucleotide evolution. Evolutionary models for each barcode were determined using MrModelTest v. 2.3 (Nylander 2004) under the Akaike Information Criterion (AIC).

MrBayes 3.2.1 (Ronquist et al. 2012) was used to analyse Bayesian Inference phylogenies and was run with four chains of 3,000,000 generations and trees were sampled every 100th generation. The initial 20% of sampled data

Table 1. GenBank and culture collection accession numbers of species included in the phylogenetic study. The newly-generated sequences are shown in bold face.

Fungal Species	Strain/Voucher No.	GenBank Accession Number			
		ITS	LSU	SSU	*tef*–1α
Alpinaria rhododendri	KT 2520	LC203335	LC203360	LC203314	LC203388
Aposphaeria corallinolutea	MFLU 15-2752	KY554202	KY554197	KY554200	KY554205
A. corallinolutea	GLMC 1355	MT153708	MT156159	–	–
Bertiella ellipsoidea	MFLU 16-0583	KX765261	KX765262	–	–
B. ellipsoidea	MFLUCC 17-2015	MG543922	MG543913	–	–
B. fici	MFLUCC 20-0229	–	MW063223	MW079351	MW183786
B. fici	NCYUCC 19-0260	–	MW063224	MW079352	MW183787
B. fici	NCYUCC 19-0290	–	MW063225	MW079353	MW183788
B. fici	**CMUB 40045**	**–**	**PP460772**	**PP460764**	**PP475453**
B. macrospora	IL 5005	–	GU385150	–	–
B. macrospora	SMH 3953	–	–	–	GU327744
Beverwykella pulmonaria	CBS 283.53	KY189974	GU301804	–	–
Byssosphaeria diffusa	AFTOL ID 1588	–	DQ678071	DQ678019	DQ677915
By. diffusa	CBS 250.62	–	–	GU205239	–
By. jamaicana	SMH 1403	–	GU385152	–	GU327746
By. jamaicana	SMH 3085	–	GU385154	–	–
By. jamaicana	SMH 3464	–	GU385153	–	–
By. macarangae	MFLUCC 17-2655	MH389782	MH389778	MH389780	MH389784
By. musae	MFLUCC 11-0146	KP744435	KP744477	KP753947	MH581149
By. phoenicis	ZHKUCC 21-0122	ON180685	ON180683	ON180691	ON243583
By. phoenicis	ZHKUCC 21-0123	ON180686	ON180684	ON180692	ON243584
By. rhodomphala	SMH3086	–	GU385155	–	–
By. rhodomphala	ANM 942	–	GU385160	–	–
By. rhodomphala	SMH 3402	–	GU385170	–	–
By. rhodomphala	GKM L153N	–	GU385157	–	GU327747
By. salebrosa	SMH 2387	–	GU385162	–	GU327748
By. schiedermayeriana	SMH 1816	–	GU385159	–	–
By. schiedermayeriana	SMH 1269	–	GU385158	–	–
By. schiedermayeriana	SMH 3157	–	GU385163	–	GU327745
By. siamensis	MFLUCC 10-0099	–	KT289895	KT289897	–
By. siamensis	MFLUCC 17-1800	MG543923	MG543914	MG543917	–
By. siamensis	**HFJAU10336**	**PP460780**	**PP460773**	**PP460765**	**PP475454**
By. taiwanense	MFLUCC 17-2643	MH389783	MH389779	MH389781	MH389785
By. villosa	GKM 204 N	–	GU385151	–	GU327751
By. poaceicola	**HFJAU10337**	**PP460781**	**PP460774**	**PP460766**	**PP475455**
By. poaceicola	**HFJAU10338**	**PP460782**	**PP460775**	**PP460767**	**PP475456**
Fusiconidium aquaticum	KUMCC 15-0300	–	KX641894	KX641895	KX641896
F. mackenziei	MFLUCC 14-0434	–	KX611112	KX611114	KX611118
Herpotrichia herpotrichoides	GKM 212N	–	GU385169	–	–
H. herpotrichoides	SMH 5167	–	GU385175	–	–
H. macrotricha	GKM 196N	–	GU385176	–	GU327755
H. macrotricha	SMH 269	–	GU385177	–	–
H. macrotricha	SMH 269	–	GU385177	–	GU327756
H. vaginatispora	MFLUCC 13-0865		KT934252	KT934256	KT934260

Fungal Species	Strain/Voucher No.	GenBank Accession Number			
		ITS	LSU	SSU	*tef*–1α
H. xiaokongense	KUMCC 21-0004	–	MZ408889	MZ408891	MZ394066
H. zingiberacearum	**HFJAU10332**	**PP460783**	**PP460776**	**PP460768**	**PP475457**
H. zingiberacearum	**HFJAU10333**	**PP460784**	**PP460777**	**PP460769**	**PP475458**
H. zingiberacearum	**HFJAU10334**	**PP460785**	**PP460778**	**PP460770**	**PP475459**
Hysterium angustatum	MFLU 16-1179	KX611363	KX611364	KX611365	–
Marjia tianschanica	TASM 6120	MG828909	MG829019	MG829126	MG829206
M. tianschanica	TASM 6121	MG828910	MG829020	MG829127	MG829206
Marjia uzbekistanica	TASM 6122	MG828911	MG829021	MG829128	MG829208
Melanocucurbitaria uzbekistanica	MFLUCC 17-0829	MG828912	MG829022	MG829129	MG829209
Melanodiplodia tianschanica	TASM 6111	MG828914	MG829023	MG829130	MG829210
Me. tianschanica	TASM 6112	MG828915	MG829024	MG829131	MG829211
Me. tianschanica	MFLUCC 17-0805	MG828913	MG829025	MG829132	MG829212
Melanomma japonicum	KT 3425	LC203320	LC203338	LC203292	LC203367
Mel. populicola	CBS 543.70	NR_170056	NG_075164	NG_070237	–
Mel. populicola	CPC 27203	MT223817	MT223910	–	–
Mel. populicola	CBS 350 82	MT223815	JF740265	–	–
Mel. populicola	CBS 130330	–	JF740328	–	–
Mel. populicola	**HFJAU10335**	**PP460786**	**PP460779**	**PP460771**	**PP475460**
Mel. pulvis pyrius	KT 2110	LC203322	LC203340	LC203294	LC203368
Mel. pulvis pyrius	KT 2113	LC203323	LC203341	LC203295	LC203369
Mel. pulvis pyrius	AH 375	LC203324	LC203342	LC203296	LC203370
Mel. pulvis pyrius	KH 27	LC203325	LC203343	LC203297	LC203371
Mel. pulvis-pyrius	CBS 124080	MH863349	GU456323	GU456302	GU456265
Monoseptella rosae	MFLUCC 17-0815	MG828916	MG829026	MG829133	MG829213
Mo. rosae	TASM 6114	MG828917	MG829027	MG829134	MG829214
Mo. tuberculata	CBS 256.84	–	GU301851	–	GU349006
Muriformistrickeria rubi	MFLUCC 15-0681	–	KT934253	KT934257	KT934261
Petrakia irregularis	CBS 306.67	NR_164281	MH870670	–	–
Phragmocephala atra	MFLUCC 15-0021	KP698721	KP698725	KP698729	–
P. garethjonesii	MFLUCC 15-0018	KP698722	KP698726	KP698730	–
Pleotrichocladium opacum	CBS 450.70	MH859791	KY853524	–	–
Pl. opacum	CBS 709.92	KY853464	KY853526	–	–
Pseudostrickeria rosae	MFLUCC 17-0643	MG828954	MG829065	MG829169	MG829234
Ps. mutabilis	SMH 1541	–	GU385209	–	–
Sarimanas pseudofluviatile	KT 760	LC001717	LC001714	LC001711	–
S. shirakamiense	KT 3000	–	LC001715	LC001712	–
Seifertia azaleae	DAOM 239136	–	EU030276	–	–
Se. shangrilaensis	MFLUCC 16-0238	–	KU954100	KU954101	KU954102
Uzbekistanica rosae-hissaricae	MFLUCC 17-0819	MG828976	MG829087	MG829187	MG829242
U. rosae-hissaricae	MFLUCC 17-0820	GU269840	MG829088	MG829188	MG829243
Xenostigmina zilleri	CBS 115685	GU269840	GU253857	LC203316	GU384553

Abbreviations: ANM, A.N. Miller; AFTOL, Assembling the Fungal Tree of Life project; CBS, Centraalbureau voor Schimmelcultures, Utrecht, The Netherlands; CPC, Working collection of Pedro Crous housed at CBS; DAOM, Plant Research Institute, Department of Agriculture (Mycology), Ottawa, Canada; GLMC, culture collections of the Senckenberg Museum of Natural History Görlitz, Germany; GKM, G.K. Mugambi; IL, I. Lopez; KUMCC, Culture Collection of Chinese Academy of Sciences, Kunming, China; KH, K. Hirayama; KT, K. Tanaka; MFLU, Mae Fah Luang University; MFLUCC, Mae Fah Luang University Culture Collection; NCYUCC, National Chiayi University Culture Collection, China; SMH, S.M. Huhndorf; ZHKUCC, Zhongkai University of Agriculture and Engineering Culture Collection, China.

were discarded as burn-in. The phylograms were visualised using the FigTree v.1.4.0 tool (Rambaut 2012) and reorganised in Adobe Illustrator® CS3 (Version 15.0.0, Adobe®, San Jose, CA). The alignments and sequences were deposited in TreeBASE, submission ID: 31212 (http://www.treebase.org/) and GenBank (https://www.ncbi.nlm.nih.gov/), respectively.

Geographical distribution and host associations of melanommataceous species

We enumerated 340 species of Melanommataceae, grouped into 36 genera, along with their geographic distribution and host associations. The necessary data were obtained from published books, publications in reputable journals, Species Fungorum (https://www.speciesfungorum.org), MycoBank (https://www.mycobank.org/), the U.S. National Fungus Collections Fungus-Host Database (Farr and Rossman 2024) and online sources (Catalogue of Life Checklist). The gathered data were mentioned with appropriate references (Table 2). In total, 296 articles were studied for information on the 340 melanommataceous species that are currently legitimate (Table 2) and accessed through Google Scholar searches. MycoBank (https://www.mycobank.org/) was used to illustrate the nomenclature validity of the taxa. However, numerous species have not been verified using molecular data, so most species should be correctly identified, based on modern taxonomic concepts. Therefore, the distribution may vary slightly.

The distribution map was prepared using MapChart programme (https://www.mapchart.net/index.html), a platform from which a personalised map of the world using different colours can be generated. The Sankey diagram was created to show the species distribution through plant host families using the free online tool SankeyMATIC by Steve Bogart (www.sankeymatic.com).

Results

Phylogenetic analyses

Phylogenetic analyses of combined LSU, SSU, ITS and *tef1-α* sequences comprised 3480 characters including gaps. *Hysterium angustatum* (MFLU 16-1179) was used as the outgroup taxon. The RAxML analysis of the combined dataset yielded a best scoring tree (Fig. 3). The final ML optimisation likelihood value was -16620.192034. There were 35.32% undetermined characters or gaps and 1071 distinct alignment patterns. Estimated base frequencies were A = 0.247534, C = 0.235205, G = 0.272353, T = 0.244907; substitution rates AC = 1.775315, AG = 3.161447, AT = 1.766474, CG = 1.002405, CT = 11.511066, GT = 1.000; proportion of invariable sites I = 0.535605; gamma distribution shape parameter α = 0.513218. The Bayesian analysis has resulted in 30,000 trees after 3,000,000 generations. Bootstrap support values for ML higher than 70% and BYPP greater than 0.90 are given above each branch respectively (Fig. 3). All analyses (ML and BYPP) showed similar topologies and concurred with previous studies (Pem et al. 2019; Kularathnage et al. 2022; Gao et al. 2023).

According to the phylogeny, our collection HFJAU10336, HFJAU10337 and HFJAU10338 cluster within *Byssosphaeria* species. HFJAU10337 and

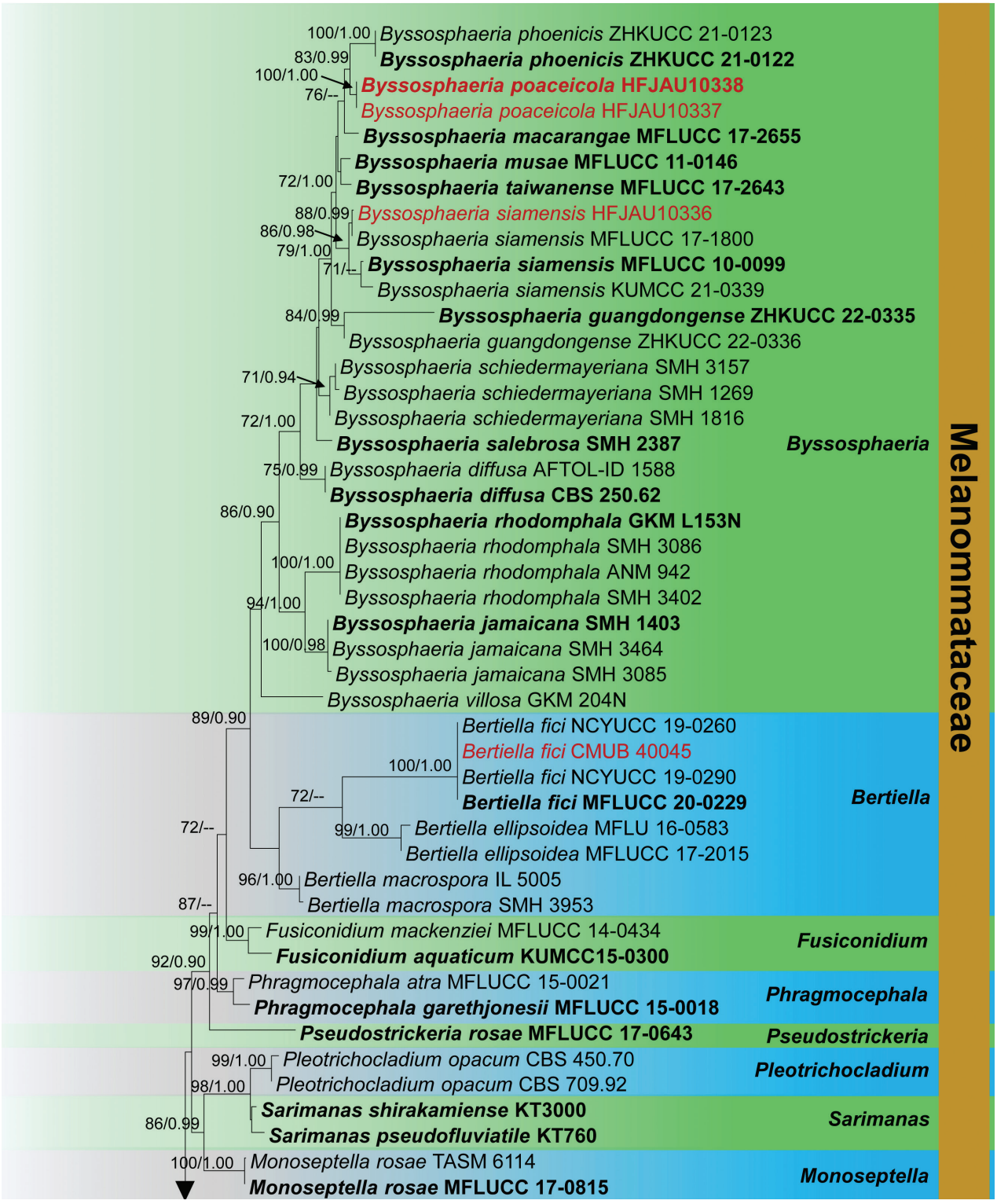

Figure 3. Phylogram generated from Maximum Likelihood analysis is based on combined LSU, SSU, ITS and *tef1-α* sequence data. The tree is rooted with *Hysterium angustatum* (MFLU 16-1179). The new isolates are in red and ex-type strains are indicated in bold face. Bootstrap support values ≥ 70% from the Maximum Likelihood (ML) and Bayesian Posterior Probabilities (BYPP) values ≥ 0.90 are given above the nodes, respectively.

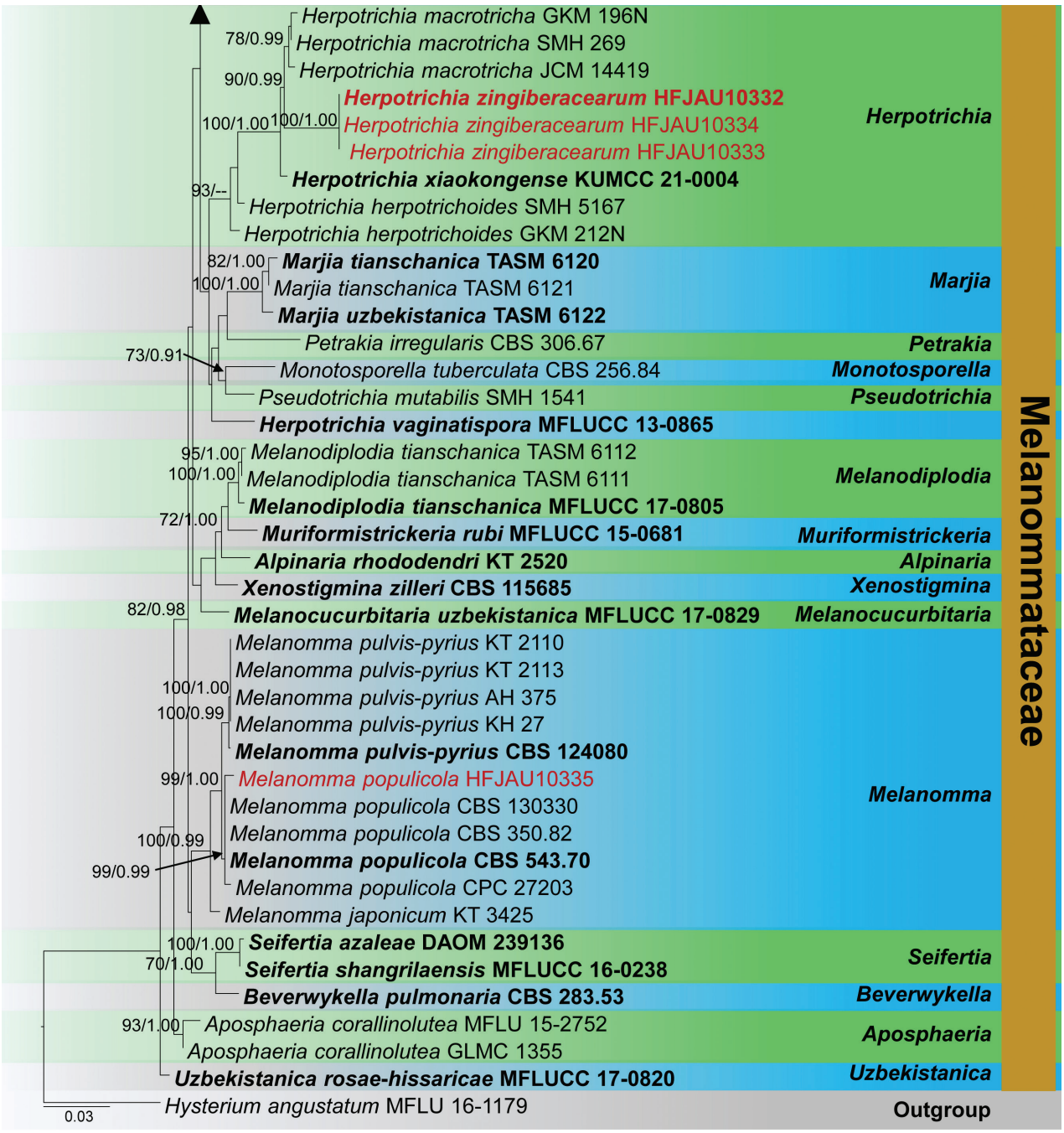

Figure 3. Continued.

HFJAU10338 cluster together and show an independent lineage, sister to *B. phoenicis* isolates (ZHKUCC 21-0122 and ZHKUCC 21-0123) with 83% ML and 0.99 BYPP statistical support. The isolate HFJAU10336 clusters with *B. siamensis* isolates (MFLUCC 10-0099, MFLUCC 17-1800 and KUMCC 21-0339) in a monophyletic clade. In addition, CBUB 40045 groups with *Bertiella fici* in a 100% ML and 1.00 BYPP supported clade. Three isolates (HFJAU10332, HFJAU10333 and HFJAU10334) cluster with *Herpotrichia* species, and show a close phylogenetic relationship with *H. melanotricha* (GKM 196N, SMH 269 and JCM 14419). As well as HFJAU10335 groups with *Melanomma populicola* (CBS 130330, CBS 350.82, CBS 543.70 and CPC 272203) in a 99% ML and 0.99 BYPP supported clade.

Table 2. Host association and geographical distribution of reported melanommataceous species.

Species	Host	Host family	Locality	References
Alpinaria rhododendri	*Rhododendron* sp.	Ericaceae	Austria and Japan	Hashimoto et al. (2017); Jaklitsch and Voglmayr (2017)
Aposphaeria allantella	*Solanum tuberosum*	Solanaceae	Germany	Farr and Rossman (2024)
Aposphaeria anomala	Unidentified host	–	Italy	Farr and Rossman (2024)
Aposphaeria arachidis	*Arachis hypogaea*	Fabaceae	India	Kulkarni (1974); Mathur (1979); Farr and Rossman (2024)
Aposphaeria bambusae	*Bambusa* sp.	Poaceae	Brazil	Bresadola (1926); Farr and Rossman (2024)
Aposphaeria bombacis	*Bombax macrocarpum*	Malvaceae	Germany	Diedicke (1912)
Aposphaeria brunneotincta	*Castanea vesca*	Fagaceae	The United States	Thaxter (1922)
Aposphaeria buddlejae	*Buddleja davidii*	Buddlejaceae	Ukraine	Farr and Rossman (2024)
Aposphaeria calligoni	*Calligonum aphyllum*	Polygonaceae	Kazakhstan	Farr and Rossman (2024)
Aposphaeria canavaliae	*Canavalia* sp.	Fabaceae	Fiji	Massee (1906); Dingley et al. (1981); Farr and Rossman (2024)
Aposphaeria caraganae	*Caragana arborescens*	Fabaceae	Russia	Farr and Rossman (2024)
Aposphaeria caricicola	*Carex rossii*	Cyperaceae	The United States	Farr and Rossman (2024)
Aposphaeria caulina	*Cerefolium sylvestre*	Apiaceae	Finland	Karsten (1905)
Aposphaeria charticola	–	–	The United States	Saccardo (1911)
Aposphaeria cladoniae	*Cladonia fimbriata*	Cladoniaceae	Germany	Allescher (1896)
Aposphaeria conica	*Quercus* sp.	Fagaceae	Italy	Saccardo and Traverso (1910)
Aposphaeria corallinolutea	*Fraxinus excelsior* and *Kerria japonica*	Oleaceae and Rosaceae	The Netherlands	De Gruyter et al. (2013)
Aposphaeria dendrophomoides	*Corylus avellana*	Betulaceae	Italy	Saccardo (1921)
Aposphaeria denudata	*Cydonia vulgaris*	Rosaceae	Hungary	Saccardo and Traverso (1910)
Aposphaeria desertorum	*Haloxylon aphyllum*	Amaranthaceae	Kazakhstan	Farr and Rossman (2024)
Aposphaeria elymi	*Elymus arenarius*	Poaceae	Germany	Diedicke (1912)
Aposphaeria ephedrae	*Ephedra* sp.	Ephedraceae	Kazakhstan and Ukraine	Hayova and Minter (2009); Farr and Rossman (2024)
Aposphaeria epicorticalis	*Corylus avellana*	Betulaceae	Italy	Saccardo (1921)
Aposphaeria eragrostidis	*Eragrostis* sp.	Poaceae	Eritrea, Ethiopia and Iraq	Castellani and Ciferri (1950); Farr and Rossman (2024)
Aposphaeria eurotiae	*Eurotia eversmanniana*	Amaranthaceae	Kazakhstan	Farr and Rossman (2024)
Aposphaeria ferrum-equinum	Unidentified host	–	Italy	Tassi (1900)
Aposphaeria freticola	*Fagus* sp. and *Nothofagus antarctica*	Fagaceae, Nothofagaceae	Argentina, Chile and Poland	Farr (1973); Mulenko et al. (2008); Farr and Rossman (2024)
Aposphaeria gallicola	Unidentified host	–	Italy	Farr and Rossman (2024)
Aposphaeria gregaria	*Salix* sp.	Salicaceae	Germany	Diedicke (1912)
Aposphaeria halimodendri	*Halimodendron halodendron*	Fabaceae	Ukraine	Farr and Rossman (2024)
Aposphaeria haloxyli	*Haloxylon aphyllum*	Amaranthaceae	Kazakhstan	Farr and Rossman (2024)
Aposphaeria hapalophragmii	*Hapalophragmium acaciae*	Fabaceae	Somalia	Trotter (1931); Mujica and Vergara (1945); Farr and Rossman (2024)

Species	Host	Host family	Locality	References
Aposphaeria henryana	*Salix alba*	Salicaceae	Italy	Farr and Rossman (2024)
Aposphaeria heveae	*Hevea brasiliensis*	Euphorbiaceae	Sri Lanka	Petch (1917)
Aposphaeria hippuridis	*Hippuris vulgaris*	Plantaginaceae	Germany	Ade (1923)
Aposphaeria hospitae	*Kleinhovia* sp.	Malvaceae	Sri Lanka	Tassi (1900)
Aposphaeria humicola	Unidentified host	–	The Netherlands	Oudemans (1902)
Aposphaeria ilicis	*Ilex aquifolium*	Aquifoliaceae	Germany	Diedicke (1912)
Aposphaeria iliensis	*Halimodendron halodendron*	Fabaceae	Kazakhstan	Farr and Rossman (2024)
Aposphaeria jubaeae	*Jubaea spectabilis*	Arecaceae	Chile	Spegazzini (1921); Farr (1973); Mujica and Vergara (1945); Farr and Rossman (2024)
Aposphaeria kiefferiana	*Quercus* sp.	Fagaceae	Italy	Farr and Rossman (2024)
Aposphaeria kravtzevii	*Eurotia eversmanniana*	Amaranthaceae	Kazakhstan	Farr and Rossman (2024)
Aposphaeria lentisci	*Pistacia* sp.	Anacardiaceae	Greece and Spain	Urries (1957); Pantidou (1973); Farr and Rossman (2024)
Aposphaeria lignicola	*Acacia arabica*	Fabaceae	Pakistan	Ahmad (1964)
Aposphaeria major	*Rubus parviflorus*	Rosaceae	The United States	Sydow and Sydow (1907)
Aposphaeria majuscula	*Vitis vinifera*	Vitaceae	France	Saccardo and Trotter (1913)
Aposphaeria martinii	*Sabal* sp.	Arecaceae	United States	Farr and Rossman (2024)
Aposphaeria mediella	*Pinus* sp.	Pinaceae	Greece, Finland and Poland	Karsten (1884); Pantidou (1973); Mulenko et al. (2008); Farr and Rossman (2024)
Aposphaeria melaleucae	*Melaleuca leucadendra*	Myrtaceae	Australia	Hennings (1903); Shivas and Alcorn (1996); Farr and Rossman (2024)
Aposphaeria mesembryanthemi	*Mesembryanthemum* sp.	Aizoaceae	Portugal	Costa and Camara (1952)
Aposphaeria mojunkumica	*Haloxylon aphyllum*	Amaranthaceae	Kazakhstan	Farr and Rossman (2024)
Aposphaeria montbretiae	*Crocosmia* sp.	Iridaceae	Azerbaijan and Georgia	Siemaszko (1923)
Aposphaeria musarum	*Musa sapientum*	Musaceae	Argentina	Farr (1973); Farr and Rossman (2024)
Aposphaeria nigra	*Betula alba*	Betulaceae	Germany	Diedicke (1912)
Aposphaeria oxalidis	*Oxalis tuberosa*	Oxalidaceae	Bolivia	Farr and Stevenson (1963); Farr and Rossman (2024)
Aposphaeria pakistanica	Unidentified host	–	Pakistan	Ahmad (1971)
Aposphaeria phellodendri	*Phellodendron amurense*	Rutaceae	Ukraine	Farr and Rossman (2024)
Aposphaeria pinea	*Pinus sylvestris*	Pinaceae	France and Germany	Saccardo (1884); Mulenko et al. (2008); Farr and Rossman (2024)
Aposphaeria pini-densiflorae	*Pinus densiflora*	Pinaceae	Japan	Sawada (1950); Farr and Rossman (2024)
Aposphaeria polonica	*Tilia platyphyllos*	Pinaceae	Poland	Mulenko et al. (2008); Farr and Rossman (2024)
Aposphaeria populea	*Populus* sp.	Salicaceae	The United Kingdom	Smith and Ramsbottom (1914); Dennis (1986)
Aposphaeria pulviscula	*Fagus sylvatica* and *Salix* sp.	Fagaceae and Salicaceae	Austria, France, Iceland, Italy, the Netherlands and Ukraine	Saccardo (1880); Spaulding (1961); Sutton (1980); Farr and Rossman (2024)

Species	Host	Host family	Locality	References
Aposphaeria punicina	*Punica granatum*	Lythraceae	China and Malta	Saccardo (1915); Tai (1979)
Aposphaeria purpurascens	*Acer pseudoplatanus*	Sapindaceae	Italy	Peyronel (1915)
Aposphaeria ramalinae	*Ramalina* sp. (lichen)	–	France	Pitard and Harmand (1911)
Aposphaeria reaumuriae	*Reaumuria* sp.	Tamaricaceae	Azerbaijan	Farr and Rossman (2024)
Aposphaeria rhois	*Rhus oxyacantha*	Anacardiaceae	Libya	El-Buni and Rattan (1981); Trotter (1912)
Aposphaeria rostrata	Unidentified host	–	The Netherlands	Oudemans (1902)
Aposphaeria rubefaciens	*Salix* sp.	Salicaceae	Italy and the Netherlands	Bubák and Kabát (1905)
Aposphaeria rudis	*Picea excelsa*	Pinaceae	Finland	Karsten (1905)
Aposphaeria salicis	*Salix* sp.	Salicaceae	Germany and India	Diedicke (1912); Mathur (1979)
Aposphaeria salicum	*Salix viminalis*	Salicaceae	Germany	Sydow and Sydow (1903)
Aposphaeria santolinae	*Santolina chamaecyparissus*	Asteraceae	Ukraine	Farr and Rossman (2024)
Aposphaeria sepulta	*Citrus aurantium*	Rutaceae	Italy	Saccardo (1884)
Aposphaeria sequoiae	*Sequoia* sp.	Cupressaceae	Denmark	Lind (1913)
Aposphaeria silenes	*Silene otites*	Caryophyllaceae	Russia	Farr and Rossman (2024)
Aposphaeria sphaerospora	*Betula alba*	Betulaceae	Italy	Peyronel (1918)
Aposphaeria striolata	*Populus deltoides*	Salicaceae	The United States	Saccardo (1916)
Aposphaeria taquarae	Bambusoideae sp.	Poaceae	Brazil	Viégas (1945)
Aposphaeria tiliana	*Tilia cordata*	Malvaceae	Ukraine	Gucevic (1977)
Aposphaeria tragopogonis	*Tragopogon dubius*	Asteraceae	Romania	Sandu-Ville and Mititiuc (1971)
Aposphaeria turmalis	*Diospyros virginiana*	Ebenaceae	The United States	Ellis and Everhart (1902); Cash (1952)
Aposphaeria ulmicola	*Ulmus* sp.	Ulmaceae	The United Kingdom	Saccardo (1884)
Aposphaeria zeae	*Zea mays*	Poaceae	Azerbaijan and Georgia	Farr and Rossman (2024)
Asymmetricospora calamicola	*Calamus caryotoides*	Arecaceae	Australia	Fröhlich and Hyde (1998); Zhang et al. (2012)
Bertiella botryosa	*Ulmus* sp.	Ulmaceae	The United States	Morgan (1904)
Bertiella ellipsoidea	Unidentified host	–	Thailand	Hyde et al. (2016)
Bertiella fici	*Cinnamomum verum*, *Ficus septica*	Lauraceae, Moraceae	China and Thailand	Tennakoon et al. (2021); this study
Bertiella gelatinosa	Unidentified host	–	Brazil	Almeida et al. (2017)
Bertiella rhodospila	*Cyrilla* sp., *Populus* sp. and *Quercus* sp.	Cyrillaceae, Fagaceae and Salicaea	The United States	Barr et al. (1986)
Bertiella striatispora	Unidentified host	–	India	Niranjan and Sarma (2019)
Bicrouania maritima	*Atraphaxis spinosa* and *Halimione portulacoides*	Amaranthaceae, Polygonaceae	France and Uzbekistan	Kohlmeyer and Volkmann-Kohlmeyer (1990); Gafforov (2017)
Byssosphaeria alnea	*Alnus* sp.	Betulaceae	The United States	Barr (1984); Farr and Rossman (2024)
Byssosphaeria erumpens	*Litsea* sp.	Lauraceae	China	Chen and Hsieh (2004); Li and Zhuang (2008); Farr and Rossman (2024)

Species	Host	Host family	Locality	References
Byssosphaeria erythrinae	*Erythrina indica*	Fabaceae	France	Barr (1984)
Byssosphaeria guangdongense	*Phoenix roebelenii*	Arecaceae	China	Xiong et al. (2023)
Byssosphaeria hainanensis	Unidentified host	–	China	Li and Zhuang (2008)
Byssosphaeria jamaicana	*Bambusa* sp., *Quercus* sp. and *Salix* sp.	Fagaceae and Poaceae, Salicaceae	China, Czech Republic, Jamaica and Mexico	Barr (1984); Sivanesan and Hsieh (1989); Wang et al. (2004); Medel (2007); Farr and Rossman (2024)
Byssosphaeria juniperi	*Juniperus* sp.	Cupressaceae	The United States	Wang et al. (2004); Farr and Rossman (2024)
Byssosphaeria macarangae	*Macaranga tanarius*	Euphorbiaceae	China	Tennakoon et al. (2018)
Byssosphaeria musae	*Musa* sp.	Musaceae	Thailand	Liu et al. (2015); Farr and Rossman (2024)
Byssosphaeria oviformis	*Saccharum arundinaceum*	Poaceae	China and Jamaica	Barr (1984); Lu et al. (2000); Wong and Hyde (2001); Farr and Rossman (2024)
Byssosphaeria phoenicis	*Phoenix roebelenii*	Arecaceae	China	Kularathnage et al. (2022)
Byssosphaeria poaceicola	*Arundo pliniana*	Poaceae	China	This study
Byssosphaeria rhodomphala	*Acer pseudoplatanus* and *Populus* sp.	Salicaceae and Sapindaceae	Brazil, China, Poland and the United States	Cooke (1887); Scheuer and Chlebicki (1997); Reblova (1997); Chen and Hsieh (2004); Wang et al. (2004)
Byssosphaeria salebrosa	*Vaccinium* sp.	Ericaceae	The United States	Barr (1984); Barr et al. (1986); Farr and Rossman (2024)
Byssosphaeria schiedermayriana	*Sambucus nigra*	Adoxaceae	Austria	Barr (1984)
Byssosphaeria semen	*Pyrus americana*	Rosaceae	The United States	Barr (1984)
Byssosphaeria siamensis	*Pandanus* sp. and *Citrus trifoliata*	Pandanaceae and Rutaceae	China and Thailand	Tian et al. (2015); Hyde et al. (2018); Farr and Rossman (2024); this study
Byssosphaeria taiwanense	*Macaranga tanarius*	Euphorbiaceae	China	Tennakoon et al. (2018)
Byssosphaeria xestothele	*Cornus florida* and *Robinia pseudoacacia*	Cornaceae and Fabaceae	Sweden and the United States	Barr (1984); Eriksson (2014); Farr and Rossman (2024)
Calyptronectria argentinensis	*Foeniculum piperitum* and *Manihot carthaginensis*	Apiaceae, Euphorbiaceae	Argentina	Spegazzini (1909); Farr (1973); Farr and Rossman (2024)
Calyptronectria indica	*Annona squamosa*	Annonaceae	India	Pande (2008)
Calyptronectria platensis	*Manihot carthagenensis*	Euphorbiaceae	Argentina	Spegazzini (1909); Farr (1973); Farr and Rossman (2024)
Camposporium antennatum	*Acacia aulacocarpa*, *Caesalpinia echinata*, *Cinnamomum japonicum*, *Cocos nucifera*, *Drymophloeus pachycladus*, *Eucalyptus globulus*, *Ficus erecta*, *Laurus nobilis*, *Machilus* sp., *Mucuna ferruginea*, *Neolitsea scrobiculata*, *Phoenix hanceana*, *Pinus massoniana*, *Quercus* sp. and *Trachycarpus fortunei*	Arecaceae, Fabaceae, Fagaceae, Lauraceae, Moraceae, Myrtaceae, and Pinaceae	California, China, the United Kingdom and Venezuela	Harkness (1884); Lu et al. (2000); Castaneda-Ruiz et al. (2003); Farr and Rossman (2024)
Camposporium appendiculatum	Unidentified host	–	China	Hyde et al. (2020)

Species	Host	Host family	Locality	References
Camposporium atypicum	*Mesua ferrea*	Calophyllaceae	India	Koukol and Delgado (2021)
Camposporium cambrense	*Alnus* sp., *Carpinus betulus*, *Fagus* sp., *Freycinetia anksia*, *Laurus nobilis* and *Quercus* sp.	Betulaceae, Fagaceae, Lauraceae, and Pandanaceae	China, New Zealand, Poland, Russia and the United Kingdom	Hughes (1951); Whitton et al. (2002); Mulenko et al. (2008); Farr and Rossman (2024)
Camposporium chinense	Unidentified host	–	China	Xu et al. (2021)
Camposporium dulciaquae	Unidentified host	–	Thailand	Calabon et al. (2021)
Camposporium fusisporum	*Pandanus* sp.	Pandanaceae	Brunei	Whitton et al. (2002)
Camposporium himalayanum	*Phoenix* sp.	Arecaceae	India	Adamcik et al. (2015)
Camposporium hyalinum	*Elaeagnus macrophylla*, and *Fagus* sp.	Elaeagnaceae and Fagaceae	The United Kingdom	Abdullah (1980); Kirk and Spooner (1984)
Camposporium hyderabadense	*Borassus flabellifer*, *Machilus thunbergii* and *Mucuna ferruginea*	Arecaceae, Fabaceae, and Lauraceae	China, India and Japan	Rao and Rao (1964); Ichinoe (1971); Farr and Rossman (2024)
Camposporium indicum	*Borassus flabellifer*	Arecaceae	India	Rao and Rao (1964)
Camposporium japonicum	*Acacia confusa*, *Betula pendula*, *Cinnamomum japonicum*, *Freycinetia arborea*, *Litchi chinensis*, *Machilus thunbergii*, *Mucuna ferruginea*, *Paulownia kawakamii* and *Quercus* sp.	Betulaceae, Lauraceae, Pandanaceae, Paulowniaceae, and Sapindaceae	China and Japan	Ichinoe (1971); Matsushima (1980); Farr and Rossman (2024)
Camposporium laundonii	*Aralia elata*, *Pasania edulis* and *Rosa* sp.	Araliaceae, Fagaceae, and Rosaceae	Japan and New Zealand	Ellis (1976); Watanabe (1993); Farr and Rossman (2024)
Camposporium lycopodiellae	*Lycopodiella inundata*	Lycopodiaceae	Germany	Hyde et al. (2020)
Camposporium marylandicum	Unidentified host	–	The United States	Shearer (1974)
Camposporium microsporum	*Borassus flabellifer*	Arecaceae	India	Rao and Rao (1964)
Camposporium multiseptatum	Unidentified host	–	China	Hyde et al. (2020)
Camposporium ontariense	*Acer saccharum* and *Freycinetia arborea*	Sapindaceae and Pandanaceae	Canada and the United States	Matsushima (1983); Whitton et al. (2002)
Camposporium pellucidum	*Betula pendula*, *Caesalpinia echinata*, *Carpodetus serratus*, *Elaeagnus* sp., *Fagus* sp., *Laurus* sp., *Pasania glabra*, *Picea abies*, *Rhopalostylis* sp. and *Sorbus aucuparia*	Areceae, Betulaceae, Elaeagnaceae, Fabaceae, Lauraceae, Pinaceae, Rosaceae, and Rousseaceae	Brazil, Japan, Poland, New Zealand, Russia and the United Kingdom	Hughes (1951); Matsushima (1983); Mulenko et al. (2008); Farr and Rossman (2024)
Camposporium quercicola	*Quercus germana*	Fagaceae	Mexico	Mercado Sierra et al. (1995)
Camposporium ramosum	*Freycinetia* sp.		Australia and the United States	Whitton et al. (2002)
Camposporium scolecosporium	Unidentified host	–	Papua New Guinea	Kobayasi (1971)
Camposporium septatum	Unidentified host	–	Thailand	Hyde et al. (2020)
Camposporium valdivianum	*Sophora microphylla*	Fabaceae	The United States	Koukol and Delgado (2021)

Species	Host	Host family	Locality	References
Camposporium verruculosum	*Clematis vitalba*	Ranunculaceae	Italy	Koukol and Delgado (2021)
Dematiomelanomma yunnanense	*Hypericum monogynum* and *Rubus parvifolius*	Hypericaceae and Rosaceae	China	Gao et al. (2023)
Exosporiella fungorum	*Thelephora* sp. (leathery earthfans/ mushroom sp.)	–	Sweden	Karsten (1892)
Fusiconidium mackenziei	*Clematis vitalba*	Ranunculaceae	Italy	Li et al. (2017)
Herpotrichia alligata	*Opuntia* sp.	Cactaceae	Sweden and the United States	Barr (1992); Farr and Rossman (2024)
Herpotrichia alpincola	*Aconitum* sp.	Ranunculaceae	Hungary and Slovakia	Rehm (1906)
Herpotrichia arizonica	*Carnegiea gigantea*	Cactaceae	The United States	Barr (1992); Farr and Rossman (2024)
Herpotrichia australis	*Sclerocarya caffra*	Anacardiaceae	South Africa	Bose (1961)
Herpotrichia bakeri	*Sambucus javanica*	Viburnaceae	Philippines	Teodoro (1937); Farr and Rossman (2024)
Herpotrichia bambusana	*Bambusa vulgaris*	Poaceae	Brazil	Hennings (1908); Eriksson and Yue (1998)
Herpotrichia boldoae	*Boldea fragrans* and *Peumus boldus*	Monimiaceae	Chile	Spegazzini (1910); Mujica and Vergara (1945); Spaulding (1961); Farr (1973); Farr and Rossman (2024)
Herpotrichia brasiliensis	Unidentified host	–	Brazil	Rick (1933)
Herpotrichia brenckleana	*Urtica gracilis*	Urticaceae	Sweden	Eriksson (2014); Farr and Rossman (2024
Herpotrichia caesalpiniae	*Caesalpinia sepiaria*	Fabaceae	South Africa	Doidge (1948); Sivanesan (1971)
Herpotrichia calamicola	*Calamus caryotoides*	Arecaceae	Australia	Fröhlich and Hyde (2000); Farr and Rossman (2024)
Herpotrichia callimorpha	*Chamaenerion angustifolium*, *Salix* sp. and *Xanthophyllum flavescens*	Onagraceae, Polygalaceae, and Salicaceae	Denmark and India	Munk (1957); Rabenhorst (1869); Pande (2008); Farr and Rossman (2024)
Herpotrichia caulogena	*Silene nutans*	Caryophyllaceae	Luxembourg	Feltgen (1903)
Herpotrichia chilensis	*Proustia pungens*	Asteraceae	Chile	Feltgen (1903); Farr (1973); Farr and Rossman (2024)
Herpotrichia cirrhostoma	Unidentified host	–	Sri Lanka	Berkeley and Broome (1873); Petch (1912)
Herpotrichia dalisayi	Unidentified host	–	The Philippines	Hyde and Aptroot (1998)
Herpotrichia decidua	Unidentified host	–	The United States	Barr (1992); Farr and Rossman (2024)
Herpotrichia detzneriae	*Detzneria tubata*	Plantaginaceae	Papua New Guinea	Kobayasi (1971); Shaw (1984); Farr and Rossman (2024)
Herpotrichia diffusa	*Juglans cinerea* and *Populus* sp.	Juglandaceae	Palestine and the United States	Ellis and Everhart (1892); Ellis (1895)
Herpotrichia ellisii	*Abies* sp.	Pinaceae	Canada	Barr (1992); Farr and Rossman (2024)
Herpotrichia ephedrae	*Ephedra distachya*	Ephedraceae	France	Kuhnholtz-Lordat and Barry (1949)
Herpotrichia fusispora	Unidentified host	–	China	Chen and Hsieh (2004); Farr and Rossman (2024)
Herpotrichia gelasinosporoides	Soil	–	India	Von Arx (1981)
Herpotrichia henkeliana	*Phragmites communis*	Poaceae	Germany	Sydow and Sydow (1921)

Species	Host	Host family	Locality	References
Herpotrichia herbarum	*Achillea millefolium*	Asteraceae		Wehmeyer (1952); Barr (1992)
Herpotrichia herpotrichoides	*Carya* sp., *Epilobium* sp., *Rhododendron hirsutum*, *Ribes* sp. and *Rubus* sp.	Ericaceae, Juglandaceae, Grossulariaceae, Onagraceae, and Rosaceae	Austria, Denmark, Germany, Poland, the United States and the United Kingdom	Cannon (1982); Barr (1984); Cannon et al. (1985); Mulenko et al. (2008); Zhang et al. (2012); Tian et al. (2015); Farr and Rossman (2024)
Herpotrichia hippocrateae	*Hippocratea grahamii*	Celastraceae	India	Tilak and Talde (1975); Pande (2008)
Herpotrichia indica	*Duranta plumieri*	Verbenaceae	India	Anahosur (1970); Pande (2008); Farr and Rossman (2024)
Herpotrichia laricina	*Larix decidua*	Pinaceae	Luxembourg	Feltgen (1901)
Herpotrichia leptospora	Unidentified host	–	–	Kirschstein (1911)
Herpotrichia lignicola	Unidentified host	–	Belgium	Bose (1961)
Herpotrichia macrotricha	*Acer spicatum*, *Agropyron repens*, *Agrostis alba*, *Arundinaria* sp., *Carex* sp., *Cocos nucifera*, *Eupatorium formosanum*, *Fagus sylvatica*, *Fraxinus* sp., *Rubus* sp. and *Solidago* sp.	Arecaceae, Asteraceae, Cupressaceae, Cyperaceae, Fagaceae, Oleaceae, Poaceae, Rosaceae, and Sapindaceae	China, India, the United Kingdom and the United States	Dennis (1978); Saccardo (1883); Barr (1968, 1984); Pande (2008); Chen and Hsieh (2004); Farr and Rossman (2024)
Herpotrichia mangrovei	Unidentified host	–	China	Jones and Vrijmoed (2003)
Herpotrichia melanotricha	*Hevea brasiliensis*	Euphorbiaceae	Congo	Saccas (1954)
Herpotrichia millettiae	*Millettia* sp.	Fabaceae	Malaysia	Sivanesan (1971)
Herpotrichia monospermatis	*Butea monosperma*	Fabaceae	India	Pande (2008); Farr and Rossman (2024)
Herpotrichia mulleri	*Artemisia nilagirica* and *Butea monosperma*	Asteraceae, Fabaceae	India	Pande (2008); Farr and Rossman (2024)
Herpotrichia myriangii	*Carica papaya*	Caricaceae	Java	Raciborski (1909)
Herpotrichia nectrioides	Melastomataceae sp.	Melastomataceae	Brazil	Rehm (1901)
Herpotrichia nigra	*Abies* sp., *Calocedrus decurrens*, *Cedrus libani*, *Chamaecyparis nootkatensis*, *Juniperus* sp., *Phyllodoce* sp., *Picea* sp., *Pinus* sp., *Pseudotsuga menziesii* and *Rhododendron* sp.	Cupressaceae, Ericaceae, and Pinaceae	Austria, Canada, France, Germany, Italy, Norway, Poland, Switzerland, Turkey, Ukraine and the United States	Shaw (1973); Ginns (1986); French (1989); Farr and Rossman (2024)
Herpotrichia nigrotuberculata	*Elaeis guineensis* and *Phyllostachys reticulata*	Arecaceae and Poaceae	Japan and Tanzania	Pirozynski (1972); Farr and Rossman (2024)
Herpotrichia nypicola	*Nypa fruticans*	Arecaceae	Malaysia	Hyde et al. (1999); Farr and Rossman (2024)
Herpotrichia occulta	*Eucalyptus* sp.	Myrtaceae	Brazil	Rick (1933)
Herpotrichia ochrostoma	*Fraxinus excelsior*	Oleaceae	Luxembourg	Feltgen (1903)
Herpotrichia palmicola	*Calamus caryotoides*, *Daemonorops* sp. and *Licuala ramsayi*	Arecaceae	Australia and China	Hyde et al. (1999); Fröhlich and Hyde 2000; Zhuang (2001); Farr and Rossman (2024)
Herpotrichia pandei	*Saccharum spontaneum*	Poaceae	India	Bose (1961)
Herpotrichia petrakiana	*Fagus sylvatica*	Fagaceae	–	Bose (1961)

Species	Host	Host family	Locality	References
Herpotrichia philippinensis	*Alstonia scholaris*	Apocynaceae	The Philippines	Rehm (1914); Teodoro (1937); Farr and Rossman (2024)
Herpotrichia pinetorum	*Herpotrichia pinetorum*	Pinaceae	Austria and India	Winter (1885); Mueller (1958); Petrak (1962); Farr and Rossman (2024)
Herpotrichia quinqueseptata	*Abies lasiocarpa*, *Larix europaea*, *Picea* sp. and *Populus tremula*	Pinaceae and Salicaceae	Canada, Czech Republic, Germany, Sweden and the United States	Shaw (1973); Minter (1981); Ginns (1986); Eriksson (2014); Farr and Rossman (2024)
Herpotrichia rara	*Tanacetum vulgare*	Asteraceae	Germany	Kirschstein (1935)
Herpotrichia rhenana	*Epilobium angustifolium*, *Rhododendron hirsutum* and *Ribes* sp.	Ericaceae, Grossulariaceae, and Onagraceae	Austria and the United States	Fuckel (1870); Remler (1979); Farr and Rossman (2024)
Herpotrichia rhodospiloides	*Populus deltoides*	Salicaceae	The United States	Peck (1909)
Herpotrichia rhodosticta	*Carex paniculata* and *Populus* sp.	Cyperaceae and Salicaceae	Germany and the United States	Saccardo (1882); Samuels (1976); Farr and Rossman (2024)
Herpotrichia setosa	*Betula glandulosa* and *Myrica gale*	Betulaceae and Myricaceae	Canada and Ireland	Barr (1992); Farr and Rossman (2024)
Herpotrichia striatispora	Soil	–	South Africa	Papendorf and Arx (1966)
Herpotrichia symphoricarpi	*Symphoricarpos* sp.	Caprifoliaceae	The United States	Barr (1984); Farr and Rossman (2024)
Herpotrichia tenuispora	*Urtica dioica*	Urticaceae	Germany	Kirschstein (1906)
Herpotrichia vaginatispora	*Trifolium* sp.	Fabaceae	Italy	Tian et al. (2015)
Herpotrichia villosa	Unidentified host	–	Brazil	Samuels and Müller (1978)
Herpotrichia xiaokongensis	*Prunus* sp.	Rosaceae	China	Hyde et al. (2021)
Herpotrichia zingiberacearum	*Hedychium coronarium*	Zingiberaceae	China	This study
Mamillisphaeria dimorphospora	Unidentified host	–	Australia	Hyde et al. (1996)
Marjia tianshanica	*Cerasus tianshanica*	Rosaceae	Uzbekistan	Wanasinghe et al. (2018)
Marjia uzbekistanica	*Rosa* sp.	Rosaceae	Uzbekistan	Wanasinghe et al. (2018)
Melanocamarosporioides ugamica	*Lonicera altmannii*	Caprifoliaceae	Uzbekistan	Pem et al. (2019)
Melanocamarosporium galiicola	*Galium* sp.	Rubiaceae	Italy	Wijayawardene et al. (2016)
Melanocucurbitaria uzbekistanica	*Acer pubescens*	Sapindaceae	Uzbekistan	Wanasinghe et al. (2018)
Melanodiplodia tianschanica	*Rosa* sp.	Rosaceae	Uzbekistan	Wanasinghe et al. (2018)
Melanomma acanthophilum	*Cereus quisco*	Cactaceae	Chile	Spegazzini (1923); Farr (1973); Farr and Rossman (2024)
Melanomma afflatum	Unidentified host	–	The United States	Shear (1941)
Melanomma anceps	Unidentified host	–	Jawa	Höhnel (1909)
Melanomma andinum	*Bulnesia retamo*	Zygophyllaceae	Argentina	Spegazzini (1909); Farr (1973); Farr and Rossman (2024)
Melanomma artemisiae-maritimae	*Artemisia maritima*	Asteraceae	Russia	Lobik (1927); Farr and Rossman (2024)
Melanomma aspegrenii	*Carpinus betulus*, *Cornus* sp. and *Fagus sylvatica*	Betulaceae, Cornaceae, and Fagaceae	Poland	Fuckel (1870); Mulenko et al. (2008); Farr and Rossman (2024)

Species	Host	Host family	Locality	References
Melanomma aurantiicola	*Citrus* sp.	Rutaceae	Paraguay	Spegazzini (1920); Farr (1973); Farr and Rossman (2024)
Melanomma aurantiiphila	*Citrus* sp.	Rutaceae	Paraguay	Spegazzini (1920); Farr (1973); Farr and Rossman (2024)
Melanomma australiense	Unidentified host	–	Australia	Hyde and Goh (1999)
Melanomma brachythele	*Sambucus* sp.	Adoxaceae	The United Kingdom	Saccardo (1878)
Melanomma bubakii	*Campanula stricta*	Campanulaceae	Turkey	Bubák (1914)
Melanomma cacheutense	*Baccharis glutinosa*	Asteraceae	Argentina	Spegazzini (1909); Farr (1973); Farr and Rossman (2024)
Melanomma caesalpiniae	*Caesalpinia cearense*	Fabaceae	Brazil	Hennings (1908)
Melanomma caryophagum	*Carya* sp. and *Juglans* sp.	Juglandaceae	The United States	Fairman (1921)
Melanomma castillejae	*Castilleja pallida*	Orobanchaceae	Siberia	Farr and Rossman (2024)
Melanomma ceratoniae	*Ceratonia siliqua*	Fabaceae	Spain	Farr and Rossman (2024)
Melanomma chilense	*Proustia pungens*	Asteraceae	Chile	Spegazzini (1910); Farr (1973); Farr and Rossman (2024)
Melanomma citricola	*Citrus medica*	Rutaceae	Bangladesh and India	Sydow et al. (1911); Rao (1969); Farr and Rossman (2024)
Melanomma conjunctum	*Thuja plicata*	Cupressaceae	The United States	Farr and Rossman (2024)
Melanomma cryptostegiae	*Cryptostegia grandiflora*	Apocynaceae	India	Pande (2008); Farr and Rossman (2024)
Melanomma cucurbitarioideum	*Pentaphylloides fruticosa*	Rosaceae	China	Yuan and Barr (1994); Farr and Rossman (2024)
Melanomma dactylosporum	Unidentified host	–	Brazil	Rehm (1901)
Melanomma dinghuense	Unidentified host	–	China	Inderbitzin and Huang (2001)
Melanomma distinctum	*Pentaphylloides fruticosa*	Rosaceae	Russia	Vasilyeva (1987)
Melanomma drimydis	*Drymis* sp.	Winteraceae	Brazil	Rehm (1901)
Melanomma dryinum	*Quercus* sp.	Fagaceae	Belgium	Mouton (1900)
Melanomma dzungaricum	*Eurotia eversmanniana*	Amaranthaceae	Kazakhstan	Vasilyeva (1987)
Melanomma ebeni	*Ebenus stellata*	Fabaceae	Iran	González Fragoso (1918)
Melanomma epiphytica	*Bambusa* sp.	Poaceae	Indonesia	Raciborski (1909); Eriksson and Yue (1998); Farr and Rossman (2024)
Melanomma gigantica	Unidentified host	–	India	Pande (1979)
Melanomma glumarum	*Oryza sativa*	Poaceae	China, India, Japan and the Philippines	Watson (1971); Reinking (1919); Farr and Rossman (2024)
Melanomma gregarium	*Populus* sp.	Salicaceae	The United States	Cash (1953); Farr and Rossman (2024)
Melanomma halimodendri	*Halimodendron halodendron*	Fabaceae	Kazakhstan	Farr and Rossman (2024)
Melanomma haloxyli	*Haloxylon aphyllum*	Amaranthaceae	Kazakhstan	Farr and Rossman (2024)
Melanomma helianthemi	*Helianthemum rupifragum*	Cistaceae	Ukraine	Gucevic (1969)
Melanomma heraclei	*Heracleum pubescens*	Apiaceae	Ukraine	Dudka et al. (2004); Farr and Rossman (2024)
Melanomma herpotrichum	*Populus* sp.	Salicaceae	Luxembourg	Feltgen (1903)
Melanomma japonicum	*Fagus crenata*	Fagaceae	Japan	Hashimoto et al. (2017); Farr and Rossman (2024)

Species	Host	Host family	Locality	References
Melanomma jenynsii	Unidentified host	–	The United Kingdom	Saccardo (1883)
Melanomma juniperi	*Juniperus virginiana*	Cupressaceae	The United States	Fairman (1905); Cash (1953); Farr and Rossman (2024)
Melanomma langloisii	*Salix nigra*	Salicaceae	The United States	Farr and Rossman (2024)
Melanomma lithophilae	*Sobolewskia lithophila*	Apocynaceae	Ukraine	Dudka et al. (2004); Farr and Rossman (2024)
Melanomma longicolle	*Acer* sp. and *Citrus limon*	Aceraceae and Rutaceae	Italy and the United Kingdom	Saccardo (1875); Farr and Rossman (2024)
Melanomma marathawadense	On paper	–	India	Tilak and Kale (1970)
Melanomma margaretae	*Dryas octopetala*	Rosaceae	Poland	Mulenko et al. (2008); Farr and Rossman (2024)
Melanomma martinianum	Unidentified host	–	New Zealand	Saccardo (1883)
Melanomma mate	*Ilex paraguensis*	Aquifoliaceae	Argentina	Spegazzini (1908); Farr (1973); Farr and Rossman (2024)
Melanomma medium	*Acer negundo*, *Calligonum* sp. and *Tamarix* sp.	Sapindaceae and Tamaricaceae	Canada, Italy and the United Kingdom	Saccardo (1878); Farr (1973); Farr and Rossman (2024)
Melanomma mindorense	*Arenga mindorensis*	Arecaceae	The Philippines	Rehm (1913)
Melanomma mojunkumica	*Haloxylon aphyllum*	Amaranthaceae	Kazakhstan	Farr and Rossman (2024)
Melanomma moravicum	Unidentified host	–	Slovakia	Farr and Rossman (2024)
Melanomma mutabile	*Solanum dulcamara*	Solanaceae	Luxembourg	Feltgen (1901)
Melanomma myricae	*Myrica gale*	Myricaceae	Sweden	Eriksson (2014); Farr and Rossman (2024)
Melanomma nigriseda	*Fagus* sp.	Fagaceae	The United States	Fairman (1922)
Melanomma obliterans	Unidentified host	–	The United Kingdom	Saccardo (1883)
Melanomma obtusissimum	Unidentified host	–	Cuba	Farr and Rossman (2024)
Melanomma oryzae	*Oryza sativa*	Poaceae	Japan	Farr and Rossman (2024)
Melanomma oxysporum	*Quercus* sp.	Fagaceae	The United States	Hawksworth (1985)
Melanomma panici-miliacei	*Panicum miliaceum*	Poaceae	Siberia	Farr and Rossman (2024)
Melanomma philippinense	Unidentified host	–	The Philippines	Sydow and Sydow (1914)
Melanomma populicola	*Cornus* sp., *Fagus sylvatica*, *Picea abies*, *Populus* sp., *Quercus* sp. and *Sorbus aucuparia*	Cornaceae, Fagaceae, Pinaceae, Rosaceae, and Salicaceae	China, Croatia, Germany and the Netherlands	Crous et al. (2020); Farr and Rossman (2024); this study
Melanomma praeandinum	*Salvia gilliesii*	Lamiaceae	Argentina	Spegazzini (1909); Farr (1973); Farr and Rossman (2024)
Melanomma pulveracea	Unidentified host	–	China	Teng (1936)
Melanomma pulvis-pyrius	*Acer* sp., *Albizia julibrissin*, *Alhagi* sp., *Alnus* sp., *Berberis* sp., *Betula* sp., *Bupleurum fruticosum*, *Campsis radicans*, *Carpinus betulus*, *Celtis australis*, *Corylus* sp., *Larix decidua* and *Pinus sylvestris*	Apiaceae, Betulaceae, Berberidaceae, Bignoniaceae, Cannabaceae, Fabaceae, Pinaceae, and Sapindaceae	Canada, Czech Republic, Japan, Poland, Russia, Scotland, Sweden and Ukraine	Mulenko et al. (2008); Hashimoto et al. (2017); Crous et al. (2020); Farr and Rossman (2024)

Species	Host	Host family	Locality	References
Melanomma pyriostictum	Unidentified host	–	The United Kingdom	Cooke (1887)
Melanomma rhododendri	*Rhododendron* sp.	Ericaceae	Austria, Belgium, Germany, Italy, Luxembourg, the Netherlands, Switzerland, the United Kingdom and the United States	Rehm (1881, 1906); Bommer and Rousseau (1890); Farr and Rossman (2024)
Melanomma ribis	*Ribes* sp.	Grossulariaceae	The United States	Barr (1990)
Melanomma rubicundum	*Lythrum* sp.	Lythraceae	Sweden	Bommer and Rousseau (1890); Farr and Rossman (2024)
Melanomma sanguinarium	Unidentified host	–	–	Saccardo (1878)
Melanomma saviczii	*Thymus pseudohumillimus*	Lamiaceae	Ukraine	Dudka et al. (2004); Farr and Rossman (2024)
Melanomma scrophulariae	*Scrophularia rupestris*	Scrophulariaceae	Ukraine	Gucevic (1967)
Melanomma sordidissimum	*Eriobotrya japonica*	Rosaceae	Argentina	Spegazzini (1909); Farr (1973); Farr and Rossman (2024)
Melanomma sparsum	*Abies* sp.	Pinaceae	Switzerland	Fuckel (1873)
Melanomma spiniferum	*Morus alba*	Moraceae	The United States	Cash (1953); Farr and Rossman (2024)
Melanomma subandinum	*Atriplex pamparum*	Amaranthaceae	Argentina	Cash (1953); Farr and Rossman (2024)
Melanomma subdispersum	*Betula* sp., and *Fagus* sp.	Betulaceae and Fagaceae	Canada, Ireland, Poland, and the United Kingdom	Conners (1967); Mulenko et al. (2008); Farr and Rossman (2024)
Melanomma submojunkumica	*Haloxylon aphyllum*	Amaranthaceae	Kazakhstan	Farr and Rossman (2024)
Melanomma thespesiae	*Thespesia* sp.	Malvaceae	India	Farr and Rossman (2024)
Melanomma trevoae	*Trevoa trinervia*	Rhamnaceae	Chile	Farr (1973); Farr and Rossman (2024)
Melanomma vile	*Quercus* sp.	Fagaceae	Sweden	Fuckel (1870)
Melanomma xylariae	Unidentified host	–	Brazil	Höhnel (1907)
Monoseptella rosae	*Rosa* sp.	Rosaceae	Uzbekistan	Wanasinghe et al. (2018)
Muriformistrickeria rosae	*Rosa* sp.	Rosaceae	Italy	Wanasinghe et al. (2018)
Muriformistrickeria rubi	*Rubus* sp.	Rosaceae	Italy	Tian et al. (2015)
Navicella costaricensis	Unidentified host	–	The United States	El-Shafie et al. (2005)
Navicella diabola	*Castanopsis* sp.	Fagaceae	China	Aptroot (2003)
Navicella pallida	*Elaeocarpus* sp.	Elaeocarpaceae	Papua New Guinea	Aptroot and Iperen (1998)
Navicella pileata	*Fraxinus* sp., *Salix fragilis*, *Tilia* sp. and *Quercus* sp.	Fagaceae, Malvaceae, Oleaceae, and Salicaceae	Finland, Lithuania and Norway	Fabre (1879); Holm and Holm (1988); Farr and Rossman (2024)
Navicella xinjiangensis	*Lonicera hispida*, *Haloxylon ammodendron*	Amaranthaceae and Caprifoliaceae	China	Yuan and Zhao (1994); Farr and Rossman (2024)
Neobyssosphaeria clematidis	*Clematis vitalba*	Ranunculaceae	The United Kingdom	Phukhamsakda et al. (2020)

Species	Host	Host family	Locality	References
Petrakia aesculi	*Aesculus turbinata*	Sapindaceae	Japan	Jaklitsch and Voglmayr (2017)
Petrakia deviata	*Acer campestre*	Sapindaceae	Georgia and Switzerland	Watzl (1937); Gross et al. (2017)
Petrakia echinata	*Acer* sp.	Sapindaceae	Italy, Slovakia, Switzerland and the United States	Sydow and Sydow (1913); Li et al. (2016a); Gross et al. (2017); Farr and Rossman (2024)
Petrakia fagi	*Fagus crenata*	Fagaceae	Japan	Beenken et al. (2020)
Petrakia greenei	*Acer saccharinum*	Sapindaceae	The United States	Beenken et al. (2020)
Petrakia irregularis	*Acer pseudoplatanus*	Sapindaceae	The Netherlands and Poland	Mulenko et al. (2008); Farr and Rossman (2024)
Petrakia juniperi	*Juniperus* sp.	Cupressaceae	Germany	Bedlan (2017)
Petrakia liobae	*Fagus sylvatica*	Fagaceae	Switzerland	Beenken et al. (2020)
Petrakia minima	*Fagus japonica*	Fagaceae	Japan	Hashimoto et al. (2017); Beenken et al. (2020)
Petrakia paracochinensis	*Miscanthus floridulus*	Poaceae	China	Wong et al. (2002)
Phragmocephala atra	*Rhopalostylis sapida* and *Urtica* sp.	Arecaceae, Urticaceae	New Zealand and the United Kingdom	Mason and Hughes (1951); McKenzie et al. (1992)
Phragmocephala elegans	*Gymnanthes lucida*	Euphorbiaceae	Brazil and Cuba	Castañeda (1985)
Phragmocephala elliptica	*Elaeagnus* sp., *Filipendula denudata*, *Laurus* sp. *Quercus robur* and *Sambucus* sp.	Adoxaceae, Elaeagnaceae, Fagaceae, Lauraceae, and Rosaceae	Canada, Russia, Ukraine and the United Kingdom	Hughes (1979); Dennis (1986); Holubtsova and Andrianova (2008); Farr and Rossman (2024)
Phragmocephala garethjonesii	Unidentified host	–	China	Su et al. (2015)
Phragmocephala glanduliformis	*Corticium coronatum*, *Picea obovate* and *Quercus* sp.	Corticiaceae, Fagaceae, and Pinaceae	Austria	Hughes (1955); Farr and Rossman (2024)
Phragmocephala hughesii	Unidentified host	–	China	Wu and Zhuang (2005)
Phragmocephala minima	*Abies balsamea* and *Fagus sylvatica*	Fagaceae and Pinaceae	Canada and the United Kingdom	Mason and Hughes (1951); Conners (1967)
Phragmocephala prolifera	*Populus tremuloides* and *Urtica dioica*	Salicaceae and Urticaceae	Belgium and Canada	Hughes (1979); Farr and Rossman (2024)
Phragmocephala stemphylioides	*Carya* sp., *Cistus* sp. and *Pistacia lentiscus*	Anacardiaceae, Cistaceae, and Juglandaceae	Brazil, Canada, China and Italy	Hughes (1958); Zhuang (2005); Lunghini et al. (2013); Farr and Rossman (2024)
Phragmotrichum andamanense	*Strobilanthes* sp.	Acanthaceae	India	Bhat and Kendrick (1993)
Phragmotrichum chailletii	*Abies* sp. and *Picea* sp.	Pinaceae	Canada, Switzerland, Romania and the United States	Kunze and Schmidt (1823); Ginns (1986); Farr and Rossman (2024)
Phragmotrichum karstenii	*Acer platanoides*	Sapindaceae	Finland	Sutton and Pirozynski (1965)
Phragmotrichum rivoclarinum	*Acer* sp., *Alnus* sp. and *Salix* sp.	Betulaceae, Salicaceae, and Sapindaceae	Canada, Italy and the United Kingdom	Sutton and Pirozynski (1966); Ginns (1986); Farr and Rossman (2024)
Phragmotrichum vassiljevae	*Alnus kamtschatica*	Betulaceae	Russia	Melnik (1984)

Species	Host	Host family	Locality	References
Pleotrichocladium opacum	Soil	–	Spain	Hernández-Restrepo et al. (2017)
Praetumpfia obducens	*Fraxinus excelsior*	Oleaceae	Austria and Sweden	Jaklitsch and Voglmayr (2017)
Pseudobyssosphaeria bambusae	*Bamboo* sp.	Poaceae	Thailand	Hyde et al. (2018)
Pseudostrickeria muriformis	*Origanum vulgare*	Lamiaceae	Italy	Tian et al. (2015)
Pseudostrickeria ononidis	*Ononis spinosa*	Fabaceae	Italy	Tian et al. (2015)
Pseudostrickeria rosae	*Rosa* sp.	Rosaceae	Italy	Wanasinghe et al. (2018)
Sarimanas pseudofluviatile	Unidentified host	–	Japan	Liu et al. (2015)
Sarimanas shirakamiense	*Swida controversa*	Cornaceae	Japan	Liu et al. (2015)
Seifertia alpina	*Rhododendron ponticum*	Ericaceae	Austria	Beenken et al. (2020)
Seifertia azaleae	*Ledum groenlandicum*, *Leucopogon costatus* and *Rhododendron* sp.	Ericaceae	Australia, Canada, China, Germany, Italy, Japan, the Netherlands, New Zealand, Panama, Switzerland, the United Kingdom and the United States	White and Hamilton (1935); Partridge and Morgan-Jones (2002); Farr and Rossman (2024)
Seifertia shangrilaensis	*Rhododendron decorum*	Ericaceae	China	Li et al. (2016b)
Tumularia aquatica	*Alnus glutinosa*, *Phragmites* sp. and *Quercus* sp.	Betulaceae, Fagaceae, and Poaceae	South Africa and the United Kingdom	Sivanesan (1984); Marvanová and Descals (1987); Farr and Rossman (2024)
Tumularia tuberculata	*Fagus sylvatica*, *Quercus* sp.	Fagaceae	Hungary	Gönczöl (1976)
Uzbekistanica pruni	*Prunus armeniaca*	Rosaceae	Russia	Hyde et al. (2020)
Uzbekistanica rosae-hissaricae	*Rosa* sp.	Rosaceae	Uzbekistan	Wanasinghe et al. (2018)
Uzbekistanica vitis-viniferae	*Vitis vinifera*	Vitaceae	Ukraine	Crous et al. (2020)
Uzbekistanica yakutkhanika	*Rosa* sp.	Rosaceae	Uzbekistan	Wanasinghe et al. (2018)
Xenostigmina aceris	*Acer macrophyllum*	Sapindaceae	The United States	Hashimoto et al. (2017)

Taxonomy

Bertiella (Sacc.) Sacc

Notes. *Bertiella* was established by Saccardo and Sydow (1899) to include *B. macrospora* as the type species. The species have superficial ascomata, cylindrical-clavate asci and hyaline, 1-septate (when immature) and pale brown, 3-septate (when mature) ascospores (Tian et al. 2015; Hongsanan et al. 2020). To the present time, there are six *Bertiella* species in Species Fungorum (2024). Of them, molecular data are available only for three species. *Bertiella* species have been reported from six different plant families, Cyrillaceae, Fagaceae, Lauraceae, Moraceae, Salicaceae and Ulmaceae (Fig. 10).

Bertiella fici **Tennakoon, C.H. Kuo & K.D. Hyde, Fungal Diversity 108: 29 (2021)**
Index Fungorum: IF555314
Facesoffungi Number: FoF09317
Fig. 4

Description. ***Saprobic*** on dead leaves of *Cinnamomum verum* J. Presl (Lauraceae). **Sexual morph:** ***Ascomata*** 160–220 × 230–280 µm ($\bar{x}$ = 180 × 240 µm, n = 15), solitary or scattered, semi-immersed to superficial, appeared as black dots on host surface, globose to subglobose, glabrous, unilocular, ostiolate. ***Peridium*** 12–20 µm wide, thick-walled, carbonaceous, composed of several layers of brown to dark brown pseudoparenchymatous cells, cells towards the inside hyaline, arranged in a ***textura angularis***, fusing at the outside indistinguishable from the host tissues. ***Hamathecium*** comprising numerous, 1–2 µm wide, hyaline, septate, cellular pseudoparaphyses. ***Asci*** 50–60 × 7.5–8.5 µm ($\bar{x}$ = 52 × 7.8 µm, n = 20), 8-spored, bitunicate, fissitunicate, cylindrical to cylindrical-clavate, short pedicellate, apically rounded, with a distinct ocular chamber. ***Ascospores*** 14–18 × 4–5 µm ($\bar{x}$ = 15 × 4.2 µm, n = 40), overlapping, 1–2-seriate, fusi-

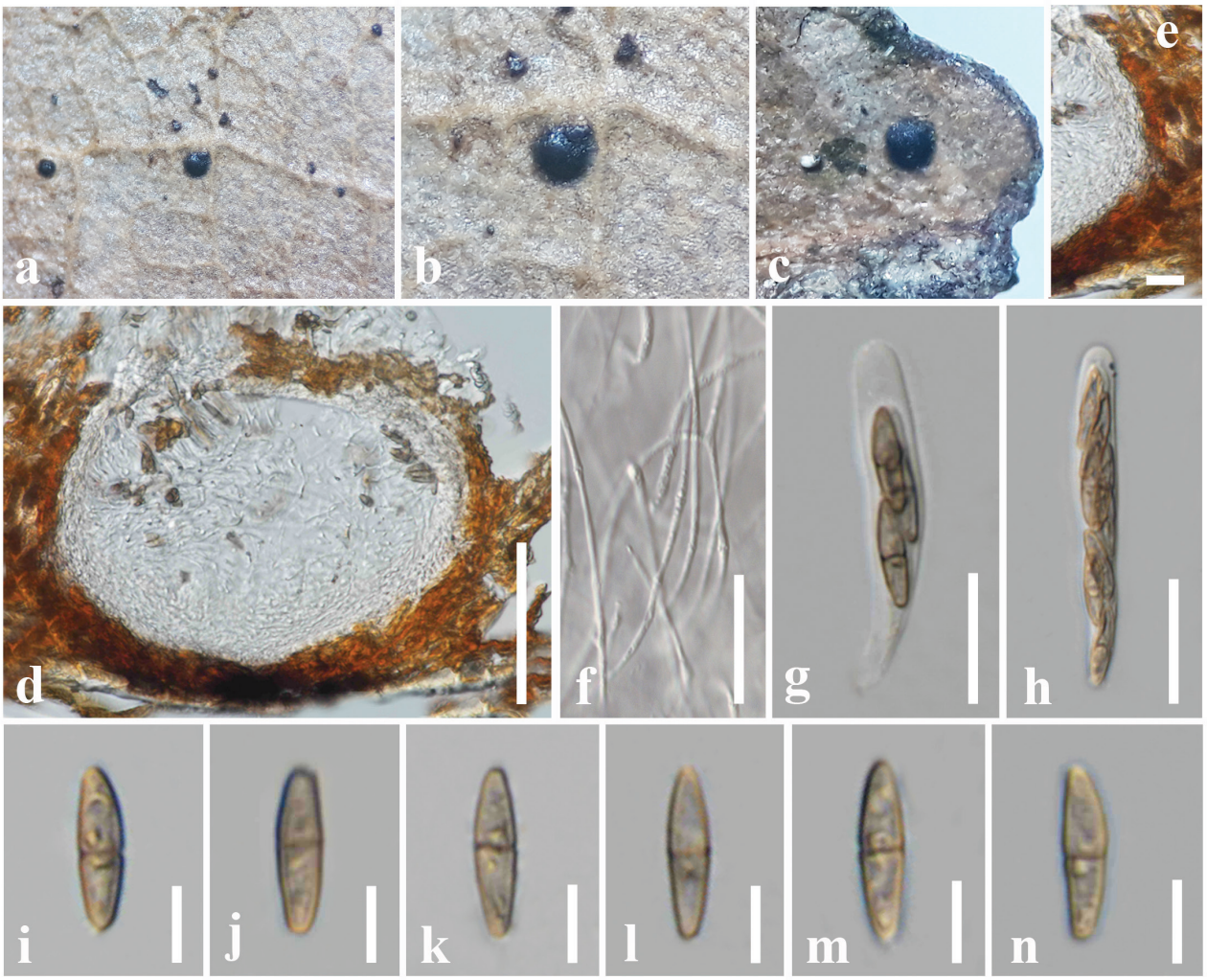

Figure 4. *Bertiella fici* (CMUB 40045, new host record) **a** appearance of ascomata on the host **b, c** close-up of ascomata **d** vertical section of an ascoma **e** peridium **f** pseudoparaphyses **g, h** asci **i–n** ascospores. Scale bars: 75 µm (**d**); 10 µm (**e**); 20 µm (**f–h**); 7 µm (**i–n**).

form, initially hyaline, becoming yellowish-brown at maturity, 1-septate, slightly curved, slightly constricted at the septum, guttulate, smooth-walled. **Asexual morph:** Undetermined.

Material examined. Thailand, Chiang Rai, Doi Mae Salong Mountain, on a dead leaf of *Cinnamomum verum* (Lauraceae), 15 June 2020, D. S. Tennakoon, DMS002 (CMUB 40045).

Known hosts. *Cinnamomum verum* and *Ficus septica* (Tennakoon et al. 2021; this study).

Known distribution. China and Thailand (Tennakoon et al. 2021; this study)

Notes. *Bertiella fici* was introduced by Tennakoon et al. (2021) from dead leaves of *Ficus septica* in China. The morphological characteristics of our collection (CMUB 40045) tally well with the *B. fici* in having solitary or scattered, semi-immersed to superficial ascomata, cylindrical to cylindrical-clavate asci and yellowish-brown, 1-septate ascospores with overlapping size ranges (Tennakoon et al. 2021). Multi-gene phylogeny (LSU, SSU, ITS and *tef1-α*) also indicates that our collection nested with *B. fici* isolates in a 100% ML and 1.00 BYPP supported clade. This was further confirmed by having only two nucleotide differences in the LSU and SSU genes between our collection and the type of *Bertiella fici*. Thus, we conclude our collection as a new host record of *Bertiella fici* from *Cinnamomum verum*. In addition, this is the first *Bertiella fici* record from Thailand.

Byssosphaeria Cooke

Notes. Cooke and Plowright (1879) established *Byssosphaeria* to accommodate *B. keithii* as the type species. *Byssosphaeria* species have superficial ascomata with bright yellow, orange or red flat apices around the ostiole, with dependent hyphal appendages that merge with the subiculum below and hyaline ascospores (Tian et al. 2015; Tennakoon et al. 2018). Species have cosmopolitan distribution as saprobes in various plant substrates (e.g. dead leaves, wood). As well, *Byssosphaeria* species have been reported from 15 plant families (Fig. 10). Currently, there are 18 accepted species in Species Fungorum (2024).

Byssosphaeria poaceicola Tennakoon & D.M. Hu, sp. nov.

Index Fungorum: IF901733
Facesoffungi Number: FoF15542
Fig. 5

Etymology. Named after the host family (Poaceae) where this fungus was collected.

Holotype. HFJAU10338.

Description. ***Saprobic*** on dead stem of *Arundo pliniana* Turra (Poaceae). **Sexual morph:** ***Ascomata*** 550–650 × 600–800 µm ($\bar{x}$ = 610 × 715 µm, n = 10), solitary to gregarious, superficial, dark brown to black, setose, coriaceous, unilocular, globose to subglobose, non-papillate, apex rounded with an orange to yellow ostiole, ostiole central, with pore-like opening, periphysate. ***Peridium*** 30–45 µm wide, thick-walled, composed of 6–7 layers of dark brown cells, orange to yellow near ostiole, arranged in ***textura angularis***. ***Hamathecium*** 1–2.5 µm wide, com-

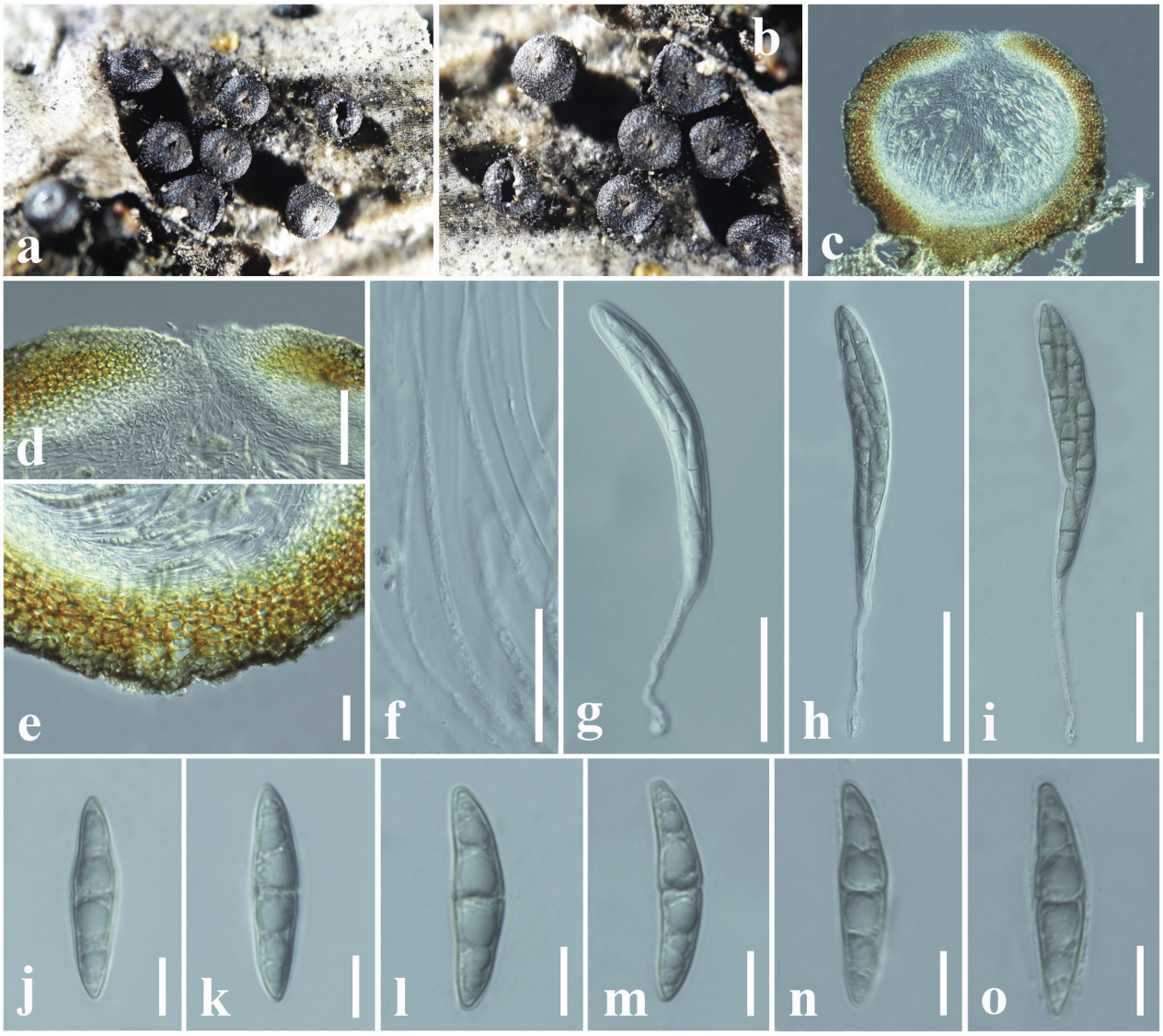

Figure 5. *Byssosphaeria poaceicola* (HFJAU10338, holotype) **a, b** appearance of ascomata on the host **c** vertical section of an ascoma **d** ostiole **e** peridium **f** pseudoparaphyses **g–i** asci **j–o** ascospores. Scale bars: 200 µm (**c**); 20 µm (**d, e**); 50 µm (**f–i**); 10 µm (**j–o**).

prising dense, filiform, anastomosing, septate, trabeculate pseudoparaphyses, embedded in a gelatinous matrix. ***Asci*** 165–180 × 12–15 µm ($\bar{x}$ = 171 × 13 µm, n = 20), 8-spored, bitunicate, fissitunicate, cylindrical clavate, apically rounded, long pedicellate (30–40 µm), with an indistinct ocular chamber. ***Ascospores*** 32–40 × 7–8 µm ($\bar{x}$ = 36 × 7.5 µm, n = 30), overlapping, 1–2-seriate, ellipsoid to fusiform, initially hyaline, pale brown when mature, 1-septate, constricted at the septum, slightly curved, guttulate, smooth-walled. ***Asexual morph:*** Undetermined.

Material examined. China, Yunnan Province, Kunming, on a dead stem of *Arundo pliniana* (Poaceae), 22 July 2016, D. S. Tennakoon, KDS30 (HFJAU10338, ***holotype***); *ibid.* 28 August 2016, KDS29 (HFJAU10337, ***paratype*).**

Notes. In the combined LSU, SSU, ITS and *tef1-α* phylogenetic analysis, two strains of *Byssosphaeria poaceicola* (HFJAU10337 and HFJAU10338) formed a monophyletic clade sister to *By. phoenicis* strains (ZHKUCC 21-0122 and ZHKUCC 21-012) with 83% ML and 0.99 BYPP statistical support. Morphologically,

they share similarities in having superficial, dark brown to black, coriaceous, non-papillate ascomata, cylindrical clavate asci and ellipsoid to fusiform, 1-septate, pale brown ascospores (Kularathnage et al. 2022). Although *Byssosphaeria poaceicola* can be distinguished from *By. phoenicis* in their size differences of asci (165–180 × 12–15 µm vs. 100–160 × 10–15 µm) and ascospores (32–40 × 7–8 µm vs. 25–30 × 5–7 µm) (Kularathnage et al. 2022). In addition, a comparison of the 497 nucleotides across the ITS (+5.8S) gene region of *By. poaceicola* and *By. phoenicis* shows 16 base pair differences (3.21%). It is interesting to notice that the *Byssosphaeria* species have not been collected much from Poaceae hosts, except for bamboo species (Jiang et al. 2022). Based on this finding, it appears that *Byssosphaeria* species can adapt to a variety of habitats, although there are limited studies to investigate their diversity on various hosts and regions.

***Byssosphaeria siamensis* Boonmee, Q. Tian & K.D. Hyde, Fungal Diversity 74: 283 (2015)**

Index Fungorum: IF551430

Facesoffungi Number: FoF01026

Fig. 6

Description. ***Saprobic*** on dead stem of *Citrus trifoliata* L. (Rutaceae). **Sexual morph:** ***Ascomata*** 250–400 × 300–500 µm ($\bar{x}$ = 320 × 410 µm, n = 10), solitary to gregarious, superficial, dark brown to black, setose, coriaceous, unilocular, globose to subglobose, non-papillate, apex rounded with an orange to yellow ostiole, ostiole central, with pore-like opening. ***Peridium*** 20–35 µm wide, thick-walled, composed of several layers of dark brown cells, orange to yellow near ostiole, arranged in ***textura angularis*** to ***textura prismatica***. ***Hamathecium*** 1–2.5 µm wide, comprising dense, filiform, anastomosing, septate, pseudoparaphyses, embedded in a gelatinous matrix. ***Asci*** 110–130 × 11–13 µm ($\bar{x}$ = 120 × 12 µm, n = 20), 8-spored, bitunicate, fissitunicate, cylindrical clavate, apically rounded, long pedicellate (20–35 µm), with an ocular chamber. ***Ascospores*** 30–40 × 6.5–8 µm ($\bar{x}$ = 31 × 7 µm, n = 30), overlapping, 1–2-seriate, ellipsoid to fusiform, initially hyaline, pale brown when mature, 1-septate, constricted at the septum, slightly curved, smooth-walled or verrucose. **Asexual morph:** Undetermined.

Material examined. China, Yunnan Province, Kunming, on a dead stem of *Citrus trifoliata* (Rutaceae), 27 July 2016, D. S. Tennakoon, KDS27 (HFJAU10336).

Known hosts. *Citrus trifoliata* (this study).

Known distribution. China, Thailand (Tian et al. 2015; Hyde et al. 2018; this study).

Notes. The morphological characteristics of our collection (HFJAU10336) similar to the type of *Byssosphaeria siamensis* in their superficial, dark brown to black, setose, non-papillate ascomata, cylindrical clavate asci and ellipsoid to fusiform, pale brown, 1-septate ascospores (Tian et al. 2015). In addition, both share overlapping size ranges of asci (110–130 × 11–13 µm vs. 112–148 × 10–16 µm) and ascospores (30–40 × 6.5–8 µm vs. 40.5–50 × 7–11 µm) (Tian et al. 2015). However, our collection is lacking a mucilaginous sheath which is present in the type species (Tian et al. 2015). According to the multi-gene phylogeny, our collection nested with *By. siamensis* isolates in 86% ML and 0.98 BYPP supported

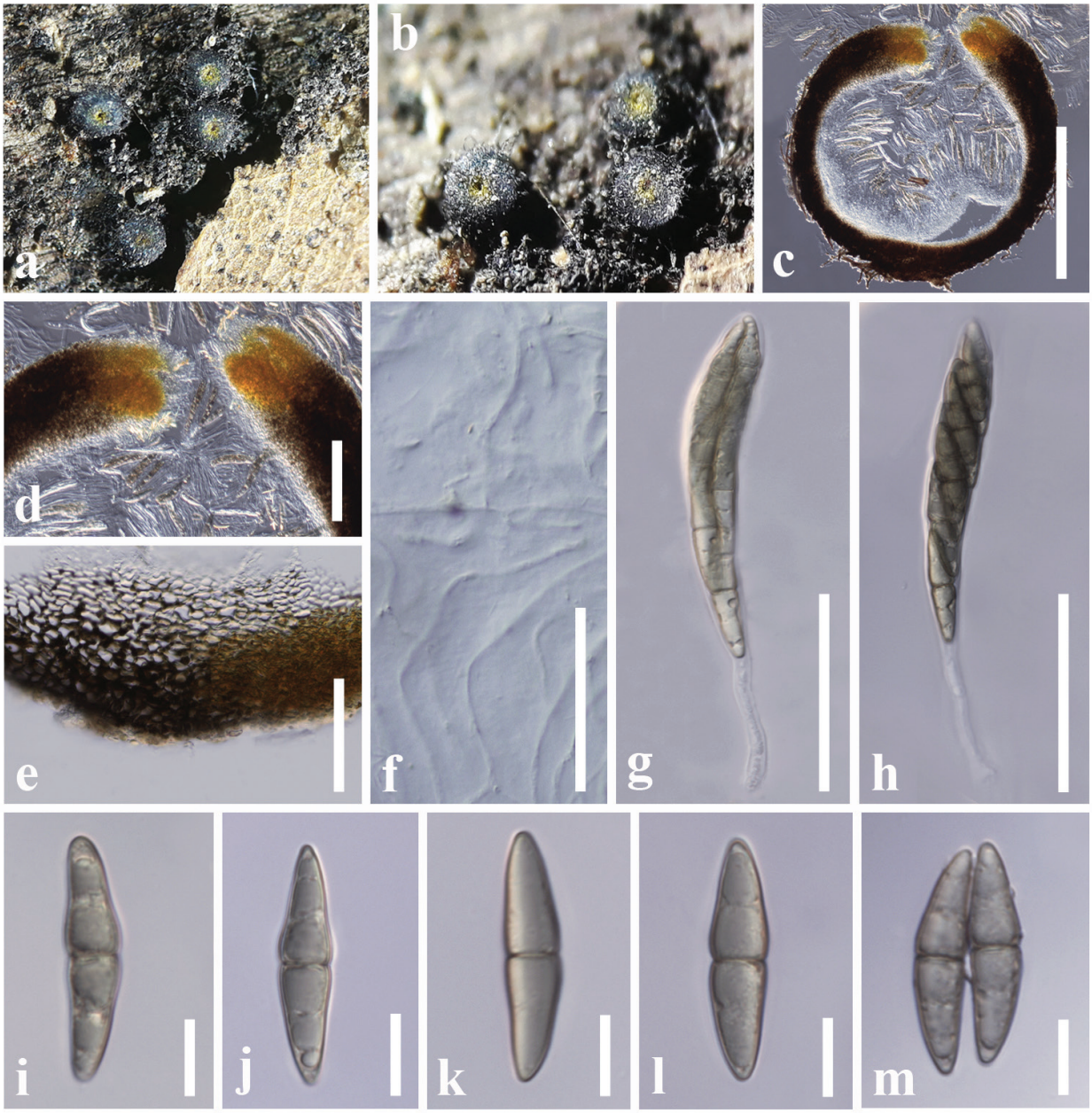

Figure 6. *Byssosphaeria siamensis* (HFJAU10336, new host record) **a** appearance of ascomata on the host **b** close-up of ascomata **c** vertical section of an ascoma **d** ostiole **e** peridium **f** pseudoparaphyses **g, h** asci **i–m** ascospores. Scale bars: 200 µm (**c**); 20 µm (**d, e**); 50 µm (**f–h**); 10 µm (**i–m**).

clade and close to the isolate MFLUCC 17-1800 with 88% ML, 0.99 BYPP support. Therefore, based on both morphology and phylogeny evidence, we introduce our collection as a new host record of *B. siamensis* from *Citrus trifoliata* in China.

Herpotrichia Fuckel

Notes. The diverse genus *Herpotrichia* was established by Fuckel (1868) to include two species, *H. rhenana* and *H. rubi*, but without designating a type species. Thus, Bose (1961) assigned *H. rhenana* as the lectotype. Subsequently, Holm (1979) assigned *H. herpotrichoides* (synonymous with *H. rubi*) as the

generic type (Cannon 1982). The species have erumpent to superficial ascomata, clavate to cylindrical asci with hyaline to pale brown, 1-septate ascospores (Sivanesan 1984; Tian et al. 2015). The asexual morph is pyrenochaeta-like with or without setae on the surface of the pycnidia (Sivanesan 1984; Hongsanan et al. 2020). *Herpotrichia* species have been reported as saprobes, mostly in dead wood substrates in 34 plant families (Fig. 10).

Herpotrichia zingiberacearum **Tennakoon & D.M. Hu, sp. nov.**
Index Fungorum: IF901734
Facesoffungi Number: FoF15543
Fig.7

Etymology. Named after the host family (Zingiberaceae) where this fungus was collected.

Holotype. HFJAU10332.

Description. ***Saprobic*** on dead stem of *Hedychium coronarium* J. Koenig (Zingiberaceae). **Sexual morph:** ***Ascomata*** 250–350 × 240–320 µm ($\bar{x}$ = 298 × 262 µm, n = 10), solitary to clustered, superficial, dark brown to black, setose, coriaceous, unilocular, globose to subglobose, rounded apex broadly cap-like, ostiolate. ***Peridium*** 15–25 µm wide, thick-walled, composed of 4–5 layers of dark brown to black cells, arranged in ***textura angularis***. ***Hamathecium*** 1–3 µm wide, comprising dense, filiform, anastomosing, septate, branched pseudoparaphyses, embedded in a gelatinous matrix. ***Asci*** 85–98 × 10–14 µm ($\bar{x}$ = 94 × 12 µm, n = 20), 8-spored, bitunicate, fissitunicate, cylindrical clavate, apically rounded, short pedicellate, with an ocular chamber. ***Ascospores*** 25–30 × 5–6 µm ($\bar{x}$ = 28 × 5.2 µm, n = 30), overlapping, 1–2-seriate, fusoid with narrowly rounded ends, hyaline, 1-septate, straight to slightly curved, constricted at the septum, with large guttules, surrounded by an expanded gelatinous sheath pointed at both ends, 2.5–4 µm wide, smooth-walled. **Asexual morph:** Undetermined.

Material examined. China, Yunnan Province, Kunming, on a dead stem of *Hedychium coronarium* (Zingiberaceae), 20 July 2016, D. S. Tennakoon, KDS12 (HFJAU10332, ***holotype***); *ibid.* 21 August 2016, KDS13 (HFJAU10333, ***paratype***); *ibid.* 25 August 2016, KDS18 (HFJAU10334, ***paratype***).

Notes. *Herpotrichia zingiberacearum* is isolated from the dead stem of *Hedychium coronarium* (Zingiberaceae). The newly-generated sequences *H. zingiberacearum* (LSU, SSU, ITS and *tef1-α*) formed a monophyletic clade closely related to *H. macrotricha* with 90% ML and 0.99 BYPP statistical support. Morphologically, they share similarities in having dark brown to black, setose, coriaceous ascomata, cylindrical clavate asci and hyaline, 1-septate ascospores (Mugambi and Huhndorf 2009). However, *H. zingiberacearum* can be distinguished from *H. macrotricha* in their smaller asci (85–98 × 10–14 µm vs. 115–145 × 11–13 µm) and ascospores (25–30 × 5–6 µm vs. 30–35 × 4–6 µm) (Tanaka and Hosoya 2006). On the other hand, *H. zingiberacearum* (HFJAU10332) differs from *H. macrotricha* (GKM 196N) by a comparison of the 694 nucleotides across the *tef1-α* gene region which shows 20 base pair differences (3.02%). This finding addresses future studies to explore the diversity of *Herpotrichia* species in different geographic regions and host plants, as these species have not previously been described from Zingiberaceae hosts (Table 2).

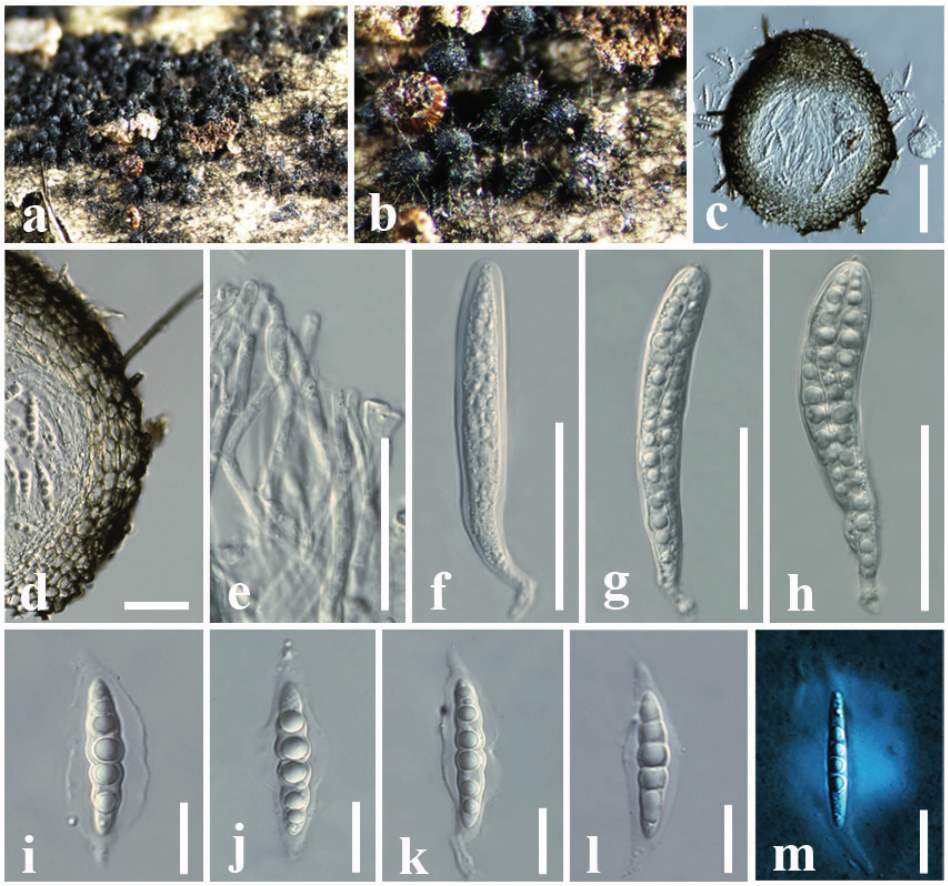

Figure 7. *Herpotrichia zingiberacearum* (HFJAU10332, holotype) **a, b** appearance of ascomata on the host **c** vertical section of an ascoma **d** peridium **e** pseudoparaphyses **f–h** asci **i–l** ascospores **m** ascospore stained in Indian ink showing a mucilaginous sheath. Scale bars: 100 µm (**c**); 20 µm (**d**); 50 µm (**e–h**); 15 µm (**i–m**).

***Melanomma* Nitschke ex Fuckel**

Notes. *Melanomma* was validly established by Fuckel (1870) with *M. pulvis-pyrius* as the type species. These species have cosmopolitan distribution worldwide and characterised in having carbonaceous ascomata and hyaline or brown, 2–3-septate ascospores (Tian et al. 2015; Crous et al. 2020). The asexual morph can be either coelomycetes or hyphomycetes (Hyde et al. 2011). Currently, 94 species are accepted in this genus (Species Fungorum 2024) and have been reported from 39 plant families (Fig. 10).

***Melanomma populicola* Crous & R.K. Schumach, Fungal Systematics and Evolution 6: 201 (2020)**
Index Fungorum: IF552757
Facesoffungi Number: FoF2887
Fig. 8

Basionym. *Aposphaeria populina* Died., Krypt.-Fl. Brandenburg (Leipzig) 9: 206 (1912).

Synonym. *Melanomma populinum* (Died.) Phukhams. & K.D. Hyde [as '*populina*'], Fungal Diversity 83: 49. 2017.

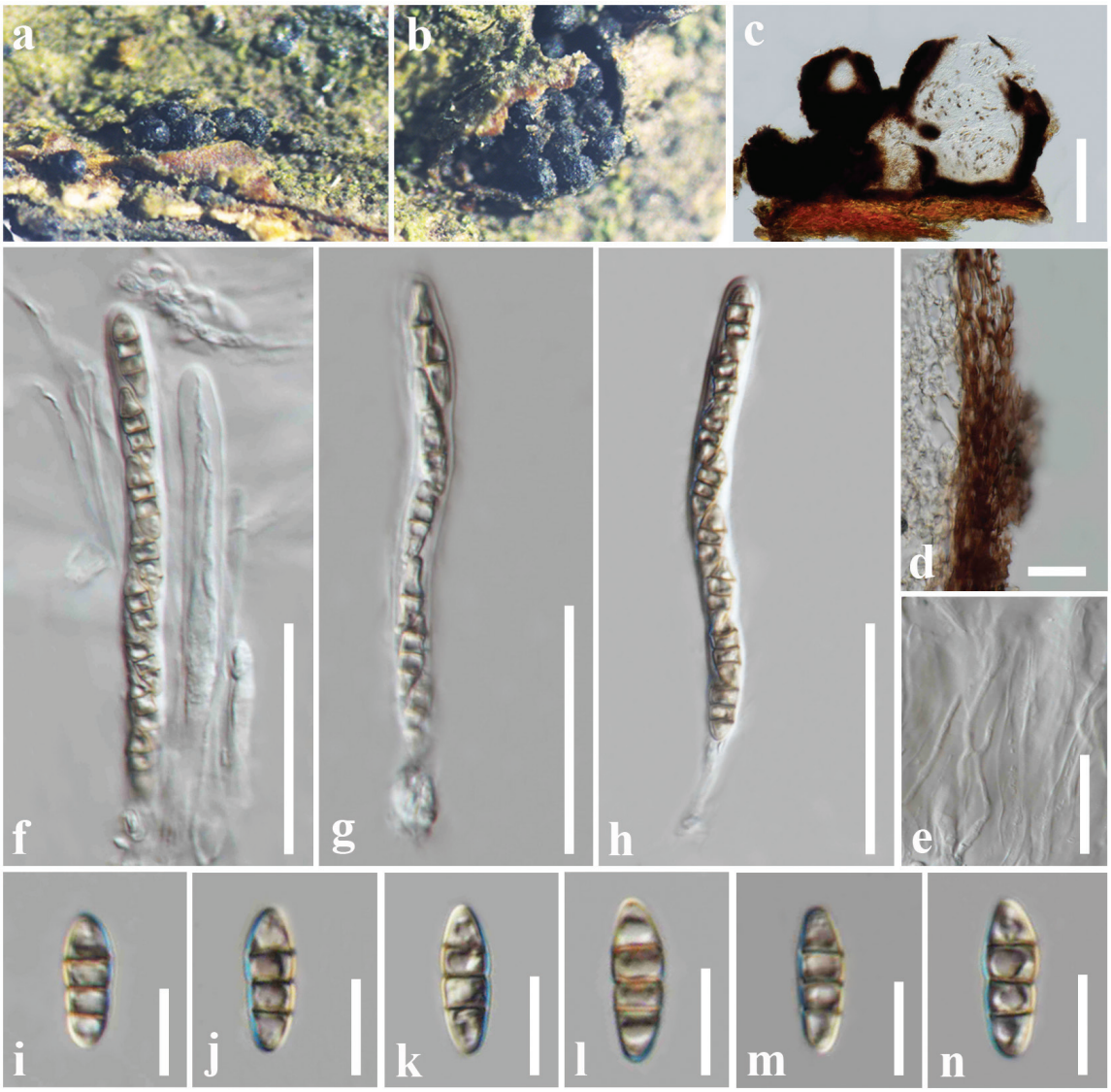

Figure 8. *Melanomma populicola* (HFJAU10335, new host record) **a** appearance of ascomata on the host **b** close-up of ascoma **c** vertical section of an ascoma **d** peridium **e** pseudoparaphyses **f–h** asci **i–n** ascospores. Scale bars: 75 µm (**c**); 10 µm (**d**); 40 µm (**e–h**); 10 µm (**i–n**).

Description. ***Saprobic*** on dead stem of *Fagus sylvatica* L. (Fagaceae). **Sexual morph:** ***Ascomata*** 130–200 × 200–300 µm ($\bar{x}$ = 150 × 255 µm, n = 15), solitary or scattered, immersed, erumpent through host surface, black, multi-loculate, globose to subglobose, ostiolate. ***Peridium*** 10–15 µm wide, thick-walled, carbonaceous, composed of several layers of light brown to dark brown pseudoparenchymatous cells, cells towards the inside hyaline, arranged in a ***textura angularis***, fusing at the outside indistinguishable from the host tissues. ***Hamathecium*** comprising numerous, 1–2 µm wide, hyaline, septate, filiform pseudoparaphyses. ***Asci*** 80–110 × 6–8 µm ($\bar{x}$ = 96 × 7 µm, n = 20), 8-spored, bitunicate, fissitunicate, cylindrical, apically rounded, short pedicellate with furcate end, with an indistinct ocular chamber. ***Ascospores*** 13–17 × 4–5.2 µm ($\bar{x}$ = 15 × 4.8 µm, n = 35), overlapping, 1–2-seriate, ellipsoid, initially hyaline, becoming light brown at maturity, 3-septate, straight to slightly curved, slightly constricted at the septa, guttulate, smooth-walled. **Asexual morph:** See Crous et al. (2020).

Material examined. China, Kunming, on a dead stem of *Fagus sylvatica* (Fagaceae), 25 July 2016, D. S. Tennakoon, KDS25 (HFJAU10335).

Known hosts. *Populus canadensis*, *Picea abies*, *Quercus* sp., *Sorbus aucuparia* (Crous et al. 2020; this study).

Known distribution. China, Germany, The Netherlands (Crous et al. 2020; this study).

Notes. *Melanomma populicola* was introduced by Diedicke (1912) as *Aposphaeria populina*, which was a phoma-like species collected from *Populus canadensis*. An epitype for *A. populina* was established by De Gruyter et al. (2013). Tibpromma et al. (2017) synonymised *A. populina* under *Melanomma* and erected as *M. populina*. Subsequently, this was validated by Crous et al. (2020) and erected as *M. populicola*. Morphological characteristics of our collection (HFJAU10335) fit well with the *M. populicola* in having black, globose to subglobose ascomata, cylindrical, apically rounded asci and ellipsoid, 3-septate, light brown ascospores. In addition, there are overlapping size ranges of asci (80–110 × 6–8 µm vs. 91–106 × 6.5–7.5 µm) and ascospores (13–17 × 4–5.2 µm vs. 15.1 × 5 µm) (Crous et al. 2020). Multi-gene phylogeny also shows that our collection groups with *M. populicola* isolates in a 99% ML and 0.99 BYPP supported clade. Therefore, we introduce our collections as a new host record of *M. populicola* from *Fagus sylvatica*.

Geographical distribution and host associations of melanommataceous species

Based on the data collected, it appears that the members of Melanommataceae are widely distributed around the world, comprising subtropical, tropical and temperate regions, such as Austria, Australia, Brazil, Canada, Finland, Germany, Japan, India, Thailand, Papua New Guinea, South Africa, Ukraine and the United States). The highest number of species have been reported from the United States (48 species). This is followed by China (35 species), Italy (30 species), India (25 species), Germany (23 species) and the United Kingdom (22 species) (indicated by red areas, Fig. 9). Moreover, Japan (17 species), Brazil (16 species), Ukraine (16 species), Canada (15 species), Kazakhstan (13 species), Poland (13 species) and Austria (11 species) are indicated by green areas (Fig. 9). Twenty-four countries have the species number range between 3 and 10, for instance Argentina, Russia and Sweden (10 species), Uzbekistan (9 species), Australia, France and Switzerland (8 species), Chile (7 species), Luxembourg, New Zealand, the Philippines and Thailand (6 species), Finland (5 species), Belgium and South Africa (4 species) and three species in nine countries (Azerbaijan, Czechia, Denmark, Georgia, Hungary, Papua New Guinea, Slovakia, Spain and Sri Lanka) (indicated by blue areas, Fig. 9). In addition, 36 countries reported two or a single species (indicated by yellow areas, Fig. 9). This may be because those countries have very limited taxonomic investigations on melanommataceous species. Consequently, it would be important to conduct more comprehensive collections, carry out more taxonomic studies and identify the species in those poorly-explored countries (e.g. African continent). In Asia, the highest number of melanommataceous species have reported from China, India and Thailand (Fig. 9), while Austria, Germany, Italy, Poland and the United Kingdom in Europe also have high numbers.

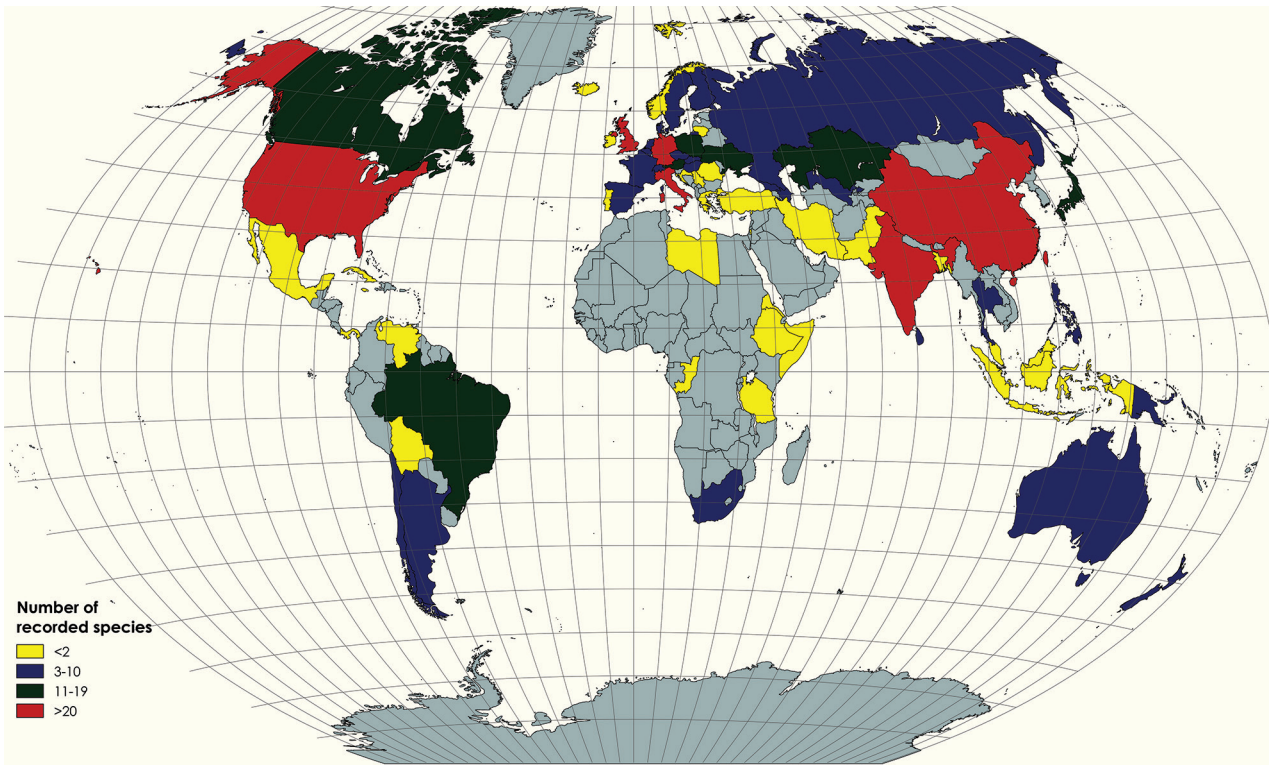

Figure 9. Distribution of so far reported species in Melanommataceae worldwide. Colour gradient shows the number of recorded species from lowest (yellow) to highest (red) and no records (grey).

Some species exist over multiple continents, while others appear to have limited distribution and are currently reported from one or a few countries (Fig. 9). Nine species of Melanommataceae are intercontinental and occur on more than five countries. Some highly diverse species include *Aposphaeria pulviscula*, *Camposporium cambrense*, *C. pellucidum*, *Herpotrichia herpotrichoides*, *H. nigra*, *H. quinqueseptata*, *Melanomma pulvis-pyrius*, *M. rhododendri* and *Seifertia azaleae* (Table 2). As well, nine species have been reported from four countries (*Byssosphaeria jamaicana*, *By. rhodomphala*, *Camposporium antennatum*, *Herpotrichia macrotricha*, *Melanomma glumarum*, *M. subdispersum*, *Petrakia echinata*, *Phragmocephala elliptica* and *Phragmotrichum chailletii*) and nine species from three countries (*Aposphaeria eragrostidis*, *A. freticola*, *A. mediella*, *Camposporium hyderabadense*, *Melanomma medium*, *M. populicola*, *Navicella pileata*, *Phragmocephala stemphylioides* and *Phragmotrichum rivoclarinum*). In contrast, the distribution of 313 species has been limited to two or to one country, based on the current information. We believe that the distribution of those species may be much higher with future collections and taxonomical investigations.

When focusing on the host association of melanommataceous species, most of have been discovered in decaying wood or submerged woody substrates (e.g. *Aposphaeria corallinolutea*, *A. rudis*, *Asymmetricospora calamicola*, *Bertiella ellipsoidea*, *Byssosphaeria juniperi*, *Calyptronectria argentinensis*, *Camposporium chinense*, *C. marylandicum*, *Herpotrichia alpincola*, *Marjia uzbekistanica*, *Melanomma dinghuense*, *Phragmocephala garethjonesii* and *Sarimanas pseudofluviatile*) (Table 2). Some species have been recorded from decaying leaves (e.g. *Bertiella fici*, *Byssosphaeria musae*, *Phragmocephala elegans*). As

well, it is noteworthy to mention that some species have been recorded from soil (e.g. *Herpotrichia gelasinosporoides*, *H. striatispora* and *Pleotrichocladium opacum*). In addition, *Aposphaeria ramalinae* has been collected from a lichen species (*Ramalina implectens*) in France (Pitard and Harmand 1911) and *Exosporiella fungorum* from a mushroom species (*Thelephora* sp. fibre vase or earth fan mushroom) in Sweden (Karsten 1892).

According to the host associations, some species of Melanommataceae are highly diverse and have been collected from more than 10 host species (e.g. *Camposporium antennatum*, *C. japonicum*, *C. pellucidum*, *Herpotrichia macrotricha*, *H. nigra* and *Melanomma pulvis-pyrius*), while some are from more than five host species (e.g. *Camposporium cambrense*, *Herpotrichia herpotrichoides*, *Melanomma populicola* and *Phragmocephala elliptica*). The highest number of melanommataceous species have reported from the plant family Fagaceae (32 species). The most common Fagaceae hosts are *Fagus* spp. (e.g. *F. crenata*, *F. sylvatica*) and *Quercus* species (e.g. *Q. germana*). This is followed by Fabaceae (24 species), Rosaceae (23 species), Salicaceae (22 species), Poaceae (19 species), Pinaceae and Arecaceae (18 species), Sapindaceae (16 species), Betulaceae (15 species), Amaranthaceae (12 species), Asteraceae (10 species), Ericaceae (9 species), Cupressaceae, Euphorbiaceae and Lauraceae (7 species), Rutaceae (6 species) and Malvaceae, Oleaceae and Pandanaceae (5 species) (Fig. 10). In addition, a range of 2–5 species have recorded from 30 plant families and single melanommataceous species have reported from 35 plant families. Thus, up to date, the species of the family have been reported from 82 plant families. However, some species have been collected from unidentified hosts and, thus, their host association remained unresolved (e.g. *Aposphaeria anomala*, *A. pakistanica*, *Bertiella ellipsoidea*, *B. gelatinosa*, *Camposporium appendiculatum* and *C. chinense*). The host specificity for most of the species has not yet been clarified, as they have been recorded from various plant families. Though, it was noted by Jaklitsch and Voglmayr (2017) that *Praetumpfia obducens* may be host specific to *Fraxinus* species.

Discussion

The members of Melanommataceae have been well-studied in last two decades, leading to many exciting discoveries (17 new genera and 76 new species), which may be mostly linked to the progress made in the DNA sequence data. The initial classification of these species was primarily based on morphological characteristics (e.g. globose or depressed ascomata, trabeculate pseudoparaphyses, fissitunicate asci, pigmented ascospores) associated with hand drawings (Saccardo 1883; Winter 1885; Morgan 1904; Spegazzini 1909; Shear 1941). However, morphology-based identification is challenging since most species can share similar characteristics, which may lead to misinterpretations. Thus, a combination of DNA-based molecular phylogeny and morphological traits has become a widely accepted tool for current fungal classifications (Tian et al. 2015; Hashimoto et al. 2017; Jaklitsch and Voglmayr 2017; Purahong et al. 2017; Kularathnage et al. 2022). Mostly, the large subunit (28S, LSU), small subunit (18S, SSU), internal transcribed spacers (ITS1–5.8S–ITS2), translation elongation factor 1 gene (*tef1-α*) and RNA polymerase second largest subunit (*rpb2*) molecular markers have been used in current phylogenetic

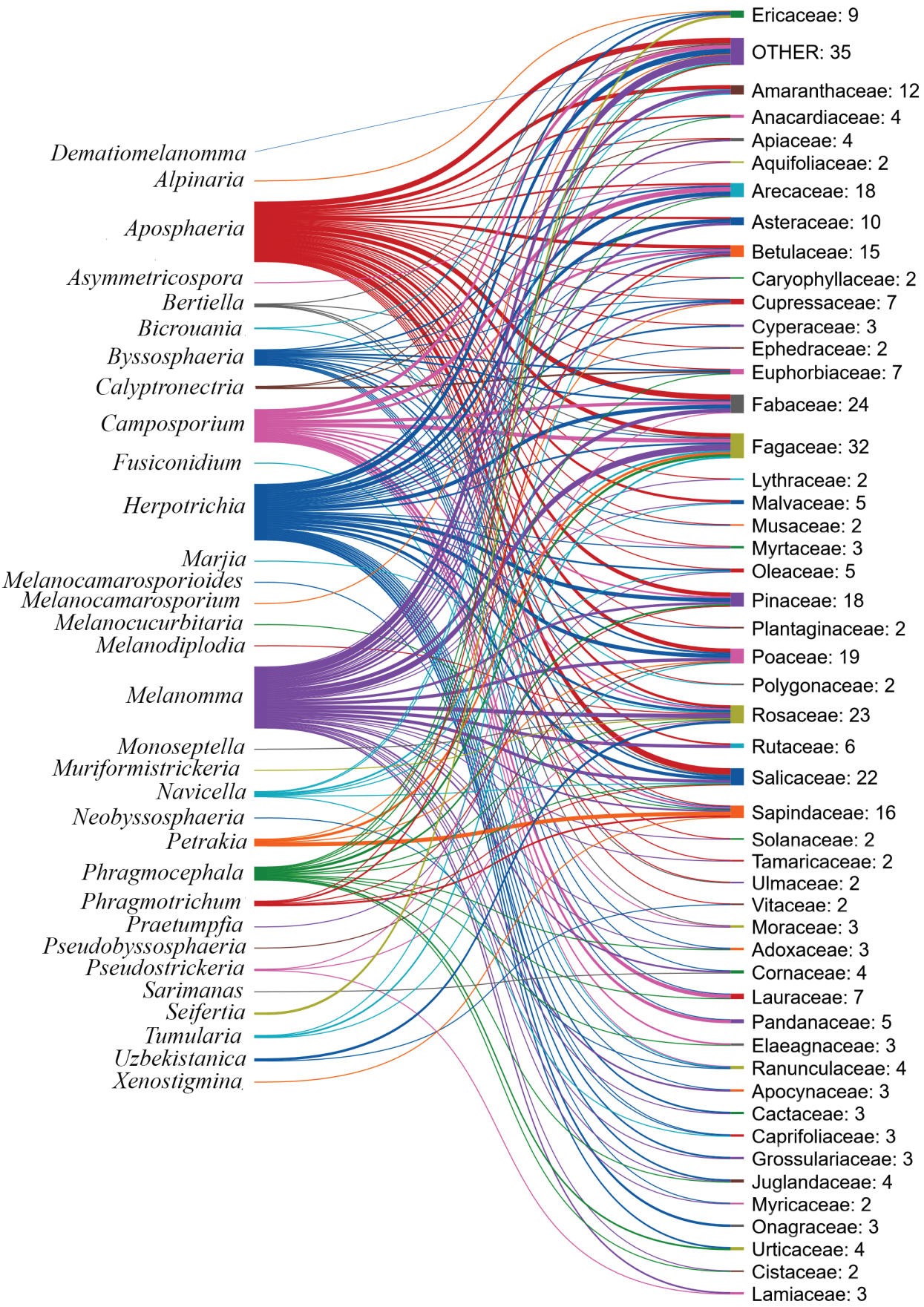

Figure 10. The melanommataceous species distribution through plant host families.

analyses of Melanommataceae (Tian et al. 2015; Tennakoon et al. 2018; Pem et al. 2019; Kularathnage et al. 2022).

Melanommataceae genera are highly varied, both morphologically and phylogenetically. Of them, some are highly diverse with numerous species (e.g. *Aposphaeria*: 83 species, *Melanomma*: 81 species, *Herpotrichia*: 61 species, *Camposporium*: 25 species, *Byssosphaeria*: 18 species and *Petrakia*: 10 species), while some have fewer species (*Phragmocephala*: 9 species, *Bertiella*: 6 species, *Navicella*: 5 species, *Phragmotrichum*: 5 species, *Uzbekistanica*: 4 species, *Calyptronectria*: 3 species, *Pseudostrickeria*: 3 species, *Seifertia*: 3 species, *Marjia*: 2 species, *Muriformistrickeria*: 2 species, *Sarimanas*: 2 species, and *Tumularia*: 2 species). In addition, some genera are monotypic and need more collections for their expansion (e.g. *Alpinaria*, *Asymmetricospora*, *Bicrouania*, *Dematiomelanomma*, *Exosporiella*, *Fusiconidium*, *Mamillisphaeria*, *Melanocamarosporioides*, *Melanocamarosporium*, *Melanocucurbitaria*, *Melanodiplodia*, *Monoseptella*, *Neobyssosphaeria*, *Pleotrichocladium*, *Praetumpfia*, *Pseudobyssosphaeria* and *Xenostigmina*). However, it is noteworthy to mention that some genera currently lack molecular data and, thus, their phylogenetic position is uncertain (e.g. *Asymmetricospora*, *Bicrouania*, *Calyptronectria*, *Exosporiella*, *Mamillisphaeria* and *Navicella*) (Hongsanan et al. 2020). As well, only two species of *Aposphaeria* have molecular data out of the 84 species listed in the Species Fungorum (2024). Consequently, to resolve their phylogenetic placements, further collections and investigations are essentially required.

In this study, we introduced two new species and three new host records collected from China and Thailand. The new species, *Byssosphaeria poaceicola* and *Herpotrichia zingiberacearum* can be distinguished from related species in their morphology and DNA molecular data. The morphological characteristics of the new host records strongly tally with their type species and phylogeny analyses also provide evidence for their placements. These new host records also demonstrate their adaptability to a broad range of habitats and there could be many more. Thus, many fungal species and host associations are waiting for us and we should undertake further explorations.

Acknowledgements

Dr. Yang Gao is thanked for his support in depositing the herbarium specimens. The authors would like to thank Shaun Pennycook (Manaaki Whenua Landcare Research, New Zealand) for his guidance on the fungal nomenclature.

Additional information

Conflict of interest

The authors have declared that no competing interests exist.

Ethical statement

No ethical statement was reported.

Funding

No funding was reported.

Author contributions

Conceptualisation, D.S.T. N.I.d.S. and D.M.H; methodology, D.S.T. and N.I.d.S; software, D.S.T. and N.I.S.; validation, K.M.T., N.I.d.S., H.Y.S., N.S., F.S.C. and D.M.H; formal analysis, D.S.T. and N.I.d.S; investigation, K.M.T., N.I.d.S., H.Y.S., N.S., F.S.C. and D.M.H; resources, D.S.T; data curation, D.S.T. and N.I.d.S; writing – original draft preparation, D.S.T., K.M.T., N.I.d.S., N.S. and D.M.H; writing – review and editing, K.M.T., N.I.d.S., H.Y.S., N.S., F.S.C. and D.M.H; supervision, D.M.H; project administration, D.M.H; funding acquisition, D.M.H. All authors have read and agreed to the published version of the manuscript.

Author ORCIDs

Danushka S. Tennakoon https://orcid.org/0000-0003-2306-1255
Kasun M. Thambugala https://orcid.org/0000-0002-6210-0504
Nimali I. de Silva https://orcid.org/0000-0002-1577-280X
Nakarin Suwannarach https://orcid.org/0000-0002-2653-1913
Dian-Ming Hu https://orcid.org/0000-0002-4750-2871

Data availability

All of the data that support the findings of this study are available in the main text.

References

Abdullah S (1980) Two hyphomycetes on litter in stagnant water from Britain. Transactions of the British Mycological Society 75(3): 514–517. https://doi.org/10.1016/S0007-1536(80)80140-9

Adamcik S, Cai L, Chakraborty D, Chen XH, Cotter HVT, Dai DQ, Dai YC, Das K, Deng C, Ghobad–Nejhad M, Hyde KD, Langer E, Latha KPD, Liu F, Liu SL, Liu T, Lv W, Lv SX, Machado AR, Pinho DB, Pereira OL, Prasher IB, Rosado AWC, Qin J, Qin WM, Verma RK, Wang Q, Yang ZL, Yu XD, Zhou LW, Buyck B (2015) Fungal biodiversity profiles 1–10. Cryptogamie. Mycologie 36(2): 121–166. https://doi.org/10.7872/crym/v36.iss2.2015.121

Ade A (1923) Mykologische Beiträge. Hedwigia 64: 286–320. https://doi.org/10.2307/911161

Ahmad S (1964) Contributions to the fungi of West Pakistan. IV. Biologia Lahore 10: 1–6.

Ahmad S (1971) Contributions to the fungi of West Pakistan. X. Biologia Lahore 17: 1–26.

Allescher A (1896) Diagnosen einiger neuer, im Jahre 1895 gesammelter Arten Bayerischer Pilze aus der Abtheilung der Fungi Imperfecti. Berichte der Bayerischen Botanischen Gesellschaft zur Erforschung der Heimischen Flora 4: 31–40.

Almeida DAC, Gusmão LFP, Miller AN (2017) A new species of *Bertiella* (Melanommataceae) from Brazil and a key to accepted species. Mycosphere: Journal of Fungal Biology 8(4): 392–396. https://doi.org/10.5943/mycosphere/8/4/1

Anahosur KH (1970) Ascomycetes of Coorg (India). III. Sydowia 24: 177–182.

Aptroot A (2003) Pyrenocarpous lichens and related non–lichenized ascomycetes from Taiwan. The Journal of the Hattori Botanical Laboratory 93: 155–173. https://doi.org/10.18968/jhbl.93.0_155

Aptroot A, Iperen A (1998) New ascomycetes and ascomycete records from Papua New Guinea. Nova Hedwigia 67(3–4): 481–497. https://doi.org/10.1127/nova.hedwigia/67/1998/481

Bánki O, Roskov Y, Döring M, Ower G, Vandepitte L, Hobern D, Remsen D, Schalk P, De Walt RE, Keping M (2023) Catalogue of Life Checklist (Version 2023-01-12). Catalogue of Life. https://doi.org/10.48580/dfqz

Barr ME (1968) The Venturiaceae in North America. Canadian Journal of Botany 46(6): 799–864. https://doi.org/10.1139/b68-111

Barr ME (1983) Muriform ascospores in class ascomycetes. Mycotaxon 18: 149–157.

Barr ME (1984) *Herpotrichia* and its segregates. Mycotaxon 20: 1–38.

Barr ME (1990) Melanommatales (Loculoascomycetes). North American Flora 13: 1–129.

Barr ME (1992) Notes on the Lophiostomataceae (Pleosporales). Mycotaxon 45: 191–221.

Barr ME, Rogerson CT, Smith SJ, Haines JH (1986) An annotated catalog of the pyrenomycetes described by Charles H. Peck. Bull. New York State Museum of Natural History 459: 1–74. https://doi.org/10.5962/bhl.title.135547

Bedlan G (2017) *Petrakia juniperi* sp. nov., ein neuer Pilzan *Juniperus* sp. Journal für Kulturpflanzen 69: 173–174.

Beenken L, Gross A, Queloz V (2020) Phylogenetic revision of *Petrakia* and *Seifertia* (Melanommataceae, Pleosporales): New and rediscovered species from Europe and North America. Mycological Progress 19(5): 417–440. https://doi.org/10.1007/s11557-020-01567-7

Berkeley MJ, Broome CE (1873) Enumeration of the fungi of Ceylon. Part II. Journal of the Linnean Society. Botany 14: 29–140. https://doi.org/10.1111/j.1095-8339.1873.tb00301.x

Bhat DJ, Kendrick B (1993) Twenty-five new conidial fungi from the Western Ghats and the Andaman Islands (India). Mycotaxon 49: 19–90.

Bommer E, Rousseau M (1890) Contributions a la Flore Mycologique de Belgique III. Bulletin de la Société royale de Botanique de Belgique 29: 205–302.

Bose SK (1961) Studies on *Massarina* Sacc. and related genera. Journal of Phytopathology 41(2): 151–213. https://doi.org/10.1111/j.1439-0434.1961.tb04048.x

Bresadola G (1926) Selecta mycologica II. Student Trent 7: 51–81.

Bubák F (1914) Fungi in 'Wissenschaftliche Ergebnisse der Expedition nach Mesopotamien'. Annalen des Naturhistorischen Museums in Wien 28: 189–218.

Bubák F, Kabát JE (1905) Vierter Beitrag zur Pilzflora von Tirol. Österreichische. Botanicheskii Zhurnal 55: 181–186. https://doi.org/10.1007/BF01793320

Calabon MS, Jones EBG, Boonmee S, Doilom M, Lumyong S, Hyde KD (2021) Five novel freshwater ascomycetes indicate high undiscovered diversity in lotic habitats in Thailand. Journal of Fungi (Basel, Switzerland) 7(2): 1–27. https://doi.org/10.3390/jof7020117

Calabon MS, Hyde KD, Jones EG, Luo ZL, Dong W, Hurdeal VG, Gentekaki E, Rossi W, Leonardi M, Thiyagaraja V, Lestari AS, Shen H-W, Bao D-F, Boonyuen N, Zeng M (2022) Freshwater fungal numbers. Fungal Diversity 114(1): 3–235. https://doi.org/10.1007/s13225-022-00503-2

Cannon PF (1982) Anote on the nomenclature of *Herpotrichia*. Transactions of the British Mycological Society 79(2): 338–339. https://doi.org/10.1016/S0007-1536(82)80123-X

Cannon PF, Hawksworth DL, Sherwood-Pike MA (1985) The British Ascomycotina. An Annotated Checklist. Commonwealth Mycological Institute, Kew, Surrey, England: 302.

Cash EK (1952) A record of the fungi named by JB Ellis (No. 2). Division of Mycology and Disease Survey, Bureau of Plant Industry, Soils, and Agricultural Engineering,

Agricultural Research Administration, US Department of Agriculture. https://doi.org/10.5962/bhl.title.149755

Cash EK (1953) A record of the fungi named by J.B. Ellis (Part 2). U.S.D.A. Special Publ. 2: 167–345.

Castañeda RF (1985) Deuteromycotina de Cuba. Hyphomycetes III: 1–42.

Castaneda-Ruiz RF, Iturriaga T, Minter DW, Saikawa M, Vidal G, Velazquez-Noa S (2003) Microfungi from Venezuela, A new species of *Brachydesmiella*, a new combination, and new records. Mycotaxon 85: 211–229.

Castellani E, Ciferri R (1950) Mycoflora Erythraea, Somala et Aethipica Suppl. 1. Atti dell'Istituto Botanico e del Laboratorio Crittogamico dell'Universita di Pavia, 52.

Chen CY, Hsieh WH (2004) *Byssosphaeria* and *Herpotrichia* from Taiwan, with notes on the taxonomic relationship between these two genera. Sydowia 56: 24–38.

Conners IL (1967) An Annotated Index of Plant Diseases in Canada and Fungi Recorded on Plants in Alaska, Canada and Greenland. Research Branch Canadian Department of Agriculture 1251: 1–381.

Cooke MC (1887) Synopsis pyrenomycetum. Grevillea 15: 80–86. https://doi.org/10.1175/1520-0493(1887)15[86:V]2.0.CO;2

Cooke MC, Plowright CB (1879) British Sphaeriacei. Grevillea 7: 77–89. https://doi.org/10.1093/nq/s5-XII.292.89b

Costa MEA, Camara MS (1952) Species Aliquae Mycologicae Lusitaniae. Portugaliae Acta Biologica Series A 3: 294–307.

Crous PW, Wingfield MJ, Schumacher RK, Akulov A, Bulgakov TS, Carnegie AJ, Jurjević Ž, Decock C, Denman S, Lombard L, Lawrence DP, Stack AJ, Gordon TR, Bostock RM, Burgess T, Summerell BA, Taylor PWJ, Edwards J, Hou LW, Cai L, Rossman AY, Wöhner T, Allen WC, Castlebury LA, Visagie CM, Groenewald JZ (2020) New and Interesting Fungi. 3. Fungal Systematics and Evolution 6(1): 157–231. https://doi.org/10.3114/fuse.2020.06.09

De Gruyter J, Woudenberg JHC, Aveskamp MM, Verkley GJM, Groenewald JZ, Crous PW (2013) Redisposition of Phoma–like anamorphs in Pleosporales. Studies in Mycology 75: 1–36. https://doi.org/10.3114/sim0004

De Silva NI, Lumyong S, Hyde KD, Bulgakov T, Phillips AJL, Yan JY (2016) Mycosphere essays 9: Defining biotrophs and hemibiotrophs. Mycosphere: Journal of Fungal Biology 7(5): 545–559. https://doi.org/10.5943/mycosphere/7/5/2

Dennis RWG (1978) British Ascomycetes. J. Cramer, Vaduz. 585.

Dennis RWG (1986) Fungi of the Hebrides. Royal Botanic Gardens, Kew: 383.

Diedicke H (1912) Sphaeropsideae. Kryptogamen–Flora der Mark Brandenburg. 9(1): 1–240.

Dingley JM, Fullerton RA, McKenzie EHC (1981) Survey of Agricultural Pests and Diseases. Technical Report Volume 2. Records of Fungi, Bacteria, Algae, and Angiosperms Pathogenic on Plants in Cook Islands, Fiji, Kiribati, Niue, Tonga, Tuvalu, and Western Samoa. Food and Agriculture Organization, 485.

Doidge EM (1948) South African Ascomycetes in the National Herbarium. Part VI. Bothalia 4(4): 837–880. https://doi.org/10.4102/abc.v4i4.1734

Dudka IO, Heluta VP, Tykhonenko YY, Andrianova TV, Hayova VP, Prydiuk MP, Dzhagan VV, Isikov VP (2004) Fungi of the Crimean Peninsula. M.G. Kholodny Institute of Botany, National Academy of Sciences of Ukraine, 452.

El-Buni AM, Rattan SS (1981) Check List of Libyan Fungi. Al Faateh University, Faculty of Science, Department of Botany, Tripoli, 169.

El-Shafie AE, Aptroot A, Al-Bahry SN, Al-Kindi AY (2005) A new species of *Navicella* from Costa Rica. Sydowia 57: 19–22.

Ellis JB (1895) Notes on some specimens of Pyrenomycetes in the Schweinitz herbarium of the Academy. Proceedings. Academy of Natural Sciences of Philadelphia 47: 20–31.

Ellis MB (1976) Dematiaceous Hyphomycetes; Commonwealth Mycological Institute, Kew, UK, 344–353. https://doi.org/10.1079/9780851983653.0000

Ellis JB, Everhart BM (1892) The North American Pyrenomycetes. Johnson Reprint Corporation. https://doi.org/10.5962/bhl.title.55690

Ellis JB, Everhart BM (1902) New Alabama fungi. Journal of Mycology 8(2): 62–73. https://doi.org/10.2307/3752297

Eriksson OE (2006) Outline of Ascomycota. Myconet 12: 1–82.

Eriksson OE (2014) Checklist of the non–lichenized ascomycetes of Sweden. Acta Universitatis Upsaliensis. Symbolae Botanicae Upsalienses 36: 499.

Eriksson OE, Yue JZ (1998) Bambusicolous pyrenomycetes, an annotated checklist. Myconet 1: 25–78.

Fabre JH (1879) Essai sur les Sphériacées du Départment de Vaucluse. Annales des Sciences Naturelles Botanique Series 6: 66–118.

Fairman CE (1905) The Pyrenomyceteae or Orleans County, New York. Proceedings of the Rochester Academy of Science. 4: 165–191.

Fairman CE (1921) The fungi of our common nuts and pits. Proceedings of the Rochester Academy of Science. 6: 73–115.

Fairman CE (1922) New or rare fungi from various localities. Proceedings of the Rochester Academy of Science 6: 117–139.

Farr ML (1973) An annotated list of Spegazzini's fungus taxa, Vol. 1. Bibliotheca Mycologica 35: 1–823.

Farr DF, Rossman AY (2024) Fungal Databases, Systematic Mycology and Microbiology Laboratory, ARS, USDA. http://nt.ars–grin.gov/fungaldatabases [accessed on 1 February 2024]

Farr ML, Stevenson JA (1963) Eine erganzungsliste bolivianischer pilze. Sydowia 17: 37–69.

Feltgen J (1901) Vorstudien zu einer Pilzflora des Grossherzogthums Luxemburg. I. Theil. – Ascomycetes. Nachträge II: 1–243.

Feltgen J (1903) Vorstudien zu einer Pilzflora des Grossherzogthums Luxemburg. I. Theil. – Ascomycetes. Nachträge III: 1–328.

French AM (1989) California Plant Disease Host Index. Calif. Dept. Food Agric., Sacramento, 394.

Fröhlich J, Hyde KD (1998) Fungi from palms. XXXIX. *Asymmetricospora* gen. et sp. nov. (Melanommataceae). Sydowia 50: 182–186.

Fröhlich J, Hyde KD (2000) Palm Microfungi. Fungal Diversity Research Series 3: 1–393.

Fuckel L (1868) Fungi rhenani exsic. 7: no. 2171.

Fuckel L (1870) Symbolae mycologicae. Beiträge zur Kenntniss der Rheinischen Pilze. Jahrbücher des Nassauischen Vereins für Naturkunde. 23–24: 1–459. https://doi.org/10.5962/bhl.title.47117

Fuckel L (1873) Symbolae mycologicae. Beiträge zur Kenntniss der rheinischen Pilze. Zweiter Nachtrag, 1–99.

Gafforov YS (2017) A preliminary checklist of Ascomycetous microfungi from southern Uzbekistan. Mycosphere: Journal of Fungal Biology 8(4): 660–696. https://doi.org/10.5943/mycosphere/8/4/12

Gao Y, Zhong T, Bhat JD, de Farias ARG, Dawoud TM, Hyde KD, Xiong W, Li Y, Gui H, Yang X, Wu S (2023) Pleomorphic *Dematiomelanomma yunnanense* gen. et sp. nov. (Asco-

mycota, Melanommataceae) from grassland vegetation in Yunnan, China. MycoKeys 98: 273–297. https://doi.org/10.3897/mycokeys.98.107093

Ginns JH (1986) Compendium of plant disease and decay fungi in Canada 1960–1980. Research Branch Canadian Department of Agriculture 1813: 416. https://doi.org/10.5962/bhl.title.58888

Glawe DA, Hummel RL (2006) North American records for *Seifertia azaleae*, cause of *Rhododendron* bud blight disease. Pacific Northwest Fungi 1: 1–6. https://doi.org/10.2509/pnwf.2006.001.005

Gönczöl J (1976) *Monotosporella tuberculata*, a new species of aquatic Hyphomycetes from Hungary. Nova Hedwigia 27: 493–500.

González Fragoso R (1918) Pugillus secundus mycetorum Persiae. Boletín de la Real Sociedad Española de Historia Natural 18: 78–85.

Gross A, Beenken L, Dubach V, Queloz V, Tanaka K, Hashimoto A, Holdenrieder O (2017) *Pseudodidymella fagi* and *Petrakia deviata*: Two closely related tree pathogens new to central Europe. Forest Pathology 47(5): e12351. https://doi.org/10.1111/efp.12351

Gucevic SA (1967) Species fungorum novae in plantis Tauriae endemicis collectae. Novosti Sistematiki Nizshikh Rastenii 4: 212–217.

Gucevic SA (1969) De speciebus fungorum novis notula. Novosti Sistematiki Nizshikh Rastenii 6: 135–142.

Gucevic SA (1977) De speciebus novis fungorum Pycnidialium e Tauria. Novosti Sistematiki Nizshikh Rastenii 14: 71–80.

Hall TA (1999) BioEdit: A user-friendly biological sequence alignment editor and analysis program for Windows 95/98/NT. Nucleic Acids Symposium Series 41: 95–98.

Harkness HW (1884) New species of California fungi. Bulletin of the California Academy of Sciences 1: 29–47.

Hashimoto A, Matsumura M, Hirayama K, Fujimoto R, Tanaka K (2017) Pseudodidymellaceae fam. nov.: Phylogenetic affiliations of mycopappus-like genera in Dothideomycetes. Studies in Mycology 87(1): 187–206. https://doi.org/10.1016/j.simyco.2017.07.002

Hawksworth DL (1985) A redisposition of the species referred to the ascomycete genus *Microthelia*. Bulletin of the British Museum for Natural History 14: 43–181.

Hawksworth DL (2001) The magnitude of fungal diversity: The 1.5 million species estimate revisited. Mycological Research 105(12): 1422–1432. https://doi.org/10.1017/S0953756201004725

Hayova VP, Minter DW (2009) *Aposphaeria ephedrae*. Descriptions of Fungi and Bacteria Set 180, 1792: 1–3. https://doi.org/10.1079/DFB/20093210586

Hennings P (1903) Fungi Australienses. Beiblatt. Hedwigia 42: 73–88. https://doi.org/10.1038/scientificamerican01311903-73

Hennings P (1908) Fungi paraënses III. Hedwigia 48: 101–117.

Hernández-Restrepo M, Gené J, Castañeda-Ruiz RF, Mena-Portales J, Crous PW, Guarro J (2017) Phylogeny of saprobic microfungi from Southern Europe. Studies in Mycology 86: 53–97. https://doi.org/10.1016/j.simyco.2017.05.002

Hill R, Leitch IJ, Gaya E (2021) Targeting Ascomycota genomes: What and how big? Fungal Biology Reviews 36: 52–59. https://doi.org/10.1016/j.fbr.2021.03.003

Höhnel F (1907) Ergebnisse der Botanischen Expedition der Kaiserlichen Akademie der Wissenschaften nach Süd–Brasilien 1901. II. Band. Thallophyta und Bryophyta. Eumycetes et Myxomycetes, 1–45.

Höhnel F (1909) Fragmente zur Mykologie. (VI. Mitteilung, Nr. 182 bis 288). Sitzungsberichte der Kaiserlichen Akademie der Wissenschaften Math. naturw. Klasse Abt. I. 118: 275–452.

Holm L (1979) Index nominum genericorum (plantarum). In: Farr ER, Leussink JA, Stafleu FA (Eds) The Hague, W. Junk, 189 pp.

Holm L, Holm K (1988) Studies in the Lophiostomataceae with emphasis on the Swedish species. Symbolae Botanicae Upsalienses 28: 1–50.

Holubtsova YI, Andrianova TV (2008) New Species of Anamorphic Fungi from Novgorod-Severskoe Poles'e (Ukraine). Mikologiâ i Fitopatologiâ 42: 28–34.

Hongsanan S, Hyde KD, Phookamsak R, Wanasinghe DN, McKenzie EHC, Sarma VV, Boonmee S, Lücking R, Pem D, Bhat DJ, Liu N, Tennakoon DS, Karunarathna A, Jiang SH, Jones EBG, Phillips AJL, Manawasinghe IS, Tibpromma S, Jayasiri SC, Sandamali D, Jayawardena RS, Wijayawardene NN, Ekanayaka AH, Jeewon R, Lu YZ, Dissanayake AJ, Zeng XY, Luo Z, Tian Q, Phukhamsakda C, Thambugala KM, Dai D, Chethana KWT, Ertz D, Doilom M, Liu JK, Pérez-Ortega S, Suija A, Senwanna C, Wijesinghe SN, Konta S, Niranjan M, Zhang SN, Ariyawansa HA, Jiang HB, Zhang JF, de Silva NI, Thiyagaraja V, Zhang H, Bezerra JDP, Miranda-Gonzáles R, Aptroot A, Kashiwadani H, Harishchandra D, Aluthmuhandiram JVS, Abeywickrama PD, Bao DF, Devadatha B, Wu HX, Moon KH, Gueidan C, Schumm F, Bundhun D, Mapook A, Monkai J, Chomnunti P, Samarakoon MC, Suetrong S, Chaiwan N, Dayarathne MC, Yang J, Rathnayaka AR, Bhunjun CS, Xu JC, Zheng J, Liu G, Feng Y, Xie N (2020) Refined families of Dothideomycetes: Dothideomycetidae and Pleosporomycetidae. Mycosphere: Journal of Fungal Biology 11(1): 1553–2107. https://doi.org/10.5943/mycosphere/11/1/13

Hughes SJ (1951) Studies on Micro-fungi. III. *Mastigosporium*, *Camposporium*, and *Ceratosporium*. Mycological Papers 36: 1–43.

Hughes SJ (1955) Microfungi. I. Cordana, Brachysporium, Phragmocephala. Canadian Journal of Botany 33(3): 259–268. https://doi.org/10.1139/b55-019

Hughes SJ (1958) Revisiones Hyphomycetum aliquot cum appendice de nominibus rejiciendis. Canadian Journal of Botany 36(6): 727–836. https://doi.org/10.1139/b58-067

Hughes SJ (1979) Relocation of species of Endophragmia auct. with notes on relevant generic names. New Zealand Journal of Botany 17(2): 139–188. https://doi.org/10.1080/0028825X.1979.10426887

Hyde KD, Aptroot A (1998) A new species of *Herpotrichia* from the tropics. Nova Hedwigia 66(1–2): 247–249. https://doi.org/10.1127/nova.hedwigia/66/1998/247

Hyde KD, Goh TK (1999) Some new melannommataceous fungi from woody substrata and a key to genera of lignicolous loculoascomycetes in freshwater. Nova Hedwigia 68: 251–272. https://doi.org/10.1127/nova.hedwigia/68/1999/251

Hyde KD, McKenzie EHC, KoKo TW (2011) Towards incorporating anamorphic fungi in a natural classification checklist and notes for 2010. Mycosphere: Journal of Fungal Biology 2: 1–88.

Hyde KD, Wong SW, Jones EBG (1996) Tropical Australian freshwater fungi. 11. *Mamillisphaeria dimorphospora* gen. et sp. nov. and notes on freshwater ascomycetes with dimoprphic ascospores. Nova Hedwigia 62: 513–520.

Hyde KD, Goh TK, Lu BS, Alias SA (1999) Eleven new intertidal fungi from *Nypa fruticans*. Mycological Research 103(11): 1409–1422. https://doi.org/10.1017/S0953756299008667

Hyde KD, Jones EBG, Liu JK, Ariyawansa HA, Boehm E, Boonmee S, Braun U, Chomnunti P, Crous PW, Dai DQ, Diederich P, Dissanayake AJ, Doilom M, Doveri F, Hongsanan S, Jayawardena RS, Lawrey JD, Li YM, Liu YX, Lücking R, Monkai J, Muggia L, Nelsen MP, Pang KL, Phookamsak R, Senanayake IC, Shearer CA, Suetrong S, Tanaka K, Thambugala KM, Wijayawardene NN, Wikee S, Wu HX, Zhang Y, Begoña AH, Alias SA, Aptroot

A, Bahkali AH, Bezerra JL, Bhat DJ, Camporesi E, Chukea E, Gueidan C, Hawksworth DL, Hirayama K, Hoog SD, Kang JK, Knudsen K, Li WJ, Li XH, Liu ZY, Mapook A, Mckenzie EHC, Miller AN, Mortimer PE, Phillips AJL, Raja HA, Scheuer C, Schumm F, Taylor JE, Tian Q, Tibpromma S, Wanasinghe DN, Wang Y, Xu JC, Yacharoen S, Yan JY, Zang M (2013) Families of Dothideomycetes. Fungal Diversity 63(1): 1–313. https://doi.org/10.1007/s13225-013-0263-4

Hyde KD, Hongsanan S, Jeewon R, Bhat DJ, McKenzie EHC, Jones EBG, Phookamsak R, Ariyawansa HA, Boonmee S, Zhao Q, Abdel-Aziz FA, Abdel-Wahab MA, Banmai S, Chomnunti P, Cui BK, Daranagama DA, Das K, Dayarathne MC, de Silva NI, Dissanayake AJ, Doilom M, Ekanayaka AH, Gibertoni TB, Go'es-Neto A, Huang SK, Jayasiri SC, Jayawardena RS, Konta S, Lee HB, Li WJ, Lin CG, Liu JK, Lu YZ, Luo ZL, Manawasinghe IS, Manimohan P, Mapook A, Niskanen T, Norphanphoun C, Papizadeh M, Perera RH, Phukhamsakda C, Richter C, de Santiago ALCMA, Drechsler-Santos ER, Senanayake IC, Tanaka K, Tennakoon TMDS, Thambugala KM, Tian Q, Tibpromma S, Thongbai B, Vizzini A, Wanasinghe DN, Wijayawardene NN, Wu HX, Yang J, Zeng XY, Zhang H, Zhang JF, Bulgakov TS, Camporesi E, Bahkali AH, Amoozegar AM, Araujo-Neta LS, Ammirati JF, Baghela A, Bhatt RP, Bojantchev S, Buyck B, da Silva GA, de Lima CLF, de Oliveira RJV, de Souza CAF, Dai YC, Dima B, Duong TT, Ercole E, Mafalda-Freire F, Ghosh A, Hashimoto A, Kamolhan S, Kang JC, Karunarathna SC, Kirk PM, Kyto¨vuori I, Lantieri A, Liimatainen K, Liu ZY, Liu XZ, Lu¨cking R, Medardi G, Mortimer PE, Nguyen TTT, Promputtha I, Raj KNA, Reck MA, Lumyong S, Shahzadeh-Fazeli SA, Stadler M, Soudi MR, Su HY, Takahashi T, Tangthirasunun N, Uniyal P, Wang Y, Wen TC, Xu JC, Zhang ZK, Zhao YC, Zhou JZ, Zhu L (2016) Fungal diversity notes 367–490: Taxonomic and phylogenetic contributions to fungal taxa. Fungal Diversity 80: 1–270. https://doi.org/10.1007/s13225-016-0373-x

Hyde KD, Chaiwan N, Norphanphoun C, Boonmee S, Camporesi E, Chethana KWT, Dayarathne MC, de Silva NI, Dissanayake AJ, Ekanayaka AH, Hongsanan S, Huang SK, Jayasiri SC, Jayawardena RS, Jiang HB, Karunarathna A, Lin CG, Liu JK, Liu NG, Lu YZ, Luo ZL, Maharachchimbura SSN, Manawasinghe IS, Pem D, Perera RH, Phukhamsakda C, Samarakoon MC, Senwanna C, Shang QJ, Tennakoon DS, Thambugala KM, Tibpromma S, Wanasinghe DN, Xiao YP, Yang J, Zeng XY, Zhang JF, Zhang SN, Bulgakov TS, Bhat DJ, Cheewangkoon R, Goh TK, Jones EBG, Kang JC, Jeewon R, Liu ZY, Lumyong S, Kuo CH, McKenzie EHC, Wen TC, Yan JY, Zhao Q (2018) Mycosphere notes 169–224. Mycosphere: Journal of Fungal Biology 9(2): 271–430. https://doi.org/10.5943/mycosphere/9/2/8

Hyde KD, Dong Y, Phookamsak R, Jeewon R, Bhat DJ, Jones EBG, Liu NG, Abeywickrama PD, Mapook A, Wei D, Perera RH, Manawasinghe IS, Pem D, Bundhun D, Karunarathna A, Ekanayaka AH, Bao DF, Li J, Samarakoon MC, Chaiwan N, Lin CG, Phutthacharoen K, Zhang SN, Senanayake IC, Goonasekara ID, Thambugala KM, Phukhamsakda C, Tennakoon DS, Jiang HB, Yang J, Zeng M, Huanraluek N, Liu JK, Wijesinghe SN, Tian Q, Tibpromma S, Brahmanage RS, Boonmee S, Huang SK, Thiyagaraja V, Lu YZ, Jayawardena RS, Dong W, Yang EF, Singh SK, Singh SM, Rana S, Lad SS, Anand G, Devadatha B, Niranjan M, Sarma VV, Liimatainen K, Aguirre-Hudson B, Niskanen T, Overall A, Alvarenga RLM, Gibertoni TB, Pfliegler WP, Horváth E, Imre A, Alves AL, da Silva Santos AC, Tiago PV, Bulgakov TS, Wanasinghe DN, Bahkali AH, Doilom M, Elgorban AM, Maharachchikumbura SSN, Rajeshkumar KC, Haelewaters D, Mortimer PE, Zhao Q, Lumyong S, Xu J, Sheng J (2020) Fungal diversity notes 1151–1276: Taxonomic and phylogenetic contributions on genera and species of fungal taxa. Fungal Diversity 100(1): 5–277. https://doi.org/10.1007/s13225-020-00439-5

Hyde KD, Suwannarach N, Jayawardena RS, Manawasinghe IS, Liao CF, Doilom M, Cai L, Zhao P, Buyck B, Phukhamsakda C, Su WX, Fu YP, Li Y, Zhao RL, He MQ, Li JX, Tibpromma S, Lu L, Tang X, Kang JC, Ren GC, Gui H, Hofstetter V, Ryoo R, Antonín V, Hurdeal VG, Gentikaki E, Zhang JY, Lu YZ, Senanayake IC, Yu FM, Zhao Q, Bao DF (2021) Mycosphere notes 325–344-Novel species and records of fungal taxa from around the world. Mycosphere: Journal of Fungal Biology 12(1): 1101–1156. https://doi.org/10.5943/mycosphere/12/1/14

Ichinoe M (1971) *Camposporium* species from Japan. Transactions of the British Mycological Society Japan 12: 79–88.

Inderbitzin P, Huang ZL (2001) *Melanomma dinghuense*, a new loculoascomycete with Munk pore–like perforations from Dinghushan Biosphere Reserve in Southern China. Mycoscience 42(2): 187–191. https://doi.org/10.1007/BF02464136

Index Fungorum (2024) Index Fungorum. http://www.indexfungorum.org/names/Names.asp [accessed 6 January 2024]

Jaklitsch WM, Voglmayr H (2017) Three former taxa of *Cucurbitaria* and considerations on *Petrakia* in the Melanommataceae. Sydowia 69: 81–95. https://doi.org/10.12905/0380.sydowia69-2017-0081

Jayasiri SC, Hyde KD, Ariyawansa HA, Bhat DJ, Buyck B, Cai L, Dai YC, Abd–Elsalam KA, Ertz D, Hidayat I, Jeewon R, Jones EBG, Bahkali AH, Karunarathna SC, Liu JK, Luangsa–ard JJ, Lumbsch HT, Maharachchikumbura SSN, McKenzie EHC, Moncalvo JM, Ghobad–Nejhad M, Nilsson H, Pang KA, Pereira OL, Phillips AJL, Raspé O, Rollins AW, Romero AI, Etayo J, Selçuk F, Stephenson SL, Suetrong S, Taylor JE, Tsui CKM, Vizzini A, Abdel–Wahab MA, Wen TC, Boonmee S, Dai DQ, Daranagama DA, Dissanayake AJ, Ekanayaka AH, Fryar SC, Hongsanan S, Jayawardena RS, Li WJ, Perera RH, Phookamsak R, de Silva NI, Thambugala KM, Tian Q, Wijayawardene NN, Zhao RL, Zhao Q, Kang JC, Promputtha I (2015) The faces of fungi database: Fungal names linked with morphology, phylogeny and human impacts. Fungal Diversity 74(1): 3–18. https://doi.org/10.1007/s13225-015-0351-8

Jiang H, Phookamsak R, Hongsanan S, Bhat DJ, Mortimer PE, Suwannarach N, Kakumyan P, Xu J (2022) A review of bambusicolous Ascomycota in China with an emphasis on species richness in southwest China. Studies in Fungi 7(1): 1–33. https://doi.org/10.48130/SIF-2022-0020

Jones EG, Vrijmoed LL (2003) Biodiversity of marine fungi in Hong Kong coastal waters. Perspectives on Marine Environment Change in Hong Kong and Southern China. Hong Kong University Press, Hong Kong, 75–92.

Jones EG, Pang KL, Abdel–Wahab MA, Scholz B, Hyde KD, Boekhout T, Ebel R, Rateb ME, Henderson L, Sakayaroj J, Suetrong S, Dayarathne MC, Kumar V, Raghukumar S, Sridhar KR, Bahkali AHA, Gleason FH, Norphanphoun C (2019) An online resource for marine fungi. Fungal Diversity 96(1): 347–433. https://doi.org/10.1007/s13225-019-00426-5

Karsten PA (1884) Fragmenta mycologica XIV. Hedwigia 23: 57–59.

Karsten PA (1892) Finlands mögelsvampar (Hyphomyctes fennici). Bidrag till Kännedom av Finlands Natur och. Folk (Kobenhavn) 51: 343–534.

Karsten PA (1905) Fungi novi nonnullis exceptis in Fennia lecti. Acta Societatis pro Fauna et Flora Fennica 27: 1–16.

Katoh K, Standley DM (2013) MAFFT multiple sequence alignment software version 7: Improvements in performance and usability. Molecular Biology and Evolution 30(4): 772–780. https://doi.org/10.1093/molbev/mst010

Kirk PM, Spooner BM (1984) An account of the fungi of Arran, Gigha and Kintyre. Kew Bulletin 38(4): 503–597. https://doi.org/10.2307/4108573

Kirschstein W (1906) Neue märkische Ascomyceten. Verhandlungen des Botanischen Vereins der Provinz Brandenburg. 48: 39–61.

Kirschstein W (1911) Sphaeriales. Kryptogamen–Flora der Mark Brandenburg 7: 164–304.

Kirschstein W (1935) Neue und seltene Ascomyceten. Annales Mycologici 33: 202–229.

Kobayasi Y (1971) Mycological reports from New Guinea and the Solomon Islands (1–11). Bulletin of the National Science Museum, Tokyo 14: 367–551.

Kohlmeyer J, Volkmann-Kohlmeyer B (1990) Revision of marine species of *Didymosphaeria* (Ascomycotina). Mycological Research 94(5): 685–690. https://doi.org/10.1016/S0953-7562(09)80669-2

Koukol O, Delgado G (2021) Why morphology matters: The negative consequences of hasty descriptions of putative novelties in asexual ascomycetes. IMA Fungus 12(1): 1–8. https://doi.org/10.1186/s43008-021-00073-z

Kuhnholtz-Lordat G, Barry JP (1949) *Quelques micromycètes* parasites intéressants du sud de la France. Bulletin de la Société Mycologique de France 65: 121–131.

Kularathnage ND, Tennakoon DS, Zhu X, Zhou J, Su B, Xie Y, Chen Q, Calabon MS, Kirk PM, Senanayake IC, Doilom M, Xu B, Dong W, Song J (2022) Reinstating *Dyfrolomyces* and introducing *Melomastia pyriformis* sp. nov. (Pleurotremataceae, Dyfrolomycetales) from Guangdong Province, China. Current Research in Environmental & Applied Mycology 13(1): 426–438. https://doi.org/10.5943/cream/13/1/16

Kulkarni RL (1974) Three fungi from groundnut leaf surface. Current Science 43: 561–562. https://doi.org/10.1016/0039-6028(74)90276-3

Kunze G, Schmidt JC (1823). Mykologische (2): 1–176. https://doi.org/10.1016/S0140-6736(02)95514-5

Li WY, Zhuang WY (2008) Notes on the genus *Byssosphaeria* (Melanommataceae) from China. Junwu Xuebao 27: 48–53.

Li GJ, Hyde KD, Zhao RL, Hongsanan S, Abdel-Aziz FA, AbdelWahab MA, Alvarado P, Alves-Silva G, Ammirati JF, Ariyawansa HA, Baghela A, Bahkali AH, Beug M, Bhat DJ, Bojantchev D, Boonpratuang T, Bulgakov TS, Camporesi E, Boro MC, Ceska O, Chakraborty D, Chen JJ, Chethana KWT, Chomnunti P, Consiglio G, Cui BK, Dai DQ, Dai YC, Daranagama DA, Das K, Dayarathne MC, De Crop E, De Oliveira RJV, de Souza CAF, de Souza JI, Dentinger BTM, Dissanayake AJ, Doilom M, Drechsler-Santos ER, Ghobad-Nejhad M, Gilmore SP, Góes-Neto A, Gorczak M, Haitjema CH, Hapuarachchi KK, Hashimoto A, He MQ, Henske JK, Hirayama K, Iribarren MJ, Jayasiri SC, Jayawardena RS, Jeon SJ, Jerônimo GH, Jesus AL, Jones EBG, Kang JC, Karunarathna SC, Kirk PM, Konta S, Kuhnert E, Langer E, Lee HS, Lee HB, Li WJ, Li XH, Liimatainen K, Lima DX, Lin CG, Liu JK, Liu XZ, Liu ZY, Luangsa-ard JJ, Lücking R, Lumbsch HT, Lumyong S, Leaño EM, Marano AV, Matsumura M, McKenzie EHC, Mongkolsamrit S, Mortimer PE, Nguyen TTT, Niskanen T, Norphanphoun C, O'Malley MA, Parnmen S, Pawłowska J, Perera RH, Phookamsak R, Phukhamsakda C, Pires-Zottarelli CLA, Raspé O, Reck MA, Rocha SCO, de Santiago ALCMA, Senanayake IC, Setti L, Shang QJ, Singh SK, Sir EB, Solomon KV, Song J, Srikitikulchai P, Stadler M, Suetrong S, Takahashi H, Takahashi T, Tanaka K, Tang LP, Thambugala KM, Thanakitpipattana D, Theodorou MK, Thongbai B, Thummarukcharoen T, Tian Q, Tibpromma S, Verbeken A, Vizzini A, Vlasák J, Voigt K, Wanasinghe DN, Wang Y, Weerakoon G, Wen HA, Wen TC, Wijayawardene NN, Wongkanoun S, Wrzosek M, Xiao YP, Xu JC, Yan JY, Yang J, Da Yang S, Hu Y, Zhang JF, Zhao J, Zhou LW, Peršoh D, Phillips AJL, Maharachchikumbura SSN (2016a) Fungal diversity notes 253–366: Taxonomic and phylogenetic contributions to fungal taxa. Fungal Diversity 78(1): 1–237. https://doi.org/10.1007/s13225-016-0366-9

Li JF, Phookamsak R, Mapook A, Boonmee S, Bhat JD, Hyde KD, Lumyong S (2016b) *Seifertia shangrilaensis* sp. nov. (Melanommataceae), a new species from Southwest China. Phytotaxa 273(1): 34–42. https://doi.org/10.11646/phytotaxa.273.1.3

Li JF, Jeewon R, Luo ZL, Phookamsak R, Bhat DJ, Mapook A, Phukhamsakda C, Camporesi E, Lumyong S, Hyde KD (2017) Morphological characterization and DNA based taxonomy of *Fusiconidium* gen. nov. with two novel taxa within Melanommataceae (Pleosporales). Phytotaxa 308(2): 206–218. https://doi.org/10.11646/phytotaxa.308.2.2

Liew ECY, Aptroot A, Hyde KD (2000) Phylogenetic significance of the pseudoparaphyses in Loculoascomycete taxonomy. Molecular Phylogenetics and Evolution 16(3): 392–402. https://doi.org/10.1006/mpev.2000.0801

Lind J (1913) Danish fungi as represented in the herbarium of E. Rostrup, 1–648. https://doi.org/10.5962/bhl.title.54591

Liu JK, Hyde KD, Jones EBG, Ariyawansa HA, Bhat DJ, Boonmee S, Maharachchikumbura SSN, McKenzie EHC, Phookamsak R, Phukhamsakda C, Shenoy BD, Abdel-Wahab MA, Buyck B, Chen J, Chethana KWT, Singtripop C, Dai DQ, Dai YC, Daranagama DA, Dissanayake AJ, Doilom M, Dsouza MJ, Fan XL, Goonasekara ID, Hirayama K, Hongsanan S, Jayasiri SC, Jayawardena RS, Karunarathna SC, Li WJ, Mapook A, Norphanphoun C, Pang KL, Perera RH, Peršoh D, Pinruan U, Senanayake IC, Somrithipol S, Suetrong S, Tanaka K, Thambugala KM, Tian Q, Tibpromma S, Udayanga D, Wijayawardene NN, Wanasinghe D, Wisitrassameewong K, Zeng XY, Abdel-Aziz FA, Adamčík S, Bahkali AH, Boonyuen N, Bulgakov T, Callac P, Chomnunti P, Greiner K, Hashimoto A, Hofstetter V, Kang JC, Lewis J, Li XH, Liu XZ, Liu ZY, Matsumura M, Mortimer PE, Rambold G, Randrianjohany E, Sato G, Sri-Indrasutdhi V, Tian CM, Verbeken A, von Brackel W, Wang Y, Wen TC, Xu JC, Yan JY, Zhao RL, Camporesi E (2015) Fungal diversity notes 1–110: Taxonomic and phylogenetic contributions to fungal species. Fungal Diversity 72(1): 1–197. https://doi.org/10.1007/s13225-015-0324-y

Lobik A (1927) Materialen zur Mykoflora des Terski Kreises. Bolezni Rast. 16: 157–199.

Lu B, Hyde KD, Ho WH, Tsui KM, Taylor JE, Wong KM, Yanna K, Zhou D (2000) Checklist of Hong Kong Fungi. Fungal Diversity Press, Hong Kong, 207.

Lunghini D, Granito VM, Di Lonardo DP, Maggi O, Persiani AM (2013) Fungal diversity of saprotrophic litter fungi in a Mediterranean maquis environment. Mycologia 105(6): 1499–1515. https://doi.org/10.3852/13-103

Marvanová L, Descals E (1987) New taxa and new combinations of 'aquatic hyphomycetes'. Transactions of the British Mycological Society 89(4): 499–507. https://doi.org/10.1016/S0007-1536(87)80084-0

Mason EW, Hughes SJ (1951) *Phragmocephala* gen. nov. Hyphomycetarum. The Naturalist London, 97–105.

Massee GE (1906) Fungi exotici, V. Bulletin of Miscellaneous Informations of the Royal Botanical Gardens Kew, 256–258. https://doi.org/10.2307/4118220

Mathur RS (1979) The Coelomycetes of India. Bishen Singh Mahendra Pal Singh, Delhi, India, 460.

Matsushima T (1980) Matsushima Mycological Memoirs No. 1. Saprophytic Microfungi from Taiwan, Part 1. Hyphomycetes. Matsushima Fungus Collection, Kobe, Japan, 82.

Matsushima T (1983) Matsushima Mycological Memoirs 3. Matsushima Mycological Memoirs 3: 1–90. https://doi.org/10.2307/3793127

McKenzie EHC, O'Sullivan PJ, Wilkie JP (1992) A list of type specimens of New Zealand fungi held in DSIR Plant Protection Herbarium (PDD). Mycotaxon 43: 77–156.

Medel R (2007) First record of the genus *Byssosphaeria* (Pleosporales) in Mexico and Venezuela. Mycotaxon 100: 247–250.

Melnik VA (1984) Coelomycetes of the SSSR. II. *Nagrajomyces dictyosoporus* Melnik gen. et sp. nov. and *Phragmotrichum vassiljevae* Melnik sp.nov. Mikologiâ i Fitopatologiâ 18: 9–14.

Mercado Sierra A, Heredia G, Mena Portales J (1995) New species of dematiaceous hyphomycetes from Veracruz, Mexico. Mycotaxon 55: 491–499.

Miller MA, Pfeiffer W, Schwartz T (2010) Creating the CIPRES Science Gateway for Inference of Large Phylogenetic Trees. SC10 Workshop on Gateway Computing Environments (GCE10). https://doi.org/10.1109/GCE.2010.5676129

Minter DW (1981) Microfungi on needles, twigs and cones of pines in Czechoslovakia. Česká Mykologie 35: 90–101.

Morgan AP (1904) New species of Pyrenomycetes. Journal of Mycology 10(4): 161–162. https://doi.org/10.2307/3752680

Mouton V (1900) Quatrième notice sur des ascomycètes nouveaux ou peu connus. Bulletin de la Société Royale de Botanique de Belgique. 39: 37–53.

Mueller E (1958) Pilze aus dem Himalaya II. Sydowia 12: 160–184.

Mugambi GK, Huhndorf SM (2009) Molecular phylogenetics of pleosporales: Melanommataceae and Lophiostomataceae re-circumscribed (Pleosporomycetidae, Dothideomycetes, Ascomycota). Studies in Mycology 64: 103–121. https://doi.org/10.3114/sim.2009.64.05

Mujica F, Vergara C (1945) Flora fungosa Chilena. Indice preliminar de los huespedes de los hongos chilenos y sus referencias bibliograficas. Imprenta Stanley, 199.

Mulenko W, Majewski T, Ruszkiewicz-Michalska M (2008) A preliminary checklist of Micromycetes in Poland. W. Szafer Institute of Botany. Polish Academy of Sciences 9: 752.

Munk A (1957) Danish Pyrenomycetes. A Preliminary Flora. Dansk Botanisk Arkiv 17: 1–491.

Niranjan M, Sarma VV (2019) New species and new records of Melanommataceae (Pleosporales) from Andaman Islands. Kavaka 52: 103–108. https://doi.org/10.36460/Kavaka/54/2020/38-42

Nylander JAA (2004) MrModeltest 2.0. Program distributed by the author. Evolutionary Biology Centre, Uppsala University.

Oudemans CAJA (1902) Contributions á la flore mycologique des Pays-Bas. XVIII. Nederlandsch Kruidkundig Archief 2: 633–781.

Pande A (1979) Ascomycetes of Western India VI. Acta Botanica Indica 7: 181–183.

Pande A (2008) Ascomycetes of Peninsular India. Scientific Publishers (India), Jodhpur, 584.

Pantidou ME (1973) Fungus-host index for Greece. Benaki Phytopathol. Institute of Kiphissia, Athens, 382.

Papendorf MC, von Arx JA (1966) *Herpotrichia striatispora* a new ascomycete from South Africa. Nova Hedwigia 12: 395–397.

Partridge EC, Morgan-Jones G (2002) Notes on hyphomycetes LXXXVIII: New genera in which to classify *Alysidium resinae* and *Pycnostysanus azaleae*, with a consideration of Sorocybe. Mycotaxon 83: 335–352.

Peck CH (1909) New species of fungi. Bulletin of the Torrey Botanical Club 36(3): 153–157. https://doi.org/10.2307/2479189

Pem D, Jeewon R, Gafforov Y, Hongsanan S, Phukhamsakda C, Promputtha I, Doilom M, Hyde KD (2019) *Melanocamarosporioides ugamica* gen. et sp. nov., a novel mem-

ber of the family Melanommataceae from Uzbekistan. Mycological Progress 18(3): 471–481. https://doi.org/10.1007/s11557-018-1448-8

Petch T (1912) Revisions of Ceylon fungi (Part III). Annals of the Royal Botanic Gardens Peradeniya 5: 265–301.

Petch T (1917) Additions to Ceylon fungi. Annals of the Royal Botanic Gardens Peradeniya 6: 195–256. https://doi.org/10.2307/4111564

Petrak F (1962) Mykologische Beitrage zur osterreichischen Flora. Sydowia 16: 155–198.

Peyronel B (1915) Primo Elenco di Funghi di val San Martino o valle della Germanasca. Memorie della Reale Accademia delle Scienze di Torino Series 66: 1–58.

Peyronel B (1918) Micromiceti di Val Germanasca. Nuovo Giornale Botanico Italiano. 25: 405–464.

Phukhamsakda C, McKenzie EHC, Phillips AJL, Jones EBG, Bhat DJ, Stadler M, Bhunjun CS, Wanasinghe DN, Thongbai B, Camporesi E, Ertz D, Jayawardena RS, Perera RH, Ekanayake AH, Tibpromma S, Doilom M, Xu JC, Hyde KD (2020) Microfungi associated with *Clematis* (Ranunculaceae) with an integrated approach to delimiting species boundaries. Fungal Diversity 102(1): 1–203. https://doi.org/10.1007/s13225-020-00448-4

Pimenta LP, Gomes DC, Cardoso PG, Takahashi JA (2021) Recent findings in azaphilone pigments. Journal of Fungi (Basel, Switzerland) 7(7): e541. https://doi.org/10.3390/jof7070541

Pirozynski KA (1972) Microfungi of Tanzania. I. Miscellaneous fungi on oil palm. Mycological Paper 129: 1–39.

Pitard CJ, Harmand J (1911) Contribution à létude des lichens des Îles Canaries. Bulletin de la Société Botanique de France 58 (Mém. 22): 1–72. https://doi.org/10.1080/00378941.1911.10829212

Purahong W, Pietsch KA, Lentendu G, Schöps R, Bruelheide H, Wirth C, Buscot F, Wubet T (2017) Characterization of unexplored deadwood mycobiome in highly diverse subtropical forests using culture-independent molecular technique. Frontiers in Microbiology 8: e574. https://doi.org/10.3389/fmicb.2017.00574

Rabenhorst GL (1869) Fungi Europaei exsiccati, Klotzschii herbarii vivi mycologici continuatio. Editio nov. Series secunda. Cent. 13(1201–no): 1300.

Raciborski M (1909) Parasitische und epiphytische Pilze Javas. Bulletin International de l'Academie des Sciences de Cracovie Classe des Sciences Mathematiques et Naturelles. 3: 346–394.

Raja HA, Paguigan ND, Fournier J, Oberlies NH (2017) Additions to *Lindgomyces* (Lindgomycetaceae, Pleosporales, Dothideomycetes), including two new species occurring on submerged wood from North Carolina, USA, with notes on secondary metabolite profiles. Mycological Progress 16(5): 535–552. https://doi.org/10.1007/s11557-017-1282-4

Rambaut A (2012) FigTree Version 1.4.0. Edinburgh: Institute of Evolutionary Biology; University of Edinburgh. http://tree.bio.ed.ac.uk/software/figtree/ [accessed January 10, 2024]

Rao VG (1969) Fungi on Citrus from India. Sydowia 23: 215–224. https://doi.org/10.3406/scrip.1969.3366

Rao RP, Rao D (1964) Some species of *Camposporium* Harkn. from India. Antonie van Leeuwenhoek 30(1): 60–64. https://doi.org/10.1007/BF02046701

Reblova M (1997) Revision and reclassification of some *Chaetosphaeria* species. Czech Mycology 50(2): 73–83. https://doi.org/10.33585/cmy.50201

Rehm H (1881) Ascomyceten in getrockneten Exemplaren herausgegeben. Berichte des Naturhistorischen Vereins Augsburg. 26: 1–132.

Rehm H (1901) Beiträge zur Pilzflora von Südamerika. XII. Sphaeriales. Hedwigia 40: 100–124.

Rehm H (1906) Beitrage zur Ascomycetenflora der Voralpen und Alpen. Plant Systematics and Evolution 56(8): 291–348. https://doi.org/10.1007/BF01672393

Rehm H (1913) Ascomycetes philippinenses – III. Philippine Journal of Science 8: 391–406.

Rehm H (1914) Ascomycetes philippinenses – V. Leaflets of Philippine Botany. 6: 2191–2237.

Rehner S (2001) Primers for Elongation Factor 1–α (EF1–α). http://ocid.NACSE.ORG/research/deephyphae/EF1primer.pdf

Reinking OA (1919) Host Index of Diseases of Economic Plants in the Philippines. Philippine Agriculturist 8: 38–54.

Remler P (1979) Ascomyceten auf Ericaceen in den Ostalpen. Bibliotheca Mycologica 68: 1–321.

Rick JE (1933) Monographia *Sphaerialium astromaticorum* Riograndensium: II. Brotéria Série Trimestral. Ciências Naturais. 2: 169–201.

Ronquist F, Teslenko M, Van Der Mark P, Ayres DL, Darling A, Höhna S, Larget B, Liu L, Suchard MA, Huelsenbeck JP (2012) MrBayes 3.2: Efficient Bayesian phylogenetic inference and model choice across a large model space. Systematic Biology 61(3): 539–542. https://doi.org/10.1093/sysbio/sys029

Saccardo PA (1875) Fungi Veneti novi vel critici. Series III. Hedwigia 14: 68–76.

Saccardo PA (1878) Fungi Italici autographice delineati a Prof. P.A. Saccardo. Patavii 1878. – Fascicoli V.–VIII. sistentes tab. 161–320. Michelia 1: 326–350.

Saccardo PA (1880) Conspectus generum fungorum Italiae inferiorum nempe ad Sphaeropsideas, Melanconieas et Hyphomyceteas pertinentium systemate sporologico dispositorum. Michelia 2: 1–38.

Saccardo PA (1882) Sylloge Pyrenomycetum. Vol. I. Sylloge Fungorum 1: 1–768.

Saccardo PA (1883) Sylloge Pyrenomycetum, Vol. II. Sylloge Fungorum 2: 1–813.

Saccardo PA (1884) Sylloge Sphaeropsidearum et Melanconiearum Omnium Hucusque Cognitarum. Sylloge Fungorum 3: 1–840.

Saccardo PA (1911) Notae mycologicae. Series XIII. Annales Mycologici 9: 249–257.

Saccardo PA (1915) Fungi ex insula Melita (Malta) lecti a Doct. Caruana–Gatto et Doct. G. Borg annis MCMXIII et MCMIV. Nuovo Giornale Botanico Italiano 22: 24–76.

Saccardo PA (1916) Notae mycologicae. Series XX. Nuovo Giornale Botanico Italiano. 23: 185–234.

Saccardo PA (1921) Notae mycologicae. Series XXIV. I. Fungi Singaporenses Barkesiani. Bolletino dell'Orto Botanico Regia dell'Universita de Napoli 6: 39–73.

Saccardo PA, Sydow P (1899) Sylloge Fungorum 14: 1–724.

Saccardo PA, Traverso JB (1910) Index Iconum Fungorum. A-L. Sylloge Fungorum 19: 1–1158.

Saccardo PA, Trotter A (1913) Supplementum Universale, Pars IX. Sylloge Fungorum 22: 1–1612.

Saccas AM (1954) Les champignons de l'hévéa en Afrique Equatoriale Française. Journal d'Agriculture Tropicale et de Botanique Appliquee 1(7): 333–355. https://doi.org/10.3406/jatba.1954.2165

Samuels GJ (1976) A revision of the fungi formerly classified as *Nectria* subgenus *Hyphonectria*. Memoirs of the New York Botanical Garden 26: 1–126.

Samuels GJ, Müller E (1978) Life–history studies of Brazilian Ascomycetes. 4. Three species of *Herpotrichia* and their Pyrenochaeta-like anamorphs. Sydowia 31: 157–168.

Sandu-Ville C, Mititiuc M (1971) Für die Wissenschaft unbekannte Pilze aus dem Gebiete des zukünftigen Stausees am Eisernen Tor. Feddes Repertorium 81(8–9): 625–627. https://doi.org/10.1002/fedr.19710810810

Sawada K (1950) Represent Forest Experiment Station, Tokyo 46: 111–150. [Fungi inhabiting on conifers in the Tohoku district. II. Fungi on various conifers except "Sugi"]

Scheuer C, Chlebicki A (1997) Recent collections of miscellaneous microfungi from South Poland. Acta Mycologica 32(2): 147–172. https://doi.org/10.5586/am.1997.014

Senanayake IC, Pem D, Rathnayaka AR, Wijesinghe SN, Tibpromma S, Wanasinghe DN, Phookamsak R, Kularathnage ND, Gomdola D, Harishchandra D, Dissanayake LS, Xiang M, Ekanayaka AH, McKenzie EHC, Hyde KD, Zhang H, Xie N (2022) Predicting global numbers of teleomorphic ascomycetes. Fungal Diversity 114(1): 237–278. https://doi.org/10.1007/s13225-022-00498-w

Shaw CG (1973) Host fungus index for the Pacific Northwest – I. Hosts. Washington State University, Agricultural Experiment Station Bulletin 765: 1–121.

Shaw DE (1984) Microorganisms in Papua New Guinea. Department of Primary Industries and Research Bulletin 33: 1–344.

Shear CL (1941) Mycological notes. V. Mycologia 33(3): 318–332. https://doi.org/10.1080/00275514.1941.12020821

Shearer CA (1974) Fungi of the Chesapeake Bay and its Tributaries IV. Three new species from the Patuxent River. Mycologia 66(1): 16–24. https://doi.org/10.1080/00275514.1974.12019568

Shivas RG, Alcorn JL (1996) A checklist of plant pathogenic and other microfungi in the rainforests of the wet tropics of northern Queensland. Australasian Mycological Society 25: 158–173. https://doi.org/10.1071/AP96029

Siemaszko W (1923) Fungi caucasici novi vel minus cogniti. II. Diagnoses specierum novarum ex Abchazia Adzariaque provenientium. Acta Societatis Botanicorum Poloniae 1(1): 1–10. https://doi.org/10.5586/asbp.1923.003

Sivanesan A (1971) The genus *Herpotrichia* Fuckel. Mycological Papers 127: 1–37.

Sivanesan A (1984) The bitunicate ascomycetes and their anamorphs. J. Cramer, Vaduz, 701.

Sivanesan A, Hsieh WH (1989) New species and new records of ascomycetes from Taiwan. Mycological Research 93(3): 340–351. https://doi.org/10.1016/S0953-7562(89)80161-3

Smith AL, Ramsbottom J (1914) New or rare microfungi. Transactions of the British Mycological Society 4: 318–330. https://doi.org/10.1016/S0007-1536(12)80035-0

Spaulding P (1961) Foreign Diseases of Forest Trees of the World. U.S.D.A. Agric. Handb. 197: 1–361.

Species Fungorum (2024) Species Fungorum. http://www.indexfungorum.org [accessed on 15 January 2024]

Spegazzini C (1908) Hongos de la yerba mate. Anales del Museo Nacional de Historia Natural Buenos Aires 17: 111–141.

Spegazzini C (1909) Mycetes Argentinenses. Series IV. Anales del Museo Nacional de Historia Natural Buenos Aires Series 3 12: 257–458.

Spegazzini C (1910) Fungi Chilenses. Contribución al Estudio de los Hongos Chilenos. Revista de la Facultad de Agronomía Universidade Nacional de La Plata 6: 1–205.

Spegazzini C (1920) Sobre algunas enfermedades y hongos que afectan las plantas de 'Agrios' en el Paraguay. Anales de la Sociedad Científica Argentina 90: 155–188.

Spegazzini C (1921) Mycetes chilenses. Boletín de la Academia Nacional de Ciencias en Córdoba 25: 1–124.

Spegazzini C (1923) Honguillos exóticos. Boletín de la Academia Nacional de Ciencias en Córdoba 26: 369–403.

Stamatakis A (2014) RAxML version 8: A tool for phylogenetic analysis and post-analysis of large phylogenies. Bioinformatics (Oxford, England) 30(9): 1312–1313. https://doi.org/10.1093/bioinformatics/btu033

Stamatakis A, Hoover P, Rougemont J (2008) A rapid bootstrap algorithm for the RAxML web servers. Systematic Biology 57(5): 758–771. https://doi.org/10.1080/10635150802429642

Su HY, Udayanga D, Luo ZL, Manamgoda DS, Zhao YC, Yang J, Liu XY, Mckenzie EHC, Zhou DQ, Hyde KD (2015) Hyphomycetes from aquatic habitats in Southern China: Species of *Curvularia* (Pleosporaceae) and *Phragmocephala* (Melannomataceae). Phytotaxa 226(3): 201–216. https://doi.org/10.11646/phytotaxa.226.3.1

Sutton BC (1980) The Coelomycetes – fungi imperfecti with pycnidia, acervuli and stromata. Commonwealth Mycological Institute, Kew, Surrey, England, 696.

Sutton BC, Pirozynski KA (1965) Notes on microfungi. II. Transactions of the British Mycological Society 48(3): 349–366. https://doi.org/10.1016/S0007-1536(65)80055-9

Sutton BC, Pirozynski KA (1966) Phragmotrichum karstenii. Transactions of the British Mycological Society 49(3): 522. https://doi.org/10.1016/S0007-1536(66)80099-2

Sydow H, Sydow P (1903) Mycotheca Germanica Fasc. II (no. 51–100). Annales Mycologici 1: 536–539.

Sydow H, Sydow P (1907) Novae fungorum species. IV. Annales Mycologici 5: 338–340.

Sydow H, Sydow P (1913) Novae fungorum species XI. Annales Mycologici 11: 402–408.

Sydow H, Sydow P (1914) Fungi from northern Palawan. Philippine Journal of Science, Section C: Botany 9: 157–189.

Sydow P, Sydow H (1921) Novae fungorum species. XVI. Annales Mycologici 18: 154–160.

Sydow H, Sydow P, Butler EJ (1911) Fungi Indiae orientalis pars III. Annales Mycologici 9: 372–421.

Tai FL (1979) Sylloge Fungorum Sinicorum. Sci. Press, Acad. Sin., Peking, 1527.

Tanaka K, Hosoya T (2006) Some new records of Loculoascomycetes from Yakushima Island, southern Japan. Bulletin of the National Science Museum, Series B (Botany) 32: 151–160.

Tassi F (1900) Novae Micromycetum species de scripta e et iconibus illustratae. Bollettino del Laboratorio de Orto Botanico Reale Universita Siena 3: 52–57.

Teng SC (1936) Additional fungi from China II. Sinensia 7: 490–527.

Tennakoon DS, Jeewon R, Kuo CH, Hyde KD (2018) Phylogenetic and morphological characterization of *Byssosphaeria macarangae* sp. nov., and *B. taiwanense* sp. nov. from *Macaranga tanarius*. Phytotaxa 364(3): 211–226. https://doi.org/10.11646/phytotaxa.364.3.1

Tennakoon DS, Kuo CH, Maharachchikumbura SSN, Thambugala KM, Gentekaki E, Phillips AJ, Bhat DJ, Wanasinghe DN, de Silva NI, Promputtha I, Hyde KD (2021) Taxonomic and phylogenetic contributions to *Celtis formosana*, *Ficus ampelas*, *F. septica*, *Macaranga tanarius* and *Morus australis* leaf litter inhabiting microfungi. Fungal Diversity 108(1): 1–215. https://doi.org/10.1007/s13225-021-00474-w

Tennakoon DS, Thambugala KM, Silva NID, Suwannarach N, Lumyong S (2022) A taxonomic assessment of novel and remarkable fungal species in Didymosphaeriaceae (Pleosporales, Dothideomycetes) from plant litter. Frontiers in Microbiology 13: e1016285. https://doi.org/10.3389/fmicb.2022.1016285

Tennakoon DS, de Silva NI, Maharachchikumbura SS, Bhat DJ, Kumla J, Suwannarach N, Lumyong S (2023) Exploring More on Dictyosporiaceae: The Species Geographical Distribution and Intriguing Novel Additions from Plant Litter. Diversity 15(3): e410. https://doi.org/10.3390/d15030410

Teodoro NG (1937) An Enumeration of Philippine Fungi. Tech. Bull. Dept. Agric. Comm. Manila 4: 1–585.

Thambugala KM, Wanasinghe DN, Phillips AJL, Camporesi E, Bulgakov TS, Phukhamsakda C, Ariyawansa HA, Goonasekara ID, Phookamsak R, Dissanayake A, Tennakoon DS (2017) Mycosphere notes 1–50: Grass (Poaceae) inhabiting Dothideomycetes. Mycosphere: Journal of Fungal Biology 8(4): 697–796. https://doi.org/10.5943/mycosphere/8/4/13

Thaxter R (1922) Reliquiae Farlowianae distributed from the Farlow Herbarium of Harvard University. Mycologia 14(3): 99–103. https://doi.org/10.1080/00275514.1922.12020377

Tian Q, Liu JK, Hyde KD, Wanasinghe DN, Boonmee S, Jayasiri SC, Luo ZL, Taylor JE, Phillips AJL, Bhat DJ, Li WJ, Ariyawansa H, Thambugala KM, Gareth Jones EB, Chomnunti P, Bahkali AH, Xu JC, Camporesi E (2015) Phylogenetic relationships and morphological reappraisal of Melanommataceae (Pleosporales). Fungal Diversity 74(1): 267–324. https://doi.org/10.1007/s13225-015-0350-9

Tibpromma S, Hyde KD, Jeewon R, Maharachchikumbura SS, Liu JK, Bhat DJ, Jones EBG, McKenzie E, Camporesi E, Bulgakov TS, Doilom M, Santiago AM, Das K, Manimohan P, Gibertoni TB, Lim YW, Ekanayaka AH, Thongbai B, Lee HB, Yang J, Kirk PM, Sysouphanthong P, Singh SK, Boonmee S, Dong W, Raj KN, Latha KP, Phookamsak R, Phukhamsakda C, Konta S, Jayasiri SC, Norphanphoun C, Tennakoon D, Li J, Dayarathne MC, Perera RH, Xiao Y, Wanasinghe DN, Senanayake IC, Goonasekara ID, Silva NI, Mapook A, Jayawardena RS, Dissanayake AJ, Manawasinghe IS, Chethana KW, Luo Z, Hapuarachchi KK, Baghela A, Soares AM, Vizzini A, Meiras-Ottoni A, Mešić A, Dutta AK, Souza CA, Richter C, Lin C, Chakrabarty D, Daranagama DA, Lima DX, Chakraborty D, Ercole E, Wu F, Simonini G, Vasquez G, Silva GA, Plautz HL, Ariyawansa HA, Lee HS, Kušan I, Song J, Sun J, Karmakar J, Hu K, Semwal KC, Thambugala KM, Voigt K, Acharya K, Rajeshkumar KC, Ryvarden L, Jadan M, Hosen MI, Mikšík M, Samarakoon MA, Wijayawardene NN, Kim NK, Matočec N, Singh PN, Tian Q, Bhatt RP, Oliveira RJ, Tulloss RE, Aamir S, Kaewchai S, Marathe SD, Khan S, Hongsanan S, Adhikari S, Mehmood T, Bandyopadhyay TK, Svetasheva TY, Nguyen TT, Antonín V, Li W, Wang Y, Indoliya Y, Tkalčec Z, Elgorban AM, Bahkali AH, Tang A, Su H, Zhang H, Promputtha I, Luangsa-Ard J, Xu J, Yan J, Kang JC, Stadler M, Mortimer PE, Chomnunti P, Zhao Q, Phillips AJ, Nontachaiyapoom S, Wen T, Karunarathna SC (2017) Fungal diversity notes 491–602: Taxonomic and phylogenetic contributions to fungal taxa. Fungal Diversity 83(1): 1–261. https://doi.org/10.1007/s13225-017-0378-0

Tilak ST, Kale SB (1970) Contribution to our knowledge of Ascomycetes of India XXIV. Sydowia 24: 81–88.

Tilak ST, Talde UK (1975) Contribution of our knowledge of Ascomycetes of India XXXV. Maharashtra Vidnyan Mandir Patrika. 10: 15–18.

Trotter A (1912) Mycetum Tripolitanorum pugillus. Annales Mycologici 10: 509–514.

Trotter A (1931) Supplementum Universale, Pars X. Myxomycetae, Myxobacteriaceae, Deuteromycetae, Mycelia sterilia. Sylloge Fungorum. 25: 1–1093.

Urries MJ (1957) Hongos Microscopicos De Canarias. El Museo Canario, 140.

Vasilyeva LN (1987) Pirenomitsety i Lokuloaskomitsety severa Dalbnego Vostoka, 1–255.

Viégas AP (1945) Alguns fungos do Brasil XI. Fungi Imperfecti (Sphaeropsidales). Bragantia 5: 717–779. https://doi.org/10.1590/S0006-87051945000900002

Vilgalys R, Hester M (1990) Rapid genetic identification and mapping of enzymatically amplified ribosomal DNA from several Cryptococcus species. Journal of Bacteriology 172(8): 4238–4246. https://doi.org/10.1128/jb.172.8.4238-4246.1990

Von Arx JA (1981) The genera of fungi sporulating in pure culture, 3rd edn. Stechert-Hafner, New York, 288.

Wanasinghe DN, Phukhamsakda C, Hyde KD, Jeewon R, Lee HB, Gareth Jones EB, Tibpromma S, Tennakoon DS, Dissanayake AJ, Jayasiri SC, Gafforov Y, Camporesi E, Bulgakov TS, Ekanayake AH, Perera RH, Samarakoon MC, Goonasekara ID, Mapook A, Li WJ, Senanayake IC, Li J, Norphanphoun C, Doilom M, Bahkali AH, Xu J, Mortimer PE, Tibell L, Tibell S, Karunarathna SC (2018) Fungal diversity notes 709–839: Taxonomic and phylogenetic contributions to fungal taxa with an emphasis on fungi on Rosaceae. Fungal Diversity 89(1): 1–236. https://doi.org/10.1007/s13225-018-0395-7

Wang YZ, Aptroot A, Hyde KD (2004) Revision of the ascomycete genus *Amphisphaeria*. Fungal Diversity Press, Hong Kong, 168.

Wang HK, Aptroot A, Crous PW, Jeewon R, Hyde KD (2007) The polyphyletic nature of Pleosporales: An example from *Massariosphaeria* based on rDNA and RBP2 gene phylogenies. Mycological Research 111(11): 1268–1276. https://doi.org/10.1016/j.mycres.2007.08.014

Watanabe T (1993) *Camposporium laundonii* on root tissue of *Aralia elata* from Japan. Transactions of the British Mycological Society, Japan 34: 71–76.

Watson AJ (1971) Foreign bacterial and fungus diseases of food, forage, and fiber crops. USDA Agricultural Research Service, 111.

Watzl O (1937) On the trees and shrubs of the region of the Khodja group drained by the Baramba and their leaf diseases. (A contribution to the flora of the south-western central Caucasus.) II. Fungi on living leaves. Beihefte zum Botanischen Centralblatt 57: 431–440.

Wehmeyer LE (1952) Some pyrenomycetous fungi from Mt. Rainier National Park. Sydowia 6: 412–428.

Wen S, Fan W, Guo H, Huang C, Yan Z, Long Y (2020) Two new secondary metabolites from the mangrove endophytic fungus Pleosporales sp. SK7. Natural Product Research 34(20): 2919–2925. https://doi.org/10.1080/14786419.2019.1598993

White RP, Hamilton CC (1935) Diseases and insect pests of *Rhododendron* and *Azalea*. New Jersey Agricultural Experiment Station 350: 1–22.

White TJ, Bruns T, Lee SJWT, Taylor JW (1990) Amplification and direct sequencing of fungal ribosomal RNA genes for phylogenetics. PCR protocols: a guide to methods and applications 18: 315–322. https://doi.org/10.1016/B978-0-12-372180-8.50042-1

Whitton SR, McKenzie EHC, Hyde KD (2002) Microfungi on the Pandanaceae: Two new species of *Camposporium* and key to the genus. Fungal Diversity 11: 177–187.

Wijayawardene NN, Hyde KD, Wanasinghe DN, Papizadeh M, Goonasekara ID, Camporesi E, Bhat DJ, McKenzie EHC, Phillips AJL, Diederich P, Tanaka K, Li WJ, Tangthirasunun N, Phookamsak R, Dai DQ, Dissanayake AJ, Weerakoon G, Maharachchikumbura SSN, Hashimoto A, Matsumura M, Bahkali AH, Wang Y (2016) Taxonomy and phylogeny of dematiaceous coelomycetes. Fungal Diversity 77(1): 1–316. https://doi.org/10.1007/s13225-016-0360-2

Wijayawardene NN, Hyde KD, Dai DQ, Sánchez-García M, Goto BT, Saxena RK, Erdoğdu M, Selçuk F, Rajeshkumar KC, Aptroot A, Błaszkowski J, Boonyuen N, da Silva GA, de Souza FA, Dong W, Ertz D, Haelewaters D, Jones EBG, Karunarathna SC, Kirk PM, Kukwa M, Kumla J, Leontyev DV, Lumbsch HT, Maharachchikumbura SSN, Marguno F, Martínez-Rodríguez P, Mešić A, Monteiro JS, Oehl F, Pawłowska J, Pem D, Pfliegler WP, Phillips AJL, Pošta A, He MQ, Li JX, Raza M, Sruthi OP, Suetrong S, Suwannarach N, Tedersoo L, Thiyagaraja V, Tibpromma S, Tkalčec Z, Tokarev YS, Wanasinghe DN, Wijesundara DSA, Wimalaseana SDMK, Madrid H, Zhang GQ, Gao Y, Sánchez-Castro I, Tang LZ, Stadler M, Yurkov A, Thines M (2022) Outline of Fungi and fungus-like taxa (2021) Mycosphere 13: 53–453. https://doi.org/10.5943/mycosphere/13/1/2

Winter G (1885) Pilze–Ascomyceten. GL Rabenhorst's Kryptogamen–Flora von Deutschland. Oesterreich und der Schweiz 1: 65–528.

Wong MKM, Hyde KD (2001) Diversity of fungi on six species of Gramineae and one species of Cyperaceae in Hong Kong. Mycological Research 105(12): 1485–1491. https://doi.org/10.1017/S0953756201004695

Wong MKM, Goh TK, McKenzie EHC, Hyde KD (2002) Fungi on grasses and sedges: *Paratetraploa exappendiculata* gen. et sp nov., *Petrakia paracochinensis* sp. nov. and *Spadicoides versiseptatis* sp. nov. (dematiaceous hyphomycetes). Cryptogamie. Mycologie 23: 195–203.

Wu WP, Zhuang WY (2005) *Sporidesmium*, *Endophragmiella* and related genera from China. Fungal Diversity Research Series 15: 1–531.

Xiong YR, Manawasinghe IS, Wanasinghe DN, Hongsanan S, Hyde KD, Biao X, Dong ZY (2023) Two new species and a new host record of Pleosporales (Dothideomycetes) from palm (Arecaceae) in Guangdong Province, China. New Zealand Journal of Botany: 1–27. https://doi.org/10.1080/0028825X.2023.2258583

Xu ZH, Sun WX, Shi XG, Zhang XG, Xia JW, Castañeda Ruíz RF, Ma J (2021) *Camposporium chinense* sp. nov. from Jiangxi, China. Mycotaxon 136(1): 73–78. https://doi.org/10.5248/136.73

Yuan ZQ, Barr ME (1994) New ascomycetous fungi on bush cinquefoil from Xinjiang, China. Sydowia 46: 329–337.

Yuan ZQ, Zhao ZY (1994) Studies on lophiostomataceous fungi from Xinjiang, China. Sydowia 46: 162–184.

Zhang Y, Crous PW, Schoch CL, Hyde KD (2012) Pleosporales. Fungal Diversity 53(1): 1–221. https://doi.org/10.1007/s13225-011-0117-x

Zhuang WY (2001) Higher Fungi of Tropical China. Mycotaxon, Ltd., Ithaca, NY, 485.

Zhuang WY (2005) Fungi of northwestern China. Mycotaxon, Ltd., Ithaca, NY, 430.

MycoKeys 106: 97–116 (2024)
DOI: 10.3897/mycokeys.106.121526

Research Article

Two new species of *Ganoderma* (Ganodermataceae, Basidiomycota) from Southwest China

Jun He[1], Xiao-Jun Li[1], Wan-Zhong Tan[1], Xiao-Qu Wu[2,3], Dan Wu[1], Zong-Long Luo[4], Qi Wu Zhou[1], E-Xian Li[2], Shu-Hong Li[2]

1 *College of Biotechnology and Engineering, West Yunnan University, Lincang 677000, Yunan, China*
2 *Biotechnology and Germplasm Resources Institute, Yunnan Academy of Agricultural Sciences, Kunming 650205, Yunnan, China*
3 *School of Agriculture, Yunan University, Kunming 650504, Yunan, China*
4 *College of Agriculture and Biological Science, Dali University, Dali 671003, Yunnan, China*

Corresponding authors: Shu-Hong Li (shuhongfungi@126.com); E-Xian Li (xiaogaogao4850@126.com)

Abstract

Ganoderma is a large and diverse genus containing fungi that cause white rot to infect a number of plant families. This study describes *G. phyllanthicola* and *G. suae* as new species from Southwest China, based on morphological and molecular evidence. *Ganoderma phyllanthicola* is characterized by dark brown to purplish black pileus surface with dense concentric furrows, pale yellow margin, irregular pileipellis cells, small pores (5–7 per mm) and ellipsoid to sub-globose basidiospores (8.5–10.0 × 6.0–7.5 µm). *Ganoderma suae* is characterized by reddish brown to oxblood red pileus surface and lead gray to greyish-white pore surface, heterogeneous context, wavy margin and almond-shaped to narrow ellipsoid basidiospores (8.0–10.5 × 5.0–7.0 µm). The phylogeny of *Ganoderma* is reconstructed with multi-gene sequences: the internal transcribed spacer region (ITS), the large subunit (nrLSU), translation elongation factor 1-α gene (TEF-1α) and the second subunit of RNA polymerase II (RPB2). The results show that *G. suae* and *G. phyllanthicola* formed two distinct line-ages within *Ganoderma*. Descriptions, illustrations and phylogenetic analyses results of the two new species are presented.

Key words: 2 new taxa, Ganodermataceae, Morphology, Phylogeny, Taxonomy

Academic editor: Zai-Wei Ge
Received: 23 February 2024
Accepted: 14 May 2024
Published: 19 June 2024

Citation: He J, Li X-J, Tan W-Z, Wu X-Q, Wu D, Luo Z-L, Zhou QW, Li E-X, Li S-H (2024) Two new species of *Ganoderma* (Ganodermataceae, Basidiomycota) from Southwest China. MycoKeys 106: 97–116. https://doi.org/10.3897/mycokeys.106.121526

Introduction

Ganodermataceae is one of the main families of polypores with fourteen accepted genera: *Amauroderma* Murrill, *Amaurodermellus* Costa-Rezende, Drechsler-Santos & Góes-Neto, *Cristataspora* Robledo & Costa-Rezende, *Foraminispora* Robledo, Costa-Rez. & Drechsler-Santos, *Furtadoella* B.K. Cui & Y.F. Sun, *Ganoderma* P. Karst., *Haddowia* Steyaert, *Humphreya* Steyaert, *Magoderna* Steyaert, *Neoganoderma* B.K. Cui & Y.F. Sun, *Sanguinoderma* Y.F. Sun, D.H. Costa & B.K. Cui, *Sinoganoderma* B.K. Cui, J.H. Xing & Y.F. Sun, *Tomophagus* Murrill and *Trachydermella* B.K. Cui & Y.F. Sun (Costa-Rezende et al. 2020; Sun et al. 2022), of which most species are classified in the genus *Ganoderma*.

The word *Ganoderma* is derived from the Greek words “Gano”, meaning “shiny”, and “derma”, meaning “skin” (Loyd et al. 2018). The genus *Ganoderma*

(Polyporales, Basidiomycota) was described by Fries (1821) based on *Polyporus lucidus* (Curtis) Fr. and typified by *Ganoderma lucidum* (Curtis) P. Karst. from Europe (Fries 1821; Karsten 1881). *Ganoderma* is a globally distributed genus of wood-decaying fungi that encompass important species for forestry, medicine, food, and cultural traditions, in which morphological delimitation has been challenging due to its large plasticity and wide distribution across various regions (Luangharn et al. 2021). In the past few decades, DNA or amino acid sequence analyses have provided effective tools for taxonomists to combine data. These modern techniques have helped to clarify the distribution of different species complexes in the genus *Ganoderma*, and have revealed some instances of misidentification (Kinge et al. 2015; Fryssouli et al. 2020).

The genus is characterized by laccate or non-laccate basidiocarps, sessile to stipitate basidiomata, white to pale yellow margin, and red-brown colored truncate double-walled basidiospores, an apical germinal pore, thin and colourless external wall (exosporium), with a brown to dark brown interwall pillars (endosporium), and the ability to cause white rot in woody plants (Karsten 1881; Moncalvo and Ryvarden 1997). Furthermore, these species hold different characteristics, such as the shape and the color of the fruit body, host specificity, and geographical origin, which are used to identify individual members of the species. The species concept in the genus *Ganoderma* is thus not universally accepted nor well established due to the highly variable morphological features of the species (Wang et al. 2014; Náplavová et al. 2020).

Currently, based on credible morphological and phylogenetic evidence, 191 species of *Ganoderma* have been described worldwide (He et al. 2022; Sun et al. 2022; Vinjusha et al. 2022; Cabarroi-Hernández et al. 2023). *Ganoderma* is economically important, due to the fact that members of the genus are regarded as valuable medicinal mushrooms (Hapuarachchi et al. 2018a). Several *Ganoderma* species are known to be prolific sources of a high number of natural bioactive compounds such as polysaccharides, triterpenoids, sterols, and secondary metabolites (Richter et al. 2015). Approximately 45 species of *Ganoderma* are recorded in Chinese Fungi (Sun et al. 2022), of which *Ganoderma lucidum* "lingzhi" and *G. sinense* which used to be listed in Chinese Pharmacopeia to prevent and treat many diseases and are listed in Chinese Pharmacopeia, and which are included in the homologous list of medicine and food (Li et al. 2018). Furthermore, *Ganoderma* was included in the American Herbal Pharmacopoeia and Therapeutic Compendium (Hapuarachchi et al. 2018b). They are commonly named as "Lingzhi" or "Rui–zhi" in China, "Youngzhi" in Korea, "Reishi" in Japan and "Ganoderma" in the USA (Liu et al. 2015). These natural bioactive compounds are used to treat and remedy many pathological diseases, including traditional medicine for treating neurasthenia, debility of prolonged illness, insomnia, arthritis, asthma, anorexia, dizziness, chronic hepatitis, hypercholesterolemia, mushroom poisoning, coronary heart disease, hypertension, prevention of acute mountain sickness, deficiency fatigue', carcinoma, and bronchial cough in the elderly (Wang et al. 2020). In addition, *Ganoderma* products come in the form of various commercial products of *Ganoderma* such as powders, dietary supplements, coffee, tea, spore products, drinks, syrup, toothpaste, soap, lotion, and capsules, and have been commercialized as effective food and drug supplements for health benefits (Lai et al. 2004).

Southwest China contains some of the highest concentrations of fungal biodiversity in the world, and Yunnan Province, in particular, has a varied topography, environmental conditions, and a variety of habitats for a diverse range of fungi (He et al. 2022). Despite the advancement in taxonomic studies of *Ganoderma* species diversity, many novel species are still being discovered (He et al. 2021; He et al. 2022). During our investigations of macrofungi in Southwest China, a couple of specimens of *Ganoderma* were collected. In the current study, the phylogenetic analyses of *Ganoderma* were carried out based on the combined sequence dataset of ITS + nLSU + TEF1–α + RPB2 gene regions. Subsequent morphological and molecular studies uncovered two undescribed species. These species are illustrated and described below.

Materials and methods

Specimen collection

During the rainy season from June 2019 to September 2023, four *Ganoderma* specimens were collected in southwest China. They were photographed in the field, then macro-mophology was described on fresh basidiomata, on the same day of collection. Specimens were there after thoroughly dried at 45 °C (Hu et al. 2022), in a thermostatic drier, stored in sealed plastic bags, and deposited in the herbarium of Kunming Institute of Botany, Chinese Academy of Sciences Academia Sinica (KUN-HKAS).

Morphological studies

Colour codes were determined following Kornerup and Wanscher (1978). For microscopic characteristics, anatomical and cytological characteristics including basidia, basidiospores, hyphal system, and pileipellis were observed and photographed using a Nikon ECLIPSE Ni-U microscope (Nikon, Japan) at magnifications up to × 1000. Tarosoft(R) Image Frame Work (IFW) was used for the measurement of photomicrographs, and Adobe Photoshop CS5 software was used to process images for making photo plates (He et al. 2021).

The following abbreviations are used: IKI = Melzer's reagent, IKI– = neither amyloid nor dextrinoid, KOH = 10% potassium hydroxide, CB = Cotton Blue, CB+ = cyanophilous. The notation [n/m/p] specifies that measurements were made on "n" basidiospores from "m" basidiomata and "p" collections. Basidiospore dimensions are given as (a) b–*av*– c (d). Where a and d refer to the lower and upper extremes of all measurements, respectively, b-c the range of 95% of the measured values, L = mean spore length (arithmetic average of all spores), W = mean spore width (arithmetic average of all spores), *Q* is the length/width ratio of basidiospores, *Qm* denotes the average of n measured basidiospores and SD is their standard deviation. Results are presented as *Q* = *Qm* ± SD.

DNA extraction, PCR amplification, and sequencing

Genomic DNA was extracted from dry specimens using the Ezup Column Fungi Genomic DNA Purification Kit following manufacturer instructions. Primers pairs for PCR were respectively ITS1F/ITS5 (White et al. 1990), LR5/LR0R (Liu

et al. 1999), TEF1–983 / TEF1–1567R (Matheny et al. 2007), and RPB2–6f / fRPB2–7cR (Liu et al. 1999), respectively. Primer sequences are available in the WASABI database at the AFTOL website (aftol.org). The PCR mixture was prepared in a 30 μL final volume, with 15 μL 2× Taq Plus Master Mix II (Sangon Biotechnology Co., Kunming, China), 12 μL ddH2O, 0.5 μL 10 μM of forward and reverse primers, 2 μL DNA. The PCR thermal cycle program for ITS and nrLSU amplification was conducted using the following profiles: 94 °C for 5 min, 35 cycles of 94 °C for 30 s, 53 °C for 50 s, 72 °C for 1 min, and 72 °C for 10 min. The PCR cycling for TEF1-α was as follows: initial denaturation at 94 °C for 5 min, followed by 35 cycles at 94 °C for 30 s, 55 °C for 30 sec and 72 °C for 1 min, and 72 °C for 10 min. The PCR cycling for RPB2 was as follows: initial denaturation at 94 °C for 5 min, followed by 35 cycles at 94 °C for 30 s, 50 °C for 50 s and 72 °C for 1 min, and 72 °C for 10 min. PCR products were checked on 1% agarose gels stained with ethidium bromide under UV light. The PCR products were purified and sequenced by the Sangon Biotech Limited Company (Shanghai, China). Raw DNA sequences were assembled and edited in Sequencher 4.1.4, and the assembled DNA sequences were deposited in GenBank (Table 1).

Sequencing and sequence alignment

Sequences newly generated in this study and sequences obtained from GenBank (Table 1) were analyzed. The related sequences were determined by using a BLAST search to reveal the closest matches with taxa in *Ganoderma* and recent relevant publications (Sun et al. 2022). Sequences were aligned using MAFFT v.7 (http://mafft.cbrc.jp/alignment/server/) (Katoh and Standley 2013) and then checked visually and manually optimized using BioEdit v.7.0.9 (Hall 1999), to allow maximum alignment and minimize gaps. Ambiguous regions were excluded from the analyses and gaps were treated as missing data. The phylogeny website tool "ALTER" (Glez-Peña et al. 2010) was used to convert the alignment fasta file to Phylip format for RAxML analysis and AliView and PAUP 4.0 b 10 were used to convert the alignment fasta file to a Nexus file for Bayesian analysis (Swofford 2003).

Phylogenetic analyses

A maximum likelihood (ML) analysis was performed at the CIPRES web portal (Miller et al. 2010) using RAxML v.8.2.12 as part of the "RAxML-HPC2 on TG" tool (Miller et al. 2010). A general time-reversible model (GTR) was applied with a discrete gamma distribution and four rate classes. Fifty thorough ML tree searches were conducted out in RAxML v.8.2.11 under the same model. One thousand non-parametric bootstrap iterations were run with the GTR model and a discrete gamma distribution. The resulting replicates were plotted onto the best scoring tree obtained previously. Since no supported conflict (BS ≥ 60%) was detected among the topologies, the four single-gene alignments were concatenated using SequenceMatrix (Vaidya et al. 2011).

The Bayesian analyses were performed using PAUP v.4.0b10 and MrBayes v.3.2 (Ronquist et al. 2012), and the best-fit model of sequences evolution was

estimated via MrModeltest 2.3 (Guindon and Gascuel 2003; Nylander 2004; Darriba et al. 2012). Markov Chain Monte Carlo (MCMC) sampling approach was used to calculate posterior probabilities (PP) (Rannala and Yang 1996). Bayesian analyses of six simultaneous Markov chains were run for one million generations and trees were sampled every 100th generation with a total of 10,000 trees. The first 2000 trees were discarded and the remaining trees were used for calculating posterior probabilities in the majority rule consensus tree.

Phylogenetic trees were visualized using FigTree v1.4.4 (http://tree.bio.ed.ac.uk/software/figtree/), and editing and typesetting was done using Adobe Illustrator CS5 (Adobe Systems Inc., USA). Sequences derived in this study were deposited in GenBank (http://www.ncbi.nlm.nih.gov). The final sequence alignments and the phylogenetic trees are available at TreeBase (http://www.treebase.org, accession number: 31439).

Results

Phylogenetic analyses

In this study, eleven sequences were newly generated from specimens of *Ganoderma* spp. and deposited in GenBank (Table 1), all collected from Yunnan Province, China. The dataset comprised combined ITS + nrLSU + TEF1-α + RPB2 sequences data from 94 specimens, representing 46 taxa in Ganodermataceae. The aligned dataset comprised 2633 characters including gaps (ITS: 1–576; nrLSU: 577–1423; TEF1-α: 1424–1959; RPB2: 1969–2633) of which *Amauroderma rugosum* Cui 9011 as the outgroup taxon (Fig. 1, Sun et al. 2020). The likelihood of the final tree was evaluated and optimized under GAMMA. The best RAxML tree with a final likelihood value of -13209.788540 is presented (Fig. 1). The matrix had 855 distinct alignment patterns, with 37.25% undetermined characters or gaps. Estimated base frequencies were as follows: A = 0.223857, C = 0.250309, G = 0.275931, T = 0.249903; substitution rates AC = 1.104623, AG = 5.821128, AT = 1.180576, CG = 1.273064, CT = 8.821984, GT = 1.000000, α = 0.169579, Tree-Length: 1.075203. Best model for the ITS + nLSU + TEF1-α + RPB2 dataset estimated and applied in the Bayesian analysis were HKY+I+G for ITS and RPB2 (Lset nst=2, rates=invgamma; Prset statefreqpr=dirichlet (1,1,1,1)), GTR+I+G for nrLSU and TEF1-α (Lset nst=6, rates=invgamma; Prset statefreqpr=dirichlet (1,1,1,1). ML analysis resulted in a similar and applied in the Bayesian in equal frequency of nucleotides. Bootstrap support values with a maximum likelihood (ML) equal to or greater than 60%, and Bayesian posterior probabilities (PP) equal to or greater than 0.90 are given above the nodes (Fig. 1).

The phylogeny demonstrated that our four *Ganoderma*-like specimens were clustered into two different lineages with high support, represented two new species, *G. phyllanthicola* (100% BS and 1.00 BP; Fig. 1) and *G. suae* (100% BS and 1.00 BPP; Fig. 1). *Ganoderma phyllanthicola* sp. nov. clustered as a sister clade with *G. castaneum* BK Cui, JH Xing & YF Sun *G. tropicum* (Jungh.) Bres. and *G. philippii* Bres. & Henn. ex Sacc. with strong statistical support (90%ML/0.99PP, Fig. 1), but forming a distinct lineage. *Ganoderma suae* sp. nov. was sister to *G. resinaceum* Boud. with high statistical support (100%ML/1.00PP, Fig. 1).

Table 1. Names, voucher numbers, origins, and their corresponding GenBank accession numbers of the taxa used in the phylogenetic analyses. The new species sequences generated sequences is show in bold, after the species name and the type specimens show "T" after the number.

Species	Voucher/strain	Origin	GenBank accession numbers			
			ITS	nLSU	TEF1–α	RPB2
Ganoderma acaciicola	Cui16815^{T}	Australia	MZ354895	MZ355005	–	MZ245384
G_acaciicola	Cui16813	Australia	MZ354893	MZ355003	–	MZ245382
G. artocarpicola	HL173^{T}	Yunnan, China	ON994239	OP456495	OP508442	OP508428
G. artocarpicola	HL188	Yunnan, China	ON994240	OP380253	OP508441	OP508427
G. aridicola	Dai12588^{T}	South Africa	KU572491	–	KU572502	–
G. austroafricanum	CBS138724^{T}	South Africa	KM507324	KM507325	–	MK611970
G. austroafricanum	CMW25884	South Africa	MH571693	–	MH567296	–
G. boninense	WD2085	Japan	KJ143906	–	KJ143925	KJ143965
G. boninense	WD2028	Japan	KJ143905	KU220015	KJ143924	KJ143964
G. bubalinomarginatum	Dai20075^{T}	Guangxi, China	MZ354926	MZ355010	MZ221637	MZ245388
G. bubalinomarginatum	Dai20074	Guangxi, China	MZ354927	MZ355040	MZ221638	MZ245389
G. carocalcareum	DMC513	Cameroon	EU089970	–	–	–
G. carocalcareum	DMC322^{T}	Cameroon	EU089969	–	–	–
G. casuarinicola	HKAS104639	Thailand	MK817650	MK817654	MK871328	MK840868
G. casuarinicola	Dai16336^{T}	Guangdong, China	MG279173	–	MG367565	MG367508
G. concinnum	Robledo3235	Brazil	MN077523	MN077557	–	–
G. concinnum	Robledo3192	Brazil	MN077522	MN077556	–	–
G. curtisii	CBS100132	NC, USA	JQ781849	–	KJ143927	KJ143967
G. curtisii	CBS100131	NC, USA	JQ781848	–	KJ143926	KJ143966
G. destructans	CBS139793^{T}	South Africa	NR132919	NG058157	–	–
G. destructans	Dai16431	South Africa	MG279177	–	MG367569	MG367512
G. dunense	CMW42150	South Africa	MG020249	–	MG020228	–
G. dunense	CMW42157^{T}	South Africa	MG020255	–	MG020227	–
G. ecuadorense	URM89449	Ecuador	MK119828	MK119908	MK121577	MK121535
G. ecuadorense	URM89441	Ecuador	MK119827	MK119907	MK121576	MK121534
G. enigmaticum	Dai15971	Africa	KU572487	–	KU572497	MG367514
G. enigmaticum	Dai15970	Africa	KU572486	–	KU572496	MG367513
G. heohnelianum	Cui13982	Guangxi, China	MG279178	–	MG367570	MG367515
G. heohnelianum	Dai11995	Yunnan, China	KU219988	KU220016	MG367550	MG367497
G. hochiminhense	MFLU19_2225	Vietnam	MN396662	MN396391	MN423177	–
G. hochiminhense	MFLU19_2224^{T}	Vietnam	MN398324	MN396390	MN423176	–
G. lingzhi	Dai20895	Liaoning, China	MZ354904	MZ355006	MZ221668	MZ245413
G. lingzhi	HL56	Yunnan, China	ON994247	OP380262	–	OP508423
G. martinicense	246TX	TX, USA	MG654185	–	MG754737	MG754858
G. martinicense	LIPSWMart0855^{T}	Martinique, France	KF963256	–	–	–
G. suae	**L4651^{T}**	**Yunnan, China**	**PP869243**	**PP869250**	**PP894782**	**PP894784**
G. suae	**L4817**	**Yunnan, China**	**PP869244**	**PP869251**	**PP894783**	–
G. mexicanum	MUCL55832	Martinique	MK531815	–	MK531829	MK531839
G. mexicanum	MUCL49453	Martinique	MK531811	–	MK531825	MK531836
G. mirabile	Cui18271	Malaysia	MZ354958	MZ355067	MZ221672	MZ345729
G. mirabile	Cui18283	Malaysia	MZ354959	MZ355069	MZ221673	MZ345730
G. mizoramense	UMNMZ5	India	KY643751	KY747490	–	–
G. mizoramense	UMNMZ4T	India	KY643750	–	–	–

Species	Voucher/strain	Origin	GenBank accession numbers			
			ITS	nLSU	TEF1–α	RPB2
G. multipileum	Cui13597	Hainan, China	MZ354899	MZ355043	MZ221675	MZ345732
G. multipileum	L4989	Yunnan, China	ON994249	OP380264	OP508447	OP508432
G. multiplicatum	CC8	China	KU569515	KU570915	–	–
G. multiplicatum	Dai17395	Brazil	MZ354903	–	MZ221678	MZ345734
G. multiplicatum	SPC9	Brazil	KU569553	KU570951	–	–
G. multiplicatum	URM83346	Brazil	JX310823	JX310837	–	–
G. myanmarense	MFLU19_2167^{T}	Myanmar	MN396330	MN428672	–	–
G. myanmarense	MFLU19_2169	Myanmar	MN396329	MN398325	–	–
G. nasalanense	GACP17060211^{T}	Laos	MK345441	MK346831	–	–
G. nasalanense	GACP17060212	Laos	MK345442	MK346832	–	–
G. orbiforme	HL43	Yunnan, China	ON994250	OP380265	OP508435	–
G. orbiforme	TNM F0018838	China	JX840350	–	–	–
G. parvulum	MUCL52655	Guiana, French	MK554770	–	MK554717	MK554755
G. parvulum	MUCL47096	Cuba	MK554783	–	MK554721	MK554742
G. philippii	Cui14443	Hainan, China	MG279188	–	MG367578	MG367524
G. philippii	MFLU19/2222	Thailand	MN401410	MN398326	MN423174	–
G. polychromum	330OR	OR, USA	MG654196	–	MG754742	–
G. polychromum	MS343OR	OR, USA	MG654197	–	MG754743	–
G. ravenelii	MS187FL	FL, USA	MG654211	–	MG754745	MG754865
G. ravenelii	NC_8349	USA	AY456341	–	–	–
G. resinaceum	LGAM462	Greece	MG706250	MG706196	MG837858	MG837821
G. resinaceum	LGAM448	Greece	MG706249	MG706195	MG837857	MG837820
G. resinaceum	MUCL38956	Netherlands	MK554772	–	MK554723	MK554747
G. resinaceum	MUCL52253	France	MK554786	–	MK554737	MK554764
G. rodriguezii	M–11926	Cuba	OQ079179	–	–	–
G. rodriguezii	269TX	USA	MG654352	–	–	–
G. ryvardenii	HKAS58053^{T}	South Africa	HM138670	–	–	–
G. ryvardenii	HKAS58054	South Africa	HM138671	–	–	–
G. sessile	113FL	FL, USA	MG654307	–	MG754748	MG754867
G. sessile	111TX	TX, USA	MG654306	–	MG754747	MG754866
G. sichuanense	Cui16343	China	MZ354928	MZ355011	MZ221692	MZ345741
G. sichuanense	Dai19651	Sri Lanka	MZ354929	MZ355031	MZ221693	MZ345742
G. sinense	Wei5327	Hainan, China	KF494998	KF495008	KF494976	MG367529
G. sinense	HL109	Yunnan, China	ON994252	OP380267	OP508438	OP508425
G. steyaertanum	MEL2382783	Australia	KP012964	–	–	–
G. steyaertanum	6WN 20B	Indonesia	KJ654462	–	–	–
G. phyllanthicola	**L4948^{T}**	**Yunnan, China**	**PP869245**	**PP869252**	–	–
G. phyllanthicola	**HL308**	**Yunnan, China**	**PP869246**	**PP869253**	–	–
G. thailandicum	HKAS104640^{T}	Thailand	MK848681	MK849879	MK875829	MK875831
G. thailandicum	HKAS104641	Thailand	MK848682	MK849880	MK875830	MK875832
G. tropicum	Dai16434	Hainan, China	MG279194	MZ355026	MG367585	MG367532
G. tropicum	HL186	Yunna, China	ON994253	OP380268	OP508440	–
G. tuberculosum	GVL40	Veracruz, Mexico	MT232634	–	–	–
G. tuberculosum	JV1607_62	Costa Rica	MZ354944	MZ355087	MZ221710	–
G. weberianum	CBS21936	Philippines	MK603804	–	MK611974	MK611972
G. weberianum	Dai19673	China	MZ354930	MZ355032	MZ221712	MZ358829
G. wiiroense	UMN21GHA^{T}	Ghana	KT952363	KT952364	–	–
G. wiiroense	UMN20GHA	Ghana	KT952361	KT952362	–	–
G. zonatum	FL03	FL_USA	KJ143922	–	KJ143942	KJ143980
G. zonatum	FL02	FL_USA	KJ143921	–	KJ143941	KJ143979
Amauroderma rugosum	Cui9011	Guangdong, China	KJ531664	–	KU572504	MG367506

Figure 1. Maximum likelihood (ML) tree based on combined ITS + nrLSU + TEF1-α + RPB2 sequence data. Bootstrap support values with a maximum likelihood (ML) equal to or greater than 60% and Bayesian posterior probabilities (PP) equal to or greater than 0.90 are given above the nodes, shown as "ML/PP". New species are indicated in bold blue.

Taxonomy

***Ganoderma phyllanthicola* J. He & S.H. Li, sp. nov.**
MycoBank No: 853508
Fig. 2

Diagnosis. Differs from other species in the genus by its sessile and coriaceous basidiomata, dark brown to purplish black pileus surface with dense concentric furrows, pale yellow margin, irregular pileipellis cells, broadly ellipsoid to subglobose basidiospores and truncated apex, exospore walls smooth, endospore walls with dense spinules.

Etymology. The epithet '*phyllanthicola*' refers to the host tree genus *Phyllanthus*.

Holotype. China. Yunnan Province., Honghe City, Mengzi County, on living tree of *Phyllanthus emblica*, alt. 1685 m, Jun He, 26 August. 2019, L4948(HKAS 123776).

Description. ***Basidiomata*** annual, sessile and broadly attached, coriaceous, hard corky to woody hard. ***Pileus*** single or dimidiate, sub-circular, flabelliform to shell-shaped, applanate, projecting up to 22 cm, 12 cm wide and 1.9 cm thick at base.

Pileus surface dark brown(8F8), purplish black(8F3) to reddish brown(6F8) and covered by a thin hard crust, laccate, glabrous and shiny, with dense concentric furrows. ***Margin*** pale yellow(4A3) to generally concolorous, entire, subacute, slightly wavy. ***Context*** up to 0.8 cm thick, homogeneous, cinnamon brown(6D7) to chestnut brown(8E5), with black melanoid lines, hard corky. ***Tubes*** 0.5–1.1 cm long, concolorous with the base of the context, corky, unstratified. ***Pores*** 5–7 per mm, circular to subcircular, dissepiments slightly thick, entire; pores surface greyish white(2B1) when fresh, orange grey(5B2) to pale brown(6D6) when bruising and drying.

***Hyphal system trimitic*.** Generative hyphae 1.0–2.0 μm in diameter, colorless, thin-walled, with clamps connections; skeletal hyphae 2.0–5.0 μm in diameter,

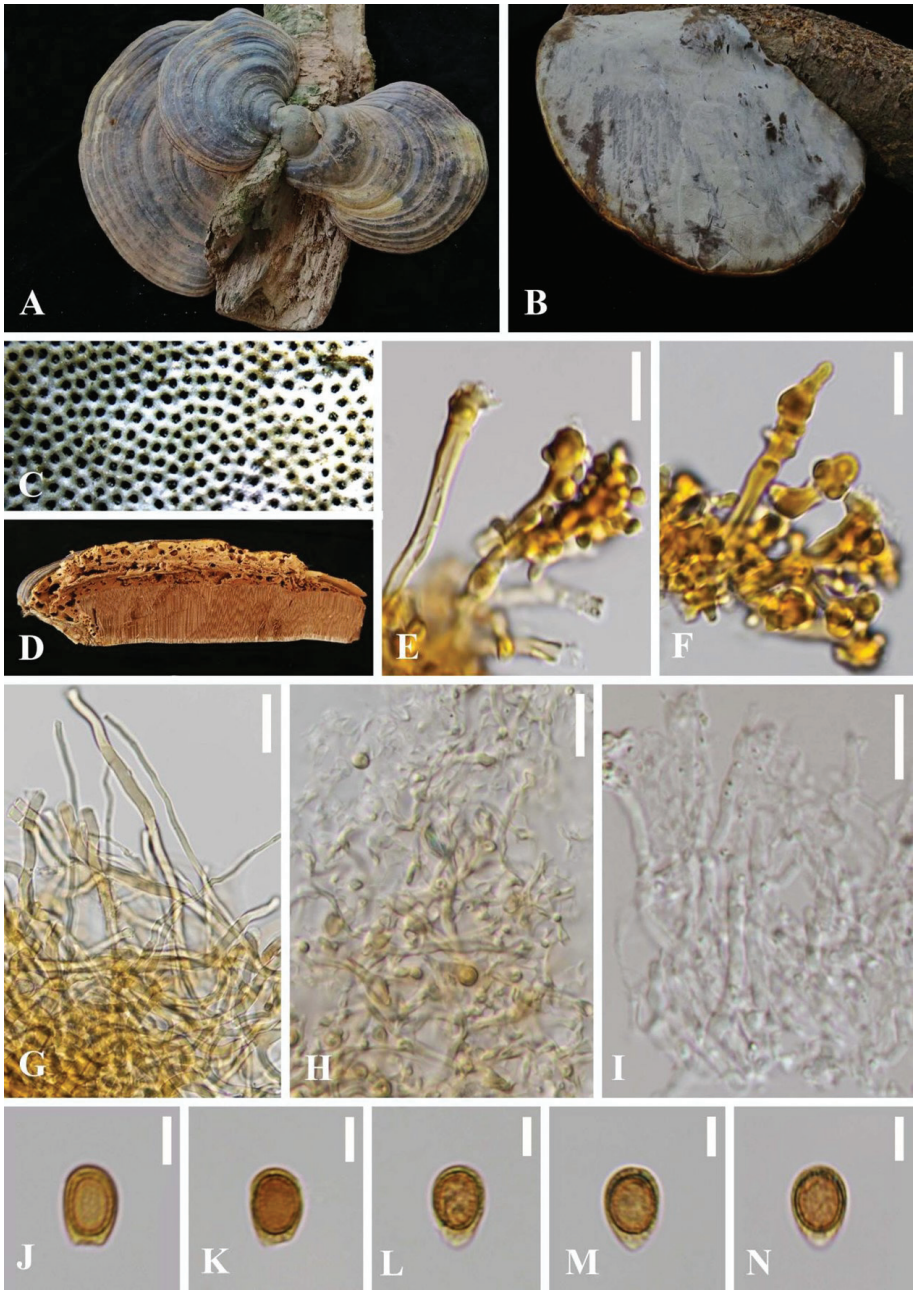

Figure 2. *Ganoderma phyllanthicola* (HKAS 123776, holotype) **A, B** basidiomata **C** pore surface **D** cut side of pileus **E, F** sections of pellis **G** skeletal hyphae from context **H** binding hyphae from context **I** generative hyphae from tubes **J–N** basidiospores. Scale bars: 20 μm (**G**); 10 μm (**E, F, H, I**); 5 μm (**J–N**).

thick-walled with a wide to narrow lumen or sub-solid, arboriform with few branches, yellowish to golden yellow; binding hyphae 1.0–3.0 µm in diameter, thick-walled, branched and flexuous, pale yellow, scarce; all the hyphae IKI–, CB+; tissues darkening in KOH.

Pileipellis a crustohymeniderm, cells 15–33 × 5–9 µm, thick-walled to sub-solid, composed of irregular, narrowly clavate end cells, straight to flexuose, smooth or with a few small apical protuberances, yellowish to golden-yellow, sometimes with apical granulations, apex slightly amyloid.

Basidiospores ellipsoid to subglobose, apex truncated or subacute, yellowish to yellowish brown, IKI–, CB+, inamyloid; double-walled with distinctly thick walls, exospore wall smooth, endospore walls with interwall pillars; (40/2/2) (8.5) 9.0–9.6–10.0 (11.0) × 6.0–6.8–7.0 (7.5) µm, L = 9.65 µm, W = 6.75 µm, *Q* = (1.24) 1.38–1.52 (1.55), *Q*m = 1.43 ± 0.07 (including myxosporium). ***Basidia*** not observed.

Additional specimens examined. China, Sichuan Province, Panzhihua City, Miyi County, on a decaying tree of *Phyllanthus* sp., alt. 1035 m, Jun-He, 15 August 2023, HL308.

Notes. In the phylogenetic analyses, *Ganoderma phyllanthicola* is clustered as a sister taxon to *G. castaneum* with strong statistical support (100% ML and 1.00PP, Fig. 1). Morphologically, both species share similar characteristics of the sessile basidiomata and non-stratified tubes. However, *G. castaneum* differs from *G. phyllanthicola* in having buff and obtuse pileus margin, regular palisade pileipellis, heterogeneous context, smaller basidiospores (6.2–8.5 × 4.2–6.3 µm) with smooth endospore walls, Sun et al. 2022). *Ganoderma tropicum* and *G. philippii* have similar homogeneous context, but *G. tropicum* has a stipitate basidiomata and buff pileus margin, samller basidiospores (6.8–10.0 × 4.0–6.4 µm), and (Steyaert 1972). *Ganoderma philippii* has wavy like pileus margin and brown context with black melanoid lines, smaller and obovoid basidiospores (6.0–8.0 × 3.0–4.0 µm, Moncalvo and Ryvarden 1997).

Ganoderma aridicola described from South Africa is similar to *G. phyllanthicola* in the sessile basidiomata with dark brown pileus surface, homogeneous context, small pores and ellipsoid basidiospores. However, *G. aridicola* differs by the distinctly stratified tubes and lacks branched or protuberant apical cells (Xing et al. 2016). Besides, the phylogenetic analyses separated *G. aridicola* and *G. phyllanthicola* (Fig. 1). *Ganoderma multiplicatum* also has pale yellow margin and irregular pileipellis cells., but it differs from *G. phyllanthicola* by the photo brown to reddish brown pileus surface, short stipe (1.8–3 cm) and ellipsoid basidiospores (6.0–10.0 × 4.5–7.0 µm, Gottlieb and Wright 1999).

***Ganoderma suae* J. He & S.H. Li, sp. nov.**
MycoBank No: 853506
Fig. 3

Diagnosis. Differs from other species in the genus by its large and substipitate basidiomata, reddish brown to oxblood red pileus surface with concentric furrows and radial rugose, whitish and wavy margin, almond-shaped basidiospores, heterogeneous context and non-stratified tubes.

Etymology. The epithet '*suae*' refers to the Chinese mycologist Prof. Hong-Yan Su, for her great contribution to the mycology.

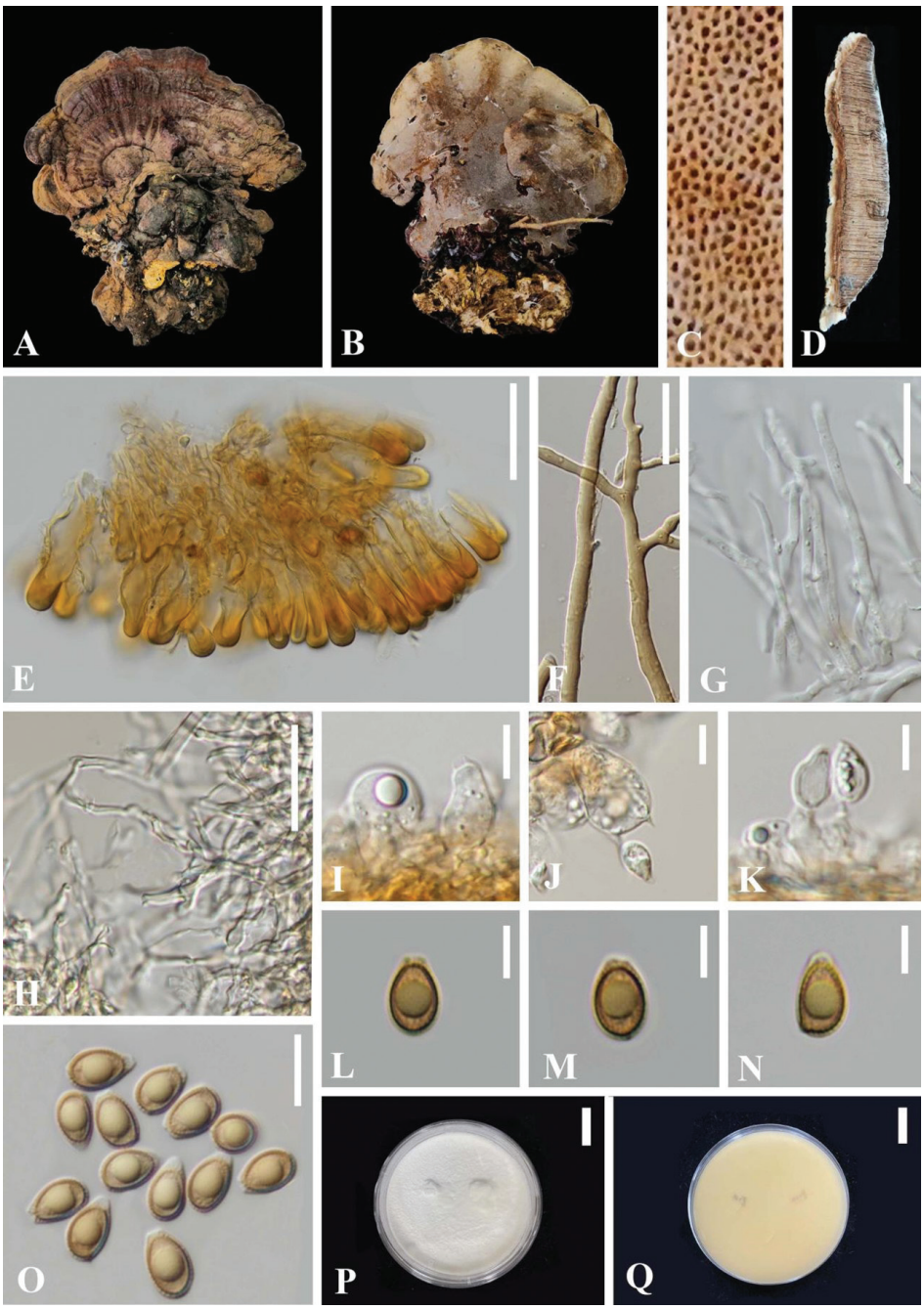

Figure 3. *Ganoderma suae* (HKAS 123791, holotype) **A, B** basidiomata **C** pore surface **D** cut side of pileus **E** sections of pellis **F** skeletal hyphae from context **E** generative hyphae from tubes **H** binding hyphae from context **I–K** basidia and basidioles **L–O** basidiospores. Scale bars: 30 μm (**E–H**); 10 μm (**I–K, O**); 5 μm (**L–N**); 20 mm (**P, Q**).

Holotype. China. Yunnan Province., Honghe City, Ivchun County, on a dead stump of a broad-leaved tree, alt. 1392 m, Jun He, 24 June 2019, L4651(HKAS 123791).

Description. ***Basidiomata*** annual, sessile to substipitate, and occasionally imbricate, woody-corky, light in weight. ***Pileus*** round-flabelliform to reniform, slightly convex to applanate; surface glabrous, projecting up to 15 cm, 10 cm wide and 2 cm thick at base. Pileus surface reddish brown(6F8) to oxblood red(9E7), weakly to strongly laccate, and covered by a thin hard crust, concentrically zonate or azonate. ***Margin*** whitish to generally concolorous, entire, acute to obtuse, smooth to irregularly wavy. ***Context*** up to 0.8 cm thick, heterogeneous, the upper layer grey-

ish white(2B1), the lower layer cinnamon brown (6D7) to chestnut brown(6F7), bearing distinct concentric growth zones, without black melanoid lines, hard corky and fibrous. ***Tubes*** 0.2–1.2 cm long, grayish brown (6B3), corky, unstratified. ***Pores*** 4–6 per mm, circular to angular, dissepiments slightly thick, entire; pore surface lead gray (2D2) to greyish white (2B1) when fresh, golden grey (4C2) to soot brown(5F5) when bruising or aging. ***Stipe*** up to 4.5 cm long and 3.0 cm diam, generally short and thick, cylindrical, horizontal or lateral, fibrous to spongy, reddish brown (6F8) to dark brown (8F8), concolorous to generally darker than pileus.

***Hyphal system trimitic*.** Generative hyphae 2.0–3.0 µm in diameter, colorless, thin-walled, hyaline, unbranched, abundant, with clamp connections; skeletal hyphae 3.0–9.0 µm in diameter, thick-walled with a narrow lumen to subsolid, non-septate, moderately branched, orange yellow to golden-yellow, predominant; binding hyphae 1.0–2.0 µm in diameter, subthick-walled to solid, non-septate, frequently branched, interwoven, colourless to yellowish, scarce, notably thinner and paler than skeletal hyphae; all the hyphae IKI–, CB+; tissues darkening in KOH.

***Culture characteristics*.** Initially, white to yellowish white, pale yellow when growing, become orange white, pale orange, light orange and some reddish yellow to dark brown around the plugged circle of active mycelium after incubation for 3 weeks.

Pileipellis a crustohymeniderm, cells 24–43 × 6–11 µm, thick-walled to sub-solid, apical cells narrowly clavate to clavate, slightly inflated, yellowish to golden-yellow, without granulations in the apex; negative or apex slightly amyloid.

Basidiospores almond-shaped to narrow ellipsoid, apex subacute, with apical germ pore, yellowish to yellowish-brown, IKI–, CB+, inamyloid; double-walled, exospore smooth, endospore with coarse echinulate, exosporium with inter-walled pillars 0.5–0.6 µm thick; (80/4/2) (8.0) 9.0–9.7–10.5 × (5.0) 5.5–6.1–6.5 (7.0) µm, L = 9.70 µm, W = 6.10 µm, *Q* = (1.38) 1.45–1.79 (1.97), *Q*m = 1.61 ± 0.13 (including myxosporium). ***Basidia*** barrel-shaped to widely clavate, colorless, with a clamp connection and four sterigmata, thin-walled, 9–18 × 9–12 µm; basidioles pear-shaped to fusiform, colourless, thin-walled, 8–14 × 6–11 µm.

Additional specimens examined. China, Yuannan Province, Lingcang City, Yun County, on a living *Quercus* sp. tree, alt. 1516 m, Jun He, 4 August 2019, L4817(HKAS 123777).

Notes. Phylogenetic analyses showed that *Ganoderma suae* clusters as a sister taxon to *G. resinaceum* with good statistical support (100% ML/1.00 PP, Fig. 1). Morphologically, *G. resinaceum* differs from *G. suae* by having smaller basidiomata, reddish brown to oxblood red pileus surface and wavy margin, homogeneous context, longer pileipellis (34–59 × 6.2–9.3 µm), and larger basidiospores (11.2–12.5 × 6.5–7.4 µm, Náplavová et al. 2020; Ryvarden 2000; Torres-Torres et al. 2012).

Ganoderma zonatum also has sessile basidiomata and a whitish pileus margin, but it differs from G. *suae* by having an apex widened to swollen of pileipellis cells (30–70 × 5–12 µm), and larger basidiospores (11.2–12.5 × 6.5–7.4 µm, Murrill 1902).

Discussion

Ganoderma has long been regarded as one of the most important genera of medicinal fungi worldwide with more than 45 species described in China. To date, 36 species of *Ganoderma* have been reported from Southwest China (Yunnan,

Tibet, Guizhou, and Sichuan), including 16 species originally described from China, namely *G. alpinum* B.K. Cui, J.H. Xing & Y.F. Sun, *G. artocarpicola* J. He & S.H. Li, *G. dianzhongense* J. He, H.Y. Su & S.H. Li, *G. ellipsoideum* Hapuar., T.C. Wen & K.D. Hyde 2018, *G. esculentum* J. He & S.H. Li, *G. leucocontextum* T.H. Li, W.Q. Deng, S. H. Wu, D. M. Wang & H.P. Hu, *G. mutabile* Y. Cao & H.S. Yuan, *G. obscuratum* J. He & S. H. Li, *G. ovisporum* H.D. Yang, T.C. Wen. *G. puerense* B.K. Cui, J.H. Xing & Y.F. Sun, *G. sanduense* Hapuar., T.C. Wen & K.D. Hyde, *G. sichuanense* J.D. Zhao & X.Q. Zhang, *G. subangustisporum* B.K. Cui, J.H. Xing & Y.F. Sun, *G. weixiense* Karun. & J.C. Xu, *G. yunnanense* J. He & S. H. Li and *G. yunlingense* B.K. Cui, J.H. Xing & Y.F. Sun (Zhao et al. 1983; Cao et al. 2012; Li et al. 2015; Hapuarachchi et al. 2019; He et al. 2021; He et al. 2022; Sun et al. 2022; Yang et al. 2022). During the last five years, the diversity of *Ganoderma* in Southwest China was mainly reported from Yunnan Province and Guizhou Province (Hapuarachchi et al. 2019; Luangharn et al. 2021; He et al. 2022; Sun et al. 2022). These studies show that there is an unrecognized diversity of *Ganoderma* species in southwest China. More potential new species of *Ganoderma* may be discovered in the future.

In this study, two new species viz *G. phyllanthicola* and *G. suae* from Southwest China are introduced based on morphology and multigene phylogeny. *Ganoderma phyllanthicola* and *G. suae* satisfied the generic concept of the genus *Ganoderma* (Karsten 1881). They comprise subglobose to ellipsoid or ovoid basidiospores, truncated, double-walled with thick walls, exospore wall semi-reticulate, endospore wall smooth or with conspicuous spinules, homogeneous or heterogeneous context and laccate with variable ornamentation pileus surface. When compared with each other, *G. phyllanthicola* and *G. suae* occupied distinct and distant positions in the multilocus phylogenetic tree, and the morphology of their basidiomata also exhibits distinct macro- and microscopic characters that can further differentiate the two species. Thus, based on convergent results from morphology and molecular data analyses, *G. phyllanthicola* and *G. suae* are considered to be new species to science.

Ganoderma phyllanthicola was closely related to *G. castaneum*, *G. philippii* and G. *tropicum* in the phylogeny inferred from the concatenated sequence data set. Morphologically, they are easily distinguishable by some macro- and microscopic characters of their basidiomata. Contrary to *G. phyllanthicola*, *G. castaneum* has a broadly attached, flabelliform, chestnut brown pileus surface with wide concentric ridges, heterogeneous context, regular palisade pileipellis cells, and broadly ellipsoid basidiospores not obviously truncated with smooth endospore walls (Sun et al. 2022; Table 2). *Ganoderma philippii* and *G. tropicum*, contrary to the new species, is characterized by flabelliform to circular, non-coriaceous basidiomata and very much smaller basidiospores (Steyaert 1972; Moncalvo and Ryvarden 1997; Table 2). Moreover, *Ganoderma enigmaticum* can be easily distinguished from *G. phyllanthicola* by the stipitate basidiomata and regular pileipellis cells (Coetzee et al. 2015). *Ganoderma orbiforme* has biannual or perennial basidiospores and longer pileipellis cells than those of *G. phyllanthicola* (Ryvarden 2000; Table 2).

Ganoderma resinaceum is known to be a Northern Hemisphere species, mainly occurring in Europe (Patouillard 1889; Moncalvo et al. 1995; Ryvarden and Melo 2014). The European specimens are easily recognized in the field by thick, soft and pale context. The first signs of genetic diversity within

Table 2. Morphological comparison of *Ganoderma phyllanthicola* sp. nov., and *G. suae* sp. nov., with their closest relatives in the combined phylogeny.

Species	Shape	Context	Pileipellis cells	Pores (per mm)	Basidiospores (µm)	Reference
Ganoderma aridicola	Sessile, dimidiate	2.4–3 µm thick, homogeneous, fuscous	cells clavate, 30–55 × 5–8 µm	6–8	9.7–11.2 × 7.0–7.8	Xing et al. 2016
G. castaneum	sessile, flabelliform	up to 1.6 cm thick, heterogeneous, the upper layer pale straw yellow, the lower layer dark brown,	composed of regular palisade, clavate end cells 25–40 × 3–5 µm	4–6	6.2–8.5 × 4.2–6.3	Sun et al. 2022
G. phyllanthicola	**sessile, sub-circular, flabelliform to shell-shaped**	**up to 0.8 cm thick, homogeneous, cinnamon brown to chestnut brown**	**composed of irregular, narrowly clavate end cells, straight to flexuous or irregular, 15–33 × 5–9 µm**	**5–7**	**8.5–11.0 × 6.0–7.5**	**this study**
G. enigmaticum	stipitate, globular	context soft, homogenous, dark brown	amyloid elements 20–46 × 5.5–9 um	3–5	8.0–11.0 × 3.5–6.0	Coetzee et al. 2015
G. lucidum	stipitate to sessile	thinner context of white to slightly cream color context	amyloid hyphal end cells up to 7–11 µm diam	4–5	7.7–11.5 × 5.2–8.4	Ryvarden and Gilbertson 1993
G. multiplicatum	sessile, flabelliform, applanate or convex	up to 2 cm thick, homogeneous, cinnamon colour, darker toward the tubes	cells clavate, cylindrical or irregular, 38–65 × 5.6–10 µm	5–6	6.0–10.0 × 4.5–7.0	Gottlieb and Wright 1999
G. orbiforme	sessile, flabelliform or spathulate	context up to 0.4–1.0 cm thick, triplex	composed of apically acanthus like branched cells, 50–100 X 6–12 µm	4–7	7.1–12.6 × 5.2–7.7	Ryvarden 2000; Wang et al. 2014
G. philippii	sessile, flabelliform to circular	up to 1.4 cm thick, homogeneous, brown	–	5–6	6.0–8.0 × 3.0–4.0	Steyaert 1972, Moncalvo and Ryvarden 1997
G. polychromum	sessile to o substipitate, flabelliform	pink buff to cinnamon buff concentric growth zones	–	4–5	10.3–18.3 × 7.0–11.9	Murrill 1908
G. resinaceum	sessile to stipitate, round-flabelliform	0.4-1.3 cm thick, homogeneous context, wood-coloured to pale tawny brown., with resinous incrustations	cells clavate, narrowly clavate, or almost cylindrical, 34–59 × 6.2–9.3 µm,	3–4	9.0–13.0 × 6.0–8.0	Steyaert 1972; Ryvarden 2000; Náplavová et al. 2020
G. sessile	sessile, pileus sometimes imbricate, conchate to flabelliform	context thin, soft corky or woody, radially fibrous, concentrically zonate, ochraceous	cylindric, smooth elements, 60–75 × 7–10 µm	4–5	12.0–16.0 × 6.0–8.0	Murrill 1902; Gottlieb and Wright 1999
G. suae	**sessile to substipitate, variable, reniform**	**up to 0.8 cm thick, heterogeneous, the upper layer greyish white, the lower layer cinnamon brown, without resinous incrustations**	**cells clavate, 24–43 × 6–11 µm**	**4–6**	**8.0–10.5 × 5.0–7.0**	**this study**
G. tropicum	usually sessile, sometimes laterally stipitate, flabelliform to shell-shaped or circular	up to 2.2 cm thick, homogeneous, dark brown	cells clavate, sometimes branched or protuberant, inflated and flexuous, 19–32 × 4–9 µm	4–6	6.8–10.0 × 4.0–6.4	Ryvarden 1981
G. vivianimercedianum	sessile to substipitate, flabelliform in pole view	1–1.5 cm thick, homogeneous, caramel above and dark brown toward the tubes,	cells clavate, apex occasionally slightly widened, 36–65 × 7.2–12 µm	3–5	9.0–12.0 × 6.0–8.0	Torres-Torres et al. 2008
G. zonatum	sessile, applanate to convex	homogeneous, slightly zonate, dark brow	cells cylindrical to clavate, 30–70 × 5–12 µm	4–5	12.0–14.0 × 6.0–9.0	Loyd et al. 2018

G. resinaceum were observed by Moncalvo (2000), and Loyd et al. (2018) showed that *G. resinaceum* sensu American *auctores* encompassed at least two distinct species, viz. *G. polychromum* and *G. sessile*. Cabarroi-Hernández et al. (2019) studies confirmed that *G. resinaceum* sensu auctores from China, East Africa, Europa, and both North and South America represented a species complex. Study of phylogenetic inferences based on multilocus sequences by Hernand éz et al. (2019) also showed that *G. resinaceum* represents a species complex.

Our results based on polygenic phylogenetic analysis also confirm that *Ganoderma resinaceum* represents a species complex, encompassing several distinct species, namely *G. platense*, *G. polychromum*, *G. sessile*, and *G. suae*. *Ganoderma suae* emerges as a newly recognized species within the *G. resinaceum* sensu complex group (Fig. 1). *Ganoderma suae* is characterized by its annual basidiomata, reddish brown to oxblood red pileus surface, heterogeneous context without resinous incrustations (without black melanoid lines), wavy margin and almond-shaped basidiospores not obviously truncated, endospore walls with dense spinules (8.0–10.5 × 5.0–7.0 µm), can be easily distinguished from *G. resinaceum* (Ryvarden 2000). Náplavová et al. 2020 confirmed the presence of two distinct genotypes (genotype A and genotype B) in European *G. resinaceum* by comparing partial sequences of the TEF1-α region and the 25 s LSU rRNA gene. Their study also showed that basidiospore sizes range between 9.6–14.4 × 6.0–8.4 µ m in genotype A and 6–12.0 × 7.2–9.6 µ m in genotype B. Besides, specimens of both genotypes share the same pileus surface (glossy with resinous layer) and almost identical coloration. Only the context color was lighter brown beige to sand yellow in genotype A and darker brown beige to ochre brown in genotype B. *Ganoderma resinaceum* from Europe has a special laccate and glossy with resinous layer pileus surface, homogeneous context, and larger basidiospores cells than those of *G. suae*. (Ryvarden 2004; Náplavová et al. 2020). Thus, *Ganoderma suae* from China and *G. resinaceum* from Europe should be recognized as two different species. Table 2 presents a morphological comparison between the new species and its closest phylogenetic neighbors. Although we are of the opinion that *G. suae* well represent a species on its own, more material, ideally from various localities, and DNA sequences, is necessary to reveal the species diversity and kinship of *G. resinaceum* complex groups.

Recent studies have shown that the specimen *G. resinaceum* collected from China is inconsistent with the original description; therefore, it is clear that *G. resinaceum* is not distributed in China (Sun et al. 2022). It's noteworthy that we have also collected a sample (HL199) from Yunnan Province, which differs from both *G. resinaceum* and *G. suae* in terms of its distinct macro-morphology and multi-gene sequences. Regrettably, the specimens were sterile and micromorphological data were missing. In the future, collecting additional specimens will be crucial for revealing the true distribution and diversity of *G. resinaceum* complex groups in China.

Acknowledgment

We would like to thank Qian-Qiu Luo, Xiao Han, Tong Lv and De-Chao Chen for their help on sample collection, DNA extraction, and PCR amplification.

Additional information

Conflict of interest

The authors have declared that no competing interests exist.

Ethical statement

No ethical statement was reported.

Funding

This research was funded by Yunnan science and technology talents and platform plan (Project ID: 202305AF150162); Central guidance for local scientific and technological development funds (Project ID: 202307AB110001); Yunnan Science Technology plan project of Science and Technology Department (Project ID: 202301BD070001-021); Lincan City Technology Innovation Talents Training Objects (Project ID 202304AC100001-RC03); Lincan City to build the national Sustainable Development agenda innovation demonstration zone science and technology project (Project ID 202204AC100001-A01).

Author contributions

Conceptualization:JH, ZLL, SHL. Formal analysis: JH. Funding acquisition: EXL, SHL, XJL. Inves tigation: JH, XQW. Methodology: JH, WZT, DW. Resources: XJL, WZT, QWZ. Software: JH. Supervision: ZLL, SHL. Writing – original draft: JH. Writing – review and editing: SHL, ZLL.

Author ORCIDs

Jun He https://orcid.org/0000-0001-7027-7206
Wan-Zhong Tan https://orcid.org/0000-0002-9355-5798
Zong-Long Luo https://orcid.org/0000-0001-7307-4885

Data availability

All of the data that support the findings of this study are available in the main text or Supplementary Information.

References

Cao Y, Yuan HS (2012) *Ganoderma mutabile* sp. nov. from southwestern China based on morphological and molecular data. Mycological Progress 12: 121–126. https://doi.org/10.1007/s11557-012-0819-9

Cabarroi-Hernández M, Villalobos-Arámbula AR, Torres-Torres MG, Decock C, Guzmán-Dávalos L (2019) The *Ganoderma weberianum-resinaceum* lineage: Multilocus phylogenetic analysis and morphology confirm *G. mexicanum* and *G. parvulum* in the Neotropics. MycoKeys 59: 95–131. https://doi.org/10.3897/mycokeys.59.33182

Cabarroi-Hernández M, Decock C, Welti S, Amalfi M, Villalobos-Arámbula A, Aliaga-Ramos D, Morera G, Macedo-Pérez E (2023) *Ganoderma* from Cuba: An approach to some species based on morphology and phylogenetic analyses. Biological Journal of the Linnean Society. Linnean Society of London 140(3): 323–357. https://doi.org/10.1093/biolinnean/blad055

Coetzee MP, Marincowitz S, Muthelo VG, Wingfield MJ (2015) *Ganoderma* species, including new taxa associated with root rot of the iconic Jacaranda mimosifolia in Pretoria, South Africa. IMA Fungus 6(1): 249–256. https://doi.org/10.5598/imafungus.2015.06.01.16

Costa-Rezende D, Robledo GL, Drechsler-Santos ER, Glen M, Gates G, de Madrignac Bonzi BR, Popoff OF, Crespo E, Góes-Neto A (2020, August) Taxonomy and phylogeny of polypores with ganodermatoid basidiospores (Ganodermataceae). Mycological Progress 19(8): 725–741. https://doi.org/10.1007/s11557-020-01589-1

Darriba D, Taboada GL, Doallo R, Posada DJ (2012) ModelTest 2: More models, new heuristics and parallel computing. Nature Methods 9(8): 772–772. https://doi.org/10.1038/nmeth.2109

Fries EM (1821) Systema mycologicum, sistens of fungorum ordines, genera et species huc usque congnitas. Vol. 1. Greifswald, Germania, 520 pp. https://doi.org/10.5962/bhl.title.5378

Fryssouli V, Zervakis GI, Polemis E, Typas MA (2020) A global meta-analysis of ITS rDNA sequences from material belonging to the genus *Ganoderma* (Basidiomycota, Polyporales) including new data from selected taxa. MycoKeys 75: 71–143. https://doi.org/10.3897/mycokeys.75.59872

Glez-Peña D, Gómez-Blanco D, Reboiro-Jato M, Fdez-Riverola F, Posada D (2010) ALTER: Program-oriented conversion of DNA and protein alignments. Nucleic Acids Research 38: 14–18. https://doi.org/10.1093/nar/gkq321

Gottlieb AM, Wright JE (1999) Taxonomy of *Ganoderma* from southern South America: Subgenus *Ganoderma.* Mycological Research 103(6): 661–673. https://doi.org/10.1017/S0953756298007941

Guindon S, Gascuel O (2003) A simple, fast, and accurate algorithm to estimate large phylogenies by maximum likelihood. Systematic Biology 52(5): 696–704. https://doi.org/10.1080/10635150390235520

Hall TA (1999) BioEdit: A user–friendly biological sequence alignment editor and analysis program for Windows 95/98/NT. Nucleic Acids Symposium Series 41: 95–98.

Hapuarachchi KK, Elkhateeb WA, Karunarathna SC, Cheng CK, Bandara AR, Kakumyan P, Hyde KD, Daba G, Wen TC (2018a) Current status of global *Ganoderma* cultivation, products, industry and market. Mycosphere 9(5): 1025–1052. https://doi.org/10.5943/mycosphere/9/5/6

Hapuarachchi KK, Karunarathna SC, McKenzie EHC, Wu XL, Kakumyan P, Hyde KD, Wen TC (2018b) High phenotypic plasticity of *Ganoderma sinense* (Ganodermataceae, Polyporales) in China. Asian Journal of Mycology 2(1): 1–47. https://doi.org/10.5943/ajom/2/1/1

Hapuarachchi KK, Karunarathna SC, Phengsintham P, Yang HD, Kakumyan P, Hyde KD, Wen TC (2019) Ganodermataceae (Polyporales): Diversity in Greater Mekong Subregion countries (China, Laos, Myanmar, Thailand and Vietnam). Mycosphere : Journal of Fungal Biology 10(1): 221–309. https://doi.org/10.5943/mycosphere/10/1/6

He J, Luo ZL, Tang SM, Li YJ, Li SH, Su HY (2021) Phylogenetic analyses and morphological characters reveal two new species of *Ganoderma* from Yunnan province. China. MycoKeys 84: 141–162. https://doi.org/10.3897/mycokeys.84.69449

He J, Han X, Luo ZL, Li EX, Tang SM, Luo HM, Niu KY, Su X, Li S-H (2022) Species diversity of *Ganoderma* (Ganodermataceae, Polyporales) with three new species and a key to *Ganoderma* in Yunnan Province, China. Frontiers in Microbiology 13: 1035434. https://doi.org/10.3389/fmicb.2022.1035434

Hu Y, Karunarathna SC, Li H, Galappaththi MC, Zhao CL, Kakumyan P, Mortimer PE (2022) The impact of drying temperature on basidiospore size. Diversity 14(4): 239. https://doi.org/10.3390/d14040239

Karsten PA (1881) Enumeratio boletinearum et polyporearum Fennicum, systemate novo dispositarium. Revue Mycologicum 3: 16–19.

Katoh K, Standley DM (2013) MAFFT multiple sequence alignment software Version 7: Improvements in performance and usability. Molecular Biology and Evolution 30(4): 772–780. https://doi.org/10.1093/molbev/mst010

Kinge T R, Mih AM, Neves MD, Sousa DR, Frota MZ (2015) Diversity and distribution of species of *Ganoderma* in south western Cameroon. Journal of Yeast and Fungal Research 6(2): 17–24. https://doi.org/10.5897/JYFR2014.0150

Kornerup A, Wanscher JH (1978) Methuen handbook of colour (3rd edn.) Methuen. London, England.

Lai T, Gao Y, Zhou SF (2004) Global marketing of medicinal Ling Zhi mushroom *Ganoderma lucidum* (W.Curt:Fr.) Lloyd (Aphyllophoromycetideae) products and safety concerns. International Journal of Medicinal Mushrooms 6(2): 189–194. https://doi.org/10.1615/IntJMedMushr.v6.i2.100

Li TH, Hu HP, Deng WQ, Wu SH, Wang DM, Tsering T (2015) *Ganoderma leucocontextum*, a new member of the *G. lucidum* complex from southwestern China. Mycoscience 56(1): 81–85. https://doi.org/10.1016/j.myc.2014.03.005

Li LF, Liu HB, Zhang QW, Li ZP, Wong TL, Fung HY, Zhang JX, Bai SP, Lu AP, Han QB (2018) Comprehensive comparison of polysaccharides from *Ganoderma lucidum* and *G. sinense*: Chemical, anti-tumor, immunomodulating and gut-microbiota modulatory properties. Scientific Reports 8(1): 6172. https://doi.org/10.1038/s41598-018-22885-7

Liu Y, Whelen S, Hall BD (1999) Phylogenetic relationships among ascomycetes: Evidence from an RNA polymerase II subunit. Molecular Biology and Evolution 16(12): 1799–1808. https://doi.org/10.1093/oxfordjournals.molbev.a026092

Liu Y, Wang Z, Zhang J (2015) Dietary Chinese herbs chemistry: Pharmacology and clinical evidence. Springer, London, 759–765. https://doi.org/10.1007/978-3-211-99448-1

Loyd AL, Barnes CW, Held BW, Schink MJ, Smith ME, Smith JA, Blanchette RA (2018) Elucidating 'lucidum': Distinguishing the diverse laccate *Ganoderma* species of the United States. PLoS ONE 13(7): e0199738. https://doi.org/10.1371/journal.pone.0199738

Luangharn T, Karunarathna SC, Dutta AK, Paloi S, Lian CK, Huyen LT, Pham HND, Hyde KD, Xu JC, Mortimer PE (2021) *Ganoderma* (Ganodermataceae, Basidiomycota) species from the Greater Mekong Subregion. Journal of Fungi 7: 1–83. https://doiorg/103390/jof7100819

Matheny PB, Wang Z, Binder M, Curtis JM, Lim YW, Nilsson RH, Hughes KW, Petersen RH, Hofstetter V, Ammirati JF, Schoch C, Langer GE, McLaughlin DJ, Wilson AW, Crane PE, Frøslev T, Ge ZW, Kerrigan RW, Slot JC, Vellinga EC, Liang ZL, Aime MC, Baroni TJ, Fischer M, Hosaka K, Matsuura K, Seidl MT, Vaura J (2007) Hibbett DS Contributions of *rpb2* and *tef1* to the phylogeny of mushrooms and allies (Basidiomycota, Fungi). Molecular Phylogenetics and Evolution 43(2): 430–451. https://doi.org/10.1016/j.ympev.2006.08.024

Miller MA, Pfeiffer W, Schwartz T (2010) Creating the CIPRES Science Gateway for inference of large phylogenetic trees In Proceedings of the 2010 Gateway Computing Environments Workshop (GCE) New Orleans LA USA 14 November, 8 pp. https://doi.org/10.1109/GCE.2010.5676129

Moncalvo JM, Wang HF, Hseu RS (1995) Phylogenetic relationships in *Ganoderma* inferred from the internal transcribed spacers and 25S ribosomal DNA sequences. Mycologia 87(2): 223–1238. https://doi.org/10.1080/00275514.1995.12026524

Moncalvo JM, Ryvarden LA (1997) A nomenclatural study of the Ganodermataceae Donk. Synopsis Fungorum 11: 1–114.

Moncalvo JM (2000) Systematics of *Ganoderma*. In: Flood P, Bridge D, Holderness M(Eds) *Ganoderma* diseases of perennial crops. CABI, Wallingford, 23–45. https://doi.org/10.1079/9780851993881.0023

Murrill WA (1902) The Polyporaceae of North America part I The genus *Ganoderma*. Bulletin of the Torrey Botanical Club 29: 599–608 https://doi.org/10.2307/2478682

Murrill WA (1908). Polyporaceae, Part 2. North American Flora 9: 73–131.

Náplavová K, Beck T, Pristaš P, Gáperová S, Šebesta M, Piknová M, Gáper J (2020) Molecular Data Reveal Unrecognized Diversity in the European *Ganoderma resinaceum*. Forests 11(8): 850. https://doi.org/10.3390/f11080850

Nylander JA (2004) A MrModeltest 20; Program Distributed by the Author; Uppsala University, Uppsala Sweden.

Patouillard NT (1889) Le genre *Ganoderma*. Bull. Soc. Mycol. Fr. 5: 64–80.

Rannala B, Yang Z (1996) Probability distribution of molecular evolutionary trees: A new method of phylogenetic inference. Journal of Molecular Evolution 43(3): 304–311. https://doi.org/10.1007/BF02338839

Richter C, Wittstein K, Kirk PM, Stadler M (2015) An assessment of the taxonomy and chemotaxonomy of *Ganoderma*. Fungal Diversity 71: 1–15. https://doi.org/10.1007/s13225-014-0313-6

Ronquist F, Teslenko M, van der Mark P, Ayres DL, Darling A, Höhna S, Larget B, Liu L, Suchard MA, Huelsenbeck JP (2012) MrBayes 32: Efficient Bayesian phylogenetic inference and model choice across a large model space. Systematic Biology 61(3): 539–542. https://doi.org/10.1093/sysbio/sys029

Ryvarden L (1981) Type studies in the Polyporaceae 12 Species described by F W Junghuhn. Persoonia 11: 369–372.

Ryvarden L (2000) Studies in neotropical polypores 2 A preliminary key to neotropical species of *Ganoderma* with a laccate pileus. Mycologia 92(1): 180–191. https://doi.org/10.1080/00275514.2000.12061142

Ryvarden L (2004) Neotropical polypores part 1. Introduction, ganodermataceae & hy-menochaetaceae. Synopsis Fungorum 19: 1–229.

Ryvarden L, Gilbertson RL (1993) European polypores Part 1 Abortiporus Lindtneria. Synopsis Fungorum 6: 1–387.

Ryvarden L, Melo I (2014) Poroid Fungi of Europe; Fungiflora. Oslo, Norway, 455.

Steyaert RL (1972) Species of *Ganoderma* and related genera mainly of the Bogor and Leiden Herbaria. Persoonia 7: 55–118.

Sun YF, Costa-Rezende DH, Xing JH, Zhou JL, Zhang B, Gibertoni TB, Gates G, Glen M, Dai Y-C, Cui B-K (2020) Multi-gene phylogeny and taxonomy of *Amauroderma* s lat (Ganodermataceae). Persoonia 44(1): 206–239. https://doi.org/10.3767/persoonia.2020.44.08

Sun YF, Xing JH, He XL, Wu DM, Song CG, Liu S, Vlasák J, Gates G, Gibertoni TB, Cui BK (2022) Species diversity systematic revision and molecular phylogeny of Ganodermataceae (Polyporales Basidiomycota) with an emphasis on Chinese collections. Studies in Mycology 101(1): 287–415. https://doi.org/10.3114/sim.2022.101.05

Swofford DL (2003) PAUP*: phylogenetic analysis using parsimony (*and other methods). Sinauer Associates Sunderland, Massachusetts. http://ciniiacjp/naid/110002665463

Torres-Torres MG, Guzmán-Dávalos L, Guggliota AM (2008) *Ganoderma vivianimercedianum* sp nov and the related species *G. perzonatum*. Mycotaxon 105: 447–454.

Torres-Torres MG, Guzmán-Dávalos L, Guggliota AM (2012) *Ganoderma* in Brazil: Known species and new records. Mycotaxon 121(1): 93–132. https://doi.org/10.5248/121.93

Vaidya G, Lohman DJ, Meier R (2011) SequenceMatrix: Concatenation software for the fast assembly of multi-gene datasets with character set and codon information. Cladistics 27(2): 171–180. https://doi.org/10.1111/j.1096-0031.2010.00329.x

Vinjusha N, Kumar TKA (2022). The Polyporales of Kerala. SporePrint Books, Calicut, Kerala, India 90–108.

Wang DM, Wu SH, Yao YJ (2014) Clarification of the Concept of *Ganoderma orbiform-e* with High Morphological Plasticity. PLoS ONE 9(5): e98733. https://doi.org/10.1371/journal.pone.0098733

Wang L, Li J, Zhang J, Li Z, Liu H, Wang Y (2020) Traditional uses chemical components and pharmacological activities of the genus *Ganoderma* P Karst: A review. RSC Advances 10(69): 84–97. https://doi.org/10.1039/D0RA07219B

White TJ, Bruns T, Lee S, Taylor J (1990) Amplification and direct sequencing of fungal ri-bosomal RNA genes for phylogenetics In: Innis MA, Gelfand DH, Sninsky JJ, White TJ (Eds) PCR protocols: a guide to methods and applications. Academic, San Diego / New York, 315–322. https://doi.org/10.1016/B978-0-12-372180-8.50042-1

Xing JH, Song J, Decock C, Cui BK (2016) Morphological characters and phylogenetic analysis reveal a new species within the *Ganoderma lucidum* complex from South Africa. Phytotaxa 266: 115–124. https://doiorg/1011646/phytotaxa26625

Yang HD, Ding Y, Wen TC, Hapuarachchi KK, Wei DP (2022) *Ganoderma ovisporum* sp. nov. (Polyporales, Polyporaceae) from Southwest China. Biodiversity Data Journal 10: 1–31. https://doi.org/10.3897/BDJ.10.e80034

Ye L, Karunarathna SC, Mortimer PE, Li HL, Qiu MH, Peng XR, Luangharn T, Li YJ, Promputtha I, Hyde K, Xu JC (2019) *Ganoderma weixiensis* (Polyporaceae Basidiomycota) a new member of the *G. lucidum* complex from Yunnan Province China. Phytotaxa 423: 75–86. https://doi.org/10.11646/phytotaxa.423.2.3

Zhao JD, Xu LW, Zhang XQ (1983) Taxonomic studies on Ganodermataceae of China II. Acta Mycologica Sinica 2: 159–167.

Supplementary material 1

Phylogenetic tree

Author: Jun He

Data type: pdf

Explanation note: Maximum likelihood (ML) tree is based on combined ITS + nrLSU + TEF1-α + RPB2 sequence data. Bootstrap support values with a maximum likelihood (ML) greater than 60% and Bayesian posterior probabilities (PP) greater than 0.90 given above the nodes, shown as “ML/PP”.

Link: https://doi.org/10.3897/mycokeys.106.121526.suppl1

MycoKeys 106: 117–132 (2024)
DOI: 10.3897/mycokeys.106.123279

Research Article

Multi-gene phylogenetic analyses revealed two novel species and one new record of *Trichobotrys* (Pleosporales, Dictyosporiaceae) from China

Wen-Jing Zhang[1], Gui-Ping Xu[2], Yu Liu[3], Yang Gao[1,4], Hai-Yan Song[4,5], Hai-Jing Hu[1,4], Jian-Ping Zhou[1,4], Ming-Hui Chen[1,4], Deng-Mei Fan[5], Dian-Ming Hu[1,4], Zhi-Jun Zhai[1,4]

1 *College of Bioscience and Bioengineering, Jiangxi Agricultural University, Nanchang, 1101 Zhimin Road, Nanchang, 330045, China*
2 *School of Biology and Biological Engineering, South China University of Technology, Guangzhou, 510006, China*
3 *Key Laboratory of Industrial Ecology and Environmental Engineering (Ministry of Education), School of Ocean Science and Technology, Dalian University of Technology, Panjin Campus, China*
4 *Jiangxi Key Laboratory for Excavation and Utilization of Agricultural Microorganisms, Jiangxi Agricultural University, Nanchang, 1101 Zhimin Road, Nanchang, 330045, China*
5 *School of Agricultural Sciences, Jiangxi Agricultural University, Nanchang, 1101 Zhimin Road, Nanchang, 330045, China*
Corresponding authors: Dian-Ming Hu (hudianming1@163.com); Zhi-Jun Zhai (zhjzh002@163.com)

Abstract

The rotting wood in freshwater is a unique eco-environment favoring various fungi. During our investigation of freshwater fungi on decaying wood, three hyphomycetes were collected from Jiangxi and Guangxi Provinces, China. Based on the morphological observations and phylogenetic analysis of a combined DNA data containing ITS, LSU, SSU and *tef1-α* sequences, two new *Trichobotrys* species, *T. meilingensis* and *T. yunjushanensis*, as well as a new record of *T. effusa*, were introduced. Additionally, a comprehensive description of the genus with both morphological and molecular data was first provided.

Key words: Freshwater hyphomycetes, phylogenetic analysis, taxonomy, *Trichobotrys*

Academic editor: Huzefa Raja
Received: 19 March 2024
Accepted: 29 May 2024
Published: 20 June 2024

Citation: Zhang W-J, Xu G-P, Liu Y, Gao Y, Song H-Y, Hu H-J, Zhou J-P, Chen M-H, Fan D-M, Hu D-M, Zhai Z-J (2024) Multi-gene phylogenetic analyses revealed two novel species and one new record of *Trichobotrys* (Pleosporales, Dictyosporiaceae) from China. MycoKeys 106: 117–132. https://doi.org/10.3897/mycokeys.106.123279

Introduction

Trichobotrys Penzig & Saccardo is a genus introduced with the discovery of the type species *Trichobotrys effusa* (Berk. & Br.) Petch from Sri Lanka, which was placed in Pleosporales genera *incertae sedis* (Pleosporales, Dothideomycetes, Ascomycota) (Petch 1924; Morgan-Jones et al. 1987). *Trichobotrys effusa* is known for producing compounds which can exhibit significant growth-inhibitory activities against the A549 lung cancer cell line (Chen et al. 2014). In addition, the bioactive compounds obtained from the deep-sea-derived fungus *T. effusa* DEFSCS021 could strongly inhibit the larvae settlement of *Bugula neritina* and *Balanus amphitrite* larvae (Sun et al. 2016).

Trichobotrys encompasses fungi characterised by their mononematous conidiophores producing catenate, dark brown, spherical and echinulate conidia on fertile, smooth, short, lateral branches with polyblastic conidiogenous cells. So far, only five species are recognised in this genus (http://www.indexfungorum.org/Names/Names.asp), namely *T. effusa*, *T. ipomoeae*, *T. pannosa*, *T. ramosa*

and *T. trechispora*. However, *T. pannosa* has been treated as a synonym of *T. effusa* (Morgan-Jones et al. 1987; D'Souza and Bhat 2001). Therefore, *Trichobotrys* is supposed to comprise four saprobic species, of which one (*T. effusa*) is from aquatic habitats and three (*T. ipomoeae*, *T. ramosa* and *T. trechispora*) are from terrestrial habitats (Petch 1917, 1924; Sawada 1959; Morgan-Jones et al. 1987; D'Souza and Bhat 2001). To date, the phylogenetic positions of representatives of *Trichobotrys* within the Ascomycota have not yet been investigated, as *T. effusa* has only ITS sequence and there are no molecular data for *T. ipomoeae*, *T. ramosa* and *T. trechispora*.

In the current study, we attempt to clarify the classification status of *Trichobotrys* through further identified materials and a more appropriate multi-gene genealogy. During our investigation of the freshwater hyphomycetes from decaying wood in Jiangxi and Guangxi provinces of China, two novel species named *T. meilingensis* and *T. yunjushanensis*, as well as a new record of *T. effusa*, are described according to morphological examination and multi-loci phylogenetic evidence.

Materials and methods

Samples collection, morphological observation and isolation

Samples of dead wood submerged in freshwater streams were collected from Jiangxi and Guangxi Provinces, China and were brought to the laboratory in plastic bags. Observations for fungi on natural substrates were made using a Nikon SMZ-1270 microscope (Nikon Corporation, Japan). With a syringe needle, the fungal structures were gathered and transferred to a small drop of distilled water on a clean slide, which was covered with a cover slide (Yang et al. 2018a). Micro-morphological characters were observed by a Nikon ECLIPSE Ni-U compound microscope (Nikon Corporation, Japan) and photographed by a Nikon DS-Fi3 camera. All measurements of the fungal structures were performed with PhotoRuler v. 1.1 software (The Genus Inocybe, Hyogo, Japan) and figures were made with Adobe Photoshop CC 2017 software (Adobe Systems, USA). Pure cultures of the fungi were obtained by the single spore isolation method (Chomnunti et al. 2014). Germinating conidia were transferred to fresh potato dextrose agar (PDA, from Beijing Bridge Technology Co., Ltd., Beijing, China) supplemented with two types of antibiotics (100 μg/mL penicillin, 50 μg/mL streptomycin), and then incubated at 25 °C for 2–3 weeks. Pure cultures were deposited at the Jiangxi Agricultural University Culture Collection (JAUCC) and specimens were stored in the Herbarium of Fungi, Jiangxi Agricultural University (HFJAU).

DNA extraction, PCR amplification and sequencing

Fresh mycelia of each strain, scraped from the growing culture with a sterile scalpel, were ground to a fine powder with liquid nitrogen to break the cells for DNA extraction. Subsequently, total genomic DNA was extracted following the modified CTAB method (Doyle and Doyle (1987). Four primer pairs, ITS1/ITS4 (White et al. 1990), LR0R/LR7 (Hopple and Vilgalys 1999), NS1/NS4 (White et al. 1990) and EF1-983F/EF1-2218R (Rehner and Buckley 2005), were used to amplify ITS, LSU, SSU and *tef1-α* gene regions, respectively. Polymerase chain reaction (PCR)

was performed in a final volume of 25 µl, containing 9.5 µl double distilled water (ddH_2O), 12.5 µl 2 × Taq PCR MasterMix (Qingke, Changsha, China), 1 µl each primer (10 µM) and 1 µl genomic DNA extract. Amplification conditions for ITS, LSU, SSU and *tef1-α* gene regions followed Zhai et al. (2022). The PCR products were sent to be sequenced by the commercial company QingKe Biotechnology Co. (Changsha, China). All sequences were edited with SeqMan v. 7.1.0 (DNASTAR, Inc, Madison, WI) and were deposited in the NCBI GenBank database (Table 1).

Data analyses

Based on ITS, LSU, SSU and *tef1-α* sequence comparison with the GenBank database, similar species in Dictyosporiaceae were found. The sequences of 37 relevant species according to the blasting result and recent publications (Tanaka and Harada 2003; Chen et al. 2014; Tanaka et al. 2015; Boonmee et al. 2016; Liu et al. 2017; Yang et al. 2018a; Chen et al. 2020) were chosen for phylogenetic analyses (Table 1) and were downloaded from GenBank. Four gene regions (ITS, LSU, SSU and *tef1-α*) were individually aligned using the online service of MAFFT v. 7 (Madeira et al. 2019) and concatenated using PhyloSuite v. 1.2.2 (Zhang et al. 2020). The alignments were checked visually and improved manually using BioEdit (Hall 1999; Liu et al. 2017).

Maximum Likelihood (ML) and Bayesian Inference (BI) were used to assess phylogenetic relationships. Maximum Likelihood (ML) analysis was conducted with RAxML v. 7.2.6 (Stamatakis and Alachiotis 2010) using the default substitution model GTR-GAMMA with rapid bootstrap analysis followed by 1000 bootstrap replicates to estimate ML bootstrap (BS) values. Bayesian Inference (BI) analysis was carried out with MrBayes v. 3.2 under partitioned models (Ronquist et al. 2012). The best-fit models of nucleotide substitutions were selected according to the Akaike information criterion (AIC) implemented in jModelTest v. 2.1.1 (Darriba et al. 2012) on XSEDE in the CIPRES web portal (Miller et al. 2010). The models for ITS, LSU, SSU and *tef1-α* datasets used for phylogenetic analysis are TIM2+I+G model (-lnL = 5321.6598), TIM2+I+G model (-lnL = 3199.3778), TIM2+I+G model (-lnL = 3481.7971) and GTR+I+G model (-lnL = 4762.6993), respectively. The data sets were run for 10,000,000 generations, with four chains, sampling trees every 1,000 generations. The first 10% trees were discarded as burn-in. Phylogenetic trees were visualized with FigTree v. 1.4.4 (Rambaut 2018), edited and beautified using Adobe Illustrator 2020 (Adobe Systems Inc., USA).

Results

Molecular phylogenetic results

According to sequence alignment analysis, the ITS sequences of the new record *Trichobotrys effusa* (JAUCC 6359 and JAUCC 6826) have only two different loci from that of *T. effusa* FS524 and three loci from that of *T. effusa* YMJ1179. The aligned sequence matrix for the combined analysis consists of ITS (574 bp), LSU (1259 bp), SSU (1459 bp) and *tef1-α* (962 bp) with a total of 4254 characters including gaps. The combined dataset shows the new species *T. meilingensis* and *T. yunjushanensis* share 98.61% (59 different loci), 98.40% (68 different loci)

Table 1. Sequences used in this study.

Species	Isolate	GenBank accession number			
		ITS	LSU	SSU	*tef1-α*
Aquadictyospora clematidis	**MFLU 172080**	**MT310592**	**MT214545**	**MT226664**	**MT394727**
Aquadictyospora lignicola	MFLUCC 17-1318	MF948621	MF948629	–	MF953164
Dendryphiella paravinosa	**CPC 26176**	**KX228257**	**KX228309**	**–**	**–**
Dendryphiella vinosa	MFLU 200444	MT907477	MT907480	–	–
Dictyocheirospora aquatica	**KUMCC 15-0305**	**KY320508**	**KY320513**	**–**	**–**
Dictyocheirospora bannica	**KH 332**	**LC014543**	**AB807513**	**AB787223**	**AB808489**
Dictyocheirospora bannica	MFLU 18-1040	MH381765	MH381774	MH381759	–
Dictyocheirospora garethjonesii	**MFLUCC 16-0909**	**KY320509**	**KY320514**	**–**	**–**
Dictyocheirospora garethjonesii	DLUCC 0848	MF948623	MF948631	–	MF953166
Dictyocheirospora pseudomusae	yone 234	LC014550	AB807520	AB797230	AB808496
Dictyocheirospora pseudomusae	KH 412	LC014549	AB807516	AB797226	AB808492
Dictyocheirospora heptaspora	DLUCC 1992	MT756244	MT756243	–	MT776563
Dictyocheirospora rotunda	**MFLUCC 14-0293**	**KU179099**	**KU179100**	**KU179101**	**–**
Dictyocheirospora rotunda	MFLUCC 17-0222	MH381764	MH381773	MH381758	MH388818
Dictyosporium alatum	**ATCC 34953**	**NR–077171**	**DQ018101**	**DQ018080**	**–**
Dictyosporium bulbosum	yone 221	LC014544	AB807511	AB797221	AB808487
Dictyosporium digitatum	KT 2660	LC014546	AB807518	AB797228	–
Dictyosporium digitatum	KH 401	LC014545	AB807515	AB797225	AB808491
Dictyosporium digitatum	yone 280	LC014547	AB807512	AB797222	AB808488
Dictyosporium elegans	NBRC 32502	DQ018087	DQ018100	DQ018079	–
Dictyosporium hughesii	KT 1847	LC014548	AB807517	AB797227	AB808493
Dictyosporium meiosporum	MFLUCC 10-0131	KP710944	KP710945	KP710946	–
Dictyosporium nigroapice	MFLUCC 17-2053	MH381768	MH381777	MH381762	MH388821
Dictyosporium olivaceosporum	**KH 375**	**LC014542**	**AB807514**	**AB797224**	**AB808490**
Dictyosporium pandanicola	MFLUCC 18-0331	MZ490792	MZ490776	–	MZ501208
Dictyosporium stellatum	**CCFC 241241**	**NR–154608**	**JF951177**	**–**	**–**
Dictyosporium strelitziae	**CBS 123359**	**NR–156216**	**FJ839653**	**–**	**–**
Dictyosporium tetrasporum	KT 2865	LC014551	AB807519	AB797229	AB808495
Dictyosporium thailandicum	MFLUCC 13-0773	KP716706	KP716707	–	–
Dictyosporium tratense	**MFLUCC 17-2052**	**MH381767**	**MH381776**	**MH381761**	**MF388820**
Digitodesmium bambusicola	CBS 110279	DQ018091	DQ018103	–	–
Gregarithecium curvisporum	**KT 922**	**AB809644**	**AB80754**	**AB797257**	**AB808523**
Jalapriya pulchra	**MFLU 17-1683**	**MF948628**	**MF948636**	**–**	**MF953171**
Jalapriya toruloides	CBS 209.65	DQ018093	DQ018104	DQ018081	–
Periconia igniaria	CBS 379.86	LC014585	AB807566	AB797276	AB808542
Periconia igniaria	CBS 845.96	LC014586	AB807567	AB797277	AB808543
Pseudocoleophoma calamagrostidis	**KT 3284**	**LC014592**	**LC014609**	**LC014604**	**LC014614**
Pseudocoleophoma flavescens	CBS 178.93	–	GU238075	GU238216	–
Pseudocoleophoma polygonicola	**KT 731**	**AB809634**	**AB807546**	**AB797256**	**AB808522**
Pseudocoleophoma zingiberacearum	NCYUCC 190054	MN615941	MN616755	–	MN629283
Pseudodictyosporium elegans	**CBS 688.93**	**MH862454**	**MH874101**	**DQ018084**	**–**
Pseudodictyosporium thailandica	**MFLUCC 16-0029**	**KX259520**	**KX259522**	**KX259524**	**KX259526**
Pseudodictyosporium wauense	**CBS 126094**	**MH864014**	**MH875472**	**–**	**–**
Trichobotrys effusa	FS524	MN545626	–	–	–
Trichobotrys effusa	YMJ1179	KJ630313	–	–	–
*Trichobotrys effusa****	JAUCC 6359	PP406377	PP407503	PP407508	PP405621
*Trichobotrys effusa****	JAUCC 6826	PP830649	PP830650	PP830652	PP845300
Trichobotrys meilingensis*	**JAUCC 4985**	**PP406380**	**PP407504**	**PP407509**	**PP405623**
*Trichobotrys meilingensis****	JAUCC 4986	PP406381	PP407505	PP407510	PP405625
Trichobotrys yunjushanensis*	**JAUCC 4987**	**PP406378**	**PP407506**	**PP407511**	**PP405622**
*Trichobotrys yunjushanensis****	JAUCC 4988	PP406379	PP407507	PP407512	PP405624

Ex-type strains or type materials are marked in bold. Newly generated sequences are indicated with "*". "–", the sequence is unavailable.

sequence similarity with *T. effusa* (JAUCC 6359 and JAUCC6826), respectively, but are less similar to *Gregarithecium curvisporu*m [95.75% (181 different loci) and 95.53% (190 different loci), respectively]. In addition, there are 57 different loci between the sequences of the two new species.

The topologies of the phylogenetic trees produced by ML and BI are congruent, and the best RAxML tree with BS and PP is shown in Fig. 1. Phylogenetic analyses indicate that the new *Trichobotrys effusa* isolates (JAUCC 6359 and JAUCC 6826) cluster with other *T. effusa* collections (FS524 and YMJ1179) in a strongly-supported monophyletic clade (BS/PP = 100/1). Moreover, *T. yunjushanensis* is sister to the *T. effusa* clade, but only with low ML bootstrap support values (BS = 43) and Bayesian posterior probabilities (PP = 0.67). However, these two species and *T. meilingensis* form a well- supported clade (BS/PP = 100/1), which is phylogenetically close to *Gregarithecium curvisporum* (BS/PP = 100/1).

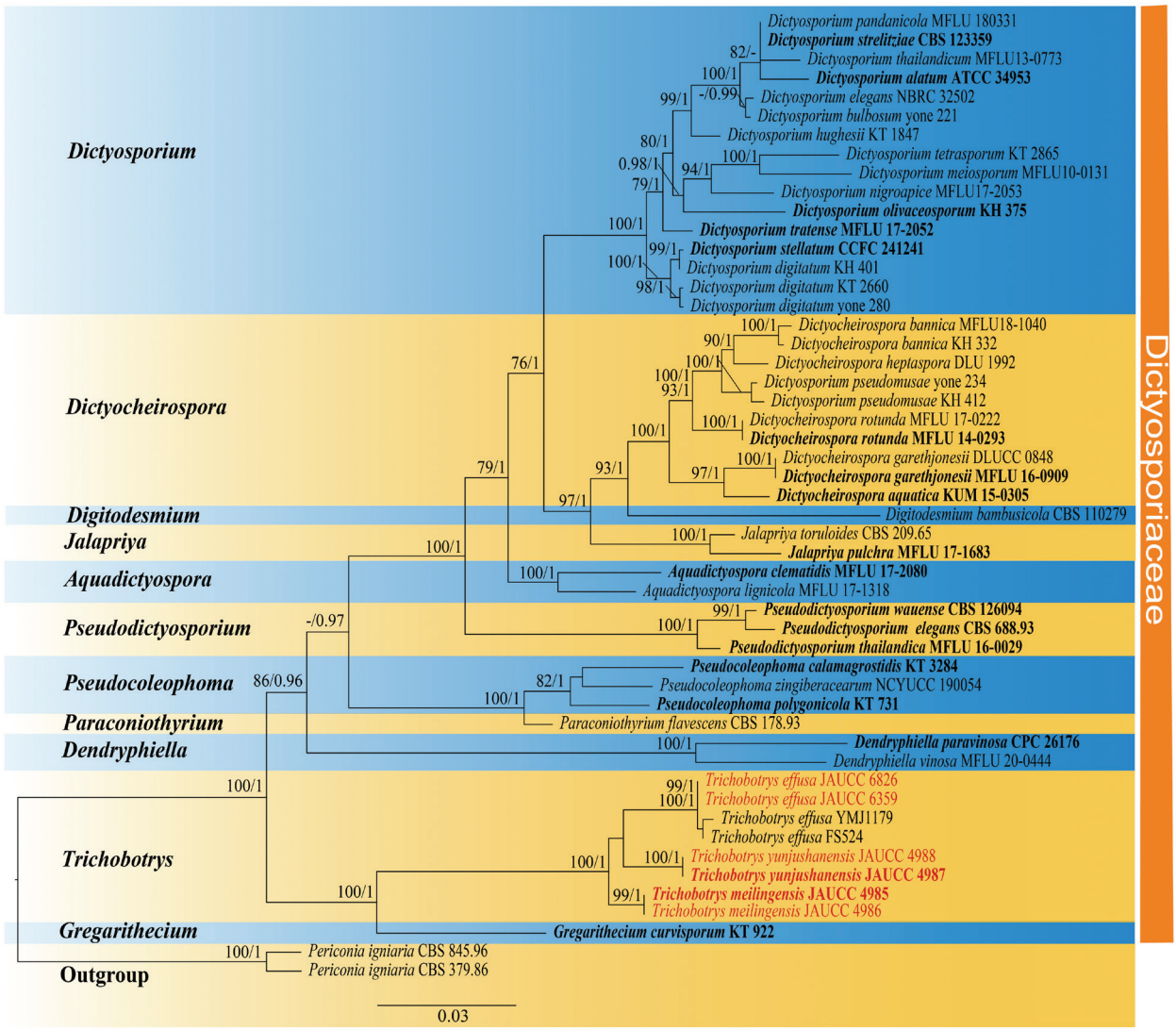

Figure 1. Phylogenetic tree of Dictyosporiaceae inferred from the combined regions (ITS-LSU-SSU-*tef1-α*) using Maximum Likelihood (ML) analysis. The *Periconia igniaria* clade was used as the outgroup. PP ≥ 0.95 and BS ≥ 75% were indicated around the branches. The new sequences generated in this study are given in red and type strains are in bold.

Taxonomy

***Trichobotrys meilingensis* G. P. Xu & Z. J. Zhai, sp. nov.**
MycoBank No: 852617
Fig. 2

Etymology. Referring to the collection site of the Meiling Mountain in Jiangxi Province, China.

Holotype. HFJAU10042.

Description. Saprobic on the stems of bamboo in freshwater habitats. **Sexual morph:** Undetermined. **Asexual morph:** Hyphomycetous. ***Colonies*** effuse, white to yellow, hairy. ***Mycelium*** partly superficial, partly immersed, gregarious and creeping, composed of septate, branched, pale brown hyphae. ***Conidiophores*** 2.5–4.5 µm wide ($\bar{x}$ = 3.5 µm, n = 20), up to 510 µm long, mononematous, variously curved, dichotomously branched in the conidiophore, septate, thick-walled, verruculose, echinulate, brown to dark brown. ***Conidiophore branches*** 15–39 × 3–4 µm ($\bar{x}$ = 24.5 × 3.4 µm, n = 15), fertile, 0–1(–2)-septate, verruculose, pale to dark brown. ***Conidiogenous cells*** 7–12 × 3–5 µm ($\bar{x}$= 9.0 × 4.0 µm, n = 10), polyblastic, integrated, erect or curved, widely distributed in the fertile branches, denticulate, hyaline to brown. ***Conidia*** 7–13 µm diam ($\bar{x}$ = 9.8 µm, n = 30), catenate, usually in branched, acropetal chains, aseptate, globose, verruculose, echinulate, sometimes guttulate, yellow brown to dark brown.

Cultural characteristics. Conidia germinating on PDA within 24 h. Colonies incubated on PDA media at 25 °C attaining 30.5 mm diam after 9 days, in natural light, circular, white, slightly cottony, yellow at the margin part, with white dense aerial mycelium; reverse yellow, white at the entire margin.

Material examined. China. Jiangxi Province: Nanchang City, Meiling Mountain, on decaying bamboo culms submerged in a freshwater stream, alt. 305 m, near 28.79°N, 115.72°E, 16 August 2021, G. P. Xu, Y. Liu and Z. J. Zhai, SLT-32 (HFJAU10042, ***holotype***), ex-type living culture, JAUCC 4985 = JAUCC 4986.

Notes. *Trichobotrys meilingensis* is similar to other species of *Trichobotrys* in having monomatous conidiophores, spherical and echinulate conidia, and polyblastic conidiogenous cells. *Trichobotrys meilingensis* is easily distinguished from *T. effusa*, *T. ipomoeae* and *T. trechispora* by its dichotomously branched conidiophores and its conidial size (7–13 µm vs. 3–4 µm, 13–15.5 µm and 3–5 µm, respectively) (Petch 1917, 1924; Sawada 1959). *Trichobotrys meilingensis* is morphologically most similar to *T. ramosa* and shares some characteristics, such as dichotomously branched conidiophores and catenate conidia. However, *T. meilingensis* has larger conidia (7–13 µm vs. 3–5 µm) and thinner conidiophores (2.5–4.5 µm vs. 8–18 µm) (D'Souza and Bhat 2001). Therefore, *T. meilingensis* can be distinguished from *T. ramosa* based on morphological characters in spite of the unavailable molecular data of the latter species. Thus, it should be identified as an independent taxon in *Trichobotrys*. A comparison of morphological features of *Trichobotrys* species is provided in Table 2.

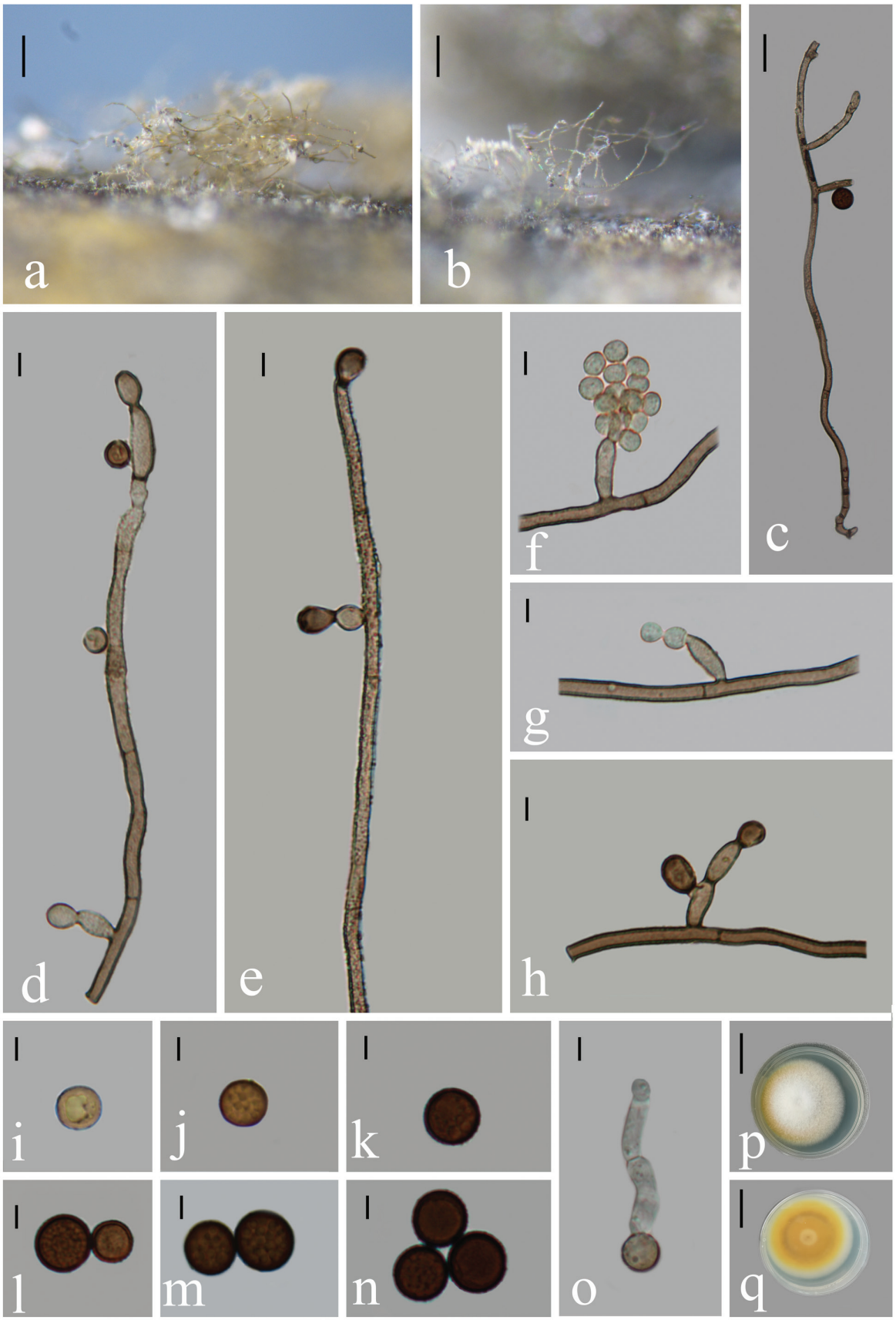

Figure 2. *Trichobotrys meilingensis* (HFJAU10042, holotype) **a, b** colonies on bamboo culms **c–e** conidiophores with conidiogenous cells **f** portion of conidiophore with fertile lateral branches **g, h** conidiogenous cells **i–n** conidia **o** germinating conidium **p, q** culture on PDA from above (**p**) and reverse (**q**). Scale bars: 100 µm (**a, b**); 20 µm (**c**); 5 µm (**d–o**); 25 mm (**p, q**).

Trichobotrys yunjushanensis **W. J. Zhang & Z. J. Zhai, sp. nov.**
MycoBank No: 852618
Fig. 3

Etymology. Referring to the collection site of the Yunjushan Mountain in Jiangxi Province, China.

Holotype. HFJAU 10044.

Description. Saprobic on decaying bamboo culms. **Sexual morph:** Undetermined. **Asexual morph:** Hyphomycetous. ***Colonies*** effuse, white, yellow to olivaceous, velvety. ***Mycelium*** mostly superficial, creeping and twining, composed of

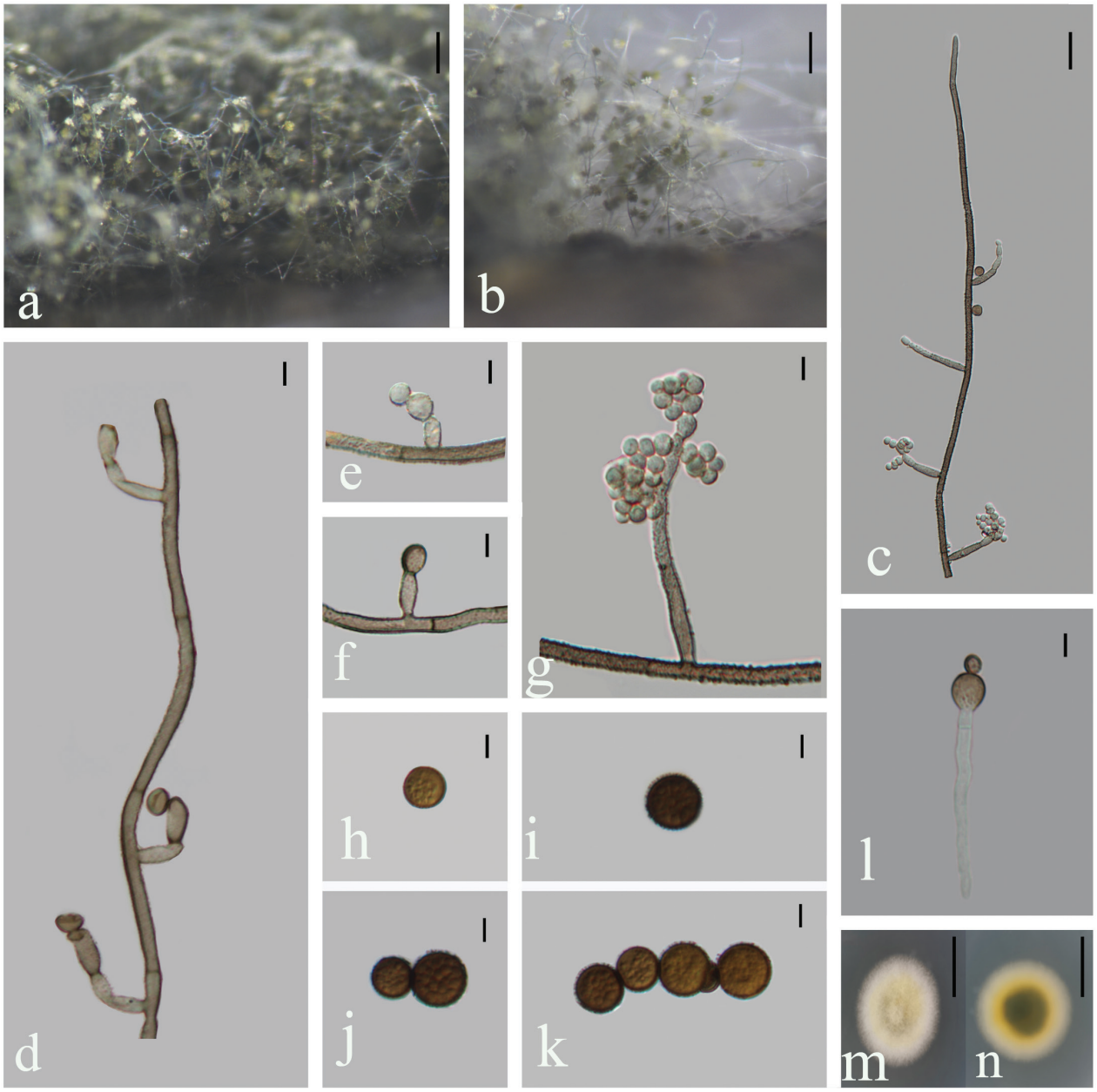

Figure 3. *Trichobotrys yunjushanensis* (HFJAU 10044, holotype) **a, b** colonies on bamboo culm **c, d** conidiophores with conidiogenous cells **e, f** conidiogenous cell with conidia **g** portion of conidiophore with fertile lateral branches **h–k** conidia **l** germinating conidium **m, n** culture on PDA from above (**m**) and reverse (**n**). Scale bars: 100 µm (**a, b**); 20 µm (**c**); 5 µm (**d–l**); 25 mm (**m, n**).

septate, brown to olivaceous, branched hyphae. ***Conidiophores*** 3–4 µm wide ($\bar{x}$ = 3.4 µm, n = 20), up to 1150 µm long, mononematous, erect, straight or flexous, septate, with fertile dichotomously branched, pale brown to olivaceous, verruculose, echinulate, thick-walled. ***Conidiophores branches*** 18–48 × 3–4 µm ($\bar{x}$ = 29.1 × 3.6 µm, n = 15), sometimes long, fertile, 0–1(–2)-septate, verruculose, rough, pale brown. ***Conidiogenous cells*** 6–11 ×3–5 µm ($\bar{x}$ = 8.5 × 4.0 µm, n = 10), integrated, polyblastic, terminal to subterminal on fertile branches, with several denticulate conidiogenous loci, hyaline to dark brown. ***Conidia*** 7–12 µm diam ($\bar{x}$ = 9.3 µm, n = 30), catenate, usually acrogenous or lateral, aseptate, spherical, verrucose, echinulate, sometimes guttulate, yellowish brown to dark brown when mature.

Cultural characteristics. Conidia germinating on PDA within 24 h. Colonies incubated on PDA media at 25 °C grow rapidly, reaching 21 mm diam after 6 days, in natural light, circular, pale on the margin, yellow at the centre, with white dense aerial mycelium; reverse yellow white to dark green. Hyphae hypline, superficial, septate but not obvious, with a layer of yellow pigment, 1.9–3.7 µm wide.

Material examined. China. Jiangxi Province: Jiujiang City, Yongxiu County, Yunjushan Mountain, on decaying bamboo culms submerged in a freshwater stream, alt. 672.5 m, 29.23°N, 115.59°E, 28 April 2020, G. P. Xu, Y. Liu and Z. J. Zhai, YJS112 (HFJAU10044, ***holotype***), ex-type living culture, JAUCC 4987 = JAUCC 4988.

Notes. In the multi-gene phylogenetic tree, *Trichobotrys yunjushanensis* groups with *T. effusa* clade with low support (BS/PP = 43/0.67), but they form a monophyletic group when including *T. meilingensis* (Fig. 1). Morphologically, *T. yunjushanensis* is distinct from the holotype of *T. effusa* by its conidial size (7–12 µm vs. 3–4 µm) and longer conidiophores (up to 1150 µm vs. up to 200 µm) (Petch 1924). *Trichobotrys yunjushanensis* is mostly similar to *T. meilingensis* and *T. ramosa* in having dichotomously branched and rough conidiophores. However, *T. yunjushanensis* can be easily distinguished from *T. ramosa* by its larger conidia (7–12 µm vs. 3–5 µm) (D'Souza and Bhat 2001). Furthermore, *T. yunjushanensis* differs from *T. meilingensis* in having longer conidiophores (up to 1150 µm vs. up to 510 µm) and is phylogenetically distinct from the latter. Therefore, both morphological characters and phylogenetic analyses supported *T. yunjushanensis* as a new taxon within *Trichobotrys*.

Trichobotrys effusa **(Berk. & Br.) Petch, Ann. R. bot. Gdns Peradeniya 9: 169 (1924)**

Fig. 4

Description. Saprobic on the stems of decaying wood in freshwater habitat. **Sexual morph:** Undetermined. **Asexual morph:** Hyphomycetous. ***Colonies*** effuse, grayish to nut brown, velvety. ***Mycelium*** mostly superficial, creeping and twining, composed of septate, branched, subhyaline to pale brown hyphae. ***Conidiophores*** 2–4 µm wide ($\bar{x}$ = 2.7 µm, n = 20), up to 650 µm long, mononematous, erect, straight or somewhat curving, columniform, moderately branched, verruculose, septate, thick-walled, echinulate, light brown to nut brown, gradually attenuated distally to an infertile, setiform apex. ***Conidiophore branches*** 7–26 × 2–4 µm ($\bar{x}$ = 14.0 × 3.2 µm, n = 16), fertile, 0–1(–2)-septate, verruculose, light brown to dark brown, individual cells typically have a slight swelling. ***Conidiogenous cells***

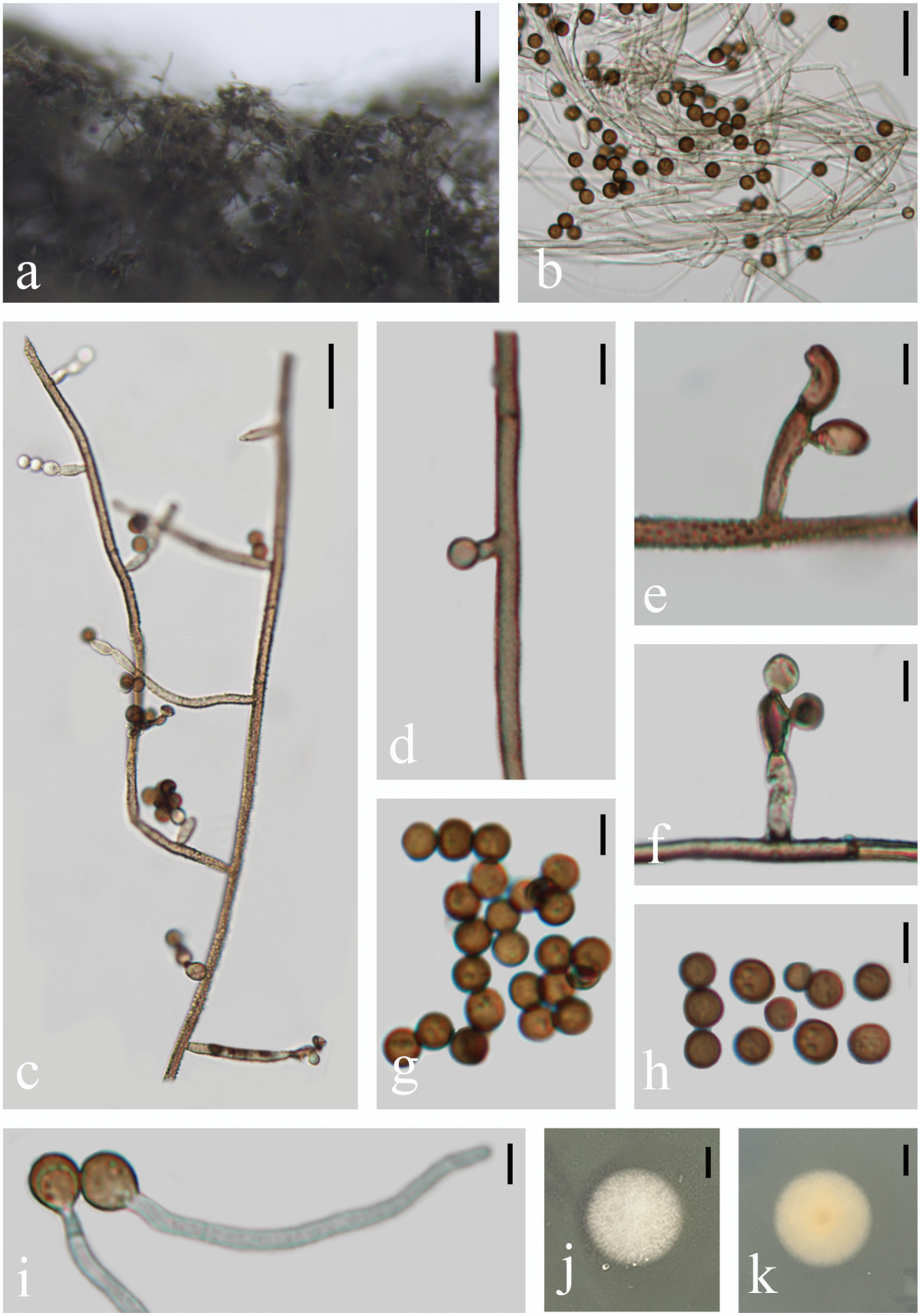

Figure 4. *Trichobotrys effusa* (HFJAU10296, HFJAU10372) **a** colonies on the substrate **b** conidiophores with conidia **c** portion of conidiophore with fertile lateral branches **d–f** conidiogenous cell with conidia **g, h** conidia **i** germinating conidia **j, k** culture on PDA from above (**j**) and reverse (**k**). Scale bars: 100 μm (**a**); 20 μm (**b, c**); 5 μm (**d–i**); 5 mm (**j, k**).

3–10.5 × 2.5–6.5 µm ($\bar{x}$ = 6.6 × 4.0 µm, n = 10), monoblastic or polyblastic, integrated and terminal on lateral branches, apical or lateral; columniform or cannulate, erect or slightly curved, with several seriated conidiogenous locations, light brown to dark brown. ***Conidia*** 3.5–5 µm diam ($\bar{x}$ = 4.4 µm, n = 30), catenulate, simple or branched apical chains, aseptate, spherical, verruculose, echinulate, sometimes guttulate, transparent to dark brown or red brown.

Cultural characteristics. Conidia germinating on PDA within 24 h. Colonies incubated on PDA media at 25 °C attaining 11.5 mm diam after 11 days, in natural light, circular, white, cottony, with white dense aerial mycelium; reverse yellow, white at the margin part.

Material examined. China. Guangxi Province: Guigang City, Pingtianshan National Forest Park, on decaying wood submerged in a freshwater stream, alt. 980.84 m, near 23.19°N, 109.51°E, 11 March 2023 and 16 May 2024, Wan Hu and Z. J. Zhai, HG13 and HG13-1 (HFJAU10296, HFJAU10372), ex-type living culture, JAUCC 6359 = JAUCC 6826.

Notes. According to phylogenetic analysis (Fig. 1), we can find that our new isolates cluster with *Trichobotrys effusa* FS524 and *T. effusa* YMJ1179 with high support (BS/PP = 100/1). Morphologically, our new collections are similar to the holotype of *T. effusa* except for the slightly larger conidia (3.5–5 µm vs. 3–4 µm), longer conidiophores (up to 650 µm vs. up to 200 µm), and slightly different colors in mycelium (grayish to nut-brown vs. dark purple-brown) (Petch 1924). The difference in color might be due to the discrepancy in incubation time and the exposure to light or different observation angles under the microscope. The differences in the size of conidiophores and conidia are also occurring in another record of *T. effusa*, in which the conidiophores and conidia are described as being up to 1000 µm long and 5–7µm in diameter, respectively (Morgan-Jones et al. 1987). The differences among the holotype and our new collections suggest that factors such as habitat and incubation time may influence the size of conidia and conidiophores. Similar observations have also been discovered in the asexual morph of other fungal species (Yang et al. 2018b; Zhang et al. 2022; Shen et al. 2024). Owing to the unavailable molecular sequences in the holotype of *T. effusa* and the deficiency of morphological descriptions about *T. effusa* FS524 and *T. effusa* YMJ1179, the possibility cannot be excluded that our new isolates are a different species to *T. effusa*. However, there are no significant morphological differences between our collections and the holotype. Therefore, we propose to identify the new collections as *T. effusa* until more strains have been examined. The new collection was collected from submerged, decaying wood in Guangxi Province, which is a new discovery in freshwater habitat in China.

Discussion

The new isolates *Trichobotrys effusa* (JAUCC 6359 and JAUCC 6826) group well with two strains (FS524 and YMJ1179) of *T. effusa* (BS/PP = 100/1). The high molecular support and morphological similarities among them indicate that they are conspecific and the two isolates (JAUCC 6359 and JAUCC 6826) are identified as a new record of *T. effusa*. Although four-loci data for *T. effusa* FS524 and *T. effusa* YMJ1179 were lacking and they were sequenced only by ITS, our result should be convincing because the fungal ITS marker generally

produces considerably more sequence variability, and thus can provide high resolution for species delimitation (Nilsson et al. 2008; Szczepańska et al. 2021). The holotype of *T. effusa* was discovered on dead bamboo from Sri Lanka (Berkeley and Broome 1873; Petch 1924). Subsequently, a series of *T. effusa* strains have been found but were mostly isolated from marine sediment samples collected in the South China Sea (Chen et al. 2014; Sun et al. 2015, 2016; Chen et al. 2020; Liu et al. 2020; Huang et al. 2023), and they were identified as *T. effusa* almost only based on ITS region sequence comparison with the GenBank database. This study is the first report of collection of *T. effusa* from the freshwater habitat and provides both molecular phylogenetical and morphological description for this species.

Two new species, *T. meilingensis* and *T. yunjushanensis*, were proposed as members of *Trichobotrys* based on four-loci (ITS, LSU, SSU and *tef1-α*) phylogenetic analyses in combination with morphological characteristics. However, the relationship between *T. yunjushanensis* and the *T. effusa* clade was unresolved due to low support value. At present, the clade including *T. meilingensis*, *T. yunjushanensis* and *T. effusa* is paraphyletic, therefore, the phylogeny relationships within this clade will become clearer with more new closely related species discovered. Besides, D'Souza and Bhat (2001) described *T. ramosa* from the forest of southern India, but no molecular data of these species are available, so it is difficult to clarify the phylogenetic relationship between this species and other taxa in *Trichobotrys*. However, *T. meilingensis* and *T. yunjushanensis* can be distinguished from *T. ramosa* by morphological characteristics. Detailed information about their morphological comparison can be obtained from the notes and Table 2 in this paper.

Trichobotrys appears as sister to *Gregarithecium* with high molecular support and is hence assigned to the family Dictyosporiaceae. The asexual morphs of *Trichobotrys* also mostly resemble other members of Dictyosporiaceae in possessing brown, cheirosporous conidia, produced from holoblastic conidiogenous cells, on micronematous conidiophores (Boonmee et al. 2016). Although we consider that species of *Trichobotrys* are closely related to *Gregarithecium*, the position of *Trichobotrys* in Dictyosporiaceae and relationship between the two genera are still doubtful due to the long branches between *Gregarithecium* and *Trichobotrys* clade and the lack of asexual morph of *Gregarithecium*. Hence, more samples closely related to *Gregarithecium* and *Trichobotrys* are required to be discovered to clarify the position of *Trichobotrys* in Dictyosporiaceae.

It has been widely reported that *Trichobotrys effusa* as the type species of *Trichobotrys* has the ability to produce diverse secondary metabolites (Chen et al. 2014; Chen et al. 2020; Huang et al. 2023; Liu et al. 2020; Sun et al. 2015, 2016). For example, Chen et al. (2014) obtained four novel aliphatic phenolic ethers with growth-inhibitory activity against the A549 lung cancer cell and Sun et al. (2016) received three new macrodiolides with antifouling activity. In this research, we introduce two novel species, *T. meilingensis* and *T. yunjushanensis*, which are both morphologically and phylogenetically similar to *T. effusa*. Furthermore, these two species both can produce yellow pigments and might have the ability to generate secondary metabolites like *T. effusa*. Therefore, future pharmacological evaluation of the two new species might be worth studying to confirm if they are similar to *T. effusa* in having similar bioactive constituents and function in secondary metabolites.

Table 2. Synopsis of morphological characteristics, habitats, hosts and district compared across *Trichobotrys* species.

Species	Conidiophores (μm)	Conidia (μm)	Conidiophores characteristics	Conidia characteristics	Habitat	Host	District	References
Trichobotrys effusa	Up to 200 × 3–4 or up to 1000 × 4–6	3–4 or 5–7	Equal, septate, with short lateral branches, thick walled, minutely verrucose	Globose, red-brown or brown, minutely verrucose	Freshwater	On fallen leaves of dead bamboo or decorticated wood	Sri Lanka and South Africa	Berkeley and Broome (1873); Petch (1924); Morgan-Jones et al. (1987)
T. effusa	**Up to 650 × 2–4**	**3.5–5**	**Mononematous, erect, with short lateral branches, verruculose, septate, thick-walled, light brown to nut brown**	**Spherical, verruculose, echinulate, transparent to dark brown or red brown**	**Freshwater**	**On Dead wood**	**China, Guangxi**	**This study**
T. ipomoeae	195–440 × 13–16	13–15.5	Simple, cylindrical, 2–3 septate, dark brown	Spherical, verrucose, brown	Terrestrial	On the leaves of *ipomoea pescaprae*	China, Taiwan	Sawada (1959)
T. meilingensis	**Up to 510 × 2.5–4.5**	**7–13**	**Mononematous, dichotomously branched in the conidiophore, septate, echinulate, brown to dark brown**	**Aseptate, globose, verruculose, echinulate, yellow brown to dark brown**	**Freshwater**	**On submerged bamboo culms**	**China, Jiangxi**	**This study**
T. ramose	330–600 × 8–18	3–5	Mononematous, erect, straight or flexous, septate, dichotomously branched in the above half, dark to reddish brown, verruculose	Dry, catenate, usually in branched, acropetal chains, spherical, dark brown, verruculose, aseptate	Terrestrial	On dead leaves of *Dendrocalamus strictus*	India, Goa	D'souza et al. (2001)
T. trechispora	Up to 1500 × 8–12	5 × 3 (oval) or 4 (spherical)	Erect, olivaceous, septate, everwhere minutely spinulose	Oval or spherical, ornamented with sharp, raised, broken ridges	Terrestrial	On dead wood	Sri Lanka, Peradeniya	Petch (1917)
T. yunjushanensis	**Up to 1150 × 3–4**	**7–12**	**Mononematous, dichotomously branched in the conidiophore, septate, echinulate, pale brown to olivaceous**	**Aseptate, spherical, verrucose, echinulate, yellowish brown to dark brown when mature**	**Freshwater**	**On submerged bamboo culms**	**China, Jiangxi**	**This study**

Acknowledgements

We are grateful to Wan Hu and Yi Yang (School of Agricultural Sciences, Jiangxi Agricultural University) for the valuable advice in the context of this study.

Additional information

Conflict of interest

The authors have declared that no competing interests exist.

Ethical statement

No ethical statement was reported.

Funding

This study was supported by the National Natural Science Foundation of China (NSFC 32070023 and NSFC 32060014), the Natural Science Foundation of Jiangxi Province (20151BAB214002) and Science and Technology Plan Project of Jiangxi Province (GJJ160417).

Author contributions

Gui-Ping Xu, Yu Liu and Zhi-Jun Zhai collected samples. Wen-Jing Zhang, Gui-Ping Xu and Yu Liu performed morphological identification, photo-plates, DNA isolation and PCR amplifcation. Wen-Jing Zhang, Gui-Ping Xu, Deng-Mei Fan and Zhi-Jun Zhai analyzed data and wrote the original draft. Yang Gao, Hai-Yan Song, Hai-Jing Hu, Jian-Ping Zhou and Ming-Hui Chen reviewed the paper. Zhi-Jun Zhai and Dian-Ming Hu designed the research and revised the manuscript. All authors approved the final manuscript version.

Author ORCIDs

Wen-Jing Zhang https://orcid.org/0009-0001-2962-498X
Deng-Mei Fan https://orcid.org/0000-0001-9825-8605
Dian-Ming Hu https://orcid.org/0000-0002-4750-2871
Zhi-Jun Zhai https://orcid.org/0009-0008-7562-9707

Data availability

All of the data that support the findings of this study are available in the main text.

References

Berkeley MJ, Broome CE (1873) Enumeration of the fungi of Ceylon, Part II. Journal of the Linnean Society. Botany 14: 100. https://doi.org/10.1111/j.1095-8339.1873.tb00301.x

Boonmee S, D'Souza MJ, Luo ZL, Pinruan U, Tanaka K, Su HY, Bhat DJ, McKenzie EHC, Jones EBG, Taylor JE, Phillips AJL, Hirayama K, Eungwanichayapant PD, Hyde KD (2016) Dictyosporiaceae fam. nov. Fungal Diversity 80(1): 457–482. https://doi.org/10.1007/s13225-016-0363-z

Chen JJ, Wang SW, Hsiao HY, Lee MS, Ju YM, Kuo YH, Lee TH (2014) Aliphatic phenolic ethers from *Trichobotrys effusa*. Journal of Natural Products 77(5): 1097–1101. https://doi.org/10.1021/np400776y

Chen SC, Liu ZM, Chen YC, Tan HB, Li SN, Liu HX, Zhang WM, Zhu S (2020) Highly substituted phenol derivatives with nitric oxide inhibitory activities from the deep-sea-

derived fungus *Trichobotrys effusa* FS524. Marine Drugs 18(3): 134. https://doi.org/10.3390/md18030134

Chomnunti P, Hongsanan S, Aguirre-Hudson B, Tian Q, Peršoh D, Dhami MK, Alias AS, Xu J, Liu X, Stadler M, Hyde KD (2014) The sooty moulds. Fungal Diversity 66(1): 1–36. https://doi.org/10.1007/s13225-014-0278-5

D'Souza MA, Bhat DJ (2001) A new species of *Trichobotrys* from the western ghat forests, India. Mycotaxon 80: 105–108.

Darriba D, Taboada GL, Doallo R, Posada D (2012) jModelTest 2: More models, new heuristics and parallel computing. Nature Methods 9(8): 772. https://doi.org/10.1038/nmeth.2109

Doyle JJ, Doyle JL (1987) A rapid DNA isolation procedure for small quantities of fresh leaf tissue. Phytochemical Bulletin 19: 11–15.

Hall TA (1999) BioEdit: a user-friendly biological sequence alignment editor and analysis program for Windows 95/98/NT. Nucleic Acids Symposium Series, 95–98.

Hopple Jr JJ, Vilgalys R (1999) Phylogenetic relationships in the mushroom genus *Coprinus* and dark-spored allies based on sequence data from the nuclear gene coding for the large ribosomal subunit RNA: Divergent domains, outgroups, and monophyly. Molecular Phylogenetics and Evolution 13(1): 1. https://doi.org/10.1006/mpev.1999.0634

Huang HB, Chen YC, Wen TY, Li SN, Liu ZM, Zhang WM, Gao XX (2023) Anti-Inflammatory phomalones from the deep-sea-derived fungus *Trichobotrys effuse* FS522. Chemistry & Biodiversity 20(12): e202301512. https://doi.org/10.1002/cbdv.202301512

Liu NG, Hongsanan S, Yang J, Lin CG, Bhat DJ, Liu JK, Jumpathong J, Boonmee S, Hyde KD, Liu ZY (2017) *Dendryphiella fasciculata* sp. nov. and notes on other *Dendryphiella* species. Mycosphere: Journal of Fungal Biology 8(9): 1575–1586. https://doi.org/10.5943/mycosphere/8/9/12

Liu HX, Chen SC, Zhang X, Dong CM, Chen YC, Liu ZM, Tan HB, Zhang WM (2020) Structural elucidation, total synthesis, and cytotoxic activity of effphenol A. Organic & Biomolecular Chemistry 18(44): 9035–9038. https://doi.org/10.1039/D0OB01985B

Madeira F, Park YM, Lee J, Buso N, Gur T, Madhusoodanan N, Basutkar P, Tivey ARN, Potter SC, Finn RD, Lopez R (2019) The EMBL-EBI search and sequence analysis tools APIs in 2019. Nucleic Acids Research 47(W1): W636–W641. https://doi.org/10.1093/nar/gkz268

Miller MA, Pfeiffer W, Schwartz T (2010) Creating the CIPRES Science Gateway for inference of large phylogenetic trees. Proceedings of the 2010 gateway computing environments workshop (GCE), New Orleans, Louisiana, 7 pp. https://doi.org/10.1109/GCE.2010.5676129

Morgan-Jones G, Sinclair RC, Eicker A (1987) Notes on Hyphomycetes. LV *Craneomvces* gen.nov. and *Trichobotrys effusa*. Mycotaxon 30: 345–350.

Nilsson RH, Kristiansson E, Ryberg M, Hallenberg N, Larsson KH (2008) Intraspecific ITS variability in the kingdom fungi as ex-pressed in the international sequence databases and its implications for molecular species identification. Evolutionary Bioinformatics Online 4: 193–201. https://doi.org/10.4137/EBO.S653

Petch T (1917) Additions to ceylon fungi. Annals of the Royal Botanic Gardens Peradeniya 6(3): 246. https://doi.org/10.2307/4111564

Petch T (1924) Revisions of ceylon fungi. Annals of the Royal Botanic Gardens Peradeniya 9: 169.

Rambaut A (2018) FigTree v1.4.4: Tree figure drawing tool. https://github.com/rambaut/figtree/releases

Rehner SA, Buckley E (2005) A Beauveria phylogeny inferred from nuclear ITS and EF1-a sequences: Evidence for cryptic diversification and links to Cordyceps teleomorphs. Mycologia 97(1): 84–98. https://doi.org/10.3852/mycologia.97.1.84

Ronquist F, Teslenko M, Van Der Mark P, Ayres DL, Darling A, Höhna S, Larget B, Liu L, Suchard MA, Huelsenbeck JP (2012) MrBayes 3.2: Efficient Bayesian phylogenetic inference and model choice across a large model space. Systematic Biology 61(3): 539–542. https://doi.org/10.1093/sysbio/sys029

Sawada K (1959) Discriptive catalogue of Taiwan (Formosan) fungi. Part XI. Special Publications of the College Agriculture National Taiwan University 8: 195.

Shen HW, Bao DF, Boonmee S, Lu YZ, Su XJ, Li YX, Luo ZL (2024) Diversity of *Distoseptispora* (Distoseptisporaceae) taxa on submerged decaying wood from the Red River in Yunnan, China. MycoKeys 102: 1–28. https://doi.org/10.3897/mycokeys.102.116096

Stamatakis A, Alachiotis N (2010) Time and memory efficient likelihood-based tree searches on phylogenomic alignments with missing data. Bioinformatics (Oxford, England) 26(12): i132–i139. https://doi.org/10.1093/bioinformatics/btq205

Sun YL, Wang J, Wang YF, Zhang XY, Nong XH, Chen MY, Xu XY, Qi SH (2015) Cytotoxic and antiviral tetramic acid derivatives from the deep-sea-derived fungus *Trichobotrys effuse* DFFSCS021. Tetrahedron 71(49): 9328–9332. https://doi.org/10.1016/j.tet.2015.10.010

Sun YL, Zhang XY, Nong XH, Xu XY, Qi SH (2016) New antifouling macrodiolides from the deep-sea-derived fungus *Trichobotrys effuse* DFFSCS021. Tetrahedron Letters 57(3): 366–370. https://doi.org/10.1016/j.tetlet.2015.12.026

Szczepańska K, Guzow-Krzemińska B, Urbaniak J (2021) Infraspecific variation of some brown Parmeliae (in Poland) – a comparison of ITS rDNA and non-molecular characters. MycoKeys 85: 127–160. https://doi.org/10.3897/mycokeys.85.70552

Tanaka K, Harada Y (2003) Pleosporales in Japan (3). The genus *Massarina*. Mycoscience 44(3): 173–185. https://doi.org/10.1007/S10267-003-0102-7

Tanaka K, Hirayama K, Yonezawa H, Sato G, Toriyabe A, Kudo H, Hashimoto A, Matsumura M, Harada Y, Kurihara Y, Shirouzu T, Hosoya T (2015) Revision of the Massarineae (Pleosporales, Dothideomycetes). Studies in Mycology 82(1): 75–136. https://doi.org/10.1016/j.simyco.2015.10.002

White TJ, Bruns TD, Lee SB, Taylor JW, Innis MA, Gelfand DH, Sninsky JJ (1990) Amplification and direct sequencing of Fungal Ribosomal RNA Genes for phylogenetics. Academic Press, San Diego, 315–322. https://doi.org/10.1016/B978-0-12-372180-8.50042-1

Yang J, Liu JK, Hyde KD, Jones EBG, Liu ZY (2018a) New species in *Dictyosporium*, new combinations in *Dictyocheirospora* and an updated backbone tree for Dictyosporiaceae. MycoKeys 36: 83–105. https://doi.org/10.3897/mycokeys.36.27051

Yang J, Maharachchikumbura SSN, Liu JK, Hyde KD, Jones EBG, Al-Sadi AM, Liu ZY (2018b) *Pseudostanjehughesia aquitropica* gen. et sp. nov. and *Sporidesmium sensu lato* species from freshwater habitats. Mycological Progress 17(5): 591–616. https://doi.org/10.1007/s11557-017-1339-4

Zhai ZJ, Yan JQ, Li WW, Gao Y, Hu HJ, Zhou JP, Song HY, Hu DM (2022) Three novel species of *Distoseptispora* (Distoseptisporaceae) isolated from bamboo in Jiangxi Province, China. MycoKeys 88: 35–54. https://doi.org/10.3897/mycokeys.88.79346

Zhang D, Gao F, Jakovlić I, Zou H, Zhang J, Li WX, Wang GT (2020) PhyloSuite: An integrated and scalable desktop platform for streamlined molecular sequence data management and evolutionary phylogenetics studies. Molecular Ecology Resources 20(1): 348–355. https://doi.org/10.1111/1755-0998.13096

Zhang H, Zhu R, Qing Y, Yang H, Li C, Wang G, Zhang D, Ning P (2022) Polyphasic identification of *Distoseptispora* with six new species from fresh water. Journal of Fungi (Basel, Switzerland) 8(10): 1063. https://doi.org/10.3390/jof8101063

MycoKeys 106: 133–151 (2024)
DOI: 10.3897/mycokeys.106.121520

Research Article

Bottlebrush and Myrtle twig canker caused by *Neopestalotiopsis* species: an emerging canker-causing group of fungi in Italy

Dalia Aiello[1], Giorgio Gusella[1], Giuseppa Rosaria Leonardi[1], Giancarlo Polizzi[1], Hermann Voglmayr[2]

1 *Dipartimento di Agricoltura, Alimentazione e Ambiente, sez. Patologia Vegetale, University of Catania, Via S. Sofia 100, 95123 Catania, Italy*

2 *Department of Botany and Biodiversity Research, University of Vienna, Rennweg 14, 1030 Vienna, Austria*

Corresponding author: Giorgio Gusella (giorgio.gusella@unict.it)

Abstract

Pestalotioid fungi were isolated in pure culture from symptomatic plants of *Callistemon laevis*, *C. viminalis*, *Luma apiculata* (marketed as "*Myrtus luma*"), *Myrtus communis* subsp. *tarentina*, and *M. communis* var. *microphylla* (*M. communis* 'Microphylla'), showing twig canker, dieback and defoliation. The isolates were identified to species by ITS, *tef1* and *tub2* sequences, which revealed the presence of six species of *Neopestalotiopsis* (*N. camelliae-oleiferae*, *N. hispanica*, *N. iberica*, *N. rosae*, *N. rosicola*, and *N. zakeelii*) and one species of *Pestalotiopsis* (*P. biciliata*). While most species were isolated only once or twice, the majority of isolates belonged to *N. rosae* (13) and *N. hispanica* (8). Pathogenicity was investigated by pathogenicity tests on all hosts, which confirmed the pathogenicity of all *Neopestalotiopsis* species on at least some of the hosts tested, while *P. biciliata* did not cause any disease symptoms. *Neopestalotiopsis hispanica* and *N. rosae* caused symptoms in all hosts of the present study, while the other *Neopestalotiopsis* species tested showed no symptoms on *Luma apiculata*.

Key words: Bottlebrush, canker, myrtle, *Neopestalotiopsis*, phylogeny

Academic editor: Nattawut Boonyuen
Received: 23 February 2024
Accepted: 18 April 2024
Published: 21 June 2024

Citation: Aiello D, Gusella G, Leonardi GR, Polizzi G, Voglmayr H (2024) Bottlebrush and Myrtle twig canker caused by *Neopestalotiopsis* species: an emerging canker-causing group of fungi in Italy. MycoKeys 106: 133–151. https://doi.org/10.3897/mycokeys.106.121520

Introduction

The Bottlebrush (*Callistemon citrinus* (Curtis.) Skeels.) and myrtle (*Myrtus communis* L.) are evergreen shrubs belonging to Myrtaceae. Bottlebrushes refer to *Callistemon* species, a group of plants native to Australia. In recent years, Australian plants, especially *Callistemon* species, have aroused interest in Mediterranean countries as ornamental plants mainly due to their aesthetic value and great adaptability to Mediterranean environmental conditions (Lippi et al. 2003).

Little is known about fungal diseases of bottlebrush. Some species of *Calonectria* (*Ca. cylindrospora*, *Ca. mexicana*, *Ca. pauciramosa*, and *Ca. pseudomexicana*) were reported causing leaf spot, blight, stem lesion and damping-off on different accessions of bottlebrushes in Europe (Pérez-Sierra et al. 2007; Polizzi et al. 2007; Vitale et al. 2013; Aiello et al. 2022) and the African continent (Lombard et al. 2011). Other causal agents of leaf spot have been reported on *C. citrinus*, including species belonging to the genera *Alternaria*, *Botryosphaeria*, *Cercospora*, *Colletotrichum*, *Phyllosticta*, and *Selenophoma* (Alfieri et al. 1984; Pennycook et al. 1989; Gadgil 2005). Recently, in Iran the new species

Xenodidymella iranica (Didymellaceae) was isolated and described from leaf spot and blight of *C. citrinus* (Ahmadpour et al. 2022). In addition, stem canker was reportedly caused by species of *Leptosphaeria* and *Phomopsis*, stem gall by *Cophinforma tumefaciens* (syn. *Sphaeropsis tumefaciens*), and root rot diseases by *Rhizoctonia solani* and species of *Phytophthora* and *Pythium* (Alfieri et al. 1984; Shivas 1989; Erwin and Ribeiro 1996; Cacciola et al. 2009).

Myrtle is widely distributed in the Mediterranean area forming spontaneous bushes, and in Italy is particularly occurring in coastal areas and islands. Two subspecies are currently accepted within this species, *Myrtus communis* subsp. *communis* and subsp. *tarentina* (Medda and Mulas 2021; POWO 2024). Myrtle is cultivated for many different purposes such as pharmaceutical, cosmetic, ornamental (especially due to high vegetative vigor, the bright green color of the leaves, and the abundant multi-colored flowering), and food industries (Mulas et al. 1998; Medda and Mulas 2021). Although myrtle is investigated worldwide under many different aspects due to its manifold uses, few data are available regarding diseases affecting this crop. Amongst fungal diseases, leaf spot and crown and root disease caused by *Ca. mexicana*, *Ca. pauciramosa*, and *Ca. pseudomexicana* have been reported in Europe (Polizzi and Crous 1999; Henricot and Beales 2003) as well as in the United States (Koike and Crous 2001) and in Tunisia (Lombard et al. 2011).

In addition, the myrtle rust disease caused by *Austropuccinia psidii* (syn. *Puccinia psidii*) (Uredinales, Pucciniaceae) is considered an important quarantine threat (Glen et al. 2007; Fensham et al. 2020), which became notorious when it started to infect various species of the Myrtaceae (Coutinho et al. 1998; Glen et al. 2007; Carnegie et al. 2010; Morin et al. 2012; Roux et al. 2013). Recently, Italian provenances of *M. communis* were shown to be highly susceptible to *Austropuccinia psidii*, highlighting a significant threat to myrtle cultivation if the pathogen were accidentally introduced to the Mediterranean (Paap et al. 2023).

In Sicily (southern Italy), recent surveys of a nursery revealed the presence of many myrtle and bottlebrush plants affected by twig cankers and dieback. Investigations conducted in recent years in Sicily, in greenhouses and also in the field, showed an increase of these symptoms in many different crops, especially ornamental plants, caused mainly by Botryosphaeriaceae spp. (Aiello et al. 2020; Gusella et al. 2021; Costanzo et al. 2022; Fiorenza et al. 2022a). Canker-causing pathogens are under investigation worldwide for many different aspects concerning the complex etiology of the diseases, their epidemiology, wide host range and difficulties in management (Guarnaccia et al. 2022). Among the canker-causing pathogens, pestalotioid fungi have been increasingly investigated in recent years (Silva et al. 2020; Diogo et al. 2021; Fiorenza et al. 2022b; Li et al. 2022; Santos et al. 2022; Zheng et al. 2023). Maharachchikumbura et al. (2014) revised *Pestalotiopsis sensu lato* dividing it into three distinct genera, *viz. Pestalotiopsis*, *Pseudopestalotiopsis*, and *Neopestalotiopsis*. These fungi are widely distributed in tropical and temperate areas and are frequently encountered as endophytes and plant pathogens causing stem-end rot, stem and leaf blight, trunk disease, and cankers (Maharachchikumbura et al. 2014). In Sicily, recent studies of young avocado trees showing canker and wood discoloration led to the identification of two *Neopestalotiopsis* species responsible for those symptoms, namely *N. rosae* and *N. siciliana* sp. nov. (Fiorenza et al. 2022b). Moreover, Fiorenza et al. (2022b) noticed frequent necroses and

cankers at the grafting point, reinforcing the assumption that the propagation processes are crucial for pestalotioid infections (Espinoza et al. 2008). Therefore, myrtle and bottlebrush plants showing symptoms of twig canker and dieback were investigated in the present study to provide a deeper insight into etiology. The aims of this study were to: ii) identify and characterize the etiological agents; ii) test their pathogenicity.

Materials and methods

Survey and fungal isolations

The survey was conducted from September 2021 in a nursery in Catania (eastern Sicily). Symptomatic plants of *Callistemon laevis*, *C. viminalis*, *Luma apiculata* (marketed as "*Myrtus luma*"), *Myrtus communis* subsp. *tarentina*, and *M. communis* var. *microphylla* (*M. communis* 'Microphylla'), showing twig canker, dieback and defoliation were brought to the laboratory of the Dipartimento di Agricoltura, Alimentazione e Ambiente for further analyses. Specifically, small pieces of diseased wood tissue from cankered twigs were surface sterilized for 1 min in 1.5% sodium hypochlorite (NaOCl), rinsed in sterile water, dried on sterile absorbent paper in a laminar flow hood and then placed on potato dextrose agar (PDA, Lickson, Italy) amended with 100 mg/L of streptomycin sulfate (Sigma-Aldrich, MO, USA) to prevent bacterial growth. The Petri plates were then incubated at 25 °C for 7 days until the fungal colonies were large enough to be examined. For *M. communis* subsp. *tarentina* and *M. communis* 'Microphylla', isolations were also conducted from the leaves as described above. Colonies of interest were transferred onto fresh PDA plates and then single hypha isolates were obtained from pure cultures. Fungal isolates were stored as mycelial plugs in sterile water in the fungal collection of the laboratory with the strain identifiers ML (isolates from *Luma apiculata*), MT (isolates from *M. communis* subsp. *tarentina*), MP (isolates from *M. communis* 'Microphylla') or CV (isolates from *Callistemon*).

DNA extraction, PCR and sequencing

A total of 26 representative isolates from *Callistemon* spp., as well as from *Luma* and *Myrtus*, were chosen for molecular and phylogenetic analysis. DNA was extracted from single hypha isolates grown on PDA. The mycelium was scraped off and processed following manufacturer's instructions of the Wizard Genomic DNA Purification Kit® (Promega Corporation, WI, USA).

The following loci were amplified and sequenced: the terminal 3' end of the small subunit nuclear ribosomal DNA (nSSU rDNA) and the complete internal transcribed spacer region (ITS1-5.8S-ITS2) of the rDNA region with primers V9G (de Hoog and Gerrits van den Ende 1998) and ITS4 (White et al. 1990); a ca 0.5 kb fragment of the translation elongation factor 1-alpha (*tef1*) gene with primers EF1-728F (Carbone and Kohn 1999) and TEFD_iR (Voglmayr et al. 2018); and a ca. 0.95 kb fragment of the beta tubulin (*tub2*) gene with primers T1D (Voglmayr et al. 2019) and BtHV2r (Voglmayr et al. 2016, 2017). PCR products were purified using enzymatic PCR cleanup (Werle et al. 1994) as described in Voglmayr and Jaklitsch (2008). DNA was cycle-sequenced using

the ABI PRISM Big Dye Terminator Cycle Sequencing Ready Reaction Kit v. 3.1 (Applied Biosystems, Warrington, U.K.) with the same primers as in PCR. Sequencing was performed on an automated DNA sequencer (3730xl Genetic Analyzer, Applied Biosystems). The resulting DNA sequences were assembled with Lasergene SeqMan Pro (DNASTAR, Madison, WI, USA). The sequences generated during the present study were deposited in Genbank (Table 1).

Analysis of sequence data

For the phylogenetic analysis, a combined matrix of ITS rDNA, *tef1* and *tub2* sequences was produced. The newly generated sequences were aligned to a representative matrix of GenBank sequences of *Neopestalotiopsis* and *Pestalotiopsis*. For *Neopestalotiopsis*, all 88 described species for which sequences were available were included in the matrix, preferentially with ex-type sequences. Sequences of the four taxa of *Pestalotiopsis* which were the closest match to the single *Pestalotiopsis* isolate of the current study were added as outgroup. The GenBank accession numbers of the sequences used in this analysis are given in Table 1.

All alignments were produced with the server version of MAFFT (www.ebi.ac.uk/Tools/mafft), checked and refined using BioEdit version 7.2.6 (Hall 1999). For some sequences, highly deviating leading or trailing sequence regions, which were likely affected by sequencing errors, were removed from the alignment, as well as primer residue sequences that were present in some GenBank sequences. The ITS rDNA, *tef1* and *tub2* matrices were combined for subsequent phylogenetic analysis.

Maximum likelihood (ML) analyses were performed with RAxML (Stamatakis 2006) as implemented in raxmlGUI 2.0 (Silvestro and Michalak 2012), using the ML + rapid bootstrap setting and the GTRGAMMA+I substitution model (selected as the best model by Modeltest) with 1000 bootstrap replicates. The matrix was partitioned for different gene regions. For evaluation and discussion of bootstrap support, values below 70% were considered low, between 70 and 90% medium/moderate, above 90% high and 100% maximum.

Maximum parsimony (MP) bootstrap analyses were performed with PAUP v. 4.0a169 (Swofford 2002), with 1 000 bootstrap replicates using five rounds of heuristic search replicates with random addition of sequences and subsequent TBR branch swapping (MULTREES option in effect, steepest descent option not in effect, COLLAPSE command set to MINBRLEN, each replicate limited to 1 million rearrangements) during each bootstrap replicate. All molecular characters were unordered and given equal weight; analyses were performed with gaps treated as missing data; the COLLAPSE command was set to minbrlen.

Table 1. Symptomatology observed on different plant species investigated in this study.

Plant species	Symptoms	Disease incidence (%)
Callistemon laevis	small twig canker; dieback and defoliation	30
C. viminalis	small twig canker; dieback and defoliation	30
Luma apiculata	small twig canker, dieback, and low defoliation	20
Myrtus communis 'Microphylla'	small twig canker, dieback, and very low defoliation	20
M. communis subsp. *tarentina*	small twig canker, dieback, and high defoliation	70

Morphological investigation

Morphology of conidia was checked from sporulated cultures on PDA, CMD (CMA: Sigma, St Louis, Missouri; supplemented with 2% (w/v) D(+)-glucose-monohydrate) or 2% MEA (2% w/v malt extract, 2% w/v agar-agar; Merck, Darmstadt, Germany) plates grown at room temperature at ambient light. Conidia, prepared in tap water on microscope slides, were investigated in a Zeiss Axio Imager. A1 compound microscope.

Pathogenicity test

To determine the ability of the fungal species to infect and induce symptoms, seven representative isolates were selected for pathogenicity tests: *Neopestalotiopsis camelliae-oleiferae* ML3, *N. hispanica* ML8, *N. iberica* MP13, *N. rosae* MT32, *N. rosicola* MP29, *N. zakeelii* MP30, and *P. biciliata* MP11 were inoculated on potted plants of *Callistemon laevis*, *C. viminalis*, *M. communis* subsp. *tarentina*, *M. communis* 'Mycrophylla', and *L. apiculata*. Each fungal species was inoculated on three plants (replicate) of each plant species. For each plant, six twigs were inoculated as sub-replicates. The inoculum consisted of a small piece (~ 0.3–0.5 mm^2) of mycelial plug from 15-day-old cultures on PDA. The bark was first gently scraped using a sterile blade and then the mycelial plug was inserted upside down onto the wound. The wounds were sealed with Parafilm to prevent desiccation. Controls consisted of sterile PDA. All inoculated plants were moved to a growth chamber with a 12 h photoperiod and maintained at 25 ± 1 °C. The plants were regularly watered and monitored weekly for development of symptoms. Final symptoms evaluation was conducted 30 days after inoculations. Re-isolations were performed as described above to fulfill Koch's postulates.

Results

Survey and fungal isolations

Symptoms observed in the nursery included twig canker, dieback, internal wood necrosis and defoliation (Fig. 1). Symptomatology details and disease incidence for each plant species are described in Table 1. Fungal isolations constantly yielded *Neopestalotiopsis*-like colonies. A total of 56 *Neopestalotiopsis*-like isolates were stored in the fungal collection.

Phylogenetic analysis and species identification

The combined multilocus matrix used for phylogenetic analyses comprised 2458 characters (539 from the ITS, 978 from *tef1*, and 941 from *tub2*), of which 414 were parsimony informative (66 from ITS, 170 from *tef1*, and 178 from *tub2*). The best ML tree (-lnL = 10329.8215) obtained by RAxML is shown in Fig. 2. While the genus *Neopestalotiopsis* and a few deeper nodes were highly supported, most of the tree backbone received little or no bootstrap support. However, the isolates of the present study could be assigned to species level, based on the results of the phylogenetic analyses (Fig. 2), viz. one species of

Figure 1. Disease symptoms caused by *Neopestalotiopsis* spp. in nursery: blight and defoliation on *Myrtus communis* subsp. *tarentina* **A–B** *Luma apiculata* **C–D** *M. communis* 'Microphylla' **E** *Callistemon viminalis* **F** and *C. laevis* **G**.

Pestalotiopsis and 6 species of *Neopestalotiopsis*: isolate MP11 was revealed as *Pestalotiopsis biciliata*, isolate MP29 as *Neopestalotiopsis rosicola*, ML3 as *N. camelliae-oleiferae*, MP13 as *N. iberica*, and the two isolates CV52 and MP30 as *N. zakeelii*. However, the majority of isolates belonged to two species, viz. eight isolates to *N. hispanica* (syn. *N. vaccinii*) and 13 to *N. rosae* (see Table 2 and Fig. 2).

These results were also confirmed by the nucleotide comparisons (Table 3), which revealed (almost) identical sequences to the ex-type strains of the respective species. While within *N. hispanica* all markers of all isolates were identical with the ex-type sequences, within *N. rosae* slight sequence differences were observed in three isolates, viz. ML1 (1 nucleotide substitution and 1 gap in ITS), CV51 and MP25 (1 gap in ITS and 1 nucleotide substitution in *tef1*). Within *N. camelliae-oleiferae*, the ITS differed from the ex-type sequence by two gaps; however, these are likely sequencing errors as they were located in polyA regions at the immediate beginning of the deposited sequence which do not sufficiently resolved by the Sanger sequencing method. In *N. zakelii*, the ITS and *tub2* sequences of our isolates differed by 3 nucleotide substitutions from the ex-type sequences; however, the difference to the second verified strain (BRIP 72271a) was much less (1 substitution in ITS, identical *tef1* and *tub2* sequences). Also, in *P. biciliata* the ITS differed by 3 and 1 nucleotide substitutions in ITS and *tef1*, respectively, but only by 1 nucleotide substitution in *tef1* from the second verified strain (CBS 790.68). The species identification of these isolates with some differences to the ex-type sequences was also confirmed by BLAST searches of *tef1* and *tub2*, in which the respective species were revealed as closest matches with 100%.

Morphology of the conidia (conidial shape, size of the conidial body, number and coloration of the conidial cells, number and length of appendages) matched the genera and species and was therefore in line with the molecular

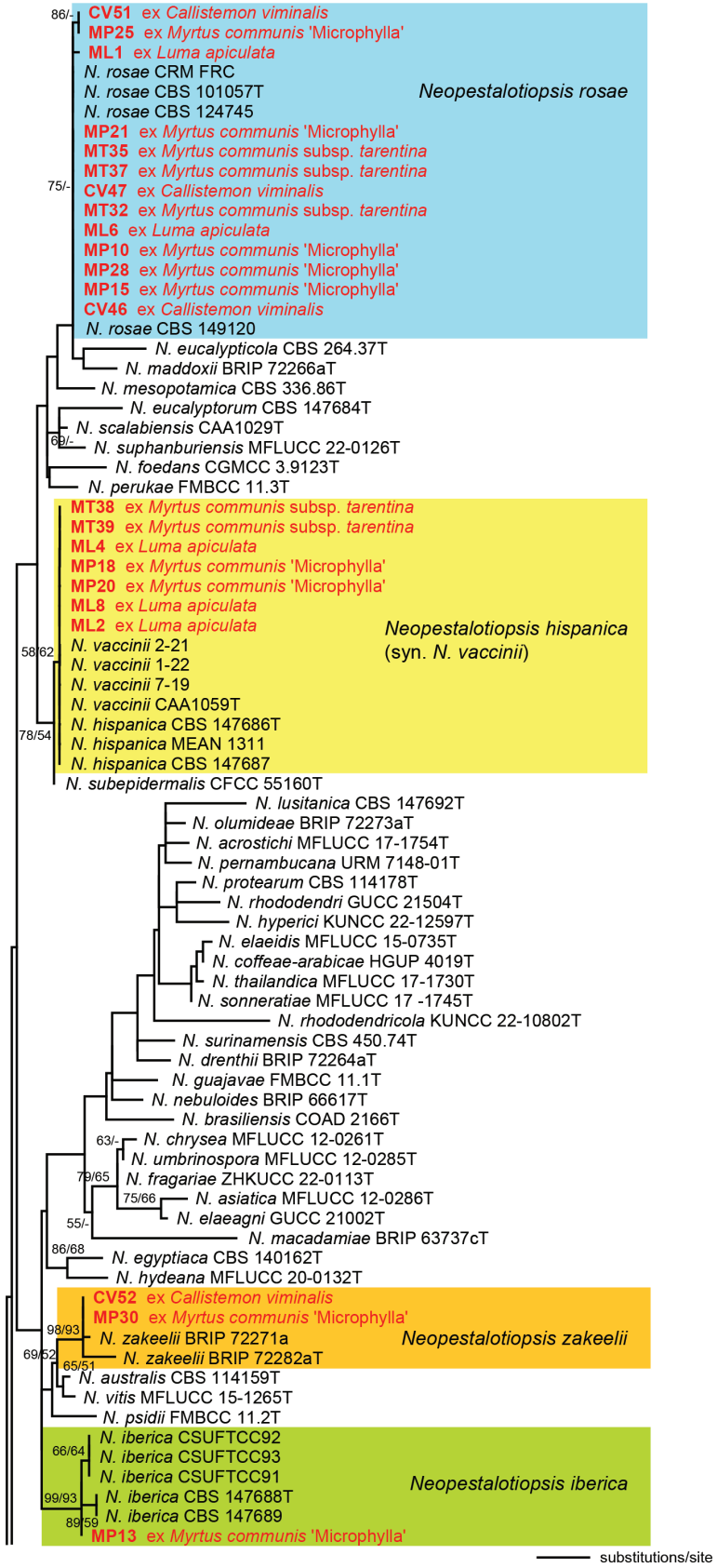

Figure 2. Phylogram of the best ML tree (-lnL = 10329.8215) revealed by RAxML from an analysis of the combined ITS-*tef1-tub2* matrix of *Neopestalotiopsis*, showing the phylogenetic position of the isolates obtained from diseased Myrtaceae. Strains marked by an "T" at the end of the strain designation represent ex-type strains. ML and MP bootstrap support above 50% are given above or below the branches. The broken branches were scaled to one-quarter.

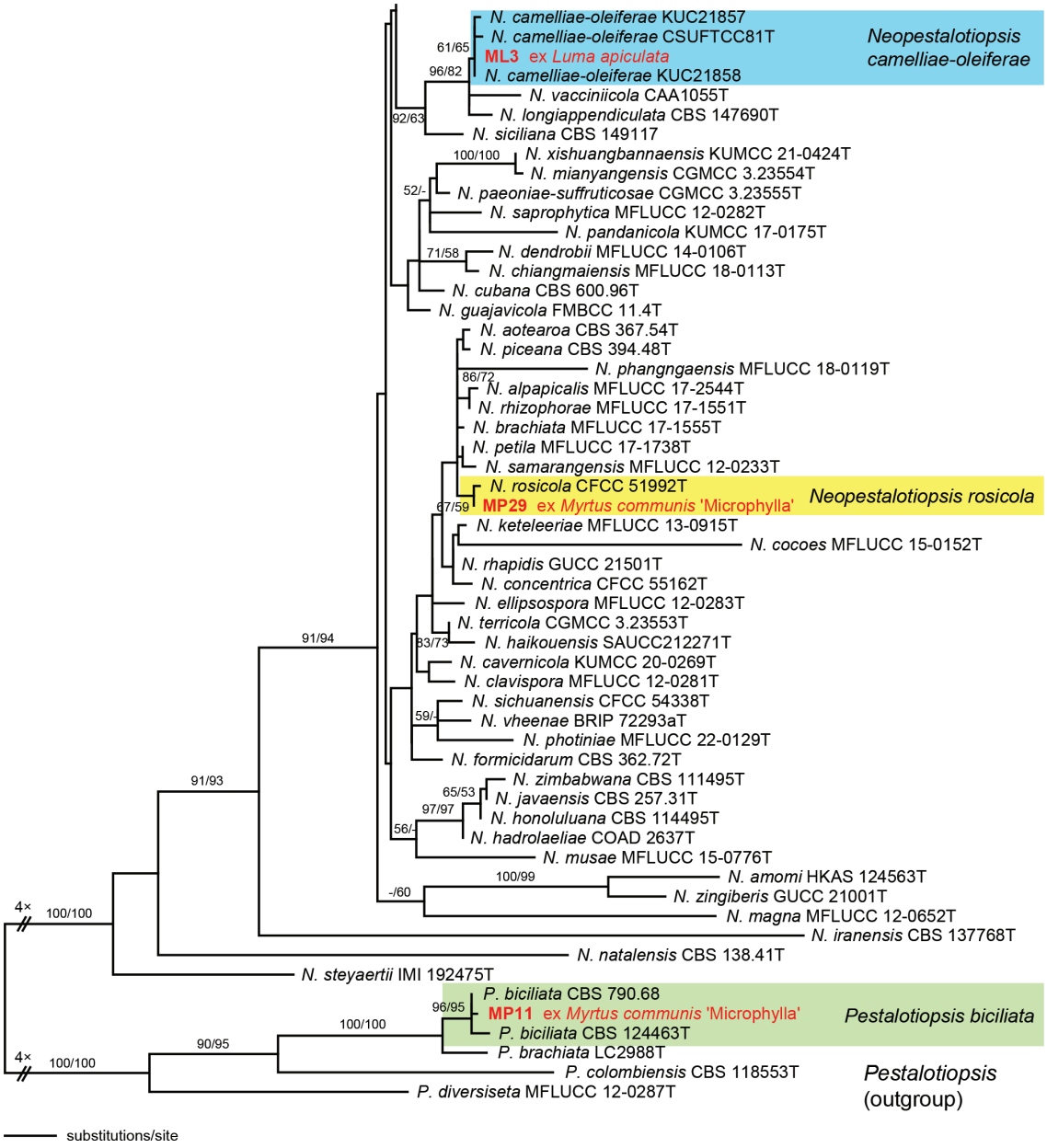

Figure 2. Continued.

identification; however, as within the genus *Neopestalotiopsis* conidial shapes and sizes largely overlap and are highly similar in the bulk of these cryptic species, no species identification is possible based on morphology.

Pathogenicity test

The results of the pathogenicity tests (disease incidence) are shown in Table 4. Although some cankers were visible after one week, the size of the twigs was too thin and small to assess the disease severity (lesion length). Only *N. rosae* and *N. hispanica* caused disease symptoms on all hosts tested, whereas *P. biciliata* did not show pathogenicity. Moreover, the isolates inoculated on wounded twigs caused similar symptoms on different host species and showed twig canker and dieback (Fig. 3).

Table 2. Isolates used in the molecular analyses in this study.

Species	Strain[1]	Host/Substrate	Origin	GenBank Accession Numbers[2]		
				ITS	*tef1*	*tub2*
Neopestalotiopsis acrostichi	MFLUCC 17-1754^T	*Acrostichum aureum*	Thailand	MK764272	MK764316	MK764338
N. alpapicalis	MFLUCC 17-2544^T	*Rhizophora mucronata*	Thailand	MK357772	MK463547	MK463545
N. amomi	HKAS 124563^T	*Amomum villosum*	China	OP498012	OP653489	OP752133
N. aotearoa	CBS 367.54^T	Canvas	New Zealand	KM199369	KM199526	KM199454
N. asiatica	MFLUCC 12-0286^T	Unidentified tree	China	JX398983	JX399049	JX399018
N. australis	CBS 114159^T	*Telopea* sp.	Australia	KM199348	KM199537	KM199432
N. brachiata	MFLUCC 17-1555^T	*Rhizophora apiculata*	Thailand	MK764274	MK764318	MK764340
N. brasiliensis	COAD 2166^T	*Psidium guajava*	Brazil	MG686469	MG692402	MG692400
N. camelliae-oleiferae	CSUFTCC81^T	*Camellia oleifera*	China	OK493585	OK507955	OK562360
N. camelliae-oleiferae	KUC21857	*Phyllostachys bambusoides*	South Korea	OR654966	OR693485	OR693494
N. camelliae-oleiferae	KUC21858	*Phyllostachys bambusoides*	South Korea	OR654967	OR693486	OR693495
N. camelliae-oleiferae	**ML3**	*Luma apiculata*	**Italy**	**PP146586**	**PP174965**	**PP197178**
N. cavernicola	KUMCC 20-0269^T	Cave rock surface	China	MW545802	MW550735	MW557596
N. chiangmaiensis	MFLUCC 18-0113^T	Dead leaves	Thailand	N/A	MH388404	MH412725
N. chrysea	MFLUCC 12-0261^T	*Pandanus* sp.	China	JX398985	JX399051	JX399020
N. clavispora	MFLUCC 12-0281^T	*Magnolia* sp.	China	JX398979	JX399045	JX399014
N. cocoes	MFLUCC 15-0152^T	*Cocos nucifera*	Thailand	NR_156312	KX789689	N/A
N. concentrica	CFCC 55162^T	*Rosa rugosa*	China	OK560707	OM622433	OM117698
N. coffeae-arabicae	HGUP 4019^T	*Coffea arabica*	China	KF412649	KF412646	KF412643
N. cubana	CBS 600.96^T	Leaf litter	Cuba	KM199347	KM199521	KM199438
N. dendrobii	MFLUCC 14-0106^T	*Dendrobium cariniferum*	Thailand	MK993571	MK975829	MK975835
N. drenthii	BRIP 72264a^T	*Macadamia integrifolia*	Australia	MZ303787	MZ344172	MZ312680
N. egyptiaca	CBS 140162^T	*Mangifera indica*	Egypt	KP943747	KP943748	KP943746
N. elaeagni	GUCC 21002^T	*Elaeagnus pungens*	China	MW930716	MZ203452	MZ683391
N. elaeidis	MFLUCC 15-0735^T	*Elaeis guineensis*	Thailand	ON650690	ON734012	N/A
N. ellipsospora	MFLUCC 12-0283^T	Dead plant materials	China	JX398980	JX399047	JX399016
N. eucalypticola	CBS 264.37^T	*Eucalyptus globulus*	N/A	KM199376	KM199551	KM199431
N. eucalyptorum	CBS 147684^T	*Eucalyptus globulus*	Portugal	MW794108	MW805397	MW802841
N. foedans	CGMCC 3.9123^T	Mangrove plant	China	JX398987	JX399053	JX399022
N. formicidarum	CBS 362.72^T	Dead *Formicidae* (ant)	Ghana	KM199358	KM199517	KM199455
N. fragariae	ZHKUCC 22-0113^T	*Fragaria* × *ananassa*	China	ON553410	ON569076	ON569075
N. guajavae	FMBCC 11.1^T	*Psidium guajava*	Pakistan	MF783085	MH460868	MH460871
N. guajavicola	FMBCC 11.4^T	*Psidium guajava*	Pakistan	MH209245	MH460870	MH460873
N. hadrolaeliae	COAD 2637^T	*Hadrolaelia jongheana*	Brazil	MK454709	MK465122	MK465120
N. haikouensis	SAUCC212271^T	*Ilex chinensis*	China	OK087294	OK104877	OK104870
N. hispanica	CBS 147686^T	*Eucalyptus globulus*	Portugal	MW794107	MW805399	MW802840
N. hispanica	CBS 147687	*Eucalyptus globulus*	Spain	MW794113	MW805401	MW802846
N. hispanica	MEAN 1311	*Eucalyptus globulus*	Portugal	MW794106	MW805400	MW802839
N. hispanica	**ML2**	*Luma apiculata*	**Italy**	**PP146593**	**PP174983**	**PP197171**
N. hispanica	**ML4**	*Luma apiculata*	**Italy**	**PP146594**	**PP174984**	**PP197172**
N. hispanica	**ML8**	*Luma apiculata*	**Italy**	**PP146596**	**PP174985**	**PP197173**
N. hispanica	**MP18**	*Myrtus communis* 'Microphylla'	**Italy**	**PP146599**	**PP174986**	**PP197174**
N. hispanica	**MP20**	*Myrtus communis* 'Microphylla'	**Italy**	**PP146600**	**PP174987**	**PP197175**
N. hispanica	**MT38**	*Myrtus communis* subsp. *tarentina*	**Italy**	**PP146606**	**PP174989**	**PP197176**
N. hispanica	**MT39**	*Myrtus communis* subsp. *tarentina*	**Italy**	**PP146607**	**PP174990**	**PP197177**

Species	Strain[1]	Host/Substrate	Origin	GenBank Accession Numbers[2]		
				ITS	*tef1*	*tub2*
N. honoluluana	CBS 114495^T	*Telopea* sp.	USA	KM199364	KM199548	KM199457
N. hydeana	MFLUCC 20-0132^T	*Artocarpus heterophyllus*	Thailand	MW266069	MW251129	MW251119
N. hyperici	KUNCC 22-12597^T	*Hypericum monogynum*	China	OP498010	OP713768	OP765908
N. iberica	CBS 147688^T	*Eucalyptus globulus*	Portugal	MW794111	MW805402	MW802844
N. iberica	CBS 147689	*Eucalyptus globulus*	Spain	MW794114	MW805403	MW802847
N. iberica	CSUFTCC91	*Camellia oleifera*	China	OK493587	OK507957	OK562362
N. iberica	CSUFTCC92	*Camellia oleifera*	China	OK493588	OK507958	OK562363
N. iberica	CSUFTCC93	*Camellia oleifera*	China	OK493589	OK507959	OK562364
N. iberica	**MP13**	*Myrtus communis* 'Microphylla'	**Italy**	**PP146587**	**PP174967**	**PP197167**
N. iranensis	CBS 137768^T	*Fragaria* × *ananassa*	Iran	KM074048	KM074051	KM074057
N. javaensis	CBS 257.31^T	*Cocos nucifera*	Indonesia	KM199357	KM199548	KM199457
N. keteleeriae	MFLUCC 13-0915^T	*Keteleeria pubescens*	China	KJ023087	KJ023089	KJ023088
N. longiappendiculata	CBS 147690^T	*Eucalyptus globulus*	Portugal	MW794112	MW805404	MW802845
N. lusitanica	CBS 147692^T	*Eucalyptus globulus*	Portugal	MW794110	MW805406	MW802843
N. macadamiae	BRIP 63737c^T	*Macadamia integrifolia*	Australia	KX186604	KX186627	KX186654
N. maddoxii	BRIP 72266a^T	*Macadamia integrifolia*	Australia	MZ303782	MZ344167	MZ312675
N. magna	MFLUCC 12-0652^T	*Pteridium* sp.	France	KF582795	KF582791	KF582793
N. mesopotamica	CBS 336.86^T	*Pinus brutia*	Turkey	KM199362	KM199555	KM199441
N. mianyangensis	CGMCC 3.23554^T	*Paeonia suffruticosa*	China	OP546681	OP723490	OP672161
N. musae	MFLUCC 15-0776^T	*Musa* sp.	Thailand	NR_156311	KX789685	KX789686
N. natalensis	CBS 138.41^T	*Acacia mollissima*	South Africa	NR_156288	KM199552	KM199466
N. nebuloides	BRIP 66617^T	*Sporobolus jacquemontii*	Australia	MK966338	MK977633	MK977632
N. olumideae	BRIP 72273a^T	*Macadamia integrifolia*	Australia	MZ303790	MZ344175	MZ312683
N. paeoniae-suffruticosae	CGMCC 3.23555^T	*Paeonia suffruticosa*	China	OP082292	OP204794	OP235980
N. pandanicola	KUMCC 17-0175^T	*Pandanus* sp.	China	N/A	MH388389	MH412720
N. pernambucana	URM 7148-01^T	*Vismia guianensis*	Brazil	KJ792466	KU306739	N/A
N. perukae	FMBCC 11.3^T	*Psidium guajava*	Pakistan	MH209077	MH523647	MH460876
N. petila	MFLUCC 17-1738^T	*Rhizophora apiculata*	Thailand	MK764276	MK764320	MK764342
N. phangngaensis	MFLUCC 18-0119^T	*Pandanus* sp.	Thailand	MH388354	MH388390	MH412721
N. photiniae	MFLUCC 22-0129^T	*Photinia serratifolia*	China	OP498008	OP753368	OP752131
N. piceana	CBS 394.48^T	*Picea* sp.	UK	KM199368	KM199527	KM199453
N. protearum	CBS 114178^T	*Leucospermum cuneiforme*	Zimbabwe	JN712498	KM199542	KM199463
N. psidii	FMBCC 11.2^T	*Psidium guajava*	Pakistan	MF783082	MH460874	MH477870
N. rhapidis	GUCC 21501^T	*Rhododendron simsii*	China	MW931620	MW980442	MW980441
N. rhizophorae	MFLUCC 17-1551^T	*Rhizophora mucronata*	Thailand	MK764277	MK764321	MK764343
N. rhododendri	GUCC 21504^T	*Rhododendron simsii*	China	MW979577	MW980444	MW980443
N. rhododendricola	KUNCC 22-10802^T	*Rhododendron* sp.	China	OK283069	OK274148	OK274147
N. rosae	CBS 101057^T	*Rosa* sp.	New Zealand	KM199359	KM199523	KM199429
N. rosae	CBS 124745	*Paeonia suffruticosa*	USA	KM199360	KM199524	KM199430
N. rosae	CRM-FRC	*Fragaria* × *ananassa*	Mexico	MN385718	MN268532	MN268529
N. rosae	AC50	*Persea americana*	Italy	ON117810	ON107276	ON209165
N. rosae	**CV46**	*Callistemon viminalis*	**Italy**	**PP146591**	**PP174971**	**PP197179**
N. rosae	**CV47**	*Callistemon viminalis*	**Italy**	**PP146592**	**PP174972**	**PP197180**
N. rosae	**CV51**	*Callistemon viminalis*	**Italy**	**PP146584**	**PP174982**	**PP197191**
N. rosae	**ML1**	*Luma apiculata*	**Italy**	**PP146583**	**PP174973**	**PP197181**
N. rosae	**ML6**	*Luma apiculata*	**Italy**	**PP146595**	**PP174974**	**PP197182**
N. rosae	**MP10**	*Myrtus communis* 'Microphylla'	**Italy**	**PP146597**	**PP174975**	**PP197183**
N. rosae	**MP15**	*Myrtus communis* 'Microphylla'	**Italy**	**PP146598**	**PP174976**	**PP197184**

Species	Strain[1]	Host/Substrate	Origin	GenBank Accession Numbers[2]		
				ITS	*tef1*	*tub2*
N. rosae	**MP21**	*Myrtus communis* 'Microphylla'	**Italy**	**PP146601**	**PP174977**	**PP197185**
N. rosae	**MP25**	*Myrtus communis* 'Microphylla'	**Italy**	**PP146588**	**PP174988**	**PP197186**
N. rosae	**MP28**	*Myrtus communis* 'Microphylla'	**Italy**	**PP146602**	**PP174978**	**PP197187**
N. rosae	**MT32**	*Myrtus communis* subsp. *tarentina*	**Italy**	**PP146603**	**PP174979**	**PP197188**
N. rosae	**MT35**	*Myrtus communis* subsp. *tarentina*	**Italy**	**PP146604**	**PP174980**	**PP197189**
N. rosae	**MT37**	*Myrtus communis* subsp. *tarentina*	**Italy**	**PP146605**	**PP174981**	**PP197190**
N. rosicola	CFCC 51992^T	*Rosa chinensis*	China	KY885239	KY885243	KY885245
N. rosicola	**MP29**	*Myrtus communis* 'Microphylla'	**Italy**	**PP146590**	**PP174968**	**PP197168**
N. samarangensis	MFLUCC 12-0233^T	*Syzygium samarangense*	Thailand	JQ968609	JQ968611	JQ968610
N. saprophytica	MFLUCC 12-0282^T	*Magnolia* sp.	China	JX398982	JX399048	JX399017
N. scalabiensis	CAA1029^T	*Vaccinium corymbosum*	Portugal	MW969748	MW959100	MW934611
N. sichuanensis	CFCC 54338^T	*Castanea mollissima*	China	MW166231	MW199750	MW218524
N. siciliana	CBS 149117	*Persea americana*	Italy	ON117813	ON107273	ON209162
N. sonneratiae	MFLUCC 17-1745^T	*Sonneronata alba*	Thailand	MK764280	MK764324	MK764346
N. steyaertii	IMI 192475^T	*Eucalytpus viminalis*	Australia	KF582796	KF582792	KF582794
N. subepidermalis	CFCC 55160^T	*Rosa rugosa*	China	OK560699	OM622425	OM117690
N. suphanburiensis	MFLUCC 22-0126^T	dead stem of unid. plant	Thailand	OP497994	OP753372	OP752135
N. surinamensis	CBS 450.74^T	Soil under *Elaeis guineensis*	Suriname	KM199351	KM199518	KM199465
N. terricola	CGMCC 3.23553^T	*Paeonia suffruticosa*	China	OP082294	OP204796	OP235982
N. thailandica	MFLUCC 17-1730^T	*Rhizophora mucronata*	Thailand	MK764281	MK764325	MK764347
N. umbrinospora	MFLUCC 12-0285^T	unidentified plant	China	JX398984	JX399050	JX399019
N. vaccinii	CAA1059^T	*Vaccinium corymbosum*	Portugal	MW969747	MW959099	MW934610
N. vaccinii	22-Jan	*Vaccinium corymbosum*	Serbia	OQ316613	OQ342778	OQ473026
N. vaccinii	21-Feb	*Vaccinium corymbosum*	Serbia	OQ316612	OQ342777	OQ473025
N. vaccinii	19-Jul	*Vaccinium corymbosum*	Serbia	OQ316611	OQ342776	OQ473024
N. vacciniicola	CAA1055^T	*Vaccinium corymbosum*	Portugal	MW969751	MW959103	MW934614
N. vheenae	BRIP 72293a^T	*Macadamia integrifolia*	Australia	MZ303792	MZ344177	MZ312685
N. vitis	MFLUCC 15-1265^T	*Vitis vinifera*	China	KU140694	KU140676	KU140685
N. xishuangbannaensis	KUMCC 21-0424^T	*Kerivoula hardwickii*	China	ON426865	OR025973	OR025934
N. zakeelii	BRIP 72282a^T	*Macadamia integrifolia*	Australia	MZ303789	MZ344174	MZ312682
N. zakeelii	BRIP 72271°	*Macadamia integrifolia*	Australia	MZ303788	MZ344173	MZ312681
N. zakeelii	**CV52**	*Callistemon viminalis*	**Italy**	**PP146585**	**PP174969**	**PP197170**
N. zakeelii	**MP30**	*Myrtus communis* 'Microphylla'	**Italy**	**PP146589**	**PP174970**	**PP197169**
N. zimbabwana	CBS 111495^T	*Leucospermum cuneiforme*	Zimbabwe	JX556231	KM199545	KM199456
N. zingiberis	GUCC 21001^T	*Zingiber officinale*	China	MW930715	MZ683389	MZ683390
Pestalotiopsis biciliata	CBS 124463^T	*Platanus* × *hispanica*	Slovakia	KM199308	KM199505	KM199399
P. biciliata	CBS 790.68	*Taxus baccata*	Netherlands	KM199305	KM199507	KM199400
P. biciliata	**MP11**	*Myrtus communis* 'Microphylla'	**Italy**	**PP146582**	**PP174966**	**PP197166**
P. brachiata	LC2988^T	*Camellia* sp.	China	KX894933	KX895150	KX895265
P. colombiensis	CBS 118553^T	*Eucalyptus grandis* × *urophylla*	Colombia	KM199307	KM199488	KM199421
P. diversiseta	MFLUCC 12-0287^T	Dead plant material	China	NR_120187	JX399073	JX399040

Table 3. Sequence comparison of differences in number of nucleotide substitutions and gaps between the sequences of isolates of the present study and the ex-type sequences of the respective species.

Species	No. of isolates	Sequence difference to ex-type strain (nucleotide substitutions/gaps)		
		ITS	*tef1*	*tub2*
Neopestalotiopsis camelliae-oleiferae	1	(2)*/0	0/0	0/0
N. hispanica (syn. *N. vaccinii*)	8	0/0	0/0	0/0
N. iberica	1	0/0	1/0	0/0
N. rosae	13	0-1/0-1	0-1/0	0/0
N. rosicola	1	0/0	1/0	0/0
N. zakeelii	2	3/0	0/0	2/0
Pestalotiopsis biciliata	1	3/0	1/1	0/0

*Gaps located at the immediate beginning of the ITS in polyA regions, likely representing sequencing errors.

Table 4. Results of pathogenicity tests conducted in this study.

Host	*Neopestalotiopsis* spp. isolates						
	N. rosae **MT32**	***N. rosicola*** **MP29**	***N. hispanica*** **ML8**	***N. iberica*** **MP13**	***N. zakeelii*** **MP30**	***N. camelliae-oleiferae*** **ML3**	***P. biciliata*** **MP11**
Callistemon laevis	+	+	+	+	+	+	-
C. viminalis	+	+	+	+	+	+	-
Luma apiculata	+	-	+	-	-	-	-
Myrtus communis 'Microphylla'	+	+	+	+	+	+	-
M. communis subsp. *tarentina*	+	+	+	+	-	+	-

"+" symptoms; "–" symptomless.

Discussion

In the present study, the following fungal species were described causing twig canker, dieback and defoliation on *Callistemon*, *Luma* and *Myrtus* spp.: *Neopestalotiopsis camelliae-oleiferae*, *N. hispanica* (syn. *N. vaccinii*), *N. iberica*, *N. rosae*, *N. rosicola*, *N. zakeelii*, and *Pestalotiopsis biciliata*. In the group of fungi characterized in this study the species *N. hispanica* and *N. rosae*, based on frequency of isolations and ability to induce symptoms in all tested plant species, probably play a key role in the disease development. *Neopestalotiopsis* species, as well as other species belonging to other taxa within the Sporocadaceae are known worldwide causing different symptoms on many hosts, such as leaf spot, flower and fruit blight, twig canker and crown rot (Rebollar-Alviter et al. 2020; Santos et al. 2022; Shahriar et al. 2022; Guterres et al. 2023). Similar symptoms to those observed in this study have been reported for *N. iberica* on *Eucalyptus globulus* in Portugal (Diogo et al. 2021) and on *Synsepalum dulcificum* in China (You et al. 2024), for *N. rosae* on blueberry in Peru, and Portugal (Rodríguez-Gálvez et al. 2020; Santos et al. 2022), and on avocado in Italy (Fiorenza et al. 2022b), for *N. rosicola* on *Rosa chinensis* in China (Jiang et al. 2018), for *N. hispanica* (syn. *N. vaccinii*) on *E. globulus* in Portugal and Spain (Diogo et al. 2021) and on blueberry in Portugal (Santos et al. 2022). However, *N. camelliae-oleiferae* was also reported causing foliar symptoms on *Camellia oleifera* in

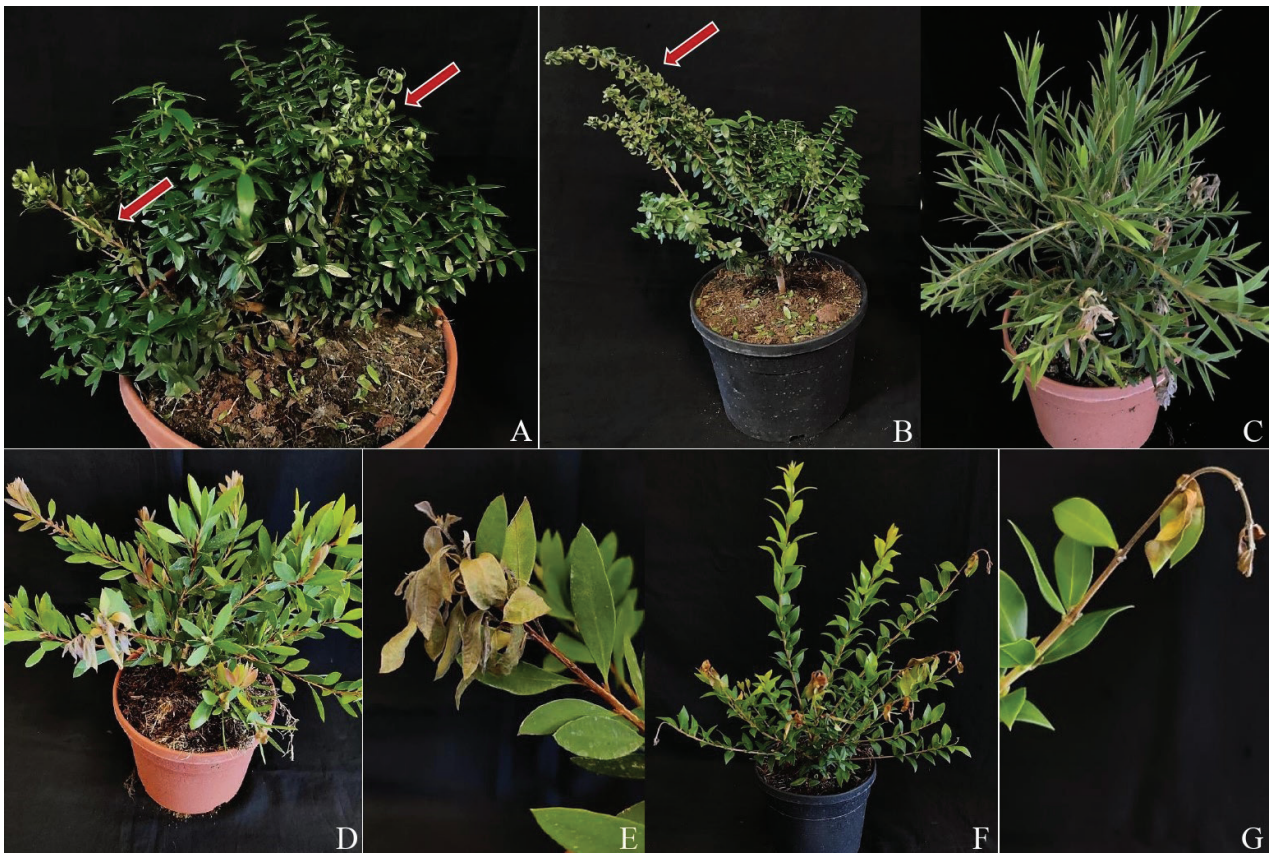

Figure 3. Symptoms caused by artificial inoculation with *Neopestalotiopsis rosae* MT32 on *Myrtus communis* 'Microphylla' **A** *Myrtus communis* subsp. *tarentina* (red arrow) **B** *Callistemon viminalis* (red arrow) **C** *Callistemon laevis* **D–E** *Luma apiculata* **F–G**.

China (Li et al. 2021), and *N. zakeelii* was described in 2021, associated with flower diseases of *Macadamia integrifolia* in Australia (Prasannath et al. 2021). Although *N. zakeelii* was reported from macadamia inflorescences showing dry flowers, Koch's postulates were not conducted and the pathogenicity was not demonstrated (Prasannath et al. 2021). In our study it is the first time that *N. zakeelii* is reported to be associated with symptoms of canker and dieback and our study confirms, for the first time, the pathogenic activity on *C. laevis* and *viminalis* and on *M. communis* 'Microphylla' causing necrotic lesions of woody tissues. On the other hand, different results have been obtained regarding pathogenicity of *P. biciliata*. This species was reported around the world causing also twig canker and dieback on different hosts such as blueberry, *Pinus pinea*, *Quercus coccifera* and *Pistacia lentiscus* (Hlaiem et al. 2022 a, b; Santos et al. 2022), whereas in our study, although isolated from cankered tissues, the tested isolate did not show any pathogenic activity on these hosts. This result is not surprising, since many other studies demonstrated that pestalotioid fungi can occur as saprobionts or generalist endophytes (Wu et al. 1982; Agarwal and Chauhan 1988; Yanna and Hyde 2002; Osono and Takeda 2006; Hu et al. 2007; Rajulu et al. 2014; Prakash et al. 2015; Park et al. 2016; Reddy et al. 2016). The results of our study showed the potential fungal diversity involved in twig canker. In fact, as highlighted in this study, to investigate these kinds of diseases, such as canker and dieback, the whole fungal diversity and the interactions among all the species involved must be taken into consideration.

Additional information

Conflict of interest

The authors have declared that no competing interests exist.

Ethical statement

No ethical statement was reported.

Funding

This research was funded by the University of Catania, Italy (PIA.CE.RI. 2020–2022 Linea 2: Research Project MEDIT-ECO-UPB: 5A722192155).

Author contributions

Conceptualisation: DA, GP. Formal analysis: GG, GRL, HV. Funding acquisition: GP. Investigation: DA, GRL, GP. Methodology: DA, GP, GRL, HV. Software: HV. Supervision: DA, GP, HV. Validation: DA, GP, HV. Writing – original draft: DA, GG, GRL, HV. Writing – review and editing: DA, GG, GRL, GP, HV.

Author ORCIDs

Dalia Aiello https://orcid.org/0000-0002-6018-6850
Giorgio Gusella https://orcid.org/0000-0002-0519-1200
Giuseppa Rosaria Leonardi https://orcid.org/0000-0002-4676-5100
Giancarlo Polizzi https://orcid.org/0000-0001-8630-2760
Hermann Voglmayr https://orcid.org/0000-0001-7666-993X

Data availability

All of the data that support the findings of this study are available in the main text

References

Agarwal AK, Chauhan S (1988) A new species of the genus *Pestalotiopsis* from Indian soil. Indian Phytopathology 41: 625–627.

Ahmadpour SA, Mehrabi-Koushki M, Farokhinejad R, Asgari B (2022) *Xenodidymella iranica* sp. nov. and new hosts of *X. glycyrrhizicola* in Iran. Tropical Plant Pathology 47(3): 430–441. https://doi.org/10.1007/s40858-022-00491-3

Aiello D, Gusella G, Fiorenza A, Guarnaccia V, Polizzi G (2020) Identification of *Neofusicoccum parvum* causing canker and twig blight on *Ficus carica* in Italy. Phytopathologia Mediterranea 59(1): 213–218. https://doi.org/10.36253/phyto-10798

Aiello D, Guarnaccia V, Vitale A, LeBlanc N, Shishkoff N, Polizzi G (2022) Impact of Calonectria diseases on ornamental horticulture: Diagnosis and Control strategies. Plant Disease 106(7): 1773–1787. https://doi.org/10.1094/PDIS-11-21-2610-FE

Alfieri Jr SA, Langdon KR, Wehlburg C, Kimbrough JW (1984) Index of Plant Diseases in Florida (Revised). Florida Department of Agriculture and Consumer Service, Division of Plant Industry. Bulletin 11: 1–389.

Cacciola SO, Scibetta S, Pane A, Faedda R, Rizza C (2009) *Callistemon citrinus* and *Cistus salvifolius*, two new hosts of *Phytophthora* taxon *niederhauserii* in Italy. Plant Disease 93(10): 1075–1075. https://doi.org/10.1094/PDIS-93-10-1075A

Carbone I, Kohn LM (1999) A method for designing primer sets for speciation studies in filamentous ascomycetes. Mycologia 91(3): 553–556. https://doi.org/10.1080/00275514.1999.12061051

Carnegie AJ, Lidbetter JR, Walker J, Horwood MA, Tesoriero L, Glen M, Priest M (2010) *Uredo rangelii*, a taxon in the guava rust complex, newly recorded on *Myrtaceae* in Australia. Australasian Plant Pathology 39(5): 463–466. https://doi.org/10.1071/AP10102

Costanzo MB, Gusella G, Fiorenza A, Leonardi GR, Aiello D, Polizzi G (2022) *Lasiodiplodia citricola*, a new causal agent of *Acacia* spp. dieback. New Disease Reports 45(2): e12094. https://doi.org/10.1002/ndr2.12094

Coutinho TA, Wingfield MJ, Alfenas AC, Crous PW (1998) Eucalyptus rust – a disease with the potential for serious international implications. Plant Disease 82(7): 819–825. https://doi.org/10.1094/PDIS.1998.82.7.819

De Hoog GS, Gerrits van den Ende AHG (1998) Molecular diagnostics of clinical strains of filamentous basidiomycetes. Mycoses 41: 183–189. https://doi.org/10.1111/j.1439-0507.1998.tb00321.x

Diogo E, Gonçalves CI, Silva AC, Valente C, Bragança H, Phillips AJ (2021) Five new species of *Neopestalotiopsis* associated with diseased *Eucalyptus* spp. in Portugal. Mycological Progress 20(11): 1441–1456. https://doi.org/10.1007/s11557-021-01741-5

Erwin DC, Ribeiro OK (1996) Phytophthora Diseases worldwide. The American Phytopathological Society, Saint Paul, Minnesota, USA, 599 pp.

Espinoza JG, Briceño EX, Keith LM, Latorre BA (2008) Canker and twig dieback of blueberry caused by *Pestalotiopsis* spp. and a *Truncatella* sp. in Chile. Plant Disease 92(10): 1407–1414. https://doi.org/10.1094/PDIS-92-10-1407

Fensham RJ, Carnegie AJ, Laffineur B, Makinson RO, Pegg GS, Wills J (2020) Imminent extinction of Australian Myrtaceae by fungal disease. Trends in Ecology & Evolution 35(7): 554–557. https://doi.org/10.1016/j.tree.2020.03.012

Fiorenza A, Aiello D, Costanzo MB, Gusella G, Polizzi G (2022a) A New Disease for Europe of *Ficus microcarpa* caused by Botryosphaeriaceae species. Plants 11(6): 727. https://doi.org/10.3390/plants11060727

Fiorenza A, Gusella G, Aiello D, Polizzi G, Voglmayr H (2022b) *Neopestalotiopsis siciliana* sp. nov. and *N. rosae* causing stem lesion and dieback on avocado plants in Italy. Journal of Fungi 8(6): 562. https://doi.org/10.3390/jof8060562

Gadgil PD (2005) Fungi on trees and shrubs in New Zealand. Fingi of New Zeland Vol. 4, Fungal Diversity Press, Hong Kong, 437 pp.

Glen M, Alfenas AC, Zauza EAV, Wingfield MJ, Mohammed C (2007) *Puccinia psidii*, a threat to the Australian environment and economy – a review. Australasian Plant Pathology 36(1): 1–16. https://doi.org/10.1071/AP06088

Guarnaccia V, Kraus C, Markakis E, Alves A, Armengol J, Eichmeier A, Compant S, Gramaje D (2022) Fungal trunk diseases of fruit trees in Europe: Pathogens, spread and future directions. Phytopathologia Mediterranea 61(3): 563–599. https://doi.org/10.36253/phyto-14167

Gusella G, Costanzo MB, Aiello D, Polizzi G (2021) Characterization of *Neofusicoccum parvum* causing canker and dieback on *Brachychiton* species. European Journal of Plant Pathology 161(4): 999–1005. https://doi.org/10.1007/s10658-021-02379-5

Guterres DC, Silva MA, Martins MD, Azevedo DMQ, Lisboa DO, Pinho DB, Furtado GQ (2023) Leaf spot caused by *Neopestalotiopsis* species on *Arecaceae* in Brazil. Australasian Plant Pathology 52(1): 47–62. https://doi.org/10.1007/s13313-022-00893-6

Hall TA (1999) BioEdit: A user-friendly biological sequence alignment editor and analysis program for Windows 95/98/NT. Nucleic Acids Symposium Series 41: 95–98. https://doi.org/10.14601/Phytopathol_Mediterr-14998u1.29

Henricot B, Beales P (2003) First record of *Cylindrocladium pauciramosum* on myrtle (*Myrtus communis*) in Portugal. Plant Pathology 52(3): 420–420. https://doi.org/10.1046/j.1365-3059.2003.00842.x

Hlaiem S, Yangui I, Della Rocca G, Barberini S, Danti R, Ben Jamaa ML (2022a) First report of *Pestalotiopsis biciliata* causing dieback on *Quercus coccifera* and *Pistacia lentiscus* in Tunisia. Canadian Journal of Plant Pathology 44(4): 534–541. https://doi.org/10.1080/07060661.2022.2032831

Hlaiem S, Yangui I, Rocca GD, Barberini S, Danti R, Jamâa MLB (2022b) First report of *Pestalotiopsis biciliata* associated with twig canker and dieback of *Pinus pinea* in Tunisia. Journal of Plant Pathology 104(1): 393–394. https://doi.org/10.1007/s42161-021-00956-5

Hu HL, Jeewon R, Zhou DQ, Zhou TX, Hyde KD (2007) Phylogenetic diversity of endophytic *Pestalotiopsis* species in *Pinus armandii* and *Ribes* spp.: Evidence from rDNA and β-tubulin gene phylogenies. Fungal Diversity 24: 1–22.

Jiang N, Bonthond G, Fan XL, Tian CM (2018) *Neopestalotiopsis rosicola* sp. nov. causing stem canker of *Rosa chinensis* in China. Mycotaxon 133(2): 271–283. https://doi.org/10.5248/133.271

Koike ST, Crous PW (2001) First report of a root and crown rot disease of myrtle in California caused by *Cylindrocladium pauciramosum.* Plant Disease 85(4): 448–448. https://doi.org/10.1094/PDIS.2001.85.4.448C

Li L, Yang Q, Li H (2021) Morphology, Phylogeny, and Pathogenicity of Pestalotioid Species on *Camellia oleifera* in China. Journal of Fungi (Basel, Switzerland) 7(12): 1080. https://doi.org/10.3390/jof7121080

Li Y, Zhang S, Wang T, Zhou S, Wu Y, Huang X, Lin H, Su X (2022) First report of *Taxus media* branch blight caused by *Neopestalotiopsis clavispora* in China. Plant Disease 106(12): 3214. https://doi.org/10.1094/PDIS-12-21-2840-PDN

Lippi G, Serra G, Vernieri P, Tognoni F (2003) Response of potted *Callistemon* species to high salinity. Acta Horticulturae 609: 247–250. https://doi.org/10.17660/ActaHortic.2003.609.36

Lombard L, Polizzi G, Guarnaccia V, Vitale A, Crous PW (2011) *Calonectria* spp. causing leaf spot, crown and root rot of ornamental plants in Tunisia. Persoonia 27(1): 73–79. https://doi.org/10.3767/003158511X615086

Maharachchikumbura SS, Hyde KD, Groenewald JZ, Xu J, Crous PW (2014) *Pestalotiopsis* revisited. Studies in Mycology 79(1): 121–186. https://doi.org/10.1016/j.simyco.2014.09.005

Medda S, Mulas M (2021) Fruit quality characters of myrtle (*Myrtus communis* L.) selections: Review of a domestication process. Sustainability 13(16): 8785. https://doi.org/10.3390/su13168785

Morin L, Aveyard R, Lidbetter JR, Wilson PG (2012) Investigating the host-range of the rust fungus *Puccinia psidii sensu lato* across tribes of the family *Myrtaceae* present in Australia. PLoS ONE 7(4): e35434. https://doi.org/10.1371/journal.pone.0035434

Mulas M, Cani MR, Brigaglia N (1998) Characters useful to cultivation in spontaneous populations of *Myrtus communis* L. Acta Horticulturae 457(457): 271–278. https://doi.org/10.17660/ActaHortic.1998.457.34

Osono T, Takeda H (2006) Fungal decomposition of *Abies* needle and *Betula* leaf litter. Mycologia 98(2): 172–179. https://doi.org/10.1080/15572536.2006.11832689

Paap T, Santini A, Rodas CA, Granados GM, Pecori F, Wingfield MJ (2023) *Myrtus communis* in Europe threatened by the pandemic and South African strains of the myrtle rust pathogen *Austropuccinia psidii* (Sphaerophragmiaceae, Pucciniales). In: Jactel H, Orazio C, Robinet C, Douma JC, Santini A, Battisti A, Branco M, Seehausen L, Kenis M (Eds) Conceptual and technical innovations to better manage invasions of alien pests and pathogens in forests. NeoBiota 84: 41–46. https://doi.org/10.3897/neobiota.84.95823

Park S, Lee SY, Lee JJ, Back CG, Ten L, Lee HB, Jung HY (2016) First report of *Neopestalotiopsis australis* isolated from soil in Korea. The Korean Journal of Mycology 44: 360–364. https://doi.org/10.4489/KJM.2016.44.4.360

Pennycook SR, Young JM, Fletcher MJ, Fry PR (1989) Plant diseases recorded in New Zealand. Vol. 3. Auckland, Plant Disease Division. D.S.I.R.

Pérez-Sierra A, Alvarez LA, Leon M, Abad-Campo P, Armengol J, Garcia-Jimenez J (2007) First report of leaf spot, blight, and stem lesions caused by *Cylindrocladium pauciramosum* on Callistemon in Spain. Plant Disease 91(8): 1057–1057. https://doi.org/10.1094/PDIS-91-8-1057C

Polizzi G, Crous PW (1999) Root and collar rot of milkwort caused by *Cylindrocladium pauciramosum*, a new record for Europe. European Journal of Plant Pathology 105(4): 407–411. https://doi.org/10.1023/A:1008759230180

Polizzi G, Vitale A, Aiello D, Dimartino MA, Parlavecchio G (2007) First report of damping-off and leaf spot caused by *Cylindrocladium scoparium* on different accessions of bottlebrush cuttings in Italy. Plant Disease 91(6): 769–769. https://doi.org/10.1094/PDIS-91-6-0769B

POWO (2024) Plants of the World Online. Facilitated by the Royal Botanic Gardens, Kew. Published on the Internet. http://www.plantsoftheworldonline.org/ [Retrieved 22 Feb. 2024]

Prakash CP, Thirumalai E, Rajulu MG, Thirunavukkarasu N, Suryanarayanan TS (2015) Ecology and diversity of leaf litter fungi during early-stage decomposition in a seasonally dry tropical forest. Fungal Ecology 17: 103–113. https://doi.org/10.1016/j.funeco.2015.05.004

Prasannath K, Shivas RG, Galea VJ, Akinsanmi OA (2021) *Neopestalotiopsis* species associated with flower diseases of *Macadamia integrifolia* in Australia. Journal of Fungi 7(9): 771. https://doi.org/10.3390/jof7090771

Rajulu MBG, Lai LB, Murali TS, Gopalan V, Suryanarayanan TS (2014) Several fungi from fire-prone forests of southern India can utilize furaldehydes. Mycological Progress 13(4): 1049–1056. https://doi.org/10.1007/s11557-014-0992-0

Rebollar-Alviter A, Silva-Rojas HV, Fuentes-Aragón D, Acosta-González U, Martínez-Ruiz M, Parra-Robles BE (2020) An emerging strawberry fungal disease associated with root rot, crown rot and leaf spot caused by *Neopestalotiopsis rosae* in Mexico. Plant Disease 104(8): 2054–2059. https://doi.org/10.1094/PDIS-11-19-2493-SC

Reddy MS, Murali TS, Suryanarayanan TS, Rajulu MG, Thirunavukkarasu N (2016) *Pestalotiopsis* species occur as generalist endophytes in trees of Western Ghats forests of southern India. Fungal Ecology 24: 70–75. https://doi.org/10.1016/j.funeco.2016.09.002

Rodríguez-Gálvez E, Hilário S, Lopes A, Alves A (2020) Diversity and pathogenicity of *Lasiodiplodia* and *Neopestalotiopsis* species associated with stem blight and dieback of blueberry plants in Peru. European Journal of Plant Pathology 157(1): 89–102. https://doi.org/10.1007/s10658-020-01983-1

Roux J, Greyling I, Coutinho TA, Verleur M, Wingfeld MJ (2013) The Myrtle rust pathogen, *Puccinia psidii*, discovered in Africa. IMA Fungus 4(1): 155–159. https://doi.org/10.5598/imafungus.2013.04.01.14

Santos J, Hilário S, Pinto G, Alves A (2022) Diversity and pathogenicity of pestalotioid fungi associated with blueberry plants in Portugal, with description of three novel species of *Neopestalotiopsis*. European Journal of Plant Pathology 162(3): 539–555. https://doi.org/10.1007/s10658-021-02419-0

Shahriar SA, Nur-Shakirah AO, Mohd MH (2022) *Neopestalotiopsis clavispora* and *Pseudopestalotiopsis camelliae-sinensis* causing grey blight disease of tea (*Camellia sinensis*) in Malaysia. European Journal of Plant Pathology 162(3): 709–724. https://doi.org/10.1007/s10658-021-02433-2

Shivas RG (1989) Fungal and bacterial diseases of plants in Western Australia. Journal of the Royal Society of Western Australia 72: 1–62.

Silva AC, Diogo E, Henriques J, Ramos AP, Sandoval-Denis M, Crous PW, Bragança H (2020) *Pestalotiopsis pini* sp. nov., an emerging pathogen on stone Pine (*Pinus pinea* L.). Forests 11(8): 805. https://doi.org/10.3390/f11080805

Silvestro D, Michalak I (2012) raxmlGUI: A graphical front-end for RAxML. Organisms Diversity and Evolution 12: 335–337. https://doi.org/10.1007/s13127-011-0056-0

Stamatakis E (2006) RAxML-VI-HPC: maximum likelihood-based phylogenetic analyses with thousands of taxa and mixed models. Bioinformatics 22: 2688–2690. https://doi.org/10.1093/bioinformatics/btl446

Swofford DL (2002) PAUP* 4.0b10: Phylogenetic analysis using parsimony (*and other methods). Sinauer Associates, Sunderland, MA. https://doi.org/10.1111/j.0014-3820.2002.tb00191.x

Vitale A, Crous PW, Lombar L, Polizzi G (2013) Calonectria diseases on ornamental plants in Europe and the Mediterranean basin: An overview. Journal of Plant Pathology 95: 463–476.

Voglmayr H, Aguirre-Hudson MB, Wagner HG, Tello S, Jaklitsch WM (2019) Lichens or endophytes? The enigmatic genus *Leptosillia* in the Leptosilliaceae fam. nov.(Xylariales), and *Furfurella* gen. nov.(Delonicicolaceae). Persoonia-Molecular Phylogeny and Evolution of Fungi 42(1): 228–60. https://doi.org/10.3767/persoonia.2019.42.09

Voglmayr H, Castlebury LA, Jaklitsch WM (2017) *Juglanconis* gen. nov. on Juglandaceae, and the new family Juglanconidaceae (Diaporthales). Persoonia 38: 136–155. https://doi.org/10.3767/003158517x694768

Voglmayr H, Friebes G, Gardiennet A, Jaklitsch WM (2018) *Barrmaelia* and *Entosordaria* in Barrmaeliaceae (fam. nov., Xylariales) and critical notes on *Anthostomella*-like genera based on multigene phylogenies. Mycological Progress 17: 155–177. https://doi.org/10.1007/s11557-017-1329-6

Voglmayr H, Gardiennet A, Jaklitsch WM (2016) *Asterodiscus* and *Stigmatodiscus*, two new apothecial dothideomycete genera and the new order Stigmatodiscales. Fungal Diversity 80: 271–284. https://doi.org/10.1007/s13225-016-0356-y

Voglmayr H, Jaklitsch WM (2008) Prosthecium species with *Stegonsporium* anamorphs on Acer. Mycological Research 112: 885–905. https://doi.org/10.1016/j.mycres.2008.01.020

White TJ, Bruns T, Lee S, Taylor J (1990) Amplification and direct sequencing of fungal ribosomal RNA genes for phylogenetics. In: Innis MA, Gelfand DH, Sninsky JJ, White TJ (Eds) PCR Protocols: a guide to methods and amplifications. Academic Press, San Diego, 315–322. https://doi.org/10.1016/B978-0-12-372180-8.50042-1

Werle E, Schneider C, Renner M, Völker M, Fiehn W (1994) Convenient single-step, one tube purification of PCR products for direct sequencing. Nucleic Acids Research 22: 4354–4355. https://doi.org/10.1093/nar/22.20.4354

Wu CG, Tseng HY, Chen ZC (1982) Fungi inhabiting on *Schoenoplectus triqueter* (L.) Palla (I). Taiwania 27: 35–38.

Yanna Ho WH, Hyde KD (2002) Fungal succession on fronds of *Phoenix hanceana* in Hong Kong. Fungal Diversity 10: 185–211.

You LQ, Senanayake IC, Liu JW, Luo M, Huang YH, Dong ZY (2024) *Neopestalotiopsis iberica* induces leaf spots on *Synsepalum dulcificum* in China. Journal of Phytopathology 172(1): e13258. https://doi.org/10.1111/jph.13258

Zheng X, Liu X, Li X, Quan C, Li P, Chang X, Gu J, Khaskheli MI, Gong G (2023) *Pestalotiopsis* species associated with blueberry leaf spots and stem cankers in Sichuan province of China. Plant Disease 107(1): 149–156. https://doi.org/10.1094/PDIS-07-21-1550-RE

MycoKeys

MycoKeys 106: 153–172 (2024)
DOI: 10.3897/mycokeys.106.117540

Research Article

Surveying lichen diversity in forests: A comparison of expert mapping and eDNA metabarcoding of bark surfaces

Lukas Dreyling[1,2], Steffen Boch[3], H. Thorsten Lumbsch[4], Imke Schmitt[1,2]

1 *Senckenberg Biodiversity and Climate Research Centre (SBiK-F), Frankfurt am Main, Germany*
2 *Goethe University Frankfurt, Institute of Ecology, Evolution and Diversity, Frankfurt am Main, Germany*
3 *WSL Swiss Federal Institute for Forest, Snow and Landscape Research, Birmensdorf, Switzerland*
4 *Collections, Conservation, and Research, The Field Museum, Chicago, IL 60605-2496, USA*

Corresponding authors: Lukas Dreyling (Lukas.Dreyling@gmx.net); Imke Schmitt (imke.schmitt@senckenberg.de)

Abstract

Lichens are an important part of forest ecosystems, contributing to forest biodiversity, the formation of micro-niches and nutrient cycling. Assessing the diversity of lichenised fungi in complex ecosystems, such as forests, requires time and substantial skills in collecting and identifying lichens. The completeness of inventories thus largely depends on the expertise of the collector, time available for the survey and size of the studied area. Molecular methods of surveying biodiversity hold the promise to overcome these challenges. DNA barcoding of individual lichen specimens and bulk collections is already being applied; however, eDNA methods have not yet been evaluated as a tool for lichen surveys. Here, we assess which species of lichenised fungi can be detected in eDNA swabbed from bark surfaces of living trees in central European forests. We compare our findings to an expert floristic survey carried out in the same plots about a decade earlier. In total, we studied 150 plots located in three study regions across Germany. In each plot, we took one composite sample based on six trees, belonging to the species *Fagus sylvatica*, *Picea abies* and *Pinus sylvestris*. The eDNA method yielded 123 species, the floristic survey 87. The total number of species found with both methods was 167, of which 48% were detected only in eDNA, 26% only in the floristic survey and 26% in both methods. The eDNA contained a higher diversity of inconspicuous species. Many prevalent taxa reported in the floristic survey could not be found in the eDNA due to gaps in molecular reference databases. We conclude that, currently, eDNA has merit as a complementary tool to monitor lichen biodiversity at large scales, but cannot be used on its own. We advocate for the further development of specialised and more complete databases.

Key words: Assessment, biodiversity, bioindicators, conservation, databases, floristic survey, identification, inventory, metabarcoding, monitoring

Academic editor: Pradeep Divakar
Received: 18 December 2023
Accepted: 10 May 2024
Published: 21 June 2024

Citation: Dreyling L, Boch S, Lumbsch HT, Schmitt I (2024) Surveying lichen diversity in forests: A comparison of expert mapping and eDNA metabarcoding of bark surfaces. MycoKeys 106: 153–172. https://doi.org/10.3897/mycokeys.106.117540

Introduction

Lichens are important components of biodiversity in forest ecosystems, where they form epiphytic communities in the canopy (Ellis 2012) and on tree trunks (Hofmeister et al. 2016). In central European forests, lichens and their symbionts are characteristic taxa of the bark surface community (Baldrian 2017; Dreyling

et al. 2022; Hofmann et al. 2023). In fact, the bark of trees has been proposed as an important part of the forest microbiome and sustains a high microbial biomass especially if lichens are present (Baldrian 2017). Temperate forests harbour more than a hundred, often several hundred species of lichen-forming fungi (Jüriado et al. 2003; Coppins and Coppins 2005; Boch et al. 2013; Lõhmus and Lõhmus 2019). The lichen communities contribute to forest ecosystem function by retaining water (Van Stan and Pypker 2015), cycling minerals and nutrients (Pike 1978; Reiners and Olson 1984; Knops et al. 1991, 1996; Campbell et al. 2010), being part of the food web and providing habitat and micro-niches for other organisms (reviewed in Ellis (2012) and Asplund and Wardle (2017)). Forest lichen communities respond to abiotic environmental changes (Miller et al. 2018; Łubek et al. 2021), as well as to forest management (Nascimbene et al. 2013; Boch et al. 2021). Some species can be used as indicators to monitor the effects of anthropogenic pollutants (Frati and Brunialti 2023). These are important reasons to survey and monitor lichen biodiversity in forests.

The assessment of lichen biodiversity can be challenging, even for taxonomic experts (Vondrák et al. 2016). Since species identification of lichenised fungi often relies only on few morphological characters (Crespo and Lumbsch 2010), considerable expertise is necessary and often requires specimen collection for ex situ identification, for example, through microscopy or chemical tests (Wright et al. 2019). As a result, the outcomes of lichen surveys are highly dependent on the training of collectors (Giordani et al. 2009). Additionally, lichen-forming fungi are a group with high potential for cryptic diversity that cannot be distinguished in the field (Crespo and Lumbsch 2010; Altermann et al. 2014).

Molecular markers are useful complementary tools to aid the identification of lichenised and non-lichenised fungi (Lücking et al. 2020). Especially, the ITS barcode marker is increasingly used for species identification and species delimitation of lichenised fungi (Schoch et al. 2012; Bradshaw et al. 2020). It has been applied to assess species diversity within geographic regions (Kelly et al. 2011), as well as within taxonomic groups, for example, Parmeliaceae (Divakar et al. 2016). While ITS barcoding works well for the majority of species, it has limitations in some taxonomic groups, for example, the genus *Cladonia*, which seems to be lacking a sufficient barcode gap at least in some species complexes (Pino-Bodas et al. 2013; Marthinsen et al. 2019) or members of Graphidaceae and Pertusariaceae, which do not amplify reliably with common ITS primers, so that their ITS is not used in multi-locus phylogenies (Schmitt and Lumbsch 2004; Rivas Plata et al. 2013) and they remain under-represented in DNA databases. A small number of studies have attempted to identify species and characterise the lichen community by metabarcoding bulk specimen collections (Wright et al. 2019; Henrie et al. 2022). They found that this method produces comparable results between minimally trained and expert collectors and thus potentially reduces the need for extensive training (Wright et al. 2019; Henrie et al. 2022). Furthermore, they concluded that metabarcoding surveys could enable a more efficient sampling over a larger spatial extent (Wright et al. 2019).

Biodiversity assessments using environmental DNA (eDNA) allow species-level identification from DNA present in environmental samples, such as water, soil or air (Taberlet et al. 2012; Yoccoz 2012). In comparison to bulk metabarcoding, this method has additional advantages, such as targeting a broader range of taxa (Taberlet et al. 2012) and being non-invasive, i.e. not

requiring destruction of specimens (Deiner et al. 2017). Despite some drawbacks, in particular due to incomplete databases and primer bias (Bellemain et al. 2010; Keck et al. 2022), eDNA has shown great potential for biodiversity assessments (Shirouzu et al. 2016; Frøslev et al. 2019). When eDNA and conventional methods were compared, species overlap was variable depending on the taxonomic group, but eDNA always identified taxa that were not picked up with other methods (Cordier et al. 2021). In a meta-analysis, eDNA was found to detect more species in general and significantly more rare species, exhibiting higher accuracy and efficiency, while being less costly than conventional biodiversity assessments (Fediajevaite et al. 2021).

In this study, we analyse the utility of eDNA – obtained from bark surfaces of tree trunks at breast height – to assess the diversity of lichen communities in central European forests. In previous studies, we have generated datasets of entire fungal communities associated with bark surfaces, based on ITS metabarcoding (Dreyling et al. 2022, 2024; Hofmann et al. 2023). Here, we use only the fraction of lichenised fungi from these datasets. The sampling sites are 150 specific plots located within the Biodiversity Exploratories (Fischer et al. 2010) in northern, central and southern Germany. We compare the results to a previous floristic survey carried out in the same plots (Boch et al. 2021). Specifically, we address the following questions: I. Which species of lichenised fungi can be identified from environmental samples via eDNA metabarcoding? II. What are the differences to the diversity obtained through an expert survey? III. Is eDNA metabarcoding a reliable tool to survey lichen diversity in forests?

Material and methods

Study sites

We surveyed communities of forest-dwelling lichen species in 150 plots, located in three regions, within the Biodiversity Exploratories framework (Fischer et al. 2010). The regions mark a south-west to north-east gradient across Germany and differ in their climate and topography. The plots within the regions were further selected along a gradient of the anthropogenic impact, i.e. forest management intensity (Fischer et al. 2010; Boch et al. 2021) and are representative for central European forest ecosystems. The South-West region is on average 2 °C colder than the North-East (6.5 °C vs. 8.5 °C) and experiences approximately twice the amount of precipitation (700–1000 mm vs. 500–600 mm; Fischer et al. (2010)). In addition, they differ in their tree species composition, with beech trees (*Fagus sylvatica*) as the dominant species in most plots across the regions. Some plots are dominated by coniferous trees, specifically Norway spruce (*Picea abies*) in the South-West region and Scots pine (*Pinus sylvestris*) in the North-East region (Schall and Ammer 2018). For both, eDNA sampling and classical lichen mapping, we surveyed a 20 m × 20 m subplot within the established 100 m × 100 m experimental plots.

eDNA sampling and processing

In each plot, we collected eDNA samples from the bark surface of six trees of the respective dominant species in May 2021. The six individual tree samples were pooled into one composite sample per plot. Since we had previously

shown large community differences between tree sizes (Dreyling et al. 2022), we included two trees each of large (> 30 cm diameter at 150 cm height), medium (15–30 cm) and small (5–15 cm) size in each sample. If this type of sampling was not possible, we included additional trees of the size class that best represented the forest in the immediate surrounding. To sample the bark surface eDNA, we moistened the bark surface with sterile water and then used a nylon-flocked medical swab (FLOQSwabs™, Copan, Brescia, Italy) to collect the bark surface biofilm (Fig. 1). We swabbed around the full tree trunk at approximately 150 cm height from the forest floor, excluding large patches of bryophytes to avoid bias due to the amplification of plant ITS, but explicitly including all other epiphytic organisms. The material collected with the swabs was fixed with 5 ml nucleic acid preservation (NAP) buffer (Camacho-Sanchez et al. 2013) in 15 ml tubes directly after sampling and placed on ice in the field. Afterwards, the samples were stored at 4 °C until DNA extraction in the following week.

Figure 1. Sampling procedure: We moistened the tree trunk on all sides at breast height and swabbed the bark surface in a zigzagging motion along a 10 cm wide band around the tree trunk. The swabbed area included smooth bark surfaces and crevices, as well as epiphytic organisms, if they were present.

A detailed description of the DNA extraction and bioinformatic processing of sequencing reads is given in Dreyling et al. (2022). In brief: We extracted DNA, from samples as well as three extraction blanks, using an extraction kit (Quick-DNA Fecal/Soil Microbe Microprep, Zymo Research Europe GmbH, Freiburg, Germany) with an additional step ensuring liberation of material from the swab. Targeting the ITS2 region, we subsequently amplified the fungal DNA in triplicate, using the universal primer pair fITS7 (GTGARTCATCGAATCTTTG) (Ihrmark et al. 2012) and ITS4 (TCCTCCGCTTATTGATATGC) (White et al. 1990). PCR reactions also included negative controls (without sample material) and multiplex controls (empty wells). We cleaned the amplicons via a magnetic bead protocol (MagSI-NGSPREP Plus, magtivio B.V., Geelen, Netherlands) and measured DNA concentration through fluorometry (Qubit dsDNA HS assay on a Qubit 3.0, Thermo Fisher Scientific, MA, United States), before equimolar pooling. The library preparation and Illumina sequencing (MiSeq 2 × 300 bp paired-end) was carried out by Fasteris SA (Plan-les-Ouates, Switzerland) according to their MetaFast Protocol, designed to avoid additional PCR bias.

We used Cutadapt (v3.3; Martin (2011)) to demultiplex the obtained sequencing reads and DADA2 (Callahan et al. 2016) to infer Amplicon Sequencing Variants (ASVs). Taxonomy was assigned against the Martin7 database (Vondrák et al. 2023) using a local BLAST (Altschul et al. 1990) search. Assignments were kept if the "percent identity" was higher than 97%. Additionally, we used the UNITE database (Abarenkov et al. 2022, Version 9.0, incl. non-fungal eukaryotic DNA as outgroups) and the NCBI nucleotide database (Sayers et al. 2022, percent identity > 97%) to assign additional taxonomy to the ASVs that could not be assigned with the Martin7 database. We used FUNGuild (Nguyen et al. 2016) to assign information on the functional guild to the additionally assigned fungal ASVs and filtered the dataset to only contain ASVs which were classified as lichenised fungi. All scripts on the bioinformatic processing, as well as the analysis, are available at Github at https://github.com/LukDrey/eDNA_lichen_survey.

Traditional floristic survey

The floristic survey was carried out in 2007 and 2008 and recorded occurrences of lichenised fungi in over 600 plots of the Biodiversity Exploratories (Boch et al. 2021), including the 150 plots of the eDNA sampling. The survey covered a comparable area of 20 m × 20 m around the plot centre, which was not fully identical, but always spatially close to the sampling area of the eDNA survey. All lichens occurring on bark (up to 2.5 m height), rocks, deadwood and soil were recorded. We did not limit the survey time per plot due to strongly varying environmental heterogeneity amongst plots. Most specimens were identified in situ, except when microscopic or chemical characters had to be assessed.

Comparison of the two methods

A number of taxonomic changes took place in the approximately 13 years between the two surveys. We accommodated for these developments by harmonising the two species lists and adopting the names accepted as the current names in MycoBank (Crous et al. 2004; Robert et al. 2013). Additionally, we

only included species from the floristic dataset, which were recorded as epiphytes in the 150 experimental plots, thus excluding species collected from rocks, deadwood and soil. A list of all species is provided as Suppl. material 1.

To allow for comparisons between the two methods, we transformed the read counts obtained through the eDNA metabarcoding to presence-absence data. Using the two presence-absence datasets, we compared the two methods and assessed the diversity and species richness found with each method. Furthermore, we calculated the number of plots in which a species was found. Finally, we selected five species to visualise geographical occurrence patterns, based on the two different assessment methods.

Results and discussion

In total, we found 167 species of lichenised fungi in the two surveys. The eDNA method found 123 species, while the traditional floristic survey recorded 87 species (Fig. 2). With the eDNA method, we found 80 species that were not found via the traditional survey methods, while with the floristic survey, we found 44 species not detected by the eDNA method. The higher number of taxa identified from the eDNA is congruent with bulk-specimen sequencing studies from other ecosystems (Wright et al. 2019). Interestingly, only 26% of the total taxa were shared between both methods, likely due to the number of small, inconspicuous genera, such as *Micarea* (Launis et al. 2019), that were only found with the eDNA (Fig. 3). The overlap between the two methods is similar to what has previously been reported for comparisons of eDNA to fruiting body surveys of forest fungi (Shirouzu et al. 2016; Frøslev et al. 2019).

In our study, several species are detected exclusively or predominantly by either of the two methods. Additionally, even the most common species are not necessarily detected by both methods. For example, out of the five most common species (Fig. 3), two were not found in the traditional floristic study,

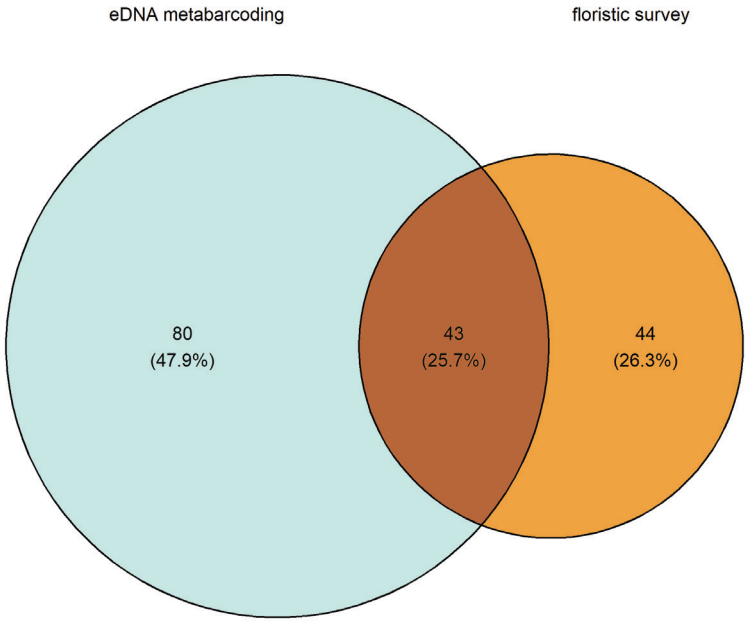

Figure 2. Number and proportion of species of lichenised fungi found either in eDNA metabarcoding or floristic survey or in both methods.

Scoliciosporum sarothamni and *Micarea czarnotae*. This result is especially striking for *S. sarothamni* which was found in 146 of 150 plots via eDNA metabarcoding, but was not identified in the floristic study. This species is very small and thus hard to find and distinguish (Kowalewska and Kukwa 2003; Dymytrova 2011). Therefore, it is plausible that it has been overlooked or simply grouped with other taxa, such as its sister species *Scoliciosporum chlorococcum*, in the floristic survey. However, *S. chlorococcum* was also highly prevalent in the eDNA study (121 occurrences), but rarely found in the floristic dataset (11 occurrences). A potential reason for *Scoliciosporum* being less prevalent in the floristic dataset is that both species have a greenish thallus and are often occurring within dominant green algal colonies, making them hard to recognise with traditional methods, especially when sterile.

Other taxa, commonly found in the eDNA metabarcoding dataset, had not been formally described at the time of the floristic survey. For example, both *Opeltiella rubrisoli* and *Micarea czarnotae* were only described in 2019 (Launis et al. 2019; Liu et al. 2019). *Micarea czarnotae* had previously been included in *M. prasina*, which was also only found in eight plots in the floristic study. In general, the eDNA dataset contained a high number of inconspicuous taxa from genera that are difficult to distinguish, such as *Micarea* (Launis et al. 2019), *Scoliciosporum* (Dymytrova 2011) and *Bacidina* (Czarnota and Guzow-Krzemińska 2018). Consistent with our findings, other studies have previously reported that eDNA was superior in revealing hidden diversity for fungi (Shirouzu et al. 2016), including lichen-forming fungi (Wright et al. 2019). An additional advantage of the eDNA approach might be the detection of taxa not directly occurring on the sampled substrate itself, for example, from propagules (Wright et al. 2019; Henrie et al. 2022).

The floristic dataset also includes numerous taxa which were not identified in the eDNA approach. For example, *Pseudosagedia aenea*, a common species found in the floristic survey (occurring in 104 plots), was not found by the eDNA metabarcoding (Fig. 3), albeit ITS sequences of this taxon are included in the sequence repositories used in this study. One potential reason is that their habitat is outside of the sampled area, for example, in the tree crowns or at the base of the tree. In fact, several species prevalent in the floristic dataset, but not the eDNA, occur in these habitats, for example, *Cladonia coniocraea* at the base of trees (Wirth et al. 2013), *Pseudevernia furfuracea* on branches in the canopy (Kranner et al. 2003) and also *P. aenea* at the stem base (Larsen et al. 2020). Therefore, restricting the eDNA sampling, or any survey, to a single forest substrate is likely insufficient to describe the full lichen diversity (see also Boch et al. (2013)).

Overall, only very few species were found in a similar number of plots with both methods (Fig. 3). The most prevalent species found with both methods were *Coenogonium pineti* and *Lepraria incana*. *Coenogonium pineti* was found in 119 plots in the floristic study and in 80 plots in the eDNA dataset. The prevalence of *L. incana* was even more similar, being found in 106 plots with floristic and 113 plots with eDNA methods. Although, both species preferentially grow at the base of trees (Lackovičová and Guttová 2005; Larsen et al. 2020), they were also often recorded with the eDNA method. It is possible that the dispersal units of these taxa (ascospores in *C. pineti* and soredia in *L. incana*) are dispersed further up the stem, for example, by wind. Furthermore, snails and slugs may play a role in distributing lichen propagules along the stem (Asplund et al. 2010; Boch et al. 2011).

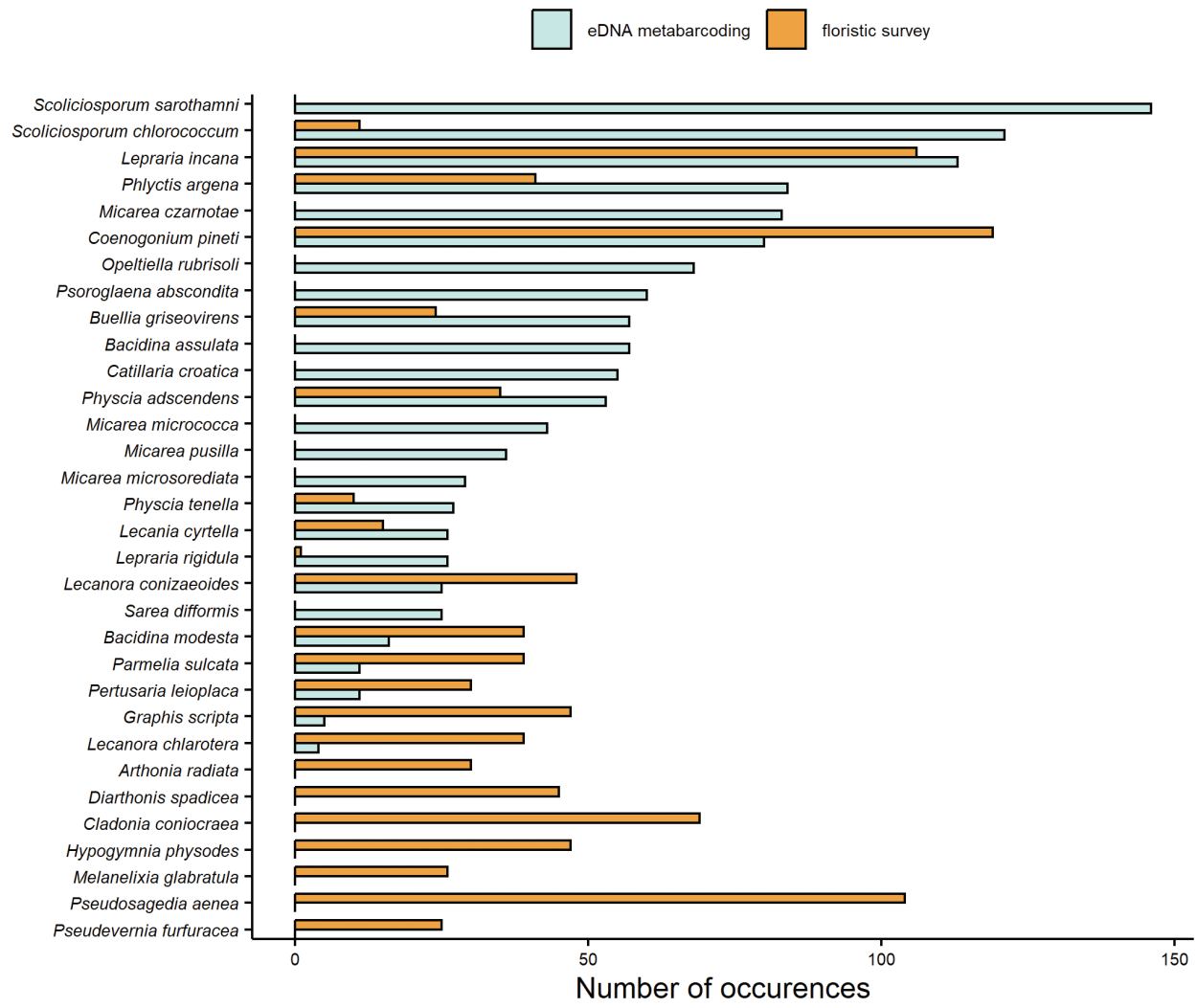

Figure 3. Most common species of lichenised fungi detected by either method (eDNA metabarcoding or floristic survey). We show taxa, which occurred in at least 25 plots (out of 150) across the three regions.

Another apparent reason for the differences in eDNA and floristic surveys are related to the databases necessary for taxonomic assignment of the metabarcoding reads. Despite large efforts in recent years towards the development of reference databases for fungal taxonomy, like the UNITE database (Abarenkov et al. 2023) or the GlobalFungi project (Větrovský et al. 2020), many gaps remain. In our study, several species, commonly found in the floristic study, have no reference sequences in the UNITE database, including *Diarthonis spadicea* and all species of the genus *Arthonia*. Previous studies have proposed to close the gaps in the reference databases by large scale sequencing of lichen herbarium specimens (Gueidan and Li 2022). Regional databases, for example, for Great Britain and Ireland (Kelly et al. 2011) or part of the western USA (Kerr and Leavitt 2023) were helpful in identifying lichen specimens, based on barcodes or bulk metabarcoding. The recently-published Martin7 database, focusing on central European lichens (Vondrák et al. 2023), greatly improved the results of the present study. It enabled the assignment of taxonomy to over 30 additional ASVs, resulting in 27 additional species compared to an initial assignment using the UNITE database.

Technical issues related to sequencing might be the reason that some species present in the floristic study could not be found in the eDNA assessment, although the ITS sequences are included in the UNITE and Martin7 databases. A search with Primer-BLAST (Ye et al. 2012) revealed that, in some cases, the primer combination used in this study could likely not amplify these species. However, some species, commonly occurring in the floristic study such as *Hypogymnia physodes* or *Pseudevernia furfuracea*, should have been amplified with the current primers, indicating other issues. A potential reason might be PCR biases influencing which taxa or groups are preferentially amplified (Bellemain et al. 2010). For example, shorter DNA fragments are usually amplified more often (Deagle et al. 2006). It is possible that we missed ITS sequences that are longer because they contain introns, a frequent and stochastic feature of the rDNAs of lichen-forming fungi (Simon et al. 2005). Furthermore, the output of the sequencing machine is limited, so that taxa with few copies might not be sequenced (Gloor et al. 2017).

There is a temporal gap of approximately 13 years between the floristic survey and the eDNA sampling, which may explain some of the observed differences, especially with regard to pollution with sulphur dioxide and nitrogen. Sulphur dioxide (SO_2) pollution has been decreasing in western Europe since the 1970s, enabling the return of many species to formerly uninhabitable ecosystems (Rose and Hawksworth 1981; Nash and Gries 2002). Conversely, species that are tolerant to acidic and sulphur-enriched conditions, for example, *Lecanora conizaeoides*, have been reported to decline in central Europe (Nash and Gries 2002; Farkas et al. 2022). In our study, the number of plots, in which *L. conizaeoides* was identified with eDNA in 2021, has halved in relation to the floristic study in 2007/2008. Today, nitrogen pollution is more important in shaping lichen communities than SO_2 pollution (Purvis et al. 2003; Hultengren et al. 2004; Pinho et al. 2008; Gadsdon et al. 2010). Temperate forests experience increased deposition of nitrogen, for example, through ammonia fertilisers or nitric oxides from fuel combustion, and nitrophytic species have increased in the recent past (Carter et al. 2017). In the present study, two species regarded as nitrophytes, *Physcia adscendens* and *P. tenella* (Gadsdon et al. 2010), have been found more frequently in the eDNA sampling than in the earlier floristic survey (Fig. 3). Interestingly, other nitrophytic species, such as *Xanthoria parietina*, *Phaeophyscia orbicularis* or *Candelariella reflexa* (Gadsdon et al. 2010), were found less frequently or not at all in the eDNA sampling (Suppl. material 1). In addition, differences between the floristic and the eDNA survey in lichen diversity and community composition might be because of successional developments or the disruption of such developments by forestry management, leading to changes in forest structure and composition, i.e. changed environmental conditions. Such changes might have been even accelerated by climate change that has been proposed to change lichen diversity and community composition (van Herk et al. 2002; Aptroot 2009; Allen and Lendemer 2016; Nascimbene et al. 2016; Nelsen and Lumbsch 2020).

The three study regions differed considerably in their lichen diversity. In the eDNA metabarcoding survey, the proportion of fungal reads assigned to lichens was highest in the south-western region with approximately 39% of the total fungal reads, 27% in the north-eastern and lowest in the central region with only 14%. On average, lichens accounted for 27% of the total fungal reads. We

observe a similar pattern in the floristic survey, where the highest number of species was also recorded in the south-western region (82 species), followed by the central and the north-eastern region (32 species). Previous studies in the Biodiversity Exploratories found similar relationships between the regions for plants (Klaus et al. 2013) and arthropods (Simons et al. 2014) that are potentially explained by differences in climate, land-use intensity or nutrient availability. In our study, the higher species richness in the South-West region is likely related to the higher annual precipitation (Fischer et al. 2010), which has been shown to positively influence lichen richness (Marini et al. 2011), but also because of the generally lower former SO_2 deposition compared to the other two regions (Umweltbundesamt 2005).

The differences amongst the three study regions are also apparent in the distribution maps of the five example species, *Buellia griseovirens*, *Graphis scripta*, *Lepraria incana*, *Phlyctis argena* and *Physcia adscendens*. These species were chosen as examples because they were amongst the most prevalent species (Fig. 3) found with both methods, but varied in how often they were recorded. In general, the highest number of plots, in which the example species were recorded, were located in the South-West region (Fig. 4A), while they did not occur in most plots of the North-East region (Fig. 4 C). If a lichen species was frequently recorded by both methods, such as *B. griseovirens*, *L. incana* and *P. argena* in the South-West (Fig. 4A), then it was also found by one of the methods in spatially close plots. In general, the lichen records do not follow a clearly distinguishable pattern of spatial clustering within the regions.

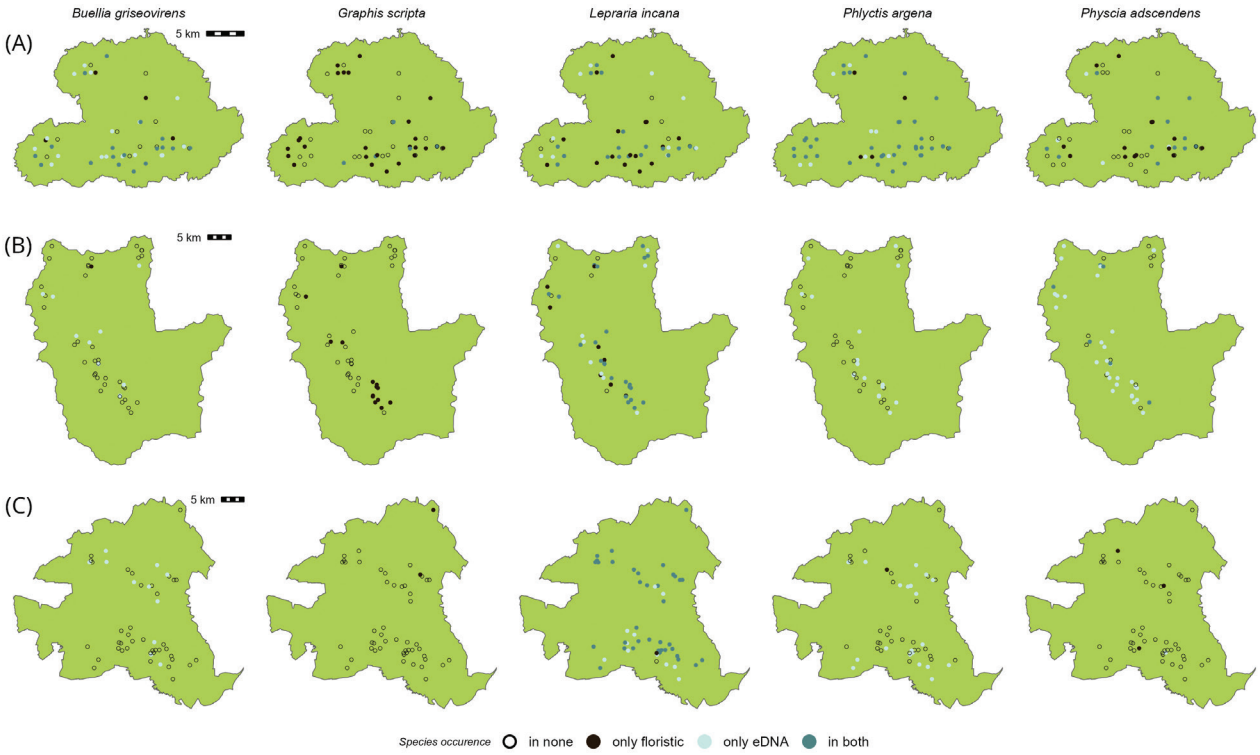

Figure 4. Distribution of five example species within the analysed forest plots of the three regions. Shown are occurrence data based on the floristic survey and eDNA metabarcoding. Each map represents one region (Biodiversity Exploratory) **A** South-West (Swabian Alb) **B** Central (Hainich-Dün) **C** North-East (Schorfheide-Chorin). Each circle depicts a 100 m × 100 m forest plot.

The detection of these five lichen species was different between the methods in the each of the regions. Of the five example species, only *L. incana* was consistently found with both methods across the three regions and consequently is one of the most prevalent species we found. *B. griseovirens* and *P. argena* were found more often in the eDNA samples and almost exclusively with eDNA in the Central and North-East regions (Fig. 4B, C). It is tempting to speculate about a northward shift of the distribution of these species considering the time difference between the two studies, which could explain the absence in the Central and North-East regions during the floristic survey. In addition, the considerably decreased pollution in these two regions might have led to the recovery of lichen communities with many species re-colonising such formerly heavily polluted areas (e.g. Gilbert (1992)).

Nevertheless, *Graphis scripta* was rarely found in the eDNA, but recorded across all three regions in the traditional survey. This pattern is likely related to the use of ITS2 as a molecular marker in the eDNA, which has previously shown low amplification rates for the genus *Graphis* (e.g. Kraichak et al. (2019)). Interestingly, *P. adscendens* was found with both methods in the South-West, purely with the eDNA in the Central and only via floristic survey in the North-East region.

Conclusions

In its current form, eDNA metabarcoding cannot be used as a stand-alone tool to survey epiphytic lichen diversity. However, it can serve as a valuable complementary tool, similarly to studies from many other taxonomic groups (Beng and Corlett 2020; Fediajevaite et al. 2021). In the long run, with more correct and more complete ITS databases, we think that the bulk of species from floristic studies can, indeed, be identified with this method. We have to be aware that there are some taxonomic groups, which have too little ITS variability or too little amplification success, to be determined with this tool. A field, which could benefit from metabarcoding of eDNA, is community ecology of lichen-forming fungi, for example, understanding communities and species assemblages of lichenised fungi, their photobiont partners and other thallus-associated microorganisms. For example, species co-occurrences, based on eDNA, could be used to explore the concept of photobiont-mediated guilds (Rikkinen 2003). We have previously shown – based on the same DNA samples used here – that the communities of fungi, green algae and bacteria present on bark surfaces, strongly affect each other's beta diversities (Dreyling et al. 2024), suggesting that functional guilds, for example, of mycobionts and their photobiont partners, might be also be detected in the present data. Taxonomic assignments need to be carefully examined to assess if assignments are sensible for the geographic region of interest. Looking forward, the recent development of lichen specific databases might solve some of these issues. If eDNA biodiversity assessments are taken beyond the description of diversity, recently developed methods circumvent this issue altogether and are able to use unclassified taxa in the prediction of ecological states (Keck et al. 2023). Future studies of lichen biodiversity could employ these methods and expand the use of lichens as modern biomonitoring agents.

Acknowledgements

We thank the managers of the three Exploratories, Max Müller, Julia Bass, Robert Künast, Anna K. Franke, Franca Marian and all former managers for their work in maintaining the plot and project infrastructure; Victoria Grießmeier for giving support through the central office, Andreas Ostrowski for managing the central data base and Markus Fischer, Eduard Linsenmair, Dominik Hessenmöller, Daniel Prati, Ingo Schöning, François Buscot, Ernst-Detlef Schulze, Wolfgang W. Weisser and the late Elisabeth Kalko for their role in setting up the Biodiversity Exploratories project. We thank the administration of the Hainich National Park, the UNESCO Biosphere Reserve Swabian Alb and the UNESCO Biosphere Reserve Schorfheide-Chorin, as well as all land owners for the excellent collaboration. Fieldwork permits were issued by the responsible state environmental offices of Baden-Württemberg, Thüringen and Brandenburg.

Additional information

Conflict of interest

The authors have declared that no competing interests exist.

Ethical statement

No ethical statement was reported.

Funding

The work has been (partly) funded by the DFG Priority Program 1374 “Infrastructure – Biodiversity- Exploratories” (SCHM 1711/8-1, FI 1246/6-1).

Author contributions

LD and IS conzeptualized the method; LD collected eDNA samples and generated the taxonomic data; SB conducted the floristic mapping; LD, SB, HTL and IS curated the species list; LD compared the datasets; LD and IS wrote the manuscript; HTL and SB provided feedback.

Author ORCIDs

Lukas Dreyling https://orcid.org/0000-0001-9839-9504
H. Thorsten Lumbsch https://orcid.org/0000-0003-1512-835X
Imke Schmitt https://orcid.org/0000-0002-7381-0296

Data availability

The raw sequencing data for this study is provided in the NCBI Sequence Read Archive under accession number SRR23371988. The code for the analysis is available at https://github.com/LukDrey/eDNA_lichen_survey.

References

Abarenkov K, Zirk A, Piirmann T, Pöhönen R, Ivanov F, Nilsson RH, Kõljalg U (2022) UNITE general FASTA release for eukaryotes. Version 27.10.2022. UNITE Community. https://doi.org/10.15156/BIO/2483913

Abarenkov K, Nilsson RH, Larsson K-H, Taylor AFS, May TW, Frøslev TG, Pawlowska J, Lindahl B, Põldmaa K, Truong C, Vu D, Hosoya T, Niskanen T, Piirmann T, Ivanov F, Zirk A, Peterson M, Cheeke TE, Ishigami Y, Jansson AT, Jeppesen TS, Kristiansson E, Mikryukov V, Miller JT, Oono R, Ossandon FJ, Paupério J, Saar I, Schigel D, Suija A, Tedersoo L, Kõljalg U (2023) The UNITE database for molecular identification and taxonomic communication of fungi and other eukaryotes: Sequences, taxa and classifications reconsidered. Nucleic Acids Research: gkad1039. https://doi.org/10.1093/nar/gkad1039

Allen JL, Lendemer JC (2016) Climate change impacts on endemic, high-elevation lichens in a biodiversity hotspot. Biodiversity and Conservation 25(3): 555–568. https://doi.org/10.1007/s10531-016-1071-4

Altermann S, Leavitt SD, Goward T, Nelsen MP, Lumbsch HT (2014) How Do You Solve a Problem like Letharia? A New Look at Cryptic Species in Lichen-Forming Fungi Using Bayesian Clustering and SNPs from Multilocus Sequence Data. PLoS One 9(5): e97556. https://doi.org/10.1371/journal.pone.0097556

Altschul SF, Gish W, Miller W, Myers EW, Lipman DJ (1990) Basic local alignment search tool. Journal of Molecular Biology 215(3): 403–410. https://doi.org/10.1016/S0022-2836(05)80360-2

Aptroot A (2009) Chapter 23 – Lichens as an Indicator of Climate and Global Change. In: Letcher TM (Ed.) Climate Change. Elsevier, Amsterdam, 401–408. https://doi.org/10.1016/B978-0-444-53301-2.00023-3

Asplund J, Wardle DA (2017) How lichens impact on terrestrial community and ecosystem properties. Biological Reviews of the Cambridge Philosophical Society 92(3): 1720–1738. https://doi.org/10.1111/brv.12305

Asplund J, Larsson P, Vatne S, Gauslaa Y (2010) Gastropod grazing shapes the vertical distribution of epiphytic lichens in forest canopies. Journal of Ecology 98(1): 218–225. https://doi.org/10.1111/j.1365-2745.2009.01584.x

Baldrian P (2017) Forest microbiome: Diversity, complexity and dynamics. FEMS Microbiology Reviews 41: 109–130. https://doi.org/10.1093/femsre/fuw040

Bellemain E, Carlsen T, Brochmann C, Coissac E, Taberlet P, Kauserud H (2010) ITS as an environmental DNA barcode for fungi: An in silico approach reveals potential PCR biases. BMC Microbiology 10(1): 189. https://doi.org/10.1186/1471-2180-10-189

Beng KC, Corlett RT (2020) Applications of environmental DNA (eDNA) in ecology and conservation: Opportunities, challenges and prospects. Biodiversity and Conservation 29(7): 2089–2121. https://doi.org/10.1007/s10531-020-01980-0

Boch S, Prati D, Werth S, Rüetschi J, Fischer M (2011) Lichen Endozoochory by Snails. PLoS One 6(4): e18770. https://doi.org/10.1371/journal.pone.0018770

Boch S, Prati D, Hessenmöller D, Schulze E-D, Fischer M (2013) Richness of Lichen Species, Especially of Threatened Ones, Is Promoted by Management Methods Furthering Stand Continuity. PLoS One 8(1): e55461. https://doi.org/10.1371/journal.pone.0055461

Boch S, Saiz H, Allan E, Schall P, Prati D, Schulze E-D, Hessenmöller D, Sparrius LB, Fischer M (2021) Direct and Indirect Effects of Management Intensity and Environmental Factors on the Functional Diversity of Lichens in Central European Forests. Microorganisms 9(2): 463. https://doi.org/10.3390/microorganisms9020463

Bradshaw M, Grewe F, Thomas A, Harrison CH, Lindgren H, Muggia L, St. Clair LL, Lumbsch HT, Leavitt SD (2020) Characterizing the ribosomal tandem repeat and its utility as a DNA barcode in lichen-forming fungi. BMC Evolutionary Biology 20: 2. https://doi.org/10.1186/s12862-019-1571-4

Callahan BJ, McMurdie PJ, Rosen MJ, Han AW, Johnson AJA, Holmes SP (2016) DADA2: High-resolution sample inference from Illumina amplicon data. Nature Methods 13(7): 581–583. https://doi.org/10.1038/nmeth.3869

Camacho-Sanchez M, Burraco P, Gomez-Mestre I, Leonard JA (2013) Preservation of RNA and DNA from mammal samples under field conditions. Molecular Ecology Resources 13(4): 663–673. https://doi.org/10.1111/1755-0998.12108

Campbell J, Fredeen AL, Prescott CE (2010) Decomposition and nutrient release from four epiphytic lichen litters in sub-boreal spruce forests. Canadian Journal of Forest Research 40(7): 1473–1484. https://doi.org/10.1139/X10-071

Carter TS, Clark CM, Fenn ME, Jovan S, Perakis SS, Riddell J, Schaberg PG, Greaver TL, Hastings MG (2017) Mechanisms of nitrogen deposition effects on temperate forest lichens and trees. Ecosphere 8(3): e01717. https://doi.org/10.1002/ecs2.1717

Coppins BJ, Coppins AM (2005) Lichens – The biodiversity value of western woodlands. Botanical Journal of Scotland 57(1–2): 141–153. https://doi.org/10.1080/03746600508685093

Cordier T, Alonso-Sáez L, Apothéloz-Perret-Gentil L, Aylagas E, Bohan DA, Bouchez A, Chariton A, Creer S, Frühe L, Keck F, Keeley N, Laroche O, Leese F, Pochon X, Stoeck T, Pawlowski J, Lanzén A (2021) Ecosystems monitoring powered by environmental genomics: A review of current strategies with an implementation roadmap. Molecular Ecology 30(13): 2937–2958. https://doi.org/10.1111/mec.15472

Crespo A, Lumbsch HT (2010) Cryptic species in lichen-forming fungi. IMA Fungus 1(2): 167–170. https://doi.org/10.5598/imafungus.2010.01.02.09

Crous PW, Gams W, Stalpers JA, Robert V, Stegehuis G (2004) MycoBank: An online initiative to launch mycology into the 21st century. Studies in Mycology 50: 19–22.

Czarnota P, Guzow-Krzemińska B (2018) *Bacidina mendax* sp. nov., a new widespread species in Central Europe, together with a new combination within the genus *Bacidina*. Lichenologist (London, England) 50(1): 43–57. https://doi.org/10.1017/S0024282917000627

Deagle BE, Eveson JP, Jarman SN (2006) Quantification of damage in DNA recovered from highly degraded samples – a case study on DNA in faeces. Frontiers in Zoology 3(1): 11. https://doi.org/10.1186/1742-9994-3-11

Deiner K, Bik HM, Mächler E, Seymour M, Lacoursière-Roussel A, Altermatt F, Creer S, Bista I, Lodge DM, de Vere N, Pfrender ME, Bernatchez L (2017) Environmental DNA metabarcoding: Transforming how we survey animal and plant communities. Molecular Ecology 26(21): 5872–5895. https://doi.org/10.1111/mec.14350

Divakar PK, Leavitt SD, Molina MC, Del-Prado R, Lumbsch HT, Crespo A (2016) A DNA barcoding approach for identification of hidden diversity in Parmeliaceae (Ascomycota): *Parmelia sensu stricto* as a case study. Botanical Journal of the Linnean Society 180(1): 21–29. https://doi.org/10.1111/boj.12358

Dreyling L, Schmitt I, Dal Grande F (2022) Tree Size Drives Diversity and Community Structure of Microbial Communities on the Bark of Beech (*Fagus sylvatica*). Frontiers in Forests and Global Change 5. https://doi.org/10.3389/ffgc.2022.858382 [October 4, 2023]

Dreyling L, Penone C, Schenk NV, Schmitt I, Dal Grande F (2024) Biotic interactions outweigh abiotic factors as drivers of bark microbial communities in central European forests. ISME Communications 4(1): ycae012. https://doi.org/10.1093/ismeco/ycae012

Dymytrova L (2011) Notes on the genus *Scoliciosporum* (Lecanorales, Ascomycota) in Ukraine. Polish Botanical Journal 56: 61–75.

Ellis CJ (2012) Lichen epiphyte diversity: A species, community and trait-based review. Perspectives in Plant Ecology, Evolution and Systematics 14(2): 131–152. https://doi.org/10.1016/j.ppees.2011.10.001

Farkas E, Varga N, Veres K, Matus G, Sinigla M, Lőkös L (2022) Distribution Types of Lichens in Hungary That Indicate Changing Environmental Conditions. Journal of Fungi (Basel, Switzerland) 8(6): 600. https://doi.org/10.3390/jof8060600

Fediajevaite J, Priestley V, Arnold R, Savolainen V (2021) Meta-analysis shows that environmental DNA outperforms traditional surveys, but warrants better reporting standards. Ecology and Evolution 11(9): 4803–4815. https://doi.org/10.1002/ece3.7382

Fischer M, Bossdorf O, Gockel S, Hänsel F, Hemp A, Hessenmöller D, Korte G, Nieschulze J, Pfeiffer S, Prati D, Renner S, Schöning I, Schumacher U, Wells K, Buscot F, Kalko EKV, Linsenmair KE, Schulze E-D, Weisser WW (2010) Implementing large-scale and long-term functional biodiversity research: The Biodiversity Exploratories. Basic and Applied Ecology 11(6): 473–485. https://doi.org/10.1016/j.baae.2010.07.009

Frati L, Brunialti G (2023) Recent Trends and Future Challenges for Lichen Biomonitoring in Forests. Forests 14(3): 647. https://doi.org/10.3390/f14030647

Frøslev TG, Kjøller R, Bruun HH, Ejrnæs R, Hansen AJ, Læssøe T, Heilmann-Clausen J (2019) Man against machine: Do fungal fruitbodies and eDNA give similar biodiversity assessments across broad environmental gradients? Biological Conservation 233: 201–212. https://doi.org/10.1016/j.biocon.2019.02.038

Gadsdon SR, Dagley JR, Wolseley PA, Power SA (2010) Relationships between lichen community composition and concentrations of NO2 and NH3. Environmental Pollution 158(8): 2553–2560. https://doi.org/10.1016/j.envpol.2010.05.019

Gilbert OL (1992) Lichen reinvasion with declining air pollution. In: Bates JW, Farmer AM (Eds) Bryophytes and Lichens in a Changing Environment. Oxford University Press. https://doi.org/10.1093/oso/9780198542919.003.0006

Giordani P, Brunialti G, Benesperi R, Rizzi G, Frati L, Modenesi P (2009) Rapid biodiversity assessment in lichen diversity surveys: Implications for quality assurance. Journal of Environmental Monitoring 11(4): 730–735. https://doi.org/10.1039/b818173j

Gloor GB, Macklaim JM, Pawlowsky-Glahn V, Egozcue JJ (2017) Microbiome Datasets Are Compositional: And This Is Not Optional. Frontiers in Microbiology 8: 2224. https://doi.org/10.3389/fmicb.2017.02224

Gueidan C, Li L (2022) A long-read amplicon approach to scaling up the metabarcoding of lichen herbarium specimens. MycoKeys 86: 195–212. https://doi.org/10.3897/mycokeys.86.77431

Henrie JR, Thomson BM, Yungfleisch AA, Kerr M, Leavitt SD (2022) Characterizing Crustose Lichen Communities – DNA Metabarcoding Reveals More than Meets the Eye. Diversity 14(9): 766. https://doi.org/10.3390/d14090766

Hofmann B, Dreyling L, Dal Grande F, Otte J, Schmitt I (2023) Habitat and tree species identity shape aboveground and belowground fungal communities in central European forests. Frontiers in Microbiology 14: 1067906. https://doi.org/10.3389/fmicb.2023.1067906

Hofmeister J, Hošek J, Malíček J, Palice Z, Syrovátková L, Steinová J, Černajová I (2016) Large beech (Fagus sylvatica) trees as 'lifeboats' for lichen diversity in central European forests. Biodiversity and Conservation 25(6): 1073–1090. https://doi.org/10.1007/s10531-016-1106-x

Hultengren S, Gralén H, Pleijel H (2004) Recovery of the Epiphytic Lichen Flora Following Air Quality Improvement in South-West Sweden. Water, Air, and Soil Pollution 154(1–4): 203–211. https://doi.org/10.1023/B:WATE.0000022967.35036.ca

Ihrmark K, Bödeker ITM, Cruz-Martinez K, Friberg H, Kubartova A, Schenck J, Strid Y, Stenlid J, Brandström-Durling M, Clemmensen KE, Lindahl BD (2012) New primers to amplify the fungal ITS2 region – evaluation by 454-sequencing of artificial and natural communities. FEMS Microbiology Ecology 82(3): 666–677. https://doi.org/10.1111/j.1574-6941.2012.01437.x

Jüriado I, Paal J, Liira J (2003) Epiphytic and epixylic lichen species diversity in Estonian natural forests. Biodiversity and Conservation 12(8): 1587–1607. https://doi.org/10.1023/A:1023645730446

Keck F, Blackman RC, Bossart R, Brantschen J, Couton M, Hürlemann S, Kirschner D, Locher N, Zhang H, Altermatt F (2022) Meta-analysis shows both congruence and complementarity of DNA and eDNA metabarcoding to traditional methods for biological community assessment. Molecular Ecology 31(6): 1820–1835. https://doi.org/10.1111/mec.16364

Keck F, Brantschen J, Altermatt F (2023) A combination of machine-learning and eDNA reveals the genetic signature of environmental change at the landscape levels. Molecular Ecology 32(17): 4791–4800. https://doi.org/10.1111/mec.17073

Kelly LJ, Hollingsworth PM, Coppins BJ, Ellis CJ, Harrold P, Tosh J, Yahr R (2011) DNA barcoding of lichenized fungi demonstrates high identification success in a floristic context. The New Phytologist 191(1): 288–300. https://doi.org/10.1111/j.1469-8137.2011.03677.x

Kerr M, Leavitt SD (2023) A Custom Regional DNA Barcode Reference Library for Lichen-Forming Fungi of the Intermountain West, USA, Increases Successful Specimen Identification. Journal of Fungi (Basel, Switzerland) 9(7): 741. https://doi.org/10.3390/jof9070741

Klaus VH, Hölzel N, Boch S, Müller J, Socher AS, Prati D, Fischer M, Kleinebecker T (2013) Direct and indirect associations between plant species richness and productivity in grasslands: Regional differences preclude simple generalization of productivity-biodiversity relationships. Preslia 85: 97–112. https://doi.org/10.7892/boris.38709

Knops JMH, Iii THN, Boucher VL, Schlesinger WH (1991) Mineral Cycling and Epiphytic Lichens: Implications at the Ecosystem Level. Lichenologist (London, England) 23(3): 309–321. https://doi.org/10.1017/S0024282991000452

Knops JMH, Nash TH III, Schlesinger WH (1996) The Influence of Epiphytic Lichens on the Nutrient Cycling of an Oak Woodland. Ecological Monographs 66(2): 159–179. https://doi.org/10.2307/2963473

Kowalewska A, Kukwa M (2003) Additions to the Polish lichen flora. Graphis Scripta.

Kraichak E, Allende L, Obermayer W, Lücking R, Lumbsch HT (2019) Scale-dependent co-occurrence patterns of closely related genotypes in a lichen species complex. Plant and Fungal Systematics 64(2): 163–172. https://doi.org/10.2478/pfs-2019-0017

Kranner I, Zorn M, Turk B, Wornik S, Beckett RP, Batič F (2003) Biochemical traits of lichens differing in relative desiccation tolerance. The New Phytologist 160(1): 167–176. https://doi.org/10.1046/j.1469-8137.2003.00852.x

Lackovičová A, Guttová A (2005) Genus *Dimerella* (Coenogoniaceae, lichenized Ascomycota) in Slovakia. Acta Botanica Croatica 64: 289–301.

Larsen HME, Hansen ES, Nord-Larsen T, Rasmussen HN (2020) Deciduous trees as lichen phorophytes: Biodiversity and colonization patterns under common garden conditions. Lichenologist (London, England) 52(3): 221–232. https://doi.org/10.1017/S0024282920000018

Launis A, Pykälä J, Boom PVD, Sérusiaux E, Myllys L (2019) Four new epiphytic species in the *Micarea prasina* group from Europe. Lichenologist (London, England) 51(1): 7–25. https://doi.org/10.1017/S0024282918000555

Liu D, Wang L, Wang XY, Hur J-S (2019) Two New Species of the Genus *Candelariella* from China and Korea. Mycobiology 47(1): 40–49. https://doi.org/10.1080/12298093.2019.1583785

Lõhmus P, Lõhmus A (2019) The Potential of Production Forests for Sustaining Lichen Diversity: A Perspective on Sustainable Forest Management. Forests 10(12): 1063. https://doi.org/10.3390/f10121063

Łubek A, Kukwa M, Jaroszewicz B, Czortek P (2021) Shifts in Lichen Species and Functional Diversity in a Primeval Forest Ecosystem as a Response to Environmental Changes. Forests 12(6): 686. https://doi.org/10.3390/f12060686

Lücking R, Aime MC, Robbertse B, Miller AN, Ariyawansa HA, Aoki T, Cardinali G, Crous PW, Druzhinina IS, Geiser DM, Hawksworth DL, Hyde KD, Irinyi L, Jeewon R, Johnston PR, Kirk PM, Malosso E, May TW, Meyer W, Öpik M, Robert V, Stadler M, Thines M, Vu D, Yurkov AM, Zhang N, Schoch CL (2020) Unambiguous identification of fungi: Where do we stand and how accurate and precise is fungal DNA barcoding? IMA Fungus 11(1): 14. https://doi.org/10.1186/s43008-020-00033-z

Marini L, Nascimbene J, Nimis PL (2011) Large-scale patterns of epiphytic lichen species richness: Photobiont-dependent response to climate and forest structure. The Science of the Total Environment 409(20): 4381–4386. https://doi.org/10.1016/j.scitotenv.2011.07.010

Marthinsen G, Rui S, Timdal E (2019) OLICH: A reference library of DNA barcodes for Nordic lichens. Biodiversity Data Journal 7: e36252. https://doi.org/10.3897/BDJ.7.e36252

Martin M (2011) Cutadapt removes adapter sequences from high-throughput sequencing reads. EMBnet.Journal 17(1): 10. https://doi.org/10.14806/ej.17.1.200

Miller JED, Root HT, Safford HD (2018) Altered fire regimes cause long-term lichen diversity losses. Global Change Biology 24(10): 4909–4918. https://doi.org/10.1111/gcb.14393

Nascimbene J, Thor G, Nimis PL (2013) Effects of forest management on epiphytic lichens in temperate deciduous forests of Europe – A review. Forest Ecology and Management 298: 27–38. https://doi.org/10.1016/j.foreco.2013.03.008

Nascimbene J, Casazza G, Benesperi R, Catalano I, Cataldo D, Grillo M, Isocrono D, Matteucci E, Ongaro S, Potenza G, Puntillo D, Ravera S, Zedda L, Giordani P (2016) Climate change fosters the decline of epiphytic *Lobaria* species in Italy. Biological Conservation 201: 377–384. https://doi.org/10.1016/j.biocon.2016.08.003

Nash TH III, Gries C (2002) Lichens as Bioindicators of Sulfur Dioxide. Symbiosis: 1–21.

Nelsen MP, Lumbsch HT (2020) A data-driven evaluation of lichen climate change indicators in Central Europe. Biodiversity and Conservation 29(14): 3959–3971. https://doi.org/10.1007/s10531-020-02057-8

Nguyen NH, Song Z, Bates ST, Branco S, Tedersoo L, Menke J, Schilling JS, Kennedy PG (2016) FUNGuild: An open annotation tool for parsing fungal community datasets by ecological guild. Fungal Ecology 20: 241–248. https://doi.org/10.1016/j.funeco.2015.06.006

Pike LH (1978) The Importance of Epiphytic Lichens in Mineral Cycling. The Bryologist 81(2): 247–257. https://doi.org/10.2307/3242186

Pinho P, Augusto S, Martins-Loução MA, Pereira MJ, Soares A, Máguas C, Branquinho C (2008) Causes of change in nitrophytic and oligotrophic lichen species in a Medi-

terranean climate: Impact of land cover and atmospheric pollutants. Environmental Pollution 154(3): 380–389. https://doi.org/10.1016/j.envpol.2007.11.028

Pino-Bodas R, Martín MP, Burgaz AR, Lumbsch HT (2013) Species delimitation in *Cladonia* (Ascomycota): A challenge to the DNA barcoding philosophy. Molecular Ecology Resources 13(6): 1058–1068. https://doi.org/10.1111/1755-0998.12086

Purvis OW, Chimonides J, Din V, Erotokritou L, Jeffries T, Jones GC, Louwhoff S, Read H, Spiro B (2003) Which factors are responsible for the changing lichen floras of London? The Science of the Total Environment 310(1–3): 179–189. https://doi.org/10.1016/S0048-9697(02)00638-1

Reiners WA, Olson RK (1984) Effects of canopy components on throughfall chemistry: An experimental analysis. Oecologia 63(3): 320–330. https://doi.org/10.1007/BF00390660

Rikkinen J (2003) Ecological and evolutionary role of photobiont-mediated guilds in lichens. Symbiosis 2003: 443–450.

Rivas Plata E, Parnmen S, Staiger B, Mangold A, Frisch A, Weerakoon G, Hernandez J, Caceres M, Kalb K, Sipman H, Common R, Nelsen M, Luecking R, Lumbsch T (2013) A molecular phylogeny of Graphidaceae (Ascomycota, Lecanoromycetes, Ostropales) including 428 species. MycoKeys 6: 55–94. https://doi.org/10.3897/mycokeys.6.3482

Robert V, Vu D, Amor ABH, van de Wiele N, Brouwer C, Jabas B, Szoke S, Dridi A, Triki M, Daoud S, Chouchen O, Vaas L, de Cock A, Stalpers JA, Stalpers D, Verkley GJM, Groenewald M, dos Santos FB, Stegehuis G, Li W, Wu L, Zhang R, Ma J, Zhou M, Gorjón SP, Eurwilaichitr L, Ingsriswang S, Hansen K, Schoch C, Robbertse B, Irinyi L, Meyer W, Cardinali G, Hawksworth DL, Taylor JW, Crous PW (2013) MycoBank gearing up for new horizons. IMA Fungus 4(2): 371–379. https://doi.org/10.5598/imafungus.2013.04.02.16

Rose CI, Hawksworth DL (1981) Lichen recolonization in London's cleaner air. Nature 289(5795): 289–292. https://doi.org/10.1038/289289a0

Sayers EW, Bolton EE, Brister JR, Canese K, Chan J, Comeau DC, Connor R, Funk K, Kelly C, Kim S, Madej T, Marchler-Bauer A, Lanczycki C, Lathrop S, Lu Z, Thibaud-Nissen F, Murphy T, Phan L, Skripchenko Y, Tse T, Wang J, Williams R, Trawick BW, Pruitt KD, Sherry ST (2022) Database resources of the national center for biotechnology information. Nucleic Acids Research 50(D1): D20–D26. https://doi.org/10.1093/nar/gkab1112

Schall P, Ammer C (2018) Stand composition based on 2nd forest inventory (abundance, basal area, crown projection area and volume) on all forest EPs, 2014 – 2018. Version 2. Biodiversity Exploratories Information System. Dataset. https://www.bexis.uni-jena.de/ddm/data/Showdata/22907

Schmitt I, Lumbsch HT (2004) Molecular phylogeny of the Pertusariaceae supports secondary chemistry as an important systematic character set in lichen-forming ascomycetes. Molecular Phylogenetics and Evolution 33(1): 43–55. https://doi.org/10.1016/j.ympev.2004.04.014

Schoch CL, Seifert KA, Huhndorf S, Robert V, Spouge JL, Levesque CA, Chen W, et al. (2012) Nuclear ribosomal internal transcribed spacer (ITS) region as a universal DNA barcode marker for Fungi. Proceedings of the National Academy of Sciences 109: 6241–6246. https://doi.org/10.1073/pnas.1117018109

Shirouzu T, Uno K, Hosaka K, Hosoya T (2016) Early-diverging wood-decaying fungi detected using three complementary sampling methods. Molecular Phylogenetics and Evolution 98: 11–20. https://doi.org/10.1016/j.ympev.2016.01.015

Simon DM, Hummel CL, Sheeley SL, Bhattacharya D (2005) Heterogeneity of intron presence or absence in rDNA genes of the lichen species *Physcia aipolia* and *P. stellaris*. Current Genetics 47(6): 389–399. https://doi.org/10.1007/s00294-005-0581-5

Simons NK, Gossner MM, Lewinsohn TM, Boch S, Lange M, Müller J, Pašalić E, Socher SA, Türke M, Fischer M, Weisser WW (2014) Resource-Mediated Indirect Effects of Grassland Management on Arthropod Diversity. PLoS ONE 9: e107033. https://doi.org/10.1371/journal.pone.0107033

Taberlet P, Coissac E, Pompanon F, Brochmann C, Willerslev E (2012) Towards next-generation biodiversity assessment using DNA metabarcoding. Molecular Ecology 21(8): 2045–2050. https://doi.org/10.1111/j.1365-294X.2012.05470.x

Umweltbundesamt (2005) 8 Daten zur Umwelt. 8: 2005. Berlin, 352 pp.

van Herk CM, Aptroot A, van Dobben HF (2002) Long-Term Monitoring in the Netherlands Suggests that Lichens Respond to Global Warming. Lichenologist (London, England) 34(2): 141–154. https://doi.org/10.1006/lich.2002.0378

Van Stan JT II, Pypker TG (2015) A review and evaluation of forest canopy epiphyte roles in the partitioning and chemical alteration of precipitation. The Science of the Total Environment 536: 813–824. https://doi.org/10.1016/j.scitotenv.2015.07.134

Větrovský T, Morais D, Kohout P, Lepinay C, Algora C, Awokunle Hollá S, Bahnmann BD, Bílohnědá K, Brabcová V, D'Alò F, Human ZR, Jomura M, Kolařík M, Kvasničková J, Lladó S, López-Mondéjar R, Martinović T, Mašínová T, Meszárošová L, Michalčíková L, Michalová T, Mundra S, Navrátilová D, Odriozola I, Piché-Choquette S, Štursová M, Švec K, Tláskal V, Urbanová M, Vlk L, Voříšková J, Žifčáková L, Baldrian P (2020) GlobalFungi, a global database of fungal occurrences from high-throughput-sequencing metabarcoding studies. Scientific Data 7(1): 228. https://doi.org/10.1038/s41597-020-0567-7

Vondrák J, Malíček J, Palice Z, Coppins B, Kukwa M, Czarnota P, Sanderson N, Acton A (2016) Methods for obtaining more complete species lists in surveys of lichen biodiversity. Nordic Journal of Botany 34(5): 619–626. https://doi.org/10.1111/njb.01053

Vondrák J, Svoboda S, Košnar J, Malíček J, Šoun J, Frolov I, Svensson M, Novotný P, Palice Z (2023) Martin7: A reference database of DNA barcodes for European epiphytic lichens and its taxonomic implications. Preslia 95(3): 311–345. https://doi.org/10.23855/preslia.2023.311

White TJ, Bruns T, Lee S, Taylor J (1990) Amplification and direct sequencing of fungal ribosomal rna genes for phylogenetics. In: Innis M, Gelfland DH, Sninsky JJ, White TJ (Eds) PCR Protocols. Academic Press, San Diego, CA, 315–322. https://doi.org/10.1016/B978-0-12-372180-8.50042-1

Wirth V, Hauck M, Schultz M (2013) Die Flechten Deutschlands. Ulmer, Stuttgart, 2 pp.

Wright B, St. Clair LL, Leavitt SD (2019) Is targeted community DNA metabarcoding suitable for biodiversity inventories of lichen-forming fungi? Ecological Indicators 98: 812–820. https://doi.org/10.1016/j.ecolind.2018.11.061

Ye J, Coulouris G, Zaretskaya I, Cutcutache I, Rozen S, Madden TL (2012) Primer-BLAST: A tool to design target-specific primers for polymerase chain reaction. BMC Bioinformatics 13(1): 134. https://doi.org/10.1186/1471-2105-13-134

Yoccoz NG (2012) The future of environmental DNA in ecology. Molecular Ecology 21(8): 2031–2038. https://doi.org/10.1111/j.1365-294X.2012.05505.x

Supplementary material 1

List of all species found in this study

Authors: Lukas Dreyling, Steffen Boch, H. Thorsten Lumbsch, Imke Schmitt

Data type: csv

Explanation note: The table contains information on wether the species was identified with either the eDNA method or the floristic survey and in how many plots it occured.

Link: https://doi.org/10.3897/mycokeys.106.117540.suppl1

MycoKeys 106: 173–200 (2024)
DOI: 10.3897/mycokeys.106.123105

Research Article

Three novel woody litter inhabiting fungi in Didymosphaeriaceae, Phaeoseptaceae and Synnemasporellaceae from Zhujiangyuan Nature Reserve, Yunnan Province, P.R. China

Gui-Qing Zhang[1], Nalin N. Wijayawardene[1,2], Li-Hong Han[1], Jaturong Kumla[3], Nakarin Suwannarach[3], Qiang Li[1], Abdallah M. Elgorban[4], Ihab M. Moussa[5], Claudia Coleine[6], Dong-Qin Dai[1]

1 *Center for Yunnan Plateau Biological Resources Protection and Utilization, College of Biological Resource and Food Engineering, Qujing Normal University, Qujing, Yunnan Province 655011, China*
2 *Tropical Microbiology Research Foundation, 96/N/10, Meemanagoda Road, 10230 Pannipitiya, Sri Lanka*
3 *Center of Excellence in Microbial Diversity and Sustainable Utilization, Chiang Mai University, Chiang Mai, Thailand*
4 *Center of Excellence in Biotechnology Research, King Saud University, Riyadh, Saudi Arabia*
5 *Department of Botany and Microbiology, College of Science, King Saud University, Riyadh 11451, Saudi Arabia*
6 *Department of Ecological and Biological Sciences, University of Tuscia, Viterbo, Italy*

Corresponding authors: Nalin N. Wijayawardene (nalinwijayawardene@yahoo.com); Dong-Qin Dai (cicidaidongqin@gmail.com)

Abstract

Zhujiangyuan Nature Reserve, located in Qujing City, Yunnan Province, China, is reported with high fauna and floral diversity, while the fungal diversity of the region is poorly documented. During the summer season in 2023, decaying wood-inhabiting microfungi were collected from different microhabitats. The novel species were identified based on morphological characteristics and phylogenetic analyses (based on combined datasets of ITS, LSU, SSU, *tef*1-α, and *rpb*2 regions). Two species belong to Dothideomycetes (*viz*., *Spegazzinia zhujiangyuanensis* **sp. nov.** and *Phaeoseptum zhujiangyuanense* **sp. nov.** in Pleosporales) while the other one resides in Sordariomycetes (*Synnemasporella fanii* **sp. nov.** in Diaporthales). The results are in conformity with the earlier studies that predicted higher fungal diversity in this region.

Key words: Morpho-molecular, new fungal species, phylogeny, taxonomy, woody fungi

Academic editor:
Chitrabhanu Sharma Bhunjun
Received: 15 March 2024
Accepted: 28 May 2024
Published: 21 June 2024

Citation: Zhang G-Q, Wijayawardene NN, Han L-H, Kumla J, Suwannarach N, Li Q, Elgorban AM, Moussa IM, Coleine C, Dai D-Q (2024) Three novel woody litter inhabiting fungi in Didymosphaeriaceae, Phaeoseptaceae and Synnemasporellaceae from Zhujiangyuan Nature Reserve, Yunnan Province, P.R. China. MycoKeys 106: 173–200. https://doi.org/10.3897/mycokeys.106.123105

Introduction

Fungi have a worldwide distribution and underpin nearly all life on the Earth (Mueller and Schmit 2007). They can grow in a wide range of habitats, including extreme environments like deserts or high salt concentrations (Raghukumar and Raghukumar 1998; Dadachova et al. 2007). Fungi exist in various lifestyles, including pathogenic, saprophytic, endophytic, and symbiotic (Naranjo-Ortiz and Gabaldón 2019). They occur as decomposers to degrade organic materials, contribute to carbon and nutrient cycling directly in ecosystems (Richards et al. 2017), and play a role in facilitating mineral cycling, accelerating rock weathering, and promoting plant growth. Currently, the estimates of fungal diversity range from 2 to 3 million. Species Fungorum (2024) (accession date: 31 May 2024) lists all accepted species of fungi, currently 161,104 species; there-

fore, over 90% of fungal species is still unknown (Hawksworth and Lücking 2017; Niskanen et al 2023). It is predicted that a number of novel taxa could be harboured in tropical regions where the environmental factors are favourable for higher diversity and continued living (Hawksworth and Lücking 2017). Wijayawardene et al. (2021) reported that Yunnan and Guizhou Provinces in China would be an important locality to explore novel taxa although it showcases subtropical climate.

The Zhujiangyuan Nature Reserve harbours abundant plant resources, with forest coverage of more than 95% and exceeding 1,000 species of plants (Wang et al. 2015). The warm climate and sufficient moisture guarantee a rich fungal diversity in Zhujiangyuan Nature Reserve. However, few studies have been carried out in the Zhujiangyuan Nature Reserve, especially on the floristic diversity of fungi.

Zhujiang is the third longest river in China, which covers about 450,000 km^2, and flows through most cities in Southern China and a wide range of areas in Northern Vietnam (Guo et al. 2023). It originates from Maxiong Mountain in Zhanyi District, Qujing City, Yunnan Province (Wang 2014). The fungal diversity of this region (i.e. Qujing City and Zhujiangyuan Nature Reserve) is not well documented. Nevertheless, recently, Doilom et al. (2021) introduced *Praeclarispora* Doilom, W. Dong, K.D. Hyde & C.F. Liao, a novel genus, with *Praeclarispora artemisiae* Doilom, W. Dong, K.D. Hyde & C.F. Liao as the type species. At the same time, Doilom et al. (2021) reported *Plenodomus artemisiae* A. Karun., Phookamsak & K.D. Hyde as a new collection from *Artemisia argyi* in Qujing City, Yunnan Province. Wijayawardene et al. (2021) introduced two new species of *Phragmocamarosporium* Wijayaw., Yong Wang bis & K.D. Hyde (*viz*., *P. magnoliae* and *P. qujingensis*) and one new species of *Lonicericola* Phookamsak, Jayasiri & K.D. Hyde (*viz*., *L. qujingensis*), collected from *Magnolia grandiflora* from Qujing Normal University garden, Qujing. Furthermore, five new host/geographical records of different taxa on *Magnolia grandiflora* collected from Qujing City, were also reported by Wijayawardene et al. (2021), *Botryosphaeria dothidea* (Moug.) Ces. & De Not. and *Shearia formosa* (Ellis & Everh.) Petr. were reported as new geographical records from China; *Diplodia mutila* (Fr.) Fr. and *D. seriata* De Not. were identified as new host records from *M. grandiflora* in China; while *Angustimassarina populi* Thambug. & K.D. Hyde was comfirmed as a new host and geographical record by Wijayawardene et al. (2021), which mentioned it is the first report of *A. populi* from China and on *M. grandiflora*.

During the summer of 2023 (July–September), we collected samples of microfungi associated with decaying wood litter in the North-east gate of Zhujiangyuan Nature Reserve. From the collected samples, we introduce three novel species belonging to *Spegazzinia* Sacc. (i.e. *S. zhujiangyuanensis* in Didymosphaeriaceae Munk, Pleosporales, Dothideomycetes O.E. Erikss. & Winka), *Phaeoseptum* Ying Zhang, J. Fourn. & K.D. Hyde (i.e. *P. zhujiangyuanense* in Phaeoseptaceae Boonmee, Thambugala & K.D. Hyde, Pleosporales, Dothideomycetes) and *Synnemasporella* X.L. Fan & J.D.P. Bezerra (i.e. *S. fanii* in Synnemasporellaceae X.L. Fan & J.D.P. Bezerra, Diaporthales Nannf., Sordariomycetes O.E. Erikss. & Winka) based on morpho-molecular analyses. The new taxa are provided with illustrations and morphological descriptions.

Materials and methodology

Sample collection

With prior permission of the management of Zhujiangyuan Nature Reserve, located in Qujing City, Yunnan Province, China, decaying wood litter samples were collected in the terrestrial habitats. The samples were stored in separate zip-lock plastic bags and transported to the microbiology laboratory of Qujing Normal University. Geographical information and sample information were recorded. Collections were maintained at room temperature (25 °C) and the samples were examined within 3–5 days.

Morphology, isolation and preservation

Fruiting bodies were examined using a Leica S8AP0 stereomicroscope with an HDMI 200C camera (Leica Corporation, Germany). Micro-morphological characters were photographed using an Olympus BX53 compound microscope (Olympus Corporation, Japan) with differential interference contrast (Olympus BX53 DIC compound microscope with an Olympus DP74 camera, Japan). Ascomata and conidiomata were sectioned by hand using a razor blade to obtain thin sections (Dai et al. 2022). All microscopic measurements were made using Tarosoft (R) Image FrameWork software (http://www.tarosoft.in.th/), and the measurements were provided as minimum–maximum values and average values. The photographic plates were edited and provided by using Adobe Photoshop CC 2018 (Adobe Systems, USA) software.

Single spore isolation was performed to obtain pure cultures following the methods described in Senanayake et al. (2020). Germinating spores were photographed, transferred to potato dextrose agar (PDA), and then incubated under the dark at 27 °C to obtain a pure culture, which were photographed to record the different characters. After a week, hyphal tips were transferred into PDA plates and grown at 27 °C in the dark.

Dried herbarium specimens and living cultures were preserved at the Mycological Herbarium of Zhongkai University of Agriculture and Engineering (MHZU) and Zhongkai University of Agriculture and Engineering (ZHKUCC), China. Duplicates of holotypes and type cultures were deposited at the Herbarium of Guizhou Medical University, Guiyang, China (GMB) and Guizhou Medical University Culture Collection (GMBCC) in Guiyang, China. Index Fungorum identifiers (2023) were obtained for the newly introduced taxa.

In the text, the following abbreviations are used: n = a number of ascospores/asci/conidiogenous cells/conidiophores/conidia measured from a given number of specimens, $\bar{x}$ = arithmetical average of sizes of all ascospores/asci/conidiogenous cells/conidia.

DNA extraction, PCR amplification and sequencing

Fresh cultures were grown on PDA in the dark at 27 °C for 15–30 days. The genomic DNA of the fungus was extracted from fresh cultures according to the specifications of the Biospin Fungal Genomic DNA Extraction Kit (bioflux ®). Both forward and reverse primers were used for the amplification of internal

Table 1. Forward and reverse primers information of ITS, LSU, SSU, *tef*1-α and *rpb*2 regions.

Locus	Primers	Reference
ITS	Forward: ITS5 TCCTCCGCTTATTGATATGC Reverse: ITS4 GGAAGTAAAAGTCGTAACAAGG	White et al. (1990)
LSU	Forward: LROR GTACCCGCTGAACTTAAGC Reverse: LR5 ATCCTGAGGGAAACTTC	Vilgalys and Hester (1990)
SSU	Forward: NS1 GTAGTCATATGCTTGTCTC Reverse: NS4 CTTCCGTCAATTCCTTTAAG	White et al. (1990)
*tef*1-α	Forward: EF1-983F GCYCCYGGHCAYCGTGAYTTYAT Reverse: EF1-2218R ATGACACCRACRGCRACRGTYTG	Rehner and Buckley (2005)
*rpb*2	Forward: fRPB2-5f GAYGAYMGWGATCAYTTYGG Reverse: fRPB2-7cr CCCATRGCTTGTYYRCCCAT	Liu et al. (1999)

Table 2. The PCR thermal cycling procedure for amplifying ITS, LSU, SSU, *tef*1-α, and *rpb*2 regions.

ITS, LSU, SSU and *tef*1-α	Initial denaturation 95 °C for 5 min. Followed by 35 cycles, denaturation at 95 °C for 30 s, annealing at 55 °C for 50 s, elongation at 72 °C for 90 s. Final extension at 72 °C for 10 min	Dai et al. (2022)
*rpb*2	Initial denaturation 95 °C for 3 min. Follow by 35 cycles, elongation at 94 °C for 1 min, annealing at 52 °C for 50 s, elongation at 72 °C for 1 min. Final extension at 72 °C for 10 min	Ma et al. (2022)

transcribed spacers (ITS), large subunit rDNA (LSU), small subunit rDNA (SSU), translation elongation factor 1-α (*tef*1-α) and RNA polymerase II second largest subunit (*rpb*2) regions are listed in Table 1. A final volume of polymerase chain reaction (PCR) was prepared, including 1 μl of DNA template, 1 μl of each forward and reverse primer, 12.5 μl of 2 × taq PCR Master Mix and 9.5 μl of double-distilled water (ddH_2O) as described by Dai et al. (2022). The PCR thermal cycling procedure for amplifying ITS, LSU, SSU, *tef*1-α and *rpb*2 regions was run under the conditions presented in Table 2. The PCR products were sent to Shanghai Sangon Biological Engineering Technology & Services Co. (Shanghai, People's Republic of China) for sequencing. All newly generated sequences were deposited in GenBank and accession numbers were obtained.

Phylogenetic analyses

Based on blast similarity and related publications, closely related sequences were downloaded from GenBank (Table 3). Single gene sequence alignment was performed by mafft v.7.215 (http://mafft.cbrc.jp/alignment/server/index.html) (Katoh and Standley 2013), and final improvements were done using BioEdit v.7.0.5.2 (Hall 2004). Alignment of ITS, LSU, SSU, *tef*1-α and *rpb*2 regions was combined with MEGA6 version 6.0 (Tamura et al. 2013). The alignment of combined datasets in FASTA format was converted to PHYLIP and NEXUS formats by using ALTER (Alignment Transformation Environment online, http://sing.ei.uvigo.es/ALTER/) (Glez-Peña et al. 2010). The online tool Findmodel (http://www.hiv.lanl.gov/content/sequence/findmodel/findmodel.html) was used to determine the best nucleotide substitution model for each partition data (Dai et al. 2022).

Table 3. Names, strain numbers, and corresponding GenBank accession numbers of taxa were used in this study.

Taxon	Strain Number	GenBank Accession Numbers			
		ITS	LSU	SSU	*tef*1-α
Didymosphaeriaceae					
Alloconiothyrium aptrootii	CBS 980.95^{T}	JX496121	JX496234	N/A	N/A
A. aptrootii	CBS 981.95	JX496122	JX496235	N/A	N/A
A. encephalarti	CPC: 35980	MN562102	MN567610	N/A	N/A
Austropleospora archidendri	MFLUCC 17-2429	MK347757	MK347974	MK347863	MK360044
A. archidendri	MFLU 22-0042	OP058964	OP059055	OP059006	OP135941
Bambusistroma didymosporum	MFLU 15-0057^{T}	KP761733	KP761730	KP761737	KP761727
B. didymosporum	MFLU 15-0058	KP761734	KP761731	KP761738	KP761728
Bimuria novae-zelandiae	CBS 107.79^{T}	MH861181	AY016356	AY016338	DQ471087
Chromolaenicola nanensis	MFLUCC 17-1473^{T}	MN325015	MN325003	MN325009	MN335648
C. nanensis	MFLUCC 17-1477	MN325014	MN325002	MN325008	MN335647
C. sapindi	KUMCC 21-0564^{T}	OP058967	OP059058	OP059009	OP135943
Cylindroaseptospora leucaenae	MFLUCC 17-2424^{T}	NR_163333	NG_066310	MK347856	MK360047
C. siamensis	MFLUCC 17-2527^{T}	MK347760	MK347976	MK347866	MK360048
Deniquelata barringtoniae	MFLUCC 11-0422^{T}	NR_111779	NG_042696	JX254656	N/A
Dictyoarthrinium vittalii	NFCCI4249^{T}	MF406218	MF182395	MF622059	MF182398
D. hydei	SQUCC 13296 ^{T}	MW077145	N/A	MW077161	MW075771
D. musae	MFLUCC 20-0105^{T}	MT482323	MT482320	MT482326	MT495602
D. musae	MFLUCC 20-0106	MT482324	MT482321	MT482327	MT495603
D. sacchari	MFLUCC 20-0107	MT482325	MT482322	MT482328	N/A
D. sacchari	CBS 529.73	N/A	MH872479	N/A	N/A
D. thailandicum	KUMCC 21-0664^{T}	OP058965	OP059056	OP059007	N/A
D. thailandicum	KUMCC 21-0665	OP058966	OP059057	OP059008	OP135942
Didymocrea sadasivanii	CBS 438.65^{T}	MH858658	DQ384103	N/A	N/A
Didymosphaeria rubi-ulmifolii	MFLUCC 14-0023^{T}	N/A	KJ436586	NG_063557	N/A
D. rubi-ulmifolii	MFLUCC 14-0024	N/A	KJ436585	KJ436587	N/A
Kalmusia italica	MFLUCC 14-0560^{T}	KP325440	KP325441	KP325442	N/A
K. variispora	CBS 121517^{T}	MH863113	MH874668	N/A	N/A
K. ebuli	CBS 123120^{T}	KF796674	JN644073	JN851818	N/A
Kalmusibambusa triseptata	MFLUCC 13-0232^{T}	KY682697	KY682695	KY682696	N/A
Karstenula lancangensis	KUMCC 21-0670^{T}	OP058969	OP059060	OP059011	N/A
K. lancangensis	KUMCC 21-0677	OP058970	OP059061	OP059012	N/A
Laburnicola hawksworthii	MFLUCC 13-0602^{T}	KU743194	KU743195	KU743196	N/A
L. muriformis	MFLUCC 14-0921^{T}	KU743200	KU743201	KU743202	N/A
Letendraea cordylinicola	MFLUCC 11-0150	KM213996	KM213999	KM214002	N/A
L. cordylinicola	MFLUCC 11-0148^{T}	NR_154118	NG_059530	KM214001	N/A
Montagnula donacina	KUMCC 21-0653	OP058961	OP059052	OP059003	OP135938
M. thailandica	MFLUCC 17-1508^{T}	MT214352	NG070949	NG070158	MT235774
Neokalmusia brevispora	KT 1466^{T}	LC014573	AB524600	AB524459	AB539112
N. scabrispora	KT 1023	LC014575	AB524593	AB524452	AB539106
Neptunomyces aureus	CMG12^{T}	MK912121	N/A	N/A	MK948000
Paracamarosporium fagi	CPC 24890	KR611886	KR611904	N/A	N/A
P. fagi	CPC 24892^{T}	KR611887	KR611905	N/A	N/A

Taxon	Strain Number	GenBank Accession Numbers			
		ITS	LSU	SSU	*tef*1-α
P. anthostomoides	MFLU 16-0172^{T}	KU743206	KU743207	KU743208	N/A
Paraphaeosphaeria rosae	MFLUCC 17-2547	MG828935	MG829044	MG829150	MG829222
P. rosae	MFLUCC 17-2549^{T}	MG828937	MG829046	MG829152	MG829223
Phaeodothis winteri	CBS 182.58	N/A	GU301857	GU296183	N/A
Pseudocamarosporium propinquum	MFLUCC 13-0544	KJ747049	KJ813280	KJ819949	N/A
P. pteleae	MFLUCC 17-0724^{T}	NR_157536	MG829061	MG829166	MG829233
Pseudopithomyces entadae	MFLUCC 17-0917^{T}	N/A	NG_066305	MK347835	MK360083
P. rosae	MFLUCC 15-0035^{T}	MG828953	MG829064	MG829168	N/A
Septofusispora thailandica	KUMCC 21-0647^{T}	OP058971	OP059062	OP059013	OP135945
S. thailandica	KUMCC 21-0652	OP058972	OP059063	OP059014	N/A
Spegazzinia bromeliacearum	URM 8084^{T}	MK804501	MK809513	N/A	N/A
S. camelliae	WNA03	MZ538526	MZ538560	N/A	MZ567102
S. camelliae	CMU328^{T}	MH734522	MH734521	MH734523	MH734524
S. deightonii	MFLUCC 20-0002^{T}	MN956768	MN956772	MN956770	MN927133
S. intermedia	CBS 249.89^{T}	MH862171	MH873861	N/A	N/A
S. jinghaensis	KUMCC 21-0495^{T}	OP058973	OP059064	OP059015	OP135946
S. jinghaensis	KUMCC 21-0496	OP058974	OP059065	OP059016	OP135947
S. lobulata	CBS 361.58^{T}	MH857812	MH869344	N/A	N/A
S. musae	MFLUCC 20-0001^{T}	MN930512	MN930514	MN930513	MN927132
S. neosundara	MFLUCC 15-0456^{T}	KX965728	KX954397	KX986341	N/A
S. radermacherae	MFLUCC 17-2285^{T}	MK347740	MK347957	MK347848	MK360088
S. tessarthra	SH 287	JQ673429	AB807584	AB797294	AB808560
S. zhujiangyuanensis	**ZHKUCC 23-1020^{T}**	**PP060498**	**PP060512**	**PP060504**	**PP035539**
S. zhujiangyuanensis	**GMBCC1002**	**PP067151**	**PP067156**	**PP066043**	**PP068812**
Tremateia arundicola	MFLU 16-1275^{T}	KX274241	KX274248	KX274254	KX284706
T. guiyangensis	GZAAS01^{T}	KX274240	KX274247	KX274253	KX284705
T. murispora	GZCC 18-2787^{T}	NR_165916	MK972751	MK972750	MK986482
Verrucoconiothyrium nitidae	CBS 119209	EU552112	EU552112	N/A	N/A
Xenocamarosporium acaciae	CBS 139895^{T}	NR_137982	NG_058163	N/A	N/A
X. acaciae	MFLUCC 17-2432	MK347766	MK347983	MK347873	MK360093
Phaeoseptaceae					
Alfoldia vorosii	CBS 145501^{T}	JN859336	MK589354	MK589346	MK599320
Amorocoelophoma cassiae	MFLUCC 17-2283^{T}	NR_163330	NG_066307	NG_065775	MK360041
Angustimassarina acerina	MFLUCC 14-0505^{T}	NR_138406	KP888637	NG_063573	KR075168
A. populi	MFLUCC 13-0034^{T}	KP899137	KP888642	NG_061204	KR075164
A. quercicola	MFLUCC 14-0506^{T}	KP899133	KP888638	NG_063574	KR075169
Crassiclypeus aquaticus	CBS 143643^{T}	LC312501	LC312530	LC312472	LC312559
Decaisnella formosa	BCC 25616	N/A	GQ925846	GQ925833	GU479851
D. formosa	BCC 25617	N/A	GQ925847	GQ925834	GU479850
Forliomyces uniseptata	MFLUCC 15-0765^{T}	NR_154006	NG_059659	NG_061234	KU727897
Gloniopsis praelonga	CBS 112415	N/A	FJ161173	FJ161134	FJ161090
Guttulispora crataegi	MFLUCC 13-0442^{T}	KP899134	KP888639	KP899125	KR075161
Halotthia posidoniae	BBH 22481	N/A	GU479786	GU479752	N/A
Hysterium angustatum	MFLUCC 16-0623	N/A	FJ161180	GU397359	FJ161096

Taxon	Strain Number	GenBank Accession Numbers			
		ITS	LSU	SSU	*tef*1-α
Lignosphaeria fusispora	MFLUCC 11-0377^{T}	NR_164233	KP888646	N/A	N/A
Mauritiana rhizophorae	BCC 28866	N/A	GU371824	GU371832	GU371817
Misturatosphaeria aurantiacinotata	GKM 1238^{T}	N/A	NG_059927	N/A	GU327761
Phaeoseptum aquaticum	CBS 123113^{T}	KY940803	JN644072	N/A	N/A
P. carolshearerianum	NFCCI-4221^{T}	MK307810	MK307813	MK307816	MK309874
P. carolshearerianum	NFCCI-4384	MK307812	MK307815	MK307818	MK309876
P. hydei	MFLUCC 17-0801^{T}	MT240622	MT240623	MT240624	MT241506
P. mali	MFLUCC 17-2108^{T}	MK659580	MK625197	N/A	MK647990
P. manglicola	NFCCI-4666^{T}	MK307811	MK307814	MK307817	MK309875
P. terricola	MFLUCC 10-0102^{T}	MH105778	MH105779	MH105780	MH105781
P. thailandicum	MFLU 19-2136	OM293749	OR211590	OM293755	OM305059
P. thailandicum	HKAS 106993	OM293750	OM293745	OM293756	OM305060
P. zhujiangyuanense	**ZHKUCC 23-1022^{T}**	**PP060500**	**PP060514**	**PP060506**	**PP035541**
P. zhujiangyuanense	**GMBCC1003**	**PP067152**	**PP067157**	**PP066044**	**PP068813**
Platystomum crataegi	MFLUCC 14-0925^{T}	KT026117	KT026109	KT026113	KT026121
Pleopunctum ellipsoideum	MFLUCC 19-0390^{T}	MK804512	MK804517	MK804514	MK828510
P. pseudoellipsoideum	MFLUCC 19-0391^{T}	MK804513	MK804518	N/A	MK828511
Pseudoaurantiascoma kenyense	GKM 1195^{T}	N/A	NG_059928	N/A	GU327767
P. cornisporum	CBS 143654^{T}	LC312515	LC312544	LC312486	LC312573
Ramusculicola thailandica	MFLUCC 13-0284^{T}	KP899141	KP888647	KP899131	KR075167
Sporormurispora atraphaxidis	MFLUCC 17-0742^{T}	NR_157546	NG_059880	NG_061296	N/A
Sulcosporium thailandicum	MFLUCC 12-0004^{T}	MG520958	KT426563	KT426564	N/A
Teichospora melanommoides	CBS 140733^{T}	NR_154632	KU601585	N/A	KU601610
T. pusilla	CBS 140731^{T}	NR_154633	KU601586	N/A	KU601605
T. rubriostiolata	CBS 140734^{T}	NR_154634	KU601590	N/A	KU601609
Thyridaria macrostomoides	GKM 1033	N/A	GU385190	N/A	GU327776
T. macrostomoides	GKM 1159	N/A	GU385185	N/A	GU327778
T. macrostomoides	GKM 224N	N/A	GU385191	N/A	GU327777
Vaginatispora appendiculata	MFLUCC 16-0314^{T}	KU743217	KU743218	KU743219	KU743220
Westerdykella ornata	CBS 379.55	AY943045	GU301880	GU296208	GU349021
Taxon	**Strain Number**	**GenBank Accession Numbers**			
		ITS	**LSU**	***tef*1-α**	***rpb*2**
Synnemasporellaceae					
Apiosporopsis carpinea	CBS 771.79	N/A	AF277130	N/A	N/A
Apiosporopsis sp.	Masuya 11Af2-1	N/A	AB669034	N/A	N/A
Apoharknessia insueta	CBS 111377^{T}	JQ706083	AY720814	N/A	N/A
A. insueta	CBS 114575	N/A	AY720813	N/A	N/A
A. asterospermum	CBS 112404	N/A	AB553745	N/A	N/A
A. asterospermum	KT2138	N/A	AB553744	N/A	N/A
Auratiopycnidiella tristaniopsidis	CBS 132180	JQ685516	JQ685522	N/A	N/A
Cainiella johansonii	Kruys 731	N/A	JF701920	N/A	N/A
Chapeckia nigrospora	AR 3809	JF681957	EU683068	N/A	N/A
Chiangraiomyces bauhiniae	MFLUCC 17-1669^{T}	MF190118	MF190064	N/A	MF377604
C. bauhiniae	MFLUCC 17-1670	MF190119	MF190065	N/A	MF377603
Chrysocrypta corymbiae	CBS 132528	JX069867	JX069851	N/A	N/A

Taxon	Strain Number	GenBank Accession Numbers			
		ITS	LSU	*tef*1-α	*rpb*2
C. koreana	CBS 143.97	KX833584	AF408378	KX833684	KX833490
C. straminea	CBS 149.22	AY339348	AF362569	KX833704	KX833506
C. wangiensis	CBS 132530	JX069873	JX069857	KX833705	KX833509
Coryneum umbonatum	AR 3541	N/A	EU683072	N/A	N/A
C. umbonatum	MFLUCC 15-1110	MF190121	MF190067	N/A	MF377610
C. umbonatum	MFLUCC 13-0658^{T}	MF190120	MF190066	N/A	MF377609
Cryphonectria macrospora	CBS 109764	EU199182	AF408340	N/A	EU220029
C. parasitica	ATCC 38755	AY141856	EU199123	EU222014	DQ862017
Cryptodiaporthe aesculi	CBS 109765	DQ323530	AF408342	GU354004	EU199138.2
C. aesculi	CBS 121905	EU254994	EU255164	DQ313558	EU219269
C. betulae	CBS 109763	EU199180	AF408375	EU221884	EU199139
C. hypodermia	AR 3552	EU199181	AF408346	N/A	EU199140
C. suffusa	CBS 109750	EU199207	AF408376	EU221945	EU199163
Cytospora elaeagni	CFCC 89633	KF765677	KF765693	KU710919	KU710956
C. leucostoma	CFCC 50468	KT732949	KT732968	N/A	N/A
Dendrostoma mali	CFCC 52102^{T}	MG682072	MG682012	MG682052	MG682032
D. osmanthi	CFCC 52106^{T}	MG682073	MG682013	MG682053	MG682033
D. quercinum	CFCC 52103^{T}	MG682077	MG682017	MG682057	MG682037
Diaporthe decedens	CBS 109772	KC343059	AF408348	N/A	N/A
D. detrusa	CBS 109770	KC343061	AF408349	KC343787	N/A
D. eres	CBS 109767	KC343075	AF408350	KC343801	N/A
Diaporthella corylina	CBS 121124	KC343004	N/A	N/A	N/A
Diaporthella sp.	CN 5	KP205483	N/A	N/A	N/A
Diaporthella sp.	CN13	KP205484	N/A	N/A	N/A
Diaporthosporella cercidicola	CFCC 51994^{T}	KY852492	KY852515	N/A	N/A
D. cercidicola	CFCC 51995	KY852493	KY852516	N/A	N/A
Diaporthostoma machili	CFCC 52100^{T}	MG682080	MG682020	MG682060	MG682040
D. machili	CFCC 52101	MG682081	MG682021	MG682061	MG682041
Disculoides eucalypti	CPC 17650	JQ685517	JQ685523	N/A	N/A
D. eucalyptorum	CBS 132184	NR_120090	JQ685524	N/A	N/A
Ditopella ditopa	CBS 109748	EU199187	EU199126	N/A	EU199145
Erythrogloeum hymenaeae	CPC 18819	JQ685519	JQ685525	N/A	N/A
G. gnomon	CBS 199.53	AY818956	AF408361	EU221885	EU219295
Harknessia eucalypti	CBS 342.97	AY720745	AF408363	N/A	N/A
Hercospora tiliae	AR 3526	N/A	AF408365	N/A	N/A
Hyaliappendispora galii	MFLUCC 16-1208	MF190149	MF190095	N/A	N/A
Juglanconis appendiculata	D96	KY427139	KY427139	KY427208	KY427189
J. juglandina	ME23	KY427150	KY427150	KY427219	KY427200
J. oblonga	ME14	KY427151	KY427151	KY427220	KY427201
J. pterocaryae	ME20	KY427155	KY427155	KY427224	KY427205
Lamproconium desmazieri	MFLUCC 14-1047	KX430132	KX430133	MF377592	N/A
L. desmazieri	MFLUCC 15-0870	KX430134	KX430135	MF377591	MF377605
Lasmenia sp.	CBS 124123	GU797406	JF838338	N/A	N/A
Lasmenia sp.	CBS 124124	JF838336	JF838341	N/A	N/A
Luteocirrhus shearii	CBS 130776	NR_120254	NG_042770	N/A	N/A

Taxon	Strain Number	GenBank Accession Numbers			
		ITS	LSU	*tef*1-α	*rpb*2
Macrohilum eucalypti	CPC 19421^{T}	KR873244	KR873275	N/A	N/A
Melanconiella ellisii	BPI 878343	JQ926271	JQ926271	JQ926406	JQ926339
M. spodiaea	MSH	JQ926298	JQ926298	JQ926431	JQ926364
Melanconis betulae	CFCC 50471	KT732952	KT732971	KT733001	KT732986
M. itoana	CFCC 50474	KT732955	KT732974	KT733004	KT732987
M. marginalis	CBS 109744	EU199197	AF408373	EU221991	EU219301
M. stilbostoma	CFCC 50475	KT732956	KT732975	KT733005	KT732988
Nakataea oryzae	CBS 243.76	KM484861	DQ341498	N/A	N/A
Ophiodiaporthe cyatheae	YMJ1364	JX570889	JX570891	N/A	JX570893
Pachytrype princeps	Rogers S	N/A	FJ532382	N/A	N/A
P. rimosa	FF1066	N/A	FJ532381	N/A	N/A
Paradiaporthe artemisiae	MFLUCC 14-0850	MF190155	MF190100	N/A	N/A
P. artemisiae	MFLUCC 17-1663	MF190156	MF190101	N/A	N/A
Phaeoappendispora thailandensis	MFLUCC 13-0161	MF190157	MF190102	N/A	MF377613
Phaeodiaporthe appendiculata	CBS 123821	KF570156	KF570156	N/A	N/A
Phragmoporthe conformis	CBS 109783	DQ323527	AF408377	N/A	N/A
Plagiostoma euphorbiae	CBS 340.78	EU199198	AF408382	N/A	DQ368643
P. salicellum	CBS 109775	DQ323529	AF408345	EU221916	EU199141
Prosopidicola mexicana	CBS 113530	AY720710	N/A	N/A	N/A
P. mexicana	CBS 113529^{T}	AY720709	KX228354	N/A	N/A
Pseudomelanconis caryae	CFCC 52110^{T}	MG682082	MG682022	MG682062	MG682042
P. caryae	CFCC 52111	MG682083	MG682023	MG682063	MG682043
Pseudoplagiostoma eucalypti	CBS 124807	GU973512	GU973606	N/A	N/A
P. eucalypti	CBS 116382	GU973514	GU973608	N/A	N/A
Pyricularia grisea	Ina168	AB026819	AB026819	N/A	N/A
Rossmania ukurunduensis	AR 3484	N/A	EU683075	N/A	N/A
Sillia ferruginea	CBS 126567	JF681959	EU683076	N/A	N/A
Stegonsporium pyriforme	CBS 124487	KF570160	KF570160	N/A	KF570190
Stilbospora macrosperma	CBS 121883	JX517290	JX517299	N/A	KF570196
Sydowiella fenestrans	CBS 125530	JF681956	EU683078	N/A	N/A
Synnemasporella aculeans	CFCC 52094	MG682086	MG682026	MG682066	MG682046
S. aculeans	CFCC 52095	MG682087	MG682027	MG682067	MG682047
S. fanii	**ZHKUCC 23-1018^{T}**	**PP060496**	**PP060510**	**PP035537**	**PP035545**
S. fanii	**GMBCC1001**	**PP067150**	**PP067155**	**PP068811**	**PP084097**
S.toxicodendri	CFCC 52097^{T}	MG682089	MG682029	MG682069	MG682049
S. toxicodendri	CFCC 52098	MG682090	MG682030	MG682070	MG682050

Note: "T" denotes ex-type. Newly generated sequences are indicated in bold. "N/A": no data available in GenBank.

Maximum-likelihood (ML) analysis was carried out via the online portal CIPRES Science Gateway v. 3.3 (Miller et al. 2010), using RAxML-HPC v.8 on XSEDE (8.2.12) tool, with the default settings but adapted: the GAMMA nucleotide substitution model and 1000 rapid bootstrap replicates.

Bayesian analysis was performed by MrBayes v. 3.0b4 (Ronquist and Huelsenbeck 2003), and the model of evolution was estimated with MrModelt-

est v. 2.2 (Nylander 2004). The posterior probabilities (PP) (Rannala and Yang 1996; Zhaxybayeva and Gogarten 2002) were determined by the following Markov chain Monte Carlo sampling (MCMC) in MrBayes v.3.0b4 (Huelsenbeck and Ronquist 2001). Six simultaneous Markov chains were run for 1,000,000 generations, with trees sampled every 100th generation. The preburn was set to 5 and the run was automatically stopped when the mean standard deviation of the split frequency reached below 0.01 (Maharachchikumbura et al. 2015).

Figtree v. 1.4.0 (http://tree.bio.ed.ac.uksoftware/figtree/) (Rambaut 2006) was used to view tree. Microsoft Office PowerPoint 2016 (Microsoft Inc., Redmond, WA, USA) was used to edit the phylogram, and then convert it to jpg. file by using the Adobe PhotoShop CC 2018 software (Jiang et al. 2021).

Results

Phylogenetic analyses

Phylogenetic analyses of *Spegazzinia*

The concatenated dataset (ITS, LSU, SSU, and *tef*1-α regions) contained 74 strains in the sequence analysis, which comprise 2988 characters with gaps. Single gene analysis was carried out and compared with each species, to compare the topology of the tree and clade stability. Two strains of *Bambusistroma didymosporum* D.Q. Dai & K.D. Hyde (MFLU 15-0057 and MFLU 15-0058) are set as the outgroup taxon. The best-scoring RAxML tree with a final likelihood value of -16559.564563 is presented. The matrix had 838 distinct alignment patterns, with 23.64% of undetermined characters or gaps. Estimated base frequencies were as follows; A = 0.238369, C = 0.251538, G = 0.273530, T = 0.236562; substitution rates AC = 1.319072, AG = 2.377467, AT = 1.425866, CG = 0.960524, CT = 6.538802, GT = 1.000000; gamma distribution shape parameter alpha = 0.188509 (Fig. 1). GTR+I+G model was selected as the best model based on MrModeltest and was used for the Bayesian analysis. Overall tree topologies based on ML and BI analyses were similar and not significantly different. In the phylogenetic analysis (Fig. 1), our new strains (ZHKUCC 23-1020 (ex-type) and GMBCC1002) belonged to the genus *Spegazzinia* (Fig. 1). Both strains grouped as the sister clade to *Spegazzinia jinghaensis* G.C. Ren & K.D. Hyde (KUMCC 21-0495 (ex-type) and KMUCC 21-0496), and phylogenetically well-distinct with high statistical values (95% ML and 1 PP; Fig. 1).

Phylogenetic analyses of *Phaeoseptum*

The concatenated dataset (ITS, LSU, SSU, and *tef*1-α regions) contained 45 strains in the sequence analysis, which comprise 3532 characters with gaps. Single gene analysis was carried out and compared with each species, to contrast the topology of the tree and clade stability. *Hysterium angustatum* Pers. (MFLUCC 16-0623) and *Gloniopsis praelonga* (Schwein.) Underw. & Earle (CBS 112415) were selected as the outgroup taxa. The best-scoring RAxML tree with a final likelihood value of -23164.186742 is presented. The matrix had 1334 distinct alignment patterns, with 25.07% of undetermined characters or gaps. Estimated base frequencies were as follows; A = 0.241078, C = 0.255689, G = 0.276841, T = 0.226392; substitution rates AC = 1.125548, AG = 2.311485,

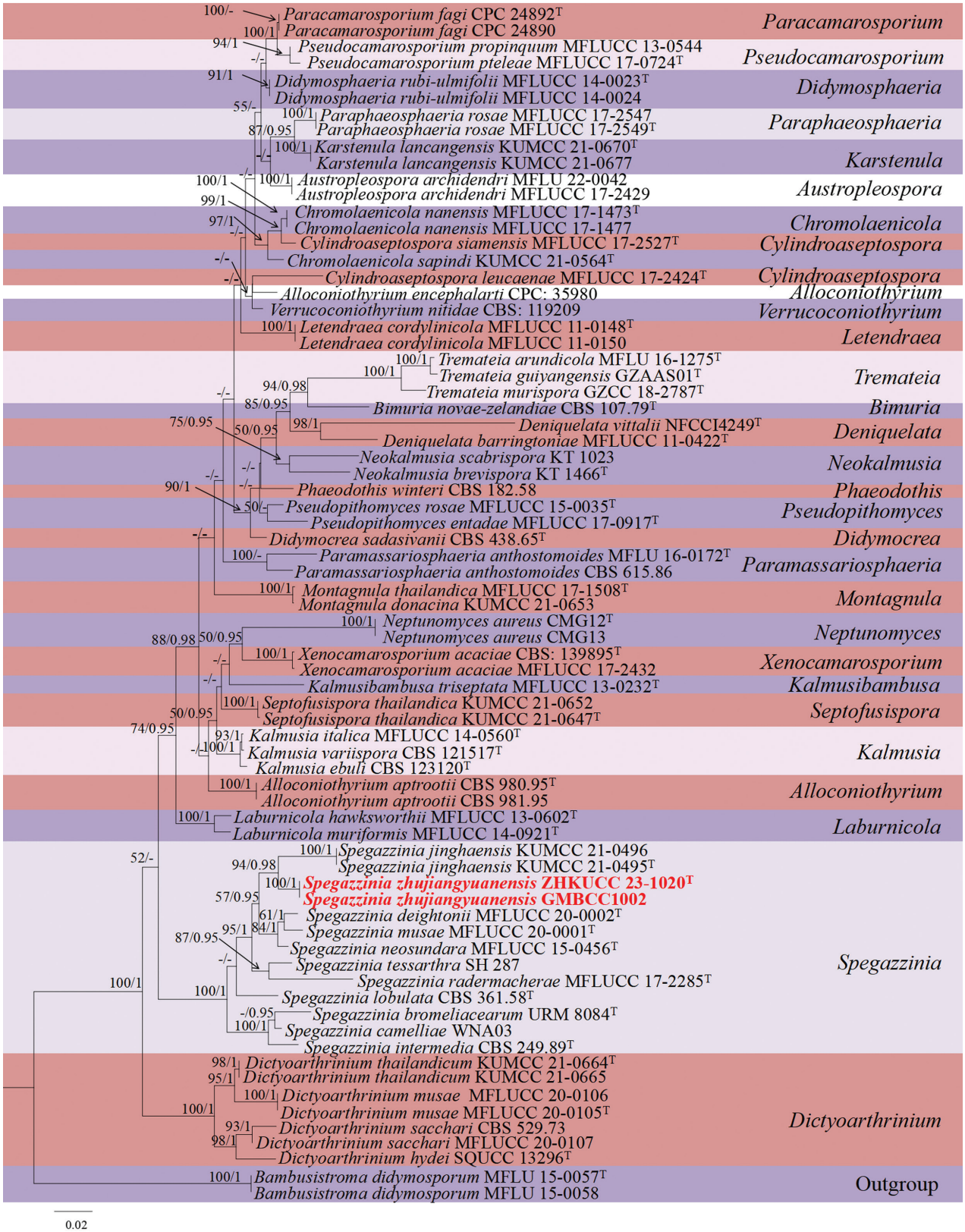

Figure 1. The phylogenetic tree from the best scoring of the RAxML analysis based on combined (ITS, LSU, SSU and *tef*1-α) is rooted to *Bambusistroma didymosporum* (MFLU 15-0057 and MFLU 15-0058). Bootstrap values for maximum likelihood (MLBP) and Bayesian posterior probabilities (BYPP) equal to or greater than 50% and 0.95 are given at the respective branches. Hyphen (-) means a value lower than 50% (BS) or 0.95 (PP). The newly generated sequences are indicated in red bold. The ex-type strains are noted with "T".

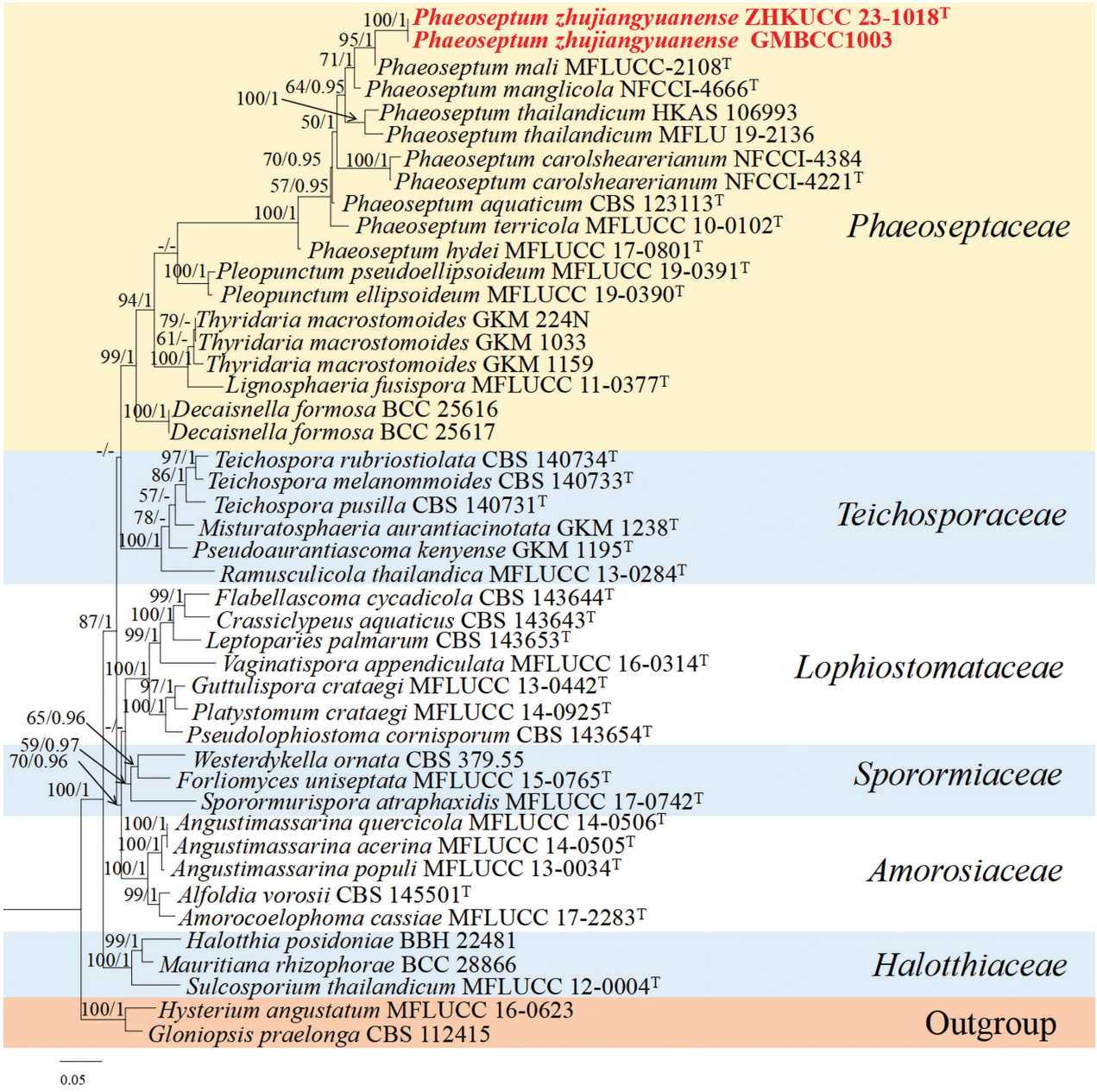

Figure 2. The phylogenetic tree from the best scoring of the RAxML analysis based on combined (ITS, LSU, SSU and *tef*1-α) is rooted to *Hysterium angustatum* (MFLUCC 16-0623) and *Gloniopsis praelonga* (CBS 112415). Bootstrap values for maximum likelihood (MLBP) and Bayesian posterior probabilities (BYPP) equal to or greater than 50% and 0.95 are given at the respective branches. Hyphen (-) means a value lower than 50% (BS) or 0.95 (PP). The newly generated sequences are indicated in red bold. The ex-type strains are indicated with "T".

AT = 1.305084, CG = 1.147813, CT = 6.370520, GT = 1.000000; gamma distribution shape parameter alpha = 0.281773 (Fig. 2). GTR+I+G model was selected as the best model based on MrModeltest and was used for the Bayesian analysis. Overall tree topologies based on ML and BI analyses were similar and not significantly different. In the phylogenetic analysis (Fig. 2), two strains of *Phaeoseptum zhujiangyuanense* (ZHKUCC 23-1022 (ex-type) and GMBCC1003) formed a monophyletic clade (100% ML, 1.00 PP). This clade formed a sister taxon to *Phaeoseptum mali* Phukhams. & K.D. Hyde (MFLUCC-2108) with 95% ML and 1.00 PP support values.

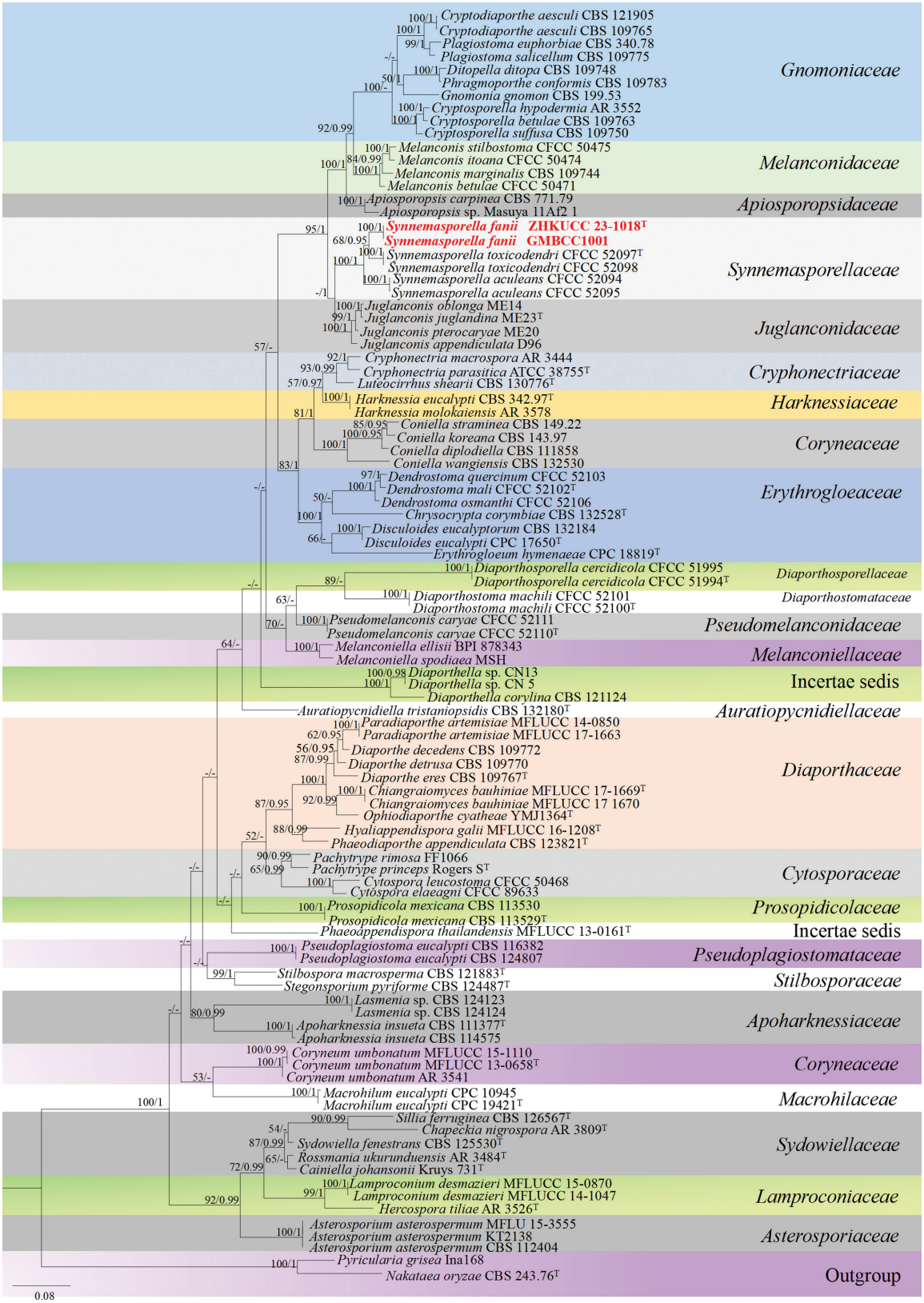

Figure 3. The phylogenetic tree from the best scoring of the RAxML analysis based on combined (ITS, LSU, *tef*1-α and *rpb*2) is rooted to *Nakataea oryzae* (CBS 243.76) and *Pyricularia grisea* (Ina168). Bootstrap values for maximum likelihood (MLBP) and Bayesian posterior probabilities (BYPP) equal to or greater than 50% and 0.95, are given at the respective branches. Hyphen (-) means a value lower than 50% (BS) or 0.95 (PP). The newly generated sequences are indicated in red bold. The ex-type strains are indicated with "T".

Phylogenetic analyses of *Synnemasporella*

The concatenated dataset (ITS, LSU, *tef*1-α and *rpb*2 regions) contained 97 strains in the sequence analysis, which comprise 2575 characters with gaps. Single gene analysis was carried out and compared with each species, to compare the topology of the tree and clade stability. *Nakataea oryzae* (Catt.) J. Luo & N. Zhang (CBS 243.76) and *Pyricularia grisea* Cooke ex Sacc. (Ina168) are set as the outgroup taxa. The best-scoring RAxML tree with a final likelihood value of -30093.037277 is presented. The matrix had 1256 distinct alignment patterns, with 32.60% of undetermined characters or gaps. Estimated base frequencies were as follows; A = 0.248601, C = 0.250906, G = 0.280824, T = 0.219669; substitution rates AC = 1.521472, AG = 3.435591, AT = 1.966143, CG = 1.205529, CT = 7.891750, GT = 1.000000; gamma distribution shape parameter alpha = 0.244582 (Fig. 3). GTR+I+G model was selected as the best model based on MrModeltest and was used for the Bayesian analysis. Overall tree topologies based on ML and BI analyses were similar and not significantly different. In the phylogenetic analysis (Fig. 3), our collection of *Synnemasporella fanii* (ZHKUCC 23-1018 (ex-type) and GMBCC1001) resided in the genus *Synnemasporella* and formed a sister clade to *S. toxicodendri* (CFCC 52097 (ex-type) and CFCC 52098) with moderate support (ML 68% and 0.95 PP).

Taxonomy

Class Dothideomycetes O.E. Erikss. & Winka
Subclass Dothideomycetidae P.M. Kirk, P.F. Cannon, J.C. David & Stalpers ex C.L. Schoch, Spatafora, Crous & Shoemaker
Pleosporales Luttrell ex M.E. Barr
Didymosphaeriaceae Munk

***Spegazzinia* Sacc.**
Index Fungorum: IF9963

Notes. The genus *Spegazzinia* was introduced by Saccardo (1880) with *S. ornata* (current name: *S. tessarthra* (Berk. & M.A. Curtis) Sacc. 1886 *fide* Saccardo 1886) as the type species. Initially, based on morphological characters with basauxic conidiogenesis, *Spegazzinia* was accommodated in Apiosporaceae, Sordariomycetes (Hyde et al. 1998). However, Tanaka et al. (2015) transferred *Spegazzinia* to Didymosphaeriaceae (Dothideomycetes) based on molecular data. Morphologically, species of *Spegazzinia* have a distinctive conidiophore ontogeny, as well as two types of conidia: α conidia are composed of 4–8 subglobose, dark cells with long spines, while β conidia are generally subspherical or broadly ellipsoid, flattened in one plane, cruciately septate or muriform, pale brown and smooth-walled (Samarakoon et al. 2020). Currently, 17 epithets are listed in Species Fungorum 2024 (accession date: 31 May 2024). Our new collection morphologically resembles *Spegazzinia s. str.* and multi-locus phylogenetic analyses confirmed that it is a novel species.

Spegazzinia zhujiangyuanensis **G.Q. Zhang, Wijayaw., & D.Q. Dai, sp. nov.**
Index Fungorum: IF901550
Fig. 4

Etymology. Named after the locality from where it was collected, Zhujiangyuan, Yunnan (China).

Holotype. MHCU 23-0273.

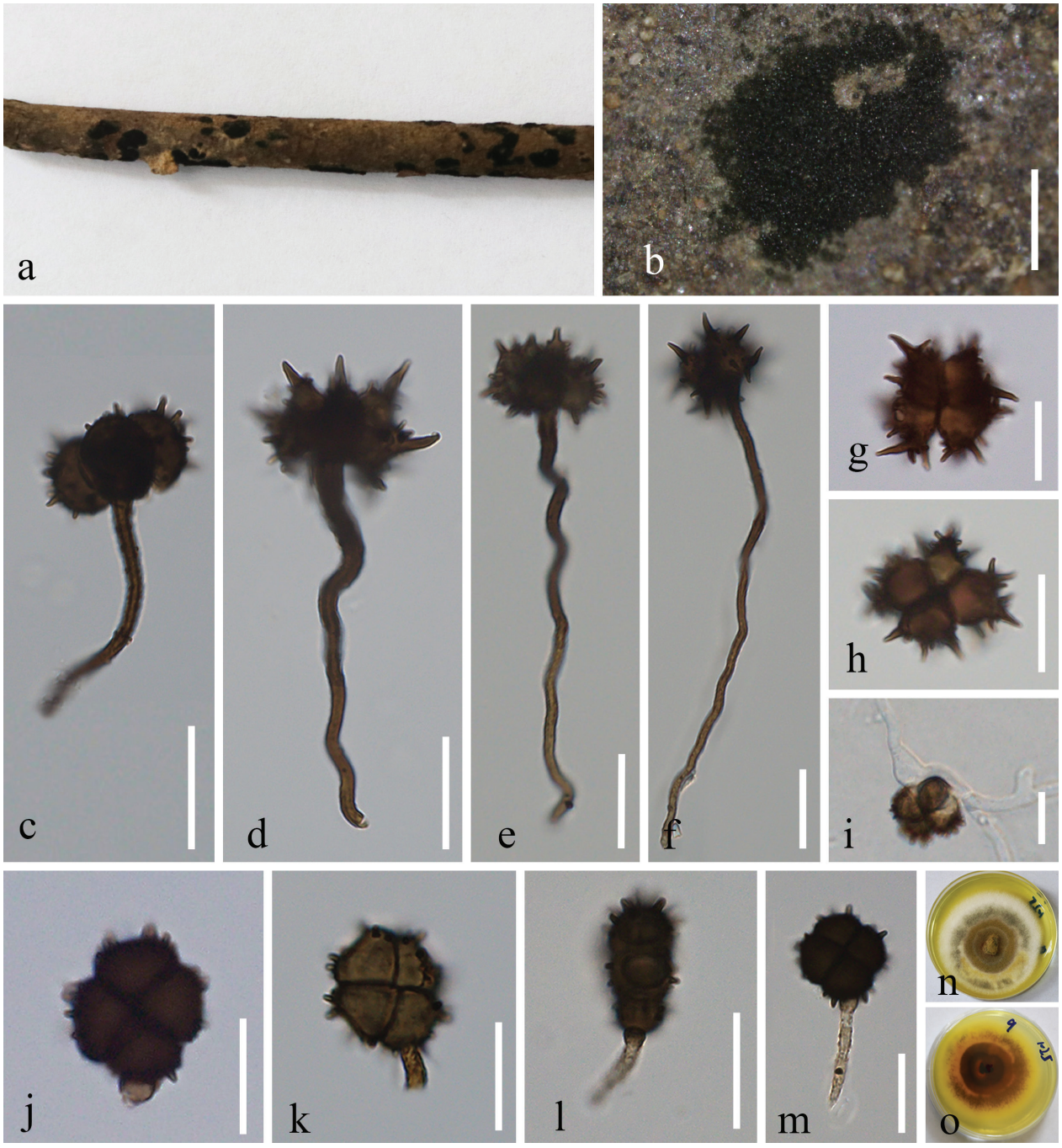

Figure 4. *Spegazzinia zhujiangyuanensis* (MHCU 23-0273, holotype) **a, b** fungal colonies on the host surface **c–f** conidiophore of α conidia and α conidia **g, h** α conidia **i** germinated α conidium **j–m** β conidia **n, o** culture characters on pda (**n** above **o** below). Scale bars: 150 μm (**b**); 25 μm (**c**); 20 μm (**d–f**); 15 μm (**g–m**).

Description. ***Saprobic*** on twigs of an unknown woody plant. **Sexual morph:** undetermined. **Asexual morph:** Hyphomycetous. ***Conidiomata*** sporodochia, powdery, dark, dense, 0.2–2 mm in diam. ***Conidiogenous cells*** 7–12 µm high × 2.5–6 µm wide ($\bar{x}$ = 9.5 × 3.5 µm; n = 10), basauxic, ampulate, subspherical, hyaline-to-light-brown, rough at surface. ***Conidiophores of α conidia*** up to 32.5–142.5 × 1.5–3.5 µm ($\bar{x}$ = 82.5 × 2.5 µm, n = 20), erect or flexuous, unbranched, dark brown. ***Conidiophores of β conidia*** 14.5–19 × 2.0–2.3 µm ($\bar{x}$ = 16.3 × 2.1 µm; n = 20), short, erect, unbranched, sub-hyaline or light brown. ***Conidia*** two types; ***α conidia*** 17.5–25 × 15.5–26 µm ($\bar{x}$ = 20.5 × 19.7 µm; n = 20), 4-celled, stellate-shaped, brown to dark-brown, globose to subglobose, with dark brown warts on the surface of some cells, with conspicuous spines, constricted at septa, 3.6–8 × 1–2.8 µm ($\bar{x}$ = 5.3 × 1.7 µm; n = 20); ***β conidia*** 12.2–16 × 12–17 µm ($\bar{x}$ = 14.1 × 14.6 µm; n = 20), 4-celled, disc-shaped, quadrangular or subspherical, pale brown at immaturity, becoming brown to dark-brown at maturity, usually attached with conidiogenous cells when detached from the conidiophore, each cell cruciately septate, turbinate, sometimes verrucose around the edges, deeply constricted at septa, flat from side view.

Culture characteristics. Conidia germinating on PDA within 24 h. Colonies growing on PDA, reaching reached 30–40 mm diam. After 14 days at 27 °C, superficial, circular, curled, producing concentric circles after 3 weeks, gradually turning brownish gray to white from middle to edge, entire white margin, periphery white at the immature stage, reverse yellowish-brown.

Material examined. China. Yunnan Province, Qujing City, Zhujiangyuan Nature Reserve, 25°30'N, 103°45'E, 01 September 2023, Gui-Qing Zhang & Dong-Qin Dai, QJNU 09 (MHCU 23-0273, ***holotype***), ex-type ZHKUCC 23-1016; *Ibid*. (GMB 1002, **isotype**), ex-isotype GMBCC1002.

GenBank numbers. Ex-type (ZHKUCC 23-1020): PP060498 (ITS); PP060512 (LSU); PP060504 (SSU); PP035539 (*tef*1-α), **ex-isotype (GMBCC1002):** PP067151 (ITS); PP067156 (LSU); PP066043 (SSU); PP068812 (*tef*1-α).

Notes. Phylogenetic analyses based on ITS, LSU, SSU, and *tef*1-α gene regions showed that our new strains (ZHKUCC 23-1020 (ex-type) and GMBCC1002) belonged to the genus *Spegazzinia* (Fig. 1). Both strains grouped as the sister clade to *S. jinghaensis* (KUMCC 21-0495 (ex-type) and KMUCC 21-0496), but phylogenetically found distinct with high statistical values (95% ML bootstrap and 1.00 PP) (Fig. 1). Morphological differences between the new taxon and *S. jinghaensis* are listed in Table 4. Therefore, based on both morpho-molecular results, we herein introduce a new species in the genus, *Spegazzinia zhujiangyuanensis*.

Table 4. Diagnostic characters of *Spegazzinia jinghaensis* and *S. zhujiangyuanensis*.

Morphological character	Species name and reference	
	Spegazzinia jinghaensis **(Ren et al. 2022)**	***S. zhujiangyuanensis*** **(This study)**
Conidiomata	Sporodochial, velvety, 2–3 mm in diam.	Sporodochial, 0.2–2 mm in diam
Conidiogenous cells	5–6 µm long × 4–5 µm wide	7–12 µm long × 2.5–6 µm wide, rough surface
Conidiophores of α conidia	80–120 × 1.4–2 µm, unbranched, dark brown	32.5–142.5 × 1.5–3.5 µm, unbranched, rough surface
Conidiophores of β conidia	3.5–8 × 2.5–3.5 µm short, erect, unbranched, sub-hyaline or light brown	14.5–19 × 2–2.3 µm, short, erect, unbranched, sub-hyaline or light brown
Culture characters	Rough surface, reverse black	With entire white margin, curled, reverse yellowish-brown

Phaeoseptaceae S. Boonmee, Thambug. & K.D. Hyde

***Phaeoseptum* Ying Zhang, J. Fourn. & K.D. Hyde**
Index Fungorum: IF561889

Notes. Zhang et al. (2013) introduced *Phaeoseptum* with *P. aquaticum* Ying Zhang, J. Fourn. & K.D. Hyde as the type species. There are seven *Phaeoseptum* epithets listed in Species Fungorum (31 May 2024). *Phaeoseptum* is characterized by immersed ascomata, cellular pseudoparaphyses, bitunicate, fissitunicate clavate, 8-spored asci, and broadly fusiform, muriform, medium brown coloured, ascospores (Zhang et al. 2013; Phukhamsakda et al. 2019). Our new collection morphologically resembles *Phaeoseptum s. str.* The phylogenetic study confirmed that the new collection represents a new species of *Phaeoseptum* (Fig. 2).

***Phaeoseptum zhujiangyuanense* G.Q. Zhang, Wijayaw., & D.Q. Dai, sp. nov.**
Index Fungorum: IF901551
Fig. 5

Etymology. named after the locality from where it was collected, Zhujiangyuan, Yunnan (China).

Holotype. MHCU 23-0275.

Description. ***Saprobic*** on dead wood branches in terrestrial habitats. **Sexual morph:** ***Ascomata*** 215–470 µm long × 150–320 µm wide ($\bar{x}$ = 340 × 225 µm, n = 20), solitary, scattered, semi-immersed to immersed, globose to subglobose, irregular, clypeate, ostiolate, sometimes erumpent as dark brown to black area from the host tissue, or sometimes with a slit-like opening. ***Ostiole*** 33–60 µm high, 15–55 µm diam., short, pale brown. ***Peridium*** 25–60 µm ($\bar{x}$ = 44 µm, n = 15) wide, comprising 4–6 layers of cells of *textura angularis*, with thick-walled and brown cells of outer layers, with thin-walled and hyaline cells of inner layers. ***Hamathecium*** composed of 1–1.5 µm ($\bar{x}$ = 1.6 µm, n = 20) wide, numerous, branched, cellular, septate, narrow pseudoparaphyses, anastomosing above the asci, and embedded in a gelatinous matrix. ***Asci*** 105–165 × 22–35 µm ($\bar{x}$ = 140 × 30 µm, n = 20), 8-spored, bitunicate, fissitunicate, cylindrical-clavate to elongate-clavate, with a distinct pedicel, apically rounded and thinned, with a distinct ocular chamber at immature stage, with a minute ocular chamber when mature. ***Ascospores*** 35–42 × 9–15 µm ($\bar{x}$ = 38 × 10 µm, n = 30), partly overlapping, uniseriate at base, 2–3-seriate above, pale to yellowish brown to medium brown from immaturity to maturity, oblong to broadly fusiform, with broadly rounded ends, slightly curved, with 7–13-transversally septa, and 5–21-vertical septa, rarely 2–5 longitudinal septa in each row, normally 1–2 longitudinal septa, but not all cells with a vertical septum in median, the septa partly pale brown, slightly constricted at septa, smooth-walled. Y-shaped septum present or absent in the end cells, with hyaline to pale brown end cells, **Asexual morph:** undetermined.

Culture characteristics. Ascospores germinating on PDA, producing germ tubes from both ends of the ascospores within 24 hours. Colonies growing on PDA, reaching reached 30–40 mm diam. after 14 days at 27 °C, surface pale brown, irregular, curled, producing concentric circles after 3 weeks, reverse warm blackish brown with olive buff at margins.

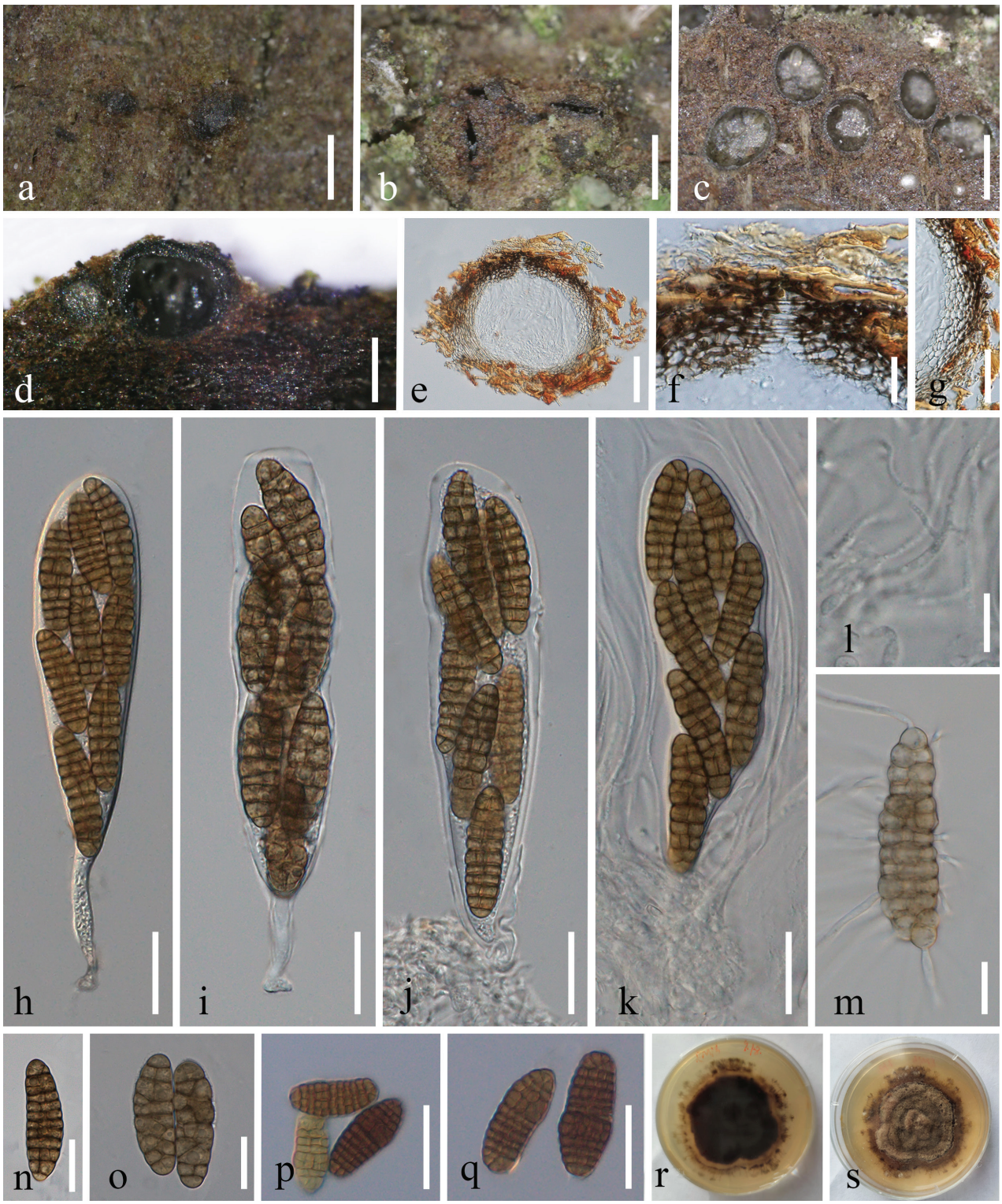

Figure 5. *Phaeoseptum zhujiangyuanense* (MHCU 23-0275, holotype) **a–c** appearance of ascomata on host substrate **d, e** vertical section of ascoma **f** ostiole **g** peridium **h–k** asci **l** pseudoparaphyses **m** germinated ascospore **n–q** ascospores **r, s** colonies on PDA (**r** above **s** below). Scale bars: 300 µm (**a–c**); 200 µm (**d, e**); 50 µm (**f, g, p, q**); 20 µm (**h–o**).

Material examined. China. Yunnan Province, Qujing City, Zhujiangyuan Nature Reserve, 25°30'N, 103°45'E, 01 September 2023, Gui-Qing Zhang & Nalin N. Wijayawardene, RM16 (MHCU 23-0275, ***holotype***), ex-type ZHKUCC 23-1022; *Ibid.* (GMB 1003, ***isotype***), ex-isotype GMBCC1003.

GenBank numbers. Ex-type (ZHKUCC 23-1022): PP060500 (ITS); PP060514 (LSU); PP060506 (SSU); PP035541 (*tef*1-α), **ex-isotype (GMBCC1003)**: PP067152 (ITS); PP067157 (LSU); PP066044 (SSU); PP068813 (*tef*1-α).

Note. The phylogenetic analyses based on a combined dataset of ITS, LSU, SSU and *tef*1-α gene regions (Fig. 2) showed that our isolates (ZHKUCC 23-1022 (ex-type) and GMBCC1003) placed in the genus *Phaeoseptum* in Didymosphaeriaceae (Fig. 2). *Phaeoseptum zhujiangyuanense* clusters with *P. manglicola* (NFCCI-4666) and *P. mali* (MFLUCC-2108) with significant support (ML 100% and 1.00 PP). Morphologically, *P. zhujiangyuanense*, *P. manglicola* Devadatha, V.V. Sarma & E.B.G. Jones and *P. mali* share similar characteristics in their ascomata, asci and ascospores, and in their overlapping dimensions. However, *P. zhujiangyuanense* is distinguishable from *P. mali* and *P. manglicola* in some characters, as shown in Table 5. Therefore, based on both morphological and phylogenetic evidences, we established this novel species in *Phaeoseptum*.

Table 5. Diagnostic characters of *Phaeoseptum mali*, *P. manglicola* and *P. zhujiangyuanense*.

Morphological character	Species name and reference		
	P. Mali **(Phukhamsakda et al. 2019)**	***P. manglicola*** **(Dayarathne et al. 2020)**	***P. zhujiangyuanense*** **(This study)**
Ascomata	Globose ascomata	Globose to subglobose or irregular, aggregate to solitary, with ostiolate	Globose to subglobose, scattered, solitary, ostiolate, with slit-like opening
Ostiole	Opened pore, ostiolate with periphyses	28–94 µm high, 39–96 µm diam	33–60 µm high, 15–55 µm diam
Peridium	5–19 µm, composed of 8–11 layers	30– 85 µm, composed 4–6 layers	25–60 µm wide, composed 4–6 layers
Asci	85–190 × 19–32 µm, cylindrical-clavate to elongate-clavate; apically rounded, ocular chamber clearly visible when immature	102–212 × 17–27.5 µm, cylindrical to clavate; apically rounded and thickened; a refractive plate in the ectoascus and a refractive apical plate in the endoascus	105–165 × 22–35 µm, cylindrical-clavate to elongate-clavate; apically rounded and thinned, with a clearly ocular chamber at immature stage
Ascospores	27–38 × 8–13 µm, broad cylindrical, broadly cylindrical, yellowish to dark brown; 11–14 transverse septa, and 1–2 longitudinal septum in each cell	27–36 × 7.5–13 µm, oblong to broadly fusiform, straight, sometimes slightly curved, hyaline, becoming pale brown to yellowish brown; 9–13 transverse septa, 1–2 longitudinal septa in each row	35–42 × 9–15 µm, oblong to broadly fusiform, slightly curved, pale to yellowish brown to brownness; 7–13-transversally septate, 5–21-vertical septate, 1–5 longitudinal septa in each row

Sordariomycetes O.E. Erikss. & Winka
Diaporthomycetidae Senan., Maharachch. & K.D. Hyde
Diaporthales Nannf
Synnemasporellaceae X.L. Fan & J.D.P. Bezerra

Fan et al. (2018) introduced this family to accommodate the holomorphic genus, *Synnemasporella* (with type species *S. toxicodendri* X.L. Fan & J.D.P. Bezerra). Currently, the family comprises only one genus (Wijayawardene et al. 2022a).

Synnemasporella **X.L. Fan & J.D.P. Bezerra**
Index Fungorum: IF823995

Notes. The genus *Synnemasporella* is a pleomorphic taxon that exhibits both sexual and asexual morphs (Fan et al. 2018). Currently, the genus comprises

two species. The asexual morphs of *S. aculeans* X.L. Fan & J.D.P. Bezerra were reported with both coelomycetous and hyphomycetous morphs (Fan et al. 2018). However, the second species *S. toxicodendri* was reported only with its hyphomycetous morph.

Synnemasporella fanii **Wijayaw., G.Q. Zhang & D.Q. Dai, sp. nov.**
Index Fungorum: IF901552
Fig. 6

Etymology. Named after Dr. Xin-Lei Fan, the mycologist who introduced the genus, to recognize his outstanding contribution to mycology in China.

Holotype. MHCU 23-0271.

Description. ***Saprobic*** on twigs of an unknown woody plant. **Sexual morph:** undetermined. **Asexual morph:** hyphomycetous. ***Conidiomata*** synnematous. ***Synnemata*** 1000–1300 µm high, 110–360 µm diam., long and determinate, pale to brown, straight, occasionally curved, composed of parallelly and compactly arranged conidiophores. ***Conidiophores*** 30–70 µm long × 4.5–6.5 µm wide, hyaline to pale brown, aggregated, straight to curved. ***Conidiogenous cells*** 1.5–3.5 × 0.5–2.5 µm, enteroblastic, with a minute collarette at the tip, hyaline to pale brown, straight to curved, cylindrical, arranged adjacent to one another at the fertile end of the synnema, with each conidiogenous cells producing one conidium. ***Conidia*** 23–37 × 11–17 µm ($\bar{x}$ = 30 × 15 µm, n = 20), cylindrical to oblong-cylindrical, 1–3 septate, slightly constricted at septa, straight to slightly curved, with a discrete hilum, smooth-walled, multiguttulate, pale brown to brown.

Culture characteristics. Conidia germinating on PDA within 24 h. Colonies growing on PDA, reaching reached 30–40 mm diam. after 14 days at 27 °C, circular, initially white, becoming sepia on the bottom after 7 days, with an irregular edge, texture uniform.

Material examined. China. Yunnan Province, Qujing City, Zhujiangyuan Nature Reserve, 25°30'N, 103°45'E, 01 September 2023, Gui-Qing Zhang & Nalin N. Wijayawardene, RM17 (MHCU 23-0271, ***holotype***), ex-type ZHKUCC 23-1018; *Ibid.* (GMB 1001, ***isotype***), ex-isotype GMBCC1001.

GenBank numbers. Ex-type (ZHKUCC 23-1018): PP060496 (ITS); PP060510 (LSU); PP035537 (*tef*1-α); PP035545 (*rpb*2), **ex-isotype (GMBCC1001):** PP067150 (ITS); PP067155 (LSU); PP068811 (*tef*1-α); PP084097 (*rpb*2).

Note. The phylogenetic analyses of the combined dataset of ITS, LSU, *rpb*2 and *tef*1-α gene regions (Fig. 3) showed that our isolates (ZHKUCC 23-1018 (ex-type) and GMBCC1001) belonged to the genus *Synnemasporella* (Fig. 3). *Synnemasporella fanii* clustered with *S. toxicodendri* (CFCC 52097 (isotype) and CFCC 52098) with moderate statistical supports (ML 68% and 0.95 PP). Morphologically, *Synnemasporella fanii* shares similar characteristics in its synnemata with *S. toxicodendri* and *S. aculeans*. Furthermore, *S. fanii* can be distinguished from *S. toxicodendri* and *S. aculeans* by having 1–3-septate conidia. Besides, in both two species of this genus, the form of the conidiogenous cells cannot be discerned well from Fan et al. (2018); it is not certain whether the two species have enteroblastic conidiogenous cells similar to our strain. The other differences are provided in Table 6. Based on morphology and phylogeny, we established this new collection as a novel species of *Synnemasporella*.

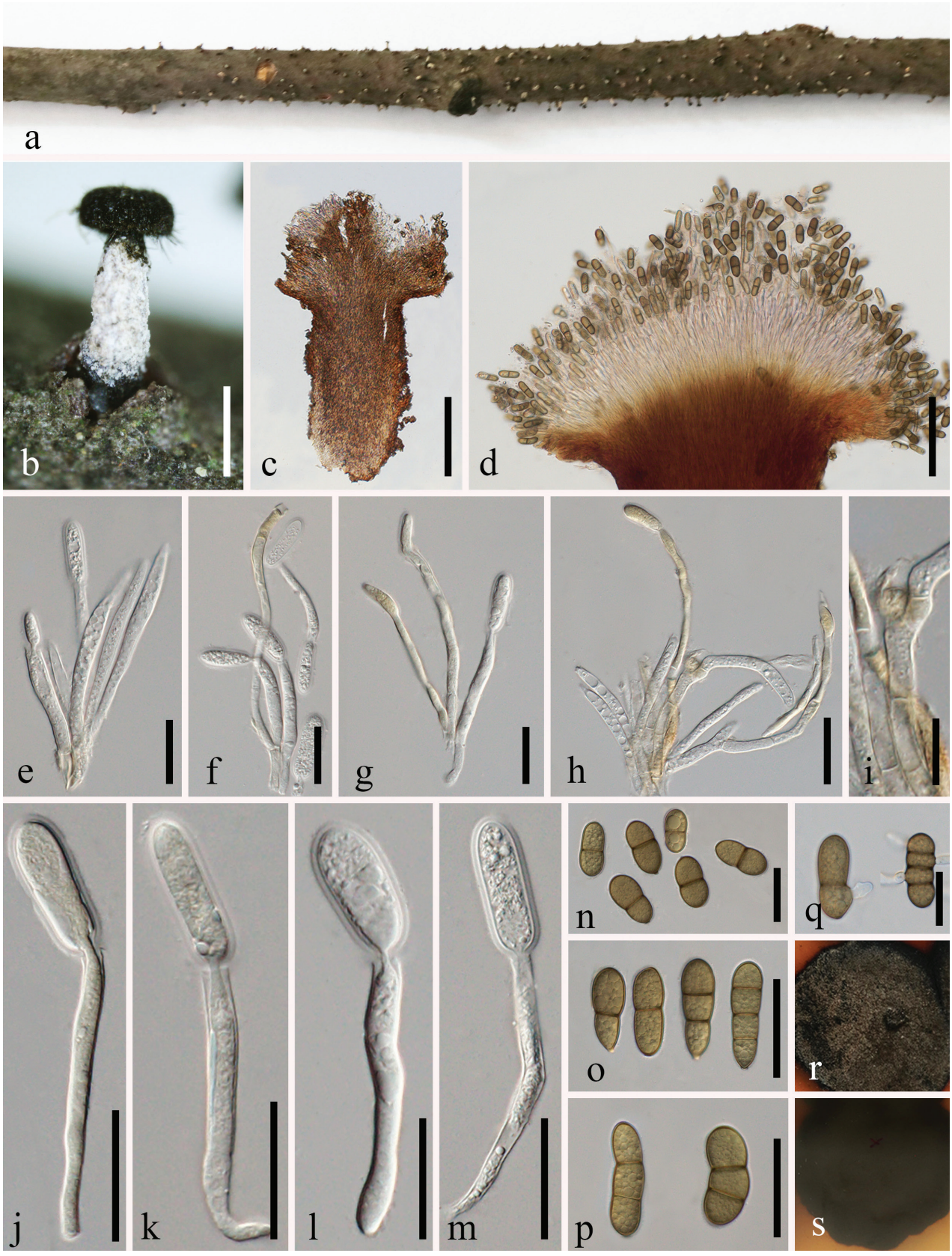

Figure 6. *Synnemasporella fanii* (MHCU 23-0271, holotype) **a, b** habit of synnemata on branches **c, d** longitudinal section of synnemata **e–h** conidiophores and conidiogenous cells **i** conidiophores showing septa **j–m** conidiogenous cells. **n–p** conidia **q** germinating conidia **r, s** colony on PDA (**r** above **s** below). Scale bars: 2 mm (**b**); 300 µm (**c**); 400 µm (**d**); 10 µm (**e, h**); 20 µm (**f, g**); 15 µm (**i**); 25 µm (**j–m, q**); 30 µm (**n–p**).

Table 6. Comparison of morphological characteristics of *Synnemasporella* species.

Morphological character	Species name and reference		
	***Synnemasporella aculeans* (Fan et al. 2018)**	***S. fanii* (This study)**	***S. toxicodendri* (Fan et al. 2018)**
Synnemata	1100–1500 µm high, 200–400 µm diam., pale to brown, straight to curved, parallel	1000–1300 µm high, 110–360 µm diam., long and determinate, pale to brown, straight, occasionally curved, parallel	1200–1800 µm high, 150–300 µm diam., pale to brown, straight to curved, parallel
Conidiophores	20–30 µm, aggregated, aseptate, straight to curved	30–70 µm long, 4.5–6.5 µm wide, aggregated, septate, straight to curved	20–30 µm, aggregated, aseptate, straight to curved
Conidiogenous cells	Cylindrical, hyaline	Cylindrical, hyaline, enteroblastic, straight to curved	Cylindrical, hyaline
Conidia	8–10(–11) × 3–3.5 µm, oblong-cylindrical, aseptate	23–37 × 11–17 µm, cylindrical to oblong-cylindrical, 1–3 septate, slightly curved	6–8 × 2.5–4 µm, cylindrical to oblong-cylindrical, aseptate
Culture characters	Regular edge; texture initially uniform, producing concentric circle on the margin after 3 days	Irregular edge, circular, initially white, becoming sepia on the bottom after one week	Irregular edge; texture initially uniform, producing concentric circles after 3 weeks

Discussion

Zhujiangyuan Nature Reserve in Yunnan Province, China, harbours a large number of native evergreen and deciduous plant species and we predict this region has higher fungal diversity, although many are yet to be discovered (Feng and Yang 2018; Luo et al. 2018; Dai et al. 2019, 2022; Wijayawardene et al. 2021, 2022c). Wijayawardene et al. (2022b) emphasized the importance of collecting materials from under-studied geographical locations as even, some extensively studied hosts could still harbour novel taxa. A few saprobic fungal taxa have been discovered on woody litter in the Zhujiangyuan Nature Reserve but leaf litter inhabiting fungi have been poorly studied in this region. Besides, less attention has been given to saprobic fungi on woody litter in riverine habitats. Thus, a comprehensive study of microfungi in this region is most warranted. Further, morphology-based taxonomic information and phylogenetic sequencing data are needed to clarify their correct taxonomy, phylogeny, and functional biodiversity.

Taxa of Didymosphaeriaceae are often reported as endophytic, pathogenic or saprobic on a wide range of plant hosts (Gonçalves et al. 2019; Hongsanan et al. 2020). Based on the morphology, and phylogenetic analyses, taxa of Didymosphaeriaceae were fairly well-studied and currently, 33 genera have been accepted in Didymosphaeriaceae (Wijayawardene et al. 2022a). However, more new taxa are waiting to be discovered from monotypic genera such as *Barria* Z.Q. Yuan, *Cylindroaseptospora* Jayasiri, E.B.G. Jones & K.D. Hyde, *Kalmusibambusa* Phook., Tennakoon, Thambug. & K.D. Hyde, *Lineostroma* H.J. Swart, *Neptunomyces* M. Gonçalves, T. Vicente & A. Alves, *Vicosamyces* Firmino, A.R. Machado & O.L. Pereira, and *Xenocamarosporium* Crous & M.J. Wingf. In this study, we introduced a novel species of *Spegazzinia*, *viz., S. zhujiangyuanensis* (ZHKUCC 23-1020 (ex-type) and GMBCC1002). Morphologically, our new collections show somewhat similar micro-morphological characters to *S. jinghaensis* (with indistinguishable conidiomata, conidiogenous cells and conidiophores of α conidia), but can be separated by its conidiophores of β conidia). Phylogenetically, our new strains *S. zhujiangyuanensis* (ZHKUCC 23-1020 (ex-type) and GMBCC1002) were grouped as the sister clade to *S. jinghaensis* (KUMCC 21-0495 (ex-type) and KMUCC 21-0496), with distinct, high statistical values (94% ML bootstrap

and 1.00 PP) (Fig. 1). Therefore, based on morphological characteristics and phylogenetic evidence (Fig. 1; based on ITS, LSU, SSU, and *tef*1-α regions), we introduce *Spegazzinia zhujiangyuanensis* as a new species.

Phaeoseptaceae was introduced by Hyde et al. (2018) to accommodate *Phaeoseptum* (type genus), *Lignosphaeria* Boonmee, Thambug. & K.D. Hyde, and *Neolophiostoma* Boonmee & K.D. Hyde. Currently, Phaeoseptaceae comprises only two genera, i.e. *Phaeoseptum* and *Pleopunctum* N.G. Liu, K.D. Hyde & J.K. Liu (Wijayawardene et al. 2022a). In this study, we introduce a novel species of *Phaeoseptum* (Phaeoseptaceae), *viz.*, *P. zhujiangyuanense*, which shares similar characteristics with *P. mali* and *P. manglicola* in their ascomata, asci and ascospore, and their overlapping dimensions, which fit the characters of *Phaeoseptum* well. However, based on morphological differences (Table 5) and phylogenetic analyses (Fig. 2), our collection can be distinguished from the other known species. Thus, we introduced *P. zhujiangyuanense* as a novel species in *Phaeoseptum*.

Synnemasporellaceae was introduced by Fan et al. (2018) to accommodate the genus *Synnemasporella*. The genus was reported with its both asexual and sexual morphs. The asexual morphs of type species of *Synnemasporella*, *S. toxicodendri* was reported with both coelomycetous and hyphomycetous morphs on the same host material (Fan et al. 2018). However, the second species, *S. aculeans* was reported only with a hyphomycetous morph. However, both species of this genus were not mentioned with the form of conidiogenous cells. In this study, our new species, *S. fanii* is found with only a hyphomycetous morph, which fits well with the characteristics of *Synnemasporella*. *Synnemasporella fanii* shares similarities with *S. toxicodendri* and *S. aculeans* in their synnemata but it can be significantly distinguished by their large-sized, 1–3-septate conidia, and possible enteroblastic conidiogenous cells. *Synnemasporella* is abundant as a hyphomycetous morph but further collections are essential to confirm this assumption.

Acknowledgments

The authors would like to thank Dr. Shaun Pennycook and Prof. Jayarama D. Bhat for their advice on nomenclature and taxonomy respectively.

Additional information

Conflict of interest

The authors have declared that no competing interests exist.

Ethical statement

No ethical statement was reported.

Funding

The authors are grateful to High-Level Talent Recruitment Plan of Yunnan Provinces ("Young Talents" Program and "High-End Foreign Experts" Program), Mee-mann Chang Academician Workstation in Yunnan Province, (Grant No. 202205AF150002), and Science and technology plan project of Science and Technology Department of Yunnan Province (Grant No. 202305AC350252, 20210BA070001-076) for support. This work

was supported by the Key Laboratory of Yunnan Provincial Department of Education of the Deep-Time Evolution on Biodiversity from the Origion of the Pearl River. Jaturong and Nakarin thank Chiang Mai University for partially support. The authors extend their appreciation to the Researchers supporting Project Number (RSPD2024R741) King Saud University, Riyadh, Saudi Arabia.

Author contributions

Data curation: LHH. Funding acquisition: AME. Project administration: IMM, QL. Writing – original draft: GQZ. Writing – review and editing: NNW, JK, NS, CC, DQD.

Author ORCIDs

Gui-Qing Zhang https://orcid.org/0000-0001-5354-0607
Nalin N. Wijayawardene https://orcid.org/0000-0003-0522-5498
Li-Hong Han https://orcid.org/0000-0002-6127-0915
Jaturong Kumla https://orcid.org/0000-0002-3673-6541
Nakarin Suwannarach https://orcid.org/0000-0002-2653-1913
Qiang Li https://orcid.org/0000-0002-9735-8214
Abdallah M. Elgorban https://orcid.org/0000-0003-3664-7853
Ihab M. Moussa https://orcid.org/0000-0001-9050-2079
Claudia Coleine https://orcid.org/0000-0002-9289-6179
Dong-Qin Dai https://orcid.org/0000-0001-8935-8807

Data availability

All of the data that support the findings of this study are available in the main text.

References

Dadachova E, Bryan RA, Huang X, Moadel T, Schweitzer AD, Aisen P, Nosanchuk JD, Casadevall A (2007) Ionizing radiation changes the electronic properties of melanin and enhances the growth of melanized fungi. PLoS One 2(5): 457. https://doi.org/10.1371/journal.pone.0000457

Dai DQ, Wijayawardene NN, Tang LZ, Liu C, Han LH, Chu HL, Wang HB, Liao CF, Yang EF, Xu RF, Li YM, Hyde KD, Bhat JD, Cannon PF (2019) *Rubroshiraia* gennova second hypocrellin-producing genus in Shiraiaceae (Pleosporales). MycoKeys 58: 1–26. https://doi.org/10.3897/mycokeys.58.36723

Dai DQ, Wijayawardene NN, Dayarathne MC, Kumla J, Han LS, Zhang GQ, Zhang X, Zhang TT, Chen HH (2022) Taxonomic and Phylogenetic Characterizations Reveal Four New Species, Two New Asexual Morph Reports, and Six New Country Records of Bambusicolous *Roussoella* from China. Journal of Fungi (Basel, Switzerland) 8(5): 532. https://doi.org/10.3390/jof8050532

Doilom M, Hyde KD, Dong W, Liao CF, Suwannarach N, Lumyong S (2021) The plant family Asteraceae is a cache for novel fungal diversity: Novel species and genera with remarkable ascospores in Leptosphaeriaceae. Frontiers in Microbiology 12: 660261. https://doi.org/10.3389/fmicb.2021.660261

Fan XL, Bezerra JD, Tian CM, Crous PW (2018) Families and genera of diaporthalean fungi associated with canker and dieback of tree hosts. Persoonia 40(1): 119–134. https://doi.org/10.3767/persoonia.2018.40.05

Feng B, Yang Z (2018) Studies on diversity of higher fungi in Yunnan southwestern China: A review. Plant Diversity 40(4): 165–171. https://doi.org/10.1016/j.pld.2018.07.001

Glez-Peña D, Gómez-Blanco D, Reboiro-Jato M, Fdez-Riverola F, Posada D (2010) ALTER: Program-oriented conversion of DNA and protein alignments. Nucleic Acids Research 38: 14–18. https://doi.org/10.1093/nar/gkq321

Gonçalves MF, Vicente TF, Esteves AC, Alves A (2019) *Neptunomyces aureus* gen. sp. nov. (Didymosphaeriaceae, Pleosporales) isolated from algae in Ria de Aveiro, Portugal. MycoKeys 60: 31–44. https://doi.org/10.3897/mycokeys.60.37931

Guo T, Tang WJ, Luo Y, Sun Q (2023) Impact Assessment of the Power Transmission and TransformationProject on the Biodiversity of the Provincial Nature Reserveof the Pearl River Source. Forest Investigation Design 52(3): 52–56+84.

Hall T (2004) BioEdit. Ibis Therapeutics, Carlsbad, CA, 92008, USA. http://www.mbio.ncsu.edu/BioEdit/bioedit.html [18 Mar 2005]

Hawksworth DL, Lücking R (2017) Fungal diversity revisited: 2.2 to 3.8 million species. Microbiology spectrum 5(4): 1–17. https://doi.org/10.1128/microbiolspec.FUNK-0052-2016

Hongsanan S, Hyde KD, Phookamsak R, Wanasinghe DN, McKenzie EHC, Sarma VV, Lücking R, Boonmee S, Bhat DJ, Liu NG, Tennakoon DS, Pem D, Karunarathna A, Jiang SH, Jones EBG, Phillips AJL, Manawasinghe IS, Tibpromma S, Jayasiri SC, Sandamali D, Jayawardena RS, Wijayawardene NN, Ekanayaka AH, Jeewon R, Lu YZ, Phukhamsakda C, Dissanayake AJ, Zeng XY, Luo ZL, Tian Q, Thambugala KM, Dai DQ, Samarakoon MC, Chethana KWT, Ertz D, Doilom M, Liu JK, Pérez-Ortega S, Suija A, Senwanna C, Wijesinghe SN, Konta S, Niranjan M, Zhang SN, Ariyawansa HA, Jiang HB, Zhang JF, Norphanphoun C, de Silva NI, Thiyagaraja V, Zhang H, Bezerra JDP, Miranda-González R, Aptroot A, Kashiwadani H, Harishchandra D, Sérusiaux E, Abeywickrama PD, Bao DF, Devadatha B, Wu HX, Moon KH, Gueidan C, Schumm F, Bundhun D, Mapook A, Monkai J, Chomnunti P, Suetrong S, Chaiwan N, Bhunjun CS, Dayarathne MC, Yang J, Rathnayaka AR, Xu J, Zheng J, Liu G, Feng Y, Xie N (2020) Refned families of Dothideomycetes: Orders and families incertae. Fungal Diversity 105: 17–318. https://doi.org/10.1007/s13225-020-00462-6

Huelsenbeck JP, Ronquist F (2001) MRBAYES: Bayesian inference of phylogenetic trees. Bioinformatics (Oxford, England) 17(8): 754–755. https://doi.org/10.1093/bioinformatics/17.8.754

Hyde KD, Fröhlich J, Taylor JE (1998) Fungi from palms XXXVI Reflections on unitunicate ascomycetes with apiospores. Sydowia 50: 21–80.

Hyde KD, Chaiwan N, Norphanphoun C, Boonmee S, Camporesi E, Chethana KWT, Dayarathne MC, de Silva NI, Dissanayake AJ, Ekanayaka AH, Hongsanan S, Huang SK, Jayasiri SC, Jayawardena RS, Jiang HB, Karunarathna A, Lin CG, Liu JK, Liu NG, Lu YZ, Luo ZL, Maharachchimbura SSN, Manawasinghe IS, Pem D, Perera RH, Phukhamsakda C, Samarakoon MC, Senwanna C, Shang QJ, Tennakoon DS, Thambugala KM, Tibpromma S, Wanasinghe DN, Xiao YP, Yang J, Zeng XY, Zhang JF, Zhang SN, Bulgakov TS, Bhat DJ, Cheewangkoon R, Goh TK, Jones EBG, Kang JC, Jeewon R, Liu ZY, Lumyong S, Kuo CH, McKenzie EHC, Wen TC, Yan JY, Zhao Q (2018) Mycosphere notes 169–224. Mycosphere: Journal of Fungal Biology 9(2): 271–430. https://doi.org/10.5943/mycosphere/9/2/8

Jiang HB, Phookamsak R, Hyde KD, Mortimer PE, Xu JC, Kakumyan P, Kumla J (2021) A taxonomic appraisal of bambusicolous fungi in Occultibambusaceae (Pleosporales, Dothideomycetes) with new collections from Yunnan Province, China. Life (Basel, Switzerland) 11(9): 932. https://doi.org/10.3390/life11090932

Katoh K, Standley DM (2013) MAFFT multiple sequence alignment software version 7: Improvements in performance and usability. Molecular Biology and Evolution 30(4): 772–780. https://doi.org/10.1093/molbev/mst010

Liu Y, Whelen S, Hall B (1999) Phylogenetic relationships among Ascomycetes: Evidence from an RNA polymerse II subunit. Molecular Biology and Evolution 16(12): 1799–1808. https://doi.org/10.1093/oxfordjournals.molbev.a026092

Luo Z, Hyde KD, Bhat DJ, Jeewon R, Maharachchikumbura SSN, Bao DF, Li WL, Su XJ, Yang XY, Su HY (2018) Morphological and molecular taxonomy of novel species Pleurotheciaceae from freshwater habitats in Yunnan China. Mycological Progress 17(5): 511–530. https://doi.org/10.1007/s11557-018-1377-6

Ma H, Song Z, Pan X, Li Y, Yang Z, Qu Z (2022) Multi-Gene Phylogeny and Taxonomy of Hypoxylon (Hypoxylaceae, Ascomycota) from China. Diversity 14(1): 37. https://doi.org/10.3390/d14010037

Maharachchikumbura SS, Hyde KD, Jones EBG, McKenzie EHC, Huang SK, Abdel-Wahab MA, Daranagama DA, Dayarathne M, Dsouza MJ, Goonasekara ID, Hongsanan S, Jayawardena RS, Kirk PM, Konta S, Liu JK, Liu ZY, Norphanphoun C, Pang KL, Perera RH, Senanayake IC, Shang Q, Shenoy BD, Xiao YP, Bahkali AH, Kang JC, Somrothipol S, Suetrong S, Wen TC, Xu JC (2015) Towards a natural classification and backbone tree for Sordariomycetes. Fungal Diversity 72(1): 199–301. https://doi.org/10.1007/s13225-015-0331-z

Miller MA, Pfeiffer W, Schwartz T (2010) Creating the CIPRES Science Gateway for inference of large phylogenetic trees. 2010 Gateway Computing Environments Workshop (GCE). New Orleans, LA, USA, 1–8. https://doi.org/10.1109/GCE.2010.5676129

Mueller GM, Schmit JP (2007) Fungal biodiversity: What do we know? What can we predict? Biodiversity and Conservation 16(1): 1–5. https://doi.org/10.1007/s10531-006-9117-7

Naranjo-Ortiz MA, Gabaldón T (2019) Fungal evolution: Major ecological adaptations and evolutionary transitions. Biological Reviews of the Cambridge Philosophical Society 94(4): 1443–1476. https://doi.org/10.1111/brv.12510

Niskanen T, Lücking R, Dahlberg A, Gaya E, Suz LM, Mikryukov V, Liimatainen K, Druzhinina I, Westrip JR, Mueller GM, Martins-Cunha K, Kirk P, Tedersoo L, Antonelli A (2023) Pushing the frontiers of biodiversity research: Unveiling the global diversity, distribution, and conservation of fungi. Annual Review of Environment and Resources 48(1): 149–176. https://doi.org/10.1146/annurev-environ-112621-090937

Nylander JAA (2004) MrModeltest 2.0. Program distributed by the author. Evolutionary Biology Centre, Uppsala University.

Phukhamsakda C, Jeewon R, McKenzie EHC, Xu JC (2019) Morphology and phylogeny of *Phaeoseptum mali* sp. nov. (Phaeoseptaceae, Pleosporales) on bark of *Malus halliana*. Asian Journal of Mycology 2(1): 118–128. https://doi.org/10.5943/ajom/2/1/6

Raghukumar C, Raghukumar S (1998) Barotolerance of fungi isolated from deep-sea sediments of the Indian Ocean. Aquatic Microbial Ecology 15(2): 153–163. https://doi.org/10.3354/ame015153

Rambaut A (2006) FigTree. Tree drawing tool version 1.4.0. University of Edinburgh: Institute of Evolutionary Biology. http://tree.bio.ed.ac.uk/software/figtree/

Rannala B, Yang Z (1996) Probability distribution of molecular evolutionary trees: a new method of phylogenetic inference. Journal of molecular evolution 43: 304–311. https://doi.org/10.1007/BF02338839

Rehner SA, Buckley E (2005) A Beauveria Phylogeny Inferred from Nuclear ITS and EF1-α Sequences: Evidence for Cryptic Diversification and Links to Cordyceps Teleomorphs. Mycologia 97(1): 84–98. https://doi.org/10.3852/mycologia.97.1.84

Richards TA, Leonard GU, Wideman JG (2017) What defines the "kingdom" fungi? The Fungal Kingdom: 57–77. https://doi.org/10.1128/9781555819583.ch3

Ronquist F, Huelsenbeck JP (2003) MrBayes 3: Bayesian phylogenetic inference under mixed models. Bioinformatics (Oxford, England) 19(12): 1572–1574. https://doi.org/10.1093/bioinformatics/btg180

Saccardo PA (1880) Fungi Dalmatici pauci ex herb. illustr. R. de Visiani addito uno alterove mycete ex Anglia et Pannonia. Michelia 2(6): 154–176. https://doi.org/10.1017/S0376892900001247

Saccardo PA (1886) Sylloge Hyphomycetum. Sylloge Fungorum 4: 1–807. https://www.biodiversitylibrary.org/item/25421#page/9/mode/1up

Samarakoon BC, Phookamsak R, Wanasinghe DN, Chomnunti P, Hyde KD, McKenzie EHC, Promputtha I, Xu JC, Li YJ (2020) Taxonomy and phylogenetic appraisal of *Spegazzinia musae* sp. nov and *S. deightonii* (Didymosphaeriaceae Pleosporales) on Musaceae from Thailand. MycoKeys 70: 19–37. https://doi.org/10.3897/mycokeys.70.52043

Senanayake IC, Rathnayaka AR, Marasinghe DS, Calabon MS, Gentekaki E, Wanasinghe DN, Lee HB, Hurdeal VG, Pem D, Dissanayake LS, Wijesinghe SN, Bundhun D, Nguyen TT, Goonasekara ID, Abeywickrama PD, Bhunjun CS, Chomnunti P, Boonmee S, Jayawardena RS, Wijayawardene NN, Doilom M, Jeewon R, Bhat JD, Zhang HX, Xie N (2020) Morphological approaches in studying fungi: Collection, examination, isolation, sporulation and preservation. Mycosphere: Journal of Fungal Biology 11(1): 2678–2754. https://doi.org/10.5943/mycosphere/11/1/20

Species Fungorum (2024) Species Fungorum-Search Page.

Tamura K, Stecher G, Peterson D, Filipski A, Kumar S (2013) MEGA6: Molecular evolutionary genetics analysis version 6.0. Molecular Biology and Evolution 30(12): 2725–2729. https://doi.org/10.1093/molbev/mst197

Tanaka K, Hirayama K, Yonezawa H, Sato G, Toriyabe A, Kudo H, Hashimoto A, Matsumura M, Harada Y, Kurihara Y, Shirouzu T, Hosoya T (2015) Revision of the Massarineae (Pleosporales, Dothideomycetes). Studies in Mycology 82(1): 75–136. https://doi.org/10.1016/j.simyco.2015.10.002

Vilgalys R, Hester M (1990) Rapid genetic identification and mapping of enzymatically amplified ribosomal DNA from several *Cryptococcus* species. Journal of Bacteriology 172(8): 4238–4246. https://doi.org/10.1128/jb.172.8.4238-4246.1990

Wang JF (2014) Research on the Development of Tourism Industry in the Area of Pearl River Sources. Journal of Qujing Normal University 33(02): 6–10.

Wang DL, Wu YM, Gao WJ (2015) Study on the Evolution of Rural Habitat in the Zhujiangyuan Nature reserve. Journal of Anhui Agriculture 43(23): 207–210.

White TJ, Bruns T, Lee S, Taylor J (1990) Amplification and direct sequencing of fungal ribosomal RNA genes for phylogenetics. In: Innis MA, Gelfand DH, Sninsky JJ, White TJ (Eds) PCR Protocols: A guide to methods and applications. Academic Press, San Diego, 315–322. https://doi.org/10.1016/B978-0-12-372180-8.50042-1

Wijayawardene NN, Dissanayake LS, Dai DQ, Xiao YP, Wen TC, Karunarathna SC, Wu HX, Zhang H, Tibpromma S, Kang JC, Wang Y, Shen XC, Tang LZ, Deng CY, Liu YX, Kang YQ (2021) Yunnan–Guizhou Plateau: A mycological hotspot. Phytotaxa 523(1): 1–31. https://doi.org/10.11646/phytotaxa.523.1.1

Wijayawardene NN, Hyde KD, Dai DQ, Sánchez-García M, Goto BT, Saxena RK, Erdoğdu M, Selçuk F, Rajeshkumar KC, Aptroot A, Błaszkowski J, Boonyuen N, da Silva GA, de Souza FA, Dong W, Ertz D, Haelewaters D, Jones EBG, Karunarathna SC, Kirk PM, Kukwa M, Kumla J, Leontyev DV, Lumbsch HT, Maharachchikumbura SSN, Marguno F, Martínez-Rodríguez P, Mešić A, Monteiro JS, Oehl F, Pawłowska J, Pem D, Pfiegler WP, Phillips AJL, Pošta A, He MQ, Li JX, Raza M, Sruthi OP, Suetrong S, Suwannarach N, Tedersoo L, Thiyagaraja V, Tibpromma S, Tkalčec Z, Tokarev YS, Wanasinghe DN,

Wijesundara DSA, Wimalaseana SDMK, Madrid H, Zhang GQ, Gao Y, Sánchez-Castro I, Tang LZ, Stadler M, Yurkov A, Thines M (2022a) Outline of Fungi and fungus-like taxa–2021. Mycosphere: Journal of Fungal Biology 13(1): 53–453. https://doi.org/10.5943/mycosphere/13/1/2

Wijayawardene NN, Phillips AJL, Pereira DS, Dai DQ, Aptroot A, Monteiro JS, Druzhinina IS, Cai F, Fan XL, Selbmann L, Coleine C, Castañeda-Ruiz RF, Kukwa M, Flakus A, Fiuza PO, Kirk PM, Kumar KCR, Arachchi ISL, Suwannarach N, Tang LZ, Boekhout T, Tan CSH, Jayasinghe RPPK, Thines M (2022b) Forecasting the number of species of asexually reproducing fungi (Ascomycota and Basidiomycota). Fungal Diversity 114(1): 463–490. https://doi.org/10.1007/s13225-022-00500-5

Wijayawardene NN, Dai DQ, Zhu ML, Wanasinghe DN, Kumla J, Zhang GQ, Zhang TT, Han LS, Tibpromma S, Chen HH (2022c) Fungi associated with dead branches of Magnolia grandiflora: A case study from Qujing, China. Frontiers in Microbiology 13: 954680. https://doi.org/10.3389/fmicb.2022.954680

Zhang Y, Fournier J, Phookamsak R, Bahkali AH, Hyde KD (2013) Halotthiaceae fam. nov. (Pleosporales) accommodates the new genus *Phaeoseptum* and several other aquatic genera. Mycologia 105(3): 603–609. https://doi.org/10.3852/11-286

Zhaxybayeva O, Gogarten JP (2002) Bootstrap, Bayesian probability and maximum likelihood mapping: Exploring new tools for comparative genome analyses. BMC Genomics 3(1): 4. https://doi.org/10.1186/1471-2164-3-4

MycoKeys 106: 201–224 (2024)
DOI: 10.3897/mycokeys.106.125831

Research Article

Morphological characteristics and phylogenetic analyses revealed four new wood inhabiting fungi (Agaricomycetes, Basidiomycota) in Xizang Autonomous Region, China

Hong-Min Zhou[1,2], Xun-Chi Zhang[2], Jie-Ting Li[3], Fang Wu[4], Chang-Lin Zhao[1,2]

1 *The Key Laboratory of Forest Resources Conservation and Utilization in the Southwest Mountains of China Ministry of Education, Key Laboratory of National Forestry and Grassland Administration on Biodiversity Conservation in Southwest China, Yunnan Provincial Key Laboratory for Conservation and Utilization of In-forest Resource, Southwest Forestry University, Kunming 650224, China*
2 *College of Forestry, Southwest Forestry University, Kunming 650224, China*
3 *Key Laboratory of Forest Ecology in Tibet Plateau, Ministry of Education, Institute of Tibet Plateau Ecology, Tibet Agricultural & Animal Husbandry University, Nyingchi, Tibet 860000, China*
4 *Institute of Microbiology, School of Ecology and Nature Conservation, Beijing Forestry University, Beijing 100083, China*

Corresponding authors: Chang-Lin Zhao (fungichanglinz@163.com); Fang Wu (fangwubjfu2014@yahoo.com)

Abstract

Four new fungi from Xizang in southwest China, *Calocera ramaria*, *Ceraceomyces rhizomorphus*, *Leptosporomyces linzhiensis*, and *Ramaria xizangensis* are described and illustrated based on the morphological and molecular evidence. *Calocera ramaria* is characterized by the ramal and bright orange basidiomata, a monomitic hyphal system with simple septa generative hyphae, usually 4-septate basidiospores; *Ceraceomyces rhizomorphus* is characterized by the cream to yellowish basidiomata with rhizomorphs, cylindrical basidiospores; *Leptosporomyces linzhiensis* is characterized by white with pink basidiomata, cylindrical to oblong ellipsoid basidiospores; *Ramaria xizangensis* is characterized by flesh pink basidiomata, branched dichotomously in 4–5 ranks, a monomitic hyphal system with clamped generative hyphae, ellipsoid to cylindrical and densely warted basidiospores.

Key words: Molecular systematic, phylogenetic analysis, taxonomy, wood-decaying fungi

This article is part of:
Diversity, taxonomy, and systematics of macrofungi from tropical Asia
Edited by Olivier Raspé, Rui-Lin Zhao, Jennifer Luangsa-ard

Academic editor: Rui-Lin Zhao
Received: 20 April 2024
Accepted: 27 May 2024
Published: 25 June 2024

Citation: Zhou H-M, Zhang X-C, Li J-T, Wu F, Zhao C-L (2024) Morphological characteristics and phylogenetic analyses revealed four new wood inhabiting fungi (Agaricomycetes, Basidiomycota) in Xizang Autonomous Region, China. MycoKeys 106: 201–224. https://doi.org/10.3897/mycokeys.106.125831

Introduction

The fruiting bodies of Basidiomycota exhibit complex forms, such as gilled, poroid, toothed, coralloid basidiomata. Numerous taxonomists have endeavored to construct a stable classification system based on these characters (Gäumann 1953). Recently, the analysis of DNA sequences has emerged as a common method for deducing fungal phylogenies and enhancing higher classification frameworks through the integration of genetic traits (Cui et al. 2019; Wijayawardene et al. 2020; Liu et al. 2023).

The abundance of biodiversity in *Abies* forests can be attributed to the plentiful presence of humus and mycorrhizal fungi, which foster an optimal environment for the proliferation of the macrofungal species. Information regarding the fungal diversity in *Abies* communities is scattered over a range of publications

(Ryvarden and Gilbertson 1993; Dai 2022). *Ceraceomyces* Jülich, a small genus characterized by yellow rhizomorphic basidiomata, was established by Jülich based on the taxon *C. tessulatus* (Cooke) Jülich (Jülich 1972). This genus, originally from North America, features annual, resupinate, pellicular basidiomata with a smooth or merulioid hymenial surface, a monomitic hyphal system, narrowly clavate basidia, and subglobose, narrowly ovate, ellipsoid to cylindrical basidiospores (Chikowski et al. 2016). Phylogenetic studies revealed that *Ceraceomyces* was polyphyletic, comprising three distinct groups. The section of *Corticium tessulatum* Cooke belonged to Polyporales, and *Ceraceomyces serpens* (Tode) Ginns and *C. eludens* K.H. Larss. were part of phlebioid clade (Larsson et al. 2004). A recent study indicated that the type species, *Corticium tessulatum* is classified under the order Amylocorticiales (Binder et al. 2010; Chikowski et al. 2016), as well as species, *C. yunnanensis* Qi Yuan & C.L. Zhao and *C. borealis* (Romell) J. Erikss. & Ryvarden (Yuan et al. 2023). Currently, eleven species are recognized in the genus *Ceraceomyces*, including *C. cystidiatus* (J. Erikss. & Hjortstam) Hjortstam, *C. eludens*, *C. microsporus* K.H. Larss. and *C. sublaevis* (Bres.) Jülich were accepted in the genus. A genus, *Crystallicutis* El-Gharabawy, Leal-Dutra & G.W. Griff. was derived from *Ceraceomyces* based on the crystals in the hymenium and subiculum of the basidiomata, which includes the brown-rot species *C. serpens* (El-Gharabawy et al. 2021). Both species *C. sulphurinus* and *C. violascens* (Fr.) Jscens were recorded in *Ceraceomyces*, are considered congeneric with *Rhizochaete* Gresl., Nakasone & Rajchenb. due to the characteristics like the rhizomorphic margin and the purple reaction in KOH.

Calocera (Fr.) Fr. is known for its distinctive characteristics, stipitate, fasciculate or scattered, gelatinous basidiomata, dendroid or staghorn-like, subclavate to clavate basidia and probasidia, as well as cylindrical to reniform, septate or non-septate basidiospores (Fisher 1931; Lowy 1971; Peng et al. 1992; Wu et al. 2011; Shirouzu et al. 2017). Recent phylogenetic analyses of the class Dacrymycetes demonstrated that *Calocera* was polyphyletic and species in the genus are scattered throughout the family Dacrymycetaceae together with most of the species of *Dacrymyces* Nees (1817: 89) as well as a few species from other genera such as *Dacryopinax* G.W. Martin (1948: 116) and *Femsjonia* Fr. (Shirouzu et al. 2007; Zamora and Ekman 2020).

The genus *Leptosporomyces* Jülich is characterized by the resupinate basidiomata, white yellow and smooth hymenial surface, a monomitic hyphal system with clamped connections, and thin-wall, smooth, acyanophilous basidiospores. Recent research has indicated that *Leptosporomyces* was polyphyletic, with two taxa, *L. galzinii* (Bourdot) Jülich and *L. raunkiaeri* (M.P. Christ.) Jülich, grouped in the order Atheliales, while *L. septentrionalis* (J. Erikss.) Krieglst. was placed in the order Amylocorticiales (Larsson 2007; Hodkinson et al. 2014; Sulistyo et al. 2021). The generic delimitation of *Fibulomyces* Jülich and *Leptosporomyces* remains controversial, with both being indistinguishable in phylogenetic and morphological analyses, leading to the former being considered as a synonym of the latter (Bernicchia and Gorjón 2010).

Ramaria Fr. ex Bonord. is a widely distributed non-gilled Basidiomycete genus (Marr and Stuntz 1973; Petersen 1981; Humpert et al. 2001). The genus is recognized by branched basidiomata, mono- to dimitic hyphal systems with clamped or simple-septate generative hyphae, and smooth to echinulate,

verrucose-reticulate or striate ornamentation basidiospores (Corner 1950; Marr and Stuntz 1973; Petersen 1981; Humpert et al. 2001). The genus has been classified into four subgenera, namely *R.* subg. *Ramaria*, *R.* subg. *Laeticolora* Marr & D.E. Stuntz, *R.* subg. *Lentoramaria* Corner, and *R.* subg. *Echinoramaria* Corner (Marr and Stuntz 1973; Humpert et al. 2001; Exeter et al. 2006; Knudson 2012; Hanif et al. 2019). Initially, *Ramaria* was treated as a subgenus within *Clavaria* (Coker 1923; Doty 1944) until Corner (1970) elevated it to genus rank. Studies based on the morphological and molecular data agree on the paraphyletic state of *Ramaria* (Humpert et al. 2001; Hosaka et al. 2006; Giachini et al. 2010).

In the present paper, species from four genera are collected from Xizang under forest of *Abies*, and the phylogenetic relationships of four taxa are still unclear. Thus, to explore the diversity and taxonomic status with different characters for those taxa will be significant for macrofungi in Xizang, and the taxonomy and phylogeny analysis show that they are new to science.

Material and method

The specimens were collected from Xizang which were deposited in the herbarium of the Southwest Forestry University (SWFC), Kunming, Yunnan Province, China. Samples were photographed when fresh in the field, and their habitats were recorded. Microscopic structures were discussed by Zhao et al. (2023). Special color terms were set by Anonymous (1969) and Petersen (1996). A Nikon Digital Sight DS-L3 or Leica ICC50 HD camera (magnification ×1,000) was used to exam hand-cut sections of basidiomata, which were first treated with 5% KOH for a few minutes and then with 1% phloxine B ($C_{20}H_4Br_4Cl_2K_2O_5$). At least 30 basidiospores of each species were examined. The values were expressed as a mean with 5% of the measurements excluded from each end of the range, given in parentheses. Stalks were excluded for basidia measurement, and the hilar appendages were excluded for basidiospore measurement.

DNA extraction, amplification, and sequencing

The CTAB rapid plant genome extraction kit-DN14 (Aidlab Biotechnologies Co., Ltd., Beijing) was used to obtain DNA from dried specimens and PCR was performed according to the manufacturer's instructions with some modifications (Yang et al. 2023). ITS were amplified using the primer pairs ITS5/ITS4 (White et al. 1990). The PCR procedure for ITS was as follows: initial denaturation at 95 °C for 3 min, followed by 35 cycles at 94 °C for 40 s, 54 °C for 45 s, and 72 °C for 1 min; and a final extension at 72 °C for 10 min. The PCR procedure for LSU was as follows: initial denaturation at 94 °C for 1 min, followed by 35 cycles at 94 °C for 30 s, 50 °C for 1 min, and 72 °C for 1.5 min; and a final extension at 72 °C for 10 min. All newly generated sequences were submitted to GenBank and are listed in Table 1.

Sequences generated for this study were aligned, with additional sequences downloaded from GenBank. Sequences were aligned using MAFFT v.7 (https://mafft.cbrc.jp/alignment/server/), adjusting the direction of nucleotide sequences according to the first sequence (accurate enough for most cases), and selecting the G-INS-i iterative refinement method (Katoh et al. 2019). Alignments were

Table 1. Taxa information and the sequences used in this study. *Newly generated sequences for this study.

Species	Locality	Voucher	ITS	LSU
Amyloathelia crassiuscula	Sweden	GB/K169-796	DQ144610	–
Amylocorticium cebennense	USA	HHB-2808	GU187505	GU187561
Amylocorticium subincarnatum	Sweden	GB/AS-95	AY463377	AY586628
Amylocorticium subsulphureum	USA	HHB-13817	GU187506	GU187562
Anomoporia bombycina	USA	CFMR L-6240	GU187508	GU187611
Anomoporia vesiculosa	China	Dai 22795	ON413718	ON413720
Athelia abscondita	USA	Goyette 633	OP877120	OP902328
Athelopsis subinconspicua	Sweden	GB0058732	LR694197	LR694174
Bondarzewia occidentalis	Canada	AFTOL-ID 452	DQ200923	DQ234539
Byssocorticium caeruleum	Canada	RS 09400 (H)	NR_121454	–
Calocera bambusicola	China	Wu 9910-12	FJ195751	–
Calocera cornea	Sweden	UPS F 940775	MN595627	MN595627
Calocera cornea	Unknown	AFTOL ID 438	AY789083	AY701526
Calocera cornea	Sweden	UPS F 940774	MN595626	MN595626
Calocera cornea	Canada	CBS 124.84	AB712437	AB472738
Calocera guepinioides	New Zealand	PDD 107969	LC131411	LC131370
Calocera guepinioides	New Zealand	PDD 107981	LC131412	LC131371
Calocera guepinioides	New Zealand	PDD 105005	LC131407	LC131366
Calocera guepinioides	New Zealand	PDD 107874	LC131409	LC131368
Calocera guepinioides	New Zealand	PDD 105033	LC131408	LC131367
Calocera guepinioides	New Zealand	PDD 107929	LC131410	LC131369
Calocera lutea	New Zealand	PDD 107841	LC131413	LC131372
Calocera lutea	New Zealand	PDD 107842	LC131414	LC131373
Calocera palmata	New Zealand	PDD 107830	LC131415	LC131374
Calocera palmata	New Zealand	PDD 107925	LC131416	LC131375
Calocera palmata	Japan	CBS 127.51	MH856777	MH868295
Calocera ramaria	China	CLZhao 31166	**PP399147**	**PP862915**
Calocera sinensis	China	MHHNU30743	MK167408	–
Calocera sinensis	China	Wu 0505-3	FJ195753	–
Calocera sinensis	China	Wu 0703-6	FJ195754	–
Calocera sinensis	China	JCH 070726	FJ195755	–
Calocera tibetica	China	Dai 20171	MW549777	MW750403
Calocera tibetica	China	Dai 20178	MW549778	MW750404
Calocera viscosa s.lat.	Sweden	UPS F-940773	MN595628	MN595628
Calocera viscosa s.lat.	Germany	FTOL ID1679	DQ520102	DQ520102
Ceraceomyces americanus	USA	FP-102188	KP135409	KP135277
Ceraceomyces atlanticus	Brazil	URM 85888	NR_153926	NG_060427
Ceraceomyces atlanticus	China	M67	OR766067	KX685874
Ceraceomyces borealis	Sweden	KHL 8432	EU118610	–
Ceraceomyces eludens	Sweden	JS 27108	AF090879	–
Ceraceomyces eludens	Sweden	JS 22780	AF090877	–
Ceraceomyces eludens	United Kingdom	KM 194563	OR907143	–
Ceraceomyces microsporus	USA	UC 2023077	KP814418	–
Ceraceomyces microsporus	Sweden	JS 27153	AF090873	–
Ceraceomyces rhizomorphus	China	CLZhao 31154	**PP399151**	–
Ceraceomyces rhizomorphus	China	CLZhao 31161	**PP399148**	–
Ceraceomyces rhizomorphus	China	CLZhao 31188	**PP399149**	**PP862917**
Ceraceomyces rhizomorphus	China	CLZhao 31197	**PP399150**	**PP862916**
Ceraceomyces sublaevis	USA	FP-101245-Sp	KP135029	GU187607
Ceraceomyces tessulatus	USA	MPN 152885038	OR680647	–
Ceraceomyces tessulatus	Sweden	KHL 16429	KU518951	–
Ceraceomyces yunnanensis	China	CLZhao 18992	OQ132519	OQ147003
Clavariadelphus amplus	China	HMAS 250466	MK705858	MK704448
Coniophora marmorata	Belgium	MUCL: 31667	GU187515	GU187571
Dacrymyces longistipitatus	New Zealand	PDD 107996	LC131425	LC131386
Dacrymyces pachysporus	New Zealand	PDD 105004	LC131429	LC131392

Species	Locality	Voucher	ITS	LSU
Dacrymyces parastenosporus	New Zealand	PDD104960	LC131431	LC131394
Dacrymyces stillatus	Sweden	UPS F-939814	MN595676	MN595676
Dacrymyces subalpinus	Japan	TUFC12834	AB712465	AB299060
Dacryonaema macnabbii	Sweden	UPS F-940949	MN595650	MN595650
Dacryonaema macnabbii	Sweden	UPS F-940951	MN595651	MN595651
Dacryonaema macrosporum	Norway	O 160045	MN595659	MN595659
Dacryonaema macrosporum	Finland	UPS F-940998	MN595660	MN595660
Dacryonaema rufum	Sweden	UPS F-941003	MN595645	MN595645
Dacryonaema rufum	Sweden	UPS F-941005	MN595646	MN595646
Dendrdacrys brasiliense	Brazil	INPA:241458	AB744230	AB723514
Dendrdacrys dendrocalami	Japan	TUFC 13914	AB712453	AB712428
Fibulomyces mutabilis	Germany	HG-B 5753 (GB)	GQ162817	–
Ganoderma resinaceum	Unknown	C45	KX371982	KX372027
Gautieria parksiana	USA	SNF 236 USA	AF377059	–
Gloeocantharellus neoechinosporus	China	GDGM 75321	MK358820	MK358815
Go. ludovicianus	USA	TFB 14476	KJ655570	KJ655580
Gomphus clavatus	Spain	MA-Fungi 48085	AJ292292	–
Hypochniciellum subillaqueatum	Sweden	KHL 8493	AY463431	AY586679
Hypochniciellum subillaqueatum	UK	KM165142	MZ159402	–
Kavinia himantia	USA	CFMR: DLL2011-079	KJ140598	–
Kavinia alboviridis	USA	CFMR: DLL2011-131	KJ140634	–
Lentaria micheneri	USA	RRD6 (TENN)	MF773634	–
Lactarius sp.	New Zealand	PDD:113066	MW683864	MW683691
Lentaria byssiseda	USA	TENN 61159	FJ596788	–
Leptosporomyces fuscostratus	USA	UC 2022884	KP814350	–
Leptosporomyces fuscostratus	Unknown	DK 16_251	OL436970	–
Leptosporomyces galzinii	Sweden	GB 0107211	LR694202	LR694180
Leptosporomyces galzinii	USA	UC 2023126	KP814291	–
Leptosporomyces linzhiensis	China	CLZhao 31174	**PP399152**	**PP862922**
Leptosporomyces linzhiensis	China	CLZhao 31183	**PP399153**	**PP862918**
Leptosporomyces linzhiensis	China	CLZhao 31187	**PP399154**	–
Leptosporomyces linzhiensis	China	CLZhao 31190	**PP399155**	–
Leptosporomyces raunkiaeri	USA	UC 2023053	KP814293	–
Leptosporomyces raunkiaeri	USA	CFMR: HHB-7628	GU187528	GU187588
Leptosporomyces septentrionalis	USA	UC 2023047	KP814348	–
Leptosporomyces septentrionalis	Sweden	GB 0090937	LR694203	LR694181
Leptosporomyces septentrionalis	Norway	JS 16122	GU187497	–
Lobulicium occultum	Sweden	KHL13496b	MT340827	–
Mythicomyces corneipes	Unknown	AFTOL-972	DQ404393	AY745707
Phaeoclavulina flaccida	Italy	AMB n. 17671	MK796107	MK796156
Phlebiella christiansenii	Finland	KHL 11689	EU118659	–
Phlebiella vaga	Sweden	KHL 11065	EU118660	EU118661
Piloderma fallax	Finland	CFMR: S-12	GU187535	–
Plicaturopsis crispa	China	LWZ 20201017-11	ON897938	ON885398
Plicaturopsis crispa	Brazil	URM 85888	NR_153926	NG_060427
Ramaria abietina	USA	u066	KY510818	–
Ramaria acrisiccescens	USA	OSC 112057	KY354738	KY354711
Ramaria admiratia	USA	TENN: 69114	NR_137862	NG_059504
Ramaria amyloidea	USA	OSC 69891	EU837196	KP637036
Ramaria apiculata var. *brunnea*	USA	CBS:149.74	MH860840	MH872577
Ramaria araiospora	Germany	OSC 108707	EU846298	–
Ramaria aurantiisiccescens	USA	OSC 104868	EU837197	–
Ramaria aurea	Italy	AMB 18352	MN637783	MN637796
Ramaria botrytis	Italy	AMB n. 18201	NR_189799	NG_241889
Ramaria botrytis	Argentina	GM 19044	OP177707	OP177871
Ramaria botrytis	USA	snf213	AF377055	–
Ramaria botrytis f. *musicolor*	Italy	ZT Myc 57160	KY626144	–
Ramaria botrytis var. *aurantiiramosa*	USA	OSC 140667	JX310410	–

Species	Locality	Voucher	ITS	LSU
Ramaria botrytis var. *aurantiiramosa*	USA	WTU-F-043053	KX574471	–
Ramaria celerivirescens	USA	OSC 140471	JX310392	JX269125
Ramaria claviramulata	USA	WTU-F-043055	KX574472	KX671009
Ramaria conjunctipes	USA	OSC: 110613	KC346861	–
Ramaria coulterae	USA	OSC 69929	EU669320	EU669320
Ramaria dendrophora	Argentina	GM 20020	OP177716	OP177880
Ramaria dendrophora	Argentina	GM 19094	OP177715	OP177879
Ramaria fennica	Italy	AMB n. 17522	MK682678	–
Ramaria flavescens	Italy	AMB 17404	KY354743	–
Ramaria flavescens	Italy	AMB 17404	MK493036	–
Ramaria flava	Italy	AMB 17393	MK493035	–
Ramaria flavinedulis	Argentina	GM 19056	OP177717	OP177881
Ramaria flavinedulis	Argentina	GM 19035	OP177720	OP177884
Ramaria flavobrunnescens var. *aromatica*	USA	AGK 059	JQ408240	–
Ramaria foetida	USA	AGK 058	JQ408239	JQ408239
Ramaria formosa	USA	OSC1064203	EU525994	–
Ramaria fumosiavellanea	USA	WTU-F-063048	MK169345	–
Ramaria gelatiniaurantia	USA	OSC 65737	KP658144	–
Ramaria inedulis	Chile	12648	OP177723	OP177887
Ramaria inedulis	Argentina	GM 19047	OP177722	OP177886
Ramaria largentii	USA	OSC 67012	KP658130	KP637058
Ramaria luteovernalis	Italy	MCVE 28637	NR_155720	KT357477
Ramaria maculatipes	USA	OSC 112051	KY354749	KY354721
Ramaria magnipes	USA	WTU-F-063057	MK169351	MK493050
Ramaria myceliosa	USA	AGK 035	JQ408230	–
Ramaria obtusissima	USA	TFB 14473	KJ655554	KJ655575
Ramaria patagonica	Argentina	403	OP177710	OP177874
Ramaria patagonica	Argentina	GM 19106	OP177713	OP177877
Ramaria pseudoflava	Italy	AMB 17392	MK493046	–
Ramaria rasilisporoides	Pakistan	MH-2013	MG760613	–
Ramaria rasilisporoides	USA	WTU-F-043029	MK169346	–
Ramaria rubella	USA	OSC 115946	EU669317	EU669343
Ramaria rubella f. *rubella*	USA	AGK 049	JQ408236	–
Ramaria rubribrunnescens	USA	OSC 119676	EU652352	EU652387
Ramaria rubribrunnescens	USA	OSC 66051	KY354750	KY354722
Ramaria sandaracina var. *sandaracina*	Canada	UBC F28386	KP454028	–
Ramaria sp.	India	KD-14-006	KT824242	–
Ramaria stricta	Germany	CBS 165.48	MH856299	–
Ramaria stricta var. *concolor*	USA	AGK 011	JQ408221	–
Ramaria stuntzii	USA	OSC 73315	KP658122	KP637048
Ramaria subbotrytis	Spain	MA-Fungi 48088	AJ408361	–
Ramaria subtilis	Spain	MA-Fungi 48055	AF442098	–
Ramaria suecica	USA	OSC 115933	KP658148	KP637079
Ramaria testaceoflava	USA	OSC 107885	KP658128	AY586708
Ramaria verlotensis	USA	WTU-F-063047	KX574480	KX671016
Ramaria xizangensis	China	CLZhao 31169	**PP399156**	**PP862919**
Ramaria xizangensis	China	CLZhao 31180	**PP399157**	**PP862920**
Ramaria xizangensis	China	CLZhao 31204	**PP399158**	**PP862921**
Ramaria formosa	Italy	AMB 18529	MT055910	MT053203
Ramaricium polyporoideum	USA	TENN: 065654	MF992160	MF992160
Stereopsis vitellina	Sweden	F 703241	LR694211	LR694189
Turbinellus floccosus	USA	MO 285170	MN319564	MN319563
Unilacryma unispora	Sweden	UPS F 941268	MN595672	MN595672
Unilacryma unispora	Sweden	UPS F 941277	MN595665	MN593500
Xenasmatella ardosiaca	Costa Rica	KHL 12928	EU118658	–
Xenasmatella ardosiaca	USA	CBS 126045	MH864060	MH875515

manually adjusted to maximize alignment and minimize gaps with BioEdit v.7.0.9 (Hall 1999). A dataset of concatenated ITS and LSU sequences was used to determine the phylogenetic position of the new species. Maximum likelihood (ML) analysis was performed using the CIPRES Science Gateway (Miller et al. 2010) based on the dataset using the RA × ML-HPC BlackBox tool, with setting RA × ML halt bootstrapping automatically and 0.25 for maximum hours and obtaining the best tree using ML search. Other parameters in ML analysis used default settings, and statistical support values were obtained using nonparametric bootstrapping with 1,000 replicates. Bayesian inference (BI) analysis based on the dataset was performed using MrBayes v.3.2.6 (Ronquist and Huelsenbeck 2012). The best substitution model for the dataset was selected by ModelFinder (Kalyaanamoorthy et al. 2017) using a Bayesian information criterion, and the model was used for Bayesian analysis. Four Markov chains were run from random starting trees. Trees were sampled every 1,000th generation. The first 25% of sampled trees were discarded as burn-in, whereas other trees were used to construct a 50% majority consensus tree and for calculating Bayesian posterior probabilities (BPPs). The aligned sequences were deposited in TreeBase (https://www.treebase.org/treebase-web/home.html; submission ID 31437).

Branches of the consensus tree that received bootstrap support for ML were greater than or equal to 75%, Bayesian posterior probabilities more than 0.9, respectively.

Result

The Phylogeny of *Calocera*

BI analysis yielded a similar topology to MP and ML analysis. Only the MP tree is provided here (Fig. 1). Branches that received bootstrap support for ML (ML-BS), and BI (BPP) greater than or equal to 75% (MP-BS and ML-BS) and 0.90 (BPP) were considered as significantly supported, respectively. The ITS and LSU dataset contains sequences from 26 fungal specimens representing twelve *Calocera* taxa. The average SD of split frequencies in BI analyses is 0.005504 (BI). The phylogenetic tree (Fig. 1) reveals the new species has close relationship with *C. tibatica*, sister to *C. viscosa* and *C. cornea*.

The Phylogeny of *Ceraceomyces*

The dataset included ITS and LSU from 29 samples representing 22 taxa. The best model for the concatenated ITS+LSU dataset estimated and applied for BI analysis was "GTR+I+G4", datatype = DNA, nucmodel = 4by4, lset nst = 6, rates = invgamma; state frequencies had a Dirichlet prior (1,1,1,1), and the distribution was approximated using four categories. BI analysis yielded a similar topology to ML analysis, with an average standard deviation of split frequencies of 0.006593. The ML tree was provided (Fig. 2). Branches that received bootstrap support for ML and BI ≥ 70%, and 0.75 were considered significantly supported, respectively.

The analysis reveals four clades (Fig. 2), in which three European species *C. eludens*, *C. microsporus*, *C. sublaevis* clustered together and *Rhizochaete americanus* (Nakasone, C.R. Bergman & Burds.) Gresl., Nakasone & Rajchenb. The core clade formed by *C. tessulatus* and *C. atlanticus*, along with

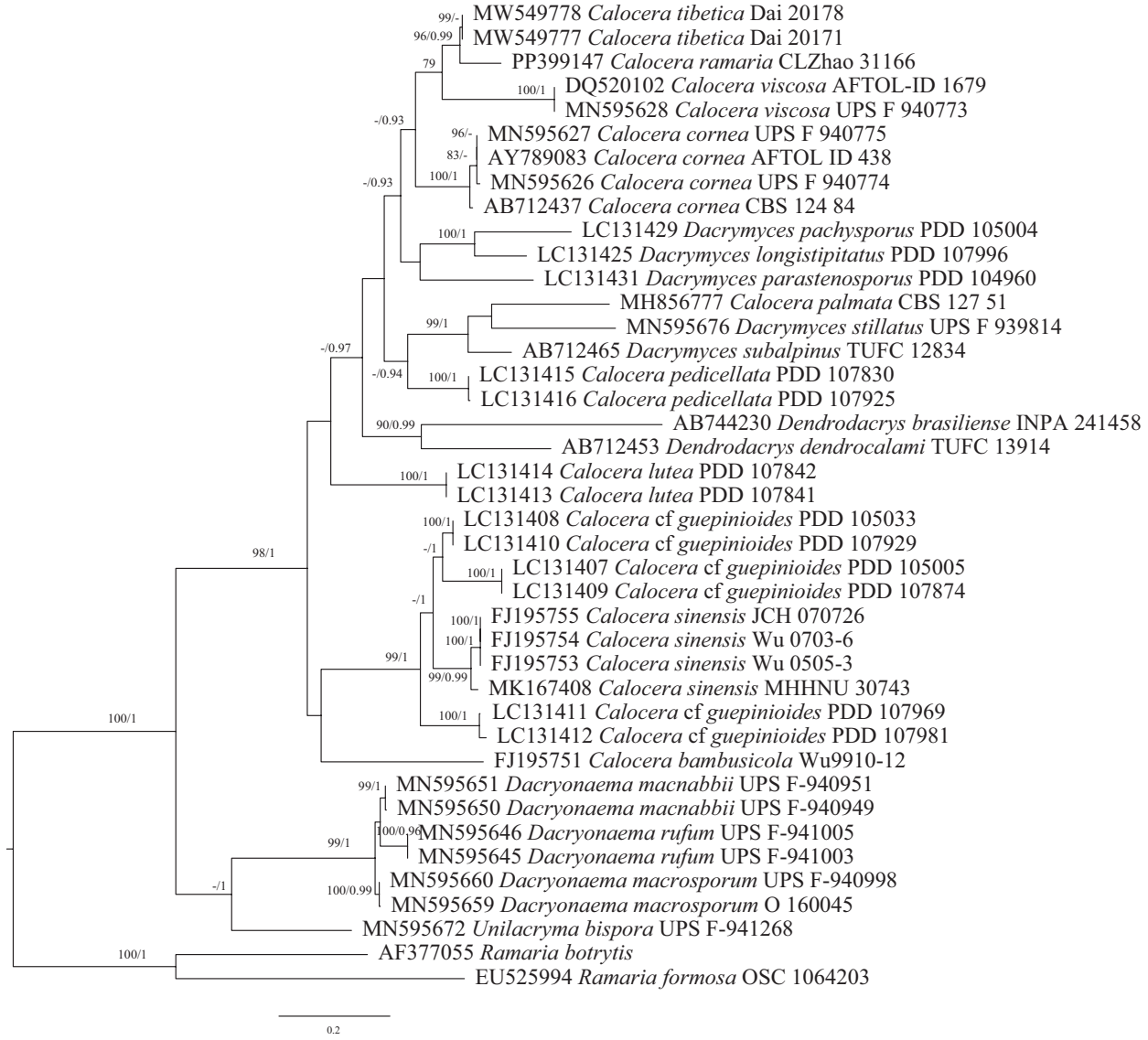

Figure 1. Phylogeny of species in *Calocera* generated by maximum likelihood based on ITS+LSU sequence data. Branches are labeled with maximum likelihood bootstrap ≥ 75% and Bayesian posterior probabilities ≥ 0.90, respectively. New species are in bold.

Hypochniciellum subillaqueatum (Litsch.) Hjortstam. Four specimens from China formed two lineages, namely *Ceraceomyces rhizomorphus* with *C. yunnanensis*, and were sister to *C. borealis*.

The Phylogeny of *Leptosporomyces*

BI analysis yielded a similar topology to MP and ML analysis, with an average standard deviation of split frequencies = 0.008841. Only the MP tree is provided here (Fig. 3). Branches that received bootstrap support for ML (ML-BS), and BI (BPP) greater than or equal to 75% (MP-BS and ML-BS) and 0.90 (BPP) were considered as significantly supported, respectively. Four previously accepted species, *L. galzinii*, *L. fuscostratus* (Jülich) Krieglst., *L. raunkiaeri*, and *L. mundus* (H.S. Jacks. & Dearden) Jülich received strong support in three lineages. The new species *L. linzhiensis* had a close relationship with *L. septentrionalis* with full support.

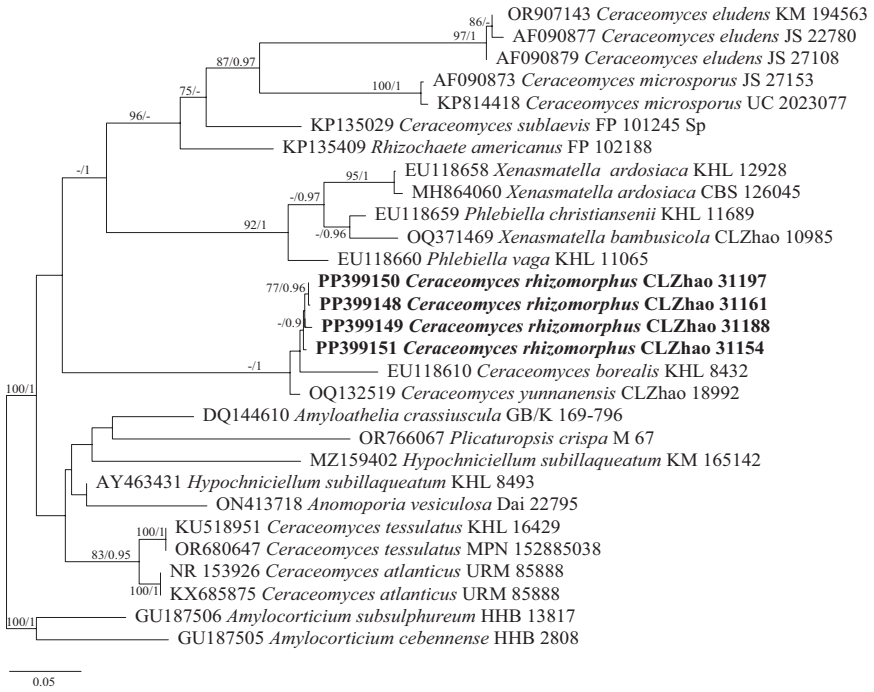

Figure 2. Phylogeny of species in *Ceraceomyces* generated by maximum likelihood based on ITS+LSU sequence data. Branches are labeled with maximum likelihood bootstrap ≥ 75% and Bayesian posterior probabilities ≥ 0.90, respectively. New species are in bold.

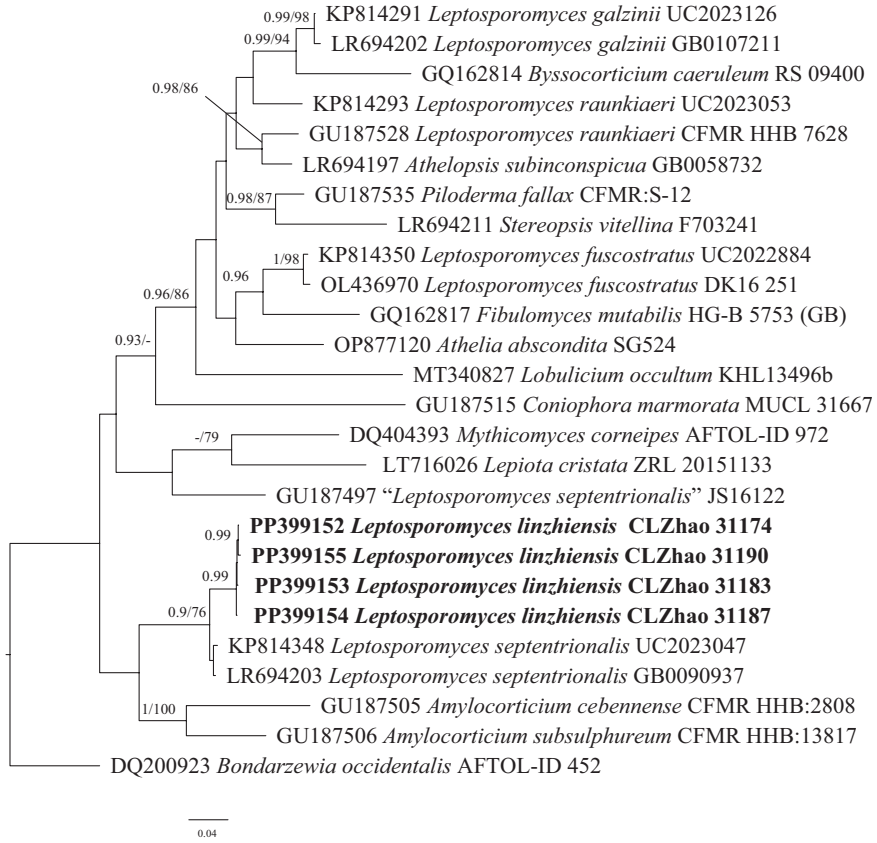

Figure 3. Phylogeny of species in *Leptosporomyces* generated by maximum likelihood based on ITS+LSU sequence data. Branches are labeled with maximum likelihood bootstrap ≥ 75% and Bayesian posterior probabilities ≥ 0.90, respectively. New species are in bold.

The Phylogeny of *Ramaria*

BI analysis yielded a similar topology to MP and ML analysis. Only the MP tree is provided here (Fig. 4). Branches that received bootstrap support for ML (ML-BS), and BI (BPP) greater than or equal to 75% (MP-BS and ML-BS) and 0.90 (BPP) were considered as significantly supported, respectively. Four clades were obtained from our phylogenetic analysis, *Ramaria* sub. *Laeticolora*, *Ramaria* Sub. *Ramaria*, *Ramaria* Sub. *Echinormaria* and *Ramaria* sub. *Lentoramaria*. The species *Ramaria xizangensis* was grouped in *Ramaria* sub. *Laeticolora* along with *R. amyloidea* Marr & D.E. Stuntz, *R. celerivescens* Marr & D.E. Stuntz, and *R. claviramulata* Marr & D.E. Stuntz.

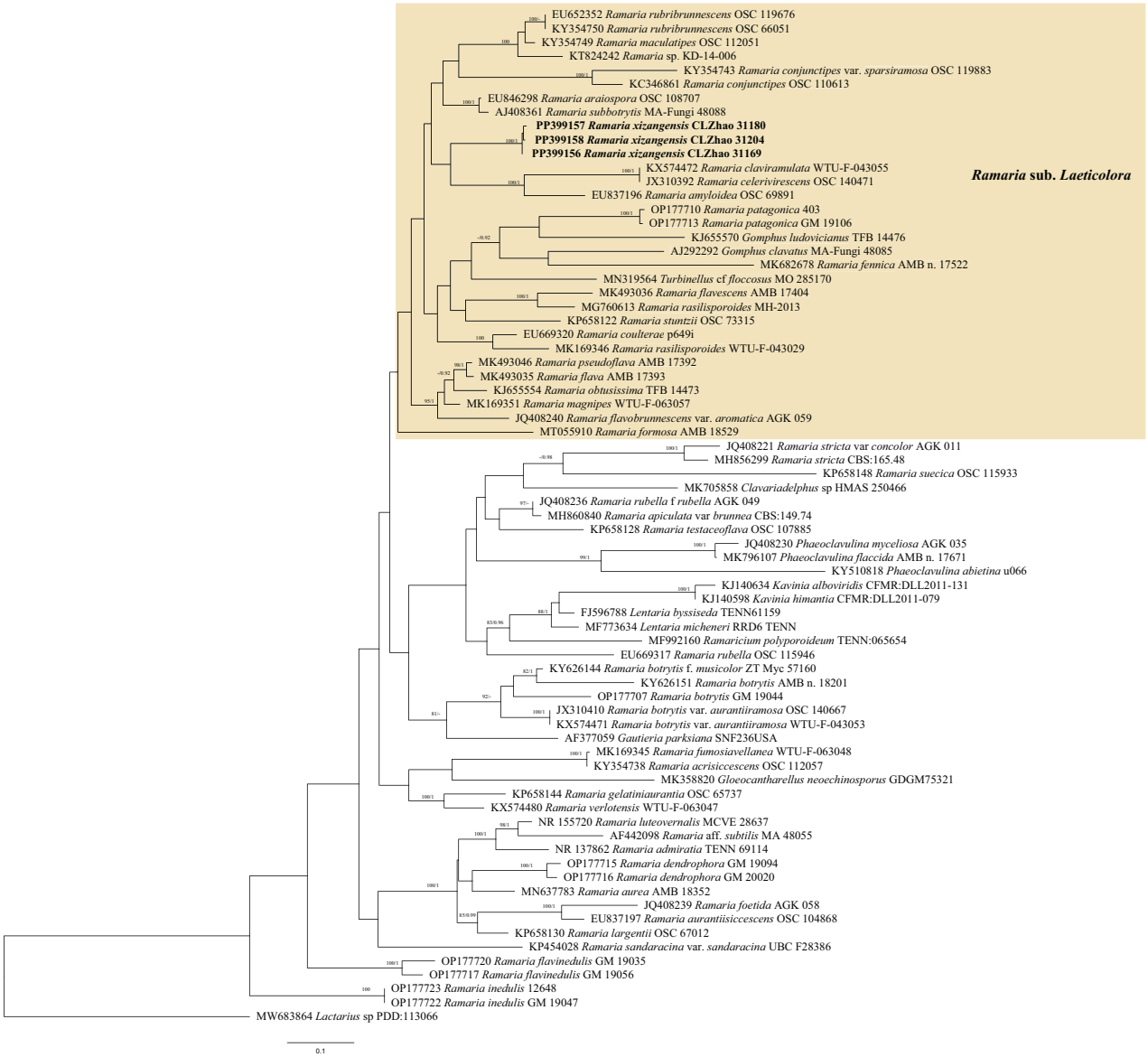

Figure 4. Phylogeny of species in the *Ramaria* generated by maximum likelihood based on ITS+LSU sequence data. Branches are labeled with maximum likelihood bootstrap ≥ 75% and Bayesian posterior probabilities ≥ 0.90, respectively. New species are in bold.

Taxonomy

Calocera ramaria **C.L. Zhao & H.M. Zhou, sp. nov.**
MycoBank No: 852565
Figs 5, 6

Holotype. China, Xizang, Linzhi, Sejila Mountain National Forest Park, 29°64'N, 94°71'E, elev. 3852 m, gregarious on humus under *Abies*, 2 August 2023, CLZhao 31166 (SWFC).

Etymology. *Ramaria* (Lat.): refers to the ramal basidiomata of the specimens.

Diagnosis. Differed from other species in having ramal basidiomata, septate hyphae, usually 4-septate basidiospores (9.2–11 × 3.9–4.4 µm).

Fruiting body. Basidiomata stipitate, gregarious, bright orange when fresh, orange brown when dry, gelatinous when soaked, corneous when dry, ramal, repeatedly branched, apically blunt, up to 6.2 cm high; stipe 0.7–1 mm in diam, become orange to reddish brown corneous when dry.

Internal features. Marginal hyphae hyaline, smooth, thin-walled, septate, simple or branched, without clamp connections, 4–5.5 µm in diam; internal hyphae hyaline, smooth or scabrous, thin- to slightly thick-walled, interwoven, with nodose-septa, without clamp connections, 2–3 µm in diam; hyphidia hyaline, smooth, thin-walled, with a simple septum at base, occasionally terminally branched; basidia hyaline, thin-walled, subclavate to clavate, without basal clamp connection, 23–31 × 2–4 µm; basidiospores hyaline, smooth, thin-walled, oblong-ellipsoid to navicular, straight or curved, apiculate, usually 4-septate when mature, occasionally 5-septate, (9.1–)9.2–11(–11.6) × (3.5–)3.9–4.4(–4.7) µm, L = 10.18 µm, W = 4.19 µm, Q = 2.43 (n = 30/1).

Ceraceomyces rhizomorphus **C.L. Zhao & H.M. Zhou, sp. nov.**
MycoBank No: 852584
Figs 7, 8

Holotype. China, Xizang, Linzhi, Sejilashan National Forest Park, 29°64'N, 94°71'E, elev. 3848 m, on the fallen branch of *Abies*, 2 August 2023, CLZhao 31188 (SWFC).

Etymology. *Rhizomorphus* (Lat.): refers to the basidiomata with rhizomorphs.

Diagnosis. Differed from other species in having merulioid, cream to yellowish basidiomata, generative hyphae with clamp connections, cylindrical basidiospores (4.7–6.2 × 1.8–2.3 µm).

Fruiting body. Basidiomata resupinate, adnate, smooth to tuberculate when fresh, merulioid upon drying, without odor or taste when fresh, up to 6 cm long, 2 cm wide, 100–200 µm thick. Hymenial surface merulioid, cream to yellowish when fresh, turn to orange yellow upon drying. Margin sterile, white, with rhizomorphs.

Hyphal structure. Hyphal system monomitic, generative hyphae with clamp connections, colorless, thin- to slightly thick-walled, branched, interwoven, 3.5–7 µm in diameter, IKI–, CB–; tissues turn black in KOH.

Hymenium. Cystidia and cystidioles absent; basidia narrowly clavate to clavate, in a dense palisade, with 4 sterigmata and a basal clamp connection,

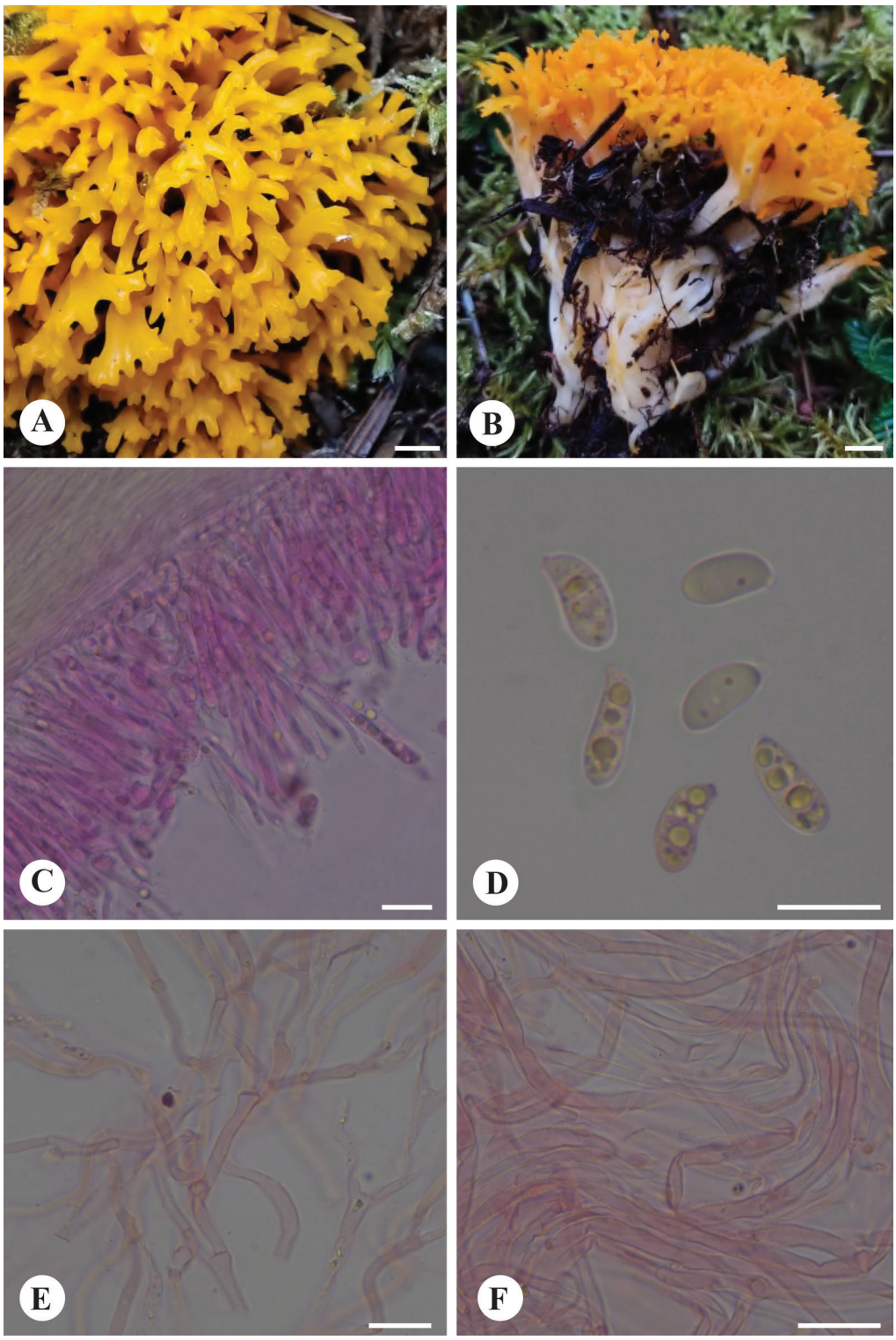

Figure 5. Basidiomata and microscopic structures of *Calocera ramaria* (holotype, CLZhao 31166, holotype) **A, B** basidiomata **C** a section of hymenium **D** basidiospores **E** marginal hyphae **F** internal hyphae. Scale bars: 1 cm (**A, B**); 10 μm (**C–F**).

16–19 × 3.5–4 μm; basidioles dominant, similar to basidia in shape, but slightly smaller.

Spores. Basidiospores cylindrical, with suprahilar depression, colorless, smooth, thin-walled, IKI–, CB–, (4.2–)4.7–6.2(–6.4) × (1.5–)1.8–2.3(–2.4) μm, L = 5.49 μm, W = 2.05 μm, Q = 2.66–2.68 (n = 60/2).

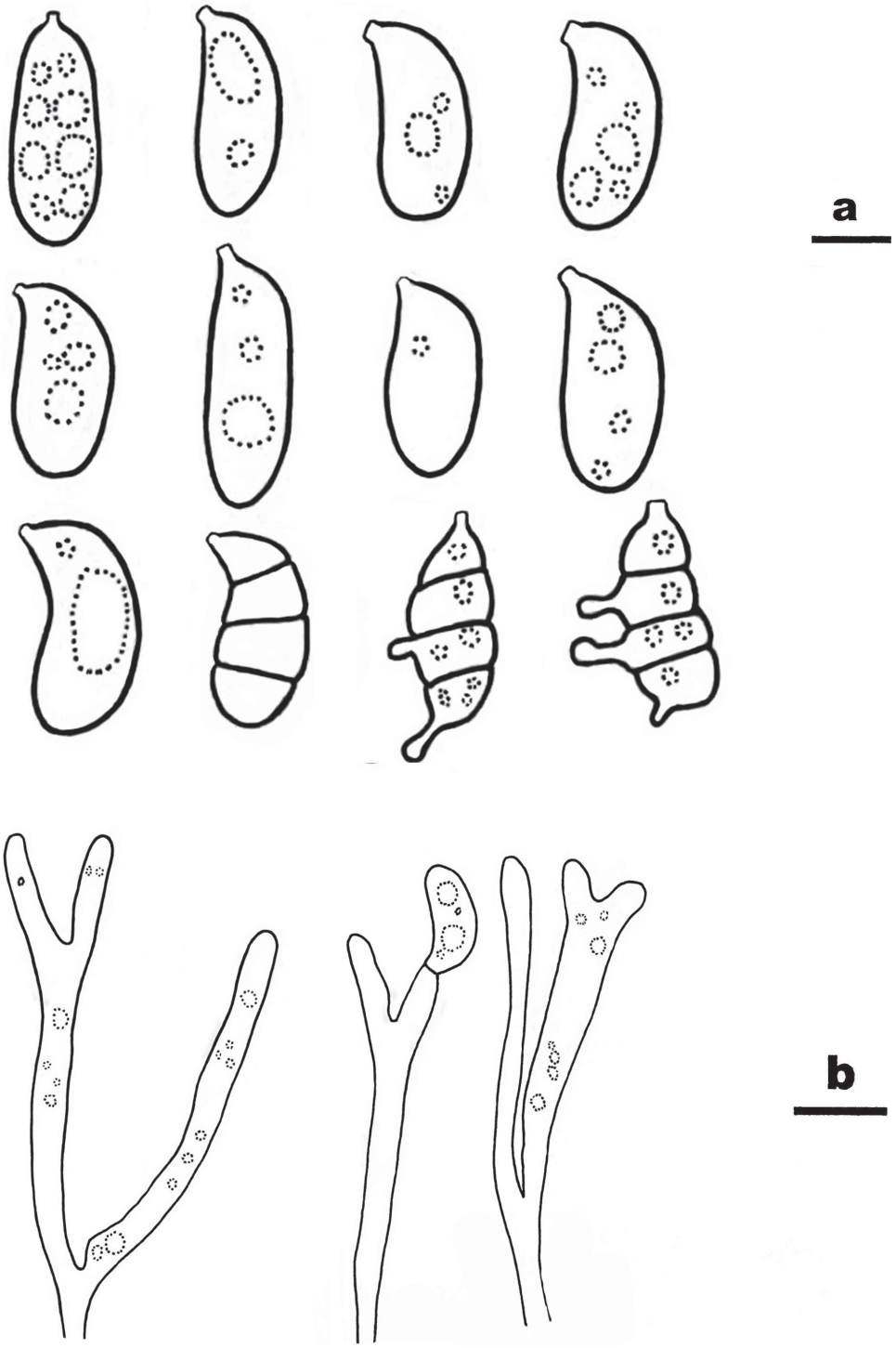

Figure 6. Microscopic structures of *Calocera ramaria* (holotype, CLZhao 31166) **a** basidiospores **b** basidia with basidiospores. Scale bars: 5 μm (**a**); 10 μm (**b**).

Additional specimens examined (*paratypes*). China. Xizang, Linzhi, Sejila Mountain National Forest Park, 29°64'N, 94°71'E, elev. 3848 m, on the trunk of *Abies*, 2 August 2023, CLZhao 31153 (SWFC); CLZhao 31154 (SWFC); CLZhao 31161 (SWFC); CLZhao 31202 (SWFC); on the fallen branch of *Abies*, 2 August 2023, CLZhao 31184 (SWFC); CLZhao 31185 (SWFC); CLZhao 31197 (SWFC).

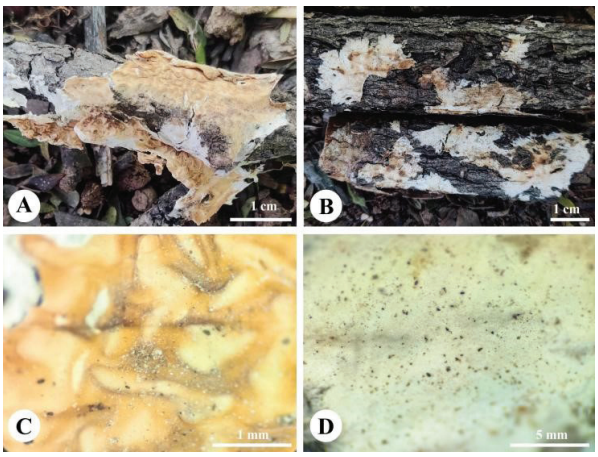

Figure 7. Basidiomata of *Ceraceomyces rhizomorphus* **A, C** CLZhao 31188 (holotype) **B, D** CLZhao 31185.

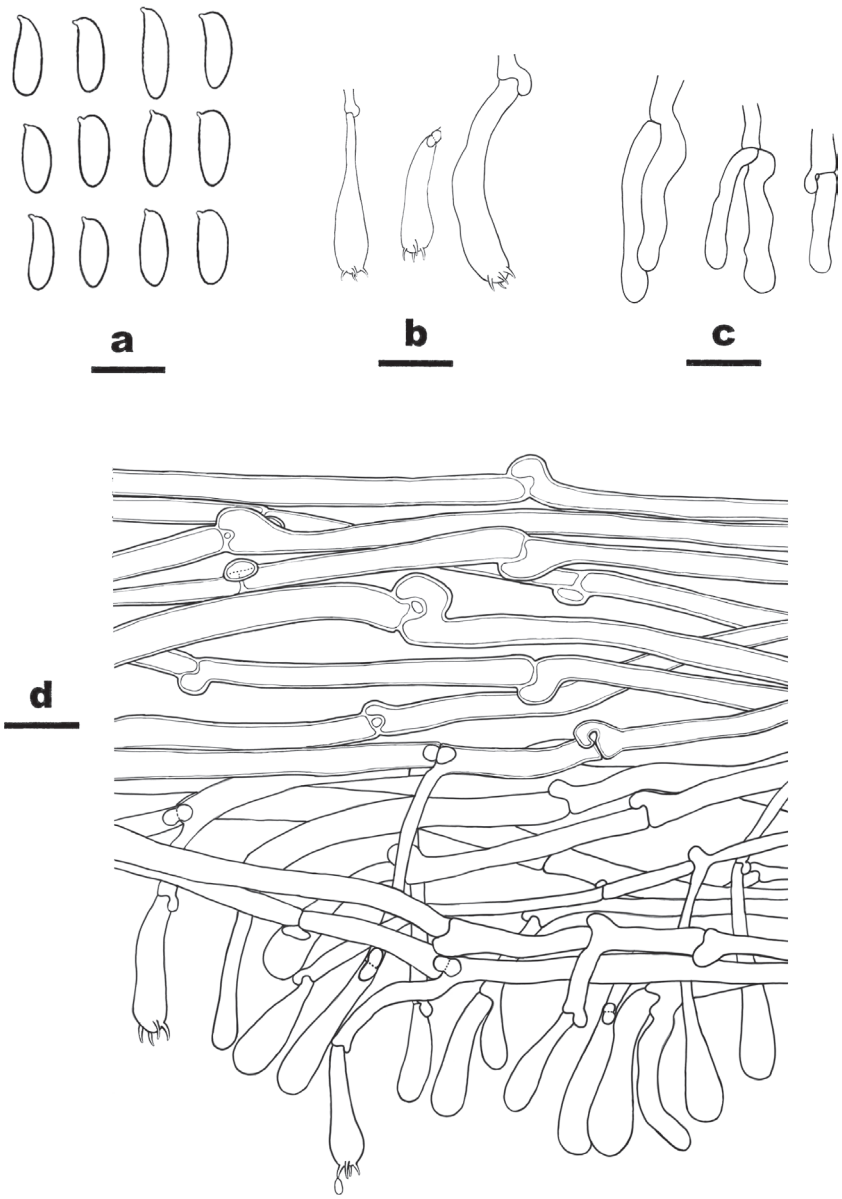

Figure 8. Microscopic structures of *Ceraceomyces rhizomorphus* (holotype, CLZhao 31216) **a** basidiospores **b** basidia **c** basidioles **d** a section of hymenium. Scale bars: 5 μm (**a**); 10 μm (**b–d**).

Leptosporomyces linzhiensis **C.L. Zhao & H.M. Zhou, sp. nov.**
MycoBank No: 852585
Figs 9, 10

Holotype. China, Xizang, Linzhi, Sjilashan Forest Park, 29°64'N, 94°71'E, elev. 3848 m, on fallen trunk of *Abies*, 2 August 2023, CLZhao 31183 (SWFC).

Etymology. *Linzhiensis* (Lat.): refers to the locality (Xizang) of the type specimens.

Diagnosis. Differed from other species in having white basidiomata, monomitic hyphal system, cylindrical to oblong ellipsoid basidiospores (3.8–4. × 1.7–2 µm).

Fruiting body. Basidiomata resupinate, athelioid, membranous upon drying, without odor or taste when fresh, up to 10 cm long, 4 cm wide, 200 µm thick. Hymenial surface smooth to cracked, white with pink tint when fresh, turning to yellowish cream upon drying. Margin sterile, white, fimbriate.

Hyphal structure. Hyphal system monomitic, generative hyphae with clamp connections, colorless, thin- to slightly thick-walled, branched, interwoven, 2–5 µm in diameter, IKI–, CB–; tissues turn black in KOH.

Hymenium. Hyphal system monomitic, generative hyphae with clamp connections, colorless, thin-walled, branched, interwoven, 2–3.5 µm in diameter, IKI–, CB–. Basidia clavate, with 4 sterigmata and a basal clamp connection, 11.5–13.5 × 3.2–3.8 µm.

Spores. Basidiospores cylindrical to oblong ellipsoid, colorless, smooth, thin-walled, IKI–, CB–, (3.5–)3.8–4.3(–4.7) × (1.7–)1.7–2(–2.3) µm, L = 4.02 µm, W = 1.88 µm, Q = 1.95–2.18 (n = 90/3).

Additional specimens examined (*paratypes*). China, Xizang, Linzhi, Sjilashan Forest Park, 22°57'N, 103°42'E, elev. 2100 m, on fallen trunk of *Abies*, 2 August 2023, CLZhao 31174 (SWFC); on fallen trunk of *Abies*, 2 August 2023, CLZhao 31187 (SWFC); on fallen trunk of *Abies*, 2 August 2023, CLZhao 31190 (SWFC).

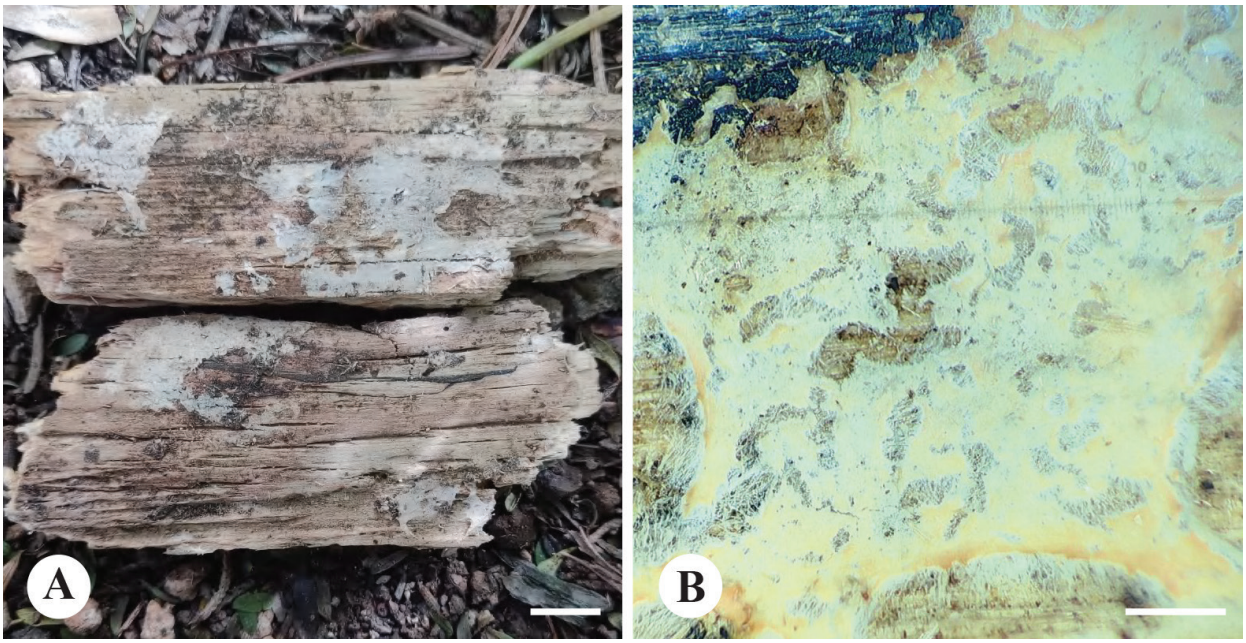

Figure 9. Basidiomata of *Leptosporomyces linzhiensis* (holotype, CLZhao 31183). Scale bars: 1 cm (**A**); 1 mm (**B**).

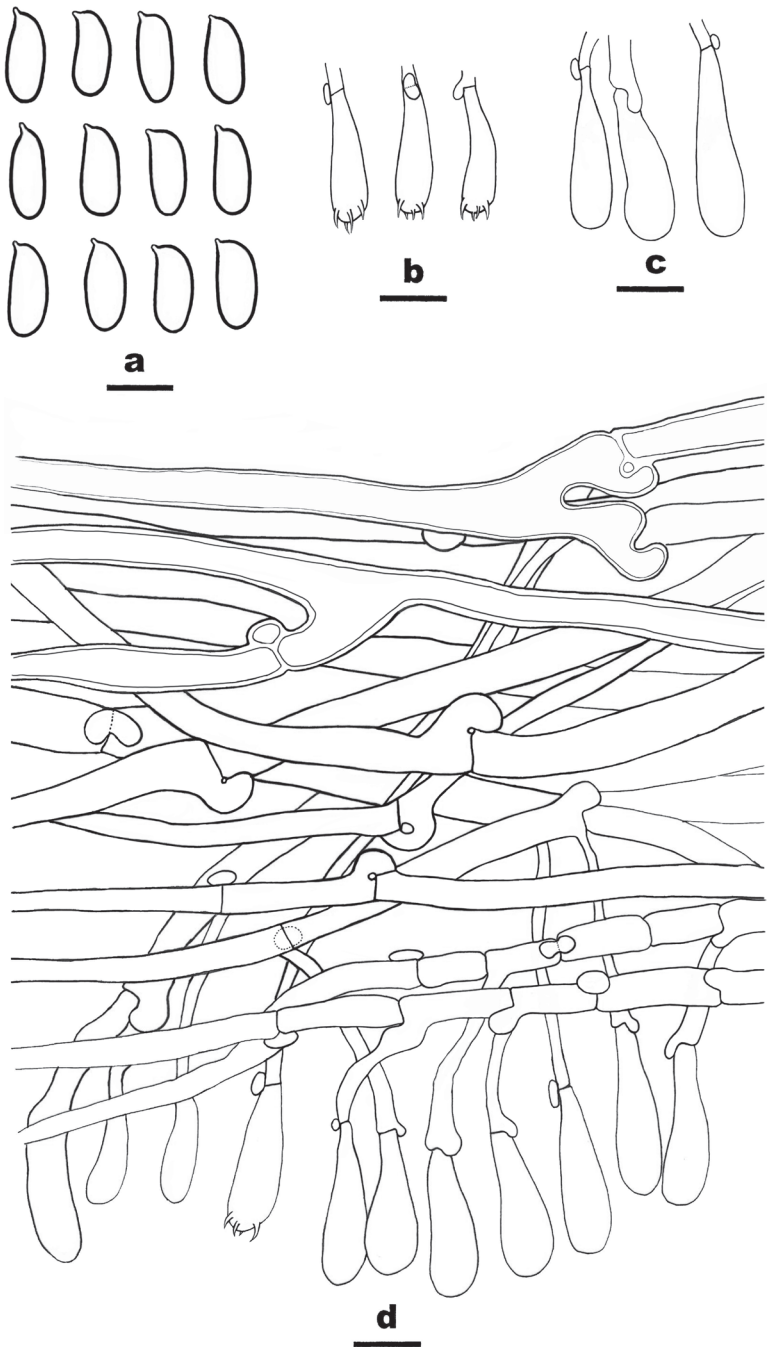

Figure 10. Microscopic structures of *Leptosporomyces linzhiensis* (holotype, CLZhao 31183) **a** basidiospores **b** basidia **c** basidioles **d** A section of hymenium. Scale bars: 5 μm (**a**); 10 μm (**b–d**).

Ramaria xizangensis **C.L. Zhao & H.M. Zhou, sp. nov.**
MycoBank No: 852586
Figs 11, 12

Holotype. China, Xizang, Linzhi, Sejila Mountain National Forest Park, 29°64'N, 94°71'E, elev. 3850 m, gregarious on the humus under *Abies*, 2 August 2023, CLZhao 31169 (SWFC).

Etymology. *Xizangensis* (Lat.): refers to the locality (Xizang) of the type specimens.

Diagnosis. Differed from other species in having flesh pink basidiomata, monomitic hyphal system, generative hyphae with clamp connections, ellipsoid to cylindrical, densely warted basidiospores (9.7–11.8 × 3.9–4.9 µm).

Fruiting body. Basidiomata solitary to gregarious, with 8 cm high × 6 cm wide at the widest point, repeat branched dichotomously in 4–5 ranks, flesh pink when fresh, become clay buff with dry; apices obtuse, orange yellow when fresh, becoming fuscous when dry. Stipe ≥ 3 cm high, compound to fasciculate in groups of 5, emerging from a common base, concolorous with the branches.

Hyphal structure. Hyphal system monomitic, generative hyphae with clamp connections, branched, walls smooth and hyaline; basal stem with tramal hyphae 4–7 µm wide and inflated ones up to 10 µm, occasionally branched, thin-walled, parallel arranged, hyaline; tramal hyphae of branches 3–4 µm wide.

Hymenium. Hymenium all along the basidiomata. Basidia clavate, in a dense palisade, with 4 sterigmata and a basal clamp connection. Basidioles elongated clavate, smooth, hyaline, contents homogeneous, 23.5–34 × 6–7 µm.

Spores. Basidiospores ellipsoid to cylindrical, densely warted, with 1–2 several guttulae, IKI–, CB–, 9.7–11.8(–12.5) × (3.8–)3.9–4.9(–5.1) µm, L = 10.69 µm, W = 4.29 µm, Q = 2.49 (n = 30/1).

Additional specimens examined (*paratypes*). China, Xizang, Linzhi, Sejila Mountain National Forest Park, 29°67'N, 94°74'E, elev. 3850 m, gregarious on the humus under *Abies*, 2 August 2023, CLZhao 31180 (SWFC); on ground in forest of *Abies*, 2 August 2023, CLZhao 31204 (SWFC).

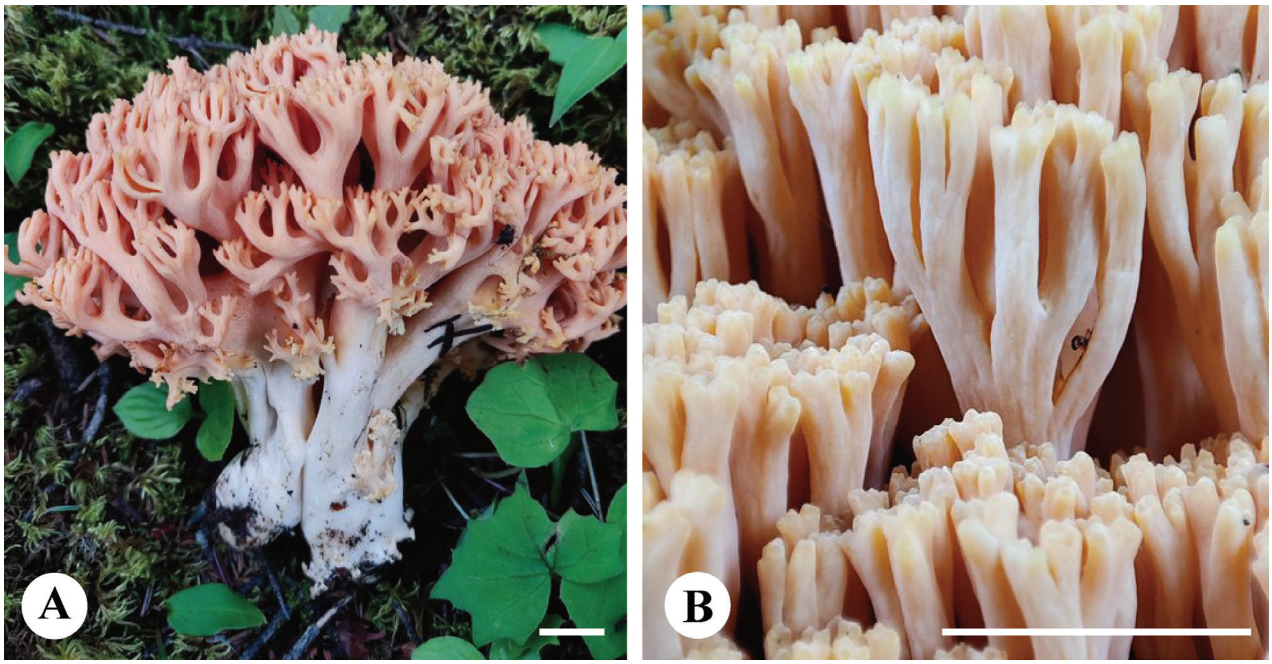

Figure 11. Basidiomata of *Ramaria xizangensis* (holotype, CLZhao 31169). Scale bars: 1 cm (**A, B**).

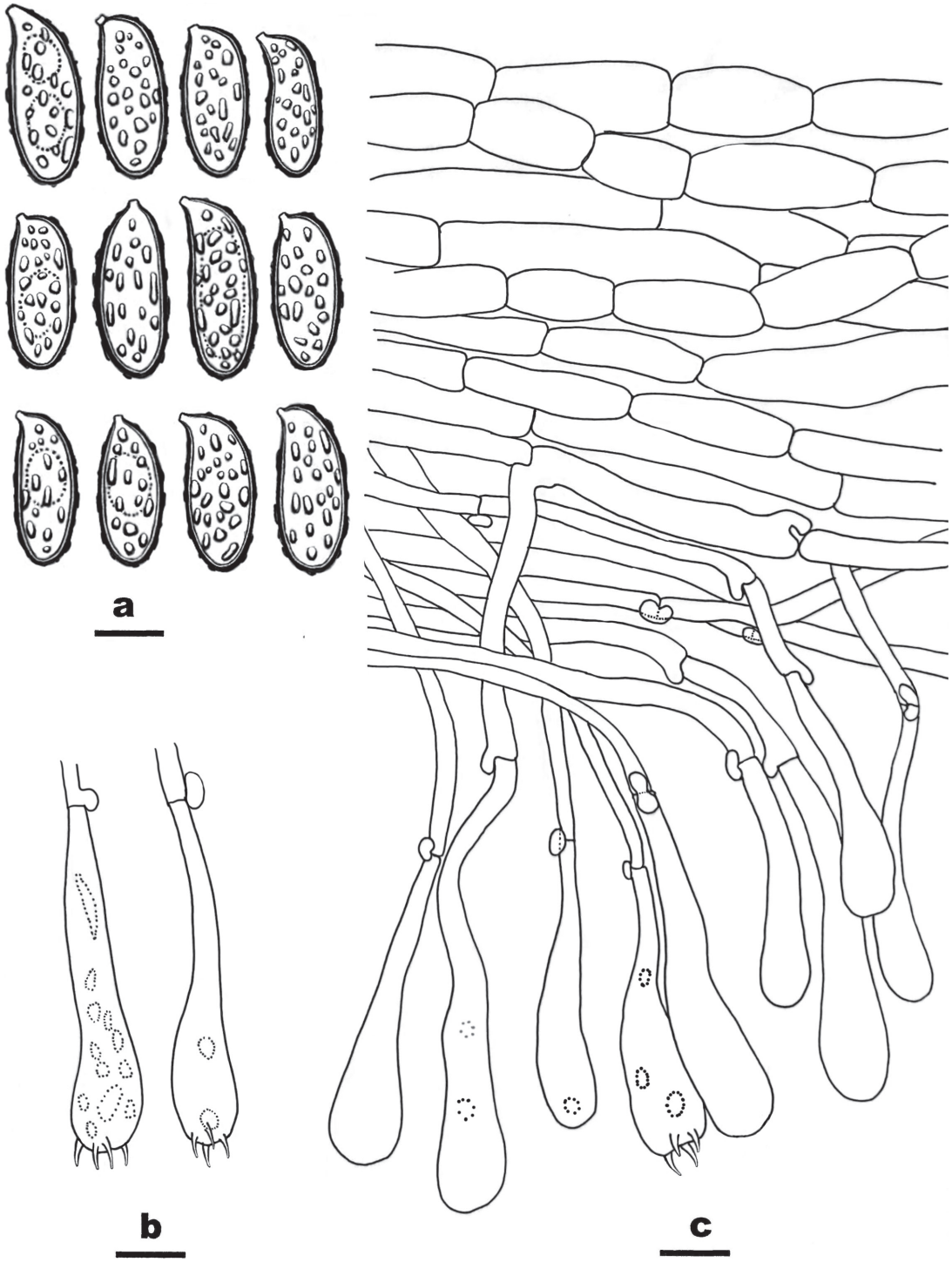

Figure 12. Microscopic structures of *Ramaria xizangensis* (CLZhao 31169, holotype) **a** basidiospores **b** basidia **c** a section of hymenium. Scale bars: 5 μm (**a**); 10 μm (**b, c**).

Discussion

Wood decay fungi encompasses the vast group of aphyllophoroid fungi with corticioid, prioid or jelly form of basidiomata (Herter 1910). This classification has historically been used to define the different families of Basidiomycetes. However, molecular studies have revealed that many of these fungi are distributed across various orders within the Basidiomycetes, including the likes

of Amylocorticiales, Atheliales, Dacrymycetales, and Gomphales (Kirk et al. 2018; Wei et al. 2022). As a result, further research is needed to elucidate the relationships and morphological variability of these taxa through phylogenetic analysis.

The Xizang Autonomous Region, situated in the southwest of China, is renowned as one of the most bio-diverse regions in the country. This is attributed to its complex topography and diverse ecosystems, making it a focal point for fungal biodiversity in China. Recently, studies focusing on fungal diversity and the ecology of Basidiomycota in Xizang were carried out (Ke 2016; Pubu et al. 2016; Wang et al. 2023). According to the study (Pubu et al. 2016), 1733 species were collected in Xizang. The fungal research indicated that Sejila Mountain National Forest Park is predominantly composed of spruce and fir trees, which provide an ideal habitat for a rich diversity of macrofungi species to flourish (Zhao and Li 1987). In our study, four species were found from Xizang, *Calocera ramaria*, *Ceraceomyces rhizomorphus*, *Leptosporomyces linzhiensis*, and *Ramaria xizangensis*.

Calocera is characterized by its yellow, gelatinous basidiomata, resembling *Dacrymyces*. However, *Dacrymyces* displays a broader range of basidiomata forms, including pulvinate, discoid, turbinate, spathulate, flabellate, and cylindrical shapes (Shirouzu et al. 2009; Fan et al. 2021), whereas *Calocera* exhibits branched, dendroid basidiomata. Our results have further confirmed that our newly discovered species features ramal basidiomata and clusters phylogenetically with *Calocera* species, placing it within the genus *Calocera*. In Xizang, two species have been identified, *C. ramaria* and *C. tibetica*, but the latter has wider basidiospores (5–6 µm vs. 3.9–4.4 µm, Fan et al. 2021). In our phylogenies, *C. viscosa* and *C. cornea* were related to *C. ramaria* (Fig. 1); however, *C. viscosa* has 1-septate mature basidiospores, and *C. cornea* differs from *C. ramaria* by its distinctly larger basidiospores (7–10 × 3–4.5 µm vs. 9.2–11 × 3.9–4.4 µm) with one septum (McNabb 1965; Shirouzu et al. 2009).

Previous research has highlighted the polyphyly of *Ceraceomyces* (Chikowski 2016; Yuan et al. 2023), and seven species are retained in *Ceraceomyces*. However, it is worth noting that authentic specimens and DNA data are lacking for *Ceraceomyces* species. Phylogenetically, *C. rhizomorphus* formed a sister group with *C. yunnanensis* and *C. borealis*, but *C. yunnanensis* has smaller basidiospores (3–4 × 1–1.5 µm vs. 4.7–6.2 × 1.8–2.3 µm, Yuan et al. 2023) and *C. borealis* has larger basidiospores (6–8 × 1.8–2 µm vs. 4.7–6.2 × 1.8–2.3 µm, Bernicchia and Gorjón 2010).

Ceraceomyces rhizomorphus and *C. tessulatus* had similar yellowish basidiomata with rhizomorphs when fresh, while *C. tessulatus* has ellipsoid and larger basidiospores (6–8 × 3.5–4.5 µm vs. 4.7–6.2 × 1.8–2.3 µm, Bernicchia and Gorjón 2010). Three known species, *C. bizonatus*, *C. reidii*, and *C. simulans* also distributed in Asia. However, *C. bizonatus* has shorter basidiospores (2.5–3.3 µm vs. 4.7–6.2 µm, Bernicchia and Gorjón 2010); *C. reidii* has larger basidiospores (11.5–15 × 4.5–6 µm vs. 4.7–6.2 × 1.8–2.3 µm, Bernicchia and Gorjón 2010); *C. simulans* has longer basidiospores (6–7 µm vs. 4.7–6.2 µm, Bernicchia and Gorjón 2010).

Leptosporomyces linzhiensis is similar to *L. thindii* in having white basidiomata and being distributed in Asia, but the latter has wider basidiospores (Prasher 2015). *Leptosporomyces linzhiensis* sisters to *L. septentrionalis* by its white ba-

sidiomata, and cylindrical basidiospores, but the latter has slightly shorter basidiospores (3–4 µm vs. 3.8–4.3 µm), and 2–4 basidia (Prasher 2015). *Leptosporomyces linzhiensis* is easily confused with *L. roseus* in, but the latter has shorter basidiospores (2–2.5 µm vs. 3.8–4.3 µm, Prasher 2015). *Leptosporomyces fuscostratus* has a broad distributional range in the northern hemisphere, but it has wider basidiospores (2–2.8 µm vs. 1.7–2 µm, Yurchenko and Wołkowycki 2022).

In our phylogeny, *Ramaria* is paraphyletic, which included four clades, *R*. sub. *Laeticolora* and *R*. sub. *Lentoramaria*, *R.* sub. *Ramaria* and R. sub. *Echinormaria*. *Ramaria xizangensis* was clustered in *Ramaria* sub. *Laeticolora* with *Ramaria amyloidea*, *R. celerivirescens* and *R. claviramulata*. However, *R. celerivirescens* has slightly wider basidiospores (4–6 µm vs. 3.9–4.9 µm, Marr and Stuntz 1973). *R. claviramulata* has cream to brownish white basidiomata. *Ramaria xizangensis* is similar to *R. indoyunnaniana* in having pink basidiomata and being distributed in Yunnan, but the latter has shorter basidiospores (7.2–8.3 µm vs. 9.7–11.8 µm, Petersen and Zang 1986).

According to our field inventory, the four Chinese new species were found in alpine zone near the Sejila Mountain, and the coniferous forest dominant by *Abies* at high altitude with cold and humid environments. Previously, numerous new species have been found in Southwest China (Dai 2022; Zhao et al. 2023), and the present paper confirms the fungal diversity is very rich in the montane forests of Southeast Xizang.

Additional information

Conflict of interest

The authors have declared that no competing interests exist.

Ethical statement

No ethical statement was reported.

Funding

The research was supported by the National Natural Science Foundation of China (Project No. 32170004); the Highlevel Talents Program of Yunnan Province (YNQR-QNRC-2018-111); the Scientific Research Fund of Yunnan Provincial Department of Education (2024J0668); Forestry Innovation Programs of Southwest Forestry University (Grant No: LXXK-2023M07).

Author contributions

Data curation: ZHM, ZCL,WF. Formal analysis: ZXC. Methodology: ZHM, ZXC, LJT. Software: ZXC, LJT. Writing - original draft: ZHM, ZCL. Writing - review and editing: ZCL, WF.

Author ORCIDs

Hong-Min Zhou https://orcid.org/0000-0002-0724-5815
Xun-Chi Zhang https://orcid.org/0000-0003-3887-0979
Fang Wu https://orcid.org/0000-0002-1455-6486
Chang-Lin Zhao https://orcid.org/0000-0002-8668-1075

Data availability

All of the data that support the findings of this study are available in the main text.

References

Anonymous (1969) Flora of British Fungi. Colour Identification Chart. Her Majesty's Stationery Office, London.

Bao Y (2020) Mycoflora Biodiversity and Genetic Variation of Macrofungi in Alpine Meadow of Tibet. Northeast Normal University.

Bernicchia A, Gorjón SP (2010) Fungi Europaei 12. Corticiaceae s.l. Edizioni Candusso, Alassio, Italy, 1008 pp.

Binder M, Larsson KH, Matheny PB, Hibbett DS (2010) Amylocorticiales ord. nov. and Jaapiales ord. nov.: Early diverging clades of Agaricomycetidae dominated by corticioid forms. Mycologia 102(4): 865–880. https://doi.org/10.3852/09-288

Chikowski R, Larsson KH, Gibertoni TB (2016) *Ceraceomyces atlanticus* (Amylocorticiales, Basidiomycota), a new species from the Atlantic Rain Forest, Brazil. Phytotaxa 296(1): 73–80. https://doi.org/10.11646/phytotaxa.296.1.5

Coker WC (1923) The *Clavarias* of the United States and Canada. Chapel Hill, 209 pp.

Corner EJH (1950) A monograph of *Clavaria* and allied genera. Annals of Botany Memoirs 1: 1–740.

Cui BK, Li HJ, Ji X, Zhou JL, Song J, Si J, Yang ZL, Dai YC (2019) Species diversity, taxonomy and phylogeny of Polyporaceae (Basidiomycota) in China. Fungal Diversity 97(1): 137–392. https://doi.org/10.1007/s13225-019-00427-4

Doty MS (1944) *Clavaria*, the species known from Oregon and the Pacific Northwest.

El-Gharabawy HM, Leal-Dutra CA, Griffith GW (2021) *Crystallicutis* gen. nov. (Irpicaceae, Basidiomycota), including *C. damiettensis* sp. nov., found on *Phoenix dactylifera* (date palm) trunks in the Nile Delta of Egypt. Fungal Biology 125(6): 447–458. https://doi.org/10.1016/j.funbio.2021.01.004

Exeter RL, Norvell L, Cazares E (2006) *Ramaria* of the Pacific Northwestern United States. United States Department of Interior, Bureau of Land Management. Salem, Oregon USA, 156 pp.

Fan LF, Wu YD, Wu F, Dai YC (2021) *Calocera tibetica* sp. nov. (Dacrymycetaceae, Dacrymycetales) from southwestern China. Phytotaxa 500: 133–141. https://doi.org/10.11646/phytotaxa.500.2.6

Fisher MC (1931) A comparative morphological study of certain species of the Dacryomycetaceae. The Proceedings 38(1): 115–125.

Gäumann EA (1953) The Fungi: a description of their morphological features and evolutionary development, (Translated by Wynd FL). Hafner Publishing, New York and London, 420 pp.

Giachini AJ, Hosaka K, Nouhra E, Spatafora J, Trappe JM (2010) Phylogenetic relationships of the Gomphales based on nuc-25S-rDNA, mit-12S-rDNA, and mit-atp6-DNA combined sequences. Fungal Biology 114(2–3): 224–234. https://doi.org/10.1016/j.funbio.2010.01.002

Hall TA (1999) Bioedit: A user-friendly biological sequence alignment editor and analysis program for Windows 95/98/NT. Nucleic Acids Symposium Series 41: 95–98.

Hanif M, Khalid AN, Exeter RL (2019) *Ramaria flavescentoides* sp. nov. with clamped basidia from Pakistan. Mycotaxon 134: 399–406. https://doi.org/10.5248/134.399

Herter WGF (1910) Autobasidiomycetes. Kryptogamen-Flora der Mark Brandenburg 6: 1–192.

Hodkinson BP, Moncada B, Lücking R (2014) Lepidostromatales, a new order of lichenized fungi (Basidiomycota, Agaricomycetes), with two new genera, *Ertzia* and *Sul-*

zbacheromyces, and one new species, *Lepidostroma winklerianum*. Fungal Diversity 64(1): 165–179. https://doi.org/10.1007/s13225-013-0267-0

Hosaka K, Bates ST, Beever RE, Castellano MA, Colgan W III, Dominguez LS, Trappe JM (2006) Molecular phylogenetics of the gomphoidphalloid fungi with an establishment of the new subclass Phallomycetidae and two new orders. Mycologia 98(6): 949–959. https://doi.org/10.1080/15572536.2006.11832624

Humpert AJ, Muench EL, Giachini AJ, Castellano MA, Spatafora JW (2001) Molecular phylogenetics of *Ramaria a*nd related genera: evidence from nuclear large subunit and mitochondrial small subunit rDNA sequences. Mycologia 93: 465–477. https://doi.org/10.2307/3761733

Jülich W (1972) Monographie der Athelieae (Corticiaceae, Basidiomycetes). Willdenowia Beiheft 7: 1–283.

Kalyaanamoorthy S, Minh BQ, Wong TKF, von Haeseler A, Jermiin LS (2017) ModelFinder: Fast model selection for accurate phylogenetic estimates. Nature Methods 14(6): 587–589. https://doi.org/10.1038/nmeth.4285

Katoh K, Rozewicki J, Yamada KD (2019) MAFFT online service: Multiple sequence alignment, interactive sequence choice and visualization. Briefings in Bioinformatics 20(4): 1160–1166. https://doi.org/10.1093/bib/bbx108

Ke ZD (2016) Studies on macrofungi diversity in Shergyla Mountain National Nature Reserve in Tibet. Jilin Agricultural University.

Kirk PM, Ainsworth GC, Cannon PF, Minter DW (2008) Ainsworth and Bisby's dictionary of fungi, 10th edn. CAB International, UK. https://doi.org/10.1079/9780851998268.0000

Knudson AG (2012) The genus *Ramaria* in Minnesota. Master of Science thesis, University of Minnesota.

Larsson KH (2007) Re-thinking the classification of corticioid fungi. Mycological Research 111(9): 1040–1063. https://doi.org/10.1016/j.mycres.2007.08.001

Larsson KH, Larsson E, Kõljalg U (2004) High phylogenetic diversity among corticoid homobasidiomycetes. Mycological Research 108(9): 983–1002. https://doi.org/10.1017/S0953756204000851

Liu S, Chen YY, Sun YF, He XL, Song CG, Si J, Liu DM, Gates G, Cui BK (2023) Systematic classification and phylogenetic relationships of the brown-rot fungi within the Polyporales. Fungal Diversity 118(1): 1–94. https://doi.org/10.1007/s13225-022-00511-2

Lowy B (1971) Tremellales. Flora Neotropica 6(8): 1–153.

Marr CD, Stuntz DE (1973) *Ramaria* of Western Washington. Bibliotheca Mycologica, Germany, 38 pp.

Martin GW (1948) New of noteworthy tropical fungi. IV. Lloydia 11(2): 111–122.

McNabb RFR (1965) Taxonomic studies in the Dacrymycetaceae 2. *Calocera* (Fries) Fries. New Zealand Journal of Botany 3: 31–58. https://doi.org/10.1080/002882 5X.1965.10428712

Miller MA, Pfeiffer W, Schwartz T (2010) Creating the CIPRES Science Gateway for inference of large phylogenetic trees. In Proceedings of the Gateway Computing Environments Workshop, New Orleans, 8 pp. https://doi.org/10.1109/GCE.2010.5676129

Nees Esenbeck, CDG (1817) System der Pilze und Schwämme, 334 pp.

Peng YB, Liu B, Li F (1992) Flora Fungorum Sinicorum Vol. 2. Tremellales et Dacrymycetales. Science Press, Beijing, 151 pp.

Petersen JH (1996) Farvekort. The Danish Mycological Society's colour-chart. Foreningen til Svampekundskabens Fremme, Greve, 6 pp.

Petersen RH (1981) Ramaria subgenus Echinoramaria. Bibliotheca Mycologia 261 pp.
Petersen RH, Zang M (1986) New or interesting clavarioid fungi from Yunnan, China. Plant Diversity 8(3): 281–294.
Prasher IB (2015) Wood-rotting non-gilled Agaricomycetes of Himalayas. Fungal Diversity Research Series, Chiang Rai, 653 pp. https://doi.org/10.1007/978-94-017-9858-7
Pubu CR, Wang M, Liu XY (2016) A review of investigation of fungi in Tibet. Mycosystema 35(9): 1025–1047. https://doi.org/10.13346/j.mycosystema.150158
Ronquist F, Huelsenbeck JP (2003) MrBayes 3: Bayesian phylogenetic inference under mixed models. Bioinformatics 19(12): 1572–1574. https://doi.org/10.1093/bioinformatics/btg180
Ryvarden L, Gilbertson RL (1993) European polypores. Part 1. Synopsis Fungorum 6: 1–387.
Shirouzu T, Hirose D, Tokumasu S (2007) Sequence analyses of the 28S rRNA gene D1/D2 region suggest *Dacrymyces* (Heterobasidiomycetes, Dacrymycetales) is polyphyletic. Mycoscience 48(6): 388–394. https://doi.org/10.1007/S10267-007-0378-0
Shirouzu T, Hirose D, Tokumasu S (2009) Taxonomic study of the Japanese Dacrymycetes. Persoonia 23(1): 16–34. https://doi.org/10.3767/003158509X468443
Shirouzu T, Hosaka K, Nam KO, Weir BS, Johnston PR, Hosoya T (2017) Phylogenetic relationships of eight new Dacrymycetes collected from New Zealand. Persoonia 38(1): 156–169. https://doi.org/10.3767/003158517X695280
Sulistyo BP, Larsson KH, Haelewaters D, Ryberg M (2021) Multigene phylogeny and taxonomic revision of Atheliales s.l.: Reinstatement of three families and one new family, Lobuliciaceae fam. nov. Fungal Biology 125(3): 239–255. https://doi.org/10.1016/j.funbio.2020.11.007
Wang SH, Li GJ, Phurbu D, He MQ, Zhang MZ, Zhu XY, Li JX, Zhao RL, Cao B (2023) Four new species of *Russula* from the Xizang Autonomous Region and other provinces of China. Mycology 15(2): 1–28. https://doi.org/10.1080/21501203.2023.2265667
Wei CL, Chen CC, He SH, Wu SH (2022) *Dendrocorticiopsis orientalis* gen. et sp. nov. of the Punctulariaceae (Corticiales, Basidiomycota) revealed by molecular data. MycoKeys 90: 19–30. https://doi.org/10.3897/mycokeys.90.84562
White TJ, Bruns T, Lee S, Taylor J (1990) Amplification and direct sequencing of fungal ribosomal RNA genes for phylogenetics. In: MA, Gefand DH, Sninsky JJ, White MJT (Eds) PCR Protocols: a guide to methods and applications; Academic Press, San Diego, 315–322. https://doi.org/10.1016/B978-0-12-372180-8.50042-1
Wijayawardene NN, Hyde KD, Al-Ani LKT, Tedersoo L, Haelewaters D, Rajeshkumar KC, Zhao RL, Aptroot A, Leontyev DV, Saxena RK, Tokarev YS, Dai DQ, Letcher PM, Stephenson SL, Ertz D, et al. (2020) Outline of fungi and fungus-like taxa. Mycosphere 11(1): 1160–1456. https://doi.org/10.5943/mycosphere/11/1/8
Wu SH, Shih K, Yu SY (2011) *Calocera bambusicola* sp. nov. and *C. sinensis* newly recorded from Taiwan. Mycotaxon 115(1): 163–169. https://doi.org/10.5248/115.163
Yang Y, Jiang Q, Li Q, Yang J, Cha L, Cheng L, Yang S, Zhao C, Zhou H (2023) Molecular systematics and taxonomic analyses of three new wood-inhabiting fungi of *Hyphoderma* (Hyphodermataceae, Basidiomycota). Journal of Fungi 9(11): 1044. https://doi.org/10.3390/jof9111044
Yuan Q, Luo KY, Zhang Y, Zhao CL (2023) Morphological characteristics and phylogenetic analyses revealed three new wood-inhabiting fungi (Agaricomycetes, Basidiomycota) in Southern China. Phytotaxa 592(3): 179–195. https://doi.org/10.11646/phytotaxa.592.3.1

Yurchenko K, Wołkowycki M (2022) New species of corticioid fungi (Basidiomycota) for Poland found in Białowieża Primeval Forest in 2018–2020. Acta Mycologica 58: 1–18. https://doi.org/10.5586/am.577

Zamora JC, Ekman S (2020) Phylogeny and character evolution in the Dacrymycetes, and systematics of Unilacrymaceae and Dacryonaemataceae fam. nov. Persoonia 44(1): 161–205. https://doi.org/10.3767/persoonia.2020.44.07

Zhao LF, Li XG (1987) Partial fungal list of Nyingchi region, Milin, Tibet. Journal of Southwest Forestry College 7(1): 55–58. [Natural Science]

Zhao CL, Qu MH, Huang RX, Karunarathna SC (2023) Multi-gene phylogeny and taxonomy of the wood-rotting fungal genus *Phlebia* sensu lato (Polyporales, Basidiomycota). Journal of Fungi 320(9): 1–41. https://doi.org/10.3390/jof9030320

MycoKeys 106: 225–250 (2024)
DOI: 10.3897/mycokeys.106.122890

Research Article

New species and records of Botryosphaeriales (Dothideomycetes) associated with tree dieback in Beijing, China

Yingying Wu[1], Cheng Peng[1], Rong Yuan[1], Mingwei Zhang[1], Yang Hu[2], Chengming Tian[1]

1 *The Key Laboratory for Silviculture and Conservation of the Ministry of Education, Beijing Forestry University, Beijing 100083, China*
2 *The Forestry Protection Station of Tonghzou Strict in Beijing, Beijing 101100, China*
Corresponding author: Chengming Tian (chengmt@bjfu.edu.cn)

Abstract

Botryosphaeriales species are important pathogens that have worldwide distribution. In this study, 23 Botryosphaeriales strains were isolated from 13 host species during a dieback disease survey in Beijing, China. Based on morphological and phylogenetic analyses, six Botryosphaeriales species were identified, including two new species named *Dothiorella hortiarborum* **sp. nov.** and *Phaeobotryon fraxini* **sp. nov.**, and four new host records: *Aplosporella ginkgonis* from *Cotinus coggygria* var. *cinereus*, *A. javeedii* from *Acer miyabei*, *Acer truncatum*, *Forsythia suspensa*, *Lagerstroemia indica*, *Sambucus williamsii*, *Syringa vulgaris*, *Ulmus pumila*, *Xanthoceras sorbifolium*, *A. yanqingensis* from *Acer truncatum*, and *Do. acericola* from *Forsythia suspensa*, *Ginkgo biloba*, and *Syringa oblata*. This study enriches the species diversity associated with tree dieback in Beijing, China, and contributes to the further study of the taxonomy of this order.

Key words: *Dothiorella*, morphology, *Phaeobotryon*, phylogeny, taxonomy

Academic editor: Ning Jiang
Received: 13 March 2024
Accepted: 2 June 2024
Published: 27 June 2024

Citation: Wu Y, Peng C, Yuan R, Zhang M, Hu Y, Tian C (2024) New species and records of Botryosphaeriales (Dothideomycetes) associated with tree dieback in Beijing, China. MycoKeys 106: 225–250. https://doi.org/10.3897/mycokeys.106.122890

Introduction

Botryosphaeriales species are important plant pathogens commonly found on the trunks and branches of woody plants (Phillips et al. 2013; Lawrence et al. 2017; Zhu et al. 2018; Zhang et al. 2021). They are associated with branch canker, dieback, decline, and death, with consequences for the ecological and economic value of the forest (Slippers and Wingfield 2007; Phillips et al. 2013; Mohali-Castillo 2023). Botryosphaeriales species occur on a wide range of hosts, in the form of endophytes on woody plants and herbs, lichens, and even seaweed leaves in marine environments, suggesting that they have great potential for research value (Yang et al. 2017; Akinsanmi et al. 2019; Zhang et al. 2021; Mohali-Castillo 2023; Rathnayaka et al. 2023).

Phylogenetic analyses of DNA sequence data have an enormous influence on the systematics and taxonomy of the order Botryosphaeriales, including redefining families and genera and identifying new species (Phillips et al. 2019; Mohali-Castillo 2023). Schoch et al. (2006) combined SSU, LSU, *tef1-α*, and *rpb2* to first propose the order Botryosphaeriales, which contains only a single family of Botryosphaeriaceae. Minnis et al. (2012) supplemented the DNA sequence data of Planistromellaceae with phylogenetic analyses combining

SSU, ITS, LSU, and *rpb1*, which introduced the family into the Botryosphaeriales. Wikee et al. (2013) reintroduced the Phyllostictaceae, grouped under Botryosphaeriales, to accommodate *Phyllosticta* using intronic genes (ITS, *act*, and *tef1-α*) and highly conserved coding regions of genes (LSU and GPDH). Slippers et al. (2013) added three new families, Aplosporellaceae (*Aplosporella* and *Bagnisiella*), Melanopsaceae (*Melanops*), and Saccharataceae (*Saccharata*), to Botryosphaeriales based on DNA sequence data of six loci (SSU, LSU, ITS, *tef1-α*, *tub2*, and mtSSU). Wyka and Broders (2016) introduced Septorioideaceae based on morphological and molecular evidence. Yang et al. (2017) mentioned that the LSU-*rpb2* combination could effectively classify taxa at the family and genus levels, and *rpb2* in combination with ITS, *tef1-α*, and *tub2* added additional resolution for species delimitation. For this reason, they combined the five fragments ITS, *tef1-α*, *tub2*, LSU, and *rpb2* to propose two new families, Endomelanconiopsisaceae and Pseudofusicoccumaceae. Therefore, Botryosphaeriales contained a total of nine families. However, Phillips et al. (2019) reassessed the families of Botryosphaeriales in terms of morphology of the sexual morphs and phylogenetic relationships of ITS and LSU sequence data, ultimately concluding that the order contained only six families (Aplosporellaceae, Botryosphaeriaceae, Melanopsaceae, Phyllostictaceae, Planistromellaceae, and Saccharataceae), with Endomelanconiopsisaceae, Pseudofusicoccumaceae, and Septorioideaceae as synonyms of existing families. Up to date, six families and 32 genera are accepted in Botryosphaeriales (https://www.outlineoffungi.org/). Of these, Botryosphaeriaceae is rich in species diversity, high in pathogenicity, and widely distributed.

Botryosphaeriaceae was first established by Theissen and Sydow (1918), containing three genera: *Botryosphaeria*, *Dibotryon*, and *Phaeobotryon*. Morphologically, Botryosphaericeae species are distinctive from other families in Botryosphaeriales by their large, ovoid to oblong, usually hyaline, aseptate ascospores (Phillips et al. 2013). Liu et al. (2012) assumed that ascospores could become pigmented and septate with age. Conidia in the asexual state of Botryosphaericeae are diverse in morphological characteristics (Phillips et al. 2005). Phylogenetically, however, there is a random distribution of hyaline or colored conidia or ascospores in the phylogenetic tree of Botryosphaericeae (Slippers et al. 2013). Therefore, accurate identification of species in the family by a single circumscription is not suitable. Currently, 22 genera and more than 200 species are contained within the family (https://www.outlineoffungi.org/). Recently, many new species have been introduced in the Botryosphaeriaceae, especially in the genera *Dothiorella* and *Phaeobotryon* (Jia et al. 2023; Li et al. 2023; Lin et al. 2023a; Wu et al. 2023).

Saccardo (1880) first established *Dothiorella* and designated *Do. pyrenophora* as the type species. Up to now, some scholars have made systematic revisions of *Dothiorella* to establish a more stable phylogenetic relationship (Dissanayake et al. 2016; Dissanayake et al. 2020; Zhang et al. 2021). The distinctive features of the genera are that the conidia are colored in the early stages of development, and with 1-septate, the sexual form of ascospores is brown and septate (Senanayake et al. 2023). The type species of the genus *Phaeobotryon* is *P. cercidis*, which is characterized by 2-septate brown ascospores with conical apiculate-elliptic to oblong or obovoid shapes at both ends and hyaline or brown conidia (Phillips et al. 2013; Fan et al. 2015b; Zhu et al. 2018; Pan et al. 2019).

In recent years, multiple studies have revealed that new species of Botryosphaeriales infest branches and trunks. Pan et al. (2019) found that *Phaeobotryon rhois* and *Diplodia quercicola* were detrimental to *Rhus typhina* and *Quercus variabilis* separately in Yudu Mountain, Beijing. *Aplosporella yanqingensis* and *Dothiorella baihuashan* are mainly recorded on Pinaceae or Cupressaceae (Lin et al. 2023a). *Lasiodiplodia regiae* caused the canker and dieback of apple trees (Wang et al. 2023). These studies suggest that Botryosphaeriales is rich in species diversity and has the potential to continue to be explored for new species. During the investigation of plant pathogens in Beijing, a higher number of diseased plant branches caused by Botryosphaeriales fungi were found. This study used phylogenetic analysis and morphological comparisons to describe new species and new host records, enriching the fungal taxa within Botryosphaeriales.

Materials and method

Sample collection and fungal isolation

A survey on dieback diseases was conducted from March to November 2023 in the Tongzhou District of Beijing, China. A total of thirteen tree species were examined, namely *Acer miyabei*, *A. truncatum*, *Cotinus coggygria* var. *cinereus*, *Forsythia suspensa*, *Fraxinus chinensis*, *Ginkgo biloba*, *Lagerstroemia indica*, *Sambucus williamsii*, *Styphnolobium japonicum*, *Syringa oblata*, *Syringa vulgaris*, *Ulmus pumila*, and *Xanthoceras sorbifolium*. Twenty specimens showing typical dieback symptoms (Fig. 1) with typical conidiomata and/or ascomata were collected. All samples were placed in paper bags and transported to the laboratory. Specimens with typical conidiomata pycnidial were selected for isolation. Removing the spore mass from conidiomata and generating single spore colonies or plating superficially sterilized diseased tissue on potato dextrose agar plates (PDA; containing 200 g potatoes, 20 g dextrose, and 20 g agar per liter) and incubating Petri dishes at 25 °C in the dark for 2–3 d. When colonies just formed, they transferred to fresh PDA Petri dishes (Crous et al. 2019). All specimens were deposited at the Museum of Beijing Forestry University (BJFC), and all cultures were preserved at the China Forestry Culture Collection Center (CFCC).

Morphological observation

Cultures were incubated on PDA at 25 °C in a 12-h day/night regime (Crous et al. 2019). After 14 days, the colonies were measured, and characteristics based on the color, shape, and sparseness of the aerial mycelium of the pathogen colonies were observed and recorded. Conidiomata were manually sectioned with a double-edged razor blade. Observations were conducted using a Leica DM 2,500 dissecting microscope (Wetzlar, Germany) and a Nikon Eclipse 80i compound microscope, equipped with differential interference contrast (DIC) illumination. Images were captured using a Nis DS-Ri2 camera with the Nikon Nis-Elements F4.30.01 software. Conidial length was measured from the base of the basal cell to the base of the apical appendage, while conidial width was measured at its widest point. A randomized selection of conidia was used for measurement (n = 50).

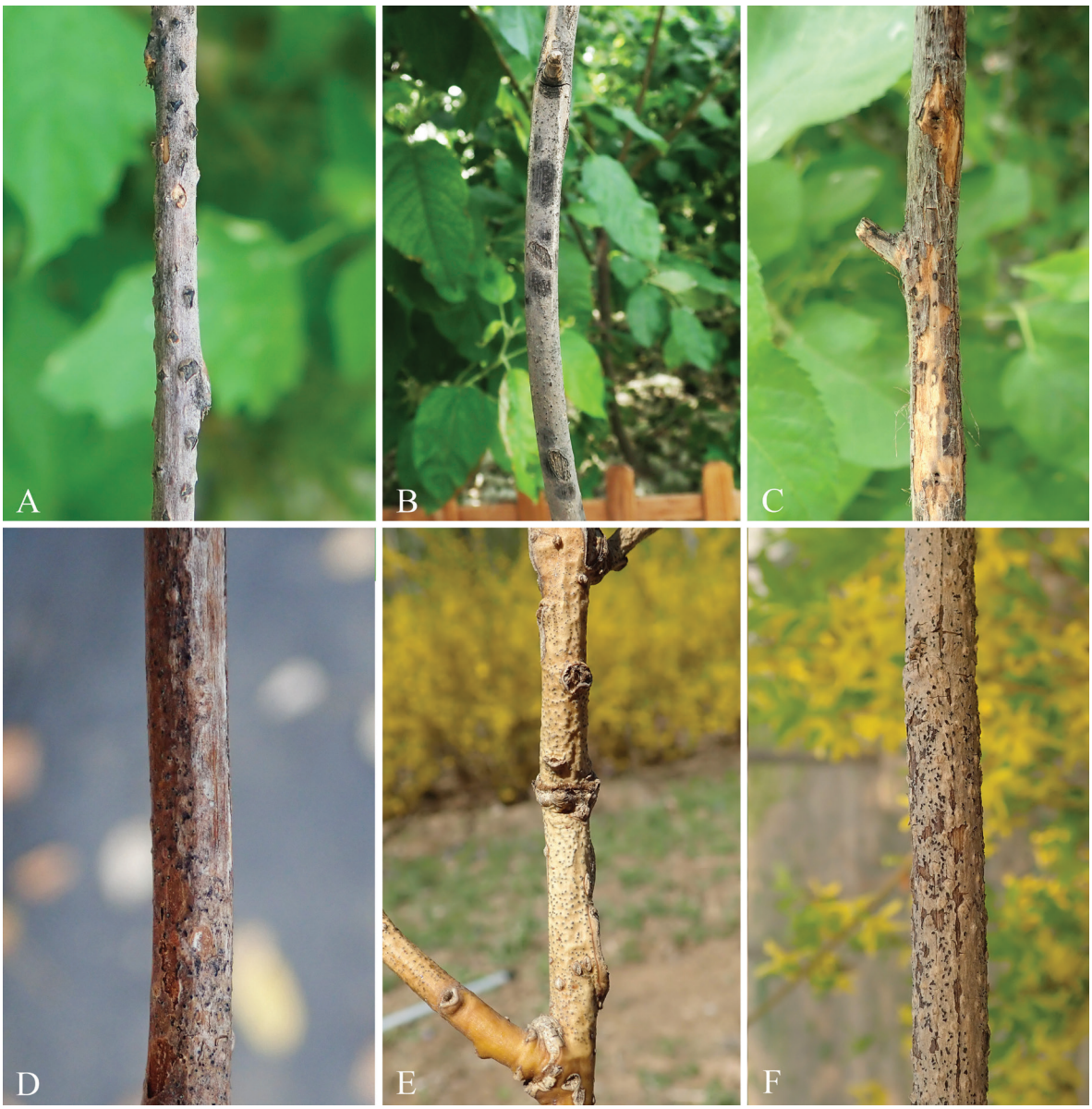

Figure 1. Disease symptoms associated with Botryosphaeriales species collected from Tongzhou District, Beijing, China **A** *Xanthoceras sorbifolium* **B** *Fraxinus chinensis* **C** *Lagerstroemia indica* **D** *Sambucus williamsii* **E** *Styphnolobium japonicum* **F** *Forsythia suspensa*.

DNA extraction, PCR amplification, and sequencing

Genetic DNA was extracted using the cetyltrime-thylammonium bromide (CTAB) method when the mycelium was well spread on the PDA. DNA samples were stored at -20 °C. The PCR reaction primers (forward and reverse) and amplification conditions are detailed in Table 1. Polymerase chain reaction (PCR) amplification was run on a PTC-200 Thermal Cycler amplifier from Bio-Rad, USA. The PCR amplification systems were all 20 µL, including 10 µL of Mix (Promega), 7 µL of double deionized water, 1 µL each of pre- and post-primers, and 1 µL of DNA template. PCR products were assayed by electrophoresis on 2% agarose gels. Amplified PCR products were sent to a commercial sequencing provider (Tsingke Biotechnology Co. Ltd., Beijing, China).

Table 1. Genes used in this study with PCR primers.

Locus	PCR primers	PCR: thermal cycles: (Annealing temp. in bold)	References
ITS	ITS1/ITS4	(95 °C: 30 s, **51 °C**: 30 s, 72 °C: 1 min) × 35 cycles	White et al. 1990
LSU	LROR/LR5	(95 °C: 45 s, **55 °C**: 30 s, 72 °C: 1 min) × 35 cycles	Vilgalys and Hester 1990
tef1-α	EF1-728F/EF1-986R	(95 °C: 15 s, **55 °C**: 30 s, 72 °C: 1 min) × 35 cycles	Carbone and Kohn 1999
tub2	Bt2a/Bt2b	(95 °C: 30 s, **55 °C**: 30 s, 72 °C: 1 min) × 35 cycles	Glass and Donaldson 1995

Phylogenetic analyses

The sequences obtained were assembled using SeqMan v. 7.1.0 software, and reference sequences from related publications (Phillips et al. 2019; Li et al. 2023; Lin et al. 2023a; Wu et al. 2023) were retrieved from the National Center for Biotechnology Information (NCBI; https://www.ncbi.nlm.nih.gov). All sequences generated in this study were submitted to GenBank (Table 2). Sequences were aligned in MAFFT v. 7 at the web server (https://mafft.cbrc.jp/alignment/server/) (Katoh and Standley 2013; Katoh et al. 2019) and further adjustments and editing of the sequences were made with MEGA v. 6 (Tamura et al. 2013). Maximum parsimony (MP), maximum likelihood (ML), and Bayesian inference (BI) were selected to construct phylogenetic trees using PAUP v. 4.0b10, PhyML 3.0, and MrBayes V3.1.2 (Huelsenbeck and Ronquist 2001; Swofford 2003; Silvestro and Michalak 2012). Phylograms were visualized with FigTree v. 1.4.0 (http://tree.bio.ed.ac.uk/software/figtree/) and additional edited with Adobe Illustrator CS v. 5 (Adobe Systems Inc., USA). Maximum-parsimony bootstrap values (MPBP) and maximum-likelihood bootstrap values (MLBP) ≥ 50% and Bayesian posterior probabilities (BYPP) ≥ 0.90 are shown for each tree.

Maximum parsimony analysis was performed using the tree bisection and reconnection (TBR) branch swapping algorithm with a heuristic search option of 1000 random-addition sequences (Swofford 2003). Max trees were set to 5000 branches of zero length, and all parsimonious trees were saved. Other measures calculated were tree length (TL), consistency index (CI), retention index (RI), and rescaled consistency (RC) (Swofford 2003). Maximum likelihood analysis was performed with the GTR GAMMA model of site substitution, including estimation of gamma-distributed rate heterogeneity and a proportion of invariant sites (Guindon et al. 2010). The branch support from MP and ML analysis was evaluated with a bootstrapping (BS) method of 1 000 replicates (Hillis and Bull 1993). The Bayesian inference analysis employing a Markov chain Monte Carlo (MCMC) algorithm was performed with Bayesian posterior probabilities (Rannala and Yang 1996). The model of nucleotide substitution was estimated by MrModeltest v.2.3 (Posada and Crandall 1998), and a weighted Bayesian analysis was considered. Two MCMC chains were run starting from random trees for 1,000,000 generations and stopped when the average standard deviation of split frequencies fell below 0.01; the trees were sampled every 100th generation. The first 25% of trees were discarded as the burn-in phase of each analysis, and the Bayesian posterior probabilities (BPP) were calculated using the remaining 7,500 trees.

Table 2. Isolates of *Aplosporella*, *Dothiorella*, and *Phaeobotryon* used in the molecular analyses in this study. Notes: NA: not applicable, Strains in this study are marked in bold, T: ex-type strains.

Species	Strain	Host	Origin	GenBank accession numbers			
				ITS	*tef1-α*	*tub2*	LSU
Aplosporella africana	CBS 121777^{T}	*Acacia mellifera*	Namibia	KF766196	EU101360	NA	NA
A. africana	CBS 1217778^{T}	*Acacia mellifera*	Namibia	EU101316	EU101361	NA	NA
A. artocarpi	CPC 22791^{T}	*Artocarpus heterophyllus*	Thailand	KM006450	KM006481	NA	NA
A. ginkgonis	CFCC 52442^{T}	*Rhus typhina*	China	MH133916	MH133950	NA	NA
A. ginkgonis	CFCC 89661^{T}	*Rhus typhina*	China	KM030583	KM030597	NA	NA
A. ginkgonis	CFCC 70746	*Cotinus coggygria* var. *cinereus*	China	PP188498	PP541796	NA	NA
A. hesperidica	CBS 732.79^{T}	*Citrus aurantium*	Buenos Aires	KX464083	NA	NA	NA
A. hesperidica	CBS 208.37	*Citrus sinensis*	Zimbabwe	JX681069	NA	NA	NA
A. javeedii	CFCC 50054^{T}	*Juniperus chinensis*	China	KP208840	KP208846	NA	NA
A. javeedii	CFCC 50052	*Gleditsia sinensis*	China	KP208838	KP208844	NA	NA
A. javeedii	CFCC 58330	*Populus canadensis*	China	OQ651161	OQ692921	NA	NA
A. javeedii	CFCC 58329	*Populus beijingensis*	China	OQ651162	OQ692922	NA	NA
A. javeedii	CFCC 58412	*Populus alba* var. *pyramidalis*	China	OQ651163	OQ692923	NA	NA
A. javeedii	CFCC 70733	*Styphnolobium japonicum*	China	PP188499	PP541797	NA	NA
A. javeedii	CFCC 70734	*Forsythia suspensa*	China	PP188500	PP541798	NA	NA
A. javeedii	CFCC 70735	*Forsythia suspensa*	China	PP188501	PP541799	NA	NA
A. javeedii	CFCC 70736	*Ulmus pumila*	China	PP188502	PP541800	NA	NA
A. javeedii	CFCC 70737	*Acer truncatum*	China	PP188503	PP541801	NA	NA
A. javeedii	CFCC 70739	*Sambucus williamsii*	China	PP188504	PP541802	NA	NA
A. javeedii	CFCC 70740	*Acer miyabei*	China	PP188505	PP541803	NA	NA
A. javeedii	CFCC 70741	*Lagerstroemia indica*	China	PP188506	PP541804	NA	NA
A. javeedii	CFCC 70742	*Xanthoceras sorbifolium*	China	PP188507	PP541805	NA	NA
A. javeedii	CFCC 70744	*Syringa vulgaris*	China	PP188508	PP541806	NA	NA
A. javeedii	CFCC 70745	*Ulmus pumila*	China	PP188509	PP541807	NA	NA
A. macropycnidia	CGMCC 3.17725^{T}	*Cerasus yedoensis*	China	KT343648	KX011176	NA	NA
A. macropycnidia	CGMCC 3.17726	*Cerasus yedoensis*	China	KT343649	KX011177	NA	NA
A. papillata	CBS 121780^{T}	*Acacia tortillas*	South Africa	EU101328	EU101373	NA	NA
A. papillata	CBS 121781	*Acacia tortillas*	South Africa	EU101329	EU101374	NA	NA
A. prunicola	CBS 121167^{T}	*Prunus persica* var. *nucipersica*	South Africa	KF766147	NA	NA	NA
A. prunicola	STE-U 6326	*Prunus persica* var. *nucipersica*	South Africa	EF564375	NA	NA	NA
A. sophorae	CPC 29688^{T}	*Sophora microphylla*	New Zealand North	KY173388	NA	NA	NA
A. thailandica	MFLU 16-0615^{T}	Dead stems	Thailand	KX423536	KX423537	NA	NA
A. yalgorensis	MUCC511^{T}	*Acacia cochlearis*	Australia	EF591926	EF591977	NA	NA
A. yalgorensis	MUCC512	*Eucalyptus gomphocephala*	Australia	EF591927	EF591978	NA	NA
A. yanqingensis	CFCC 58791^{T}	*Platycladus orientalis*	China	OQ651164	OQ692924	NA	NA
A. yanqingensis	CFCC 58792^{T}	*Platycladus orientalis*	China	OQ651165	OQ692925	NA	NA
A. yanqingensis	CFCC 70743	*Acer truncatum*	China	PP188510	PP541808	NA	NA
A. yanqingensis	CFCC 70738	*Acer truncatum*	China	PP188511	PP541809	NA	NA
Alanomyces indica	CBS 134264^{T}	Soil	India	HF563622	AB872219	NA	NA
Dothiorella alpina	CGMCC 3-18001^{T}	*Platycladus orientalis*	China	KX499645	KX499651	NA	NA
Do. acacicola	CBS 141295^{T}	*Acacia mearnsii*	Réunion	KX228269	KX228376	NA	NA
Do. acericola	KUMCC 18-0137^{T}	*Acer palmatum*	China	MK359449	MK361182	NA	NA
Do. acericola	CFCC 70755	*Forsythia suspensa*	China	PP188520	PP766251	PP566659	NA
Do. acericola	CFCC 70760	*Ginkgo biloba*	China	PP188521	PP766252	PP566660	NA
Do. acericola	CFCC 70761	*Syringa oblata*	China	PP188522	PP766253	PP566661	NA

Species	Strain	Host	Origin	GenBank accession numbers			
				ITS	*tef1-α*	*tub2*	LSU
Do. albiziae	MFLUCC 22-0057^{T}	*Albizia lebbeck*	Thailand	ON751762	ON799588	ON799590	NA
Do. alpina	CFCC 58299^{T}	*Populus szechuanica*	China	OQ651166	OQ692932	OQ692926	NA
Do. americana	CBS 128309^{T}	*Vitis species and Vitis vinifera*	USA: Missouri	HQ288218	HQ288262	HQ288297	NA
Do. baihuashanensis	CFCC 58549^{T}	*Juniperus chinensis*	China	OQ651167	OQ692933	OQ692927	NA
Do. baihuashanensis	CFCC 58788^{T}	*Juniperus chinensis*	China	OQ651168	OQ692934	OQ692928	NA
Do. brevicollis	CBS 130411 = CMW 36463^{T}	*Acacia karroo*	South Africa	JQ239403	JQ239390	JQ239371	NA
Do. californica	CBS 119635	*Laurus nobilis*	Turkey	MT587396	MT592108	MT592579	NA
Do. californica	CBS 141587^{T}	*Umbellularia californica*	USA	KX357188	KX357211	KX357165	NA
Do. camelliae	CMGCC 3.24158^{T}	*Camellia oleifera*	China	OQ190531	OQ241464	OQ275064	NA
Do. capri-amissi	CBS 121763 = CMW 25403 = CAMS 1158^{T}	*Acacia erioloba*	South Africa	EU101323	EU101368	KX464850	NA
Do. capri-amissi	CBS 121878 = CMW 25404 = CAMS 1159^{T}	*Acacia erioloba*	South Africa	EU101324	EU101369	KX464851	NA
Do. casuarinae	CBS 120688 = CMW 4855^{T}	*Casuarina* sp.	Australia	DQ846773	DQ875331	DQ875340	NA
Do. casuarinae	CBS 120689 = CMW 4856	*Casuarina* sp.	Australia	DQ846772	DQ875332	DQ875339	NA
Do. casuarinae	CBS 120690 = CMW 4857	*Casuarina* sp.	Australia	DQ846774	DQ875333	DQ875341	NA
Do. citricola	CBS 124728 = ICMP 16827	*Citrus sinensis*	New Zealand	EU673322	EU673289	KX464852	NA
Do. citricola	CBS 124729 = ICMP 16828^{T}	*Citrus sinensis*	New Zealand	EU673323	EU673290	KX464853	NA
Do. citrimurotticola	BE5 = CGMCC3.20392^{T}	*Citrus unshiu*	China	MW880663	MW884166	MW884195	NA
Do. citrimurotticola	BE8 = CGMCC3.20394	*Citrus reticulatachen* × *C. sinensis*	China	MW880661	MW884164	MW884193	NA
Do. diospyricola	CBS 145972	*Diospyros mespiliformis*	South Africa	MT587398	MT592110	MT592581	NA
Do. dulcispinae	CBS 121764 = CMW 25406 = CAMS 1159	*Acacia mellifera*	Namibia	EU101299	EU101344	KX464854	NA
Do. dulcispinae	CBS 130413 = CMW 36460^{T}	*Acacia karroo*	South Africa	JQ239400	JQ239387	JQ239373	NA
Do. eriobotryae	CBS 140852^{T}	*Eriobotrya japonica*	Spain	KT240287	KT240262	MT592582	NA
Do. franceschinii	CBS 147722	*Rhamnus alaternus*	Italy	OP999677	OQ067247	NA	NA
Do. guttulata	MFLUCC 17-0242	*Alnus glutinosa*	Italy	KY797637	NA	NA	NA
Do. heterophyllae	CMW 46458^{T}	*Acacia heterophylla*	Réunion	MN103794	MH548348	MH548324	NA
Do. hortiarborum	CFCC 70756^{T}	*Fraxinus chinensis*	China	PP188523	PP723042	PP566662	NA
Do. hortiarborum	CFCC 70757	*Fraxinus chinensis*	China	PP188524	PP723043	PP566663	NA
Do. hortiarborum	CFCC 70758	*Lagerstroemia indica*	China	PP188525	PP723044	PP566664	NA
Do. hortiarborum	CFCC 70759	*Lagerstroemia indica*	China	PP188526	PP723045	PP566665	NA
Do. iberica	CBS 113188 = DA-1	*Quercus suber*	Spain	AY573198	EU673278	EU673097	NA
Do. iberica	CBS 113189 = DE-14	*Quercus ilex*	Spain	AY573199	AY573230	KX464855	NA
Do. iberica	CBS 115041 = CAP 145^{T}	*Quercus ilex*	Spain	AY573202	AY573222	EU673096	NA
Do. irannica	CBS 124722 = CJA 153 = IRAN 1587C^{T}	*Olea europaea*	Iran, Golestan	KC898231	KC898214	KX464856	NA
Do. koae	CMW 48017^{T}	*Acacia koa*	Hawaiian Is.	MH447652	MH548338	MH548327	NA
Do. lampangensis	MFLUCC 18-0232^{T}	Rutaceae	Thailand	MK347758	MK340869	MK412874	NA
Do. longicollis	CBS 122066 = CMW 26164	*Terminalia* sp.	Australia	EU144052	EU144067	KX464857	NA
Do. longicollis	CBS 122067 = CMW 26165	*Lysiphyllum cunninghamii*	Australia	EU144053	EU144068	KX464858	NA
Do. longicollis	CBS 122068 = CMW 26166^{T}	*Lysiphyllum cunninghamii*	Australia	EU144054	EU144069	KF766130	NA
Do. magnoliae	CFCC51563^{T}	*Magnolia grandiflora*	China	KY111247	KY213686	NA	NA
Do. mangifericola	CBS 124727^{T}	*Mangifera indica*	Iran	KC898221	KX464614	NA	NA
Do. mangifericola	IRAN 1584C	*Mangifera indica*	Iran	MT587407	MT592119	NA	NA
Do. moneti	WAC 13154 = MUCC 505^{T}	*Acacia rostellifera*	Australia	EF591920	EF591971	EF591954	NA
Do. neclivorem	DAR 80992^{T}	*Vitis vinifera*	Australia	KJ573643	KJ573640	KJ577551	NA
Do. oblonga	CBS 121765 = CMW 25407 = CAMS 1162^{T}	*Acacia mellifera*	South Africa	EU101300	EU101345	KX464862	NA
Do. oblonga	CBS 121766 = CMW 25408 = CAMS 1163	*Acacia mellifera*	South Africa	EU101301	EU101346	KX464863	NA
Do. obovata	MFLUCC22-0058^{T}	*Pavonia odorata*	Thailand	ON751763	ON799589	ON799591	NA

Species	Strain	Host	Origin	GenBank accession numbers			
				ITS	*tef1-α*	*tub2*	LSU
Do. omnivora	CBS 124717 = CJA 214 = IRAN 1570C	*Juglans regia*	Iran	KC898233	KC898216	KX464865	NA
Do. omnivora	CBS 392.80	–	France	KX464133	KX464626	KX464897	NA
Do. omnivora	CBS 124716 = CJA 241 = IRAN 1573C	*Juglans regia*	Iran	KC898232	KC898215	KX464864	NA
Do. omnivora	CBS 242.51	–	Italy	EU673317	EU673284	EU673105	NA
Do. omnivora	CBS 188.87	*Juglans regia*	France	EU673316	EU673283	EU673119	NA
Do. parva	CBS 124720 = CJA 27 = IRAN 1579C^{T}	*Corylus* sp.	Iran	KC898234	KC898217	KX464866	NA
Do. parva	CBS 124721 = CJA 35	*Corylus* sp.	Iran	KX464123	KX464615	KX464867	NA
Do. parva	CBS 125580	*Corylus avellana*	Austria	KX464124	KX464616	KX464868	NA
Do. plurivora	CBS 124724 = CJA 254 = IRAN 1557C^{T}	*Citrus* sp.	Iran	KC898225	KC898208	KX464874	NA
Do. pretoriensis	CBS 130404 = CMW 36480^{T}	*Acacia karroo*	South Africa	JQ239405	JQ239392	JQ239376	NA
Do. prunicola	CBS 124723 = CAP 187 = IRAN 1541C^{T}	*Prunus dulcis*	Portugal	EU673313	EU673280	EU673100	NA
Do. rhamni	MFLUCC 14-0902^{T}	*Rhamnus cathartica*	South European Russia	MF398893	MF398945	NA	NA
Do. rosulata	CBS 121760 = CMW 25389 = CAMS 1444^{T}	*Acacia karroo*	Namibia	KF766227	EU101335	KX464877	NA
Do. rosulata	CBS 121761 = CMW 25392 = CAMS 1147	*Acacia mellifera*	South Africa	EU101293	EU101338	KX464878	NA
Do. rosulata	CBS 121762 = CMW 25395 = CAMS 1150	*Acacia mellifera*	South Africa	EU101319	EU101364	KX464879	NA
Do. rosulata	CBS 500.72	*Medicago sativa*	South Africa	EU673318	EU673285	EU673118	NA
Do. santali	WAC 13155 = MUCC 509^{T}	*Santalum acuminatum*	Australia	EF591924	EF591975	EF591958	NA
Do. saprophytica	MFLUCC 23-0210	–	Thailand	OR527239	OR532455	OR532454	NA
Do. sarmentorum	IMI 63581b	*Ulmus* sp.	UK: England	AY573212	AY573235	EU673102	NA
Do. sempervirentis	IRAN 1581C = CBS 124719	*Cupressus sempervirens*	Iran	KC898237	KC898220	KX464885	NA
Do. sempervirentis	IRAN 1583C = CBS 124718 = CJA 264^{T}	*Cupressus sempervirens*	Iran	KC898236	KC898219	KX464884	NA
Do. sp.	CBS 121783 = CMW 25432 = CAMS 1187	*Acacia mearnsii*	South Africa	EU101333	EU101378	KX464859	NA
Do. sp.	CBS 121784 = CMW 25430 = CAMS 1185	*Acacia mearnsii*	South Africa	EU101331	EU101376	KX464860	NA
Do. sp.	CBS 121785 = CMW 25433 = CAMS 1188	*Acacia mearnsii*	South Africa	EU101334	EU101379	KX464861	NA
Do. striata	CBS 124730 = ICMP 16819	*Citrus sinensis*	New Zealand	EU673320	EU673287	EU673142	NA
Do. striata	CBS 124731 = ICMP 16824^{T}	*Citrus sinensis*	New Zealand	EU673321	EU673288	EU673143	NA
Do. styphnolobii	Cr01^{T}	*Styphnolobium japonicum*	Crym	MH880849	MK069594	NA	NA
Do. symphoricarpicola	CPC 33923^{T}	*Symphoricarpos*	Italy	MT587414	MT592126	MT592606	NA
Do. tectonae	MFLUCC18-0232^{T}	*Tectona grandis*	Thailand	KM396899	KM409637	KM510357	NA
Do. thailandica	CBS 133991 = CPC 21557 = MFLUCC 11-0438	*Dead bamboo culm*	Thailand	JX646796	JX646861	JX646844	NA
Do. thripsita	CBS 125445 = BRIP 51876a^{T}	*Acacia harpophylla*	Australia	KJ573642	KJ573639	KJ577550	NA
Do. ulmacea	CBS 141414^{T}	*Ulmus laevis*	Germany	MT587415	MT592127	MT592608	NA
Do. uruguayensis	CBS 124908 = CMW 26763^{T}	*Hexachlamis edulis*	Uruguay	EU080923	EU863180	KX464886	NA
Do. vidmadera	CBS 621.74	*Pyrus communis*	Switzerland	KX464129	KX464621	KX464887	NA
Do. vidmadera	CBS 725.79^{T}	*Pyrus malus*	Switzerland	KX464130	KX464622	KX464888	NA
Do. vinea-gemmae	DAR 81012^{T}	*Vitis vinifera*	Australia	KJ573644	KJ573641	KJ577552	NA
Do. viticola	CBS 117009^{T}	*Vitis vinifera*	Spain	AY905554	AY905559	EU673104	NA
Do. westralis	WA10NO01^{T}	*Vitis vinifera*	Australia	HM009376	HM800511	NA	NA
Do. yunnana	CGMCC 3-17999^{T}	*Camellia* sp.	China	KX499643	KX499649	NA	NA
Do. yunnana	CGMCC 3-18000	*Camellia* sp.	China	KX499644	KX499650	NA	NA
Do. zanthoxyli	CMGCC 3.24159^{T}	*Zanthoxylum bungeanum*	Sichuan	OQ190536	OQ241468	OQ275069	NA

Species	Strain	Host	Origin	GenBank accession numbers			
				ITS	*tef1-α*	*tub2*	LSU
Neofusicoccum luteum	CBS 562.92^{T}	*Actinidia deliciosa*	New Zealand	MH862376	KX464690	KX464968	NA
Neofusicoccum parvum	CMW 9081^{T}	*Populus nigra*	New Zealand	AY236943	AY236888	AY236917	NA
Phaeobotryon aplosporum	CFCC 53774	*Syzygium aromaticum*	China	MN215836	MN205996	NA	MN215871
P. aplosporum	CFCC 53775^{T}	*Rhus typhina*	China	MN215837	NA	NA	MN215872
P. aplosporum	CFCC 53776	*Rhus typhina*	China	MN215838	MN205997	NA	MN215873
P. aplosporum	CFCC 58596	*Juglans mandshurica*	China	OQ651169	NA	NA	OQ652540
P. aplosporum	CFCC 58784	*Juglans mandshurica*	China	OQ651170	NA	NA	OQ652541
P. cupressi	CBS 124700 = IRAN 1455C^{T}	*Cupressus sempervirens*	Iran	FJ919672	FJ919661	NA	KX464538
P. cupressi	CBS 124701 = IRAN 1458C	*Cupressus sempervirens*	Iran	FJ919671	FJ919660	NA	KX464539
P. fraxini	CFCC 70762^{T}	*Fraxinus chinensis*	China	PP188527	PP505782	NA	PP177348
P. fraxini	CFCC 70763	*Fraxinus chinensis*	China	PP188528	PP505783	NA	PP177349
P. juniperi	JU001^{T}	*Juniperus formosana*	China	OP941637	OP948218	NA	OP941644
P. juniperi	JU005	*Juniperus formosana*	China	OP941638	OP948219	NA	OP941645
P. mali	XJAU 2930^{T}	*Malus pumila*	China	MW326854	MW509519	NA	MW367101
P. mali	XJAU 2772	*Juglans regia*	China	MW326853	MW509520	NA	MW367094
P. mali	XJAU 2782	*Malus 'Royalty'*	China	MW326852	MW509516	NA	MW367092
P. mali	XJAU 3094	*Elaeagnus angustifolia*	China	MW326858	MW509517	NA	MW367100
P. mali	XJAU 3100	*Rhus typhina*	China	MW326878	MW509518	NA	MW367093
P. mamane	CBS 122980 = CPC 12440^{T}	*Sophora chrysophylla*	USA	EU673332	EU673298	NA	EU673248
P. mamane	CPC 12442	*Sophora chrysophylla*	USA	EU673333	EU673299	NA	DQ377899
P. negundinis	CAA 797	*Acer negundo*	Russia	KX061513	KX061507	NA	NA
P. negundinis	CAA 798	*Ligustrum vulgare*	Russia	KX061514	KX061508	NA	NA
P. negundinis	CAA 799	*Forsythia intermedia*	Russia	KX061515	KX061509	NA	NA
P. negundinis	CPC 33384	*Acer nugundo*	Ukraine	MT587542	MT592276	NA	MT587323
P. negundinis	CPC 33388	*Dead stem*	Ukraine	MT587543	MT592277	NA	MT587324
P. negundinis	CPC 34752	*Acer negundo*	Ukraine	MT587544	MT592278	NA	MT587325
P. negundinis	MFLUCC 15-0436^{T}	*Acer negundo*	Russia	KU820970	KU853997	NA	NA
P. platycladi	CFCC 58799^{T}	*Platycladus orientalis*	China	OQ651172	OQ692930	NA	OQ652543
P. platycladi	CFCC 58800	*Platycladus orientalis*	China	OQ651173	OQ692931	NA	OQ652544
P. rhoinum	CFCC 52449	*Rhus typhina*	China	MH133923	MH133957	NA	MH133940
P. rhoinum	CFCC 52450^{T}	*Rhus typhina*	China	MH133924	MH133958	NA	MH133941
P. rhois	CFCC 89662 = CCTCC AF2014017^{T}	*Rhus typhina*	China	KM030584	KM030598	NA	KM030591
P. rhois	CFCC 89663 = CCTCC AF2014016	*Rhus typhina*	China	KM030585	KM030599	NA	KM030592
P. rhois	CFCC 58679^{T}	*Populus alba* var. *pyramidalis*	China	OQ651171	OQ692929	NA	OQ652542
P. spiraeae	CFCC 53925^{T}	*Spiraea salicifolia*	China	OM049420	NA	NA	OM0049432
P. spiraeae	CFCC 53926	*Spiraea salicifolia*	China	OM049421	NA	NA	OM0049433
P. spiraeae	CFCC 53927	*Spiraea salicifolia*	China	OM049422	NA	NA	OM0049434
P. ulmi	94-13	*Ulmus pumila*	USA	AF243398	NA	NA	NA
P. ulmi	CBS 114123 = UPSC 2552	*Ulmus glabra*	Sweden	MT587539	MT592273	NA	MT587320
P. ulmi	CBS 138854 = CPC 24264^{T}	*Ulmus laevis*	Germany	MT587540	MT592274	NA	MT587321
P. ulmi	CBS 123.30 = ATCC 24443	*Ulmus* sp.	USA	KX464232	KX464766	NA	DQ377861
P. ulmi	CBS 174.63	*Ulmus glabra*	Finland	MT587541	MT592275	NA	MT587322
P. ulmi	CMH 299	*House dust*	USA	KF800390	NA	NA	NA
P. ulmi	PB_11f	*Ulmus glabra*	Poland	MK134682	NA	NA	NA
Alanphillipsia aloeicola	CBS 138896 = CPC 23674^{T}	*Aloe* sp.	South Africa	KP004444	MT592027	NA	KP004472

Result

Phylogenetic analysis

The BLAST results indicated that the 23 isolates resided in *Aplosporella*, *Dothiorella*, and *Phaeobotryon* (14 for *Aplosporella*, 7 for *Dothiorella*, and 2 for *Phaeobotryon*). Separate phylogenetic trees for each of the three genera were constructed in this study.

In *Aplosporella*, the combined ITS and *tef1-α* dataset consists of 944 characters, including alignment gaps (508 for ITS and 436 for *tef1-α*), of which 794 are constant and 60 are variable parsimony uninformative characters. MP analysis with the remaining 90 parsimony-informative characters resulted in one equally parsimonious tree: tree length (TL) = 230; consistency index (CI) = 0.817; retention index (RI) = 0.896; and rescaled consistency index (RC) = 0.732. In ML analysis based on the combined gene dataset, the matrix had 193 distinct alignment patterns. Estimated base frequencies are as follows: A = 0.217607, C = 0.264598, G = 0.259539, T = 0.258256, AC = 2.784746, AG = 2.845183, AT = 1.353935, CG = 1.848853, CT = 4.935430, GT = 1.000000, gamma distribution shape parameter: α = 0.157110, and likelihood value of ln: -2 499.855852. The maximum likelihood (ML) and Bayesian methods (BI) for phylogenetic analyses have the same topology and terminal clades. Fourteen isolates were distributed in *Aplosporella*, aggregated with three known species, *A. javeedii*, *A. yanqingensis*, and *A. ginkgonis*, separately (Fig. 2). The single gene tree for ITS and *tef1-α* of *Aplosporella* is shown in Suppl. material 1.

In *Dothiorella*, sequences of the combined ITS, *tef1-α*, and *tub2* were aligned; the dataset consists of 1,319 characters, including alignment gaps (534 for ITS, 369 for *tef1-α*, and 416 for *tub2*), of which 905 are constant and 107 are variable parsimony uninformative characters. MP analysis with the remaining 307 parsimony-informative characters resulted in one equally parsimonious tree: tree length (TL) = 1,282; consistency index (CI) = 0.477; retention index (RI) = 0.824; and rescaled consistency index (RC) = 0.394. In ML analysis based on the combined gene dataset, the matrix had 601 distinct alignment patterns. Estimated base frequencies are as follows: A = 0.206208, C = 0.312741, G = 0.250328, T = 0.230723, AC = 0.833804, AG = 2.174710, AT = 1.041501, CG = 0.791470, CT = 3.735830, GT = 1.000000, gamma distribution shape parameter: α = 0.215045, and likelihood value of ln: -8 567.497788. Three of the seven isolates were of the known species *Dothiorella acericola*, and the other four isolates formed a separate clade for designation as new species based on phylogenetic analysis (Fig. 3). The single gene tree for ITS, *tef1-α*, and *tub2* of *Dothiorella* is shown in Suppl. material 2.

In *Phaeobotryon*, the combined ITS, LSU, and *tef1-α* dataset consists of 1,394 characters, including alignment gaps (494 for ITS, 333 for LSU, and 567 for *tef1-α*), of which 1,218 are constant and 56 are variable parsimony uninformative characters. MP analysis with the remaining 120 parsimony-informative characters resulted in one equally parsimonious tree: tree length (TL) = 259; consistency index (CI) = 0.799; retention index (RI) = 0.913; and rescaled consistency index (RC) = 0.730. In ML analysis based on the combined gene dataset, the matrix had 239 distinct alignment patterns. Estimated base frequencies are as follows: A = 0.224820, C = 0.266099, G = 0.277247, T = 0.231833, AC = 0.602998, AG = 2.181745, AT = 0.500445, CG = 0.607508, CT = 4.549533, GT = 1.000000, gamma distribution shape parameter: α = 0.020014, and likelihood

value of ln: -3 357.887099. Eight isolates were assigned to *Phaeobotryon*, one isolate aggregated with *P. mali*, and two isolates stood alone, not branching off from known species, representing a new species (Fig. 4). The single gene tree for ITS, LSU, and *tef1-α* of *Phaeobotryon* is shown in Suppl. material 3.

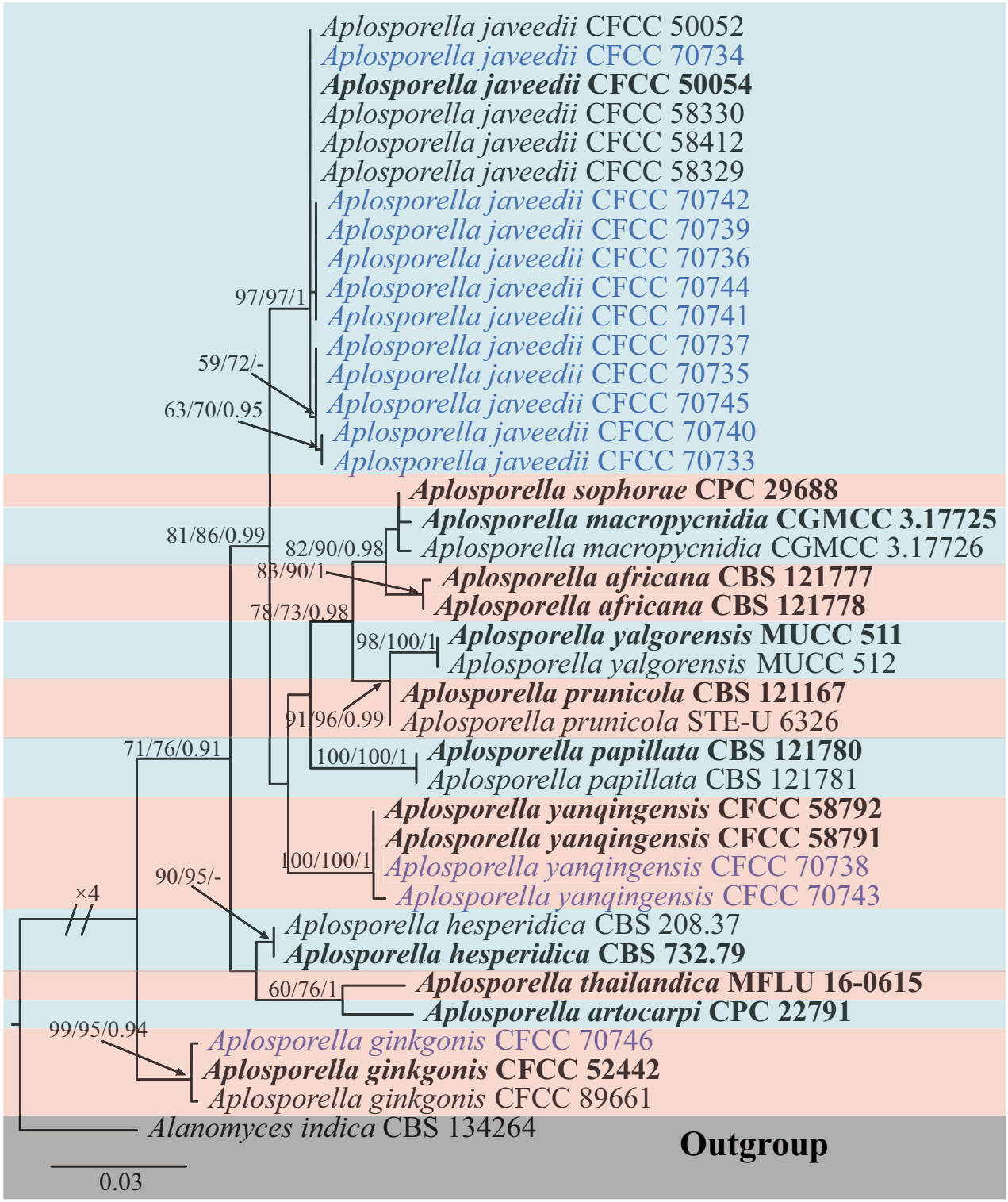

Figure 2. Phylogram generated from RAxML analysis based on ITS with *tef1-α* sequence data of *Aplosporella* isolates. The tree was rooted in *Alanomyces indica* (CBS 134264). The MP, ML (≥ 50%), and BI (≥ 0.9) bootstrap supports are given near the nodes, respectively. Isolates from this study are marked in blue, and ex-type strains are marked in bold.

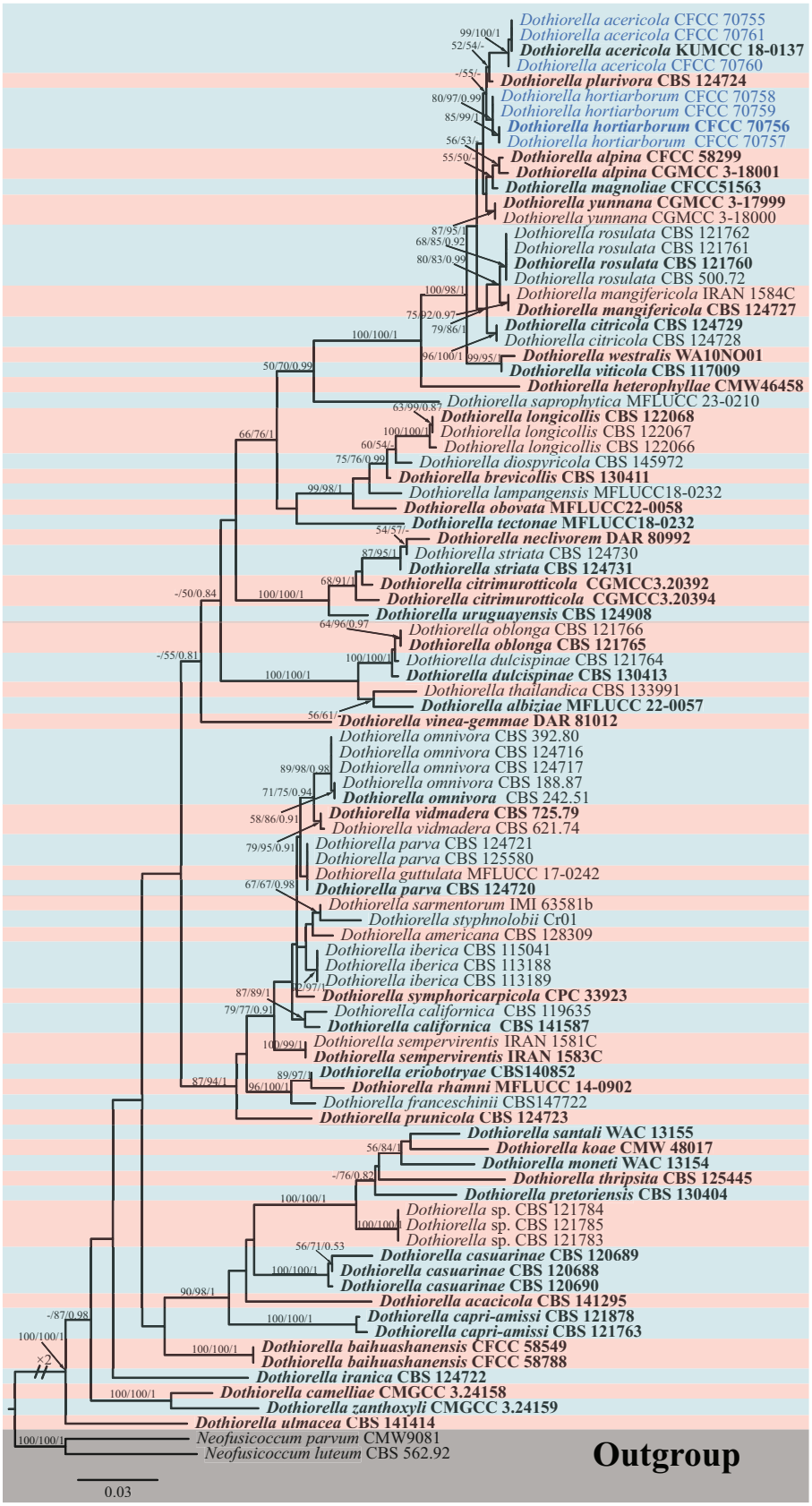

Figure 3. Phylogram generated from RAxML analysis based on ITS, *tef1-α*, and *tub2* sequence data of *Dothiorella* isolates. The tree was rooted in *Neofusicoccum luteum* (CBS 562.92) and *Neofusicoccum parvum* (CMW9081). The MP, ML (≥ 50%), and BI (≥ 0.9) bootstrap supports are given near the nodes, respectively. Isolates from this study are marked in blue, and ex-type strains are marked in bold.

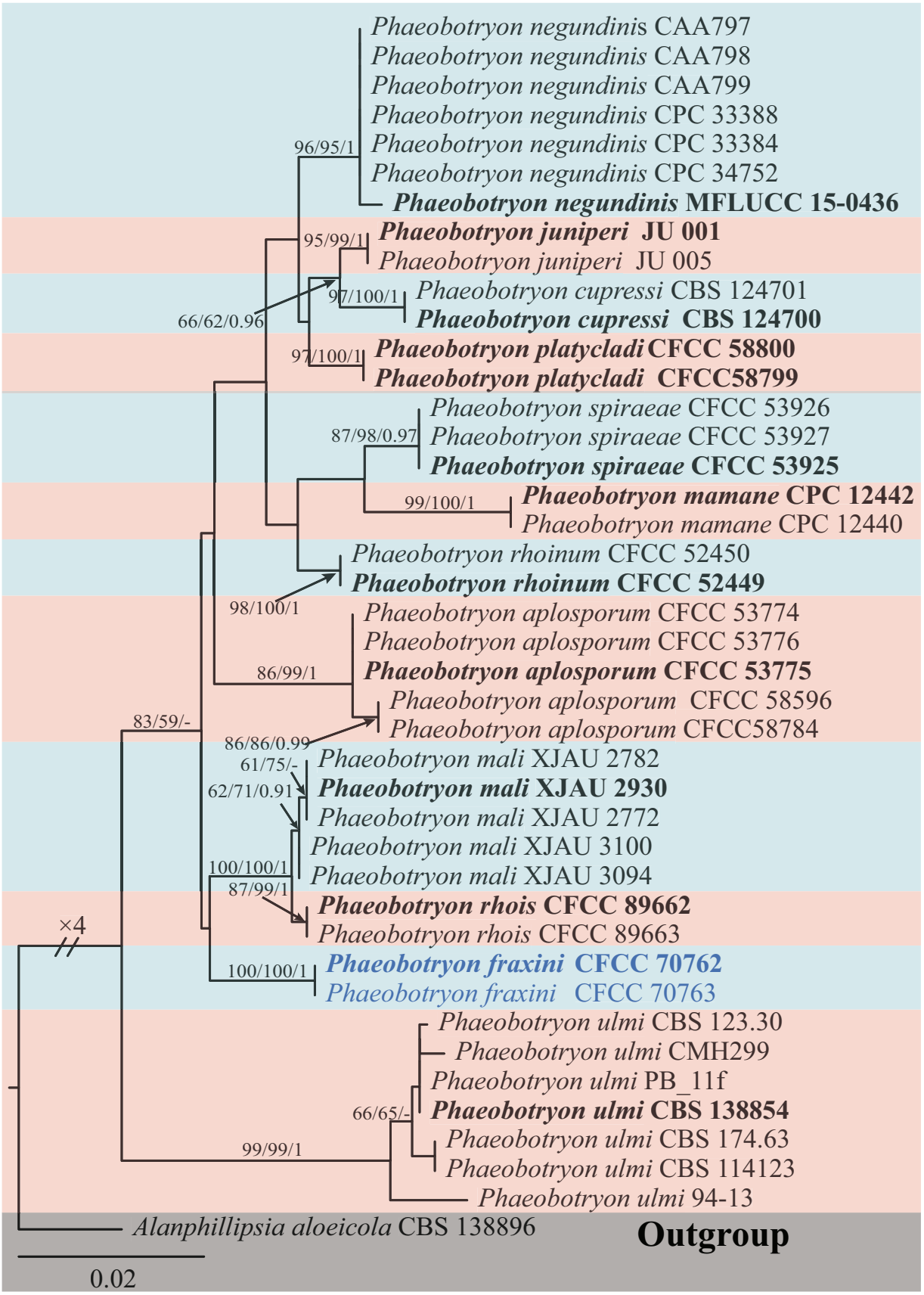

Figure 4. Phylogram generated from RAxML analysis based on ITS, LSU, and *tef1-α* sequence data of *Phaeobotryon* isolates. The tree was rooted in *Alanphillipsia aloeicola* (CBS 138896). The MP, ML (≥ 50%), and BI (≥ 0.9) bootstrap supports are given near the nodes, respectively. Isolates from this study are marked in blue, and ex-type strains are marked in bold.

Taxonomy

Aplosporella ginkgonis C.M. Tian, Z. Du & K.D. Hyde, Mycosphere 8(2): 1249 (2017)

Description. See Du et al. 2017.

Material examined. China, Beijing City, Tongzhou District, Majuqiao Wetland Park, 39°46'12"N, 116°37'12"E, on the disease branches of *Cotinus coggygria* var. *cinereus*, 2 May 2023, Y.Y. Wu, BJFC-S1931, living culture CFCC 70746.

Notes. *Aplosporella ginkgonis* was first reported in Gansu Province, China, causing canker and dieback disease in *Ginkgo biloba* and *Morus alba* (Du et al. 2017). Zhu et al. (2018) and Li et al. (2023) discovered the species on *Rhus typhina* and *Zanthoxylum bungeanum*, respectively, extending its host range. In the present study, one isolate (CFCC 70746) was identified as *A. ginkgonis* based on the phylogenetically highly supported clade with 99% MP, 95% ML, and 0.94 BYPP values (Fig. 2) and morphological characteristics. This is the first report of *A. ginkgonis* on *Cotinus coggygria* var. *cinereus*.

Aplosporella javeedii Jami, Gryzenh., Slippers & M.J. Wingf., Fungal Biology 118(2): 174 (2013)

Description. See Fan et al. 2015.

Material examined. China, Beijing City, Tongzhou District, Hougezhuang Plain Forest, 29°50'24"N, 116°54'00"E, on the dead branches of *Styphnolobium japonicum*, 8 April 2023, C.M. Tian, S.J. Li & Y.Y. Wu, BJFC-S1932, living culture CFCC 70733; *ibid*. on the dead branches of *Forsythia suspensa*, BJFC-S1933, living culture CFCC 70734; *ibid*. on the dead branches of *Forsythia suspensa*, BJFC-S1934, living culture CFCC 70735; *ibid*. on the dead branches of *Ulmus pumila*, BJFC-S1935, living culture CFCC 70736; China, Beijing City, Tongzhou District, Central Green Forest Park, 39°52'16"N, 116°42'04"E, from branches of *Acer truncatum*, 12 April 2023, C.M. Tian, Y.M. Liang, C. Peng, Y. Hu & Y.Y. Wu, BJFC-S1936, living culture CFCC 70737; China, Beijing City, Tongzhou District, Central Green Forest Park, 39°52'16"N, 116°42'04"E, on the dead branches of *Sambucus williamsii*, 19 April 2023, C.M. Tian, C. Peng, R. Yuan, M.W. Zhang & Y.Y. Wu, BJFC-S1937, living culture CFCC 70739; *ibid*. on the dead branches of *Acer miyabei*, BJFC-S1938, living culture CFCC 70740; *ibid*. on the dead branches of *Lagerstroemia indica*, BJFC-S1939, living culture CFCC 70741; *ibid*. on the dead branches of *Xanthoceras sorbifolium*, BJFC-S1940, living culture CFCC 70742; China, Beijing City, Tongzhou District, Majuqiao Wetland Park, 39°46'12"N, 116°37'12"E, from branches of *Syringa vulgaris*, 2 May 2023, Y.Y. Wu, BJFC-S1941, living culture CFCC 70744, *ibid*. on the dead branches of *Ulmus pumila*, BJFC-S1942, living culture CFCC 70745.

Notes. *Aplosporella javeedii* was initially reported on *Celtis africana* and *Searsia lancea* in South Africa (Jami et al. 2014). Fan et al. (2015a) recorded this species in China for the first time, associating it with the canker or dieback disease

of five hosts: *Albizia julibrissin*, *Broussonetia papyrifera*, *Gleditsia sinensis*, *Juniperus chinensis*, and *Styphnolobium japonicum*. *Aplosporella javeedii* is widespread on host plants of more than 10 families (Fan et al. 2015a; Zhu et al. 2018; Pan et al. 2019; Lin et al. 2023a). In this study, we report new host records for this species, including *Acer miyabei*, *Acer truncatum*, *Forsythia suspensa*, *Lagerstroemia indica*, *Sambucus williamsii*, *Syringa vulgaris*, *Ulmus pumila*, and *Xanthoceras sorbifolium*.

Aplosporella yanqingensis **L. Lin & X.L. Fan, MycoKeys 97: 9 (2023)**

Description. See Lin et al. 2023a.

Material examined. China, Beijing City, Tongzhou District, Central Green Forest Park, 39°52'16"N, 116°42'04"E, on the dead branches of *Acer truncatum*, 12 April 2023, C.M. Tian, Y.M. Liang, C. Peng, Y. Hu & Y.Y. Wu, BJFC-S1943, living culture CFCC 70743; *ibid*. BJFC-S1944, living culture CFCC 70738.

Notes. *Aplosporella yanqingensis* was first discovered on the branches of *Platycladus orientalis* in Beijing (Lin et al. 2023a). In this study, the two isolates (CFCC 70738 and CFCC 70743) from *Acer truncatum* formed a clade with 100% MP, 100% ML, and 1.00 BYPP values in the multi-locus phylogenetic tree with *A. yanqingensis* (Fig. 2). Compared with the description of Lin et al. (2023a), this study has shorter conidia and thinner conidiogenous cells (11.0–16.5 × 6.0–9.0 µm vs. 16.0–21.5 × 6.0–9.5 µm and 5.0–20.5 × 1.0–2.0 µm vs. 6.0–13.5 × 2.0–3.0 µm). Thus, these isolates were identified as *A. yanqingensis*, and herewith we are providing a new host record for *A. yanqingensis*, *Acer truncatum*.

Dothiorella acericola **Phookamsak, Tennakoon & K.D. Hyde, Fungal Diversity 95: 78 (2019)**

Description. See Pan et al. 2021.

Material examined. China, Beijing City, Tongzhou District, Hougezhuang Plain Forest, 29°50'24"N, 116°54'00"E, on the dead branches of *Forsythia suspensa*, 8 April 2023, C.M. Tian, S.J. Li & Y.Y. Wu, BJFC-S1948, living culture CFCC 70755; China, Beijing City, Tongzhou District, Majuqiao Wetland Park, 39°46'12"N, 116°37'12"E, on the dead branches of *Ginkgo biloba*, 2 May 2023, Y.Y. Wu, BJFC-S1949, living culture CFCC 70760; *ibid*. on the dead branches of *Syringa oblata*, BJFC-S1950, living culture CFCC 70761.

Notes. Based on phylogenetic analyses (Fig. 3), three isolates in this study clustered with *Dothiorella acericola* and formed a clade with 99% MP, 100% ML, and 1.00 BYPP values. *Dothiorella acericola* is reported to be associated with the canker disease of *Acer palmatum* in China (Phookamsak et al. 2019). Pan et al. (2021, 2023) found that *Do. acericola* infests *Ziziphus jujuba* and *Koelreuteria paniculata* branches. The fungus was also recorded on dead branches of *Euonymus japonicus* (Lin et al. 2023b). This is the first discovery of this fungus in the host families Oleaceae and Ginkgoaceae.

Dothiorella hortiarborum **Y.Y. Wu & C.M. Tian, sp. nov.**
MycoBank No: 851826
Fig. 5

Etymology. "Hort" means "garden," and "arbor" means "tree" in Latin. Collected from *Fraxinus chinensis* and *Lagerstroemia indica*, both of which are landscaping and greening trees.

Holotype. China, Beijing City, Tongzhou District, Central Green Forest Park, 39°52'16"N, 116°42'04"E, on the dead branches of *Fraxinus chinensis*, 19 April 2023, C.M. Tian, C. Peng, R. Yuan, M.W. Zhang & Y.Y. Wu (holotype BJFC-S1951, ex-type cultures CFCC 70756).

Description. ***Sexual morph*****:** Not observed. ***Asexual morph*****:** ***Conidiomata*** pycnidial, scattered to aggregated, immersed to semi-immersed in bark, globose to subglobose, dark gray to black, unilocular, 260–450 µm diam. ***Disc*** black, ovoid, 310–330 µm diam. ***Ostioles*** single, light gray, circular, central, papillate, 30–45 µm diam. ***Locules*** single, black, oval, 100–380 µm, ***Conidiophores*** reduced to conidiogenous cells. ***Conidiogenous cells*****:** hyaline, smooth, thin-walled, holoblastic, cylindrical to subcylindrical, 4.5–11.0 × 2.0–4.0 µm (av. ± S.D.= 6.8 ± 1.3 × 2.9 ± 0.5 µm). ***Conidia*** initially hyaline, then producing light yellow pigmentation, uneven surface, thick-walled, dark brown when matrues, 1-septate, constricted at the septum, smooth, ovoid with a broadly rounded apex, truncate base. 10.0–19.0 × 6.0–11.0 µm (av. ± S.D.= 14.9 ± 2.6 × 8.1 ± 1.0 µm).

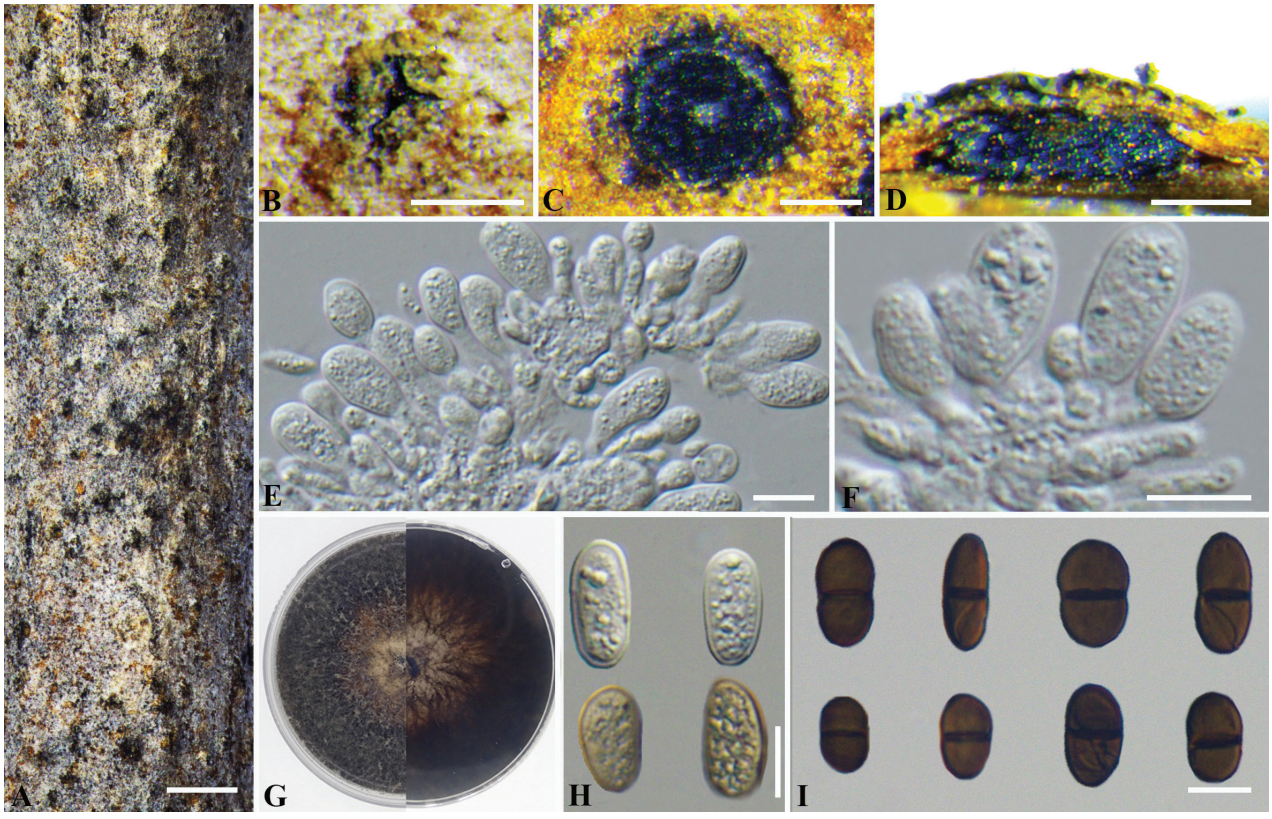

Figure 5. *Dothiorella hortiarborum* (BJFC-S1951) **A, B** habit of conidiomata on branch **C** transverse section of conidioma **D** longitudinal section through conidioma **E, F** conidiogenous cells and conidia **G** top (left) and bottom (right) sides of colonies on potato dextrose agar (PDA) **H, I** conidia. Scale bars: 1000 µm (**A**); 200 µm (**B–D**); 10 µm (**E–F, H–I**).

Culture characters. Colonies on PDA with aerial mycelium gray-green, thick and dense, fluffly, margin with undulate and irregular, reverse with inky blue pigment accumulation, reaching 60 mm diam in 7 days at 25 °C.

Other material examined. China, Beijing City, Tongzhou District, Central Green Forest Park, 39°52'16"N, 116°42'04"E, on the dead branches of *Fraxinus chinensis*, 19 April 2023, C.M. Tian, C. Peng, R. Yuan, M.W. Zhang & Y.Y. Wu, BJFC-S2366, living culture CFCC 70757; China, Beijing City, Tongzhou District, Central Green Forest Park, 39°52'16"N, 116°42'04"E, on the dead branches of *Lagerstroemia indica*, 19 April 2023, C.M. Tian, C. Peng, R. Yuan, M.W. Zhang & Y.Y. Wu, BJFC-S1952, living culture CFCC 70758; *ibid*. BJFC-S2367, living culture CFCC 70759.

Notes. *Dothiorella hortiarborum* formed an independent clade with 87% MP, 97% ML, and 0.99 BYPP values and is distinct from *Do. acericola* and *Do. plurivora* in the multi-locus analyses (Fig. 3). Morphologically, *Do. hortiarborum* can be distinguished from *Do. acericola* by shorter conidia (Phookamsak et al. 2019) and *Do. plurivora* by smaller conidia (10.0–19.0 × 6.0–11.0 µm vs. 22.3–22.7 × 10.8–11.2 µm) (Abdollahzadeh et al. 2014). Additionally, *Do. hortiarborum* differs from *Do. acericola* in *tef1-α* (five bp difference from 170 characters, with 97.1% similarity, including no gaps) sequences, and *Do. plurivora* in *tef1-α* (one bp difference from 254 characters, with 99.6% similarity, including one gap), *tub2* (three bp difference from 370 characters, with 99.2% similarity, including one gap) sequences.

***Phaeobotryon fraxini* Y.Y. Wu & C.M. Tian, sp. nov.**
MycoBank No: 851827
Fig. 6

Etymology. Named after the host, *Fraxinus chinensis*.

Holotype. China, Beijing City, Tongzhou District, Central Green Forest Park, 39°52'16"N, 116°42'04"E, on the dead branches of *Fraxinus chinensis*, 19 April 2023, C.M. Tian, C. Peng, R. Yuan, M.W. Zhang & Y.Y. Wu (holotype BJFC-S1953, ex-type cultures CFCC 70762).

Description. *Sexual morph*: Not observed. ***Asexual morph*: *Conidiomata*** pycnidial, scattered, occasionally aggregated, superficial or immersed, globose, dark brown to black, unilocular, 200–360 µm diam. ***Disc*** inconspicuous. ***Ostioles*** single, brown or black, circular, central, papillate, 40–85 µm diam. ***Locules*** single, globose, 100–170 µm, ***Conidiophores*** reduced to conidiogenous cells. ***Conidiogenous cells*** hyaline, smooth, thin-walled, holoblastic, cylindrical, formed from the cells lining the inner walls of the locules, 7.0–14.0 × 1.0–5.0 µm (av. ± S.D.= 10.6 ± 2.0 × 3.1 ± 0.8 µm). ***Conidia*** initially hyaline, smooth, thin-walled, then gradually producing light yellow pigment, becoming yellow or light brown, occasionally with bubbles, mature with 1-septate, brownish yellow to dark brown, oblong, obtuse, rounded at both ends, 13.0–20.0 × 7.0–10.0 µm (av. ± S.D.= 17.6 ± 1.3 × 8.7 ± 0.7 µm).

Culture characters. Colonies on PDA with aerial gray-white mycelium, thick and dark black at the edge, thin and paler in color in the center, fluffly, entire margin, reverse with black pigment accumulation, reaching 60 mm diam in 7 days at 25 °C.

Other material examined. China, Beijing City, Tongzhou District, Central Green Forest Park, 39°52'16"N, 116°42'04"E, on the dead branches of *Fraxinus chinensis*, 19 April 2023, C.M. Tian, C. Peng, R. Yuan, M.W. Zhang & Y.Y. Wu, BJFC-S2368, living culture CFCC 70763.

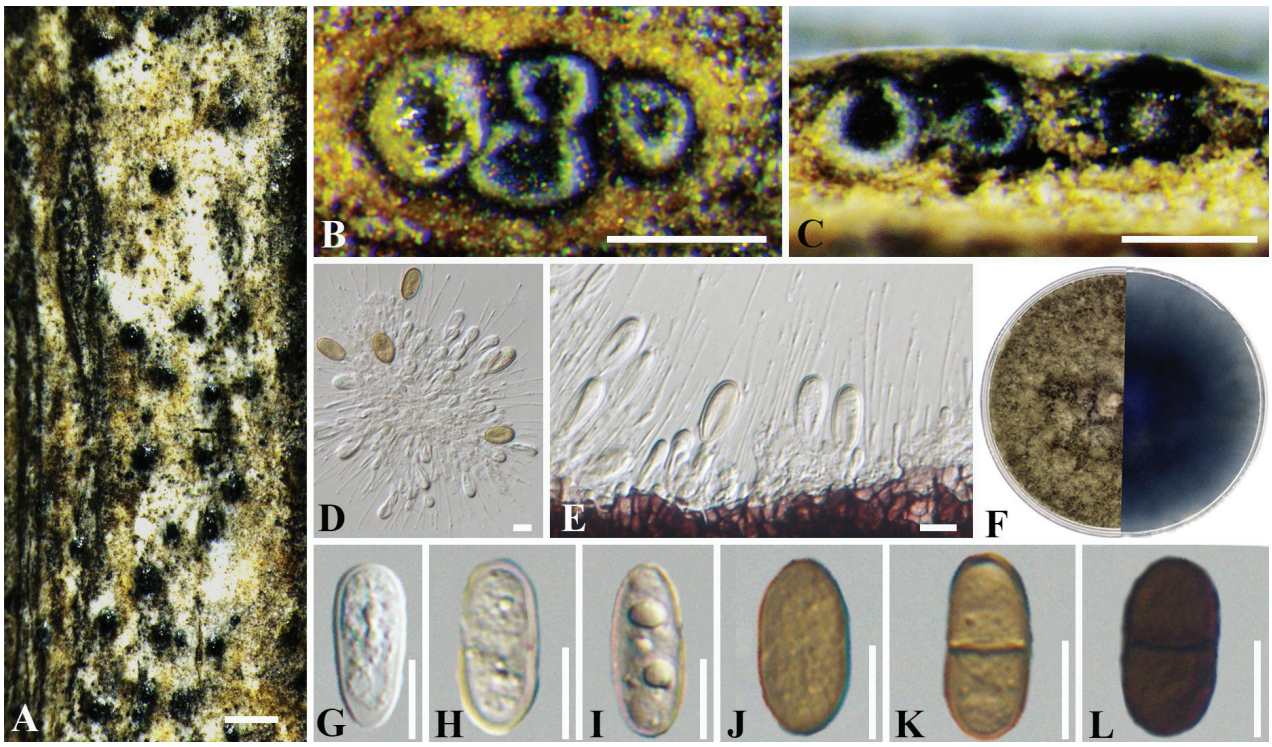

Figure 6. *Phaeobotryon fraxini* (BJFC-S1953) **A** habit of conidiomata on branch **B** transverse section of conidioma **C** longitudinal section through conidioma **D, E** conidiogenous cells and conidia **F** top (left) and bottom (right) sides of colonies on potato dextrose agar (PDA) **G-L** conidia. Scale bars: 500 μm (**A**); 200 μm (**B, C**); 10 μm (**D, E, G–L**).

Notes. Based on multi-locus phylogenetic analysis, the two isolates cluster separately in a high-supported clade with 100% MP, 100% ML, and 1.00 BYPP value (Fig. 4). In the phylogenetic analysis, *Phaeobotryon fraxini* showed a close relationship to *P. mali* and *P. rhois*. These three species could be distinguished based on ITS, *tef1-α*, and LSU loci from *P. mali* by nineteen bp (6/465 in ITS; 10/184 in *tef1-α*; 3/559 in LSU) and *P. rhois* by twenty-two bp (7/465 in ITS; 12/184 in *tef1-α*; 3/559 in LSU). Moreover, *P. fraxini* differs from *P. mali* and *P. rhois* in having smaller conidia (13.0–20.0 × 7.0–10.0 μm vs. 22.0–31.5 × 12–16.5 μm for *P. mali* and 20–25 × 10–12 μm for *P. rhois*) (Fan et al. 2015b; Jia et al. 2023) (Table 3). Therefore, *P. fraxini* is introduced as a novel species.

Table 3. Comparison of species in *Phaeobotryon*.

Species	Host	Location	Conidial size	Septation	Reference
Phaeobotryon aplosporum	*Rhus typhina*	China	17–19 × 5.5–7	aseptate	Pan et al. 2019
P. mali	*Malus pumila*	China	22.0–31.5 × 12–16.5	1-septate	Jia et al. 2023
P. cupressi	*Cupressus sempervirens*	Iran	24.1–25 × 12.2–12.5	1(–2)-septate	Abdollahzadeh et al. 2009
P. fraxini	*Fraxinus chinensis*	China	13–20 × 7–10	1-septate	This study
P. juniperi	*Juniperus formosana*	China	24.5–27.5 × 12.0–13.5	1-septate	Peng et al. 2023
P. mamane	*Sophora chrysophylla*	USA	35–38 × 14–15	1(–2)-septate	Phillips et al. 2008
P. negundinis	*Acer negundo*	Russia	16–24.5 × 7.9–11.5	aseptate	Daranagama et al. 2016
P. platycladi	*Platycladus orientalis*	China	23.0–31.0 × 9.5–12.5	aseptate or 1-septate	Lin et al. 2023a
P. rhoinum	*Rhus typhina*	China	19–21 × 7.5–9	1-septate	Zhu et al. 2018
P. rhois	*Rhus typhina*	China	20–25 × 10–12	1-septate	Fan et al. 2015b
P. spiraeae	*Spiraea salicifolia*	China	23.5–28.5 × 8.5–13.5	aseptate	Jin and Karunarathna 2021
P. ulmi	*Ulmus laevis*	Germany	28.5–32.5 × 16.5–18.5	aseptate or 1-septate	Zhang et al. 2021

Discussion

In this paper, 23 Botryosphaeriales isolates were identified as six species based on multi-locus phylogenetic analyses. These species included two new species, namely *Dothiorella hortiarborum* and *Phaeobotryon fraxini*, and four new hosts: *Aplosporella ginkgonis* on *Cotinus coggygria* var. *cinereus*; *A. javeedii* on *Acer miyabei*; *Acer truncatum*; *Forsythia suspensa*; *Lagerstroemia indica*; *Sambucus williamsii*; *Syringa vulgaris*; *Ulmus pumila*; *Xanthoceras sorbifolium*; *A. yanqingensis* on *Acer truncatum*; and *Do. acericola* on *Forsythia suspensa*; *Ginkgo biloba*; and *Syringa oblata*. The six fungal species identified in this study involve a total of 13 different hosts, which elucidates the wide range of hosts of Botryospaeriales.

Aplosporella is the type genus of Aplosporellaceae (Slippers et al. 2013). The distinctive morphological feature of *Aplosporella* species is that both ascospores and conidia are aseptately hyaline to pigmented (Slippers et al. 2013; Phillips et al. 2019). In this study, a total of three new host record species of the genus were identified, including *A. ginkgonis*, *A. javeedii*, and *A. yanqingensis*. *Aplosporella javeedii* has the highest isolation rate and the widest host range, involving five orders of host plants, including Dipsacales, Fabales, Lamiales, Myrtales, and Rosales. Currently, this species is mainly found in warm temperate and tropical regions (Fan et al. 2015a; Zhu et al. 2018), and further exploration is needed to determine whether the geographic range of *A. javeedii* is related to climate.

Dothiorella was considered a synonym of *Diplodia* based on a broad morphological concept (Crous and Palm 1999). Phillips et al. (2005) compared the morphological characteristics again and found that the conidia of *Dothiorella* were brown, with 1-septate in early development, and the conidia still adhered to the conidiogenous cells. In contrast, the conidia of *Diplodia* become black and septate after being excreted from the conidiomata. Crous et al. (2006) confirmed these morphological differences. Therefore, *Dothiorella* is regarded as an independent genus in the Botryosphaeriaceae. In this study, the conidia of *Do. hortiarborum* are transparent and aseptate when attached to conidiogenous cells. After being released by the conidiomata, the conidia bear yellowish pigment or become brown with a 1-septate. In recent years, many new species of *Dothiorella* have been published with conidial morphology similar to *Do. hortiarborum* (Li et al. 2023; Lin et al. 2023a; Wu et al. 2023). These suggest that the morphological characteristics of *Dothiorella* are not always stable. Thus, it is not accurate to rely solely on the morphology of conidia for *Dothiorella*; combining phylogenetic analysis and the size of conidia of neighboring species is necessary. *Dothiorella* species have been reported on more than 20 host plants in China (https://fungi.ars.usda.gov/). This study has expanded its host range in Oleaceae plants (*Do. acericola* in *Forsythia suspensa*, *Ginkgo biloba* and *S. oblata*, and *Do. hortiarborum* in *Fraxinus chinensis*).

Currently, many *Dothiorella* species have been recorded from *Fraxinus*, distributed mainly in regions such as Europe and North America (Table 4). In this study, a new species, *Do. hortiarborum*, from *F. chinensis*, was introduced in China. However, based on morphological and DNA sequence data, *Do. hortiarborum* shows significant differences from other species in *Fraxinus*. Phylogenetic analysis showed that *Do. hortiarborum* belongs to a different lineage from *Do. omnivora*, *Do.* sp.,

Table 4. Comparison of species from *Fraxinus* in *Dothiorella*.

Specise	Host	Location	Conidial size	Septation	Reference
Dothiorella concaviuscula	*Fraxinus viridis*	USA	4–6 × 2.5–3	no description	Jepson 1896
Do. fraxini	*Fraxinus* sp.	Belgium	26–30 × 12	1-septate	Saccardo 1892
Do. fraxinicola	*Fraxinus* sp.	USA	18–30 × 6–7	no description	Ellis and Everhart 1895
Do. hortiarborum	*Fraxinus chinensis*	China	10.0–19.0 × 6.0–11.0	1-septate	This study
Do. omnivora	*Fraxinus excelsior*	Bosnia	19.3–25.5 × 7.5–10.6	1-septate	Linaldeddu et al. 2016
Do. sp.	*Fraxinus excelsior*	Bosnia, Herzegovina	11–14 × 6–8	2–4-septate	Zlatković et al. 2016
Do. vidmadera	*Fraxinus ornus*	Australia	21.2–21.9 × 9.6–9.8	1-septate	Pitt et al. 2013

and *Do. vidmadera* (Fig. 3), while distinguishing them based on the size of conidia and the number of septates (Table 4). *Do. concaviuscula*, *Do. fraxini*, and *Do. fraxinicola* were not available for sequence information due to their earlier publication; however, *Do. hortiarborum* can also be easily distinguished from them based on their documented conidia size. In addition, *Do. lagerstroemiae* and *Do. hortiarborum* were both isolated from *Lagersiroemia alba*, but its conidia were significantly smaller than *Do. hortiarborum* (8.3–10 × 3.5–4 µm vs. 10.0–19.0 × 6.0–11.0 µm).

Phaeobotryon species have more overlapping morphological characters, with 1(–2) septate or aseptate conidia and similar pigmentation variations. For example, *P. cupressi* and *P. juniperi* have overlapping sizes of conidia (24.1–25 × 12.2–12.5 µm vs. 24.5–27.5 × 12.0–13.5 µm), *P. rhoinum* and *P. rhois* are derived from the same host and geographic origin, and the conidia have 1-septate (Table 3). So, morphology combined with phylogenetics to further clarify the affinities between species is essential. Furthermore, Phaeobotryon species were reported on a variety of hosts and considered to be potential or opportunistic pathogens (Weiland et al. 2016; Zhu et al. 2020; Ilyukhin and Ellouze 2023; Jia et al. 2023). In this study, *P. fraxini* was isolated only from dead *Fraxinus chinensis*; more extensive specimen collection was needed to confirm its distribution characteristics and pathogenicity.

Although Botryosphaeriales recorded many fungi on Index Fungorum (https://www.indexfungorum.org/), only some species are now recognized. Mainly due to the early records of many species, the lack of model specimens, or the low quality of specimens, it is difficult to obtain strains and DNA data. Therefore, more detailed sampling is needed to revise the classification system of related taxa in Botryosphaeriales.

Additional information

Conflict of interest

The authors have declared that no competing interests exist.

Ethical statement

No ethical statement was reported.

Funding

This study is financed by National Natural Science Foundation of China (Project No.: 32371887), Survey of Insect and Pathogen Diversity in Beijing Municipal Administrative Center.

Author contributions

Conceptualization, Yingying Wu and Chengming Tian; data curation, Yingying Wu; funding acquisition, Chengming Tian; investigation, Yingying Wu, Cheng Peng, Rong Yuan, Mingwei Zhang, Yang Hu; project administration, Chengming Tian; resources, Yingying Wu, Cheng Peng, Rong Yuan, Mingwei Zhang, Yang Hu; supervision, Chengming Tian; writing-original draft, Yingying Wu; writing-review and editing, Yingying Wu, Cheng Peng, and Chengming Tian. All authors have read and agreed to the published version of the manuscript.

Author ORCIDs

Yingying Wu https://orcid.org/0009-0007-5095-2738
Rong Yuan https://orcid.org/0009-0006-5597-7531
Chengming Tian https://orcid.org/0000-0002-3352-7664

Data availability

All of the data that support the findings of this study are available in the main text or Supplementary Information.

References

Abdollahzadeh J, Goltapeh EM, Javadi A, Shams-Bakhsh M, Zare R, Phillips AJL (2009) *Barriopsis iraniana* and *Phaeobotryon cupressi*: Two new species of the Botryosphaeriaceae from trees in Iran. Persoonia 23(1): 1–8. https://doi.org/10.3767/003158509X467552

Abdollahzadeh J, Javadi A, Zare R, Phillips AJL (2014) A phylogenetic study of *Dothiorella* and *Spencermartinsia* species associated with woody plants in Iran, New Zealand, Portugal and Spain. Persoonia 32(1): 1–12. https://doi.org/10.3767/003158514X678606

Akinsanmi OA, Daniel R, Shivas R (2019) Introduction to special issue on Botryosphaeriales. Australasian Plant Pathology 48(1): 1–2. https://doi.org/10.1007/s13313-018-0610-8

Carbone I, Kohn LM (1999) A method for designing primer sets for speciation studies in filamentous ascomycetes. Mycologia 91(3): 553–556. https://doi.org/10.1080/00275514.1999.12061051

Crous PW, Palm ME (1999) Reassessment of the anamorph genera *Botryodipoldia. Dothiorella* and *Fusicoccum.* Sydowia 52: 167–175.

Crous PW, Slippers B, Wingfield MJ, Rheeder J, Marasas WF, Philips AJL, Alves A, Burgess T, Barber P, Groenewald JZ (2006) Phylogenetic lineages in the Botryosphaeriaceae. Studies in Mycology 55(1): 235–253. https://doi.org/10.3114/sim.55.1.235

Crous PW, Verkleij GJM, Groenewald JZ, Houbraken J (2019) Westerdijk Laboratory Manual Series No. 1. Fungal biodiversity. CBS Laboratory Manual Series, 2nd edn. Westerdijk Fungal Biodiversity Institute.

Daranagama DA, Thambugala KM, Campino B, Alves A, Bulgakov TS, Phillips AJL, Liu XZ, Hyde KD (2016) *Phaeobotryon negundinis* sp. nov. (Botryosphaeriales) from Russia. Mycosphere : Journal of Fungal Biology 7(7): 933–941. https://doi.org/10.5943/mycosphere/si/1b/2

Dissanayake AJ, Bhunjun CS, Maharachchikumbura SSN, Liu JK (2020) Applied aspects of methods to infer phylogenetic relationships amongst fungi. Mycosphere : Journal of Fungal Biology 11(1): 26532677. https://doi.org/10.5943/mycosphere/11/1/18

Dissanayake AJ, Phillips A, Li X, Hyde KD (2016) Botryosphaeriaceae: Current status of genera and species. Mycosphere : Journal of Fungal Biology 7(7): 1001–1073. https://doi.org/10.5943/mycosphere/si/1b/13

Du Z, Fan XL, Yang Q, Hyde KD, Tian CM (2017) *Aplosporella ginkgonis* (Aplosporellaceae, Botryosphaeriales), a new species isolated from *Ginkgo biloba* in China. Mycosphere 8(2): 1246–1252. http://www.mapress.com/j/pt/. https://doi.org/10.5943/mycosphere/8/2/8

Ellis JB, Everhart BM (1895) New species of fungi from various localities. Proceedings of the Academy of Natural Sciences of Philadelphia: 413–441.

Fan XL, Hyde KD, Liu JK, Liang YM, Tian CM (2015b) Multigene phylogeny and morphology reveal *Phaeobotryon rhois* sp. nov. (Botryosphaeriales, Ascomycota). Phytotaxa 205(2): 90–98. https://doi.org/10.11646/phytotaxa.205.2.2

Fan XL, Qin Y, Cao B, Liang YM, Tian CM (2015a) New record of *Aplosporella javeedii* on five hosts in China based on multi–gene analysis and morphology. Mycotaxon 130(3): 749–756. https://doi.org/10.5248/130.749

Glass NL, Donaldson GC (1995) Development of primer sets designed for use with the PCR to amplify conserved genes from filamentous ascomycetes. Applied and Environmental Microbiology 61(4): 1323–1330. https://doi.org/10.1128/aem.61.4.1323-1330.1995

Guindon S, Dufayard JF, Lefort V, Anisimova M, Hordijk W, Gascuel O (2010) New algorithms and methods to estimate maximum-likelihood phylogenies: Assessing the performance of PhyML 3.0. Systematic Biology 59(3): 307–321. https://doi.org/10.1093/sysbio/syq010

Hillis DM, Bull JJ (1993) An empirical test of bootstrapping as a method for assessing confidence in phylogenetic analysis. Systematic Biology 42(2): 182–192. https://doi.org/10.1093/sysbio/42.2.182

Huelsenbeck JP, Ronquist F (2001) MRBAYES: Bayesian inference of phylogenetic trees. Bioinformatics 17(8): 754–755. https://doi.org/10.1093/bioinformatics/17.8.754

Ilyukhin E, Ellouze W (2023) First report of *Phaeobotryon negundinis* associated with twig and branch dieback of *Malus domestica* trees in southern Ontario, Canada and worldwide. Journal of Plant Pathology 105(1): 355–356. https://doi.org/10.1007/s42161-022-01272-2

Jami F, Slippers B, Wingfeld MJ (2014) Botryosphaeriaceae species overlap on four unrelated, native South African hosts. Fungal Biology 118(2): 168–179. https://doi.org/10.1016/j.funbio.2013.11.007

Jepson WL (1896) Erythea: A Journal of Botany, West American and General. University of California, California 4: 1–200.

Jia H, Li M, Wang C, Ma R (2023) Species diversity of *Phaeobotryon* associated with tree canker and dieback diseases in Xinjiang, China. Forests 14(5): 864. https://doi.org/10.3390/f14050864

Jin XC, Karunarathna SC (2021) Looking for the undiscovered asexual taxa: Case studies from lesser studied life modes and habitats. Mycosphere 12(1): 1290–1333. https://doi.org/10.5943/mycosphere/12/1/17

Katoh K, Rozewicki J, Yamada KD (2019) MAFFT online service: multiple sequence alignment, interactive sequence choice and visualization. Briefings in bioinformatics 20(4): 1160–1166. https://doi.org/10.1093/bib/bbx108

Katoh K, Standley DM (2013) MAFFT multiple sequence alignment software version 7: improvements in performance and usability. Molecular biology and evolution 30(4): 772–780. https://doi.org/10.1093/molbev/mst010

Lawrence DP, Peduto Hand F, Gubler WD, Trouillas FP (2017) Botryosphaeriaceae species associated with dieback and canker disease of bay laurel in northern California with the description of *Dothiorella californica* sp. nov. Fungal Biology 121(4): 347–360. https://doi.org/10.1016/j.funbio.2016.09.005

Li WL, Liang RR, Dissanayake AJ, Liu JK (2023) Botryosphaerialean fungi associated with woody oil plants cultivated in Sichuan Province, China. MycoKeys 97: 71–116. https://doi.org/10.3897/mycokeys.97.103118

Lin L, Bai YK, Pan M, Tian CM, Fan XL (2023a) Morphology and molecular analyses reveal three new species of Botryosphaeriales isolated from diseased plant branches in China. MycoKeys 97: 1–19. https://doi.org/10.3897/mycokeys.97.102653

Lin L, Pan M, Gao H, Tian C, Fan XL (2023b) The potential fungal pathogens of *Euonymus japonicus* in Beijing, China. Journal of Fungi 9(2): 271. https://doi.org/10.3390/jof9020271

Linaldeddu BT, Deidda A, Scanu B, Franceschini A, Alves A, Abdollahzadeh J, Phillips AJL (2016) Phylogeny, morphology and pathogenicity of Botryosphaeriaceae, Diatrypaceae and Gnomoniaceae associated with branch diseases of hazelnut in Sardinia (Italy). European Journal of Plant Pathology 146(2): 259–279. https://doi.org/10.1007/s10658-016-0912-z

Liu JK, Phookamsak R, Doilom M, Wikee S, Li YM, Ariyawansha H, Boonmee S, Chomnunti P, Dai DQ, Jayarama D (2012) Towards a natural classification of Botryosphaeriales. Fungal Diversity 57(1): 149–210. https://doi.org/10.1007/s13225-012-0207-4

Minnis AM, Kennedy AH, Grenier DB, Palm ME, Rossman AY (2012) Phylogeny and taxonomic revision of the Planistromellaceae including its coelomycetous anamorphs: Contributions towards a monograph of the genus *Kellermania.* Persoonia 29(1): 11–28. https://doi.org/10.3767/003158512X658766

Mohali-Castillo SR (2023) A review of Botryosphaeriales in Venezuela with special reference to woody plants. Annals of Forest Research 66(1): 35–62. https://doi.org/10.15287/afr.2023.2492

Pan M, Lin L, Tian CM, Fan XL (2023) Identification and pathogenicity of six fungal species causing canker and dieback disease on golden rain tree in Beijing, China. Mycology 14(1): 37–51. https://doi.org/10.1080/21501203.2022.2096144

Pan M, Tian CM, Fan XL (2021) Two fungal species associated with canker disease of Jujube tree in China. Mycoasia 3: 1–21. https://doi.org/10.59265/mycoasia.2021-03

Pan M, Zhu HY, Bezerra JD, Bonthond G, Tian CM, Fan XL (2019) Botryosphaerialean fungi causing canker and dieback of tree hosts from Mount Yudu in China. Mycological Progress 18(11): 1341–1361. https://doi.org/10.1007/s11557-019-01532-z

Peng C, Shi TY, Xia GC, Tian CM (2023) A new species of *Phaeobotryon* from galls of *Juniperus formosana* branches in China. Journal of Fungal Research 21(1–3): 31–41. https://doi.org/10.13341/j.jfr.2023.0004 [in Chinese]

Phillips AJL, Alves A, Abdollahzadeh J, Slippers B, Wingfield MJ, Groenewald JZ, Crous PW (2013) The Botryosphaeriaceae: Genera and species known from culture. Studies in Mycology 76(1): 51–167. https://doi.org/10.3114/sim0021

Phillips AJL, Alves A, Pennycook S, Johnston P, Ramaley A, Akulov A, Crous PW (2008) Resolving the phylogenetic and taxonomic status of dark–spored teleomorph genera in the Botryosphaeriaceae. Persoonia 21(1): 29–55. https://doi.org/10.3767/003158508X340742

Phillips AJL, Hyde KD, Alves A, Liu JK (2019) Families in Botryosphaeriales: A phylogenetic, morphological and evolutionary perspective. Fungal Diversity 94(1): 1–22. https://doi.org/10.1007/s13225-018-0416-6

Phillips AJL, Rumbos IC, Alves A, Correia A (2005) Morphology and phylogeny of *Botryosphaeria dothidea* causing fruit rot of olives. Mycopathologia 159(3): 433–439. https://doi.org/10.1007/s11046-005-0256-2

Phookamsak R, Hyde KD, Jeewon R, Bhat DJ, Jones EBG, Maharachchikumbura SSN, Raspe´ O, Karunarathna DS, Wanasinghe DN, Hongsanan S, Doilom M, Tennakoon

DS, Machado AR, Firmino AL, Ghosh A, Karunarathna A, Mešić A, Dutta AK, Thongbai B, Devadatha B, Norphanphoun C, Senwanna C, Wei D, Pem D, Ackah FK, Wang G-N, Jiang H-B, Madrid H, Lee HB, Goonasekara ID, Manawasinghe IS, Kušan I, Cano J, Gené J, Li J, Das K, Acharya K, Raj KNA, Latha KPD, Chethana KWT, He M-Q, Dueñas M, Jadan M, Martín MP, Samarakoon MC, Dayarathne MC, Raza M, Park MS, Telleria MT, Chaiwan N, Matočec N, de Silva NI, Pereira OL, Singh PN, Manimohan P, Uniyal P, Shang Q-J, Bhatt RP, Perera RH, Alvarenga RLM, Nogal-Prata S, Singh SK, Vadthanarat S, Oh S-Y, Huang S-K, Rana S, Konta S, Paloi S, Jayasiri SC, Jeon SJ, Mehmood T, Gibertoni TB, Nguyen TTT, Singh U, Thiyagaraja V, Sarma VV, Dong W, Yu X-D, Lu Y-Z, Lim YW, Chen Y, Tkalčec Z, Zhang Z-F, Luo Z-L, Daranagama DA, Thambugala KM, Tibpromma S, Camporesi E, Bulgakov TS, Dissanayake AJ, Senanayake IC, Dai DQ, Tang L-Z, Khan S, Zhang H, Promputtha I, Cai L, Chomnunti P, Zhao R-L, Lumyong S, Boonmee S, Wen T-C, Mortimer PE, Xu J (2019) Fungal diversity notes 929–1035: Taxonomic and phylogenetic contributions on genera and species of fungi. Fungal Diversity 95(1): 1–273. https://doi.org/10.1007/s13225-019-00421-w

Pitt WM, Úrbez-Torres JR, Trouillas FP (2013) *Dothiorella vidmadera*, a novel species from grapevines in Australia and notes on Spencermartinsia. Fungal Diversity 61(1): 209–219. https://doi.org/10.1007/s13225-013-0244-7

Posada D, Crandall KA (1998) Modeltest: Testing the model of DNA substitution. Bioinformatics 14(9): 817–818. https://doi.org/10.1093/bioinformatics/14.9.817

Rannala B, Yang Z (1996) Probability distribution of molecular evolutionary trees: A new method of phylogenetic inference. Journal of Molecular Evolution 43(3): 304–311. https://doi.org/10.1007/BF02338839

Rathnayaka AR, Chethana KT, Phillips AJ, Liu JK, Samarakoon MC, Jones EG, Karunarathna SC, Zhao CL (2023) Re-evaluating Botryosphaeriales: Ancestral state reconstructions of selected characters and evolution of nutritional modes. Journal of Fungi 9(2): 184. https://doi.org/10.3390/jof9020184

Saccardo PA (1880) Conspectus generum fungorum Italiae inferiorum nempe ad Sphaeropsideas, Melanconieas et Hyphomyceteas pertinentium systemate sporologico dispositorum. Michelia 2: 1–38.

Saccardo PA (1892) Sylloge Fungorum omnium hucusque cognitorum. Typis Seminarii, Padua 10: 1–964.

Schoch CL, Shoemaker RA, Seifert KA, Hambleton S, Spatafora JW, Crous PW (2006) A multigene phylogeny of the Dothideomycetes using four nuclear loci. Mycologia 98(6): 1041–1052. https://doi.org/10.1080/15572536.2006.11832632

Senanayake IC, Ross W, Leonardi M, Weir A, McHugh M, Rajeshkumar KC, Verma RK, Karunarathna SC, Tibpromma S, Ashtekar N, Ashtamoorthy SK, Raveendran S, Kour G, Singh A, Peña-Lastra DLP, Mateos A, Kolařík M, Antonín V, Ševčíková H, Esteve-Raventós E, Larsson E, Pancorbo F, Moreno G, Altés A, Turégano Y, Du TY, Lu L, Li QR, Kang JC, Gunaseelan S, Kezo K, Kaliyaperumal M, Fu J, Samarakoon MC, Gafforov Y, Teshaboeva S, Kunjan PC, Chamaparambath A, Flakus A, Etayo J, Rodriguez-Flakus P, Zhurbenko MP, Silva NI, Tennakoon DS, Latha KPD, Manimohan P, Raj KNA, Calabon MS, Ahmadpour A, Heidarian Z, Alavi Z, Alavi F, Ghosta Y, Azizi R, Luo M, Zhao MP, Kularathnage ND, Hua L, Yang YH, Liao CF, Zhao HJ, Lestari AS, Jayasiri SC, Yu FM, Lei L, Liu JW, Karimi O, Tang SM, Sun YR, Wang Y, Zeng M, Htet ZH, Linaldeddu BT, Alves A, Phillips AJL, Bregant C, Montecchio L, Kesel AD, Hustad VP, Miller AN, Fedosova AG, Kučera V, Raza M, Hussain M, Chen YP, Thiyagaraja V, Gomdola D, Rathnayaka AR, Dissanayake AJ, Suwannarach N, Hongsanan S, Maharachchikumbura SSN, Dissanayake LS, Wijayawardene NN, Phookamsak R, Lumyong S, Jones EBG,

Yapa N, Wanasinghe DN, Xie N, Doilom M, Manawasinghe IS, Liu JK, Zhao Q, Xu B, Hyde KD, Song J (2023) Fungal diversity notes 1611–1716: Taxonomic and phylogenetic contributions on fungal genera and species emphasis in south China. Fungal Diversity 122(1): 1–243. https://doi.org/10.1007/s13225-023-00523-6

Silvestro D, Michalak I (2012) raxmlGUI: A graphical front–end for RAxML. Organisms, Diversity & Evolution 12(4): 335–337. https://doi.org/10.1007/s13127-011-0056-0

Slippers B, Boissin E, Phillips AJL, Groenewald JZ, Lombard L, Wingfield MJ, Postma A, Burgess T, Crous PW (2013) Phylogenetic lineages in the Botryosphaeriales: A systematic and evolutionary framework. Studies in Mycology 76(1): 31–49. https://doi.org/10.3114/sim0020

Slippers B, Wingfield MJ (2007) Botryosphaeriaceae as endophytes and latent pathogens of woody plants: Diversity, ecology and impact. Fungal Biology Reviews 21(2–3): 90–106. https://doi.org/10.1016/j.fbr.2007.06.002

Swofford DL (2003) PAUP^* Phylogenetic Analysis Using Parsimony (^* and Other Methods). Version 4. http://paup.csit.fsu.edu/

Tamura K, Stecher G, Peterson D, Filipski A, Kumar S (2013) MEGA6: Molecular evolutionary genetics analysis version 6.0. Molecular Biology and Evolution 30(12): 2725–2729. https://doi.org/10.1093/molbev/mst197

Theissen F, Sydow H (1918) Vorentwürfe zu den Pseudosphaeriales. Annales Mycologici 16:1–34.

Vilgalys R, Hester M (1990) Rapid genetic identification and mapping of enzymatically amplified ribosomal DNA from several *Cryptococcus* species. Journal of Bacteriology 172(8): 4238–4246. https://doi.org/10.1128/jb.172.8.4238-4246.1990

Wang Y, Xie S, Cao J, Zhao H, Yin X, Guo Y, Xu C, Guo L, Wu H, Zhang M (2023) *Lasiodiplodia regiae* sp. nov.: A new species causing canker and dieback of fruit trees in China. Phytopathology 113(7): 1210–1221. https://doi.org/10.1094/PHYTO-06-22-0231-R

Weiland JE, Sniezko RA, Wiseman MS, Serdani M, Putnam ML (2016) First report of *Phaeobotryon cupressi* causing canker of *Calocedrus decurrens* (incense-cedar) in Oregon. Plant Disease 100(8): 1793–1793. https://doi.org/10.1094/PDIS-03-16-0313-PDN

White TJ, Bruns T, Lee S, Taylor JW (1990) Amplification and direct sequencing of fungal ribosomal RNA genes for phylogenetics. In: Innis MA, Gelfand DH, Sninsky JJ, White TJ (Eds) PCR Protocols: a Guide to Methods and Applications. New York. https://doi.org/10.1016/B978-0-12-372180-8.50042-1

Wikee S, Lombard L, Nakashima C, Motohashi K, Chukeatirote E, Cheewangkoon R, McKenzie EHC, Hyde KD, Crous PW (2013) A phylogenetic re–evaluation of *Phyllosticta* (Botryosphaeriales). Studies in Mycology 76(1): 1–29. https://doi.org/10.3114/sim0019

Wu N, Dissanayake AJ, Du HZ, Liu JK (2023) Morpho–phylogenetic evidence reveals novel species and new records of Botryosphaeriaceae in China and Thailand. Journal of Fungi 9(11): 1051. https://doi.org/10.3390/jof9111051

Wyka SA, Broders KD (2016) The new family Septorioideaceae, within the Botryosphaeriales and *Septorioides strobi* as a new species associated with needle defoliation of *Pinus strobus* in the United States. Fungal Biology 120(8): 1030–1040. https://doi.org/10.1016/j.funbio.2016.04.005

Yang T, Groenewald JZ, Cheewangkoon R, Jami F, Abdollahzadeh J, Lombard L, Crous PW (2017) Families, genera, and species of Botryosphaeriales. Fungal Biology 121(4): 322–346. https://doi.org/10.1016/j.funbio.2016.11.001

Zhang W, Groenewald JZ, Lombard L, Schumacher RK, Phillips AJL, Crous PW (2021) Evaluating species in Botryosphaeriales. Persoonia 46(1): 63–115. https://doi.org/10.3767/persoonia.2021.46.03

Zhu HY, Tian CM, Fan XL (2018) Studies of botryosphaerialean fungi associated with canker and dieback of tree hosts in Dongling Mountain of China. Phytotaxa 348(2): 63–76. https://doi.org/10.11646/phytotaxa.348.2.1

Zhu W, Liu X, Liu J, Wang Y, Peng X (2020) Morphological identification of the branch wilt pathogen of *Ulmus pumila* L. Forest Engineering 36(1): 19–24. https://www.researchgate.net/publication/228478725

Zlatković M, Keča N, Wingfield MJ, Jami F, Slippers B (2016) Botryosphaeriaceae associated with the die-back of ornamental trees in the Western Balkans. Antonie van Leeuwenhoek 109(4): 543–564. https://doi.org/10.1007/s10482-016-0659-8

Supplementary material 1

Aplosporella

Authors: Yingying Wu, Cheng Peng, Rong Yuan, Mingwei Zhang, Yang Hu, Chengming Tian

Data type: pdf

Link: https://doi.org/10.3897/mycokeys.106.122890.suppl1

Supplementary material 2

Dothiorella

Authors: Yingying Wu, Cheng Peng, Rong Yuan, Mingwei Zhang, Yang Hu, Chengming Tian

Data type: pdf

Link: https://doi.org/10.3897/mycokeys.106.122890.suppl2

Supplementary material 3

Phaeobotryon

Authors: Yingying Wu, Cheng Peng, Rong Yuan, Mingwei Zhang, Yang Hu, Chengming Tian

Data type: pdf

Link: https://doi.org/10.3897/mycokeys.106.122890.suppl3

MycoKeys 106: 251–264 (2024)
DOI: 10.3897/mycokeys.106.125693

Research Article

Phylogeny and taxonomy of two new species in Dictyosporiaceae (Pleosporales, Dothideomycetes) from Guizhou, China

Yao Feng[1,2], Zuo-Yi Liu[2], Xiao-Fang Chen[3], Mi-Lian Yang[1], Zhi-Yuan Zhang[4], Ya-Ya Chen[5,6]

1 *School of Chinese Ethnic Medicine, Guizhou Minzu University, Guiyang, Guizhou 550025, China*
2 *Guizhou Key Laboratory of Agricultural Biotechnology, Guizhou Academy of Agricultural Sciences, Guiyang, Guizhou 550025, China*
3 *Bijie Medical College, Bijie, Guizhou 551700, China*
4 *College of Eco-Environmental Engineering, Guizhou Minzu University, Guiyang, Guizhou 550025, China*
5 *Institute of Crop Germplasm Resources, Guizhou Academy of Agricultural Sciences, Guiyang, Guizhou 550025, China*
6 *Ministry of Agriculture and Rural Affairs, Key Laboratory of Crop Cenetic Resources and Germplasm Innovation in Karst Region, Guiyang, Guizhou 550009, China*
Corresponding authors: Zhi-Yuan Zhang (zzymetac16@163.com); Ya-Ya Chen (wmlove@163.com)

Abstract

Two novel species within the family Dictyosporiaceae are described and illustrated from terrestrial habitats on dead culms of bamboo and an unidentified plant, respectively. Through morphological comparisons and the multi-locus phylogenetic analyses of combined LSU, ITS, SSU, and *tef1-α* sequence dataset, two species, *Gregarithecium bambusicola*, *Pseudocoleophoma paraphysoidea* are identified. Phylogenetically, both species clustered into a monophyletic clade with strong bootstrap support. *Gregarithecium bambusicola* **sp. nov.** can be distinguished from other species within the genus based on its almost straight ascospores. *Pseudocoleophoma paraphysoidea* **sp. nov.** differs from other species in its conidiogenous cells intermixed with paraphyses, longer conidiogenous cells and larger conidia. The identification of this lineage contributes to our understanding of the classification of Dictyosporiaceae.

Key words: 2 new species, *Gregarithecium*, multi-locus, new taxa, *Pseudocoleophoma*, taxonomy

Academic editor: Kevin D. Hyde
Received: 18 April 2024
Accepted: 9 June 2024
Published: 27 June 2024

Citation: Feng Y, Liu Z-Y, Chen X-F, Yang M-L, Zhang Z-Y, Chen Y-Y (2024) Phylogeny and taxonomy of two new species in Dictyosporiaceae (Pleosporales, Dothideomycetes) from Guizhou, China. MycoKeys 106: 251–264. https://doi.org/10.3897/mycokeys.106.125693

Introduction

Boonmee et al. (2016) established the family Dictyosporiaceae, with the type genus *Dictyosporium*, based on morphology and multi-locus phylogenetic analysis. Members of Dictyosporiaceae are mostly saprobic, globally distributed and commonly found in terrestrial and aquatic habitats (Boonmee et al. 2016, 2021). The main diagnostic criteria of Dictyosporiaceae are immersed to erumpent or superficial, subglobose to globose, dark brown to black ascomata, bitunicate asci with septate, hyaline, sheathed ascospores; the asexual morphs are cheirosporous hyphomycetes (Boonmee et al. 2016; Tennakoon et al. 2019; Hongsanan et al. 2020). Currently, Dictyosporiaceae comprises 18 genera (Hongsanan et al. 2020; Tian et al. 2022; Wijayawardene et al. 2022).

Tanaka et al. (2015) erected the genus *Gregarithecium* and *Pseudocoleophoma* within Dictyosporiaceae, with *Gregarithecium curvisporum* and

Pseudocoleophoma calamagrostidis as the type species, respectively. *Gregarithecium* is characterized by immersed to erumpent, grouped ascomata with fissitunicate, cylindrical, short-stalked asci, broadly fusiform, hyaline ascospore with a median septum, surrounded by an entire sheath (Tanaka et al. 2015; Tennakoon et al. 2019; Lu et al. 2022). *Pseudocoleophoma* is characterized by ostiolar ascomata; brown and polygonal to rectangular cells of peridium; cylindrical to clavate and fissitunicate asci with numerous pseudoparaphyses; fusiform, and septate ascospores, with an apparent sheath (Tanaka et al. 2015; Lu et al. 2022). The asexual morph of *Pseudocoleophoma* is pycnidial, which is characterized by subglobose conidiomata, doliiform and phialidic conidiogenous cells, and cylindrical or oblong, hyaline, aseptate, smooth-walled conidia (Jiang et al. 2021). Currently, only one species is accepted in the genus *Gregarithecium*, while *Pseudocoleophoma* has 13 records listed in Index Fungorum.

In this study, we introduce two new taxa (*Gregarithecium bambusicola* and *Pseudocoleophoma paraphysoidea*) belonging to Dictyosporiaceae, collected from landscape plants in Guizhou Province, China. Morphological observations and phylogenetic analyses were conducted to clarify the classification of these species and their evolutionary relationships with closely related species. Detailed descriptions of the morphological features of these species along with their molecular characterization are provided.

Materials and methods

Sample collection, Fungal isolation and morphological studies

Fresh fungal specimens were collected in Guizhou Province, China. The specimens were examined by using a stereomicroscope (Motic SMZ 168). Freehand sections of ascomata and other fungal structures were photographed using a Nikon ECLIPSE Ni compound microscope fitted with a Nikon DS-Ri2 digital camera. Measurements for all structural components were made with Tarosoft Image FrameWork software (IFW 0.97 version) (Liu et al. 2010). Single spore isolations were carried out following the approaches in Chomnunti et al. (2014). Type specimens were deposited in the herbarium of Guizhou Academy of Agriculture sciences (GZAAS), Guiyang, China. All living cultures were stored in a metabolically inactive state (i.e., kept in sterile 30% glycerol in a –80 °C freezer), which were deposited in Guizhou Culture Collection (GZCC), Guiyang, China. Facesoffungi (http://www.facesoffungi.org/) numbers were obtained as in Jayasiri et al. (2015). The new species are registered in Index Fungorum (2024, http://www.indexfungorum.org/).

DNA extraction, PCR amplification and sequencing

Fungal mycelia were scraped with a surgical knife from the pure culture which was growing on potato dextrose agar (PDA) for one week at 25 °C in dark. The total genomic DNA was conducted by using Ezup Column Fungi Genomic DNA Purification Kit (Sangon Biotech, China) from fresh fungal mycelia. Four gene regions, internal transcribed spacer (ITS), large subunit rDNA (LSU), small subunit rDNA (SSU) and the translation elongation factor 1-alpha (*tef1-α*) were amplified

Table 1. Sequences of primers used in this study.

Molecular marker	Primer name	Primer sequence (5´–3´)	Reference
SSU	NS1	GTAGTCATATGCTTGTCTC	White et al. 1990
	NS4	CTTCCGTCAATTCCTTTAAG	White et al. 1990
ITS	ITS1 (*Gregarithecium*)	TCCGTAGGTGAACCTGCG	White et al. 1990
	ITS4	TCCTCCGCTTATTGATATGC	White et al. 1990
	ITS5 (*Pseudocoleophoma*)	GGAAGTAAAAGTCGTAACAAGG	White et al. 1990
LSU	LR5	ATCCTGAGGGAAACTTC	Vilgalys and Hester 1990
	LR0R	ACCCGCTGAACTTAAGC	Vilgalys and Hester 1990
tef1-α	983F	GCYCCYGGHCAYCGTGAYTTYAT	Rehner and Buckley 2005
	2218R	ATGACACCRACRGCRACRGTYTG	Rehner and Buckley 2005

and sequenced using primers listed in Table 1. Polymerase chain reaction (PCR) was carried out in a 25 µL reaction volume, which contained 12.5 µL 2 × PCR Master Mix (Sangon Biotech, China), 8.5 µL ddH_2O, 1 µL of each primer and 2 µL DNA template. The amplification conditions for all four loci consisted of initial denaturation at 95 °C for 5 min; followed by 35 cycles of 1 min at 94 °C, 1 min at 52 °C, and 1.5 min at 72 °C, and a final extension period of 10 min at 72 °C. PCR products were analyzed using 1.2% agarose electrophoresis gel stained with ethidium bromide and sequenced by Sangon Biotech (Shanghai) Co., Ltd, China. New generated nucleotide sequences were submitted in GenBank (Table 2).

Phylogenetic analyses

Phylogenetic analyses of Dictyosporiaceae were performed based on ITS, LSU, SSU, and *tef1-α* sequence data. The representative taxa of Dictyosporiaceae (Table 2) were referred to BLAST (https://blast.ncbi.nlm.nih.gov/Blast.cgi) result and relevant publications (Lu et al. 2022; Tian et al. 2022). Sequences were aligned using MAFFT v. 7 (Katoh and Standley 2013). Manual adjustments were performed when it is necessary using BioEdit v. 7.0 (Hall 1999). Phylogenetic analyses of maximum likelihood (ML) and Bayesian inference (BI) were conducted based on combined datasets.

ML analysis was performed with raxmlGUI v. 1.3 (Silvestro and Michalak 2012) and the topology was evaluated using 1,000 ultrafast bootstrap replicates. The phylogenetic analyses were performed for Bayesian inference in MrBayes 3.2.6. The model of evolution was estimated by ModelTest 2. The Markov chain Monte Carlo (MCMC) sampling in MrBayes 3.2.6 was used to determine the posterior probabilities (PP). Every 100th generation was sampled as a tree with 1,000,000 generations running for six MCMC chains (Huelsenbeck and Ronquist 2001; Zhaxybayeva and Gogarten 2002; Nylander 2004). Phylogenetic trees were viewed with FigTree v1.4.2 (Rambaut 2012) and edited using Adobe Illustrator 2021 (2.6.0.44) and Adobe Photoshop CS6 software (Adobe Systems, USA).

Results

Phylogenetic analyses

To determine the phylogenetic placement of the new taxa within the family Dictyosporiaceae, a dataset consisting of combined LSU, ITS, SSU, and *tef1-α* sequences was analyzed, including a total of 52 taxa. *Murilentithecium clematidis* (MFLUCC

Table 2. GenBank accession numbers of the sequences used in this study.

Taxa	Voucher/Culture	GenBank accession numbers			
		LSU	ITS	SSU	*tef1-α*
Aquadictyospora clematidis	MFLUCC 17-2080	MT214545	MT310592	MT226664	MT394727
Aquadictyospora lignicola	MFLUCC 17-1318 **T**	MF948629	MF948621	–	MF953164
Aquaticheirospora lignicola	HKUCC 10304	AY736378	AY864770	AY736377	–
Cheirosporium triseriale	HMAS 180703 **T**	EU413954	EU413953	–	–
Dendryphiella fasciculata	MFLUCC 17-1074 **T**	MF399214	MF399213	–	–
Dendryphiella paravinosa	CBS 141286 **T**	KX228309	KX228257	–	–
Dictyocheirospora bannica	KH 332	AB807513	LC014543	–	AB808489
Dictyocheirospora pseudomusae	yone 234	AB807520	LC014550	AB797230	AB808496
Dictyocheirospora rotunda	MFLUCC 14-0293 **T**	KU179100	KU179099	KU179101	–
Dictyosporium appendiculatum	KUMCC 17-0311	MH376715	MH388343	–	–
Dictyosporium digitatum	KUMCC 17-0269	MH376716	MH388344	MH388311	MH388378
Dictyosporium guttulatum	KUMCC 17-0288	MH376717	MH388345	MH388312	MH388379
Dictyosporium hongkongensis	KUMCC 17-0268	MH376718	MH388346	MH388313	MH388380
Digitodesmium chiangmaiense	KUN-HKAS 102163	MK571766	–	MK571775	–
Digitodesmium polybrachiatum	CoAD 3175	MW879317	MW879319	MW879326	–
Digitodesmium polybrachiatum	COAD 3174	MW879316	MW879318	MW879325	–
Gregarithecium bambusicola	**GZCC 21-0713 T**	**PP639379**	**PP639375**	**PP661224**	**PP624323**
Gregarithecium bambusicola	**GZCC 21-1120**	**PP639380**	**PP639376**	**PP661225**	**PP624324**
Gregarithecium curvisporum	KT 922 **T**	AB807547	AB809644	AB797257	AB808523
Immotthia bambusae	KUNHKAS 112012 **T**	MW489450	MW489455	MW489461	MW504646
Jalapriya pulchra	MFLUCC 15-0348 **T**	KU179109	KU179108	KU179110	–
Jalapriya pulchra	MFLUCC 17-1683	MF948636	MF948628	–	MF953171
Murilentithecium clematidis	MFLUCC 14-0561	KM408758	KM408756	–	KM454444
Murilentithecium clematidis	MFLUCC 14-0562 **T**	KM408759	KM408757	NG_061185	KM454445
Neodendryphiella mali	CBS 139.95 **T**	LT906657	LT906655	–	–
Neodigitodesmium cheirosporum	UESTCC 22.0020	ON595713	ON595714	ON595712	ON595700
Pseudocoleophoma bauhiniae	MFLUCC 17-2580	MK347952	MK347735	MK347843	MK360075
Pseudocoleophoma bauhiniae	MFLUCC 17-2586 **T**	MK347953	MK347736	MK347844	MK360076
Pseudocoleophoma calamagrostidis	KT 3284 **T**	LC014609	LC014592	LC014604	LC014614
Pseudocoleophoma clematidis	MFLUCC 17-2177 **T**	NG_073844	MT310596	MT226667	MT394730
Pseudocoleophoma flavescens	CBS 178.93	GU238075	–	GU238216	–
Pseudocoleophoma guizhouensis	MFLU 18-2262	OP099522	OR225073	OR134444	OR140434
Pseudocoleophoma heteropanacicola	ZHKUCC 23-0880 **T**	OR365486	OR365486	–	OR700204
Pseudocoleophoma paraphysoidea	**GZCC 21-0711 T**	**PP639377**	**PP639373**	**PP661222**	**PP624321**
Pseudocoleophoma paraphysoidea	**GZCC 21-0712**	**PP639378**	**PP639374**	**PP661223**	**PP624322**
Pseudocoleophoma polygonicola	KT 731 **T**	AB807546	AB809634	AB797256	–
Pseudocoleophoma puerensis	ZHKUCC 22-0204 **T**	OP297769	OP297799	OP297783	OP321568
Pseudocoleophoma puerensis	ZHKUCC 22-0205	OP297770	OP297800	OP297784	OP321569
Pseudocoleophoma rhapidis	ZHKUCC 21-0124 **T**	ON244661	ON244664	ON244667	–
Pseudocoleophoma rusci	MFLU 16-0292	MT183514	MT185549	MT214983	–
Pseudocoleophoma rusci	MFLUCC 16-1444 **T**	NG_073840	NR_170045	NG_070346	–
Pseudocoleophoma typhicola	MFLUCC 16-0123 **T**	KX576656	KX576655	–	–
Pseudocoleophoma yunnanensis	ZHKUCC 22-0200 **T**	OP297765	OP297795	OP297779	OP321564
Pseudocoleophoma yunnanensis	ZHKUCC 22-0201	OP297766	OP297796	OP297780	OP321565
Pseudocoleophoma zingiberacearum	NCYUCC 19-0054 **T**	MN616755	MN615941	–	MN629283
Pseudoconiothyrium broussonetiae	CPC 33570	NG_066331	NR_163377	–	–
Pseudodictyosporium thailandica	MFLUCC 16-0029 **T**	KX259522	KX259520	–	KX259526
Pseudodictyosporium wauense	NBRC 30078	DQ018105	DQ018098	–	–
Pseudodictyosporium wauense	DLUCC 0801	MF948630	MF948622	–	MF953165
Verrucoccum coppinsii	SPO 2343	MT918765	MT918780	MT918773	–
Verrucoccum hymeniicola	CBS 845.96	AB807567	LC014586	AB797277	AB808543
Vikalpa australiensis	HKUCC 8797 **T**	–	DQ018092	–	–

Notes: "**T**" stands for Ex-type strains. Sequences highlighted in bold were generated in this study.

14-0561 and MFLUCC 14-0562) was used as the outgroup taxa for the analysis. The concatenated alignment comprises 3,376 characters (LSU: 1–803; ITS: 804–1,340; SSU: 1,341–2,338; *tef1-α*: 2,339–3,376) including gaps. Maximum likelihood and Bayesian analyses were performed, respectively, and presented consistent topologies. Bayesian posterior probabilities were calculated with a final average standard deviation of split frequencies of less than 0.01. The best scoring RAxML tree (Fig. 1) was built with a final likelihood value of -18784.512555. Estimated base frequencies were as follows: A = 0.236875, C = 0.246782, G = 0.270789, T = 0.245554; substitution rates AC = 1.688035, AG = 3.527408, AT = 2.540885, CG = 1.033994, CT = 9.137618, GT = 1.000000. The gamma distribution shape parameter alpha is equal to 0.178657 and the Tree-Length equal to 2.160218.

Taxonomy

***Gregarithecium bambusicola* Y. Feng & Z. Y. Liu, sp. nov.**
Index Fungorum: IF901991
Facesoffungi Number: FoF15871
Fig. 2

Etymology. The epithet refers to the species inhabiting on bamboo.

Holotype. GZAAS 21-0199.

Diagnosis. ***Saprobic*** on dead bamboo culms, the surface of the host has a withered spot with a central protrusion. **Sexual morph:** ***Ascomata*** 386–658 × 129–237 µm (av. 487 × 169 µm, n= 10), scattered to gregarious, immersed with only ostiolar necks visible on the host surface or erumpent, globose to hemispherical with flattened base in section. ***Peridium*** composed of several layers of hyaline to dark brown cells of ***textura angularis***. ***Hamathecium*** comprising dense, hyaline, branched and anastomosed, septate pseudoparaphyses. ***Asci*** 75–104 µm × 17–26 µm (av. 91 × 20 µm, n = 10), 8- spored, cylindrical, fissitunicate, rounded at the apex with a shallow ocular chamber, small stalk at the base. ***Ascospores*** 25–27 × 5–7 µm (av. 26 × 6 µm, n = 10), biseriate, fusiform, hyaline, mostly straight, septum and constricted, smooth, guttulate, with a distinct gelatinous sheath. **Asexual morph:** undetermined.

Culture characteristics. ***Ascospores*** germinating on WA within 12 h. Colonies slow growing on PDA at 25 °C, reaching 2 cm diam. in 1 week at 25 °C. Colonies irregular circular, entire edge, white, off-white in reverse.

Material examined. China, Guizhou Province, Xingyi City, on dead culms of bamboo, 2 May 2019, Yao Feng, XY-40 (holotype GZAAS 21-0401, ex-type living culture GZCC 21-1120), *ibid.*, XY-40b (isotype GZAAS21-0401, living culture GZCC21-1120).

Notes. The genus *Gregarithecium* comprises a single species, *G. curvisporum*, which was collected from the culms of *Sasa* sp. (Tanaka et al. 2015). In this study, two new strains clustered in a single clade with high support value (98/1.00), and were closely related to *G. curvisporum* (Fig. 1). *Gregarithecium bambusicola* resembles the type species in having cylindrical asci and transparent fusiform, guttulate ascospores surrounded by an entire sheath (Tanaka et al. 2015). However, unlike the curved ascospores observed in *G. curvisporum*, *G. bambusicola* has predominantly straight ascospores (Tanaka et al. 2015). Furthermore, the ascospores of *G. curvisporum* have three septa after

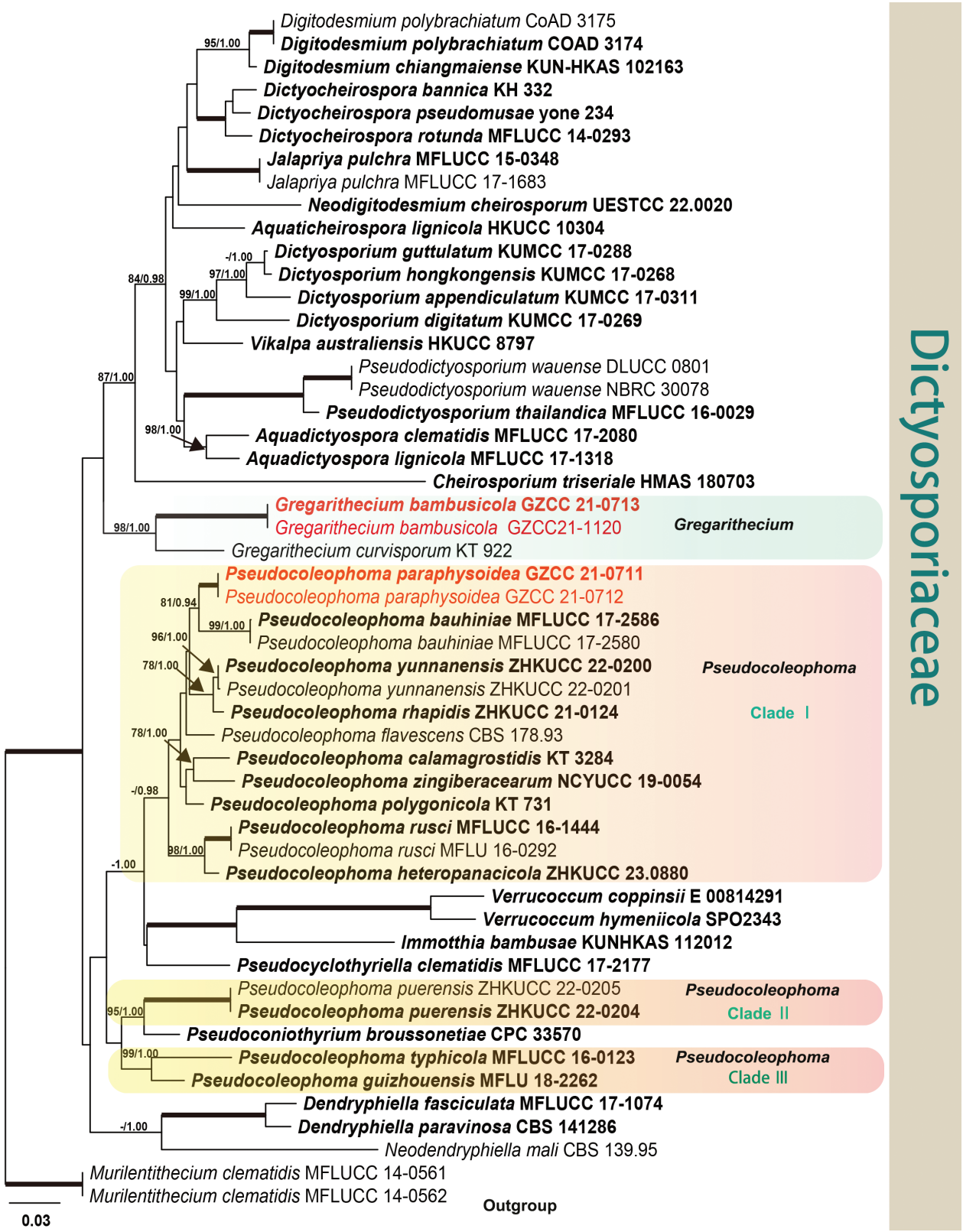

Figure 1. Phylogram based on the maximum likelihood (ML) analysis using the LSU, ITS, SSU, and *tef1-α* sequences of Dictyosporiaceae. Bootstrap support values for ML equal to or greater than 75% and the Bayesian posterior probabilities equal to or higher than 0.95 PP are indicated above the nodes as ML/PP. Ex-type strains are in black bold and the new taxa are highlighted in bold and red.

Figure 2. Morphology of *Gregarithecium bambusicola* (GZAAS 21-0199, holotype) **A, B** appearance of ascomata on host **C** vertical section of ascoma **D** peridium **E** pseudoparaphyses **F–I** asci **J–M** ascospores. Scale bars: 50 µm (**C**); 30 µm (**D**); 20 µm (**F–I**); 10 µm (**E, J–M**).

maturation, which is not seen in *G. bambusicola* (Tanaka et al. 2015). In addition, they can be distinguished by their low sequence similarities. In a comparison of LSU, ITS, SSU, and *tef1-α* nucleotides, *G. bambusicola* (Type strain GZCC 21-0713) has 98%, 87%, 99% and 94% similarity, in LSU (782/800 bp, 2 gaps), ITS (420/484 bp, 5 gaps), SSU (527/534 bp, no gap), and *tef1-α* (780/834 bp, no gap), which is different from *G. curvisporum* (Type strain KT 922).

Pseudocoleophoma paraphysoidea **Y. Feng & Z. Y. Liu, sp. nov.**
Index Fungorum: IF901990
Facesoffungi Number: FoF15872
Fig. 3

Etymology. The epithet refers to the species having paraphyses.

Holotype. GZAAS 21-0197.

Diagnosis. ***Saprobic*** on decaying wood in terrestrial habitats, and immersed in host epidermis. At maturity, the fruiting body breaks through host epidermis. **Sexual morph:** undetermined. **Asexual morph:** ***Conidiomata*** dark brown to black, pycnidial, solitary to gregarious, globose to subglobose, apapillate, ostiolate. ***Conidiomatal wall*** comprising several layers of cells of ***textura angularis***, with inner layers comprising hyaline to dark brown and outer layers composed of dark brown to black cells. ***Conidiogenous cells*** 11–27 × 3–5 µm (av. 21 × 4 µm, n = 20), hyaline, enteroblastic, phialidic, with minute collarette, doliiform, ampulliform, arising from the innermost layer of the pycnidial wall, intermixed with hyaline, filamentous, septate paraphyses. ***Conidia*** 12–15 (–23) × 2–4 µm (av. 14 × 3 µm, n = 30), hyaline, smooth, cylindrical to subcylindrical or fusiform, straight or slightly curved, aseptate, guttulate at both ends.

Culture characteristics. ***Conidia*** germinating on WA within 12 h and germ tubes produced from the basal end. After transfer to the PDA, the colonies grew rapidly, reaching 5 cm diam. in 1 week at 25 °C. Part of the mycelia grew on the surface of the medium, compact, violet, with a light-colored rim, and part of the mycelia remained immersed in the medium. The central area of the colony on the back was reddish-brown, the middle white, and the edge light-colored.

Material examined. China, Guizhou Province, Guiyang City, Guizhou Academy of Agricultural Sciences, on dead culms of an unidentified plant, 18 June 2018, Zuo-Peng Liu, NK-1 (holotype GZAAS 21-0197, ex-type living culture GZCC 21-0711). China, Guizhou Province, Xingyi City, on dead culms of an unidentified plant, 7 August 2019, Yao Feng XY19-13 (paratype GZAAS 21-0198, living culture GZCC 21-0712).

Notes. The multi-locus phylogenetic analyses showed that the new isolates GZCC 21-0711 and GZCC 21-0711 (*Pseudocoleophoma paraphysoidea*) formed a single clade and clustered together with high support value 81/0.94 (Fig. 1). *Pseudocoleophoma paraphysoidea* differs from *P. bauhiniae* in its conidiogenous cells intermixed with paraphyses, longer conidiogenous cells (11–27 × 3–5 µm vs. 2.5–5.5 × 2–3 µm) and larger conidia (12–15 × 2–4 µm vs. 7.5–11 × 2–3 µm) (Jayasiri et al. 2019). In addition, they can be distinguished by their low sequence similarities. In a comparison of LSU, ITS, SSU, and *tef1-α* nucleotides, *P. paraphysoidea* (type strain GZCC 21-0711) has 99%, 97%, 99% and 93% similarity, in LSU (789/795 bp, no gap), ITS (490/503 bp, 2 gaps), SSU

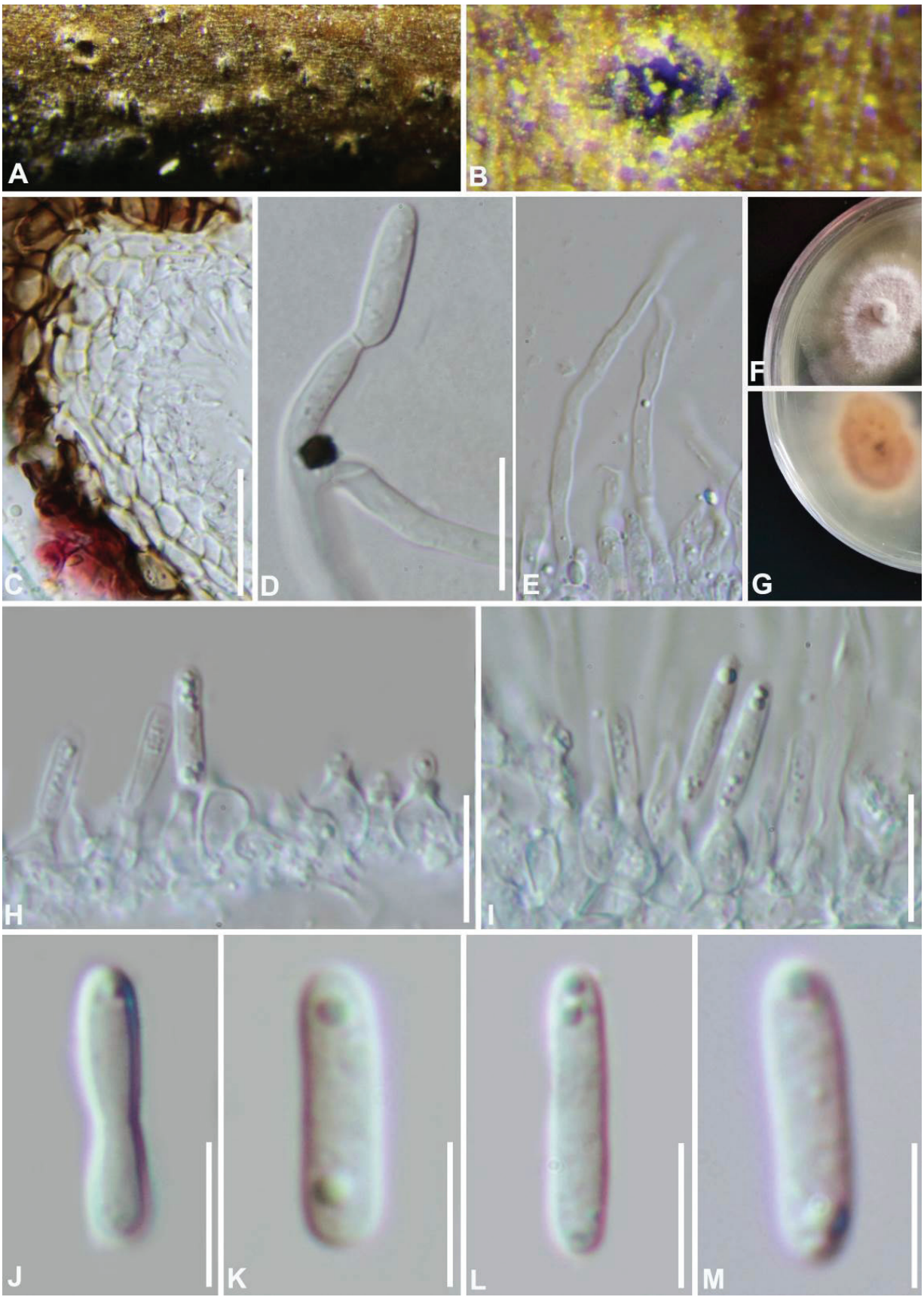

Figure 3. Morphology of *Pseudocoleophoma paraphysoidea* (GZAAS 21-0197, holotype) **A, B** appearance of pycnidia on host **C** peridium **D** germinating conidium **E** paraphyses **F, G** culture **H, I** conidiogenous cells and conidia **J–M** conidia. Scale bars: 20 µm (**C**); 10 µm (**D, H, I**); 5 µm (**J–M**).

(1008/1010 bp, one gap), and *tef1-α* (815/878 bp, no gap), which is different from *P. bauhiniae* (Type strain MLFUCC 17-2586).

Key to the genus *Pseudocoleophoma*

1 Asexual and sexual morph produced **2**
– Asexual or sexual morph produced **3**
2 Ascospores 1-septate, with sheath **4**
– Ascospores 1–3-septate, without sheath ..... ***P. bauhiniae***
3 Asexual morph produced **5**
– Sexual morph produced **6**
4 Ascomata 160–220 × 140–200 µm, scattered ..... ***P. calamagrostidis***
– Ascomata 280–350 × 230–310 µm, scattered to 2–4-gregarious ..... ***P. polygonicola***
5 Conidia aseptate **7**
– Conidia 1-euseptate ..... ***P. typhicola***
6 Ascospores fusiform **8**
– Ascospores narrowly ellipsoid or oblong ..... ***P. puerensis***
7 Conidiomata ostiolate **9**
– Conidiomata apapillate, ostiole **10**
8 Ascospores 1-septate **11**
– Ascospores 3-septate ..... ***P. heteropanacicola***
9 Conidia 20–25 × 10–15 µm, oblong to obovoid ..... ***P. rhapidis***
– Conidia 8–14 × 3–6 µm, cylindrical to subcylindrical or fusiform ..... ***P. rusci***
10 Conidiomata solitary to gregarious **12**
– Conidiomata solitary ..... ***P. zingiberacearum***
11 Ascomata gregarious, scattered; Asci clavate ..... ***P. guizhouensis***
– Ascomata solitary or scattered; Asci clavate to cylindrical, fissitunicate ..... ***P. yunnanensis***
12 Conidiogenous cells globose to doliiform; conidia ellipsoidal ..... ***P. flavescens***
– Conidiogenous cells doliiform, ampulliform; conidia cylindrical to subcylindrical or fusiform ..... ***P. paraphysoidea***

Discussion

In this study, *Gregarithecium bambusicola* and *Pseudocoleophoma paraphysoidea* are described as two new species in Dictyosporiaceae based on phylogenetic analysis and morphological features. The phylogenetic analysis revealed their distinct genetic relationships and their placement within the family Dictyosporiaceae. Dictyosporiaceae has a diverse species distribution in dead leaves of *Alauraceous* tree, leaves of *Citrus sinensis*, submerged wood, soil and other hosts. The discovery of the new species is of great significance to the species diversity, classification and geographical distribution of Dictyosporiaceae.

The genus *Pseudocoleophoma* has 13 species in Index Fungorum. Among these species, four species were described based on the sexual morph (*viz*. *P. guizhouensis*, *P. heteropanacicola*, *P. puerensis*, and *P. yunnanensis*), five species were based on asexual morph (*viz*. *P. flavescens*, *P. typhicola*, *P. rhapidis*, *P. rusci*, and *P. zingiberacearum*), only three species have been reported for both the holomorphs (*viz*. *P. bauhiniae*, *P. calamagrostidis*, and *P. polygonicola*) (Tanaka et al. 2015; Jayasiri et

al. 2019; Jiang et al. 2021). Jiang et al. (2021) synonymized *Pseudocoleophoma clematidis* as *Pseudocyclothyriella clematidis* based on phylogenetic analysis, and transferred *Immotthia* from Teichosporaceae to Dictyosporiaceae.

In our phylogenetic analysis, *Pseudocoleophoma* was divided into three clades (Fig. 1). Clade I comprised ten species (including *P. paraphysoidea*), but with lower support in the phylogenetic tree. Clade II comprises two isolates (ZHKUCC 22-0205 and ZHKUCC 22-0204) of *P. puerensis* and closely related to *Pseudoconiothyrium* (Fig. 1). Furthermore, Clade III is composed of *P. typhicola* and *P. guizhouensis* (Fig. 1). The confusing relationship of these three clades to *Immotthia*, *Verrucoccum*, *Pseudoconiothyrium*, and *Pseudocyclothyriella* demonstrates that *Pseudocoleophoma* is polyphyletic, which are consistent with previous studies (Dong et al. 2023; Zhang et al. 2023).

Morphologically, the species in clade I had morphological features typical of *Pseudocoleophoma*. Clade II includes only one species, *P. puerensis*, which has been reported to have a sexual morphology that is distinct from members of *Pseudocoleophoma* due to its brown spores (Lu et al. 2022). *Pseudocoleophoma typhicola* in clade III is different from members of *Pseudocoleophoma* in its septate conidia (Hyde et al. 2016), but *P. guizhouensis*, a sister clade, has been reported as a sexual morph, which are consistent with *Pseudocoleophoma*. Further research is needed to elucidate the relationship among *Pseudocoleophoma*, *Immotthia*, *Verrucoccum*, *Pseudoconiothyrium*, and *Pseudocyclothyriella*.

Additional information

Conflict of interest

The authors have declared that no competing interests exist.

Ethical statement

No ethical statement was reported.

Funding

This work was financially supported by the Science Research Youth Program in Colleges and Universities (Qiankeji [2022]153), the Foundation of Guizhou in University for Doctoral Research Start-up Project (GZMUZK[2024]QD49), the Bijie Technology Innovation Platform and talent Team (Bikehe [2023] No. 66), the Guizhou Provincial Science and Technology Projects (ZK[2024] 541) and the Funded Project of Guizhou Minzu University (No.GZMUZK[2022]YB16).

Author contributions

The individual contributions are as follows: Yao Feng, Zhi-Yuan Zhang and Ya-Ya Chen conceptualized the study, performed microscopical examinations of fungal specimens, wrote, edited, and reviewed the manuscript. Yao Feng and Zhi-Yuan Zhang conducted phylogenetic studies. Yao Feng wrote, reviewed, and edited the manuscript. Xiao-Fang Chen and Mi-Li-an Yang prepared figures. Ya-Ya Chen and Zuo-Yi Liu reviewed the manuscript and provided funding. All authors have read and agreed to the published version of the manuscript.

Author ORCIDs

Yao Feng https://orcid.org/0000-0002-0888-8775
Zuo-Yi Liu https://orcid.org/0000-0001-5348-8458

Xiao-Fang Chen https://orcid.org/0009-0000-9962-7644
Mi-Lian Yang https://orcid.org/0000-0003-3511-3630
Zhi-Yuan Zhang https://orcid.org/0000-0003-2031-7518
Ya-Ya Chen https://orcid.org/0000-0002-8293-168X

Data availability

All of the data that support the findings of this study are available in the main text.

References

Boonmee S, D'souza MJ, Luo ZL, Pinruan U, Tanaka K, Su H, Bhat DJ, McKenzie EHC, Jones EBG, Taylor JE, Phillips AJL, Hirayama K, Eungwanichayapant PD, Hyde KD (2016) Dictyosporiaceae fam. nov. Fungal Diversity 80(1): 457–482. https://doi.org/10.1007/s13225-016-0363-z

Boonmee S, Wanasinghe DN, Calabon MS, Huanraluek N, Chandrasiri SKU, Jones GEB, Rossi W, Leonardi M, Singh SK, Rana S, Singh PN, Maurya DK, Lagashetti AC, Choudhary D, Dai YC, Zhao CL, Mu YH, Yuan HS, He SH, Phookamsak R, Jiang HB, Martín MP, Dueñas M, Telleria MT, Kałucka IL, Jagodziński AM, Liimatainen K, Pereira DS, Phillips AJL, Suwannarach N, Kumla J, Khuna S, Lumyong S, Potter TB, Shivas RG, Sparks AH, Vaghefi N, Abdel-Wahab MA, Abdel-Aziz FA, Li GJ, Lin WF, Singh U, Bhatt RP, Lee HB, Nguyen TTT, Kirk PM, Dutta AK, Acharya K, Sarma VV, Niranjan M, Rajeshkumar KC, Ashtekar N, Lad S, Wijayawardene NN, Bhat DJ, Xu RJ, Wijesinghe SN, Shen HW, Luo ZL, Zhang JY, Sysouphanthong P, Thongklang N, Bao DF, Aluthmuhandiram JVS, Abdollahzadeh J, Javadi A, Dovana F, Usman M, Khalid AN, Dissanayake AJ, Telagathoti A, Probst M, Peintner U, Garrido-Benavent I, Bóna L, Merényi Z, Boros L, Zoltán B, Stielow JB, Jiang N, Tian CM, Shams E, Dehghanizadeh F, Pordel A, Javan-Nikkhah M, Denchev TT, Denchev CM, Kemler M, Begerow D, Deng CY, Harrower E, Bozorov T, Kholmuradova T, Gafforov Y, Abdurazakov A, Xu JC, Mortimer PE, Ren GC, Jeewon R, Maharachchikumbura SSN, Phukhamsakda C, Mapook A, Hyde KD (2021) Fungal diversity notes 1387–1511: Taxonomic and phylogenetic contributions on genera and species of fungal taxa. Fungal Diversity 111(1): 1–335. https://doi.org/10.1007/s13225-021-00489-3

Chomnunti P, Hongsanan S, Aguirre-Hudson B, Tian Q, Peršohm D, Dhami MK, Alias AS, Xu JC, Liu XZ, Stadler M, Hyde KD (2014) The sooty moulds. Fungal Diversity 66(1): 1–36. https://doi.org/10.1007/s13225-014-0278-5

Dong W, Hyde KD, Jeewon R, Liao CF, Zhao HJ, Kularathnage ND, Li H, Yang YH, Pem D, Shu YX, Gafforov Y, Manawasinghe IS, Doilom M (2023) Mycosphere notes 449–468: Saprobic and endophytic fungi in China, Thailand, and Uzbekistan. Mycosphere: Journal of Fungal Biology 14(1): 2208–2262. https://doi.org/10.5943/mycosphere/14/1/26

Hall TA (1999) BioEdit: A user-friendly biological sequence alignment editor and analysis program for Windows 95/98/NT. Nucleic Acids Symposium Series 41: 95–98.

Hongsanan S, Hyde KD, Phookamsak R, Wanasinghe DN, McKenzie EHC, Sarma VV, Boonmee S, Lücking R, Bhat DJ, Liu NG, Tennakoon DS, Pem D, Karunarathna A, Jiang SH, Jones EBG, Phillips AJL, Manawasinghe IS, Tibpromma S, Jayasiri SC, Sandamali DS, Jayawardena RS, Wijayawardene NN, Ekanayaka AH, Jeewon R, Lu YZ, Dissanayake AJ, Zeng XY, Luo ZL, Tian Q, Phukhamsakda C, Thambugala KM, Dai DQ, Chethana KWT, Samarakoon MC, Ertz D, Bao DF, Doilom M, Liu JK, Pérez-Ortega S, Suija A, Senwanna C, Wijesinghe SN, Konta S, Niranjan M, Zhang SN, Ariyawansa HA, Jiang HB, Zhang JF, Norphanphoun C, de Silva NI, Thiyagaraja V, Zhang H, Bezerra JDP, Miranda-González R, Aptroot A, Kashiwadani H, Harishchandra D, Sérusiaux E, Aluthmuhandiram JVS,

Abeywickrama PD, Devadatha B, Wu HX, Moon KH, Gueidan C, Schumm F, Bundhun D, Mapook A, Monkai J, Chomnunti P, Suetrong S, Chaiwan N, Dayarathne MC, Yang J, Rathnayaka AR, Bhunjun CS, Xu JC, Zheng JS, Liu G, Feng Y, Xie N (2020) Refined families of Dothideomycetes: Dothideomycetidae and Pleosporomycetidae. Mycosphere: Journal of Fungal Biology 11(1): 1553–2107. https://doi.org/10.5943/mycosphere/11/1/13

Huelsenbeck JP, Ronquist F (2001) MRBAYES: Bayesian inference of phylogenetic trees. Bioinformatics (Oxford, England) 17(8): 754–755. https://doi.org/10.1093/bioinformatics/17.8.754

Hyde KD, Hongsanan S, Jeewon R, Bhat DJ, McKenzie EHC, Jones EBG, Phookamsak R, Ariyawansa HA, Boonmee S, Zhao Q, Abdel-Aziz FA, Abdel-Wahab MA, Banmai S, Chomnunti P, Cui BK, Daranagama DA, Das K, Dayarathne MC, de Silva NI, Dissanayake AJ, Doilom M, Ekanayaka AH, Gibertoni TB, Goes Neto A, Huang SK, Jayasiri SC, Jayawardena RS, Konta S, Lee HB, Li WJ, Lin CG, Liu JK, Lu YZ, Luo ZL, Manawasinghe IS, Manimohan P, Mapook A, Niskanen T, Norphanphoun C, Papizadeh M, Perera RH, Phukhamsakda C, Richter C, de Santiago ALCM, Drechsler-Santos ER, Senanayake IC, Tanaka K, Tennakoon TMDS, Thambugala KM, Tian Q, Tibpromma S, Thongbai B, Vizzini A, Wanasinghe DN, Wijayawardene NN, Wu HX, Yang J, Zeng XY, Zhang H, Zhang JF, Bulgakov TS, Camporesi E, Bahkali AH, Amoozegar MA, Araujo-Neta LS, Ammirati JF, Baghela A, Bhatt RP, Bojantchev D, Buyck B, de Silva GA, de Lima CLF, de Oliveira RJV, de Souza CAF, Dai YC, Dima B, Duong TT, Ercole E, Mafalda-Freire F, Ghosh A, Hashimoto A, Kamolhan S, Kang JC, Karunarathna SC, Kirk PM, Kytovuori I, Lantieri A, Liimatainen K, Liu ZY, Liu XZ, Lucking R, Medardi G, Mortimer PE, Nguyen TTT, Promputtha I, Raj KNA, Reck MA, Lumyong S, Shahzadeh-Fazeli SA, Stadler M, Soudi MR, Su HY, Takahashi T, Tangthirasunun N, Uniyal P, Wang Y, Wen TC, Xu JC, Zhang ZK, Zhao YC, Zhou JL, Zhu L (2016) Fungal diversity notes 367–490: Taxonomic and phylogenetic contributions to fungal taxa. Fungal Diversity 80: 1–270. https://doi.org/10.1007/s13225-016-0373-x

Jayasiri SC, Hyde KD, Ariyawansa HA, Bhat DJ, Buyck B, Cai L, Dai YC, Abd-Elsalam KA, Ertz D, Hidayat I, Jeewon R, Jones EBG, Bahkali AH, Karunarathna SC, Liu JK, Luangsa-ard JJ, Lumbsch HT, Maharachchikumbura SSN, McKenzie EHC, Moncalvo JM, Ghobad-Nejhad M, Nilsson H, Pang K, Pereira OL, Phillips AJL, Raspé O, Rollins AW, Romero AI, Etayo J, Selçuk F, Stephenson SL, Suetrong S, Taylor JE, Tsui CKM, Vizzini A, Abdel-Wahab MA, Wen TC, Boonmee S, Dai DQ, Daranagama DA, Dissanayake AJ, Ekanayaka AH, Fryar SC, Hongsanan S, Jayawardena RS, Li WJ, Perera RH, Phookamsak R, De Silva NI, Thambugala KM, Tian Q, Wijayawardene NN, Zhao RL, Zhao Q, Kang JC, Promputtha I (2015) The Faces of Fungi database: Fungal names linked with morphology, phylogeny and human impacts. Fungal Diversity 74(1): 3–18. https://doi.org/10.1007/s13225-015-0351-8

Jayasiri SC, Hyde KD, Jones EBG, McKenzie EHC, Jeewon R, Phillips AJL, Bhat DJ, Wanasinghe DN, Liu JK, Lu YZ, Kang JC, Xu J, Karunarathna SC (2019) Diversity, morphology and molecular phylogeny of Dothideomycetes on decaying wild seed pods and fruits. Mycosphere: Journal of Fungal Biology 10(1): 1–186. https://doi.org/10.5943/mycosphere/10/1/1

Jiang HB, Jeewon R, Karunarathna SC, Phukhamsakda C, Doilom M, Kakumyan P, Suwannarach N, Phookamsak R, Lumyong S (2021) Reappraisal of *Immotthia* in Dictyosporiaceae, Pleosporales: Introducing *Immotthia bambusae* sp. nov. and *Pseudocyclothyriella clematidis* comb. et gen. nov. based on morphology and phylogeny. Frontiers in Microbiology 12: 656235. https://doi.org/10.3389/fmicb.2021.656235

Katoh K, Standley DM (2013) MAFFT multiple sequence alignment software version 7: Improvements in performance and usability. Molecular Biology and Evolution 30(4): 772–780. https://doi.org/10.1093/molbev/mst010

Liu JK, Chomnunti P, Cai L, Phookamsak R, Chukeatirote E, Jones EBG, Moslem M, Hyde KD (2010) Phylogeny and morphology of *Neodeightonia palmicola* sp. nov. from palms. Sydowia 62(2): 261–276. https://doi.org/10.1016/j.riam.2010.07.001

Lu L, Karunarathna SC, Dai D-Q, Xiong Y-R, Suwannarach N, Stephenson SL, Elgorban AM, Al-Rejaie S, Jayawardena RS, Tibpromma S (2022) Description of four novel species in Pleosporales associated with coffee in Yunnan, China. Journal of Fungi (Basel, Switzerland) 8(10): 1113. https://doi.org/10.3390/jof8101113

Nylander JAA (2004) MrModeltest v2. Program distributed by the author. Evolutionary Biology Centre, Uppsala University.

Rambaut A (2012) FigTree, version 1.4. 2. University of Edinburgh, Edinburgh.

Rehner SA, Buckley E (2005) A *Beauveria* phylogeny inferred from nuclear ITS and EF1-α sequences: Evidence for cryptic diversification and links to *Cordyceps* teleomorphs. Mycologia 97(1): 84–98. https://doi.org/10.3852/mycologia.97.1.84

Silvestro D, Michalak I (2012) raxmlGUI: A graphical front-end for RAxML. Organisms, Diversity & Evolution 12(4): 335–337. https://doi.org/10.1007/s13127-011-0056-0

Tanaka K, Hirayama K, Yonezawa H, Sato G, Toriyabe A, Kudo H, Hashimoto A, Matsumura M, Harada Y, Kurihara Y, Shirouzu T, Hosoya T (2015) Revision of the Massarineae (Pleosporales, Dothideomycetes). Studies in Mycology 82(1): 75–136. https://doi.org/10.1016/j.simyco.2015.10.002

Tennakoon D, Bhat D, Kuo C, Hyde KD (2019) Leaf litter saprobic Dictyosporiaceae (Pleosporales, Dothideomycetes): *Pseudocoleophoma zingiberacearum* sp. nov. from *Hedychium coronarium*. Kavaka 53: 1–7. https://doi.org/10.36460/Kavaka/53/2019/1-7

Tian WH, Chen YP, Sajeewa Maharachchikumbura S (2022) *Neodigitodesmium*, a novel genus of family Dictyosporiaceae from Sichuan Province, China. Phytotaxa 559(2): 176–184. https://doi.org/10.11646/phytotaxa.559.2.6

Vilgalys R, Hester M (1990) Rapid genetic identification and mapping of enzymatically amplified ribosomal DNA from several *Cryptococcus* species. Journal of Bacteriology 172(8): 4238–4246. https://doi.org/10.1128/jb.172.8.4238-4246.1990

White TJ, Bruns T, Lee S, Taylor J (1990) Amplification and direct sequencing of fungal ribosomal RNA genes for phylogenetics. In: Innis MA, Gelfand DH, Sninsky JJ, White TJ (Eds) PCR protocols: a guide to methods and applications, Academic Press, San Diego, 315–322. https://doi.org/10.1016/B978-0-12-372180-8.50042-1

Wijayawardene N, Hyde KD, Dai D, Sánchez-García M, Goto B, Saxena R, Erdogdu M, Selçuk F, Rajeshkumar K, Aptroot A, Błaszkowski J, Boonyuen N, da Silva GA, de Souza FA, Dong W, Ertz D, Haelewaters D, Jones EBG, Karunarathna SC, Kirk PM, Kukwa M, Kumla J, Leontyev DV, Lumbsch HT, Maharachchikumbura SSN, Marguno F, Martínez-Rodríguez P, Mešić A, Monteiro JS, Oehl F, Pawłowska J, Pem D, Pfliegler WP, Phillips AJL, Pošta A, He MQ, Li JX, Raza M, Sruthi OP, Suetrong S, Suwannarach N, Tedersoo L, Thiyagaraja V, Tibpromma S, Tkalčec Z, Tokarev YS, Wanasinghe DN, Wijesundara DSA, Wimalaseana SDMK, Madrid H, Zhang GQ, Gao Y, Sánchez-Castro I, Tang LZ, Stadler M, Yurkov A, Thines M (2022) Outline of Fungi and fungus-like taxa – 2021. Mycosphere: Journal of Fungal Biology 13(1): 53–453. https://doi.org/10.5943/mycosphere/13/1/2

Zhang JF, Liu JK, Hyde KD, Chen YY, Ran HY, Liu ZY (2023) Ascomycetes from karst landscapes of Guizhou Province, China. Fungal Diversity 122(1): 1–160. https://doi.org/10.1007/s13225-023-00524-5

Zhaxybayeva O, Gogarten JP (2002) Bootstrap, Bayesian probability and maximum likelihood mapping: Exploring new tools for comparative genome analyses. BMC Genomics 3(1): 4. https://doi.org/10.1186/1471-2164-3-4

MycoKeys 106: 265–285 (2024)
DOI: 10.3897/mycokeys.106.125920

Research Article

Pezizomycotina species associated with rotten plant materials in Guizhou Province, China

Shamin Fu[1,2,3], Jing-E Sun[2,3], Entaj Tarafder[2,4], Nalin N. Wijayawardene[5], Yan Hu[6], Yong Wang[2,4], Yan Li[1]

1 *The Key Laboratory of Plant Resources Conservation and Germplasm Innovation in Mountainous Region (Ministry of Education), College of Life Sciences/ Institute of Agro-Bioengineering, Guizhou University, Guiyang 550025, China*
2 *College of Agriculture, Guizhou University, Guiyang Guizhou 550025, China*
3 *Guizhou Zhunongjia Agricultural Science and Technology Service Co., Ltd, Guiyang, Guizhou 550025, China*
4 *Institute of Plant Health and Medicine, College of Agriculture, Guizhou University, Guiyang Guizhou 550025, China*
5 *Center for Yunnan Plateau Biological Resources Protection and Utilization, College of Biological Resource and Food Engineering, Qujing Normal University, Qujing, Yunnan 655011, China*
6 *Weining Branch, Bijie Tobacco Company, Bijie, 553100, China*

Corresponding authors: Yan Li (yli@gzu.edu.cn); Yong Wang (yongwangbis@aliyun.com)

Abstract

Nine Pezizomycotina strains were isolated from rotten dead branches and leaves collected from Guizhou Province. To obtain their accurate taxonomic placement, we provided the morphological characteristics of conidiophore cells and conidia. Phylogenetic relationships, based on ITS, *rpb2*, SSU, LSU and *tub2* gene sequences, confirmed our strains represented three novel species, *Peglionia falcata*, *Neoascochyta pseudofusiformis* and *Neomicrosphaeropsis cylindrica*. *Peglionia falcata* produced falcate conidia and *Neoa. pseudofusiformis* generated fusiform conidia, while *Neom. cylindrica* possessed cylindrical conidia. The phylogenetic results also supported them as novel taxa. All the new species in the present study were found as saprophytic on forest litter with high rainfall, which suggest they may have a certain effect on nutrient decomposition and redistribution in forest ecosystems. Thus, it opened a way for further research on related ecological roles and their application production.

Key words: Ascomycota, morphology, phylogeny, taxonomy, three new taxa

Academic editor:
Chayanard Phukhamsakda
Received: 22 April 2024
Accepted: 12 June 2024
Published: 27 June 2024

Citation: Fu S, Sun J-E, Tarafder E, Wijayawardene NN, Hu Y, Wang Y, Li Y (2024) Pezizomycotina species associated with rotten plant materials in Guizhou Province, China. MycoKeys 106: 265–285. https://doi.org/10.3897/mycokeys.106.125920

Introduction

Pezizomycotina is the largest subphylum of Ascomycota (Spatafora et al. 2006; Wijayawardene et al. 2022a), which is large and diverse (the 10th edition of Ainsworth & Bisby's Dictionary of the Fungi estimates close to 70,000 Pezizomycetes species) (Charley and David 2017). These taxa often exist as saprophytes fed by herbivore faeces or grow on woody and non-woody plant tissues. However, some can also be pathogenic to some plants and animals or symbiotic with some plants as endophytes (Money 2016). Fungal studies, related to ascomycetous taxa have been extensively carried out in China and many novel taxa are introduced annually (Hyde et al. 2016; Wijayawardene et al. 2022b).

The genus *Peglionia* (Goidànich 1934) is distinguished from *Circinotrichum* and *Gyrothrix* by the branching pattern of the setae (Hernández-Restrepo et al. 2022). According to Hernández-Restrepo et al., *Gyrothrix verticiclada* (CBS 127654 phenotype, CBS 140226 and CBS 148329) clustered with *G. hughesii* in the phylogenetic tree as a distinct branch, which were defined as a new genus (*Peglionia*) (Hernández-Restrepo et al. 2022). *Peglionia verticiclada* (type species) is characterised by the production of curved conidia and setae with verticillate and straight branches at the apex and never circinate as in *Circinotrichum*, *Gyrothrix* or other members of Xylariales. In terms of morphological characteristics, the conidiogenous cells of *Peglionia* vary from inverted clavate to lagenate, appearing hyaline or subhyaline. The conidia are attached to the tips of the conidiogenous cells, presenting a dry sickle shape, without septa and presenting hyaline (Hernández-Restrepo et al. 2022).

Neomicrosphaeropsis (Didymellaceae) was introduced by Thambugala et al. (2017) based on morphology and molecular data; meanwhile, *Phoma tamaricicola* were recollected and accommodated to *Neomicrosphaeropsis*. There are currently 11 epithets in the genus *Neomicrosphaeropsis* in Mycobank (www.mycobank.org), but *Neom. cystisi*, *Neom. cystisicola*, *Neom. cytisina* and *Neom. minima* have been transferred to *Microsphaeropsis* (Wijayawardene et al. 2022b). This genus contains some pathogens or endophytes (Wijayawardene et al. 2017). In terms of morphological features, the conidiophores of the genus *Neomicrosphaeropsis* appear pustulate, almost submerged in agar and slightly vesicular. The outer wall of the conidiophore ranges from light to dark brown. Conidiogenous cells are cylindrical, appear hyaline, have a smooth surface and are aggregated singly or in multiples. Conidia are hyaline to light brown, with a smooth outer wall and are ovate to ellipsoid (Thambugala et al. 2017).

Chen et al. (2015) introduced *Neoascochyta* to accommodate taxa that morphologically resemble to *Ascochyta*, but phylogenetically distinct. *Neoascochyta* belongs to the Didymellaceae family and species in this family are primarily parasitic on wood and dead herbaceous stems or leaves (Hyde et al. 2013). Currently, 20 *Neoascochyta* species have been listed in MycoBank database (2024). This genus is morphologically characterised by pseudothecial ascomata, cylindrical to subclavate asci, cylindrical to ovoid, hyaline 1-septate ascospores. The asexual morph is coelomycetous and is characterised by pycnidial conidiomata, pseudoparenchymatous wall, obpyriform or ampulliform to doliiform conidiogeneous cells and hyaline fusoid to cylindrical, obclavate-ovoid to ellipsoidal conidia (Chen et al. 2015).

The purpose of this study was to introduce three new Pezizomycotina taxa collected in Guizhou Province, viz. *Peglionia falcata*, *Neoascochyta pseudofusiformis* and *Neomicrosphaeropsis cylindrica*. The present study was of great significance to enrich the diversity of Pezizomycotina in southwest China on the basis of morphological description and phylogeny combined with ITS, LSU, *tub2* and *rpb2* sequence data analysis. Meanwhile, since all three new species identified are saprophytic fungi, which play an important role in the process of organic matter decomposition, they can be further studied for their ecological effects, which will provide an important theoretical and practical basis for relevant applied research and potential value exploration, based on their roles in natural ecosystems.

Materials and methods

Fungal sampling, isolating and morphology

Sample collection was carried out in the summer of 2023, in a mountain forest in Yunyan District of Guiyang City, Guizhou Province, which was at a time of high rainy weather, with a large area covered by various kinds of vegetation. Decayed plant tissue samples were collected from the moist soil surface and brought back to the laboratory in self-sealing bags. The specimens were then examined for their macroscopic characteristics using a Nikon SMZ 745 series stereomicroscope and photographed, using a Canon 700D digital camera. Pure cultures were obtained using a single spore isolation method as described in (Senanayake et al. 2020). The germinated spores were transferred to fresh potato dextrose agar (PDA) plates and incubated at 25 °C for 14 days. Micro-morphological structures were photographed using a Nikon digital camera (Canon 700D) that was attached to a light microscope (Nikon Ni). Fruiting bodies on natural substrates were observed using a Zeiss Scope5 compound microscope Axioscope 5 (Carl Zeiss Microscopy GmbH, Jena, Germany) with the microscope techniques of differential interference contrast light (DIC) and photographed using an AxioCam 208 colour (Carl Zeiss Microscopy GmbH, Jena, Germany) camera and saved as JPG files. Approximately 30 morphological measurements of new species were made of each feature using the ZEN 3.0 (blue edition) (Jena, Germany) software.

Type specimens were deposited in the Herbarium of the Department of Plant Pathology, Agricultural College, Guizhou University (**HGUP**). Ex-type cultures were deposited in the Culture Collection at the Department of Plant Pathology, Agriculture College, Guizhou University, P.R. China (**GUCC**). Taxonomic information of the new species was submitted to MycoBank (www.mycobank.org) and accession numbers are provided in the Taxonomy section of this paper.

DNA extraction, polymerase chain reaction (PCR) amplification

The fungal strains were cultured on potato dextrose agar (**PDA**) (c = 40.1 g/l) medium in an incubator at 25 °C for 7 days and the mycelium was scraped with a sterile scalpel. Total DNA was extracted with a (Biomiga#GD2416, San Diego, California, USA) BIOMIGA Fungus Genomic DNA Extraction Kit (GD2416) following the manufacturer's protocol. Five loci (ITS, *tub2*, SSU, LSU and *rpb2*) were selected for the total DNA extracted. Amplification was undertaken of forward and reverse primers, including the internal transcribed spacer regions (**ITS**), partial beta-tubulin gene (*tub2*), partial large subunit nrRNA gene (**LSU**), 18S small subunit ribosomal RNA (**SSU**) and partial DNA-directed RNA polymerase II second largest subunit (*rpb2*) gene using the primer pairs ITS5/ITS4 (White et al. 1990), Bt2a/Bt2b (Woudenberg et al. 2009), LR0R/LR5 (Vilgalys and Hester 1990), NS1/NS4 (White et al. 1990) and RPB2-5F2/RPB2-7cR (Liu et al. 1999), respectively. Amplification reactions profiles for LSU, ITS, and *tub2* gene followed to Chen et al. (2015) and SSU accorded to White et al. (1990). The amplification for *rpb*2 was performed according to an improved protocol (Crous et al. 2013). PCR products were sequenced by SinoGegoMax (Beijing, China). The consensus sequences were assembled from forward and reverse sequences using Seqman Pro v. 10.0.1 (DNASTAR, Madison, USA). Novel sequences generated in this study were deposited in GenBank (http://www.ncbi.nlm.nih.gov) and their accession numbers are shown in Table 1.

Table 1. Taxa and corresponding GenBank accession numbers of sequences used in the phylogenetic analysis T = ex-holotype strain, F = non-type strain, ET = ex-epitype strain.

Current name	Old name	Strain number	T/F	Host	Country	GenBank Accession Numbers				
						ITS	LSU	*tub2*	*rpb2*	SSU
Circinotrichum circinatum	*"Gyrothrix circinata"*	CBS 140217	F	Unidentified	Malawi	ON400747	ON400800	–	ON399330	–
	"Gyrothrix circinata"	CBS 140218	F	Unidentified	Malawi	ON400748	ON400801	–	ON399331	–
	"Gyrothrix circinata"	CBS 140229	F	Unidentified	Zimbabwe	ON400751	ON400804	–	ON399335	–
	"Gyrothrix circinata"	CBS 140230	F	Unidentified	Zimbabwe	ON400752	ON400805	–	ON399334	–
	"Gyrothrix circinata"	CBS 140219	F	Unidentified	Malawi	ON400749	ON400802	–	ON399332	–
	"Gyrothrix circinata"	CBS 140220	F	Unidentified	Malawi	ON400750	ON400803	–	ON399333	–
	"Gyrothrix circinata"	CBS 148325	F	Unidentified	USA	ON400745	ON400798	–	ON399329	–
	"Gyrothrix sp."	CBS 140235	F	Unidentified	Brazil	ON400746	ON400799	–	ON399336	–
	"Gyrothrix circinata"	CBS 148326	F	Unidentified	Australia	ON400743	ON400796	–	ON399328	–
	"Gyrothrix circinata"	CBS 148327	F	*Hakea* sp.	Australia	ON400744	ON400797	–	ON399327	–
	"Gyrothrix sp."	CPC 26309	F	*Erica* sp.	France	ON400742	ON400795	–	ON399326	–
Circinotrichum maculiforme	*Circinotrichum maculiforme*	CBS 122758	F	Unidentified	Spain	KR611875.1	KR611896.1	–	ON399337	–
	Circinotrichum maculiforme	CBS 140016	ET	*Loranthus* sp.	Czech Republic	KR611874.1	KR611895.1	–	ON399338	–
	Circinotrichum maculiforme	CBS 140225	F	Unidentified	Cuba	ON400753	ON400806	–	ON399339	–
	Circinotrichum sp.	CPC 29975	F	*Cornus sanguinea*	France	ON400754	ON400807	–	ON399340	–
"Ceratocladium microspermum"	*"Ceratocladium microspermum"*	CBS 488.77	F	*Quercus* sp.	Slovakia	ON400740	ON400793	–	ON399324	–
Circiontrichum australiense	*"Gyrothrix podosperma"*	CBS 148706	T	Unidentified	Australia	ON400741	ON400794	–	ON399325	–
	Coniocessia nodulisporioides	CBS 125776	F	Unidentified	Unknown	MH863754.1	MH875222.1	–	–	–
	Coniocessia nodulisporioides	CBS 125777	F	Unidentified	Unknown	MH863755.1	MH875223.1	–	–	–
Coniocessia cruciformis	*Coniocessia cruciformis*	CBS 125769	F	*Triticum aestivum*	Iran	MH863750.1	MH875218.1	–	–	–
Pirozynkiomyces brasiliensis	*"Gyrothrix circinata"*	CBS 112314	T	Unidentified	Brazil	ON400767	ON400819	–	ON399341	–
Circinotrichum sinense	*Circinotrichum sinense*	UAMH 11913	T	*Camellia cuspidata*	China	KY994106.1	KY994107.1	–	–	–
Hansfordia pruni	*Hansfordia pruni*	CBS 125775	F	*Prunus persica*	Italy	MH863753.1	MH875221.1	–	–	–
	Hansfordia pruni	CBS 125767	F	*Prunus persica*	Italy	MH863748.1	MH875216.1	–	–	–
	Hansfordia pruni	CBS 125768	F	*Prunus persica*	Italy	MH863749.1	MH875217.1	–	–	–
	Selenodriella fertilis	CBS 772.83	F	Unidentified	Unknown	KP859055.1	KP858992.1	–	–	–
	Selenodriella fertilis	CPC 16273	F	Unidentified	Unknown	ON400771	ON400823	–	ON399358	–
	Selenodriella fertilis	CBS 144589	F	Unidentified	Unknown	MK442624.1	MK442560.1	–	–	–
Circinotrichum rigidum	*"Circinotrichum rigidum"*	CBS 148328	F	*Eucalyptus* sp.	Australia	ON400772	ON400824	–	ON399359	–

Current name	Old name	Strain number	T/F	Host	Country	GenBank Accession Numbers				
						ITS	LSU	*tub2*	*rpb2*	SSU
Selenodriella brasiliana	*"Circinotrichum australiense"*	CBS 140227	T	Unidentified	Brazil	ON400769	ON400821	–	ON399356	–
	"Circinotrichum sp.*"*	CBS 140236	F	Unidentified	Brazil	ON400770	ON400822	–	ON399357	–
Selenodriella cubensis	*Selenodriella cubensis*	CBS 683.96	T	Unidentified	Cuba	KP859053.1	KP858990.1	–	–	–
Peglionia verticiclada	*"Gyrothrix verticiclada"*	CBS 101171	F	Unidentified	Venezuela	ON400766	ON400818	–	ON399355	–
	"Gyrothrix verticiclada"	CBS 140226	F	Unidentified	Venezuela	ON400764	ON400816	–	ON399354	–
	"Gyrothrix verticiclada"	CBS 127654	ET	*Smilax aspera*	Italy	ON400763	ON400815	–	ON399352	–
	"Gyrothrix verticiclada"	CBS 148329	F	*Eucalyptus* sp.	Australia	ON400765	ON400817	–	ON399353	–
	***Peglionia falcat*a**	**GUCC 23-0042**	**T**	**Unidentified**	**China**	**PP295269**	**PP314032**	–	**PP396044**	–
	Peglionia falcata	**GUCC 23-0043**	**F**	**Unidentified**	**China**	**PP295270**	**PP314033**	–	**PP396045**	–
	Peglionia falcata	**GUCC 23-0044**	**F**	**Unidentified**	**China**	**PP295271**	**PP349828**	–	**PP396046**	–
	Microdochium lycopodinum	CBS 125585	F	Unidentified	Unknown	NR_145223.1	KP858952.1	–	KP859125.1	–
	Idriella lunata	CBS 204.56	F	*Fragaria chiloensis var. ananass*a	USA	MH857584.1	MH869129.1	–	–	–
	Zygosporium pseudomassoni	CBS 146059	F	Unidentified	Unknown	NR_166342.1	NG_068340.1	–	MN556815.1	–
	Zygosporium mycophilum	CBS 894.69	F	Unidentified	Unknown	MH859474.1	MH871255.1	–	–	–
	Monosporascus cannonballus	ATCC 26931	T	*Cucumis melo*	USA	NR_111370.1	–	–	–	–
	Monosporascus nordestinus	CMM 4846	F	*Trianthema portulacastrum*	Brazil	MG735241	MG748810.1	–	–	–
	Monosporascus caatingaensis	CMM 4833	F	*Boerhavia diffusa*	Brazil	MG735228.1	MG748797.1	–	–	–
	Diatrypella vulgaris	CBS 128329	F	*Citrus paradisi*	Australia	MH864880.1	MH876328.1	–	–	–
	Diatrype disciformis	CBS 197.49	F	Unidentified	Unknown	–	DQ470964.1	–	DQ470915.1	–
	Acrocordiella occulta	CBS 140500	F	Unidentified	Unknown	KT949893.1	MH878156.1	–	–	–
	Neomicrosphaeropsis alhagi-pseudalhagi	MFLUCC 17-0825	T	*Alhagi pseudalhagi*	Uzbekistan	MH069664	MH069670	MH069689	–	MH069676
	Neomicrosphaeropsis elaeagni	MFLUCC 17-0740	T	*Elaeagnus angustifoli*a	Russia	MH069666	MH069672	MH069691	–	MH069678
	Neomicrosphaeropsis italica	MFLUCC 15-0485	T	*Tamarix* sp.	Italy	KU900318	KU729854	–	–	KU900309
	Neomicrosphaeropsis italica	MFLUCC 16-0284	F	*Tamarix* sp.	Italy	KU900321	KU900296	KX453299	–	KU900311
	Neomicrosphaeropsis italica	MFLUCC 15-0484	F	*Tamarix* sp.	Italy	KU900319	KU729853	KX453298	–	–
	Neomicrosphaeropsis italica	MFLUCC 15-0487	F	*Tamarix* sp.	Italy	KU900320	KU729852	–	–	KU900310
	Neomicrosphaeropsis juglandis	MFLUCC 18-0795	T	*Juglans regia*	Turkey	MN244223	MN244206	MN871954	–	MN244183
	Neomicrosphaeropsis novorossica	MFLUCC 14-0578	T	*Tamarix ramosissima*	South European Russia	KX198709	KX198710	–	–	KX198711

Current name	Old name	Strain number	T/F	Host	Country	GenBank Accession Numbers				
						ITS	LSU	*tub2*	*rpb2*	SSU
	Neomicrosphaeropsis rossica	MFLUCC 14-0586	T	*Tamarix ramosissima*	South European Russia	KU752192	KU729855	–	–	KU870914
	Neomicrosphaeropsis tamaricicola	MFLUCC 14-0443	F	*Tamarix* sp.	Italy	KU900322	KU729851	–	–	KU900312
	Neomicrosphaeropsis tamaricicola	MFLUCC 14-0439	F	*Tamarix* sp.	Italy	KU900323	KU729858	–	–	KU900313
	Neomicrosphaeropsis tamaricicola	MFLUCC 14-0602	T	*Tamarix* sp.	Italy	KM408753	KM408754	MH069692	–	KM408755
	Neomicrosphaeropsis cylindrica	**GUCC23-0048**	**T**	**Unidentified**	**China**	**PP314028**	**PP314039**	**PP396056**	**PP396050**	**PP316087**
	Neomicrosphaeropsis cylindrica	**GUCC23-0049**	**F**	**Unidentified**	**China**	**PP314030**	**PP316086**	**PP396057**	**PP396051**	**PP316089**
	Neomicrosphaeropsis cylindrica	**GUCC23-0050**	**F**	**Unidentified**	**China**	**PP314031**	**PP316082**	**PP396058**	**PP396052**	**PP316088**
Microsphaeropsis minima	*Neomicrosphaeropsis minima*	MFLUCC 13-0394	F	*Verbascum* sp.	Italy	KX572336	KX572341	–	–	KX572346
Microsphaeropsis cytisina	*Neomicrosphaeropsis cytisina*	MFLU 16-1364	T	*Cytisus scoparius*	Italy	KX611243	KX611241			KX611242
Microsphaeropsis cystisicola	*Neomicrosphaeropsis cystisicola*	MFLUCC 18-0355	T	*Cytisus* sp.	Italy	MH069665	MH069671	MH069690	–	–
Microsphaeropsis cytisi	*Neomicrosphaeropsis cystisi*	MFLUCC 13-0396	T	*Cytisus* sp.	Italy	KX572337	KX572342	–	–	KX572347
	Microsphaeropsis fusca	CBS 116670	T	Sarothamnus scoparius	The Netherlands	MN973573	MT018220	–	MT018220	–
	Microsphaeropsis rafniae	CMW 57792	T	Rafnia amplexicaulis	South Africa	OR209698	OR209716	–	OR211858	–
	Microsphaeropsis viridis	CBS 763.73	F	Populus tremula	France	MN973561	MN943768	–	MT018210	–
	Microsphaeropsis taxicola	CBS 469.80	F	Rhus typhina	The Netherlands	MN973565	MN943772	–	MT018210	–
	Neodidymelliopsis ranunculi	MFLUCC 13-0490	T	Unidentified	Italy	MN944410	MT020377	–	–	KX572348
	Neoascochyta adenii	CBS 142108	T	*Adenium obesum*	Thailand	KY173423	KY173514	KY173607	–	–
	Neoascochyta argentina	CBS 112524	T	*Triticum aestivum*	Argentina	KT389524	KT389742	KT389822	–	–
	Neoascochyta cylindrispora	CBS 142456	T	*Homo sapiens*	USA	LT592963	LN907502	LT593032	–	–
	Neoascochyta dactylidis	MFLUCC 13-0495	T	*Dactylis glomerata*	Italy	NR_170041	–	–	–	–
	Neoascochyta desmazieri	CBS 297.69	T	*Lolium perenne*	Germany	KT389508	KT389726	KT389806	–	–
	Neoascochyta desmazieri	CBS 758.97	F	Unidentified	Norway	KT389509	KT389727	KT389807	–	–
	Neoascochyta desmazieri	CBS 247.79	F	Gramineae	Austria	KT389507	KT389725	KT389805	–	–
	Neoascochyta europaea	CBS 820.84	T	*Hordeum vulgare*	Germany	KT389511	KT389729	KT389809	–	–
	Neoascochyta europaea	CBS 819.84	F	*Hordeum vulgare*	Germany	KT389510	KT389728	KT389808	–	–
	Neoascochyta exitialis	CBS 812.84	F	*Hordeum vulgare*	Germany	KT389517	KT389735	KT389815	–	–
	Neoascochyta exitialis	CBS 811.84	F	*Secale cereale*	Germany	KT389516	KT389734	KT389814	–	–
	Neoascochyta exitialis	CBS 389.86	F	*Triticum aestivum*	Switzerland	KT389515	KT389733	KT389813	–	–
	Neoascochyta exitialis	CBS 113693	F	*Allium* sp.	Sweden	KT389513	KT389731	KT389811	–	–

Current name	Old name	Strain number	T/F	Host	Country	GenBank Accession Numbers				
						ITS	LSU	*tub2*	*rpb2*	SSU
	Neoascochyta exitialis	CBS 110124	F	*Triticum* sp.	Netherlands	KT389512	KT389730	KT389810	–	–
	Neoascochyta fuci	CMG 47/ MUM19.41	T	*Fucus* sp.	Portugal	MN053014	–	MN066618	–	–
	Neoascochyta fuci	CMG 48	F	*Fucus* sp.	Portugal	MN053015	–	MN066619	–	–
	Neoascochyta fusiformis	CBS 876.72	T	*Triticum* sp.	South Africa	KT389527	KT389745	KT389825	–	–
	Neoascochyta graminicola	CBS 816.84	F	*Hordeum vulgare*	Germany	KT389523	KT389741	KT389821	–	–
	Neoascochyta graminicola	CBS 815.84	F	*Hordeum vulgare*	Germany	KT389522	KT389740	KT389820	–	–
	Neoascochyta graminicola	CBS 447.82	F	*Triticum aestivum*	Germany	KT389520	KT389738	KT389818	–	–
	Neoascochyta graminicola	CBS 301.69	F	*Lolium multiflorum*	Germany	KT389519	KT389737	KT389817	–	–
	Neoascochyta graminicola	CBS 102789	F	*Lolium perenne*	New Zealand	KT389518	KT389736	KT389816	–	–
	Neoascochyta humicola	CBS 127323	T	Unidentified	USA	MN973628	MN943837	MT005740	–	–
	Neoascochyta longispora	CBS 113420	T	*Cerastium semidecandrum*	New Zealand	MN973629	MN943838	MT005741	–	–
	Neoascochyta mortariensis	CBS 516.81	T	Gramineae	Italy	KT389525	KT389743	KT389823	–	–
	Neoascochyta paspali	CBS 560.81	T	*Paspalum dilatatum*	New Zealand	FJ427048	GU238124	FJ427158	–	–
	Neoascochyta paspali	CBS 561.81	F	*Lolium perenne*	New Zealand	GU237889	–	GU237640	–	–
	Neoascochyta paspali	ICMP 6614	F	*Paspalum dilatatum*	New Zealand	KT309957	–	KT309539	–	–
	Neoascochyta paspali	ICMP 6819	F	*Dactylis glomerata*	New Zealand	KT309992	–	KT309572	–	–
	Neoascochyta paspali	ICMP 6615	F	*Lolium perenne*	New Zealand	KT309958	–	KT309540	–	–
	Neoascochyta rosicola	MFLUCC 15-0048	T	*Rosa canina*	Italy	MG828921	MG829031	–	–	–
	Neoascochyta soli	LC 8165	T	Unidentified	China	KY742121	KY742275	KY742363	–	–
	Neoascochyta soli	LC 8166	F	Unidentified	China	KY742122	KY742276	KY742364	–	–
	Neoascochyta tardicrescens	CBS 689.97	T	Unidentified	Norway	KT389526	KT389744	KT389824	–	–
	Neoascochyta triticicola	CBS 544.74	T	*Triticum aestivum*	South Africa	GU237887	EU754134	GU237488	–	–
	Neoascochyta yunnanensis	YCW1883	T	*Camellia sinensis*	China	OP648090	OP837280	OP854553		
	Neoascochyta zhejiangensis	YCW1361	T	*Camellia sinensis*	China	OP648091	OP083837281	OP854554		
	Neoascochyta pseudofusiformis	**GUCC 23-0045**	**T**	**Unidentified**	**China**	**PP314026**	**PP314037**	**PP396053**	**PP396047**	**PP345789**
	Neoascochyta pseudofusiformis	**GUCC 23-0046**	**F**	**Unidentified**	**China**	**PP314027**	**PP314038**	**PP396054**	**PP396048**	**PP301319**
	Neoascochyta pseudofusiformis	**GUCC 23-0047**	**F**	**Unidentified**	**China**	**PP314029**	**PP314036**	**PP396055**	**PP396049**	**PP301320**
	Vandijckomycella joseae	CBS 143011	T	Unidentified	Unknown	NR_168247	NG_068687	–	–	–
	Vandijckomycella snoekiae	CBS 144954	T	Unidentified	Unknown	NR_168248	NG_068688	MN824765	–	–

Sequence alignment and phylogenetic analyses

After primary BLAST alignment, all our nine isolates could not be affiliated to any of the currently-known species. Thus, the related sequences were added to the sequence alignment for phylogenetic analyses. Available sequences of species in relative genera containing ex-type or representative isolates were downloaded from GenBank (Table 1) according to previous publications (Li et al. 2018, 2020; Vu et al. 2019; Chen et al. 2020; Chu et al. 2021; Yukako et al. 2021). Alignments for the individual locus matrices were generated with the online version of MAFFT v. 7.307 (Katoh et al. 2019). The alignments were checked visually and improved manually where necessary using BioEdit v. 7.0.5.2 (Hall 1999). Ambiguous regions were excluded from the analyses and gaps were treated as missing data. Sequence matrix v. 1.7.8 was used to concatenate the aligned sequences (Vaidya et al. 2011). In Fig.

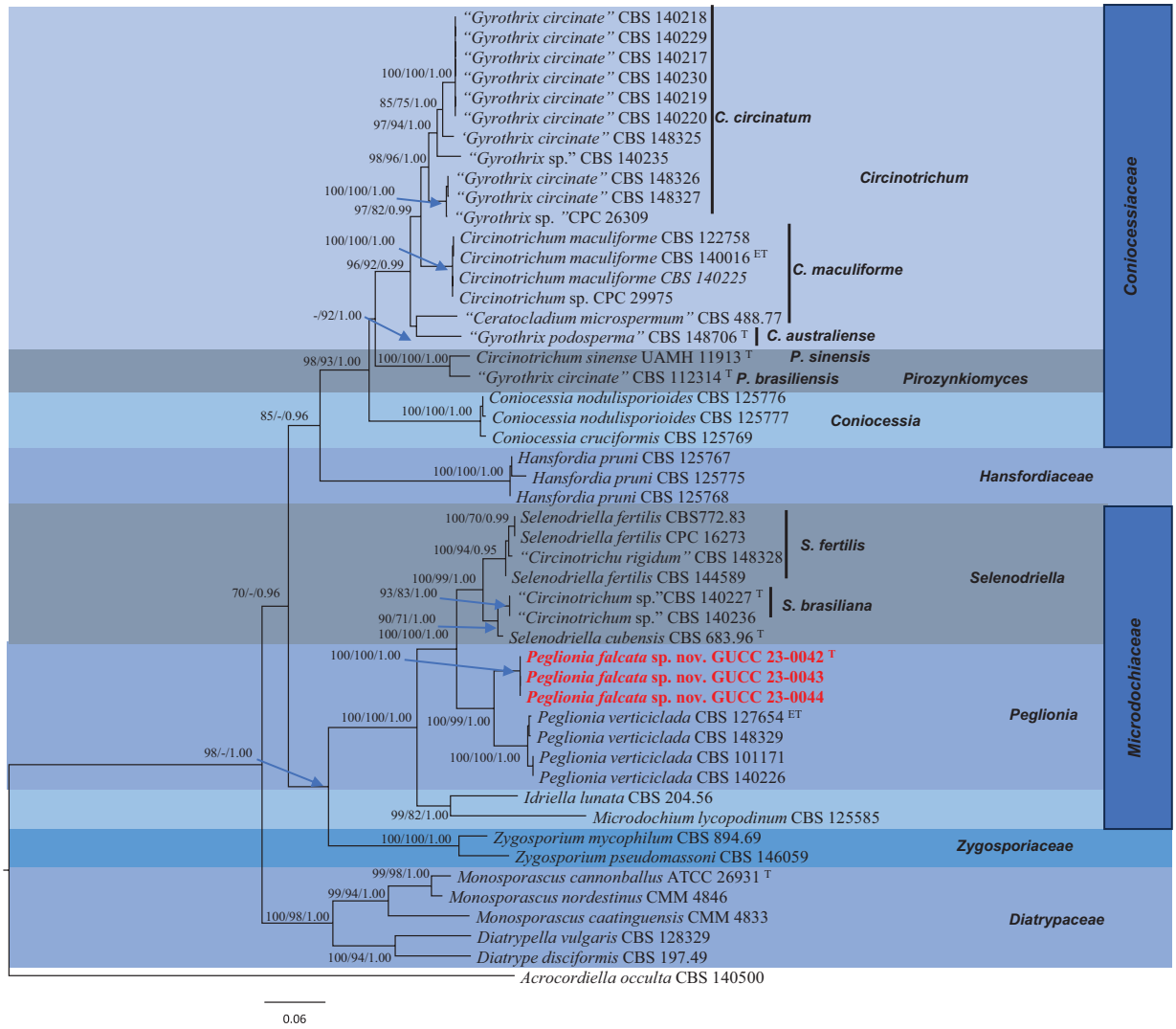

Figure 1. Trees resulting from ML analysis of the combined ITS, *rpb*2 and LSU sequence alignment for forty-nine isolates in Coniocessiaceae and Microdochiaceae. RAxML and MP bootstrap support values (ML, MP ≥ 70%) and Bayesian posterior probability (PP ≥ 0.95) are denoted on the nodes (ML/MP/PP). The tree was rooted to *Acrocordiella occulta* (CBS 140500). New species are highlighted in red. The scale bar indicates 0.06 expected changes per site. T = ex-holotype strain, ET = ex-epitype strain.

1, *Acrocordiella occulta* (CBS 140500) was selected as outgroup, in Fig. 2, *Vandijckomycella joseae* (CBS 143011) and *V. snoekiae* (CBS 144954) were selected as outgroup and, in Fig. 3, *Neodidymelliopsis ranunculi* (MFLUCC 13-0490) was selected as outgroup. Maximum Likelihood (ML), Maximum Parsimony (MP) and Bayesian Inference (BI) were used to place the newly-discovered strains into a phylogenetic framework and estimate their phylogenetic relationships. ML analysis was performed using IQ-TREE (Nguyen et al. 2015; Trifinopoulos et al. 2016) on the IQ-TREE web server (http://iqtree.cibiv.univie.ac.at, 17 February 2024). The MP analysis was implemented to test the discrepancy of the ITS, *rpb2*, LSU, SSU and *tub2* sequence datasets

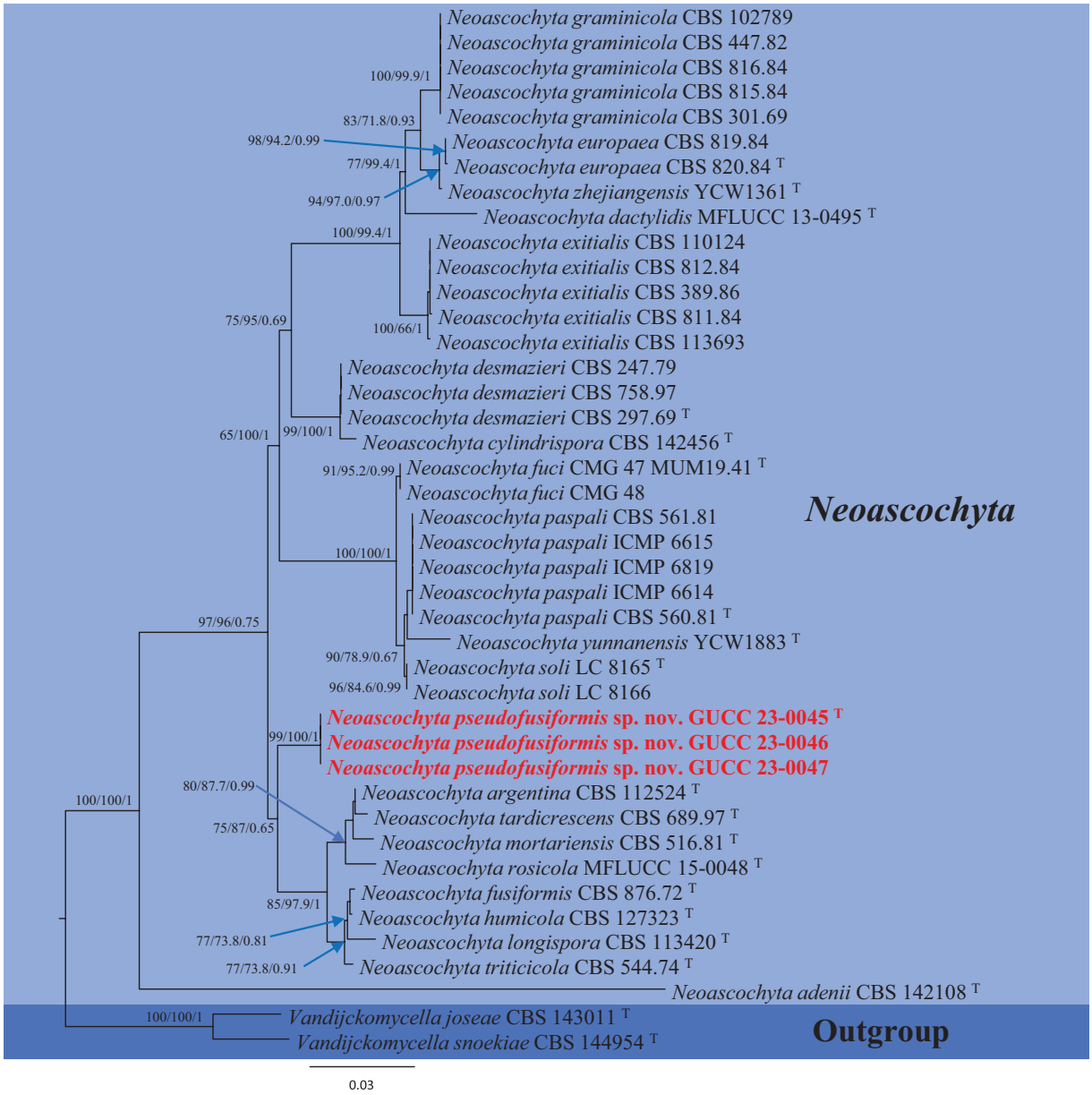

Figure 2. Trees resulting from ML analysis of the combined ITS, *tub2* and LSU sequence alignment for thirty-seven isolates in *Neoascochyta*. RAxML and MP bootstrap support values (ML, MP ≥ 65%) and Bayesian posterior probability (PP ≥ 0.65) are denoted on the nodes (ML/MP/PP). The tree was rooted to *Vandijckomycella joseae* (CBS 143011) and *Vandijckomycella snoekiae* (CBS 144954). New species are highlighted in red. The scale bar indicates 0.03 expected changes per site. T = ex-holotype strain.

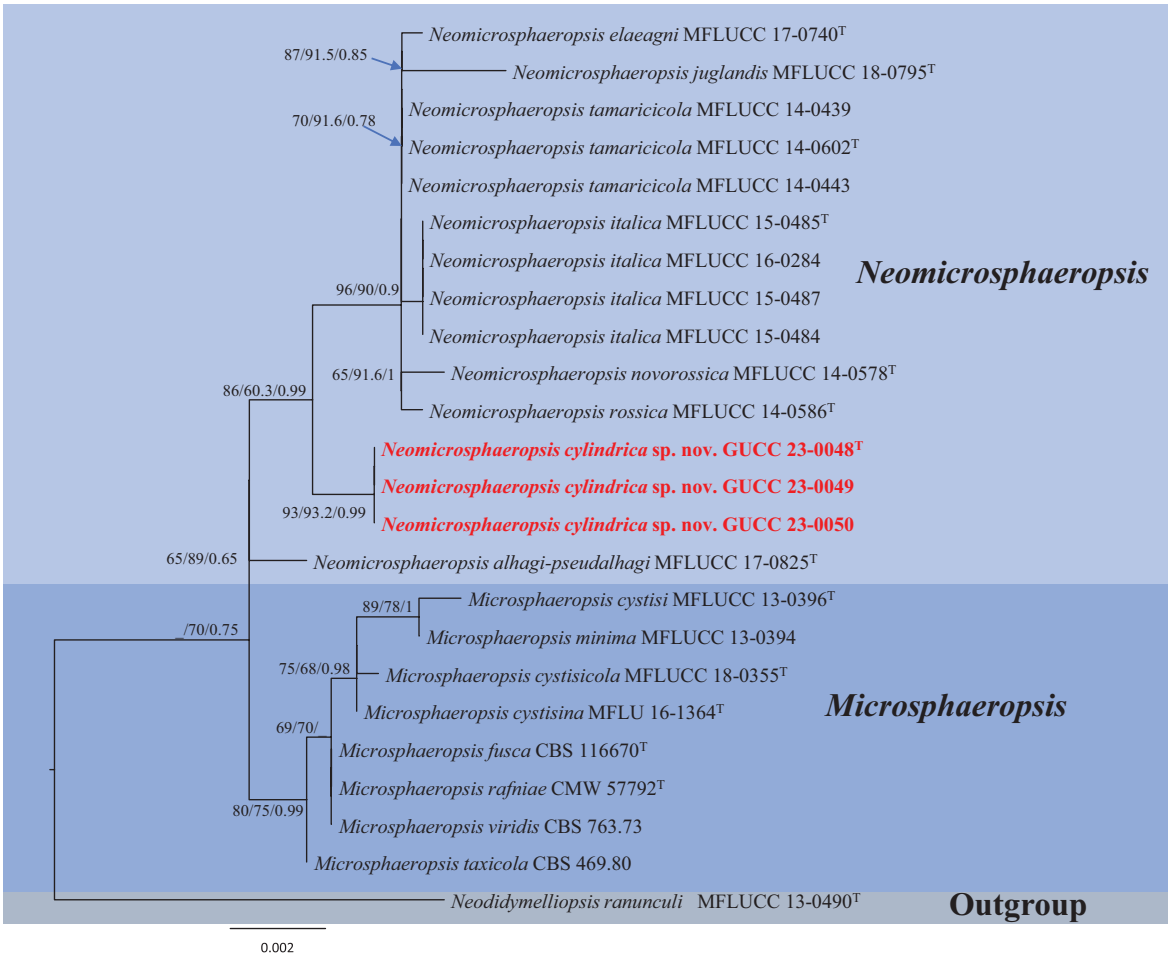

Figure 3. Trees resulting from ML analysis of the combined ITS, SSU and LSU sequence alignment for twelve isolates in *Neomicrosphaerops*is and eight isolates in *Microsphaeropsis*. RAxML and MP bootstrap support values (ML, MP ≥ 60%) and Bayesian posterior probability (PP ≥ 0.65) are denoted on the nodes (ML/MP/PP). The tree was rooted to *Neodidymelliopsis ranunculi* (MFLUCC13-0490). New species are highlighted in red. The scale bar indicates 0.002 expected changes per site. T = ex-holotype strain.

with PAUP v. 4.0b10 (Swofford 2002). Gaps were treated as missing data, which were interpreted as uncertainty of multistate taxa. MP trees were generated using the heuristic search option with tree bisection re-connection (TBR) branch swapping. "Maxtrees" was set to 5000, the tree length (TL), consistency index (CI), homoplasy index (HI), retention index (RI) and rescaled consistency index (RC) were calculated. BI was performed using six Markov Chain Monte Carlo runs for 5,000,000 generations, sampling every 1000 generations. The first 25% resulting trees were discarded as the burn-in phase of each analysis.

Results

In the phylogenetic analyses, the MP, ML and Bayesian results obtained similar topologies, thus the ML topologies were edited and shown as Figs 1–3. For the *Peglionia* and related genera (Fig. 1), the combined data matrix of ITS–LSU–*rpb*2 consisted of 2366 characters (ITS: 761, LSU: 885 and *rpb*2: 720), amongst which 612 are parsimony informative characters. Maximum Parsimo-

ny analysis with the following parameters: TL = 2197; CI = 0.5294; HI = 0.4706; RI = 0.8182; and RC = 0.4331 indicated that *Peglionia falcata* strains (GUCC-0042, GUCC-0043 and GUCC-0044) without the DNA base differences in three loci formed an independent branch (ML = 100, MP = 100, PP = 1.00) and maintained a close relationship to *P. verticiclada* (CBS 127654, CBS 148329, CBS 101171 and CBS 140226) (ML = 100, MP = 99, PP = 1.00).

The combined data matrix of *Neoascochyta* (ITS–LSU–*tub*2) yielded 1784 characters (ITS: 489, LSU: 959 and *tub*2: 336). The MP analysis, based on 194 parsimony informative characters (1480 characters were constant and 110 variable characters), produced the phylogenetic tree with the following parameters: TL = 562; CI = 0.6975; HI = 0.3025; RI = 0.8932; and RC = 0.6230. The result (Fig. 2) displayed that *Neoascochyta pseudofusiformis* (GUCC23-0045, GUCC23-0046 and GUCC23-0047) formed an independent branch without the DNA base differences in three loci supported by strong statistic data (ML = 99, MP = 100, PP = 1.00) and were adjacent to the branch of *Neoascochyta argentina* CBS 112524 and *N. tardicrescens* (CBS 689.97) (ML = 75, MP = 87, PP = 0.65).

In Fig. 3, the combined data matrix of *Neomicrosphaeropsis* (ITS–LSU–SSU) including 2328 characters (ITS: 484, LSU: 833 and SSU: 1011), only had 17 parsimony informative characters. The MP analysis (TL = 51; CI = 0.8627; HI = 0.1373; RI = 0.9136; and RC = 0.7882) indicated the three strains of *Neomicrosphaeropsis cylindrica* (GUCC 23-0048, GUCC 23-0049 and GUCC 23-0050) as a branch without genetic distance (ML = 93, MP = 93.2, PP = 0.99) adjoining to the clade (ML = 86, MP = 60.3, PP = 0.99) including *Neom. rossica*, *Neom. novorossica* and *Neom. italica*. The phylogenetic placements of these novel taxa were also supported by DNA base-pair differences (Table 2).

Table 2. The DNA base differences of our isolates and related taxa in different loci.

Species	Strain number	ITS (1–761 characters)	LSU (762–1646 characters)	*rpb*2 (1647–2366 characters)
Peglionia falcata	GUCC-0042	0	0	0
Peglionia falcata	GUCC-0043	0	0	0
Peglionia falcata	GUCC-0044	0	0	0
Peglionia verticiclada	CBS 127654	20 (gaps: 4)	13 (gap: 0)	69 (gap: 0)
Peglionia verticiclada	CBS 101171	19 (gaps: 4)	17 (gap: 1)	65 (gap: 0)
Peglionia verticiclada	CBS 683.96	36 (gaps: 7)	25 (gaps: 2)	/
Peglionia verticiclada	CBS 140227	39 (gaps: 6)	26 (gaps: 2)	84 (gap: 0)
Species	**Strain number**	**ITS (1–489 characters)**	**LSU (490–1448 characters)**	***tub*2 (1449–1784 characters)**
***Neoascochyta pseudofusiformi*s**	GUCC23-0045	0	0	0
Neoascochyta pseudofusiformis	GUCC23-0046	0	0	0
Neoascochyta pseudofusiformis	GUCC23-0047	0	0	0
Neoascochyta soli	LC 8166	24 (gap: 3)	16 (gap: 0)	35 (gap: 1)
Neoascochyta argentina	CBS 112524	18 (gap: 0)	2 (gap: 0)	29 (gap: 1)
Neoascochyta tardicrescens	CBS 689.97	23 (gap: 0)	2 (gap: 0)	30 (gap: 1)
Neoascochyta mortariensis	CBS 516.81	20 (gap: 0)	2 (gap: 0)	30 (gap: 1)
Neoascochyta rosicola	MFLUCC 15-0048	24 (gaps: 0)	3 (gap: 0)	/
Species	**Strain number**	**ITS (1–484 characters)**	**LSU (485–1317)**	**SSU (1318–2328 characters)**
Neomicrosphaeropsis cylindrica	GUCC 23-0048	0	0	0
Neomicrosphaeropsis cylindrica	GUCC 23-0049	0	0	0
Neomicrosphaeropsis cylindrica	GUCC 23-0050	0	0	0
Neomicrosphaeropsis rossica	MFLUCC 14-0586	4 (gap:0)	4 (gap: 0)	1 (gap: 1)
Neomicrosphaeropsis novorossica	MFLUCC 14-0578	5 (gap:0)	3 (gap: 0)	1 (gap: 0)
Neomicrosphaeropsis alhagi-pseudalhagi	MFLUCC 17-0825	5 (gaps:0)	2 (gap: 0)	0

Taxonomy

***Peglionia falcata* S.M. Fu & Yong Wang bis, sp. nov.**
MycoBank No: 854204
Facesoffungi Number: FoF15890
Fig. 4

Etymology. In reference to the fungus, which produced falcate conidia.

Diagnosis. *Peglionia falcata* is characterised by dry falcate meriform spores (24.1 × 2.9 µm; L/W = 8.005).

Type. China, Guizhou Province, Guiyang City, 26°57'N, 106°72'E, from rotten dead branch, 19 July 2023, S.M. Fu, HGUP 23-0013 (holotype), ex-type culture GUCC23-0042.

Culture characteristics. Colonies on PDA, after 8 d, 20–25 mm diam., scarce aerial mycelium, dark brown, white to the periphery, margin entire, reverse dark brown. Occasionally, when a seta bears only two apical branches, one or both can be once forked. Conidiogenous cells polyblastic, obclavate to lageniform, hyaline to subhyaline. Conidia adherent in a continuous white layer on the conidiogenous cells, dry falcate, non-septate, hyaline. Chlamydospores (in culture) in chains, subglobose to irregularly-shaped, subhyaline to brown. Sexual morph not observed. Colonies hypophyllous, scattered, up to 1 mm wide, occasionally larger by confluence, velvety, black when sterile and whitish within when sporulating profusely. Conidiogenous cells obclavate to lageniform, hyaline to subhyaline, distally with a somewhat irregular contour, 5–16.5 × 4–7 µm ($\bar{x}$ = 9.8 × 5.3 µm, n = 20). Conidia adherent in a continuous white layer on the conidiogenous cells, falcate, non-septate, hyaline,18–30 × 2.5–3.5 µm ($\bar{x}$ = 24.1 × 2.9 µm, n = 30).

Habit. On rotten dead branches.

Distribution. China, Guizhou Province, Guiyang City

Other materials examined. China, Guizhou Province, Guiyang City, 26°57'N, 106°72'E, from rotten dead branch, 19 July 2023, S.M. Fu, HGUP 23-0013, living culture GUCC23-0042, GUCC23-0043 and GUCC23-0044.

Notes. In morphology, *Peglionia falcata* differs to *P. verticiclada* by its larger conidiogenous cells (4–7 µm wide vs. 3–5 µm wide in *P. verticiclada*) and larger conidia (18–30 µm vs. 17–22 µm in *P. verticiclada*) (Hernández-Restrepo et al. 2022). The phylogenetic analyses and DNA base differences (Table 2) also supported *P. falcata* as a novel taxon was distinct from *P. verticiclada*.

***Neoascochyta pseudofusiformis* S.M. Fu & Yong Wang bis, sp. nov.**
MycoBank No: 854206
Facesoffungi Number: FoF15891
Fig. 5

Etymology. In reference to the fungus, which produced fusiform conidia morphologically similar to *Neoascochyta fusiformis*.

Diagnosis. *Neoascochyta pseudofusiformis* is characterised by oval to fusiform conidia (3.6 × 1.9; L/W = 1.896) with moderate growth rate.

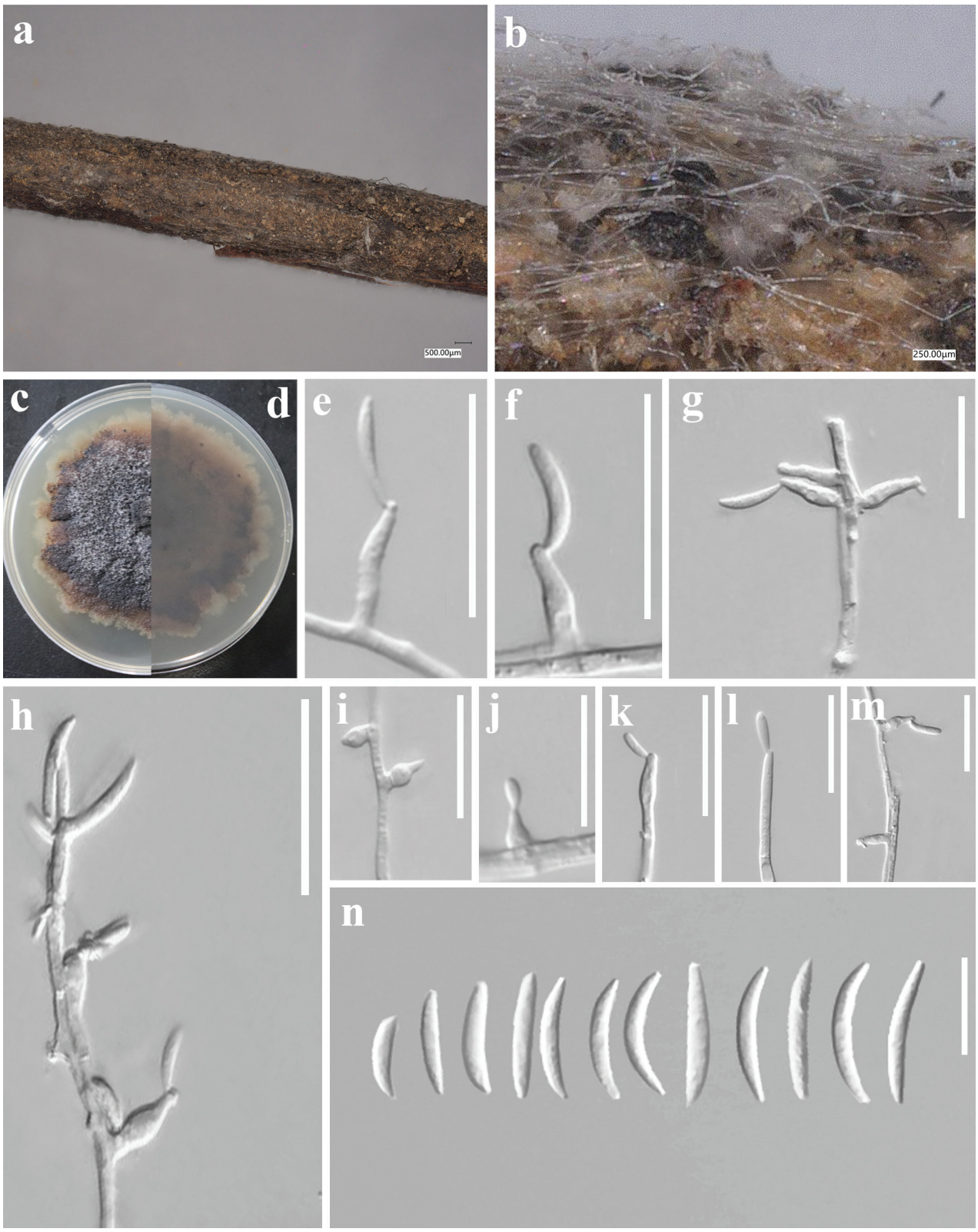

Figure 4. *Peglionia falcata* (GUCC23-0042) **a, b** appearance on host surface **c, d** culture characteristics on PDA (**c** above view **d** reverse view) **e–m** conidiophores, conidiogenous cells and conidia **n** conidia. Scale bars: 20 μm (**e–n**).

Type. China, Guizhou Province, Guiyang City, 26°57'N, 106°72'E, from rotten dead branch, 19 July 2023, S.M. Fu, HGUP 23-0014 (holotype), ex-type culture GUCC23-0045.

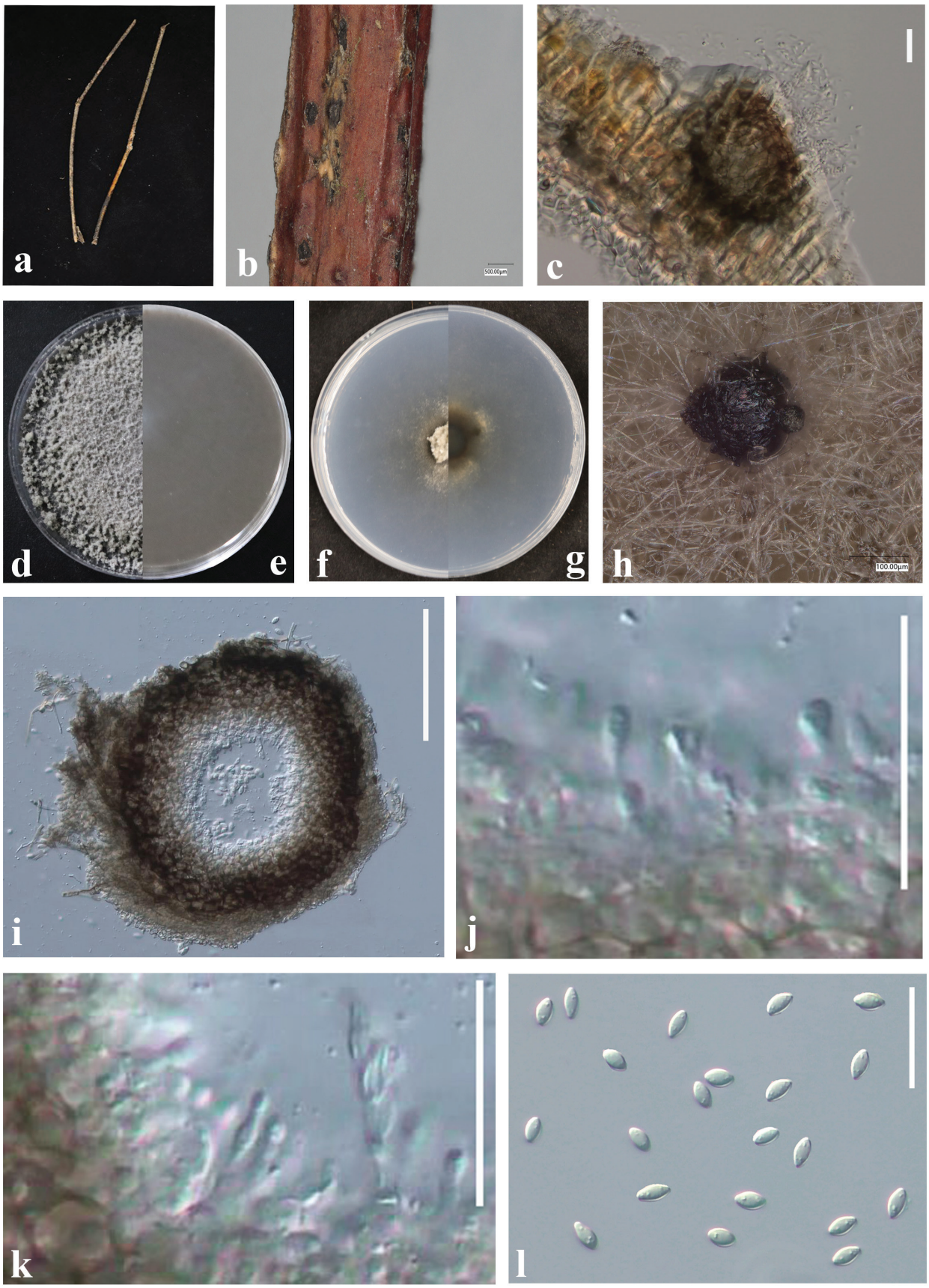

Figure 5. *Neoascochyta pseudofusiformis* (GUCC 23-0045) **a, b** appearance on host surface **c** colonies on host surface **d–g** culture characteristics on PDA, WA (**d, f** above view **e, g** reverse view) **h** colonies on WA **i–k** conidiophores, conidiogenous cells and conidia **l** conidia. Scale bars: 20 µm (**i–l**).

Culture characteristics. Colonies on PDA, 70–75 mm diam. after 7 d, margin regular, covered by floccose aerial mycelium, greyish-olivaceous, with flat and greenish-black flat mycelium near the margin; reverse black olivaceous. Mycelium is light to dark grey, separated, smooth, thin to thick wall. Acicular conidium, grey to dark grey, solitary or conjunctival, immersed in culture (WA), glabrous, subglobular, 100–250 × 90–130 µm, with a single pore neck; The angular textured cylindrical wall consists of 2 to 4 layers of flat polygonal cells 10–50 µm thick. The meristem cells are biparental, transparent, smooth-walled, pot or spherical, 3 × 5 µm wide. The conidia are 0–1 septum, transparent, smooth, thick-walled, mostly fusiform or slightly allantoic, 3.0–4.5 × 1.5–2.5 µm ($\bar{x}$ = 3.6 × 1.9 µm, n = 30).

Habit. On rotten dead branches.

Distribution. China, Guizhou Province, Guiyang City

Other materials examined. China, Guizhou Province, Guiyang City, 26°57'N, 106°72'E, from rotten dead branches, 19 July 2023, S.M. Fu, HGUP 23-0014, living culture GUCC23-0045, GUCC23-0046 and GUCC23-0047.

Notes. The present taxon differs morphologically to related species by conidial size range (3.0–4.5 × 1.5–2.5 µm vs. 16.5–27 × 5–8.5 µm in *N. argentina* and 2.5–3.5 × 1.0–1.5 µm in *N. tardicrescens*) (Chen et al. 2017; Valenzuela-Lopez et al. 2018). In phylogeny, our novel taxon maintained a close relationship to *N. argentina* CBS 112524 and *N. tardicrescens* CBS 689.97; however, DNA base differences (Table 2) supported that they belonged to different taxa.

***Neomicrosphaeropsis cylindrica* S.M. Fu & Yong Wang bis, sp. nov.**

MycoBank No: 854207

Facesoffungi Number: FoF15892

Fig. 6

Etymology. In reference to the fungus, which produced cylindrical conidia.

Diagnosis. *Neomicrosphaeropsis cylindrica* is characterised by broadly cylindrical conidia (15.4 × 3.4; L/W = 4.574) with moderate growth rate.

Type. China, Guizhou Province, Guiyang City, 26°57'N, 106°72'E, from rotten dead leaves, 19 July 2023, S.M. Fu, HGUP 23-0015 (holotype), ex-type culture GUCC23-0048.

Culture characteristics. Saprobic on dead leaves. Colony on PDA, 35–38 mm diameter, after 7 days, dense low-altitude hypha, light yellow, centre with abundant stigma; Turning light yellow to rose light yellow, the centre of concentric circles is darker; on MEA, after 7 days, 28–30 mm, the edge is intact, dense hypoxic mycelium, the edge is yellowish; reverse rose-yellowish to yellowish at margin with abundant scattered on stigma; Conidia cylindrical, spherical to kettle-shaped, 200–350 µm in diameter, tan to black, solitary, population centre abundant, banded, glabrous, without papillae; the cell wall is angular textured, light brown, bifid, cylindrical, thin-walled, transparent. Conidia occasionally septate, 12.5–18.5 × 2.4–4.0 µm ($\bar{x}$ = 15.4 × 3.4 µm, n = 30), cylindrical, transparent, thin-walled.

Sexual stage. Not observed.

Habit. On rotten dead leaves.

Distribution. China, Guizhou Province, Guiyang City.

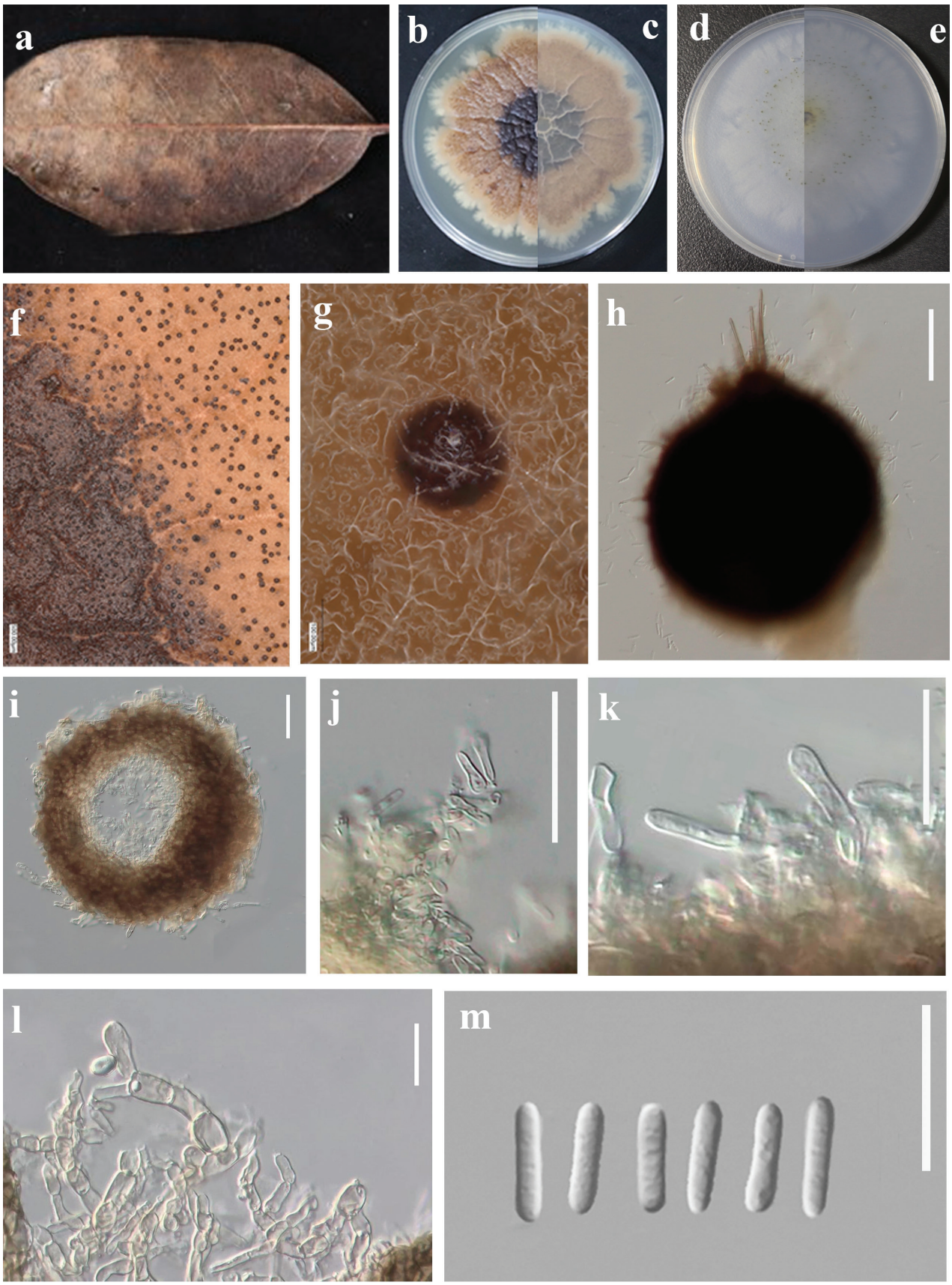

Figure 6. *Neomicrosphaeropsis cylindrica* (GUCC 23-0048) **a** appearance on host surface **b–e** culture characteristics on PDA, WA (**b–d** above view **c–e** reverse view) **f–g** colonies on PDA **h–l** conidiophores, Conidiogenous cells and Conidia **m** conidia. Scale bars: 100 μm (**h**); 50 μm (**i–k**); 20 μm (**l–m**).

Other materials examined. China, Guizhou Province, Guiyang City, 26°57'N, 106°72'E, from rotten dead leaf, 19 July 2023, S.M. Fu, HGUP 23-0015, living culture GUCC23-0048, GUCC23-0049 and GUCC23-0050.

Notes. *Neomicrosphaeropsis cylindrica* (GUCC 23-0048) formed a clade with *N. rossica* (MFLUCC 14-0586) and *N. alhagi-pseudalhagi* (MFLUCC 17-0825) (Fig. 3). However, by morphological comparison, our species produced obviously longer conidia than *N. rossica* (12.5–18.5 × 2.4–4.0 µm vs. 4.4–5.7 × 2.9–3.9 µm) and smaller conidia than *N. alhagi-pseudalhagi* (12.5–18.5 × 2.4–4.0 µm vs. 30–45 × 18–22 µm) (Thambugala et al. 2017; Wanasinghe 2018).

Discussion

According to Hernández-Restrepo et al. (2022), four strains of *Peglionia verticiclada* totally originated from decayed plant tissues in Europe and Australia. Our *Peglionia* species was also collected from rotten dead branches, which was the first discovery in China. In the database of Index Fungorum, *Neoascochyta* has 20 epithets and three of them were described by Chinese mycologists (Chen et al. 2017; Wang et al. 2024). Interestingly, the plant hosts of *Neoascochyta* spp. were mostly reported in the Gramineae family, such as *Triticum* sp., *Hordeum* sp. and *Paspalum* sp. (Chen et al. 2015, 2017; Hou et al. 2020). However, only two taxa (*Neoascochyta soli* and our *N. pseudofusiformis*) were both isolated from Guizhou, China and related to saprobic environments (Chen et al. 2017). In the test of inhibiting the germination of rust spores, the number of rust spots on leaves were significantly reduced after *Neoascochyta* treatment, which may provide a potential biological control method against rust diseases (Wilson et al. 2020). *Neomicrosphaeropsis cylindrica* was also the first species in *Neomicrosphaeropsis* to be discovered and described in China. This genus presented high correlations with alcohol and acids and was the highest contributors to the generation of volatile compounds, especially during alcohol production (Ma et al. 2021). Members of this genus were mostly obtained from Salicaceae as saprophytic fungi (Hyde et al. 2016; Thambugala et al. 2017). All our three Pezizomycotina taxa were isolated from rotten branches or leaves, which indicated that the diversity of this fungal group in Guizhou was relatively high. Thus, there was a need for a more comprehensive investigation.

Additional information

Conflict of interest

The authors have declared that no competing interests exist.

Ethical statement

No ethical statement was reported.

Funding

This research is supported by the following projects: National Natural Science Foundation of China (No. 31972222, 31660011), Program of Introducing Talents of Discipline to Universities of China (111 Program, D20023), Talent project of Guizhou Science and Technology Cooperation Platform ([2017]5788-5, [2019]5641, [2019]13),

Guizhou Science, Technology Department of International Cooperation Base project ([2018]5806), the project of Guizhou Provincial Education Department ([2021]001) and Guizhou Science and Technology Innovation Talent Team Project ([2020]5001).

Author contributions

Conceptualization: YH. Data curation: SF. Formal analysis: NNW. Funding acquisition: YW, YL. Investigation: ET. Methodology: JES. Supervision: YW. Writing - original draft: SF.

Author ORCIDs

Shamin Fu https://orcid.org/0009-0000-2829-7967
Jing-E Sun https://orcid.org/0000-0002-5226-5743
Entaj Tarafder https://orcid.org/0000-0002-3680-3433
Nalin N. Wijayawardene https://orcid.org/0000-0003-0522-5498
Yong Wang https://orcid.org/0000-0003-3831-2117
Yan Li https://orcid.org/0000-0003-2227-008X

Data availability

All of the data that support the findings of this study are available in the main text.

References

Charley GPM, David AF (2017) Chapter Six - multiple approaches to phylogenomic reconstruction of the fungal kingdom. Advances in Genetics 100: 211–266. https://doi.org/10.1016/bs.adgen.2017.09.006

Chen Q, Jiang JR, Zhang GZ, Crous PW (2015) Resolving the *Phoma enigma*. Studies in Mycology 82(1): 137–217. https://doi.org/10.1016/j.simyco.2015.10.003

Chen Q, Hou LW, Duan WJ, Crous PW, Cai L (2017) Didymellaceae revisited. Studies in Mycology 87(1): 105–159. https://doi.org/10.1016/j.simyco.2017.06.002

Chen YY, Dissanayake AJ, Liu ZY, Liu JK (2020) Additions to Karst Fungi 4: *Botryosphaeria* spp. associated with woody hosts in Guizhou province, China including *B. guttulata* sp. nov. Phytotaxa 454(3): 186–202. https://doi.org/10.11646/phytotaxa.454.3.2

Chu RT, Dou ZP, He W, Zhang Y (2021) Two novel species of *Botryosphaeria* causing stem canker of blueberries from China. Mycosystema 40: 473–486. https://doi.org/10.13346/j.mycosystema.200333

Crous PW, Braun U, Hunter GC, Wingfield MJ, Verkley GJM, Shin HD, Nakashima C, Groenewald JZ (2013) Phylogenetic lineages in *Pseudocercospora*. Studies in Mycology 75: 37–114. https://doi.org/10.3114/sim0005

Goidànich G (1934) Un nouvo genere di Demaziacee amerospore. Malpighia 33: 1–7.

Hall TA (1999) BioEdit: A user-friendly biological sequence alignment editor and analysis program for windows 95/98/NT. Nucleic Acids Symposium Series 41: 95–98. https://doi.org/10.1021/bk-1999-0734.ch008

Hernández-Restrepo M, Decock CA, Costa MM, Crous PW (2022) Phylogeny and taxonomy of *Circinotrichum*, *Gyrothrix*, *Vermiculariopsiella* and other setose hyphomycetes. Persoonia 49(1): 99–135. https://doi.org/10.3767/persoonia.2022.49.03

Hou LW, Groenewald JZ, Pfenning LH, Yarden O, Crous PW, Cai L (2020) The phoma-like dilemma. Studies in Mycology 96: 309–396. https://doi.org/10.1016/j.simyco.2020.05.001

Hyde KD, Jones EBG, Liu J, Ariyawansa H, Boehm E, Boonmee S, Braun U, Chomnunti P, Crous PW, Dai D, Diederich P, Dissanayake A, Doilom M, Doveri F, Hongsanan S, Jay-

awardena R, Lawrey JD, Li Y, Liu Y, Lücking R, Monkai J, Muggia L, Nelsen MP, Pang K, Phookamsak R, Senanayake IC, Shearer CA, Suetrong S, Tanaka K, Thambugala KM, Wijayawardene NN, Wikee S, Wu H, Zhang Y, Aguirre-Hudson B, Alias SA, Aptroot A, Bahkali AH, Bezerra JL, Bhat DJ, Camporesi E, Chukeatirote E, Gueidan C, Hawksworth DL, Hirayama K, De Hoog S, Kang J, Knudsen K, Li W, Li X, Liu Z, Mapook A, Mckenzie EHC, Miller AN, Mortimer PE, Phillips AJL, Raja HA, Scheuer C, Schumm F, Taylor JE, Tian Q, Tibpromma S, Wanasinghe DN, Wang Y, Xu J, Yacharoen S, Yan J, Zhang M (2013) Families of Dothideomycetes. Fungal Diversity 63(1): 1–313. https://doi.org/10.1007/s13225-013-0263-4

Hyde KD, Hongsanan S, Jeewon R, Bhat JD, McKenzie CHE, Jones GBE, Phookamsak R, Ariyawansa HA, Boonmee S, Zhao Q, Abdel-Aziz FA, Abdel-Wahab MA, Banmai S, Chomnunti P, Cui B, Daranagama DA, Das K, Dayarathne MC, de Silva NI, Dissanayake AJ, Doilom M, Ekanayaka AH, Gibertoni TB, Góes-Neto A, Huang S, Jayasiri SC, Jayawardena RS, Konta S, Lee HB, Li W, Lin C, Liu J, Lu Y, Luo Z, Manawasinghe IS, Manimohan P, Mapook A, Niskanen T, Norphanphoun C, Papizadeh M, Perera RH, Phukhamsakda C, Richter C, de Santiago ALCM, Drechsler-Santos ER, Senanayake IC, Tanaka K, Tennakoon TMDS, Thambugala KM, Tian Q, Tibpromma S, Thongbai B, Vizzini A, Wanasinghe DN, Wijayawardene NN, Wu H, Yang J, Zeng X, Zhang H, Zhang J, Bulgakov TS, Camporesi E, Bahkali AH, Amoozegar MA, Araujo-Neta LS, Ammirati JF, Baghela A, Bhatt RP, Bojantchev D, Buyck B, Da Silva GA, de Lima CLF, de Oliveira RJV, de Souza CAF, Dai Y, Dima B, Duong TT, Ercole E, Mafalda-Freire F, Ghosh A, Hashimoto A, Kamolhan S, Kang J, Karunarathna SC, Kirk PM, Kytövuori I, Lantieri A, Liimatainen K, Liu Z, Liu X, Lücking R, Medardi G, Mortimer PE, Nguyen TTT, Promputtha I, Raj KNA, Reck MA, Lumyong S, Shahzadeh-Fazeli SA, Stadler M, Soudi MR, Su H, Takahashi T, Tangthirasunun N, Uniyal P, Wang Y, Wen T, Xu J, Zhang Z, Zhao Y, Zhou J, Zhu L (2016) Fungal diversity notes 367–490: Taxonomic and phylogenetic contributions to fungal taxa. Fungal Diversity 80: 1–270. https://doi.org/10.1007/s13225-016-0373-x

Katoh K, Rozewicki J, Yamada KD (2019) MAFFT online service: Multiple sequence a2gnment, interactive sequence choice and visualization. Briefings in Bioinformatics 20(4): 1160–1166. https://doi.org/10.1093/bib/bbx108

Li GQ, Liu FF, Li JQ, Liu QL, Chen SF (2018) Botryosphaeriaceae from *Eucalyptus* plantations and adjacent plants in China. Persoonia 40(1): 63–95. https://doi.org/10.3767/persoonia.2018.40.03

Li GQ, Slippers B, Wingfield MJ, Chen SF (2020) Variation in Botryosphaeriaceae from *Eucalyptus* plantations in Yunnan Province in southwestern China across a climatic gradient. IMA Fungus 11(1): 22. https://doi.org/10.1186/s43008-020-00043-x

Liu YJ, Whelen S, Hall BD (1999) Phylogenetic relationships among ascomycetes: Evidence from an RNA polymerase II subunit. Molecular Biology and Evolution 16(12): 1799–1808. https://doi.org/10.1093/oxfordjournals.molbev.a026092

Ma Y, Li T, Xu X, Ji Y, Jiang X, Shi X, Wang B (2021) Investigation of volatile compounds, microbial succession, and their relation during spontaneous fermentation of Petit Manseng. Frontiers in Microbiology 12: 717387. https://doi.org/10.3389/fmicb.2021.717387

Money P (2016) Chapter 1-Fungal Diversity. In: Watkinson SC, Boddy L, Money NP (Eds) The Fungi (3rd edn.), 36 pp. https://doi.org/10.1016/B978-0-12-382034-1.00001-3

Nguyen LT, Schmidt HA, Von Haeseler A, Minh BQ (2015) IQ-TREE: A fast and effective stochastic algorithm for estimating maximum-likelihood phylogenies. Molecular Biology and Evolution 32(1): 268–274. https://doi.org/10.1093/molbev/msu300

Senanayake IC, Rathnayake AR, Marasinghe DS, Calabon MS, Gentekaki E, Lee HB, Hurdeal VG, Pem D, Dissanayake LS, Wijesinghe SN, Bundhun D, Nguyen TT, Goonasekara ID, Abeywickrama PD, Bhunjun CS, Jayawardena RS, Wanasinghe DN, Jeewon R, Bhat DJ, Xiang MM (2020) Morphological approaches in studying fungi: Collection, examination, isolation, sporulation and preservation. Mycosphere 11(1): 2678–2754. https://doi.org/10.5943/mycosphere/11/1/20

Spatafora J, Sung G, Johnson D, Hesse C, O'Rourke B, Serdani M, Spotts R, Lutzoni F, Valerie H, Miadlikowska J, Reeb V, Gueidan C, Fraker E, Lumbsch T, Lücking R, Schmitt I, Hosaka K, Aptroot A, Roux C, Schoch C (2006) A five-gene phylogeny of Pezizomycotina. Mycologia 98(6): 1018–1028. https://doi.org/10.1080/15572536.2006.11832630

Swofford DL (2002) PAUP*: Phylogenetic analysis using parsimony (and other methods), version 4.0 b10. Sinauer Associates, Sunderland, UK.

Thambugala MK, Daranagama AD, Phillips LJA, Bulgakov TS, Bhat DJ, Camporesi D, Bahkali AH, Eungwanichayapant PD, Liu ZY, Hyde KD (2017) Microfungi on *Tamarix*. Fungal Diversity 82(1): 239–306. https://doi.org/10.1007/s13225-016-0371-z

Trifinopoulos J, Nguyen LT, von Haeseler A, Minh BQ (2016) W-IQ-TREE: A fast online phylogenetic tool for maximum likelihood analysis. Nucleic Acids Research 44(W1): W232–W235. https://doi.org/10.1093/nar/gkw256

Vaidya G, Lohman DJ, Meier R (2011) Sequence Matrix: Concatenation software for the fast assembly of multi-gene datasets with character set and codon information. Cladistics 27(2): 171–180. https://doi.org/10.1111/j.1096-0031.2010.00329.x

Valenzuela-Lopez N, Cano-Lira J, Guarro J, Sutton DA, Wiederhold N, Crous PW, Stchigel AM (2018) Coelomycetous Dothideomycetes with emphasis on the families Cucurbitariaceae and Didymellaceae. Studies in Mycology 90(1): 1–69. https://doi.org/10.1016/j.simyco.2017.11.003

Vilgalys R, Hester M (1990) Rapid genetic identification and mapping of enzymatically amplified ribosomal DNA from several *Cryptococcus* species. Journal of Bacteriology 172(8): 4238–4246. https://doi.org/10.1128/jb.172.8.4238-4246.1990

Vu D, Groenewald M, Vries MD, Stielow B, Eberhardt U, Al-Hatmi A, Groenewald JZ, Cardinali G, Houbraken J, Boekhout T, Crous PW, Robert V, Verkley GJM (2019) Large-scale generation and analysis of filamentous fungal DNA barcodes boosts coverage for kingdom fungi and reveals thresholds for fungal species and higher taxon delimitation. Studies in Mycology 92(1): 135–154. https://doi.org/10.1016/j.simyco.2018.05.001

Wanasinghe DN (2018) Taxonomic circumscription and phylogenetics of novel Didymellaceous taxa with brown muriform spores. Studies in Fungi 3(1): 152–175. https://doi.org/10.5943/sif/3/1/17

Wang Y, Tu Y, Chen X, Jiang H, Ren H, Lu Q, Wei C, Lv W (2024) Didymellaceae species associated with tea plant (*Camellia sinensis*) in China. MycoKeys 105: 217–251. https://doi.org/10.3897/mycokeys.105.119536

White TJ, Bruns T, Lee S, Taylor J (1990) Amplification and direct sequencing of fungal ribosomal RNA genes for phylogenetics. In: Innes MA, Gelfand DH, Sninsky JJ, White TJ (Eds) PCR protocols: a guide to methods and applications. Academic Press, San Diego, CA, 315–322. https://doi.org/10.1016/B978-0-12-372180-8.50042-1

Wijayawardene NN, Hyde KD, Rajeshkumar KC, Hawksworth DL, Madrid H, Kirk PM, Braun U, Singh RV, Crous PW, Kukwa M, Lücking R, Kurtzman CP, Yurkov A, Haelewaters D, Aptroot A, Lumbsch HT, Timdal E, Ertz D, Etayo J, Phillips AJL, Groenewald JZ, Papizadeh M, Selbmann L, Dayarathne MC, Weerakoon G, Jones EBG, Suetrong S, Tian Q, Castañeda-Ruiz RF, Bahkali AH, Pang K-L, Tanaka K, Dai DQ, Sakayaroj J, Hujslová M,

Lombard L, Shenoy BD, Suija A, Maharachchikumbura SSN, Thambugala KM, Wanasinghe DN, Sharma BO, Gaikwad S, Pandit G, Zucconi L, Onofri S, Egidi E, Raja HA, Kodsueb R, Cáceres MES, Pérez-Ortega S, Fiuza PO, Monteiro JS, Vasilyeva LN, Shivas RG, Prieto M, Wedin M, Olariaga I, Lateef AA, Agrawal Y, Fazeli SAS, Amoozegar MA, Zhao GZ, Pfliegler WP, Sharma G, Oset M, Abdel-Wahab MA, Takamatsu S, Bensch K, de Silva NI, De Kesel A, Karunarathna A, Boonmee S, Pfister DH, Lu Y-Z, Luo Z-L, Boonyuen N, Daranagama DA, Senanayake IC, Jayasiri SC, Samarakoon MC, Zeng X-Y, Doilom M, Quijada L, Rampadarath S, Heredia G, Dissanayake AJ, Jayawardana RS, Perera RH, Tang LZ, Phukhamsakda C, Hernández-Restrepo M, Ma X, Tibpromma S, Gusmao LFP, Weerahewa D, Karunarathna SC (2017) Notes for genera: Ascomycota. Fungal Diversity 86(1): 1–594. https://doi.org/10.1007/s13225-017-0386-0

Wijayawardene NN, Hyde KD, Dai DQ, Sanchez-Garcia M, Tomio Goto B, Saxena RK, Erdoğdu M, Selcuk F (2022a) Outline of Fungi and fungus-like taxa – 2021. Mycosphere 13(1): 53–453. https://doi.org/10.5943/mycosphere/13/1/2

Wijayawardene NN, Phillips AJL, Pereira DS, Dai DQ, Aptroot A, Monteiro JS, Druzhinina IS, Cai F, Fan X, Selbmann L, Coleine C, Castañeda-Ruiz R, Kukwa M, Flakus A, Oliveira Fiuza P, Kirk PM, Rajesh Kumar KC, Ileperuma Arachchi IS, Suwannarach N, Thines M (2022b) Forecasting the number of species of asexually reproducing fungi (Ascomycota and Basidiomycota). Fungal Diversity 114(1): 463–490. https://doi.org/10.1007/s13225-022-00500-5

Wilson A, Cuddy WS, Park RF, Harm GFS, Priest MJ, Bailey J, Moffitt MC (2020) Investigating hyperparasites as potential biological control agents of rust pathogens on cereal crops. Australasian Plant Pathology 49(3): 231–238. https://doi.org/10.1007/s13313-020-00695-8

Woudenberg JHC, Aveskamp MM, Gruyter J, Spiers AG, Crous PW (2009) Multiple *Didymella* teleomorphs are linked to the *Phoma clematidina* morphotype. Persoonia 22(1): 56–62. https://doi.org/10.3767/003158509X427808

Yukako H, Yuho A, Atsuko S, Nami U, Chiharu N (2021) Taxonomical study of noteworthy species of *Botryosphaeria* in Japan. Mycobiology 49(2): 122–132. https://doi.org/10.1080/12298093.2021.1895486

MycoKeys 106: 287–301 (2024)
DOI: 10.3897/mycokeys.106.117205

Research Article

Multi-locus molecular phylogenetic analysis reveals two new species of *Amphichorda* (Bionectriaceae, Hypocreales)

Zhi-Qin Wang[1,2*], Jing Zhao[1,2*], Quan-Ying Dong[1,2], Yao Wang[1,2], Ying-Ling Lu[1,2], Run Luo[1,2], Hong Yu[1,2]

1 *Yunnan Herbal Laboratory, College of Ecology and Environmental Sciences, Yunnan University, Kunming, Yunnan, China*
2 *The International Joint Research Center for Sustainable Utilization of Cordyceps Bioresources in China and Southeast Asia, Yunnan University, Kunming, Yunnan, China*

Corresponding author: Hong Yu (hongyu@ynu.edu.cn, herbfish@163.com)

Abstract

Amphichorda has been previously accepted as a member of the Cordycipitaceae and currently it is considered a member of the Bionectriaceae. The substrates of *Amphichorda* were complex and varied, being mainly animal faeces. This study reports two new species of *Amphichorda* from Yunnan Province in south-western China. Based on the five-gene (nr*SSU*, nr*LSU*, *tef-1α*, *rpb1* and *rpb2*) sequence and ITS data phylogenetic analysis, two new species, namely *A. excrementa* and *A. kunmingensis*, are proposed and a detailed description of the new species is provided. *Amphichorda excrementa* and *A. kunmingensis* were isolated from animal faeces in the park. The morphological characteristics of two novel species and seven known species in *Amphichorda* are also compared.

Key words: Coprophilous fungi, diversity, morphology, new taxa, taxonomy

Academic editor:
Nalin Wijayawardene
Received: 11 December 2023
Accepted: 6 May 2024
Published: 3 July 2024

Citation: Wang Z-Q, Zhao J, Dong Q-Y, Wang Y, Lu Y-L, Luo R, Yu H (2024) Multi-locus molecular phylogenetic analysis reveals two new species of *Amphichorda* (Bionectriaceae, Hypocreales). MycoKeys 106: 287–301. https://doi.org/10.3897/mycokeys.106.117205

Introduction

Amphichorda Fr. was established to accommodate the type species *A. felina* (DC.) Fr., which was isolated from cat dung and previously classified in the genus *Clavaria* (Lamarck 1815; Fries 1825). At the present, seven species of the *Amphichorda* are now validly published (Zhang et al. 2017, 2021; Guerra-Mateo et al. 2023; Liu et al. 2023; Leão et al. 2024). The traditional phylogenetic placement of the genus *Amphichorda* was considered in the family Cordycipitaceae (Hypocreales). The Cordycipitaceae is the most complex group in the order Hypocreales because of its varied morphological characteristics and wide-ranging hosts and some genera present numerous taxonomical problems (Wang et al. 2020; Guerra-Mateo et al. 2023). In the studies of Zhang et al. (2017, 2021) and Liu et al. (2023) which report new species of the genus *Amphichorda*, the phylogenetic position of *Amphichorda* belongs to the Cordycipitaceae. However, Guerra-Mateo et al. (2023) conducted the phylogenetic analysis based on the nuclear ribosomal internal transcribed spacer region (ITS) and the nuclear ribosomal large subunit (nr*LSU*), considered *Amphichorda* to belong to the family Bionectriaceae and determined *Amphichorda* has close phylogenetic

* These authors contributed equally to this work.

relationships with the genera *Hapsidospora* and *Nigrosabulum*. Leão et al. (2024) also proving the genus *Amphichorda* belongs to the family Bionectriaceae.

The taxonomic status of the type species has been controversial since the original description of the type species of the *Amphichorda*. *Amphichorda felina* was classified as *Beauveria* in 1980 (Carmichael et al. 1980). However, early phylogenetic analyses showed that *Beauveria felina* was distant from other *Beauveria* species and that it was morphologically distinguished from other *Beauveria* species by the absence of elongate conidiogenous cells with apical denticulate rachis (Rehner et al. 2011; Zhang et al. 2017; Liu et al. 2023). The type strain of *A. felina* (= *B. felina*) seems to be unknown (Guerra-Mateo et al. 2023). *Isaria cretacea* J.F.H. Beyma type strain CBS 250.34 was considered to be the type strain of *A. felina* since *I. cretacea* was synonymised with *A. felina* (De Hoog 1972; Zhang et al. 2021; Guerra-Mateo et al. 2023). However, the criteria required for fungal epitypification were the substrate and geographic similarity (Guerra-Mateo et al. 2023). The substrate and geography were different between *A. felina* and the strain CBS 250.34, so this strain has not been designated as the epitype of *A. felina* (Lendemer 2020). Guerra-Mateo et al. (2023) proposed that the strain CBS 250.34 can be accepted as a reference to stabilise the nomenclature of *A. felina*, but should be avoided to indicate it as a type strain of *A. felina* (Zhang et al. 2017, 2021; Wang et al. 2020; Liu et al. 2023).

During the surveys of entomopathogenic fungi from two regions in Yunnan Province, China, the animal faeces were collected and three strains were isolated from the specimens. Based on morphological evidence together with the five-gene (nr*SSU*, nr*LSU*, *tef-1α*, *rpb1* and *rpb2*) sequence and ITS data analyses of some genera in Bionectriaceae, it was shown that the three strains belong to the genus *Amphichorda*. On the basis of its morphological characteristics and multi-locus molecular phylogenetic analyses, two new species were described. Furthermore, the morphological characteristics of two novel species and seven known species in *Amphichorda* were compared.

Materials and methods

Fungal collection and isolation

The specimens were collected in Kunming City, Yunnan Province, China in July 2019. In the field, it was placed in sterilised plastic pipes and brought to the laboratory for isolation. In order to obtain axenic cultures, part of the surface tissue of the specimen was cut off with a sterilised dissecting knife and then placed into a flask containing 10 ml of sterilised water and glass beads. Then the suspension was shaken for 10 min and diluted 50 times. Finally, the diluted suspension was applied on Petri dishes with potato dextrose agar (PDA: fresh potato 200 g/l, dextrose 20 g/l and agar 18 g/l) containing 0.1 g/l streptomycin and 0.05 g/l tetracycline. Then the Petri dish was placed in a room at 15 °C to allow it to grow, during which time the growing fungi were transferred one by one to new Petri dishes. After isolation into pure cultures, they were transplanted to a PDA slant and stored at 4 °C. The specimens were deposited in the Yunnan Herbal Herbarium (YHH) of Yunnan University, China. The strain was deposited at the Yunnan Fungal Culture Collection (YFCC) of Yunnan University, China. The culture of the *Amphichorda felina* (CBS 250.34) was obtained from

the culture collection (CBS) of the Westerdijk Fungal Biodiversity Institute (WI) in Utrecht, the Netherlands. The obtained strain CBS 250.34 was inoculated into PDA medium and re-cultured.

Morphological observations

Colonies were incubated on PDA for three weeks in an incubator at 25 °C. The photograph was taken morphologically using a Canon 750 D camera (Canon Inc., Tokyo, Japan). The anamorphs (Conidiophores, Phialides and Conidia) in culture were observed using a light microscope (Olympus BX53). The growth rate of colonies was calculated using the method of Liu and Hodge (2005) and it was categorised as: fast-growing (30–35 mm in diameter), moderately growing (20–30 mm in diameter) and slow-growing (< 20 mm in diameter).

DNA extraction, PCR and sequencing

The genomic DNA was extracted from axenic living cultures using the Genomic DNA Purification Kit (Qiagen GmbH, Hilden, Germany) according to the manufacturer's instructions. The five-gene (nr*SSU*, nr*LSU*, *tef-1α*, *rpb1* and *rpb2*) and ITS were sequenced and the following primer pairs were used for PCR amplification. The nuclear ribosomal internal transcribed spacer region (ITS) was amplified with the primer pairs ITS4/ITS5 (White et al. 1990). The nuclear ribosomal small and large subunit (nr*SSU* and nr*LSU*) were amplified with the primer pairs nr*SSU*-CoF/nr*SSU*-CoR and LR5/LR0R, respectively (Vilgalys and Hester 1990; Rehner and Samuels 1994; Wang et al. 2015a). The translation elongation factor 1α (*tef-1α*) was amplified with the primers EF1α-EF and EF1α-ER (Bischof et al. 2006; Sung et al. 2007). The largest and second subunits of RNA polymerase II (*rpb1* and *rpb2*) were amplified with the primers RPB1-5'F/RPB1-5'R and RPB2-5'F/RPB2-5'R, respectively (Bischof et al. 2006; Sung et al. 2007). The polymerase chain reaction (PCR) matrix was performed in a final volume of 50 µl and the detailed information was described by Wang et al. (2022). Amplification reactions were performed in the BIORAD T100TM thermal cycler (BIO-RAD Laboratories, Hercules, CA, United States). The PCR reactions followed the procedures of Wang et al. (2015b) and the PCR products were sequenced by the Beijing Genomics Institute (Chongqing, China).

Phylogenetic analyses

Based on the six-locus molecular, including ITS, nr*SSU*, nr*LSU*, *tef-1α*, *rpb1* and *rpb2*, phylogenetic analyses were performed using datasets retrieved from GenBank and those generated in this work. The DNA sequences newly generated have been submitted to GenBank. The sequences downloaded from the GenBank database were based on a previous study by Hou et al. (2023) and Leão et al. (2024). The taxonomic information and corresponding GenBank accession numbers used are provided in Table 1. Sequences were aligned with MEGA v.6.06 and used to remove poorly-aligned regions and for manual adjustment (Tamura et al. 2013). Six-locus molecular were concatenated together using Phylosuite v.1.2.2 (Zhang et al. 2020). The Maximum Likelihood (ML) tree was performed using IQ-tree v.2.1.3 and the Bayesian Inference (BI) tree was performed using MrBayes v.3.2.2

Table 1. Species information and corresponding GenBank accession numbers of *Amphichorda* and close relative genera used in this study.

Species	Strain	ITS	nr*SSU*	nr*LSU*	*tef-1α*	*rpb1*	*rpb2*
Alloacremonium humicola	CBS 613.82	NR_189433	–	NG_229089	OQ470786	–	OQ453888
Alloacremonium ferrugineum	CBS 102877	NR_189432	–	NG_228721	OQ470785	–	OQ453887
*Amphichorda cavernicol*a	CGMCC3.19571	MK329056	–	MK328961	MK335997	–	–
Amphichorda cavernicola	LC12481	MK329057	–	MK328962	MK335998	–	–
Amphichorda cavernicola	LC12553	MK329059	–	MK328964	MK336000	–	–
Amphichorda cavernicola	LC12560	MK329061	–	MK328966	MK336002	–	–
Amphichorda coprophila	CBS 247.82 ^{T}	MH861494	–	MH873238	OQ954487	–	–
Amphichorda coprophila	CBS 424.88	OQ942929	–	OQ943166	OQ954488	–	–
Amphichorda excrementa	**YFCC AECCS848^{T}**	-	**OR913433**	**OR913439**	**OR917446**	**OR917451**	**OR917443**
Amphichorda felina	CBS 250.34	MH855498	–	OQ943167	OQ954490	–	–
Amphichorda felina	**CBS 250.34**	-	**OR913436**	**OR913440**	**OR917447**	**OR917450**	**OR917444**
Amphichorda felina	CBS 648.66	OQ942930	–	MH870575	OQ954491	–	–
Amphichorda guana	CGMCC3.17908^{T}	KU746665	KY883262	KU746711	KX855211	KY883202	KY883228
Amphichorda guana	CGMCC3.17909	KU746666	KY883263	KU746712	KX855212	KY883203	–
Amphichorda kunmingensis	**YFCC AKYYH8414^{T}**	-	**OR913435**	**OR913438**	**OR917448**	**OR917452**	–
Amphichorda kunmingensis	**YFCC AKYYH8487**	-	**OR913434**	**OR913437**	**OR917449**	**OR917453**	**OR917445**
Amphichorda littoralis	FMR 17952	OQ942925	–	OQ943162	OQ954483	–	–
Amphichorda littoralis	FMR 19404^{T}	OQ942924	–	OQ943161	OQ954482	–	–
Amphichorda littoralis	FMR 19611	OQ942926	–	OQ943163	OQ954484	–	–
Amphichorda monjolensis	COAD 3124	OQ288256	–	OQ288260	OR454090	–	OQ405040
Amphichorda monjolensis	COAD 3125	OQ288257	–	–	–	–	OQ405041
Amphichorda monjolensis	COAD 3120	OQ288258	–	–	–	–	OQ405042
Amphichorda yunnanensis	KUMCC 21-0414	ON426823	–	–	OR025977	OR022016	OR022041
Amphichorda yunnanensis	KUMCC 21-0415	ON426824	–	–	OR025976	OR022015	OR022040
Amphichorda yunnanensis	KUMCC 21-0416^{T}	-	–	–	OR025975	OR022014	OR022039
Bulbithecium ammophilae	CBS 178.78	NR_189437	–	NG_242039	OQ470793	–	OQ453895
Bulbithecium arxii	CBS 737.84	NR_145040	–	HQ232159	OQ470794	–	OQ451834
Bulbithecium borodinense	CBS 101148	OQ429506	–	HQ232003	–	–	–
Bulbithecium ellipsoideum	CBS 993.69	NR_189438	–	NG_242040	OQ470796	–	OQ453896
Bulbithecium hyalosporum	CBS:318.91	MH862256	AF096172	OQ055419	OQ470797	–	OQ453897
Bulbithecium pinkertoniae	CBS 157.70	NR_159611	NG_062816	NG_058554	OQ470799	–	OQ453898
Bulbithecium spinosum	CBS 136.33	OQ429512	NG_062819	NG_056971	OQ470802	–	OQ453899
Bulbithecium truncatum	CBS 113718	NR_189439	–	NG_242041	OQ470803	–	OQ453900
Claviceps purpurea	SA cp11	-	EF469122	EF469075	EF469058	EF469087	EF469105
Geosmithia lavendula	CBS 344.48	MH856380	–	MH867927	–	–	–
Geosmithia pallidum	CBS 260.33	OQ429599	–	OQ055509	OQ470909	–	OQ453998
Hapsidospora chrysogena	CBS 144.62	NR_189452	NG_062810	HQ232017	OQ470953	–	OQ454043
Hapsidospora flava	CBS 596.70	NR_189453	NG_062812	NG_056983	OQ470957	–	OQ454047
Hapsidospora globosa	CBS 512.70	NR_160124	–	NG_064081	OQ470963	–	OQ454053
Hapsidospora inversa	CBS 517.70	NR_189454	–	OQ055565	OQ470967	–	OQ454057
Hapsidospora irregularis	CBS 510.70	NR_160123	–	MH871595	OQ470968	–	OQ454058
Hapsidospora stercoraria	CBS 516.70	OQ429662	–	OQ055568	OQ470970	–	OQ454060
Hapsidospora variabilis	CBS 100549	NR_189456	–	NG_229091	OQ470971	–	OQ454061
*Myriogenospora atramentos*a	AEG 96-32	-	AY489701	AY489733	AY489628	AY489665	DQ522455

Species	Strain	ITS	nr*SSU*	nr*LSU*	*tef-1α*	*rpb1*	*rpb2*
Ovicillium subglobosum	CBS 101963	NR_154335	–	NG_069329	OQ471085	–	OQ454170
Ovicillium attenuatum	CBS 399.86	NR_154333	–	NG_229092	OQ471083	–	OQ454168
Proxiovicillium blochii	CBS 427.93	-	HQ232182	HQ232001	–	–	–
Proxiovicillium lepidopterorum	CBS 101239	NR_189482	–	NG_242070	OQ471145		OQ454214
Proliferophialis apiculata	CBS 303.64	NR_189480	–	NG_242064	OQ471122	–	OQ454207
Proliferophialis apiculata	CBS 397.78	OQ429798	–	OQ055694	–	–	OQ454209
Stilbocrea macrostoma	CBS 141849	OQ429874	–	OQ430123	–	–	OQ454273
Stilbocrea walteri	CBS 144627	NR_160063	–	NG_242075	–	–	–
Waltergamsia parva	CBS 381.70A	NR_163808	–	NG_242083	OQ471279	–	OQ454346
Waltergamsia pilosa	CBS 124.70	NR_163809	–	OQ430199	OQ471282	–	OQ454349

Boldface: data generated in this study; ^{T}: ex-type culture.
A.E.G: A. E. Glenn personal collection; CBS: the culture collection of the Westerdijk Fungal Biodiversity Institute (WI); CGMCC: the China General Microbiological Culture Collection Center; COAD: the Laboratório de Micologia e Etiologia de Doenças Fúngicas de Plantas and Coleção Octávio Almeida Drummond; FMR: the culture collection of the Faculty of Medicine in Reus; KUMCC: the Kunming Culture Collection; LC: personal culture collection held in the lab of Dr Lei Cai; YFCC: the Yunnan Fungal Culture Collection (YFCC) of Yunnan University.

(Ronquist et al. 2012; Nguyen et al. 2015). The best-fitting likelihood model for BI and ML analyses was selected using ModelFinder (Kalyaanamoorthy et al. 2017). In the phylogenetic tree of *Amphichorda* and some other genera, the TN+F+I+G4 model was selected as the optimal model for the ML analyses, with 5000 ultrafast bootstraps (Hoang et al. 2017) in a single run. The GTR+F+I+G4 model was selected as the optimal model for the BI analysis and the four Markov Chain Monte Carlo chains run for 2 million generations from a random start tree with a sampling frequency of 100 generations, in which the initial 25% of sampled data were discarded as burn-in. Phylogenetic trees were visualised in FigTree v.1.4.3 and edited in Adobe Illustrator CS6. The values of ML bootstrap proportions (BP) (≥ 70%) and the BI posterior probability (PP) (≥ 0.70) are indicated at the nodes (BP/PP).

Results

Sequencing and phylogenetic analyses

The phylogenetic tree was inferred using 54 strains of 12 genera from Bionectriaceae and Clavicipitaceae, including *Alloacremonium*, *Amphichorda*, *Bulbithecium*, *Claviceps*, *Geosmithia*, *Hapsidospora*, *Myriogenospora*, *Ovicillium*, *Proxiovicillium*, *Proliferophialis*, *Stilbocrea* and *Waltergamsia*. Two strains (*Claviceps purpurea* SA cp11 and *Myriogenospora atramentosa* AEG 96-32) of Clavicipitaceae were selected as the outgroup. The final length of the six-locus molecular sequence concatenated dataset was 5,798 bp, including 766 bp for ITS, 1,391 bp for nr*SSU*, 859 bp for nr*LSU*, 850 bp for *tef-1α*, 781 bp for *rpb1* and 1,151 bp for *rpb2*. Phylogenetic trees from the BI and ML analyses exhibited similar topologies that had ten recognised, statistically well-supported clades in Bionectriaceae. The four strains were clustered in the genus *Amphichorda* based on the phylogenetic analyses of the combined dataset (Fig. 1). Our ML and BI analyses showed that two new species (i.e. *A. excrementa* and *A. kunmingensis*) and one known species were recognised. The new species, *A. excrementa* and *A. kunmingensis*, were well-supported by bootstrap proportions (BP = 90% and BP = 82%, respectively) and posterior probabilities (PP = 1.00 and PP = 0.96, respectively).

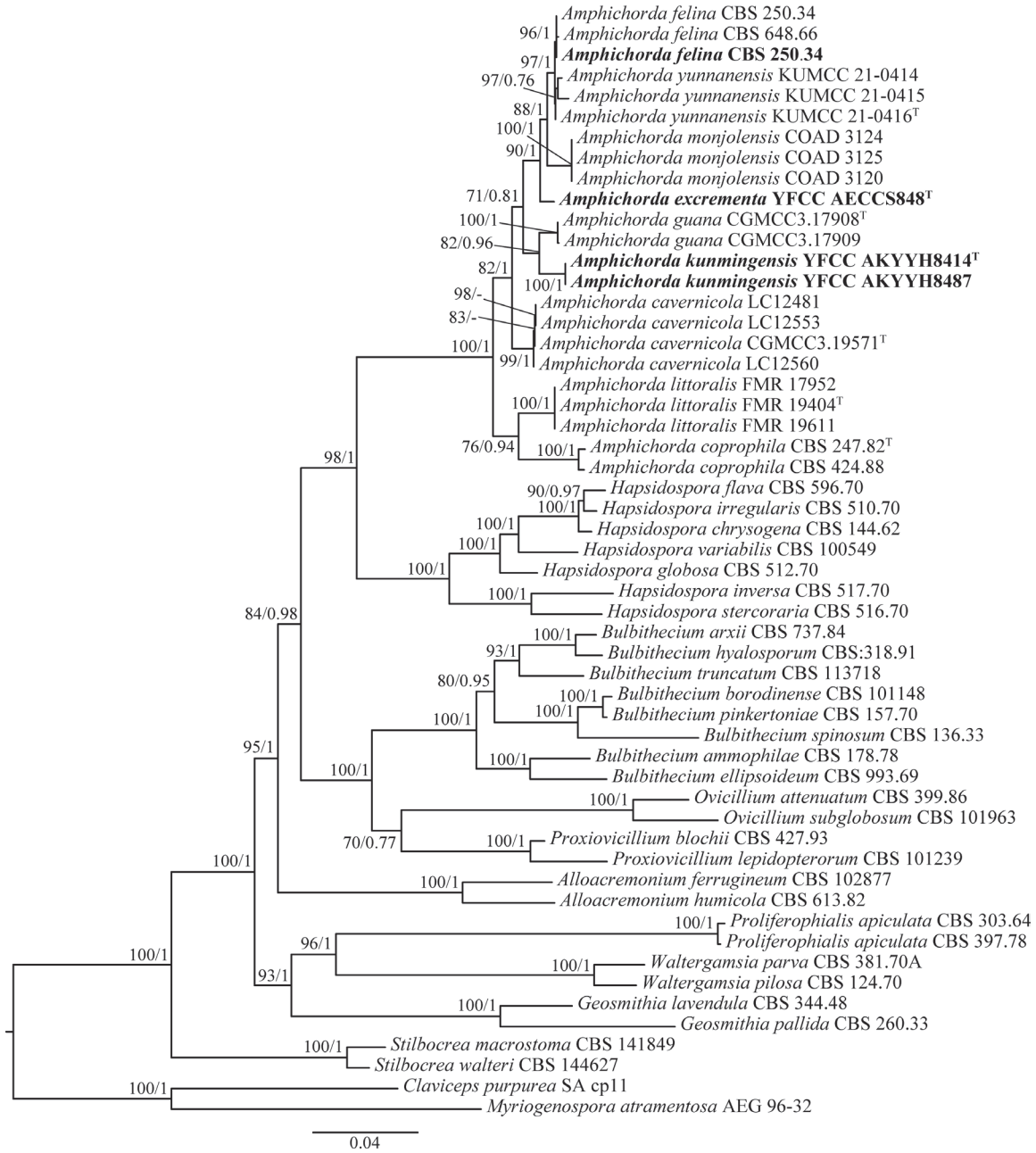

Figure 1. Phylogenetic tree of *Amphichorda* and close relative genera was constructed, based on Maximum Likelihood (ML) and Bayesian Inference (BI) analysis using six-locus molecular (ITS, nr*SSU*, nr*LSU*, *tef-1a*, *rpb1* and *rpb2*) sequences. The values of ML bootstrap proportions (BP) (≥ 70%) and the BI posterior probability (PP) (≥ 0.70) are indicated at the nodes (BP/PP). The new taxa were highlighted in bold.

Taxonomy

Amphichorda excrementa **Hong Yu bis, Z.Q. Wang, Q.Y. Dong & Y. Wang, sp. nov.**
MycoBank No: 851377
Fig. 2

Etymology. Refers to the excrement material from which this fungus was isolated.

Type. China, Yunnan Province, Kunming City, Changchongshan Country Park, 11 July 2019, Hong Yu and Yao Wang (YHH AECCS200777, ***holotype***; YFCC AECCS848, ex-type).

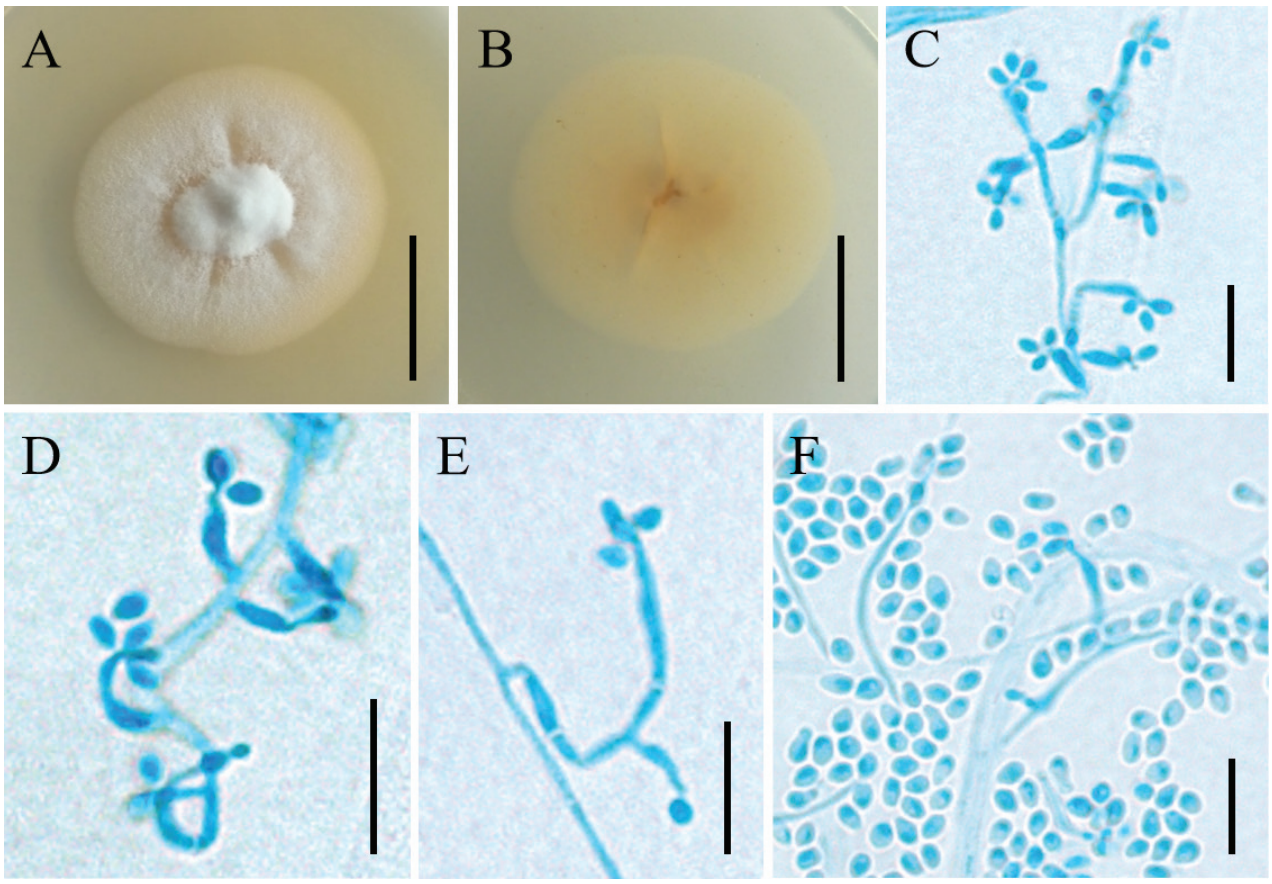

Figure 2. Morphology of *Amphichorda excrementa* **A, B** colony character on PDA medium after 30 d (**A** obverse **B** reverse) **C–F** conidiophores, conidiogenous cells and conidia. Scale bars: 2 cm (**A, B**); 10 μm (**C–F**).

Description. ***Sexual morph*:** Undetermined. ***Asexual morph*:** Colonies on PDA attaining a diameter of 42–44 mm after a month at 25 °C, white to cream, with high mycelial density, cottony, with a yellow margin, reverse pale yellow. ***Hyphae*** branched, smooth-walled, septate, hyaline, 0.6–1.3 μm wide. Cultures readily produced phialides and conidia after 3 weeks on potato dextrose agar at room temperature. ***Conidiophores*** arising laterally from hyphae, cylindrical, straight or slightly curved, hyaline and occasionally branched. ***Phialides*** arising laterally from aerial hyphae, occasionally solitary, mostly in whorls of 2–3 on lateral branches from the mycelia, basal portion cylindrical or flask-shaped, usually curved, 4.1–13.9 × 1.3–2.1 μm, tapering abruptly towards the apex, have a distinctly thin neck. ***Conidia*** 1.7–3.0 × 1.2–2.5 μm, one-celled, smooth-walled, hyaline, globose to elliptical, single. ***Chlamydospores*** not observed.

Substrate. Animal faeces.

Distribution. China.

Commentary. Phylogenetic analyses showed that *Amphichorda excrementa* formed a separate clade with statistical support from the BI posterior probabilities (PP = 1.00) and the ML bootstrap proportions (BP = 90%) and was closely related to *A. felina*, *A. yunnanensis* and *A. monjolensis*. However, *A. excrementa* can be distinguished from three species by morphological differences. The phialides of *A. excrementa* were longer (4.1–13.9 × 1.3–2.1 μm) than those of *A. felina* (1.5–8.5 × 1.8–2.9 μm) and the conidia were smaller than those of *A. felina* (1.7–3.0 × 1.2–2.5 μm vs. 2.5–4.7 × 2–3.5 μm). The phialides of

A. excrementa were longer (4.1–13.9 × 1.3–2.1 μm) than those of *A. yunnanensis* (4–12 × 1–4 μm) and the conidia were smaller than those of *A. felina* (1.7–3.0 × 1.2–2.5 μm vs. 2–5 × 2–4 μm). The conidia of *A. monjolensis* were longer than those of *A. excrementa* (2.8–3.7 × 1.8–2.9 μm vs. 1.7–3.0 × 1.2–2.5 μm).

***Amphichorda felina* (DC.) Fr., Syst. orb. veg. (Lundae) 1: 170 (1825).**
MycoBank No: 562082
Fig. 3

Description. The morphological description of this study is based on the specimen, CBS 250.34. ***Sexual morph*:** Undetermined. ***Asexual morph*:** Colonies on PDA attaining a diameter of 36–38 mm after a month at 25 °C, white to creamy-white, hard texture, felt-like, reverse black-brown, many conidia assemble to form powder. ***Hyphae*** branched, smooth-walled, septate, hyaline, 1.2–2.4 μm wide. ***Phialides*** arising laterally from aerial hyphae, erect or irregularly curved, 1.5–4.1 × 1.8–2.9 μm. ***Conidia*** 2.9–4.7 × 2.4–3.5 μm, one-celled, smooth-walled, hyaline, broadly ellipsoid or subglobose, single or aggregated into spheres. ***Chlamydospores*** not observed.

Substrate. Pupa of *Anaitis efformata*, rabbit dung, mouldy leaves, porcupine dung, cat dung.

Distribution. Argentina, Britain, France, Germany.

Commentary. Guerra-Mateo et al. (2023) proposed that the strain CBS 250.34 can be accepted as a reference to stabilise the nomenclature of *Amphichorda felina* and thus the genus *Amphichorda*, but should be avoided to indicate it as a type strain. In this study, the strain, CBS 250.34, was available in the CBS culture collection and morphological observations were made. Its morphology was generally consistent with those described by De Hoog (1972), with one difference being that this study extended the phialides (1.5–8.5 × 1.8–2.9 μm) and conidia size range of this species (2.5–4.7 × 2–3.5 μm).

***Amphichorda kunmingensis* Hong Yu bis, Z.Q. Wang, Q.Y. Dong & Y. Wang, sp. nov.**
MycoBank No: 851378
Fig. 4

Etymology. Named from the location Kunming City where the species was collected.

Type. China, Yunnan Province, Kunming City, Wild Duck Lake Forest Park, 16 July 2019, Hong Yu and Yao Wang (YHH AKYYH200704, ***holotype***; YFCC AKYYH8414, ex-type).

Description. *Sexual morph*: Undetermined. ***Asexual morph*:** Colonies on PDA attaining a diameter of 52–54 mm after a month at 25 °C, white to pale grey, with low mycelial density, lanose. ***Hyphae*** hyaline, branched, smooth-walled, septate, 0.7–1.9 μm wide. Cultures readily produced phialides and conidia after 3 weeks on potato dextrose agar at room temperature. ***Phialides*** arising laterally from aerial hyphae, solitary, occasionally in simple whorls on lateral branches from the mycelia, basal portion cylindrical or fusiform, straight or

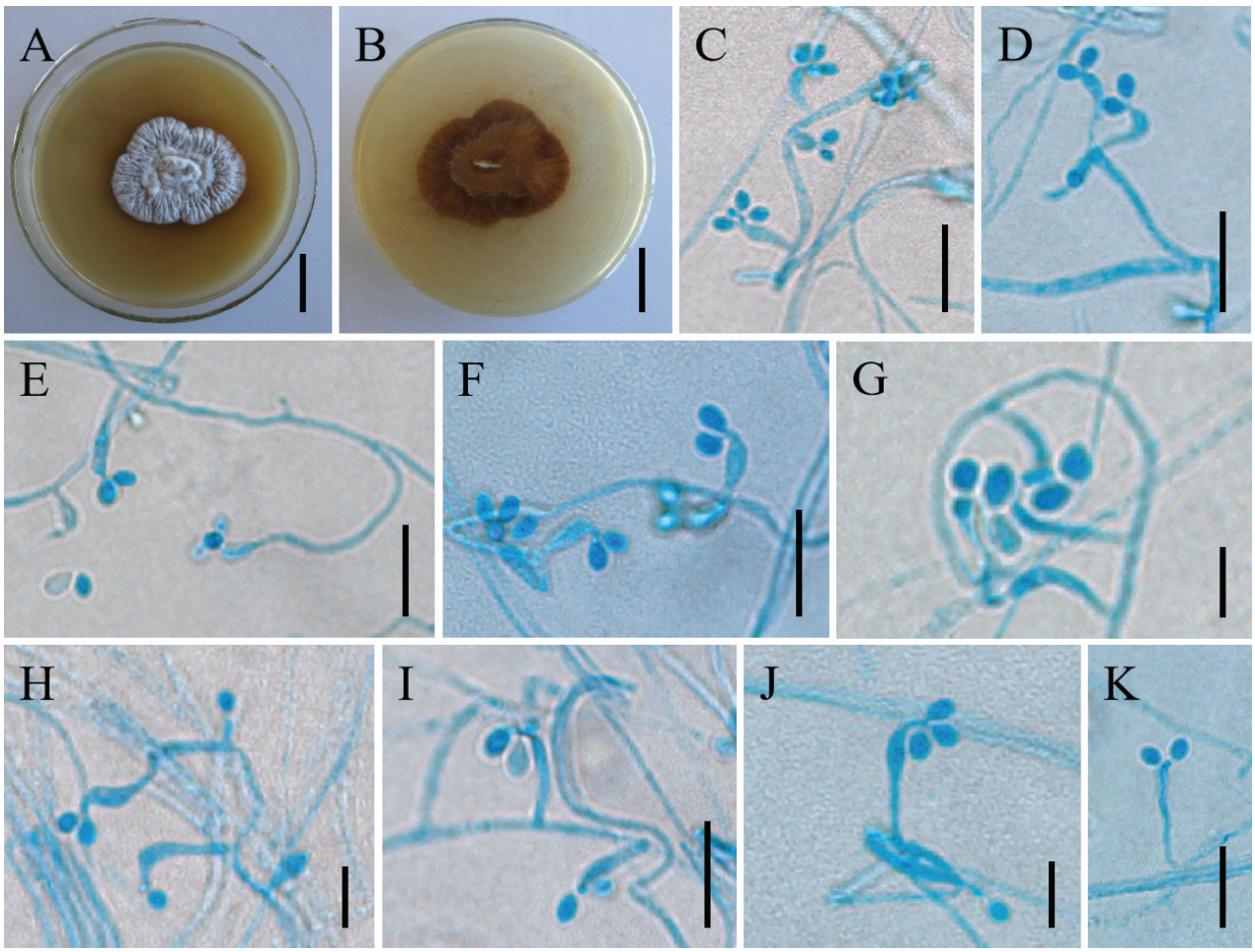

Figure 3. Morphology of *Amphichorda felina* **A, B** colony character on PDA medium after 30 d (**A** obverse **B** reverse) **C–K** conidiophores, conidiogenous cells and conidia. Scale bars: 2 cm (**A, B**); 10 μm (**C–F, I, K**); 5 μm (**G–H, J**).

irregularly bent, 6.1–17.5 × 1.4–2.9 μm. ***Conidia*** 2.3–4.2 × 1.6–3.0 μm, one-celled, smooth-walled, hyaline, globose to elliptical, single or aggregating in small heads at the apex of conidiogenous cells. ***Chlamydospores*** not observed.

Substrate. Animal faeces.

Distribution. China.

Other material examined. China, Yunnan Province, Kunming City, Wild Duck Lake Forest Park, 16 July 2019, Hong Yu and Yao Wang (YHH AKYYH200776, paratype; YFCC AKYYH8487, ex-paratype).

Commentary. Three species of *Amphichorda* were from China and *A. yunnanensis* was distributed in Yuxi City, Yunnan Province. The two new species in this study were from Kunming City, Yunnan Province. According to the phylogenetic tree, the new species, *A. kunmingensis*, forms a separate branch in *Amphichorda* and is sister to *A. guana*. However, it differs from *A. guana* by its smaller conidia. Although *A. kunmingensis*, *A. excrementa* and *A. yunnanensis* were all collected from Yunnan, their morphology was quite different (see Table 2). *Amphichorda kunmingensis* differs from *A. excrementa* in its usually curved and longer phialides (6.1–17.5 × 1.4–2.9 μm vs. 4.1–13.9 × 1.3–2.1 μm) and larger conidia (2.3–4.2 × 1.6–3.0 μm vs. 1.7–3.0 × 1.2–2.5 μm). *Amphichorda kunmingensis* differs from *A. yunnanensis* in the shape of its phialides and narrower conidia.

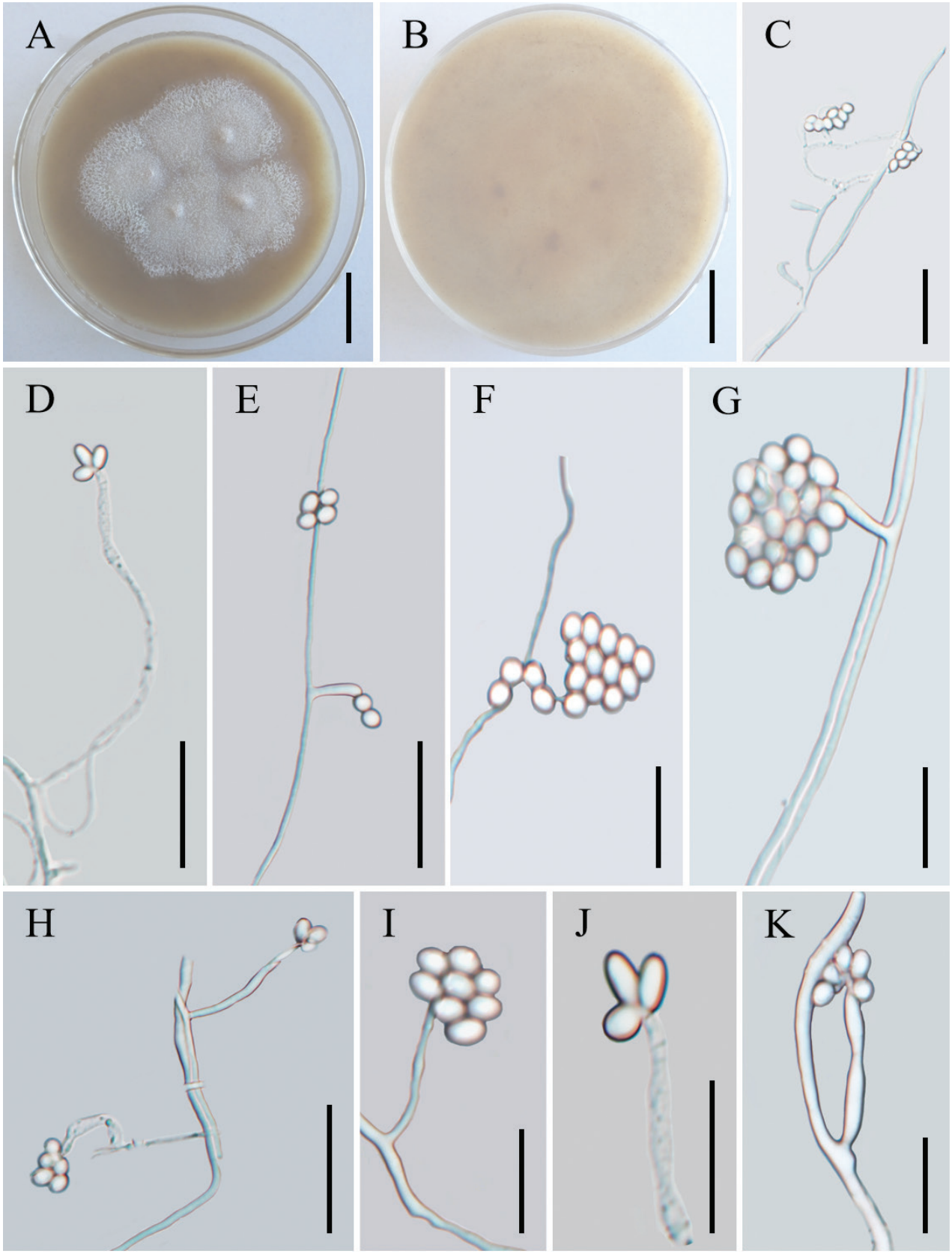

Figure 4. Morphology of *Amphichorda kunmingensis* **A, B** colony character on PDA medium after 30 d (**A** obverse **B** reverse) **C–K** conidiogenous cells and conidia. Scale bars: 2 cm (**A, B**); 20 μm (**C–E, H**); 10 μm (**F–G, I–K**).

Discussion

The phylogenetic analyses, based on the five-gene (nr*SSU*, nr*LSU*, *tef-1α*, *rpb1* and *rpb2*) sequence and ITS data were conducted and *Amphichorda excrementa* and *A. kunmingensis* were introduced. The morphological characteristics of the new species are similar to those of other *Amphichorda* species. Its conidiophores straight or slightly curved; phialides solitary, simple whorls or several whorls, straight or irregularly bent, usually curved, tapering abruptly towards the apex; conidia solitary or clumped, one-celled, shape variable (Table 2). They were similar to those of *Beauveria* and all species of *Amphichorda* do not have the elongate conidiogenous cells with apical denticulate rachis that are characteristic of *Beauveria*.

Table 2. Geographical location, hosts/substrates and asexual morphology of *Amphichorda*.

Species	Country	Host/Substrate	Conidiophores	Phialides (μm)	Conidia (μm)	References
Amphichorda cavernicola	China	Bird faeces; soil; plant debris; animal faeces; bat guano	Cylindrical, straight or slightly curved, occasionally branched	Fusiform or ellipsoidal, straight or irregularly bent, 4.5–8.0 × 2.0–3.0	Broadly ellipsoidal to subglobose, 2.5–4.0 × 2.0–3.5	Zhang et al. (2021)
A. coprophila	Canada; England	Chipmunk, rabbit and porcupine dung	Straight or flexuous, unbranched, bearing lateral or terminal conidiogenous cells, arranged singly or in whorls	Flask-shaped, usually with a strongly bent neck, 6–10 × 2–2.5	Subglobose to somewhat ellipsoidal, 3.5–5.5 × 2–3	Guerra-Mateo et al. (2023)
A. excrementa	**China**	Animal faeces	**Cylindrical, straight or slightly curved, occasionally branched**	**Occasionally solitary, mostly in whorls of 2–3, basal portion cylindrical or flask-shaped, usually curved, 4.1–13.9 × 1.3–2.1**	**Globose to elliptical 1.7–3.0 × 1.2–2.5**	**In this study**
A. felina	Britain, Germany, Argentina, France	Pupa of *Anaitis efformata*; rabbit dung; mouldy leaves; porcupine dung; cat dung	Straight	Solitarily or in small groups, consisting of a swollen, flask-shaped or curved, occasionally elongate basal part, 1.5–8.5 × 1.8–2.9	Subglobose, ellipsoidal or ovoidal, sometimes with a pointed base, 2.5–4.7 × 2–3.5	De Hoog (1972); **In this study**
A. guana	China	Bat guano	Straight or slightly curved	Fusiform or ellipsoidal, straight or irregularly bent, 7–10 × 2–3	Broadly ellipsoid to subglobose, 4.5–5.5 × 3.5–5	Zhang et al. (2017)
A. kunmingensis	**China**	**Animal faeces**	**-**	**Solitary, occasionally in simple whorls, basal portion cylindrical or fusiform, straight or irregularly bent, 6.1–17.5 × 1.4–2.9**	**Globose to elliptical 2.3–4.2 × 1.6–3.0**	**In this study**
A. littoralis	Spain	Sediments; fragment of floating rubber tire	Straight or flexuous, commonly unbranched, bearing lateral or terminal conidiogenous cells, arranged singly or in whorls of 2–4	Flask-shaped, usually with a strongly bent neck, 6–10 (–11.5) × 1.5–2	Subglobose, 3–4 × 2.5–3	Guerra-Mateo et al. (2023)
A. monjolensis	Brazil	on PDA plate consumed by an insect	Cylindrical, bearing one or more conidiogenous cells, straight or slightly bent, solitary or synnematous, sometimes branched	Flask-shaped, straight or irregularly bent, 3.1–6.1 × 2.7–5.1	Holoblastic, 2.8–3.7×1.8–2.9	Leão et al. (2024)
A. yunnanensis	China	Wing surfaces of *Rhinolophus*	Cylindrical, straight or slightly curved, branched	Monoblastic to polyblastic, ampulliform to flask-shaped, 4–12 × 1–4	Globose to oval, slightly ellipsoid, 2–5 × 2–4	Liu et al. (2023)

The species of *Amphichorda* has an extremely wide distribution, including Argentina, Canada, China, France, Germany, Great Britain, Spain (Table 2). Amongst the *Amphichorda* species, *A. felina*, *A. cavernicola*, *A. guana* and *A. monjolensis* were found in caves, especially *A. felina*, which was widely distributed in caves (Vanderwolf et al. 2013; Zhang et al. 2017, 2021; Vanderwolf et al. 2018; Leão et al. 2024). *Amphichorda littoralis* was found in Mediterranean coast sediments at 20 m depth (Guerra-Mateo et al. 2023). In contrast to the particular ecology of caves and the sea, *A. coprophila* was isolated from rabbit, chipmunk and porcupine dung and *A. yunnanensis* was isolated from the wing surfaces of *Rhinolophus affinis* (Guerra-Mateo et al. 2023; Liu et al. 2023). *Amphichorda excrementa* and *A. kunmingensis* were isolated from animal faeces in the Park. The substrates of *Amphichorda* were complex and varied, being mainly animal faeces, i.e. bird, cat, bat, chipmunk, rabbit and porcupine dung, but they have also been isolated in the pupa of *Anaitis efformata*, mouldy leaves, plant debris, sediments, fragments of floating rubber tyres, wing surfaces of *Rhinolophus* and soil. Most species of the genus *Amphichorda* have been isolated on animal faeces and are quite unique to their parasitic environments. This is unique to the biological characteristics and ecological habits for the genus *Amphichorda*.

Coprophilous fungi, particularly coprophilous ascomycetes, will be a rich source of antibiotics and other biologically important secondary metabolites (Bills et al. 2013). Species of the genus *Amphichorda* tend to have special physiological and metabolic characteristics due to the uniqueness of their growth environment. Additionally, some of their species have been reported to have high application value, such as *A. felina*, which was a well-known producer of insecticidal cyclodepsipeptide and cyclosporin C (Langenfeld et al. 2011; Chung et al. 2013; Xu et al. 2018). Furthermore, the study by Liang et al. (2021) successfully established a genetic transformation system in *A. guana* strain LC5815, which facilitated the development of bioactive secondary metabolites in fungi. Two new species of the genus *Amphichorda*, described in the present study, were isolated from animal faeces and may have good potential for natural product research.

Additional information

Conflict of interest

The authors have declared that no competing interests exist.

Ethical statement

No ethical statement was reported.

Funding

This work was supported by the National Natural Science Foundation of China (No. 31870017).

Author contributions

Data curation: QYD. Investigation: YW. Visualization: RL, YLL. Writing - original draft: ZQW. Writing - review and editing: JZ, HY.

Author ORCIDs

Zhi-Qin Wang https://orcid.org/0000-0001-9022-3635
Hong Yu https://orcid.org/0000-0002-2149-5714

Data availability

All of the data that support the findings of this study are available in the main text.

References

Araújo JPM, Lebert BM, Vermeulen S, Brachmann A, Ohm RA, Evans HC, de Bekker C (2022) Masters of the manipulator: Two new hypocrealean genera, *Niveomyces* (Cordycipitaceae) and *Torrubiellomyces* (Ophiocordycipitaceae), parasitic on the zombie ant fungus *Ophiocordyceps camponoti-floridani*. Persoonia 49(1): 171–194. https://doi.org/10.3767/persoonia.2022.49.05

Belyagoubi L, Belyagoubi-Benhammou N, Jurado V, Dupont J, Lacoste S, Djebbah F, Ounadjela FZ, Benaissa S, Habi S, Abdelouahid DE, Saiz-Jimenez C (2018) Antimicrobial activities of culturable microorganisms (Actinomycetes and Fungi) isolated from Chaabe Cave, Algeria. International Journal of Speleology 47(2): 189–199. https://doi.org/10.5038/1827-806X.47.2.2148

Bills GF, Gloer JB, An Z (2013) Coprophilous fungi: Antibiotic discovery and functions in an underexplored arena of microbial defensive mutualism. Current Opinion in Microbiology 16(5): 549–565. https://doi.org/10.1016/j.mib.2013.08.001

Bischof JF, Rehner SA, Humber RA (2006) *Metarhizium frigidum* sp. nov.: A cryptic species of *M. anisopliae* and a member of the *M. favoviride* Complex. Mycologia 98(5): 737–745. https://doi.org/10.1080/15572536.2006.11832645

Carmichael JW, Kendrick WB, Conners IL, Sigler L (Eds) (1980) Genera of Hyphomycetes. University of Alberta Press.

Chung YM, El-Shazly M, Chuang DW, Hwang TL, Asai T, Oshima Y, Ashour ML, Wu YC, Chang FR (2013) Suberoylanilide hydroxamic acid, a histone deacetylase inhibitor, induces the production of anti-inflammatory cyclodepsipeptides from *Beauveria felina*. Journal of Natural Products 76(7): 1260–1266. https://doi.org/10.1021/np400143j

De Hoog GS (1972) The Genera *Beauveria*, *Isaria*, *Tritirachium* and *Acrodontium* gen. nov. Studies in Mycology 1: 1–41.

Fries EM (1825) Systema orbis vegetabilis: Primas Lineas Novae Constructionis Periclitatur; E Typographia Academica. Lunde, Norway 1: 170.

Guerra-Mateo D, Gené J, Baulin V, Cano-Lira JF (2023) Phylogeny and Taxonomy of the Genus *Amphichorda* (Bionectriaceae): An Update on *Beauveria*-like Strains and Description of a Novel Species from Marine Sediments. Diversity 15(7): 795. https://doi.org/10.3390/d15070795

Hoang DT, Chernomor O, von Haeseler A, Minh BQ, Vinh LS (2017) UFBoot2: Improving the ultrafast bootstrap approximation. Molecular Biology and Evolution 35(2): 518–522. https://doi.org/10.1093/molbev/msx281

Hou LW, Giraldo A, Groenewald JZ, Rämä T, Summerbell RC, Huang GZ, Cai L, Crous PW (2023) Redisposition of acremonium-like fungi in Hypocreales. Studies in Mycology 105(1): 23–203. https://doi.org/10.3114/sim.2023.105.02

Kalyaanamoorthy S, Minh BQ, Wong TKF, von Haeseler A, Jermiin LS (2017) ModelFinder: Fast model selection for accurate phylogenetic estimates. Nature Methods 14(6): 587–589. https://doi.org/10.1038/nmeth.4285

Lamarck JB (1815) Flore Françoise ou Descriptions Succinctes de Toutes les Plantes Qui Croissent Naturellement en France, Disposées Selon Une Nouvelle Méthode D'Analyse, et Précédées Par un Exposé des Principes Élémentaires de la Botanique. Libraire Chez Desray, Paris, vol. 6, 30 pp. https://doi.org/10.5962/bhl.title.112968

Langenfeld A, Blond A, Gueye S, Herson P, Nay B, Dupont J, Prado S (2011) Insecticidal cyclodepsipeptides from *Beauveria felina*. Journal of Natural Products 74(4): 825–830. https://doi.org/10.1021/np100890n

Leão AF, Condé TO, Dutra YLG, Rosado AWC, Grazziotti PH, Neves SC, Fraga LMS, Kasuya MCM, Pereira OL (2024) *Amphichorda monjolensis* sp. nov., a new fungal species isolated from a Brazilian limestone cave, with an update on acremonium-like species in Bionectriaceae. Brazilian Journal of Microbiology. https://doi.org/10.1007/s42770-024-01289-y

Lendemer JC (2020) Epitypes are forever: Best Practices for an Increasingly Misused Nomenclatural Action. Taxon 69(5): 849–850. https://doi.org/10.1002/tax.12289

Liang M, Li W, Qi D, Chen C, Cai L, Yin B. (2021) Establishment of a genetic transformation system in guanophilic fungus *Amphichorda guana*. Journal of Fungi 7: 138. https://doi.org/10.3390/jof7020138

Liu M, Hodge KT (2005) *Hypocrella zhongdongii* sp. nov., the teleomorph of *Aschersonia incrassata*. Mycological Research 109: 818–824. https://doi.org/10.1016/10.1017/S095375620500290X

Liu XF, Tibpromma S, Hughes AC, Chethana KWT, Wijayawardene NN, Dai DQ, Du TY, Elgorban AM, Stephenson SL, Suwannarach N, Xu JC, Lu L, Xu RF, Maharachchikumbura SSN, Zhao CL, Bhat DJ, Sun YM, Karunarathna SC, Mortimer PE (2023) Culturable mycota on bats in central and southern Yunnan Province, China. Mycosphere 14(1): 497–662. https://doi.org/10.5943/mycosphere/14/1/7

Nguyen LT, Schmidt HA, von Haeseler A, Minh BQ (2015) IQ-TREE: A fast and efective stochastic algorithm for estimating maximum likelihood phylogenies. Molecular Biology and Evolution 32(1): 268–274. https://doi.org/10.1093/molbev/msu300

Rehner SA, Samuels GJ (1994) Taxonomy and phylogeny of *Gliocladium* analysed from nuclear large subunit ribosomal DNA sequences. Mycological Research 98(6): 625–634. https://doi.org/10.1016/S0953-7562(09)80409-7

Rehner SA, Minnis AM, Sung GH, Luangsa-ard JJ, Devotto L, Humber RA (2011) Phylogeny and systematics of the anamorphic, entomopathogenic genus *Beauveria*. Mycologia 103(5): 1055–1073. https://doi.org/10.3852/10-302

Ronquist F, Teslenko M, van der Mark P, Ayres DL, Darling A, Höhna S, Larget B, Liu L, Suchard MA, Huelsenbeck JP (2012) MrBayes 3.2: Efcient Bayesian phylogenetic inference and model choice across a large model space. Systematic Biology 61(3): 539–542. https://doi.org/10.1093/sysbio/sys029

Sung GH, Hywel-Jones NL, Sung JM, Luangsa-Ard JJ, Shrestha B, Spatafora JW (2007) Phylogenetic classifcation of *Cordyceps* and the clavicipitaceous fungi. Studies in Mycology 57: 5–59. https://doi.org/10.3114/sim.2007.57.01

Tamura K, Stecher G, Peterson D, Filipski A, Kumar S (2013) MEGA6: Molecular Evolutionary Genetics Analysis Version 6.0. Molecular Biology and Evolution 30(12): 2725–2729. https://doi.org/10.1093/molbev/mst197

Vanderwolf KJ, Malloch D, Mcalpine DF, Forbes GJ (2013) A world review of fungi, yeasts, and slime molds in caves. International Journal of Speleology 42(1): 77–96. https://doi.org/10.5038/1827-806X.42.1.9

Vilgalys R, Hester M (1990) Rapid genetic identifcation and mapping of enzymatically amplifed ribosomal DNA from several *Cryptococcus* species. Journal of Bacteriology 172(8): 4238–4246. https://doi.org/10.1128/jb.172.8.4238-4246.1990

Wang YB, Yu H, Dai YD, Wu CK, Zeng WB, Yuan F, Liang ZQ (2015a) *Polycephalomyces agaricus*, a new hyperparasite of *Ophiocordyceps* sp. infecting melolonthid larvae in southwestern China. Mycological Progress 14(9): 70. https://doi.org/10.1007/s11557-015-1090-7

Wang YB, Yu H, Dai YD, Chen ZH, Zeng WB, Yuan F, Liang ZQ (2015b) *Polycephalomyces yunnanensis* (Hypocreales), a new species of *Polycephalomyces* parasitizing *Ophiocordyceps nutans* and stink bugs (Hemipteran adults). Phytotaxa 208: 34–44. https://doi.org/10.11646/phytotaxa.208.1.3

Wang YB, Wang Y, Fan Q, Duan DE, Zhang GD, Dai RQ, Dai YD, Zeng WB, Chen ZH, Li DD, Tang DX, Xu ZH, Sun T, Nguyen TT, Tran NL, Dao VM, Zhang CM, Huang LD, Liu YJ, Zhang XM, Yang DR, Sanjuan T, Liu XZ, Yang ZL, Yu H (2020) Multigene phylogeny of the family Cordycipitaceae (Hypocreales): New taxa and the new systematic position of the Chinese cordycipitoid fungus *Paecilomyces hepiali*. Fungal Diversity 103(1): 1–46. https://doi.org/10.1007/s13225-020-00457-3

Wang ZQ, Wang Y, Dong QY, Fan Q, Dao VM, Yu H (2022) Morphological and Phylogenetic Characterization Reveals Five New Species of *Samsoniella* (Cordycipitaceae, Hypocreales). Journal of Fungi (Basel, Switzerland) 8(7): 747. https://doi.org/10.3390/jof8070747

White TJ, Bruns TD, Lee SB, Taylor JW (1990) Amplifcation and direct sequencing of fungal ribosomal RNA genes for phylogenetics. In: Innis MA, Gelfand DH, Sninsky JJ, White TJ (Eds) PCR protocols: a guide to methods and applications. Academic, New York, 315–322. https://doi.org/10.1016/B978-0-12-372180-8.50042-1

Xu L, Li Y, Biggins JB, Bowman BR, Verdine GL, Gloer JB, Alspaugh JA, Bills GF (2018) Identifcation of cyclosporin C from *Amphichorda felina* using a *Cryptococcus neoformans* differential temperature sensitivity assay. Applied Microbiology and Biotechnology 102(5): 2337–2350. https://doi.org/10.1007/s00253-018-8792-0

Zhang ZF, Liu F, Zhou X, Liu XZ, Liu SJ, Cai L (2017) Culturable mycobiota from Karst caves in China, with descriptions of 20 new species. Persoonia 39(1): 1–31. https://doi.org/10.3767/persoonia.2017.39.01

Zhang D, Gao FL, Jakovlić I, Zou H, Zhang J, Li WX, Wang GT (2020) PhyloSuite: An integrated and scalable desktop platform for streamlined molecular sequence data management and evolutionary phylogenetics studies. Molecular Ecology Resources 20(1): 348–355. https://doi.org/10.1111/1755-0998.13096

Zhang ZF, Zhou SY, Eurwilaichitr L, Ingsriswang S, Raza M, Chen Q, Zhao P, Liu F, Cai L (2021) Culturable mycobiota from Karst caves in China II, with descriptions of 33 new species. Fungal Diversity 106(1): 29–136. https://doi.org/10.1007/s13225-020-00453-7

MycoKeys 106: 303–325 (2024)
DOI: 10.3897/mycokeys.106.127355

Research Article

Phylogenomics, taxonomy and morphological characters of the Microdochiaceae (Xylariales, Sordariomycetes)

Zhao-Xue Zhang[1], Yu-Xin Shang[1], Meng-Yuan Zhang[1], Jin-Jia Zhang[1], Yun Geng[2], Ji-Wen Xia[1], Xiu-Guo Zhang[1]

1 *Shandong Provincial Key Laboratory for Biology of Vegetable Diseases and Insect Pests, College of Plant Protection, Shandong Agricultural University, Taian, 271018, China*

2 *Institute of Crop Germplasm Resources, Shandong Academy of Agricultural Sciences, Jinan, 250100, China*

Corresponding author: Xiu-Guo Zhang (sdau613@163.com)

Abstract

Species of the family Microdochiaceae (Xylariales, Sordariomycetes) have been reported from worldwide, and collected from different plant hosts. The proposed new genus and two new species, *viz.*, *Macroidriella* **gen. nov.**, *M. bambusae* **sp. nov.** and *Microdochium australe* **sp. nov.**, are based on multi-locus phylogenies from a combined dataset of ITS rDNA, LSU, RPB2 and TUB2 with morphological characteristics. *Microdochium sinense* has been collected from diseased leaves of *Phragmites australis* and this is the first report of the fungus on this host plant. Simultaneously, we annotated 10,372 to 11,863 genes, identified 4,909 single-copy orthologous genes, and conducted phylogenomic analysis based on genomic data. A gene family analysis was performed and it will expand the understanding of the evolutionary history and biodiversity of the Microdochiaceae. The detailed descriptions and illustrations of species are provided.

Key words: Microdochiaceae, multigene phylogeny, new taxa, phylogenomics, taxonomy

This article is part of:
Exploring the Hidden Fungal Diversity: Biodiversity, Taxonomy, and Phylogeny of Saprobic Fungi
Edited by Samantha C. Karunarathna, Danushka Sandaruwan Tennakoon, Ajay Kumar Gautam

OPEN ACCESS

Academic editor:
Danushka Sandaruwan Tennakoon
Received: 12 May 2024
Accepted: 20 June 2024
Published: 3 July 2024

Citation: Zhang Z-X, Shang Y-X, Zhang M-Y, Zhang J-J, Geng Y, Xia J-W, Zhang X-G (2024) Phylogenomics, taxonomy and morphological characters of the Microdochiaceae (Xylariales, Sordariomycetes). MycoKeys 106: 303–325. https://doi.org/10.3897/mycokeys.106.127355

Introduction

Microdochium Syd. & P. Syd., is the type genus of the family Microdochiaceae Hern.-Restr., Crous & J.Z. Groenew. This was first described by Syd. & P. Syd. (Sydow 1924). The holotype collection of the type species of *Microdochium*, *M. phragmitis* Syd. & P. Syd. was obtained in Germany from the leaves of *Phragmites australis* (Sydow 1924). *Microdochium* species were collected as endophytes, plant pathogens, and saprophytes, and were frequently isolated from different plant hosts (Von Arx 1987; Glynn et al. 2005; Jewell and Hsiang 2013; Mandyam et al. 2013; Hiruma et al. 2018; Liang et al. 2019; Lu et al. 2023; Zhang et al. 2023a). Prior research has indicated that the classification of *Microdochium* within the Amphisphaeriaceae is supported by its morphological similarities (Parkinson et al. 1981; Samuels and Hallett 1983; Von Arx 1984; Jaklitsch and Voglmayr 2012). Hernández-Restrepo et al. (2016) was proposed that *Idriella* and *Microdochium* may be closely related genera. Their phylogenetic analysis revealed that *Idriella*, *Microdochium*, and *Selenodriella* formed a distinct

monophyletic group within the Xylariales. Therefore, Hernández-Restrepo et al. (2016) established the new family Microdochiaceae to encompass this clade.

Currently, there are approximately 68 species of *Microdochium* listed in the Index Fungorum (2024), with 45 species being accepted. *Microdochium* has a diverse range of hosts that are widely distributed worldwide (Zhang et al. 2017; Crous et al. 2018, 2019, 2021; Marin-Felix et al. 2019; Huang et al. 2020). However, only a few species of *Microdochium* have the capability to cause diseases, primarily impacting grasses and cereals. Zhang et al. (2015) identified *Microdochium paspali* Syd. & P. Syd., which was responsible for causing leaf blight on *Paspalum vaginatum* Sw. Liang et al. (2019) identified *Mi. poae* J.M. Liang & Lei Cai, which induced leaf blight disease in turf grasses like *Poa pratensis* and *Agrostis stolonifera* L. Stewart et al. (2019) identified *Mi. sorghi* U. Braun, which was responsible for the development of zonate leaf spots and decay on sorghum species. *Mi. albescens* (Thüm.) Hern.-Restr. & Crous was the causative agent of leaf scald and grain discoloration in rice, leading to a global decrease in rice yield (Dirchwolf et al. 2023). *Mi. bolleyi* (R. Sprague) de Hoog & Herm.-Nijh. was cited as the cause of root necrosis and basal rot in creeping bent grass (Hong et al. 2008). In addition to this, some species of *Microdochium* occur as endophytes or saprophytes. Liu et al. (2022) identified three species, *Microdochium miscanthi* S.B. Liu, X.Y. Liu, Z. Meng & X.G. Zhang, *Mi. sinense* S.B. Liu, X.Y. Liu, Z. Meng & X.G. Zhang, and *Mi. hainanense* S.B. Liu, X.Y. Liu, Z. Meng & X.G. Zhang, isolated from *Miscanthus sinensis* Anderss. and *Phragmites australis* (Cav.) Trin. ex Steud in Hainan, China. Zhang et al. (2023a) collected novel species (*Mi. bambusae* J. Zhang, Z.X. Zhang, & Z. Li, *Mi. nannuoshanense* J. Zhang, Z.X. Zhang, & Z. Li, and *Mi. phyllosaprophyticum* J. Zhang, Z.X. Zhang, & Z. Li) from leaves of Bambusaceae plant as a saprobe.

With the advent of the sequencing era, genomics is increasingly being utilized for phylogenetic studies and can offer additional insights into pathogenic mechanisms (Manamgoda et al. 2011; Schoch et al. 2012; Jeewon et al. 2013; David et al. 2016; Mesny et al. 2021; Tsers et al. 2023). However, at present, only the genome information of three species of this taxon (*Microdochium*) can be retrieved from the NCBI database (https://www.ncbi.nlm.nih.gov/, accessed on 30 April 2024). In this study, we explored the species diversity of *Microdochium* and described one new species and one new host record based on the molecular phylogenetic analyses and morphological observations. In addition, we conducted genome and transcriptome sequencing of the new species, aiming to conduct phylogenetic analysis, and gene structure annotation at the genomic level. By comparing and analyzing the obtained data with existing species genome information, we aim to reveal the genetic relationship and functional differences between the new species and other species. This will gain a more comprehensive understanding of the biological characteristics and evolutionary history of the new taxa.

Materials and methods

Morphological study

During a series of field visits in 2023 in Hainan Province, China, plant specimens with necrotic spots were collected. Even though specimens harbor multiple fungi, we managed to obtain pure colonies through the single spore

isolation (Senanayake et al. 2020) and tissue isolation techniques (Zhang et al. 2023a). We retrieved small fragments (5 × 5 mm) from the damaged leaf edges, treated them by immersion in a 75% ethanol solution for 60 s, followed by rinsing in sterile distilled water for 45 s and a 10% sodium hypochlorite solution for 45 s. Subsequently, specimens were rinsed three times in sterile deionized water for 30 s. The processed fragments were then placed on sterile filter paper to remove excess moisture before being transferred onto PDA for incubation at 24 °C for 3 days. The hyphal tips from growing colonies were transferred to fresh PDA plates. Images were captured using a Sony Alpha 6400L digital camera (Sony Group Corporation, Tokyo, Japan) on days 7 and 14. Microscopic examination of the fungal structures was conducted using an Olympus SZ61 stereo microscope and an Olympus BX43 microscope (Olympus Corporation, Tokyo, Japan), along with BioHD-A20c color digital camera (FluoCa Scientific, China, Shanghai) for recording. All fungal strains were preserved in 15% sterilized glycerol at 4 °C, with each strain stored in three 2.0 mL tubes for future studies. Structural measurements were carried out using Digimizer software (v5.6.0), with a minimum of 25 measurements taken for each characteristic such as conidiophores, conidiogenous cells, and conidia. Specimens were deposited in the HSAUP (Herbarium of Plant Pathology, Shandong Agricultural University) and HMAS (Herbarium Mycologicum Academiae Sinicae), while living cultures were stored in the SAUCC (Shandong Agricultural University Culture Collection) for preservation and further research purposes. Taxonomic information of the new taxa was submitted to MycoBank (http://www.mycobank.org).

DNA extraction, amplification and sequencing

Fungal DNA was extracted from fresh mycelia grown on PDA using either the CTAB method or a kit method (OGPLF-400, GeneOnBio Corporation, Changchun, China) (Guo et al. 2000; Zhang et al. 2023a). Four gene regions, LSU, ITS, RPB2, and TUB2 were amplified using the primer pairs listed in Suppl. material 1 (Vilgalys et al. 1990; White et al. 1990; Liu et al. 1999; Sung et al. 2007; Jewell et al. 2013). The amplification reaction was conducted in a 25 μL reaction volume, consisting of 12.5 μL 2 × Hieff Canace® Plus PCR Master Mix (Shanghai, China) (with dye) (Yeasen Biotechnology, Cat No. 10154ES03), 0.5 μL each of forward and reverse primer, and 0.5 μL template genomic DNA, with the volume adjusted to 25 μL using distilled deionized water. PCR products were separated and purified using 1% agarose gel and GelRed (TsingKe, Qingdao, China), and UV light was used to visualize the fragments. Gel extraction was performed using a Gel Extraction Kit (Cat: AE0101-C) (Shandong Sparkjade Biotechnology Co., Ltd., Jinan, China). The purified PCR products were subjected to bidirectional sequencing by Biosune Company Limited (Shanghai, China). The raw data (trace data) were analyzed using MEGA v. 7.0 to obtain consistent sequences (Kumar et al. 2016). All sequences generated in this study were deposited in GenBank under the accession numbers provided in Table 1. The abbreviations of the genera names used in our study are as follows: *I.* = *Idriela*; *S.* = *Selenodriella*; *Ma.* = *Macroidriella*; *Mi.* = *Microdochium*.

Table 1. GenBank accession number of the taxa used in phylogenetic reconstruction.

Species	Strain no.	GenBank accession number				References
		ITS	LSU	RPB2	TUB2	
Cryptostroma corticale	CBS 218.52	HG934112	MH868531	HG934118	HG934104	Vu et al. (2019)
Idriela lunata	CBS 204.56*	KP859044	KP858981	–	–	Hernández-Restrepo et al. (2016)
	CBS 177.57	KP859043	KP858980	–	–	
I. chlamydospora	CGMCC 3.20778*	OL897016	OL897058	–	ON569069	Zhang et al. (2023b)
	GZUIFR 21.922	OL897017	OL897059	–	ON569070	
I. multiformispora	CGMCC 3.20779*	OL897018	OL897060	ON568988	ON569071	
	GZUIFR 21.924	OL897019	OL897061	ON568989	ON569072	
	GZUIFR 21.925	OL897020	OL897062	ON568990	ON569073	
Macroidriella bambusae	**SAUCC 6792-1***	**PP716851**	**PP716512**	**PP729053**	**PP729058**	**This study**
	SAUCC 6792-2	**PP716852**	**PP716513**	**PP729054**	**PP729059**	
	SAUCC 6792-5	**PP716853**	**PP716514**	**PP729055**	**PP729060**	
	SAUCC 6113-1	**PP716854**	**PP716515**	**PP729056**	**PP729061**	
	SAUCC 6113-3	**PP716855**	**PP716516**	**PP729057**	**PP729062**	
Microdochium albescens	CBS 243.83	KP858994	KP858930	KP859103	KP859057	Hernández-Restrepo et al. (2016)
	CBS 291.79	KP858996	KP858932	KP859105	KP859059	
Mi. australe	**SAUCC 6322-5-1***	**PP695312**	**PP702043**	**PP716780**	**PP716787**	**This study**
	SAUCC 6151-1	**PP695313**	**PP702044**	**PP716779**	**PP716788**	
Mi. bambusae	SAUCC 1862-1*	OR702567	OR702576	OR715785	PP445175	Zhang et al. (2023a)
	SAUCC 1866-1	OR702568	OR702577	OR715786	PP445176	
Mi. bolleyi	CBS 540.92	KP859010	KP858946	KP859119	KP859073	Hernández-Restrepo et al. (2016)
	CPC 25994	KP859018	KP858954	KP859127	KP859074	
Mi. chrysanthemoides	CGMCC 3.17929*	KU746690	KU746736	–	KU746781	Zhang et al. (2017)
Mi. chrysopogonis	GDMCC 3.683	MT988022	MT988024	MW002442	MW002441	Lu et al. (2023)
	LNU-196	MT988020	MT988023	MW002445	MW002442	
Mi. chuxiongense	YFCC 8794*	OK586161	OK586160	OK584019	OK556901	Tang et al. (2022)
Mi. citrinidiscum	CBS 109067*	KP859003	KP858939	KP859112	KP859066	Hernández-Restrepo et al. (2016)
Mi. colombiense	CBS 624.94*	KP858999	KP858935	KP859108	KP859062	
Mi. dawsoniorum	BRIP 65649*	MK966337	–	–	–	Crous et al. (2020)
Mi. fisheri	CBS 242.90*	KP859015	KP858951	KP859124	KP859078	Hernández-Restrepo et al. (2016)
Mi. graminearum	CGMCC 3.23525*	OP103966	OP104016	OP236027	–	Gao et al. (2022)
	CGMCC 3.23524	OP103965	OP104015	OP236026	–	
Mi. hainanense	SAUCC 210782	OM956296	OM959324	OM981154	OM981147	Liu et al. (2022)
	SAUCC 210781*	OM956295	OM959323	OM981153	OM981146	
Mi. indocalami	SAUCC 1016*	MT199884	MT199878	MT510550	MT435653	Huang et al. (2020)
Mi. insulare	BRIP 75114a	OQ917075	OQ892168	OQ889560		-
Mi. lycopodinum	CBS 146.68	KP858993	KP858929	KP859102	KP859056	Hernández-Restrepo et al. (2016)
	CBS 122885*	KP859016	KP858952	KP859125	KP859080	
Mi. maculosum	COAD 3358*	Ok966954	Ok966953	OL310501	–	Crous et al. (2021)
Mi. majus	CBS 741.79	KP859001	KP858937	KP859110	KP859064	Hernández-Restrepo et al. (2016)
Mi. miscanthi	SAUCC 211092*	OM956214	OM957532	OM981148	OM981141	Liu et al. (2022)
	SAUCC 211093	OM956215	OM957533	OM981149	OM981142	
Mi. musae	CBS 143499	MH107894	MH107941	–	–	Crous et al. (2018)
	CBS 143500*	MH107895	MH107942	MH108003	–	
Mi. nannuoshanense	SAUCC 2450-1*	OR702569	OR702578	OR715787	PP445177	Zhang et al. (2023a)
	SAUCC 2450-3	OR702570	OR702579	OR715788	PP445178	

Species	Strain no.	GenBank accession number				References
		ITS	LSU	RPB2	TUB2	
Mi. neoqueenslandicum	CBS 445.95	KP858997	KP858933	KP859106	KP859060	Hernández-Restrepo et al. (2016)
	CBS 108926*	KP859002	KP858938	KP859111	KP859065	
Mi. nivale	CBS 116205*	KP859008	KP858944	KP859117	KP859071	
Mi. nivale var. majus	CBS 177.29	MH855031	MH866500	–	–	Vu et al. (2019)
Mi. nivale var. nivales	CBS 288.50	–	MH868135	–	–	
Mi. novae-zelandiae	CPC 29376*	LT990655	–	LT990641	LT990608	Marin-Felix et al. (2019)
	CPC 29693	LT990656	–	LT990642	LT990609	
Mi. paspali	HK-ML-1371	KJ569509	–	–	KJ569514	Zhang et al. (2015)
	CBS 138620*	KJ569513	–	–	KJ569518	
Mi. phyllosaprophyticum	SAUCC 3583-1*	OR702571	OR702580	OR715789	PP445179	Zhang et al. (2023a)
	SAUCC 3583-6	OR702572	OR702581	OR715790	PP445180	
Mi. phragmitis	CBS 285.71*	KP859013	KP858949	KP859122	KP859077	Hernández-Restrepo et al. (2016)
	CBS 423.78	KP859012	KP858948	KP859121	KP859076	
Mi. poae	CGMCC 3.19170*	MH740898	–	MH740906	MH740914	Liang et al. (2019)
	LC 12115	MH740901	–	MH740909	MH740917	
	LC 12116	MH740902	–	MH740910	MH740918	
Mi. ratticaudae	BRIP 68298*	MW481661	MW481666	MW626890	–	Crous et al. (2021)
Mi. rhopalostylidis	CBS 145125*	MK442592	MK442532	MK442667	–	Crous et al. (2019)
Mi. salmonicolor	NC14-294	MK836110	MK836108	–	–	Das et al. (2020)
Mi. seminicola	CBS 139951*	KP859038	KP858974	KP859147	KP859101	Hernández-Restrepo et al. (2016)
	CPC 26001	KP859025	KP858961	KP859134	KP859088	
	DAOM 250161	KP859034	KP858970	KP859143	KP859097	
Mi. shilinense	CGMCC 3.23531*	OP103972	OP104022	–	OP242834	Gao et al. (2022)
Mi. sinense	SAUCC 211097*	OM956289	OM959225	OM981151	OM981144	Liu et al. (2022)
	SAUCC 211098	OM956290	OM959226	OM981152	OM981145	
	SAUCC 3922-1	**PP695314**	**PP702045**	**PP716781**	**PP716789**	**This study**
	SAUCC 3922-3	**PP695315**	**PP702046**	**PP716782**	**PP716790**	
Mi. sorghi	CBS 691.96	KP859000	KP858936	KP859109	KP859063	Hernández-Restrepo et al. (2016)
Mi. tainanense	CBS 269.76*	KP859009	KP858945	KP859118	KP859072	
	CBS 270.76	KP858995	KP858931	KP859104	KP859058	
Mi. trichocladiopsis	CBS 623.77*	KP858998	KP858934	KP859107	KP859061	
Mi. yunnanense	SAUCC 1011*	MT199881	MT199875	MT510547	MT435650	Huang et al. (2020)
	SAUCC 1012	MT199882	MT199876	MT510548	MT435651	
Selenodriella cubensis	CBS 683.96	KP859053	KP858990	–	–	Hernández-Restrepo et al. (2016)
S. fertilis	CBS 772.83	KP859055	KP858992	–	–	Hernández-Restrepo et al. (2016)

Notes: Ex-type or ex-epitype strains are marked with "*" and the new species described in this study was marked in bold.

Library construction, quality control and whole-genome sequencing

Library construction and sequencing were carried out by Novogene Co., Ltd. (Beijing, China). Obtain FASTQ format data, which included sequence information and corresponding sequencing quality information (Cock et al. 2010). Preprocess the raw data that were obtained from the sequencing platform using fastp (https://github.com/OpenGene/fastp) to obtain clean data for subsequent analysis (Chen et al. 2018). Clean data were deposited in the National Center for Biotechnology Information (NCBI) under BioProject PRJNA1105317.

Genome assembly and annotation

Genome data were assembled using the software SPAdes v 3.12.0 (Bankevich et al. 2012). Genome annotation mainly included three aspects: a. Masking of repetitive sequences (RepeatMasker version v4.1.4; RepeatModeler v2.0.3, https://www.repeatmasker.org/); b. Annotation of non-coding RNA (RNAmmer v1.2; tRNAscan-SE v2.0); c. Annotation of gene structure (RNA-seq prediction: Trinity v2.14.0, HISAT2 v2.2.1, StringTie v2.2.0; Ab inito prediction: BRAKER2; Homology protein prediction: GeMoMa v1.9) (Grabherr et al. 2011; Pertea et al. 2015; Keilwagen et al. 2016, 2018; Bruna et al. 2021). The final genome and annotation files were integrated using EVM and PASA (Haas et al. 2008, 2011).

Phylogeny

The generated consensus sequences were subjected to Megablast searches to identify closely related sequences in the NCBI's GenBank nucleotide database (Zhang et al. 2000). Newly generated sequences in this study were aligned with related sequences retrieved from GenBank (Table 1) using MAFFT 7 (Katoh et al. 2019; http://mafft.cbrc.jp/alignment/server/) online service with the default strategy and corrected manually used MEGA 7. For phylogenetic analyses, we operated following the methods by Zhang et al. (2023a), single and concatenated ITS rDNA, LSU, RPB2 and TUB2 sequence alignments were subjected to analysis by maximum likelihood (ML) and Bayesian Inference (BI) algorithms, respectively. ML and BI were run on the CIPRES Science Gateway portal (https://www.phylo.org/, accessed on 30 April 2023) or offline software (ML was operated in RAxML-HPC2 on XSEDE v8.2.12, and BI analysis was operated in MrBayes v3.2.7a with 64 threads on Linux). For ML analyses, the default parameters were used and 1,000 rapid bootstrap replicates were run with the GTR+G+I model of nucleotide evolution; BI analysis was performed using a fast bootstrap algorithm with an automatic stop option (Zhang et al. 2023a). The GTR+I+G model was recommended for LSU, RPB2, and TUB2, while SYM+I+G was suggested for ITS. The Markov chain Monte Carlo (MCMC) analysis of the five concatenated genes was conducted over 1,130,000 generations, yielding 22,602 trees. Following the discard of the initial 5,650 trees generated during the burn-in phase, the remaining trees were used to compute posterior probabilities in the majority rule consensus trees.

For phylogenomic analyses, the genome sequences were submitted to GenBank under the accession numbers in Table 2. The final annotated data were processed to retain the coding protein genes and the longest transcript. Extracted all coding protein genes to identify gene families and single copy orthologous genes using OrthoFinder v2.5.5 (https://github.com/davidemms/OrthoFinder), according to the method by Emms and Kelly (2015, 2019). Multiple sequence alignment was used ParaAT v1.0 (https://ngdc.cncb.ac.cn/tools/paraat) and merged into supergene using seqkit v2.7.0 (https://github.com/shenwei356/seqkit) (Zhang et al. 2012; Shen et al. 2016). Phylogenomic analysis was carried out following the methods by Stamatakis et al. (2014), using RAxML-NG v1.2.1 (https://github.com/amkozlov/raxml-ng) with the LG+G8+F model and 100 bootstrap replications. All resulted trees were plotted using FigTree v. 1.4.4 (http://tree.bio.ed.ac.uk/software/figtree) or ITOL: Interactive Tree of Life (https://itol.embl.de/, accessed on 20 October 2023) (Letunic and Bork 2021) and the layout of the trees was edited in Adobe Illustrator CC 2019.

Table 2. BioSample and SRA NCBI number of the taxa used in phylogenomic reconstruction in this study.

Species	Strains	BioSample	SRA NCBI*	References
Asterophora parasitica	AP01	SAMN09737569	SRS3956156	
Cryphonectria parasitica	EP155	SAMN02744051	SRS6915724	Crouch et al. 2020
Diaporthe eres	CBS 160.32	SAMN21449118	SRS10459569	Hilário et al. 2022
Macroidriella bambusae	**SAUCC 6792-1**	**SAMN41099213**	**SRR28834790**	**This study**
Microdochium australe	**SAUCC 6322-5-1**	**SAMN41099214**	**SRR28834789**	**This study**
Mi. bambusae	**SAUCC 1862-1**	**SAMN41099215**	**SRR28834788**	**This study**
Mi. bolleyi	J235TASD1	SAMN04386150	SRS1667728	David et al. 2016
Mi. nannuoshanense	**SAUCC 2450-1**	**SAMN41099216**	**SRR28834787**	**This study**
Mi. nivale	F00608	SAMN26062287	SRS14642463	Tsers et al. 2023
Mi. phyllosaprophyticum	**SAUCC 3583-1**	**SAMN41099217**	**SRR28834786**	**This study**
Mi. trichocladiopsis	MPI-CAGE-CH-0230	SAMN06297163	SRS2394902	Mesny et al. 2021
Pestalotiopsis fici	W106-1	SAMN02369365		Wang et al. 2015
Xylaria flabelliformis	G536	SAMN11912834	SRS4852315	

Species information described in this study is marked in bold.

Results

Phylogenetic and phylogenomic analyses

A total of 80 isolates representing species within the Microdochiaceae family used for phylogenetic analysis. One strain of *Cryptostroma corticale* (CBS 218 52) was used as an outgroup taxon. The final alignment comprised 3,386 concatenated characters, spanning from positions 1 to 553 (ITS), 554 to 1,827 (LSU), 1,828 to 2,676 (RPB2), and 2,677 to 3,386 (TUB2). The maximum likelihood (ML) optimization likelihood was calculated to be -23041.844775. The matrix exhibited 1,071 distinct alignment patterns, with 25.57% of characters or gaps remaining undetermined. MrModelTest suggested that Dirichlet base frequencies be utilized for the ITS, LSU, RPB2, and TUB2 data partitions. The alignment exhibited a total of 876 unique site patterns (ITS: 287, LSU: 186, RPB2: 386, TUB2: 213). The topology of the ML tree corroborated that of the tree obtained from Bayesian inference; therefore, only the ML tree is depicted (Fig. 1). Based on the four-gene phylogeny (Fig. 1), the 80 strains were classified into 47 species. To enhance the visual appeal and conciseness of the phylogenetic tree, 39 strains were collapsed within it (The complete ML phylogenetic tree is available in the Suppl. material 5). Among them, five strains (SAUCC 6792-1, SAUCC 6792-2, SAUCC 6792-5, SAUCC 6113-1 and SAUCC 6113-3) identified a new genus, *Macroidriella* gen. nov., with solid support (98% MLBV and 1.0 BIPP), and *M. bambusae* sp. nov. (SAUCC 6792-1) as the type species. Two strains (SAUCC 6322-5-1 and SAUCC 6151-1) identified as *Microdochium australe* sp. nov.

We sequenced the genomes of six species in Microdochiaceae for phylogenomic analyses, and downloaded the published genomes of four species from in NCBI Datasets (https://www.ncbi.nlm.nih.gov/datasets/). *Xylaria flabelliformis* G536 was used as an outgroup taxon. Based on 4,909 clusters of orthologous proteins, the ML tree is depicted (Fig. 2). The phylogenomic tree was divided into two clades (excepted outgroup), viz, clade 1 (*Microdochium nannuoshanense* SAUCC 2450-1, *Mi. phyllosaprophyticum* SAUCC 3583-1, *Mi. australe* SAUCC 6322-5-1 and *Mi. bambusae* SAUCC 1862-1) and clade 2 (*Mi. nivale* F00608, *Mi. bolleyi* J235TASD1, *Mi. trichocladiopsis* MPI-CAGE-CH-0230 and *Macroidriella bambusae*

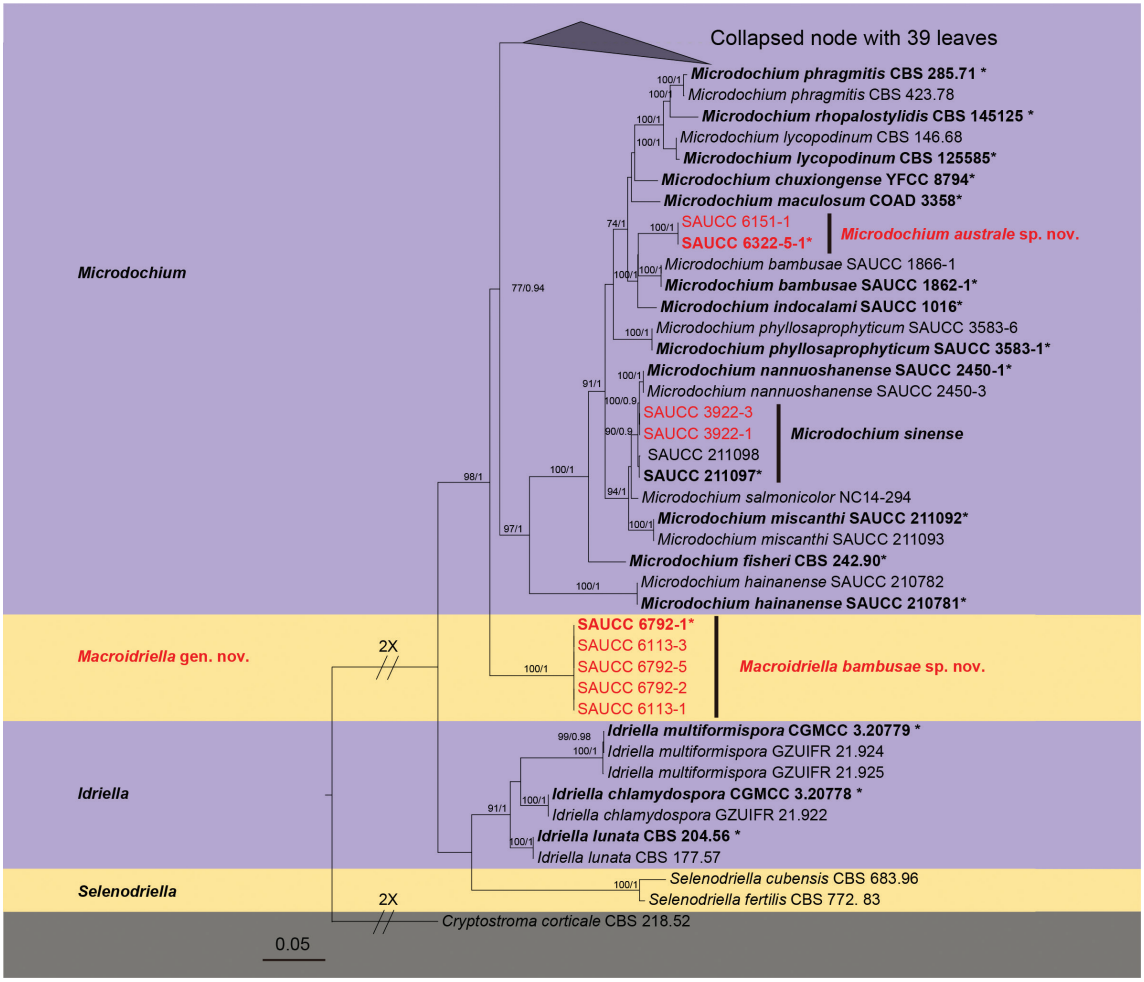

Figure 1. A maximum likelihood tree was constructed using a combined dataset of ITS, LSU, RPB2, and TUB2 sequence data. Branch support values, shown as ML/BIPP, are indicated above the nodes: MLBV ≥ 70% on the left and BIPP ≥ 0.90 on the right. Ex-type cultures are denoted in bold and marked with an asterisk (*). Strains from the current study are highlighted in red. The tree was rooted with *Cryptostroma corticale* (CBS 218.52). The scale bar at the bottom center represents 0.05 substitutions per site.

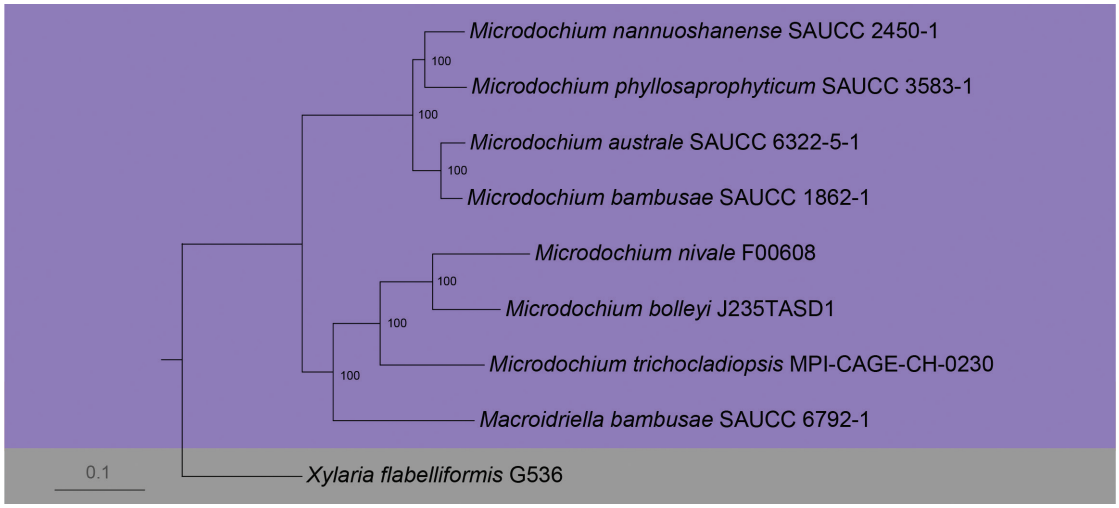

Figure 2. A Maximum Likelihood phylogenomic tree was constructed using a combined 4,909 clusters of orthologous proteins. Maximum Likelihood bootstrap values (≥ 70%) are indicated along branches. Genera are highlighted in different colors. The scale bar at the bottom represents 0.1 substitutions per site.

SAUCC 6792-1). The branch length of all four strains was < 0.1 in clade 1, indicating that their evolutionary distance was relatively close compared to clade 2 (each strain's branch was > 0.1). Due to limited genomic data, *Macroidriella bambusae* (SAUCC 6792-1) was not individually clustered, but the evolutionary distance of *Macroidriella bambusae* is relatively far compared to other species.

Annotations and comparative analysis

After structural annotation of the genomic data, we conducted a statistical summary, including, number of genes, total number of cds, total number of exons, total number of introns, total cds length, total exon length and total intron length (Suppl. material 2). Due to the limited genomic data available for Microdochiaceae, we will conduct gene family analysis by comparing the self-tested data of the new genus (*Macroidriella*) with genomic data from the orders of Diaporthales (*Cryphonectria parasitica* EP155 and *Diaporthe eres* CBS 160.32), Xylariales (*Pestalotiopsis fici* W106-1 and *Xylaria flabelliformis* G536), and the Basidiomycota (*Asterophora parasitica* AP01). The intersections of gene family among the six representative strains (≤ 6) are 3431, the maximum number (508) of gene family intersections between *Macroidriella bambusae* and *Microdochium trichocladiopsis*, and the minimum number (4) of gene family intersections between *Macroidriella bambusae* and *Asterophora parasitica* (Fig. 3a). The intersections of gene family among the seven representative strains are 3,291, the unique number of genes in *Asterophora parasitica* was 513 (maximum), the unique number of genes in *Macroidriella bambusae* was 42 (minimum) (Fig. 3b). We have presented the number of single-copy genes, multi-copy genes and so on for the seven representative strains (Fig. 3c).

Taxonomy

***Macroidriella* Z.X. Zhang, J. W. Xia & X.G. Zhang, gen. nov.**
MycoBank No: 853699

Type species. *Macroidriella bambusae* Z. X. Zhang, J. W. Xia & X. G. Zhang.

Etymology. Referring to the composed of "Macro-" and "-idriella" (Similar in morphology to *Idriella* and bigger than *Idriella* in conidia).

Description. Genus of Microdochiaceae. ***Endogenic*** on diseased leaves of Bambusaceae sp. ***Sporodochia*** yellowish brown, slimy. ***Conidiophores*** are indistinct and often reduced to conidiogenous cells. ***Conidiogenous cells*** are straight or slightly branched, smooth, curved, mono- or polyblastic, terminal, hyaline, septate, cylindrical and ampulliform. ***Conidia*** are solitary, hyaline, lunate, curved, mooned, multi-guttulate, apex rounded, base usually flattened. Sexual morphs were not observed, chlamydospores were not observed.

Notes. In the phylogenetic tree (Fig. 1), *Macroidriella* is allied to *Idriella*, *Microdochium* and *Selenodriella*, but forms a separate lineage with good statistical support (98% MLBV and 1.0 BIPP). In morphology, the conidia of *Macroidriella* are predominantly lunate and curved, unlike the elliptical conidia of *Microdocium*, suggesting a genus of its own, because it is similar to *Idriella* in morphology (but the conidia of *Macroidriella* are longer than *Idriella*), both being lunate conidia, it is named *Macroidriella* gen. nov.

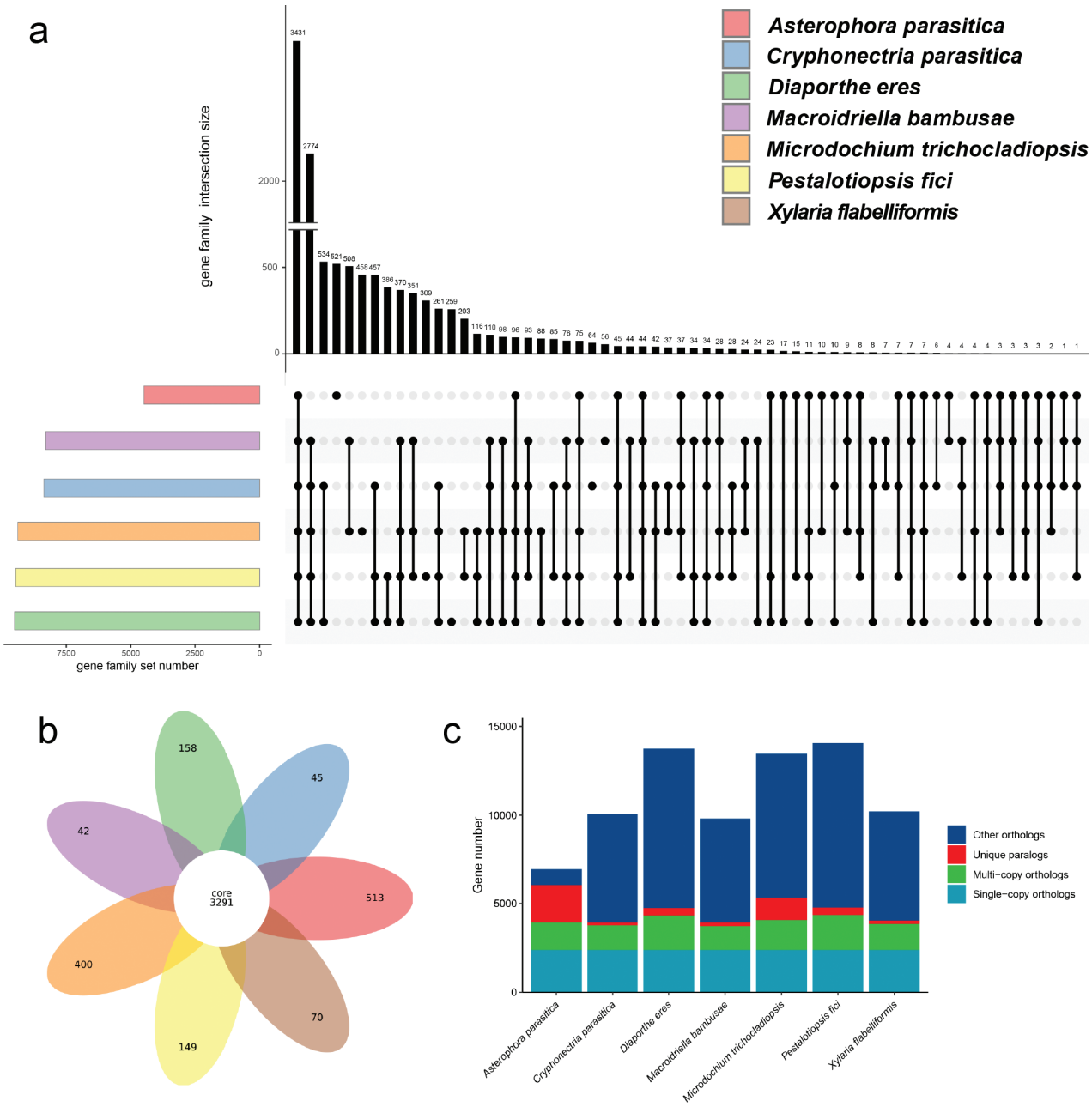

Figure 3. Gene family analysis of *Macroidriella* **a** UpSet plot of six strains, showing the intersection counts between different strains in the form of a bar graph **b** petal plot of seven strains, the center of the petal represents the number of shared genes **c** bar chart of homologous genes for each strain.

Macroidriella bambusae **Z.X. Zhang & X.G. Zhang, sp. nov.**
MycoBank No: 853712
Fig. 4

Type. China, Hainan Province, Danzhou City: Hainan tropical botanical garden, on diseased leaves of Bambusaceae sp., 15 October 2023, Z. X. Zhang (HMAS 352974, holotype), ex-holotype living culture SAUCC 6792-1.

Etymology. Referring to the species name of the host plant Bambusaceae sp.

Description. ***Endogenic*** on diseased leaves of Bambusaceae sp. ***Mycelia*** are superficial and immersed, 2–3.5 µm wide, branched, membranous and hyaline.

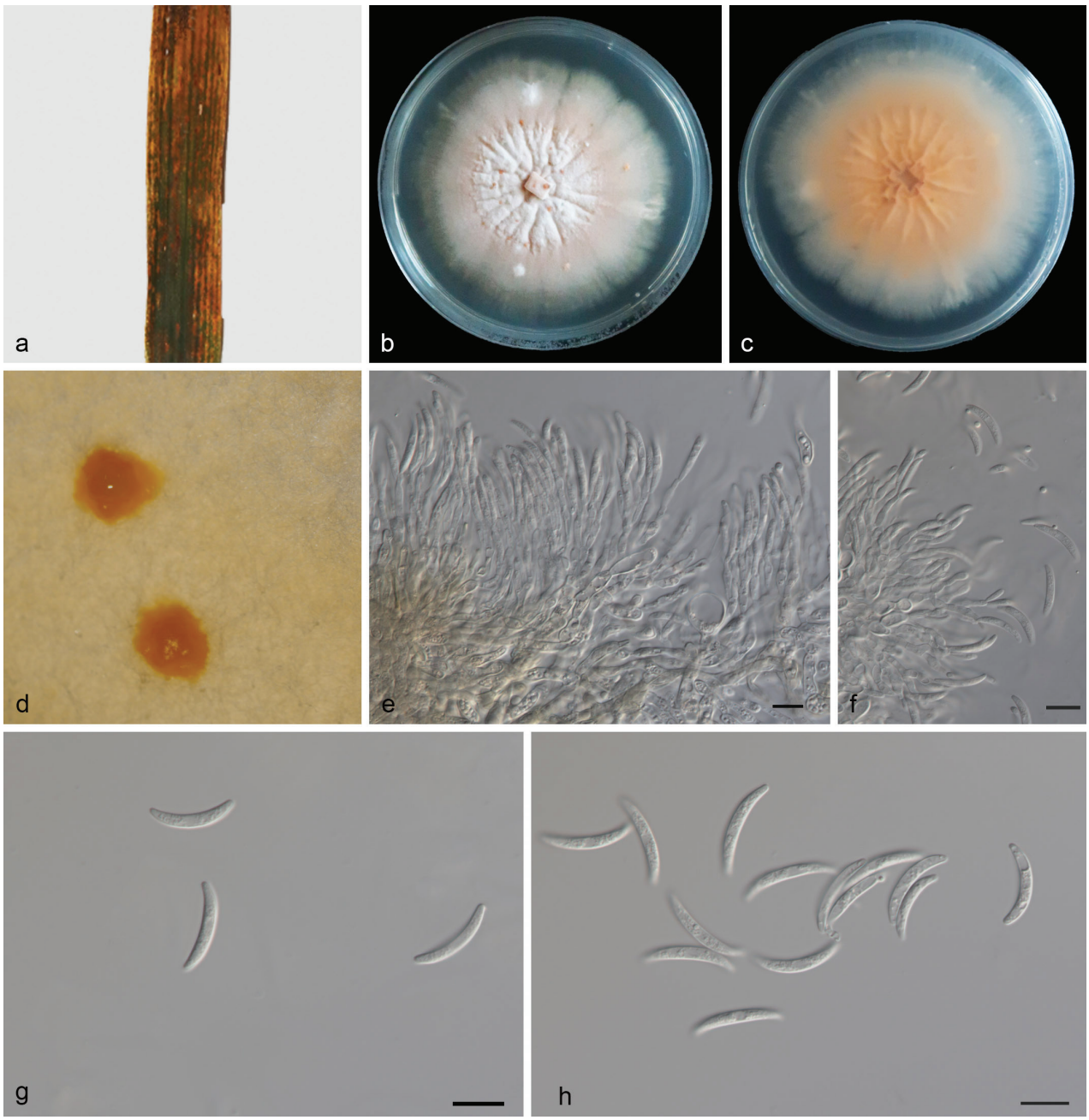

Figure 4. *Macroidriella bambusae* (HMAS 352974, holotype) **a** a leaf of Bambusaceae sp. **b, c** colonies on PDA from above and below after 14 days **d** colony overview **e, f** conidiogenous cells and conidia **g, h** conidia. Scale bars: 10 μm (**e–h**).

Sporodochia yellowish brown, slimy. ***Conidiophores*** are indistinct and often reduced to conidiogenous cells. Conidiogenous cells are straight or slightly curved, 10.4–15 × 1.7–2.8 μm, mono- or polyblastic, terminal, hyaline, septate, cylindrical and smooth. ***Conidia*** are solitary, hyaline, lunate, curved, mooned, 16.5–21.7 × 2–2.8 μm, multi-guttulate, apex rounded, base usually flattened. Sexual morphs were not observed, chlamydospores were not observed, see Fig. 4.

Culture characteristics. Cultures incubated on PDA at 25 °C in darkness, reaching 63–70 mm diam., had a growth rate of 4.5–5.0 mm/day after 14 days, with moderate aerial mycelia, the center and edges are milky white, with a yellow-brown color in the middle, and sporodochia are observed.

Additional material studied. China, Hainan Province, Danzhou City, Hainan tropical botanical garden, on diseased leaves of Bambusaceae sp., 15 October 2023, Z. X. Zhang (HSAUP 6792-2), living culture SAUCC 6792-2; *ibid*, (HSAUP 6792-5), living culture SAUCC 6792-5; on dead leaves, 15 October 2023, Z. X. Zhang (HSAUP 6113-1), living culture SAUCC 6113-1; *ibid*., (HSAUP 6113-3), living culture SAUCC 6113-3.

Notes. Phylogenetic analyses showed that *Macroidriella bambusae* formed an independent clade (Fig. 1), and closely related to *Idriella multiformispora* (lunate, curved-shaped conidia) and *Microdochium bolleyi*. The *Ma. bambusae* was distinguished from *I. multiformispora* (CGMCC 3.20779) by 60/520, 22/1222, 74/848 and 57/710 base-pair differences, from *Mi. bolleyi* (CBS 540.92) by 40/514, 19/765, 138/850 and 51/710 base pairs in ITS, LSU, RPB2 and TUB2 sequences, respectively. Morphologically, *Ma. bambusae* (16.5–21.7 × 2–2.8 μm) longer than *I. multiformispora* (8.5–13.5 × 1.0–2 μm) and *Mi. bolleyi* (5–8.7 × 1.6–2.3 μm) in conidia. Therefore, we describe this fungus as a novel species.

***Microdochium australe* Z.X. Zhang, & X.G. Zhang, sp. nov.**
MycoBank No: 853695
Fig. 5

Type. China, Hainan Province, Jianfengling National Forest Park, on diseased leaves of *Phragmites australis*, 13 October 2023, Z. X. Zhang (HMAS 352973, holotype), ex-holotype culture SAUCC 6322-5-1.

Etymology. Referring to the species name of the host plant *Phragmites australis*.

Description. ***Endogenic*** on diseased leaves of *Phragmites australis*. ***Mycelia*** are superficial and immersed, 3–3.3 μm wide, branched, membranous and hyaline. ***Sporodochia*** black, aggregative or solitary. ***Conidiophores*** are indistinct and often reduced to conidiogenous cells. ***Conidiogenous cells*** are straight or slightly curved, 15.4–23.5 × 2.8–4 μm, terminal, hyaline, septate, ampulliform or obpyriform, smooth. ***Conidia*** are solitary, hyaline, straight to slight curved, oblong to ellipsoid, 11.3–16.1 × 2.5–3.7 μm, multi-guttulate, (2)3-septate, apex rounded, base usually flattened. Sexual morphs were not observed, chlamydospores were not observed, see Fig. 5.

Culture characteristics. Cultures incubated on PDA at 25 °C in darkness, reaching 73–76 mm diam., had a growth rate of 5.2–5.4 mm/day after 14 days, with moderate aerial mycelia, milky white to grey-white, with regular margin, and sporodochia are observed, reverses black to brown in the centre, with grey-white and regular margin.

Additional material studied. China, Hainan Province, Jianfengling National Forest Park, on saprophytic leaves, 13 October 2023, Z. X. Zhang (HSAUP 6151-1), living culture SAUCC 6151-1.

Notes. Phylogenetic analyses showed that *Microdochium australe* sp. nov. formed an independent clade closely related to *Microdochium bambusae* and *Microdochium indocalami* (Fig. 1). *Mi. australe* was distinguished from *Mi. bambusae* (SAUCC 1862-1) by 47/503, 2/836, 56/848 and 17/710 base pair differences, from *Mi. bambusae* and *Mi. indocalami* (SAUCC 1016) by 52/503, 2/848, 44/840 and 17/708 base pairs in ITS, LSU, RPB2 and TUB2 sequences, respectively. Morphologically, *Mi. australe* (11.3–16.1 × 2.5–3.7 μm, (2)3-septate) differs from *Mi. bambusae* (13.0–17 × 2.5–3.5 μm, aseptate) and *Mi. indocalami* in conidia (13–15.5 × 3.5–5.5 μm, 3-septate), and, therefore, we described this fungus as a novel species.

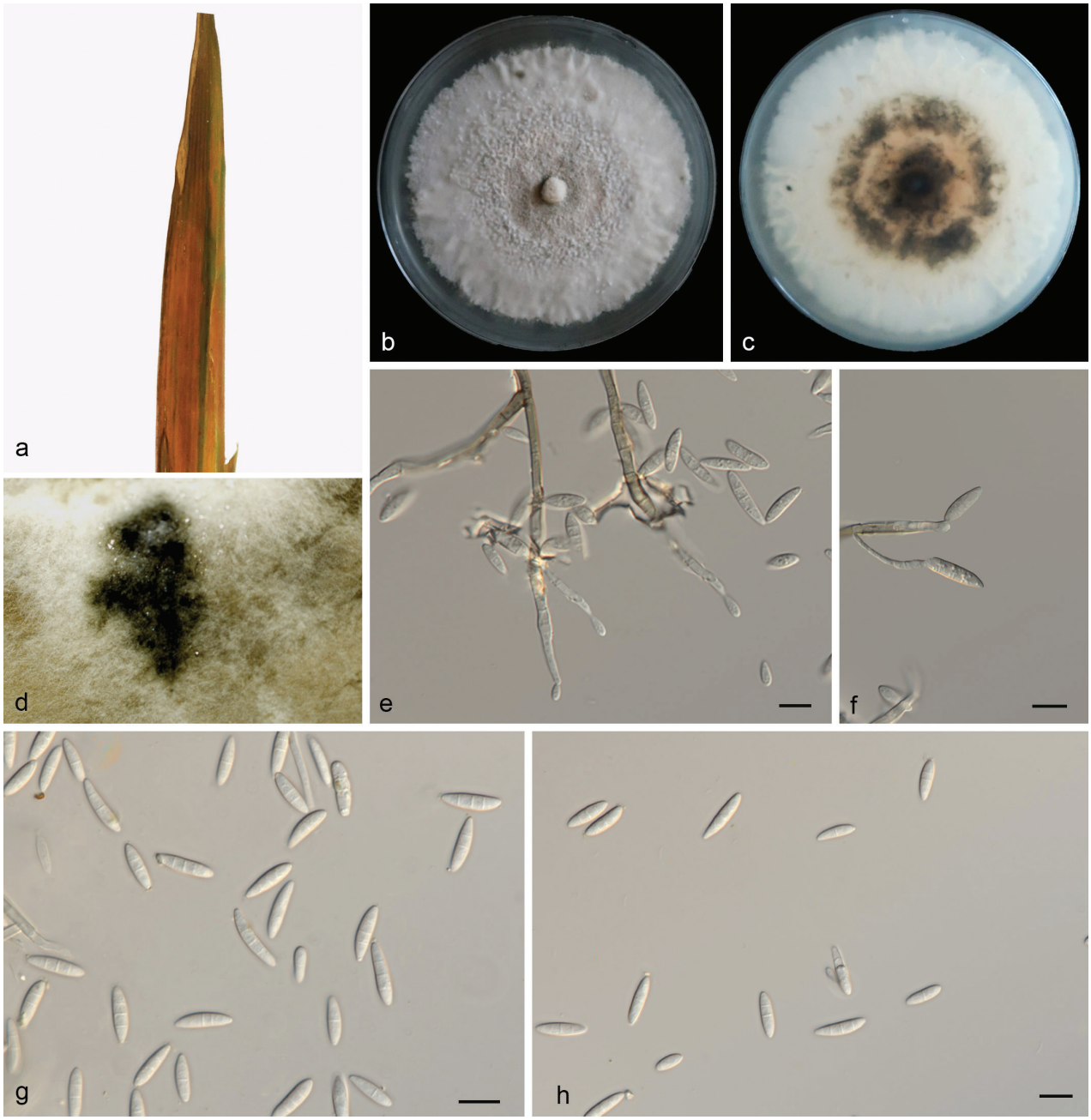

Figure 5. *Microdochium australe* (HMAS 352973, holotype) **a** a leaf of *Phragmites australis* **b, c** colonies on PDA from above and below after 14 days **d** colony overview **e, f** conidiogenous cells and conidia **g, h** conidia. Scale bars: 10 μm (**e–h**).

Microdochium sinense **S.B. Liu, X.Y. Liu, Z. Meng & X.G. Zhang, J. Fungi 2022, 8, 577.**
Fig. 6

Material examined. China, Hainan Province, Jianfengling National Forest Park, on diseased leaves of *Phragmites australis*, 12 April 2023, Z. X. Zhang (HSAUP 3922-1), living culture SAUCC 3922-1; *ibid*., (HSAUP 3922-3), living culture SAUCC 3922-3.

Description. ***Endogenic*** on diseased leaves of *Phragmites australis*. ***Mycelia*** are superficial and immersed, 2.1–2.9 μm wide, branched, membranous and hyaline. ***Conidia*** are solitary, hyaline, straight, oblong to ellipsoid,

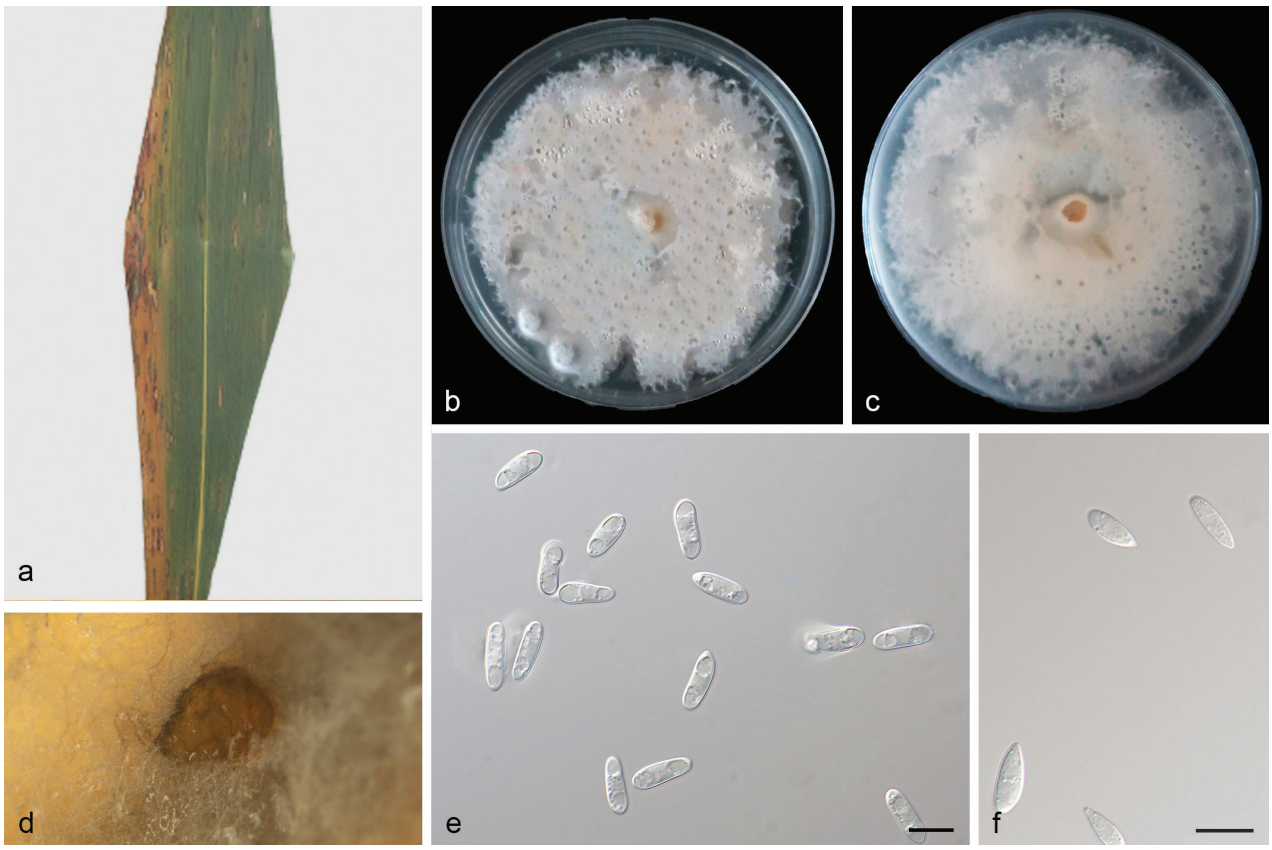

Figure 6. *Microdochium sinense* **a** diseased symptoms on a leaf of *Phragmites australis* **b, c** colonies on PDA from above and below after 14 days **d** conidiomata on PDA **e, f** conidia. Scale bars: 10 µm (**e–f**).

12.3–15 × 3.5–5.6 µm, multi-guttulate, apex rounded, base usually flattened. ***Conidiophores*** were not observed, chlamydospores were not observed, sexual morphs were not observed, see Fig. 6.

Culture characteristics. Cultures incubated on PDA at 25 °C in darkness, reach-ing 72–76 mm diam., had a growth rate of 5.1–5.4 mm/day after 14 days, with moder-ate aerial mycelia, milky white to grey-white, with irregular margin, reverses light brown in the centre, with grey-white and regular margin.

Notes. Phylogenetic analyses of four combined genes (ITS, LSU, RPB2 and TUB2) showed that SAUCC 3922-1 and SAUCC 3922-3 clustered with the type collection of *Microdochium sinense* with strong support (Fig. 1). We, therefore, identified the isolated strains (SAUCC 3922-1 and SAUCC 3922-3) as *Mi. sinense*. Morphologically, the conidia of the both (newly isolated and type) were similar (12.3–15 × 3.5–5.6 vs. 11.5–19.34 × 2.8–5.4 µm).

Discussion

The establishment of the family Microdochiaceae by Hernández-Restrepo et al. (2016) to encompass the clade consisting of *Idriella*, *Microdochium*, and *Selenodriella* within the Xylariales highlights the importance of phylogenetic analysis in understanding the evolutionary relationships among fungi. This new classification helps to better organize and categorize fungal species based on their genetic relatedness and morphological characteristics (Hernández-Restrepo et al. 2016; Liang et al. 2019; Huang et al. 2020; Liu et al. 2022; Lu et al.

2023; Zhang et al. 2023a). In the recent study, nine strains isolated from two host plants, *Phragmites australis* and Bambusaceae sp., were introduced into a new genus, *Macroidriella* and two new species, *Macroidriella bambusae* and *Microdochium australe*. The Global Biodiversity Information Facility (GBIF) currently hosts 1,594 georeferenced records of Microdochiaceae species worldwide (https://www.gbif.org/, accessed on April 30, 2024). The distribution of this family is predominantly in the United States, Europe, and Oceania, with fewer occurrences in Asia.

In the recent study of the family, *Microdochium* emerged as a prominent research focus, with 12 species of this genus documented across five Provinces (Guizhou, Hainan, Henan, Shandong, and Yunnan) since the beginning of the 21st century in China (Zhang et al. 2015; Liang et al. 2019; Huang et al. 2020; Gao et al. 2022; Liu et al. 2022; Tang et al. 2022). *Microdochium* species have been identified on a variety of host families (10 families), with over half of the fungi associated with Poaceae plants. In contrast, *Idriella* and *Selenodriella* have been less extensively studied, with *Idriella* having only two reported species since the turn of the 21st century. Through the joint analysis of multiple gene fragments and genomes, the position of new taxa can be better determined, especially through phylogenomic analyses, which was provided with more robust support values. Comparative analysis will help us determine the position of the *Macroidriella* genus on the evolutionary tree and its relationship with other fungi. By comparing the genomic data of different fungi, we can identify common gene families and infer their evolutionary relationships. Through comparative genomic analysis, it can be observed that *Macroidriella* has 42 unique single-copy orthologous genes. *Asterophora* shares only 4 single-copy orthologous genes with *Macroidriella*, which also indicates that their relationship is very distant (belonging to different fungal phyla).

This study represents a pioneering effort in Microdochiaceae as it integrates multi-gene fragments with genomic data to unveil the phylogenetic relationships within the family. By combining these diverse datasets, a comprehensive understanding of the evolutionary history of Microdochiaceae is achieved, shedding new light on its genetic landscape and evolutionary dynamics.

Acknowledgements

We would like to express our gratitude to Jie Zhang, a master's student at Shandong Agricultural University, for her assistance in this study.

Additional information

Conflict of interest

The authors have declared that no competing interests exist.

Ethical statement

No ethical statement was reported.

Funding

This research was supported by National Natural Science Foundation of China (nos. 32100016, 32270024, U2002203 and 32370001).

Author contributions

Sampling, molecular biology analysis: Zhao-Xue Zhang and Yu-Xin Shang; fungal isolation: Yu-Xin Shang and Jin-Jia Zhang; description and phylogenetic analysis: Meng-Yuan Zhang; microscopy: Yun Geng; writing—original draft preparation: Zhao-Xue Zhang; writing—review and editing, Ji-Wen Xia and Xiu-Guo Zhang. All authors read and approved the final manuscript.

Author ORCIDs

Zhao-Xue Zhang https://orcid.org/0000-0002-4824-9716
Ji-Wen Xia https://orcid.org/0000-0002-7436-7249

Data availability

All of the data that support the findings of this study are available in the main text or Supplementary Information.

References

Bankevich A, Nurk S, Antipov D, Gurevich AA, Dvorkin M, Kulikov AS, Lesin VM, Nikolenko SI, Pham S, Prjibelski AD, Pyshkin AV, Sirotkin AV, Vyahhi N, Tesler G, Alekseyev MA, Pevzner PA (2012) SPAdes: A new genome assembly algorithm and its applications to single-cell sequencing. Journal of Computational Biology 19(5): 455–477. https://doi.org/10.1089/cmb.2012.0021

Bruna T, Hoff KJ, Stanke M, Lomsadze A, Borodovsky M (2021) BRAKER2: Automatic eukaryotic genome annotation with GeneMark-EP+ and AUGUSTUS supported by a protein database. NAR Genomics and Bioinformatics 3(1): lqaa108. https://doi.org/10.1093/nargab/lqaa108

Chen SF, Zhou YQ, Chen YR, Gu J (2018) fastp: An ultra-fast all-in-one FASTQ preprocessor. Bioinformatics 34(17): i884–i890. https://doi.org/10.1093/bioinformatics/bty560

Cock PJA, Fields CJ, Goto N, Heuer ML, Rice PM (2010) The Sanger FASTQ file format for sequences with quality scores, and the Solexa/Illumina FASTQ variants. Nucleic Acids Research 38(6): 1767–1771. https://doi.org/10.1093/nar/gkp1137

Crouch JA, Dawe A, Aerts A, Barry K, Churchill ACL, Grimwood J, Hillman BI, Milgroom MG, Pangilinan J, Smith M, Salamov A, Schmutz J, Yadav JS, Grigoriev IV, Nuss DL (2020) Genome Sequence of the Chestnut Blight Fungus *Cryphonectria parasitica* EP155: A Fundamental Resource for an Archetypical Invasive Plant Pathogen. Phytopathology 110(6): 1180–1188. https://doi.org/10.1094/PHYTO-12-19-0478-A

Crous PW, Schumacher RK, Wingfield MJ, Akulov A, Denman S, Roux J, Braun U, Burgess TI, Carnegie AJ, Váczy KZ, Guatimosim E, Schwartsburd PB, Barreto RW, Hernández-Restrepo M, Lombard L, Groenewald JZ (2018) New and interesting fungi 1. Fungal Systematics and Evolution 1(1): 169–215. https://doi.org/10.3114/fuse.2018.01.08

Crous PW, Schumacher RK, Akulov A, Thangavel R, Hernández-Restrepo M, Carnegie AJ, Cheewangkoon R, Wingfield MJ, Summerell BA, Quaedvlieg W, Coutinho TA, Roux J, Wood AR, Giraldo A, Groenewald JZ (2019) New and interesting fungi 2. Fungal Systematics and Evolution 3(1): 57–134. https://doi.org/10.3114/fuse.2019.03.06

Crous PW, Wingfield MJ, Chooi YH, Gilchrist CLM, Lacey E, Pitt JI, Roets F, Swart WJ, Cano-Lira JF, Valenzuela-Lopez N, Hubka V, Shivas RG, Stchigel AM, Holdom DG, Jurjević Ž, Kachalkin AV, Lebel T, Lock C, Martín MP, Tan YP, Tomashevskaya MA, Vitelli JS, Baseia IG, Bhatt VK, Brandrud TE, De Souza JT, Dima B, Lacey HJ, Lombard L, Johnston PR, Morte A, Papp V, Rodríguez A, Rodríguez-Andrade E, Semwal KC, Tegart L, Abad ZG,

Akulov A, Alvarado P, Alves A, Andrade JP, Arenas F, Asenjo C, Ballarà J, Barrett MD, Berná LM, Berraf-Tebbal A, Bianchinotti MV, Bransgrove K, Burgess TI, Carmo FS, Chávez R, Čmoková A, Dearnaley JDW, Santiago ALCMA, Freitas-Neto JF, Denman S, Douglas B, Dovana F, Eichmeier A, Esteve-Raventós F, Farid A, Fedosova AG, Ferisin G, Ferreira RJ, Ferrer A, Figueiredo CN, Figueiredo YF, Reinoso-Fuentealba CG, Garrido-Benavent I, Cañete-Gibas CF, Gil-Durán C, Glushakova AM, Gonçalves MFM, González M, Gorczak M, Gorton C, Guard FE, Guarnizo AL, Guarro J, Gutiérrez M, Hamal P, Hien LT, Hocking AD, Houbraken J, Hunter GC, Inácio CA, Jourdan M, Kapitonov VI, Kelly L, Khanh TN, Kisło K, Kiss L, Kiyashko A, Kolařík M, Kruse J, Kubátová A, Kučera V, Kučerová I, Kušan I, Lee HB, Levicán G, Lewis A, Liem NV, Liimatainen K, Lim HJ, Lyons MN, Maciá-Vicente JG, Magaña-Dueñas V, Mahiques R, Malysheva EF, Marbach PAS, Marinho P, Matočec N, McTaggart AR, Mešić A, Morin L, Muñoz-Mohedano JM, Navarro-Ródenas A, Nicolli CP, Oliveira RL, Otsing E, Ovrebo CL, Pankratov TA, Paños A, Paz-Conde A, Pérez-Sierra A, Phosri C, Pintos Á, Pošta A, Prencipe S, Rubio E, Saitta A, Sales LS, Sanhueza L, Shuttleworth LA, Smith J, Smith ME, Spadaro D, Spetik M, Sochor M, Sochorová Z, Sousa JO, Suwannasai N, Tedersoo L, Thanh HM, Thao LD, Tkalčec Z, Vaghefi N, Venzhik AS, Verbeken A, Vizzini A, Voyron S, Wainhouse M, Whalley AJS, Wrzosek M, Zapata M, Zeil-Rolfe I, Groenewald JZ (2020) Fungal Planet description sheets: 1042–1111. Persoonia 44(1): 301–459. https://doi.org/10.3767/persoonia.2020.44.11

Crous PW, Cowan DA, Maggs-Kölling G, Yilmaz N, Thangavel R, Wingfield MJ, Noordeloos ME, Dima B, Brandrud TE, Jansen GM, Morozova OV, Vila J, Shivas RG, Tan YP, Bishop-Hurley S, Lacey E, Marney TS, Larsson E, Le Floch G, Lombard L, Nodet P, Hubka V, Alvarado P, Berraf-Tebbal A, Reyes JD, Delgado G, Eichmeier A, Jordal JB, Kachalkin AV, Kubátová A, Maciá-Vicente JG, Malysheva EF, Papp V, Rajeshkumar KC, Sharma A, Spetik M, Szabóová D, Tomashevskaya MA, Abad JA, Abad ZG, Alexandrova AV, Anand G, Arenas F, Ashtekar N, Balashov S, Bañares Á, Baroncelli R, Bera I, Biketova AY, Blomquist CL, Boekhout T, Boertmann D, Bulyonkova TM, Burgess TI, Carnegie AJ, Cobo-Diaz JF, Corriol G, Cunnington JH, da Cruz MO, Damm U, Davoodian N, de A Santiago ALCM, Dearnaley J, de Freitas LWS, Dhileepan K, Dimitrov R, Di Piazza S, Fatima S, Fuljer F, Galera H, Ghosh A, Giraldo A, Glushakova AM, Gorczak M, Gouliamova DE, Gramaje D, Groenewald M, Gunsch CK, Gutiérrez A, Holdom D, Houbraken J, Ismailov AB, Istel Ł, Iturriaga T, Jeppson M, Jurjević Ž, Kalinina LB, Kapitonov VI, Kautmanová I, Khalid AN, Kiran M, Kiss L, Kovács Á, Kurose D, Kušan I, Lad S, Læssøe T, Lee HB, Luangsa-Ard JJ, Lynch M, Mahamedi AE, Malysheva VF, Mateos A, Matočec N, Mešić A, Miller AN, Mongkolsamrit S, Moreno G, Morte A, Mostowfizadeh-Ghalamfarsa R, Naseer A, Navarro-Ródenas A, Nguyen TTT, Noisripoom W, Ntandu JE, Nuytinck J, Ostrý V, Pankratov TA, Pawłowska J, Pecenka J, Pham THG, Polhorský A, Pošta A, Raudabaugh DB, Reschke K, Rodríguez A, Romero M, Rooney-Latham S, Roux J, Sandoval-Denis M, Smith MT, Steinrucken TV, Svetasheva TY, Tkalčec Z, van der Linde EJ, V D Vegte M, Vauras J, Verbeken A, Visagie CM, Vitelli JS, Volobuev SV, Weill A, Wrzosek M, Zmitrovich IV, Zvyagina EA, Groenewald JZ (2021) Fungal Planet description sheets: 1182–1283. Pers. Mol. Phylogeny Evol. Fungi. 46: 313–528. https://doi.org/10.3767/persoonia.2021.46.11

Das K, Lee SY, Jung HY (2020) Molecular and morphological characterization of two novel species collected from soil in Korea. Mycobiology 48(1): 9–19. https://doi.org/10.1080/12298093.2019.1695717

David AS, Haridas S, LaButti K, Lim J, Lipzen A, Wang M, Barry K, Grigoriev IV, Spatafora JW, May G (2016) Draft Genome Sequence of *Microdochium bolleyi*, a Dark Septate Fungal Endophyte of Beach Grass. Genome Announcements 4(2): e00270–e16. https://doi.org/10.1128/genomeA.00270-16

Dirchwolf PM, Moschini RC, Gutiérrez SA, Carmona MA (2023) Modelling of the effects of environmental factors on rice grain discoloration incidence in Corrientes province, Argentina. Journal of Phytopathology 171(1): 12–22. https://doi.org/10.1111/jph.13150

Emms DM, Kelly S (2015) OrthoFinder: Solving fundamental biases in whole genome comparisons dramatically improves orthogroup inference accuracy. Genome Biology 16(1): 157. https://doi.org/10.1186/s13059-015-0721-2

Emms DM, Kelly S (2019) OrthoFinder: Phylogenetic orthology inference for comparative genomics. Genome Biology 20(1): 238. https://doi.org/10.1186/s13059-019-1832-y

Gao Y, Ren G, Wanasinghe DN, Xu J, Gomes De Farias AR, Gui H (2022) Two New Species and a New Record of *Microdochium* from Grasses in Yunnan Province, South-West China. Journal of Fungi (Basel, Switzerland) 8(12): 1297. https://doi.org/10.3390/jof8121297

Glynn NC, Hare MC, Parry DW, Edwards SG (2005) Phylogenetic analysis of EF-1 alpha gene sequences from isolates of *Microdochium nivale* leads to elevation of varieties Majus and Nivale to species status. Fungal Biology 109: 872–880. https://doi.org/10.1017/S0953756205003370

Grabherr MG, Haas BJ, Yassour M, Levin JZ, Thompson DA, Amit I, Adiconis X, Fan L, Raychowdhury R, Zeng Q, Chen Z, Mauceli E, Hacohen N, Gnirke A, Rhind N, di Palma F, Birren BW, Nusbaum C, Lindblad-Toh K, Friedman N, Regev A (2011) Full-length transcriptome assembly from RNA-seq data without a reference genome. Nature Biotechnology 29(7): 644–652. https://doi.org/10.1038/nbt.1883

Guo LD, Hyde KD, Liew ECY (2000) Identification of endophytic fungi from Livistona chinensis based on morphology and rDNA sequences. New Phytologist 147(3): 617–630. https://doi.org/10.1046/j.1469-8137.2000.00716.x

Haas BJ, Salzberg SL, Zhu W, Pertea M, Allen JE, Orvis J, White O, Buell CR, Wortman JR (2008) Automated eukaryotic gene structure annotation using EVidenceModeler and the Program to Assemble Spliced Alignments. Genome Biology 9(1): R7. https://doi.org/10.1186/gb-2008-9-1-r7

Haas BJ, Zeng Q, Pearson MD, Cuomo CA, Wortman JR (2011) Approaches to Fungal Genome Annotation. Mycology 2(3): 118–141. https://doi.org/10.1080/21501203.2011.606851

Hernández-Restrepo M, Groenewald JZ, Crous PW (2016) Taxonomic and phylogenetic re-evaluation of *Microdochium*, *Monographella* and *Idriella*. Persoonia 36(1): 57–82. https://doi.org/10.3767/003158516X688676

Hilário S, Gonçalves MFM, Fidalgo C, Tacão M, Alves A (2022) Genome Analyses of Two Blueberry Pathogens: *Diaportheamygdali* CAA958 and *Diaporthe eres* CBS 160.32. Journal of Fungi (Basel, Switzerland) 8(8): 804. https://doi.org/10.3390/jof8080804

Hiruma K, Kobae Y, Toju H (2018) Beneficial associations between Brassicaceae plants and fungal endophytes under nutrient-limiting conditions: Evolutionary origins and host–symbiont molecular mechanisms. Current Opinion in Plant Biology 44: 145–154. https://doi.org/10.1016/j.pbi.2018.04.009

Hong SK, Kim WG, Choi HW, Lee SY (2008) Identification of *Microdochium bolleyi* associated with basal rot of creeping bent grass in Korea. Mycobiology 36(2): 77–80. https://doi.org/10.4489/MYCO.2008.36.2.077

Huang ST, Xia JW, Zhang XG, Sun WX, Li Z (2020) Two new species of *Microdochium* from *Indocalamus longiauritus* in south-western China. MycoKeys 72: 93–108. https://doi.org/10.3897/mycokeys.72.55445

Index Fungorum (2024) Index Fungorum. http://www.indexfungorum.org/ [April 30, 202]

Jaklitsch WM, Voglmayr H (2012) Phylogenetic relationships of five genera of Xylariales and *Rosasphaeria* gen. nov. (Hypocreales). Fungal Diversity 52(1): 75–98. https://doi.org/10.1007/s13225-011-0104-2

Jeewon R, Ittoo J, Mahadeb D, Jaufeerally-Fakim Y, Wang HK, Liu AR (2013) DNA based identification and phylogenetic characterisation of endophytic and saprobic fungi from *Antidesma madagascariense*, a medicinal plant in Mauritius. Journal of Mycology 781914: 10. https://doi.org/10.1155/2013/781914

Jewell LE, Hsiang T (2013) Multigene differences between *Microdochium nivale* and *Microdochium majus*. Botany 91(2): 99–106. https://doi.org/10.1139/cjb-2012-0178

Katoh K, Rozewicki J, Yamada KD (2019) MAFFT online service: multiple sequence alignment, interactive sequence choice and visualization. Briefings in Bioinformatics 20: 1160–1166. https://doi.org/10.1093/bib/bbx108

Keilwagen J, Wenk M, Erickson JL, Schattat MH, Grau J, Hartung F (2016) Using intron position conservation for homology-based gene prediction. Nucleic Acids Research 44(9): e89. https://doi.org/10.1093/nar/gkw092

Keilwagen J, Hartung F, Paulini M, Twardziok SO, Grau J (2018) Combining RNA-seq data and homology-based gene prediction for plants, animals and fungi. BMC Bioinformatics 19(1): 189. https://doi.org/10.1186/s12859-018-2203-5

Kumar S, Stecher G, Tamura K (2016) MEGA7: Molecular Evolutionary Genetics Analysis Version 7.0 for Bigger Datasets. Molecular Biology and Evolution 33(7): 1870–1874. https://doi.org/10.1093/molbev/msw054

Letunic I, Bork P (2021) Interactive Tree of Life (iTOL) v5: An online tool for phylogenetic tree display and annotation. Nucleic Acids Research 49(W1): 293–296. https://doi.org/10.1093/nar/gkab301

Liang JM, Li GS, Zhao MQ, Cai L (2019) A new leaf blight disease of turfgrasses caused by *Microdochium poae* sp. nov. Mycologia 111(2): 265–273. https://doi.org/10.1080/00275514.2019.1569417

Liu SB, Liu XY, Zhang ZX, Xia JW, Zhang XG, Meng Z (2022) Three new species of *Microdochium* (Sordariomycetes, Amphisphaeriales) on *Miscanthus sinensis* and *Phragmites australis* from Hainan, China. Journal of Fungi (Basel, Switzerland) 8(6): 577. https://doi.org/10.3390/jof8060577

Liu YJ, Whelen S, Hall BD (1999) Phylogenetic Relationships among Ascomycetes: evidence from an RNA polymerse II subunit. Molecular Biology and Evolution 16(12): 1799–1808. https://doi.org/10.1093/oxfordjournals.molbev.a026092

Lu X, Mai M, Tan W, Zhang M, Xie J, Lu Y, Niu XL, Zhang W (2023) Identification and fungicide sensitivity of *Microdochium chrysopogonis* (Ascomycota, Amphisphaeriaceae), a new species causing tar spot of *Chrysopogon zizanioides* in southern China. MycoKeys 100: 205–232. https://doi.org/10.3897/mycokeys.100.112128

Manamgoda DS, Cai L, Bahkali AH, Chukeatirote E, Hyde KD (2011) Cochliobolus: An overview and current status of species. Fungal Diversity 51(1): 3–42. https://doi.org/10.1007/s13225-011-0139-4

Mandyam KG, Roe J, Jumpponen A (2013) *Arabidopsis thaliana* model system reveals a continuum of responses to root endophyte colonization. Fungal Biology 117(4): 250–260. https://doi.org/10.1016/j.funbio.2013.02.001

Marin-Felix Y, Hernández-Restrepo M, Wingfield MJ, Akulov A, Carnegie AJ, Cheewangkoon R, Gramaje D, Groe-newald JZ, Guarnaccia V, Halleen F, Lombard L, Luangsa-ard J, Marincowitz S, Moslemi A, Mostert L, Quaedvlieg W, Schumacher RK, Spies CFJ, Thangavel R, Taylor PWJ, Wilson AM, Wingfield BD, Wood AR, Crous PW (2019)

Genera of phytopathogenic fungi: GOPHY 2. Studies in Mycology 92(1): 47–133. https://doi.org/10.1016/j.simyco.2018.04.002

Mesny F, Miyauchi S, Thiergart T, Pickel B, Atanasova L, Karlsson M, Hüttel B, Barry KW, Haridas S, Chen C, Bauer D, Andreopoulos W, Pangilinan J, LaButti K, Riley R, Lipzen A, Clum A, Drula E, Henrissat B, Kohler A, Grigoriev IV, Martin FM, Hacquard S (2021) Genetic determinants of endophytism in the Arabidopsis root mycobiome. Nature Communications 12(1): 7227. https://doi.org/10.1038/s41467-021-27479-y

Parkinson VO, Sivanesan A, Booth C (1981) The perfect state of the rice leaf-scald fungus and the taxonomy of both the perfect and imperfect states. Transactions of the British Mycological Society 76(1): 59–69. https://doi.org/10.1016/S0007-1536(81)80009-5

Pertea M, Pertea GM, Antonescu CM, Chang TC, Mendell JT, Salzberg SL (2015) StringTie enables improved reconstruction of a transcriptome from RNA-seq reads. Nature Biotechnology 33(3): 290–295. https://doi.org/10.1038/nbt.3122

Samuels GJ, Hallett IC (1983) *Microdochium stoveri* and *Monographella stoveri*, new combinations for *Fusarium stoveri* and *Micronectriella stoveri*. Transactions of the British Mycological Society 81(3): 473–483. https://doi.org/10.1016/S0007-1536(83)80115-6

Schoch CL, Seifert KA, Huhndorf S, Robert V, Spouge JL, André Levesque C, Chen W, et al. (2012) Nuclear ribosomal internal transcribed spacer (ITS) region as a universal DNA barcode marker for Fungi. Proceedings of the National Academy of Sciences of the United States of America 109(16): 6241–6246. https://doi.org/10.1073/pnas.1117018109

Senanayake IC, Rathnayaka AR, Marasinghe DS, Calabon MS, Gentekaki E, Lee HB, Hurdeal VG, Pem D, Dissanayake LS, Wijesinghe SN, Bundhun D, Nguyen TT, Goonasekara ID, Abeywickrama PD, Bhunjun CS, Jayawardena RS, Wanasinghe DN, Jeewon R, Bhat DJ, Xiang MM (2020) Morphological approaches in studying fungi: Collection, examination, isolation, sporulation and preservation. Mycosphere 11(1): 2678–2754. https://doi.org/10.5943/mycosphere/11/1/20

Shen W, Le S, Li Y, Hu FQ (2016) SeqKit: A Cross-Platform and Ultrafast Toolkit for FASTA/Q File Manipulation. PLoS ONE 11(10): e0163962. https://doi.org/10.1371/journal.pone.0163962

Stamatakis A (2014) RAxML version 8: A tool for phylogenetic analysis and post-analysis of large phylogenies. Bioinformatics 30(9): 1312–1313. https://doi.org/10.1093/bioinformatics/btu033

Stewart S, Rodríguez M, Mattos N, Abreo E, Stewart S, Rodríguez M, Mattos N, Abreo E (2019) First report of zonate leaf spot in sorghum caused by *Microdochium sorghi* in Uruguay. Agrociencia (Montevideo) 23(2): 94–98. https://doi.org/10.31285/AGRO.23.74

Sung GH, Sung JM, Hywel-Jones NL, Spatafora JW (2007) A multi-gene phylogeny of Clavicipitaceae (Ascomycota, Fungi): identification of localized incongruence using a combinational bootstrap approach. Molecular Phylogenetics and Evolution 44(3): 1204–1223. https://doi.org/10.1016/J.YMPEV.2007.03.011

Sydow H (1924) Mycotheca germanic. Fasc. XLII–XLV (No. 2051–2250). Annls Mycol 22: 257–268.

Tang D, Zou W, Wang Y, Huang OU, Yu H (2022) Morphology and phylogeny of *Microdochium chuxiongense* sp. nov., a fungus from Southwest China. Phytotaxa 555(2): 147–158. https://doi.org/10.11646/phytotaxa.555.2.3

Tsers I, Marenina E, Meshcherov A, Petrova O, Gogoleva O, Tkachenko A, Gogoleva N, Gogolev Y, Potapenko E, Muraeva O, Ponomareva M, Korzun V, Gorshkov V (2023) First genome-scale insights into the virulence of the snow mold causal fungus *Microdochium nivale*. IMA Fungus 14(1): 2. https://doi.org/10.1186/s43008-022-00107-0

Vilgalys R, Hester M (1990) Rapid genetic identification and mapping of enzymatically amplified ribosomal DNA from several *Cryptococcus species*. J. Bacteriol 172: 4238–4246. https://doi.org/10.1128/jb.172.8.4238-4246.1990

Von Arx JA (1984) Notes on *Monographella* and *Microdochium*. Transactions of the British Mycological Society 83(2): 373–374. https://doi.org/10.1016/S0007-1536(84)80168-0

Von Arx JA (1987) Plant pathogenic fungi. Nova Hedwigia 87: 1–288.

Vu D, Groenewald M, De VM, Gehrmann T, Stielow B, Eberhardt U, Al-Hatmi A, Groenewald JZ, Cardinali G, Houbraken J, Boekhout T, Crous PW, Robert V, Verkley GJM (2019) Large-scale generation and analysis of filamentous fungal DNA barcodes boosts coverage for kingdom fungi and reveals thresholds for fungal species and higher taxon delimitation. Studies in Mycology 2019(92): 135–154. https://doi.org/10.1016/j.simyco.2018.05.001

Wang X, Zhang X, Liu L, Xiang M, Wang W, Sun X, Che Y, Guo L, Liu G, Guo L, Wang C, Yin WB, Stadler M, Zhang X, Liu X (2015) Genomic and transcriptomic analysis of the endophytic fungus *Pestalotiopsis fici* reveals its lifestyle and high potential for synthesis of natural products. BMC Genomics 16(1): 28. https://doi.org/10.1186/s12864-014-1190-9

White T, Burns T, Lee S, Taylor J (1990) Amplification and direct sequencing of ribosomal RNA genes for phylogenetics. In: Innis MA (Ed.) PCR Protocols: A Guide to Methods and Applications. Academic Press, New York, 315–322. https://doi.org/10.1016/B978-0-12-372180-8.50042-1

Zhang Z, Schwartz S, Wagner L, Miller W (2000) A greedy algorithm for aligning DNA sequences. Journal of Computational Biology 7: 203–214. https://doi.org/10.1089/10665270050081478

Zhang Z, Xiao JF, Wu JY, Zhang HY, Liu GM, Wang XM, Dai L (2012) ParaAT: A parallel tool for constructing multiple protein-coding DNA alignments. Biochemical and Biophysical Research Communications 419(4): 779–781. https://doi.org/10.1016/j.bbrc.2012.02.101

Zhang W, Nan ZB, Tian P, Hu MJ, Gao ZY, Li M, Liu GD (2015) *Microdochium paspali*, a new species causing seashore paspalum disease in southern China. Mycologia 107(1): 80–89. https://doi.org/10.3852/14-119

Zhang ZF, Liu F, Zhou X, Liu XZ, Liu SJ, Cai L (2017) Culturable Mycobiota from karst caves in China, with descriptions of 20 new species. Persoonia 39(1): 1–31. https://doi.org/10.3767/persoonia.2017.39.01

Zhang J, Zhang ZX, Li DH, Xia JW, Li Z (2023a) Three New Species of *Microdochium* (Microdochiaceae, Xylariales) on Bambusaceae sp. and Saprophytic Leaves from Hainan and Yunnan, China. Journal of Fungi 9(12): 1176. https://doi.org/10.3390/jof9121176

Zhang ZY, Li X, Chen WH, Liang JD, Han YF (2023b) Culturable fungi from urban soils in China II, with the description of 18 novel species in Ascomycota (Dothideomycetes, Eurotiomycetes, Leotiomycetes and Sordariomycetes). MycoKeys 98: 167–220. https://doi.org/10.3897/mycokeys.98.102816

Supplementary material 1

The PCR primers, sequence and cycles used in this study

Authors: Zhao-Xue Zhang, Yu-Xin Shang, Meng-Yuan Zhang, Yun Geng, Ji-Wen Xia, Xiu-Guo Zhang

Data type: docx

Link: https://doi.org/10.3897/mycokeys.106.127355.suppl1

Supplementary material 2

GenBank accession number of the taxa used in phylogenetic reconstruction

Authors: Zhao-Xue Zhang, Yu-Xin Shang, Meng-Yuan Zhang, Yun Geng, Ji-Wen Xia, Xiu-Guo Zhang

Data type: docx

Link: https://doi.org/10.3897/mycokeys.106.127355.suppl2

Supplementary material 3

The sequence of phylogenetic analysis

Authors: Zhao-Xue Zhang, Yu-Xin Shang, Meng-Yuan Zhang, Yun Geng, Ji-Wen Xia, Xiu-Guo Zhang

Data type: txt

Link: https://doi.org/10.3897/mycokeys.106.127355.suppl3

Supplementary material 4

The sequence of phylogenomic analysis

Authors: Zhao-Xue Zhang, Yu-Xin Shang, Meng-Yuan Zhang, Yun Geng, Ji-Wen Xia, Xiu-Guo Zhang

Data type: txt

Link: https://doi.org/10.3897/mycokeys.106.127355.suppl4

Supplementary material 5

The complete ML phylogenetic tree

Authors: Zhao-Xue Zhang, Yu-Xin Shang, Meng-Yuan Zhang, Yun Geng, Ji-Wen Xia, Xiu-Guo Zhang

Data type: pdf

Link: https://doi.org/10.3897/mycokeys.106.127355.suppl5

MycoKeys 106: 327–354 (2024)
DOI: 10.3897/mycokeys.106.123484

Research Article

A phylogenetic study of *Micarea melaeniza* and similar-looking species (Pilocarpaceae) unveils hidden diversity and clarifies species boundaries and reproduction modes

Annina Kantelinen[1], Måns Svensson[2], Jiří Malíček[3], Jan Vondrák[3,4], Göran Thor[5], Zdeněk Palice[3], Stanislav Svoboda[3], Leena Myllys[1]

1 *Botany and Mycology Unit, Finnish Museum of Natural History, University of Helsinki, P.O. Box 7, FI-00014 Helsinki, Finland*
2 *Museum of Evolution, Uppsala University, Norbyvägen 16, SE-752 36 Uppsala, Sweden*
3 *Czech Academy of Sciences, Institute of Botany, Zámek 1 252 43, Průhonice, Czech Republic*
4 *Department of Botany, Faculty of Science, University of South Bohemia, CZ-37005 České Budějovice, Czech Republic*
5 *Department of Ecology, Swedish University of Agricultural Sciences, P.O. Box 7044, SE-750 07 Uppsala, Sweden*
Corresponding author: Annina Kantelinen (annina.kantelinen@helsinki.fi)

Abstract

Micarea (Ascomycota, Pilocarpaceae) is a large cosmopolitan genus of crustose lichens. We investigated molecular systematics and taxonomy of the poorly known *Micarea melaeniza* group focussing on *M. melaeniza*, *M. nigella* and *M. osloensis*. A total of 54 new sequences were generated and using Bayesian and maximum likelihood analysis of two markers (nuITS and mtSSU), we discovered two previously unrecognized phylogenetic lineages, one of which is described here as *Micarea eurasiatica* Kantelinen & G. Thor, **sp. nov.**, morphologically characterized by pycnidia that are sessile to emergent, cylindrically shaped, with greenish-black K+ olive green, wall pigmentation and containing large mesoconidia up to 6 µm in length. The species is known from Japan and Finland. In addition, we show that the reproduction biology of *M. osloensis* has been poorly understood and that the species often occurs as an anamorph with stipitate pycnidia. We present a species synopsis and notes on pigments. Our research supports previous results of asexuality being an important reproductive strategy of species growing on dead wood.

Key words: Biodiversity, DNA-barcoding, lichenized ascomycete, new species, overlooked taxa, reproduction mode

Academic editor: Thorsten Lumbsch
Received: 19 March 2024
Accepted: 6 June 2024
Published: 5 July 2024

Citation: Kantelinen A, Svensson M, Malíček J, Vondrak J, Thor G, Palice Z, Svoboda S, Myllys L (2024) A phylogenetic study of *Micarea melaeniza* and similar-looking species (Pilocarpaceae) unveils hidden diversity and clarifies species boundaries and reproduction modes. MycoKeys 106: 327–353. https://doi.org/10.3897/mycokeys.106.123484

Introduction

Species of the genus *Micarea* Fr. are lichenized ascomycetes belonging to the family Pilocarpaceae. Currently, more than 140 species are known, and new species are continually described (e.g., Czarnota 2007; Czarnota and Guzow-Krzemińska 2010; Sérusiaux et al. 2010; Guzow-Krzemińska et al. 2016, 2019; van den Boom et al. 2017; Kantvilas and Coppins 2019; Launis and Myllys 2019; Launis et al. 2019a, b; van den Boom et al. 2020; Vondrák et al. 2022; Index Fungorum 2023). *Micarea* species are globally distributed with representatives found on all continents. These species occur across a wide range

of habitats and grow on substrates such as bark, dead wood, rocks, soil and bryophytes. Some *Micarea* species are specialized and prefer specific habitats, such as dead wood in old-growth forests (Fig. 1). Their typical substrate has acidic pH (e.g. Coppins 1983; Czarnota 2007).

Despite the diversity and global presence of *Micarea* species, they are often overlooked and poorly understood. Several factors contribute to the challenge of identifying them. First, they are typically small. Second, *Micarea* exhibits a wide range of sexual and asexual propagules, including ascospores, three types of conidia (micro-, meso-, and macroconidia), and thallus fragments called goniocysts which likely serve as asexual propagules including both symbiotic partners. Some *Micarea* species are primarily sexual, while others often lack sexual structures but form numerous pycnidia where asexual conidia are produced (e.g. Coppins 1983; Czarnota 2007; Kantelinen et al. 2022a). Third, some *Micarea* species display intraspecific colour variations, which depend on light exposure and corresponding pigment levels. For example, the Sedifolia-grey pigment, commonly found in the apothecia of *Micarea* species, varies in concentration from light grey in shaded situations to almost black in well-lit habitats (Coppins 1983; Czarnota 2007; Launis et al. 2019a, 2019b). Due to these challenges, identifying *Micarea* species typically requires careful examinations of microscopic features, chemical testing (spot tests and TLC) and/or DNA sequencing.

Significant progress in the understanding of species boundaries and diversity within *Micarea* has been achieved through the application of molecular methods (Czarnota and Guzow-Krzemińska 2010; Sérusiaux et al 2010; Guzow-Krzemińska et al. 2016; van den Boom et al. 2017; Launis et al. 2019 a, b). However, some infra-generic groups in *Micarea* have been more studied than others. One group that remains poorly understood and has been sequenced only rarely is *Micarea melaeniza* Hedl. and similar species, i.e. *M. anterior* (Nyl.) Hedl., *M. botryoides* (Nyl.) Coppins, *M. deminuta* Coppins, *M. denigrata* (Fr.) Hedl., *M. melaeniza*, *M. misella* (Nyl.) Hedl., *M. nigella* Coppins, *M. olivacea* Coppins and *M. osloensis* (Th. Fr.) Hedl.. These species share morphological characteristics, such as a thin or endosubstratal thallus, small (0.1–0.3 mm wide) dark apothecia and/or dark stipitate mesopycnidia, as well as often simple to one septate ascospores. Furthermore, *M. botryoides*, *M. deminuta*, *M. melaeniza*, *M. nigella*, *M. olivacea* and *M. osloensis* are similar in having dark hypothecium and dimorphic paraphyses. The Cinereorufa-green (K+ green, HNO_3+ purple) and Superba-brown (K–, HNO_3–) pigments are often present, as well as sometimes Melaena-red (K+ green, HNO_3+ purple-red). Most of these species are obligate or facultative lignicoles (Coppins 1983, Czarnota 2007). Despite their morphological and ecological similarities, all the species are not necessarily closely related (Coppins 1983; Andersen and Ekman 2005; Sérusiaux et al. 2010).

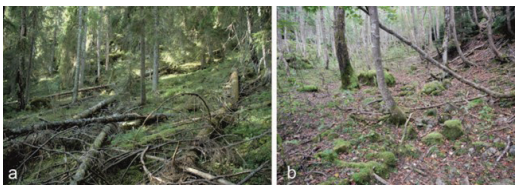

Figure 1. Typical habitats for species in the *M. melaeniza* group in boreal and boreonemoral forests **a** Koli National Park, Eastern Finland (photo: Kantelinen) **b** Nikko National Park, Central Honshu, Japan near the type locality of *M. eurasiatica* sp. nov. (photo: Thor).

We aim to clarify the molecular systematics and morphology of the poorly known *M*. *melaeniza* and its similar-looking species, focusing especially on *M*. *melaeniza*, *M*. *nigella* and *M*. *osloensis*, species that are morphologically challenging to identify. We use phenotypic characters and sequence data from two loci (nuITS and mtSSU). Additionally, we also address the species´ reproduction biology. Our study generates reliable sequences of several rarely collected species and furthers understanding on lichen diversity in boreal, boreonemoral and hemiboreal forests especially on dead wood and conifer bark.

Materials and methods

A substantial portion of the sequenced specimens in this study were collected from southern and central Finland as part of a research project that investigated lichen diversity on dead wood (years 2012–2014, Kantelinen et al. 2022b). Logs and stumps of decaying *Picea abies* trees in decay stages 2, 3, 4 and 5 were inventoried (following Renvall 1995).

In addition, specimens were obtained from the Czech Republic, Japan, Russian Caucasus, Sweden and Ukraine. These specimens were collected from dead wood and bark and sequenced when possible. Geo-coordinates are given in the format WGS84. Relevant specimens were also looked for amongst fresh *Micarea* collections from Australia, Brazil, Kenya, Rwanda and Tasmania with no success. Herbarium collections and type specimens from the herbaria FR, H, PRA, RBGE, S and UPS were studied.

Species identification

Specimens were identified with a dissecting (Leica S4E) and compound (Leica DM750) microscopes. Anatomical characters and ascospore dimensions were measured in water and K. The number of measured ascospores and conidia depended on their availability, but usually 10–30 were measured and the rest were examined superficially to ensure that they fell into the same size category. To detect and determine the insoluble pigments present in the specimens chemical spot tests with 10% potassium hydroxide (K) and sodium hypochlorite (C) and nitric acid (HNO_3) were used (Orange et al. 2010). Fresh material was often not sufficient for thin-layer chromatography (TLC). The specimens are generally quite small and have no or thin thallus, meaning that a substantial part of the collection would need to be taken for TLC. No secondary substances have previously been detected in *M*. *melaeniza*, *M*. *nigella* or *M*. *osloensis*, nor in the similar-looking species *M*. *anterior*, *M*. *misella* and *M*. *substipitata* Palice & Vondrák (Coppins 1983; Czarnota 2007; Vondrák et al. 2022). Thus, TLC is of limited practical value in the study of this species group.

Total genomic DNA was extracted from lichen structures (apothecia, pycnidia and/or thallus) in labs in Finland and the Czech Republic. In Finland, extractions were conducted using DNeasy® Blood & Tissue kit by Qiagen following the manufacturer´s instructions with the following exceptions. Lichen structures of approximately 0.5–1 mm in diam. were ground with mini-pestles in 40 µl of lysis buffer, after which 140 µl of the buffer was added by simultaneously flushing lichen fragments from the mini-pestle. The extracted DNA was eluted in 50 µl of the eluation buffer. Samples were incubated for 5 minutes and centrifuged. After

the first elution, a second elution was performed to increase sample availability by adding another 50 µl of the elution buffer, incubated for 5 minutes and centrifuged. The two elutions were stored in the freezer in separate microcentrifuge tubes. In the Czech Republic, extractions were conducted using ISOLATE II DNA Plant Kit (Bioline) according to the manufacturer´s protocol using a cetyltrimethylammonium bromide (CTAB)-based protocol (Aras and Cansaran 2006).

In Finland, PCR reactions were prepared using PuReTaq Ready-To-Go PCR beads (GE Healthcare). The 25 µl reaction volume contained 19 µl dH2O, 0.4 µM of each primer and 4 µL extracted DNA. The ITS and mtSSU regions were used for species identification. PCR was run under the following conditions: initial denaturation for 10 min at 95 °C followed by six cycles of 1 min at 95 °C (denaturation), 1 min at 62 °C (annealing), and 1 min 45 s at 72 °C (extension); for the remaining 35 cycles, the annealing temperature was decreased to 56 °C; the PCR program ended with a final extension of 10 min at 72 °C. The primers used were ITS1LM and ITS2KL (Myllys et al. 1999), and mrSSU1 and mrSSU3R (Zoller et al. 1999) and they were used for PCR amplification and sequencing. In the Czech Republic, PCR reactions for Malíček´s specimens were prepared following the protocol in Malíček et al. (2023). For Vondrák´s and Palice´s specimens PCR reactions were prepared as follows: Polymerase chain reactions were performed in a reaction mixture containing 2.5 mmol/l MgCl2, 0.2 mmol/l of each dNTP, 0.3 µmol/l of each primer, 0.5 U Tag polymerase (TOP-Bio, Praha, Czech Republic) in the manufacturer's reaction buffer, and sterile water to make up a final volume of 10 µl. The ITS and mtSSU regions were used for species identification. PCR was run under the following conditions: for ITS initial denaturation for 3 min at 94 °C followed by 30 cycles of 30 sec at 94 °C (denaturation), 30 sec at 56 °C (annealing), and 2 min at 72 °C (extension); the PCR program ended with a final extension of 7 min at 72 °C. For mtSSU initial denaturation for 10 min at 94 °C followed by 40 cycles of 30 sec at 94 °C (denaturation), 30 sec at 58 °C (annealing), and 2 min at 72 °C (extension); the PCR program ended with a final extension of 7 min at 72 °C. The primers used were ITS1F (White et al. 1990) and ITS4 (Gardes and Bruns 1993), and mrSSU1 (Zoller et al. 1999) and mrSSU7 (Zhou and Stanosz 2001), and they were used for PCR amplification and sequencing.

Phylogenetic analyses

To examine the phylogenetic position of our study species within *Micarea* s. lat., we ran a preliminary analysis of an mtSSU data matrix using *Psora decipiens* (Hedw.) Hoffm. from the family Psoraceae as an outgroup, based on the studies by Andersen and Ekman (2005) and Sérusiaux et al. (2010). In the phylogeny (tree not shown) our new samples fall outside of *Micarea* s. str. (i.e. the *M*. *prasina* group) and close to *M*. *doliiformis* (Coppins & P. James) Coppins & Sérus., *M*. *paratropa* (Nyl.) Alstrup, *M*. *assimilata* (Nyl.) Coppins and *Leimonis erratica* (Körb.) R.C. Harris & Lendemer (see phylogeny in Sérusiaux et al. 2010).

The final phylogenies, including 29 newly generated mtSSU and 25 ITS sequences (Table 1), were first aligned with MUSCLE v.3.8.31 (Edgar 2004) using the European Molecular Biology Laboratory, European Bioinformatics Institute's (EMBL-EBI) freely available web server (http://www.ebi.ac.uk/Tools/msa/muscle/). Based on our previous studies (Launis et al. 2019 a, b) and our preliminary phylogenetic reconstruction of the genus, *M*. *byssacea* and *M*. *prasina* belonging to

Table 1. List of *Micarea* specimens used in the phylogenetic analysis with locality, voucher information and GenBank accession numbers.

Taxon	Locality	Voucher information, sequence ID	mtSSU	ITS
M. anterior	Finland	Kantelinen 199 (H), A265	PP811702	PP811675
M. botryoides	Norway	Andersen 79b (BG)	AY567741	AY756471
M. byssacea	Finland	Kantelinen (Launis) 289103 (H), A98	MG707768	MG521562
M. contexta	Finland	Kantelinen 1914 (H), A569	PP811722	PP811692
M. deminuta	Japan	Thor 40245 (UPS), A926	PP811719	PP811689
M. deminuta	Czech Republic	Palice 6745 & Vořišková (PRA)	AY756446	AY756474
M. denigrata	Finland	Kantelinen 723 (H), A686	PP811721	PP811691
M. doliiformis	UK, Wales	Orange, LG database 29 (LG)	GU138666	
M. doliiformis	UK	Andersen 178a (BG)		HQ650654
M. eurasiatica sp. nov.	Finland	*Kantelinen* 2729 (H), A466	PP811712	PP811684
M. eurasiatica sp. nov.	Japan	*Thor* 40053 (UPS) A914, holotype	PP811720	PP811690
M. eximia	Finland	Kantelinen 3785 (H), A785	MT982134	MT981600
M. globulosella	Finland	Kantelinen (Launis) 67114 (H), A243	MG707744	MG521547
M. incrassata	Finland	*Kantelinen* 90 (H), A90	MT982132	MT981598
Micarea sp.	Finland	*Kantelinen* 2640 (H), A487	PP811703	PP811676
M. melaeniza	Finland	*Kantelinen* 2430 (H), A772	PP811709	PP811682
M. melaeniza	Ukraine	*Vondrák* 21921 (PRA)	PP811724	PP811694
M. melaeniza	Russia	*Vondrák* 23358 (PRA)	PP811725	PP811695
M. melaeniza (*M. nigella* in GenBank)	Czech Republic	*Palice* 32013 (PRA)	OQ646318	
M. misella	Finland	*Kantelinen* (Launis) 108111 (H), A264	MG707742	MG521545
M. nigella	Finland	*Kantelinen* 1971 (H), A589	PP811706	PP811679
M. nigella	Finland	*Kantelinen* 1974 (H), A588	PP811714	PP811686
M. nigella	Finland	*Kantelinen* 1921 (H), A572	PP811715	PP811687
M. nigella	Czech Republic	*Malíček* 16287	PP811726	PP811696
M. nigella	Czech Republic	*Malíček* 14664	PP811729	PP811698
M. osloensis	Finland	*Kantelinen* 1685 (H), A574	PP811704	PP811677
M. osloensis	Finland	*Kantelinen* 1865 (H), A575	PP811705	PP811678
M. osloensis	Finland	*Kantelinen* 1909 (H), A583	PP811717	
M. osloensis	Finland	*Kantelinen* 2899 (H), A736	PP811716	PP811688
M. osloensis	Finland	*Kantelinen* 1923 (H), A573	PP811713	PP811685
M. osloensis	Finland	*Kantelinen* 1686 (H), A768	PP811708	PP811681
M. osloensis	Finland	*Kantelinen* 2643 (H), A484	PP811710	PP811683
M. osloensis	Finland	*Kantelinen* 2003 (H), A594	PP811707	PP811680
M. osloensis	Finland	*Kantelinen* 2648 (H), A485		PP811693
M. osloensis	Czech Republic	*Malíček* 16281	PP811730	
M. osloensis (*M. melaeniza* in GenBank)	Czech Republic	*Palice* 30267 (PRA)	OQ646316	
M. osloensis (*M. nigella* in GenBank)	Czech Republic	*Palice* 30266 (PRA)	OQ646320	OQ717948
M. osloensis	Sweden	*Svensson* 4385 (UPS), C792	PP811718	
M. osloensis	Russia	*Vondrák 22836* (*PRA*)	PP811723	
M. osloensis (*M. melaeniza* in GenBank)	Czech Republic	*Vondrak* 25774 (PRA)	OQ646315	OQ717944
M. osloensis	Czech Republic	*Vondrák* 19007 (PRA)	PP811727	PP811697
M. osloensis	Czech Republic	*Vondrák* 22217 (PRA)	PP811728	
M. prasina	Finland	*Kantelinen* (*Launis*) 265101 (H), A92	MG707747	MG521549
M. substipitata	Finland	*Kantelinen* 2700 (H), A469	PP811711	

Micarea s. str. were selected as outgroups. We ran separate single-marker analyses by using MrBayes3.2.7a and did not detect conflicting clades between the analyses, although missing data was higher in the ITS matrix, and hence decided to concatenate the data by using Mesquite v. 3.61 (Maddison and Maddison 2023). The two-locus data matrix from sequences of 43 specimens included 1245 aligned nucleotide characters, with 707 positions in the mtSSU and 537 positions in the ITS regions. The hypervariable region at the end of the mtSSU was removed from the analyses. *Micarea doliiformis* is represented by sequences from two specimens that were combined as one, the other specimen represented by an mtSSU sequence and another by ITS sequence (see Table 1). The data matrix was subjected to Bayesian inference using MrBayes (v. 3.2.7a) (Ronquist and Huelsenbeck 2003) and to maximum likelihood (ML) analysis using freely available IQ-Tree 1.6.12 (Trifinopoulos et al. 2016) web server (http://iqtree.cibiv.univie.ac.at/). For the Bayesian analysis, substitution models were selected by having the MCMC procedure sample across models (Huelsenbeck et al. 2004). The convergence of the four parallel runs was checked after 2000000 generations using Tracer (v. 1.5) (Rambaut et al. 2018) and graphed using FigTree (v. 1.4.4). For the ML analysis, model TIM2+F+I+G4 was chosen by having IQ-Tree run the best-fitting substitution model for our one partition matrix, and branch lengths were assumed to be proportional across subsets. Node support was estimated with 1000 bootstrap replicates using the ultrafast bootstrap algorithm. The alignment is available from the Dryad Digital Repository https://doi.org/10.5061/dryad.79cnp5j44.

Results

We present the first molecular phylogeny of *M. melaeniza* and similar-looking species. We recorded 72 specimens of the *M. melaeniza* group of which 26 were sequenced successfully. In addition, we downloaded sequences from GenBank (Table 1). The topologies of the Bayesian and ML analyses showed no conflict and hence only the Bayesian tree is shown (Fig. 2).

The phylogenies are well-supported and resolved into 18 taxa. *Micarea misella*, *M. globulosella*, *M. eximia* and *M. botryoides* form basal nodes for the phylogeny. The remaining taxa resolve into four clades that include the *M. melaeniza* group and its sister groups. The *M. melaeniza* group, delimited in this study, includes six monophyletic taxa, i.e. *M. deminuta*, *M. melaeniza*, *M. nigella*, *M. osloensis* and two undescribed species, each represented by two specimens. We describe the first as *M. eurasiatica* Kantelinen & G. Thor, sp. nov., but refrain from describing the other because of insufficient material and sequence data ("Kantelinen 2640 and Kantelinen 1870"; sequences from the latter specimen are not of sufficient quality and therefore not included in the final analyses even though it formed a monophyletic clade in preliminary analysis). Based on our results the similar looking *M. anterior*, *M. contexta* and *M. subtipitata* are not included in the *M. melaeniza* group. Instead, they form a sister clade to this group, but the relationship receives no support and is based on limited taxon sampling. Several outgroups, including *M. incrassata*, *M. doliiformis*, and *Lecania cyrtella* have been tested but the overall topology of the phylogeny has not changed. The main distinguishing morphological characters are presented in the species synopsis Table 2. Pigments are presented in Table 3.

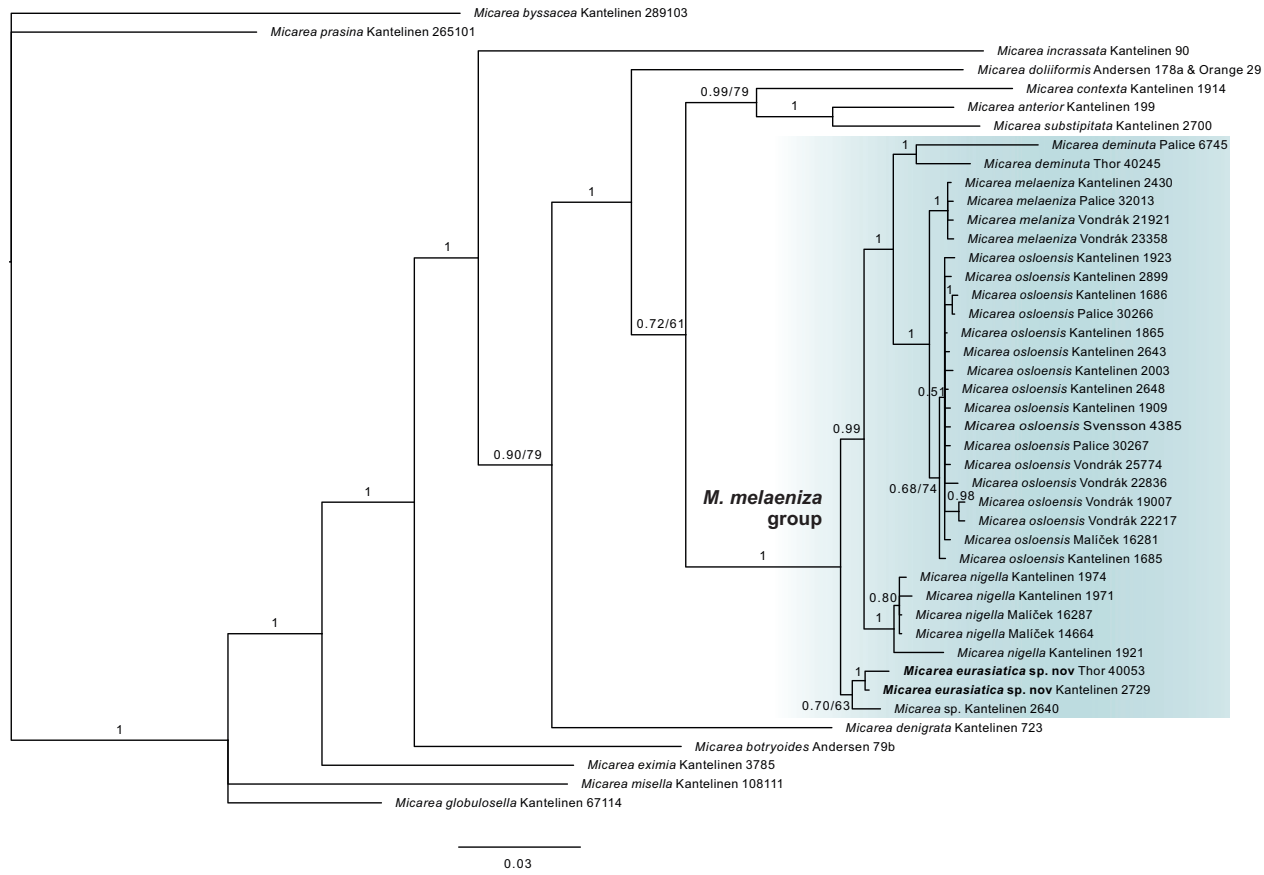

Figure 2. Bayesian tree of the *Micarea melaeniza* -group and similar-looking species based on mtSSU and ITS sequences. Bayesian posterior probabilities are always indicated near the branches together with bootstrap support when less than 80 (e.g. 0.70/63).

In addition to our specimens, we downloaded *M. melaeniza* and *M. nigella* sequences from Genbank. Based on our phylogenetic analyses, all of them fall inside *Micarea osloensis* (OQ646318, OQ646320, OQ717948, OQ646315, OQ717944, OQ646316, in addition OQ717947 and OQ646319 are identical with others and excluded from our final analysis because of repetition). Three sequences from Genbank were left out from our analyses (AY756488, AY756484, OQ717944), because they are substantially different compared to the other sequences in the *M. melaeniza* group and hence the alignment and phylogenetic analysis became unreliable. Based on blast searches AY756484 is a species of *Lepraria*, AY756488 perhaps *Micarea melaena* or *M. nitschkeana*, and OQ717944 an uncultured fungus.

Our data include a taxon with a high morphological resemblance to *Micarea osloensis*, a species found only twice before in years 1874 and 2007. Unfortunately, we were not successful in sequencing the old collections. Despite the high morphological resemblance, our new specimens have some subtle differences compared to the type. The type specimen of *M. osloensis* is a fertile specimen with apothecia, whereas our specimens are usually asexual with pycnidia. The specimens are mostly dimorphic, meaning that the existing sequenced specimens are usually either sexual or asexual, and rarely both. In addition, some of the fresh material is with Cinereorufa green pigment which is not present in the type. See taxonomy section for further info.

Table 2. Species synopsis representing key morphological characters based on our study and literature (Hedlund 1892; Coppins 1983; Czarnota 2007).

	reproduction	anatomical coloration	spores (simple, if not mentioned otherwise)	paraphyses (µm wide)	mesopycnidia	mesoconidia	K-reaction
Micarea anterior	pycnidia, ap quite rare	(orange-/reddish-)brown	8–12(–12.5) × 3–4(–4.8) µm 0–1(–2) sept.	one type: 1–1.5 µm, sometimes upper part 2.5–3 µm	stipitate, brown from base and black from the top, up to 250 µm tall (Finnish specimens); sessile to stipitate, pallid, often with reddish-brown blotches, up to 250 µm tall (Coppins 1983); dilute brownish (Czarnota 2007)	3.5–4.5 × 1.2–1.5 µm	no reaction or dulling
M. contexta	apothecia, pycnidia rare	dark green, purple	7–13(–14) × 3–4.6 µm	two types: : thick 1.5–2.0 µm; thin less than 1 µm	sessile to emergent, c. 40 µm diam.	4.2–5.0 × 1.2–1.5 µm	K+ green
M. deminuta (TYPE)	apothecia	dark-brown epihymenium, brown-black (not warm) [dark ± reddish brown / Coppins 1995] hypothecium	7–11(–11.8) × 4–5(–5.5) µm; (5.8–)7.7–10.1(–11.5) × (3.2–)3.7–4.5(–4.8) µm (Coppins 1995)	two types: thick 1.5–2.0(–3.0) µm; thin 0.8–1.0 µm	no emergent/stalked pycnidia	not reported	K+ green
M. deminuta (sensu Czarnota 2007)	apothecia, pycnidia rare	olivaceous epihymenium (with dull brown to brown-black streaks in hymenium), brown-black hypothecium	(7.2–)8.2–11.3(–11.8) × (4.1–)4.4–5.5(–6.1) µm	two types: thick (1-)1.2–2.0 µm; thin 0.8–1.0 µm	emergent, often with gaping ostioles, black-brown with brown to olive-brown walls	(4.9–)5.5–8(–8.1) × 1.5–1.8 um	K- or K+ dull olive grey [=K+ green]
M. misella	pycnidia, ap not always present	dark olive-brown epihymenium, hyaline hymenium and hypothecium	6–9(–10) × (2–)2.5–3.5(–4) µm; 0(–1) sept.	one type: (0.8–)1–1.2(–1.5) µm	brown to black, glossy, stipitate up to 300 µm tall, walls olive, olive-brown	3.5–5(–6.5) × 1.2–1.4(–1.7) µm	K+ violet
M. melaeniza (TYPE)	ap and pycnidia	brownish-black, greenish	5–9.0 × 2.5–3.8 µm	two types: thick c. 2 µm; thinner c. 0.7–1 µm	black, stipitate up to 300 µm tall, upper part of the walls greenish-brown and lower part reddish-brown sometimes growing from the same base	3–3.5 × 1.75 µm	K+ green, or rarely K–
M. melaeniza (sequenced)	pycnidia, ap rare	brownish-black, greenish, rarely purplish tone	5–9.0 × 2.5–3.8 µm	two types: thick c. 2 µm; thinner c. 0.7–1 µm	black, stipitate up to 300 µm tall, upper part of the walls greenish-brown and lower part reddish-brown, rarely purplish tone, sometimes growing from the same base	2.5–3.5 × 1.2–1.8 µm	K+ green, or rarely K–
M. nigella (TYPE)	ap and pycnidia	brownish-black, often purple tinge	6.5–12 × 2.5–4 µm	two types: thick 2–3 µm; thinner c. 0.7–1 µm	black, stipitate, purplish-brown according to the description, but the type specimen is not clearly purplish, but walls are instead brown-black to slightly greenish-black	3.4–4.3 (–4.5) × 1.2–1.6 (–1.8) µm	K+ green
M. nigella (sequenced)	pycnidia, no ap	brownish-black, often purple tinge	none	none	black, stipitate, walls brownish black or often purplish black, sometimes growing from the same base	(3.5–)3.8–4.5 × 1.2–1.5(–1.8) µm	K+ green

	reproduction	anatomical coloration	spores (simple, if not mentioned otherwise)	paraphyses (µm wide)	mesopycnidia	mesoconidia	K-reaction
M. olivacea (TYPE)	ap and pycnidia	olivaceous, olive-brown	(7–)9–12.3 × 2.5–3.5 µm	two types: thick 2–3 µm; thinner c. 1–1.2 µm	sordid green, numerous, inconspicuous, +/-immersed	3.4–4.3 × 1.2–1.6 µm	K+ green
M. osloensis (TYPE)	ap, no pycnidia	warm brown tones	6–9.5(–10) × 3–4 µm	two types: mostly 2–3 µm, unevenly shaped, sometimes branched; thinner 1.5–1.8 µm	not seen	not seen	No reaction
M. osloensis (sequenced)	pycnidia, ap few	warm brown and olivaceous tones	7–10 × 3.0–3.5 (–4.0) µm	two types: thick 2–3 µm often uneven in shape; thinner c. 1–1.5 µm	often numerous and crowded, simple or branched from the base, emergent or shortly stalked up to 180 µm, dark brown to blackish, walls greenish black to greenish brown from the top with a warm brown lower part	3.5–4.5(–5) × 1.2–1.5(–1.8) µm	No reaction, or K+ green epihymenium
M. eurasiatica sp. nov.	pycnidia, ap few	greenish black, dark brown	(6–)7–9 × 3–4 µm	two types: thick 2–3 µm sometimes branched; thinner c. 0.7–1.5 µm	sessile to emergent, 50–80 (–100) µm tall, 30–45 µm wide	4.5–6.0 × 1.2–1.5(–1.8) µm	K+ green
M. sp. (Kantelinen 2640)	pycnidia, ap few	brownish-black, greenish-black, violet-black	none seen	two types	sessile (to emergent), c. 50 µm tall, 50 µm wide	4.2–5.0 × 1.2–1.5 µm	K+ green
M. substipitata	pycnidia, ap not always present	pallid to whitish, hyaline	7–10 (–11) × 2.2–3.5 (–3.8) µm (0–) 1 sept.	two types: mostly 0.9–1.3 µm; rarely thicker 1.5–2.0 µm	sessile to shortly stipitate, white, up to 250 µm tall	2.5–3.5(–4) × 1.0–1.5 µm	No reaction

Table 3. Pigments found in apothecia and pycnidia based on our study and literature (Hedlund 1892; Coppins 1983; Czarnota 2007).

	Cinereorufa-green [Pigment A] *K+* green intensifying, HNO_3+ purple	Melaena-red [Pigment B] *K+* dull sordid green, HNO_3+ purple-red	Melaenida-red [Pigment C] *K+* purplish-red, HNO_3 -	Superba-brown [within Pigment F] No reaction in *K* or HNO_3
M. deminuta	x			x
M. melaeniza	x	(x)	(x)	x
M. nigella	x	x	x	
M. osloensis (type)				x
M. osloensis (new)	(x)			x
M. eurasiatica sp. nov	x		(x)	x

Taxonomy

***Micarea eurasiatica* Kantelinen & G. Thor, sp. nov.**
MycoBank No: 854181
Fig. 3A, B

Type. Japan, Honshu, Gunma Prefecture, Katashina-mura, Nikko National Park, 4.7 km E of Marunuma Kogen Ski Resort, 550 m S of the parking lot at the start of the trail up to the summit of Mt. Oku-Shirane, along the trail. Open forest with mainly deciduous trees. On *Tsuga diversifolia* log. 36.81573°N, 139.37823°E (± 10 m), elevation 1791 m. 2019. Thor 40053 (Holotype UPS). DNA sample A914.

Description. *Thallus* endoxylic. Photobiont micareoid, 4–7 µm.

Apothecia few, immarginate, convex, black, matt, 0.1–0.2 mm in diam. Hymenium 25–40 µm tall, hyaline or tinged green, K+ greenish when tinged, sometimes with darker vertical streaks. Epihymenium black to blackish-green, K+ green, HNO_3+ purple (Cinereorufa-green). Asci clavate, 28–38 × 11–14 µm. Ascospores ellipsoid to ovoid, simple, (6–)7–9 × 3–4 µm. Paraphyses numerous, of two types: 1. evenly distributed, branched, thin, c. 0.7–1.5 µm wide, 2. evenly distributed, stout, sometimes branched, 2–3 µm wide, not always coated in pigment. Hypothecium c. 35–45 µm tall, dark brown, K – (Superba-brown), or sometimes with a slight purple tinge (Melaenida-red), hyphae coated with dark brown pigment. Excipulum not evident.

Mesopycnidia few to abundant, sessile to emergent, cylindrical in shape, 50–80(–100) µm tall, 30–45 µm wide, black, walls greenish black, K+ green, HNO_3+ purple (Cinereorufa-green), sometimes merged from base, usually extruding white mass of conidia that sometimes merge with neighbouring conidial mass. Mesoconidia ellipsoid-cylindrical, (4–)4.5–6.0 × 1.2–1.5(–1.8) µm. Micro- or macropycnidia not seen.

***Chemistry*.** Material not sufficient for TLC.

Crystalline granules not present in apothecia or pycnidia.

Habitat and distribution. *M. eurasiatica* is currently known from Finland and Japan. In Finland, the species was collected in a shaded and dense, *Picea abies* dominated managed forest. In Japan, the species occurred in a semiopen forest with mainly deciduous trees. On both occasions, the species was found growing on dead wood.

Notes. *M. eurasiatica* is currently known from two collections. The type collection has abundant mesopycnidia, and additionally few small apothecia.

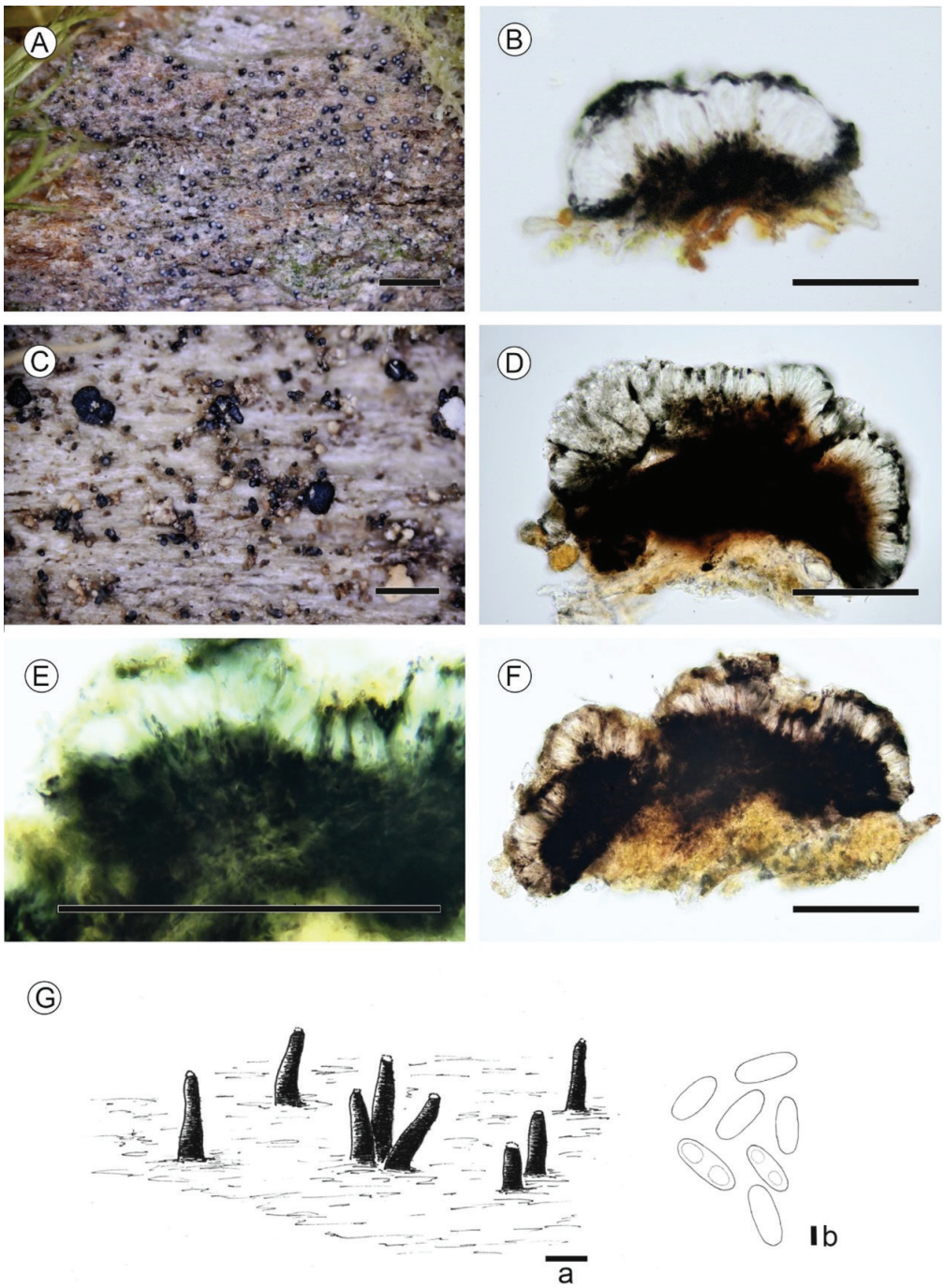

Figure 3. Morphological and anatomical features **A, B** *Micarea eurasiatica* sp. nov. (Thor 40053) **A** habit **B** apothecial section in water **C, D** *Micarea melaeniza* (Holotype) **C** habit, apothecia and pycnidia **D** apothecial section in water **E–G** *Micarea nigella* (Holotype) **E** apothecial section in K **F** apothecial section in water **G** drawing of *M. nigella* pycnidia on dead wood (Kantelinen 1974, H), Ga.) Mesopycnidia extruding mesoconidia, Gb.) Mesoconidia are cylindrical, ellipsoid, sometimes biguttulate. Photos and drawing Kantelinen. Scale bars: Habit 0.5 mm (**A, C**); Apothecial sections 100 µm (**B, C, E, F**); Drawing Ga 100 µm, Gb 1 µm.

The other collection has only pycnidia. The most important diagnostic characters are the combination of sessile to emergent pycnidia that are cylindrical in shape, greenish-black pycnidial walls, large mesoconidia (up to 6 µm in length) and a K+ olive green reaction (Cinereorufa-green). If apothecia are present, they are 0.1–0.2 mm wide, have greenish-black epihymenium (K+ green,

Cinereorufa-green) and dark brown hypothecium (K– or sometimes slightly K+ purple if Melaenida-red present). *Micarea eurasiatica* resembles other often asexual *Micarea* species on dead wood such as *M. melaeniza*, *M. misella*, *M. olivacea* and *M. osloensis*. *Micarea eurasiatica* differs from *M. melaeniza* by having shorter mesopycnidia, longer mesoconidia (*M. melaeniza*: (3–)3.5–4.5 × 1.2–1.8 µm, *M. eurasiatica*: (4–)4.5–6.0 × 1.2–1.5(–1.8) µm), and a more greenish black wall colouration in the pycnidia with no brown tones. *Micarea misella* has a K+ violet reaction (Sedifolia-grey) instead of K+ olive green and its mesopycnidia are brownish-black and taller (Coppins 1983; Czarnota 2007). *Micarea olivacea* has rather similar short mesopycnidia that react K+ green, but the wall of pycnidia is olive-brown and the mesoconidia are shorter than those of *M. eurasiatica* (*M. olivacea*: 3.4–4.3 × 1.2–1.6 µm, *M. eurasiatica*: (4–)4.5–6.0 × 1.2–1.5(–1.8) µm) (Coppins 1983). *Micarea osloensis*, on the other hand, has a warm brown wall colouration and usually no K reaction.

Additional specimen studied. Finland, Uusimaa, Tuusula, W of Korso, shaded and dense *Picea abies* dominated managed forest (plot 2), on wood of fallen *Picea abies* (decay stage 2), 60.3544°N, 25.0322°E, 2013, Kantelinen 2729 (DNA A466), H.

***Micarea melaeniza* Hedl.**
MycoBank No: 368074
Fig. 3C, D

Type. Bih. Kongl. Svenska Vetensk.Akad. Hand. III, 18: 96 (1892). Type: Sweden, Helsinglandiæ [= Hälsingland], Jerfsö [= Järvsö], VIII 1891. J. T. Hedlund (S L1471! – lectotype, designated by Coppins 1983 [ICN Art. 9.10], further specified here [ICN Art. 9.17], S L1472!, UPS L-005556!, UPS L-171894!, LD 1056591!, isolectotypes).

Description. ***Thallus*** endoxylic. Photobiont micareoid, 4–7 µm.

Apothecia absent to numerous (mostly rare), immarginate, subglobose, often becoming tuberculate, black, matt, 0.1–0.3 mm in diam. Hymenium (25–)28–42 µm tall, hyaline or tinged aeruginose green, olive, or rarely purplish brown, often with darker vertical streaks. Epihymenium irregularly pigmented aeruginose green, or rarely sordid brown, sometimes with a purplish tinge. Epihymenium and hymenium K+ olive green, HNO_3 purple (Cinereorufa-green), or rarely K–. Asci clavate, 22–35 × 10–12 µm. Ascospores ellipsoid to usually ovoid, simple, 5–9 × 2.5–4.0 µm. Paraphyses numerous, of two types: 1.) evenly distributed, branched, thin, c. 0.7–1 µm wide, 2.) scattered or in small fascicles, stout, c. 2 µm wide, coated by greenish pigment. Hypothecium c. 60–120 µm tall, dark brown (Superba-brown), sometimes greenish or with a reddish tinge, often K+ olive green in the upper part (reaction in the greenish Cinereorufa-green pigment), hyphae coated with dark brown pigment. Excipulum not evident.

Mesopycnidia always present, usually numerous, black, sessile or more usually stalked and then 80–300 µm tall, 40–70 µm in diam., stalks simple or branched from the base bearing up to four pycnidia, upper part of the walls greenish-brown and lower part reddish-brown, K+ dull green (the greenish pigment) or sometimes K–. Mesoconidia ellipsoid to short cylindrical 2.5–3.5 × 1.2–1.8 µm. Micro- or macropycnidia not seen.

Crystalline granules not present in apothecia, pycnidia or thallus.

Chemistry no substances detected by TLC (information based on Coppins 1983 and Czarnota 2007).

***Typification*.** In his original description of *Micarea melaeniza*, Hedlund (1892) cited material that he had collected in Järvsö in Hälsingland, but without giving further specimen data. There are five specimens of *M. melaeniza* in S, LD and UPS collected by Hedlund in Järvsö in August 1891 and which all are likely to be part of the original material. Coppins (1983) cited a 'holotype' in S, which constitutes a lectotypification following ICN Art. 9.10. There is, however, an additional specimen in S (S L1472) with the same label data, and as Coppins (1983) did not indicate which of these specimens he considered to be the holotype, the lectotypification effectively concerns both specimens. We therefore further specify this by here designating the specimen S L1471 as the lectotype. This specimen was likely the one referred to as holotype by Coppins, as annotation slips from him are included in the envelope. It should be noted that all five type specimens of *M. melaeniza* are homogeneous.

Habitat and distribution. *M. melaeniza* occurs on lignum of conifer stumps and logs. Based on sequenced specimens and type, the species is currently known from the Czech Republic, Finland, Sweden, Ukraine and the Russian Caucasus. In addition, *M. melaeniza* has been reported from Alaska (Spribille et al. 2020), Austria (Berger and Türk 1991, this study) and Mongolia (Palka and Śliwa 2006). Further, it might have been reported as *M. nigella* and could be found after revising specimens.

Notes. In his monograph of European *Micarea* species, Coppins (1983) accepted *M. melaeniza*, and in his interpretation, the species is characterized by having a hymenium with green pigmentation, a dark brown hypothecium without any reaction with K, and black stalked pycnidia containing comparatively short conidia. In the same work, the new species *M. nigella* was described, which should differ from *M. melaeniza* by having a purplish brown, K+ green pigment in the hymenium, hypothecium and pycnidial tissues, and slightly larger mesoconidia (*M. melaeniza*: 2.3–3.6 × 1–1.3 µm vs. *M. nigella*: 3.4–4.3 × 1.2–1.6 µm; Coppins 1983). Czarnota (2007) noted that the amount of purple, K+ green pigment varied considerably in Polish collections determined as *M. nigella*, and suggested that *M. melaeniza* and *M. nigella* could be conspecific. He further noted that Hedlund's original description could be interpreted as indicating the presence of another pigment, the purple, K+ purple pigment and suggested that the differences between Hedlund's and Coppins' descriptions could be due to the studied material having aged (Czarnota 2007).

In our interpretation, *M. melaeniza* is a species with mostly two pigments: (i) a blackish-green, usually K+ green intensifying pigment, mostly located to the epihymenium but sometimes also in the hymenium and the upper part of the hypothecium (Cinereorufa-green) and (ii) a dark brown, K– pigment in the hypothecium (possibly Superba-brown). The description in Coppins (1983) fits our interpretation quite well, except that the specimens have a K+ greenish reaction due to Cinereorufa-green pigment that is not mentioned by Coppins (l.c.) but is, on the other hand, mentioned in the original description of the species by Hedlund (1892) and seen by us in the type specimen. Pigmentation of *M. melaeniza* may be more complex, however. One specimen from the Czech Republic (ZP32013) shows patchily purplish, K+ dark green pigment that might

be the Melaena-red pigment (in apothecia concentrated mainly in hymenium as darker streaks). This specimen was originally downloaded to GenBank as *M. nigella*, but it is monophyletic with *M. melaeniza* in our phylogenetic analyses. More sequenced specimens are needed to understand better the pigment profile of *M. melaeniza*.

We considered the possibility of *M. melaeniza* and *M. nigella* being synonymous. A careful study of the type specimens showed morphological differences, e.g. in the size of conidia and pigmentation of apothecia and pycnidia. A brown or purple-brown, K+ green pigment in the hymenium, hypothecium and pycnidia walls (Melaena-red) of *M. nigella* is an important difference between *M. melaeniza* and *M. nigella*, although this is not true for all the studied specimens as was mentioned above. The difference in pigmentation is also visible in nitric acid, i.e. in *M. melaeniza* the hypothecium is mostly HNO_3– (rarely HNO_3 intensifying red), and in *M. nigella* HNO_3+ purple-red. Compared to *M. melaeniza*, *M. nigella* also has longer conidia (3.4–4.5 × 1.2–1.6 µm), slightly shorter hymenium (up to 30 µm) and wider paraphyses (up to 3 µm), as also shown by Coppins (1983).

The molecular study supports the distinction of *M. melaeniza* and *M. nigella* (Fig. 2). Our sequenced specimens form two monophyletic clades, and these specimens are morphologically similar with the type specimens (except for ZP32013 discussed above).

In external appearance, *M. melaeniza* also resembles *M. botryoides*, *M. eurasiatica*, *M. misella* and *M. osloensis*. *Micarea botryoides* is usually not lignicolous, has longer ascospores (8–13(–16) × 2.3–3.7(–4) µm) that are often septate, and longer mesoconidia (Coppins 1983). *Micarea eurasiatica* has similar pigmentation like *M. melaeniza*, but the shape of apothecia is different (adnate vs subglobose), its pycnidia are sessile and mesoconidia are longer (up to 6 µm). *Micarea misella*, on the other hand, can be microscopically distinguished from *M. melaeniza* by the olivaceous pigment that reacts violet instead of dull green in K, and by its hyaline hypothecium (Coppins 1983). *Micarea osloensis* is similar to *M. melaeniza* in many characters, and is a close relative based on our phylogenetic study. However, *M. osloensis* has shorter pycnidia (max. 180 µm), longer mesoconidia 3.5–4.5(–5) × 1.2–1.5 (–1.8) µm, and apothecia and pycnidia are mostly K– (although a higher concentration of Cinereorufa-green pigment is known to occur in some of the C-European specimens).

Additional specimens studied. Austria, Niederösterreich, Ybbstaler Alpen, Wildnisgebiet Dürrenstein, Lunz am See Rothwald, Kleiner Urwald, primeval beech dominated forest on a crest above the valley of Moderbach brook, 47°46'31.0"N, 15°06'10.5"E, 1010 m, on wood of snag of *Picea abies*, 2022, Malíček 16229, Berger, Palice & Vondrák, hb Malíček.

Czech Republic, S Bohemia, Šumava Mts, Volary, České Žleby: Radvanovický hřbet - E foothill, managed spruce forest with left old beeches on E-NE-facing slope, 48°54'02"N, 13°48'28"E, on decaying wood of (?)*Picea* stump, 820 m, 2021, Palice 32013, PRA (in GenBank as *M. nigella*: OQ646318); ibid., Horní Vltavice, Zátoň: Jilmová skála Nature Monument, scree old-growth forest (150–200 years old) with maple, beech, sycamore, silver fir etc., 48°57'13"N, 13°47'48"E, 1000–1030 m, on decaying stump, 2014, Malíček 7322, hb Malíček.

Finland, Uusimaa, Vantaa, Herukkapuro nature reserve (plot 1), old-growth forest, on wood of a dead stump of *Picea abies* (decay stage 5), WGS84 60.3215°N, 24.7658°E, 2013, Kantelinen 2430 (DNA A772), H.

Ukraine, Ukrainian Carpathians, Nadvirna, Bystrytsia, in valley of stream Dzhurbzinets, c. 3 km south of village Maksymets, 48°28'30"N, 24°18'23"E, 1005 m, on soft wood of coniferous (*Picea*?) stump, 2019, Vondrák 21921, PRA.

Russia, Russian Western Caucasus, Adler, Krasnaya Polyana, primeval fir-beech forest below timberline, 43°41'50"N, 40°21'25"E, 1690 m, on soft rotten wood of *Abies* snag, 2019, Vondrák 23358, PRA.

Sweden, Ångermanland, Långsele par., VII. 1891. Hedlund, UPS (L-171893).

Micarea nigella Coppins

Fig. 3E, F, G

Micarea nigella Coppins. Bull. Brit. Mus. Nat. Hist. 11(2): 163 (1983). Type: Denmark, Jylland, c. 16 km N of Hobro, Rold Skov, Torstedlund Skov, on conifer stump, lignum, 1979, Coppins 4429 (RBGE! – holotype).

Description. ***Thallus*** endoxylic or thin green-grey layer on top of substrate. Photobiont micareoid, 4–7 µm.

Apothecia absent to numerous (mostly rare), immarginate, subglobose, often becoming tuberculate, black, matt, 0.1–0.3 mm in diam. Hymenium 25–30 µm tall, hyaline or tinged dull brown or purplish brown, K+ sordid green, HNO_3+ purple-red (Melaena-red), often with darker vertical streaks. Epihymenium irregularly pigmented brown to purplish-brown (Melaena-red), sometimes dark greenish, K+ olive green, HNO_3+ purple (Cinereorufa-green). Asci clavate, 22–30 × 10–12 µm. Ascospores ellipsoid to usually ovoid, simple, 6.5–12 × 2.5–4.0 µm. Paraphyses of two types: 1.) evenly distributed, branched, thin, c. 0.7–1 µm wide, 2.) scattered or in small fascicles, stout, 2–3 µm wide, coated by dark pigment. Hypothecium c. 70–120(–160) µm tall, dark brown with variable amount of purplish tone, K+ olive green, HNO_3+ purple-red (Melaena-red), hyphae coated with a dark brown pigment. Excipulum not evident.

Mesopycnidia always present, usually numerous, black, sessile or more usually stalked and then 80–300 µm tall, 40–80 µm in diam., stalks simple or branched from the base bearing up to four pycnidia, walls brownish black to purplish black, sometimes olivaceous from the top, K+ dull green and HNO_3+ purple-red especially in the brown parts (Melaena-red). Mesoconidia ellipsoid or short cylindrical 3.5–4.5(–5) × 1.2–1.8 µm. Micro- or macropycnidia not seen.

Crystalline granules not present in apothecia, pycnidia or thallus.

Chemistry no substances detected by TLC (information based on Coppins 1983 and Czarnota 2007).

Habitat and distribution. *Micarea nigella* occurs mainly on lignum of conifer stumps or fallen trunks, sometimes spreading from wood to dead bryophytes. Based on sequenced specimens and the type material, the species is known from the Czech Republic, Denmark (holotype), Great Britain (paratypes), Finland and Sweden. In addition, *M. nigella* has previously been reported from boreal and temperate forests in north-western, central and eastern Europe (e.g. Czarnota 2007).

Notes. In external appearance, *M. nigella* resembles *M. melaeniza*. The differences between these two species are discussed in detail under *M. melaeniza* and Coppins (1983). The species also resembles *M. botryoides*, *M. misella*

and *M. osloensis*. *Micarea botryoides* is usually not lignicolous and prefers rain-sheltered microhabitats on various substrata, it has slightly taller pycnidia (up to 400 µm) and longer ascospores (8–13(–16) × 2.3–4 µm) that are often septate (e.g. Coppins 1983). Microscopically, *M. misella* can be distinguished by the olivaceous pigment that reacts violet instead of dull green in K, and by its hyaline hypothecium (Coppins 1983; Czarnota 2007). *Micarea osloensis*, on the other hand, is usually K– and its pycnidia are shorter. However, our study includes specimens that are difficult to identify by morphological characters, especially between *M. melaeniza*, *M. nigella* and *M. osloensis*.

One of the distinguishing characteristics of *M. nigella* is the Melaena-red pigment (K+ green, HNO_3+ purple-red) in the hymenium, hypothecium and pycnidia. In the literature, the pigment is described as `purple` (Coppins 1983; Meyer and Printzen 2000; Czarnota 2007). However, based on our study, the pigment is mostly brown, sometimes with a purplish tinge. The holotype of *M. nigella* has the Melaena-red pigment, that looks brown with a purplish tinge, but of our three sequenced specimens (Fig. 2, Table 1), one (collection Kantelinen 1971) has no purplish tone, whereas the other two collections (Kantelinen 1974, 1921) have easily detected amounts of purple. Interpreting the colouration can be difficult and confusing, but maybe a helpful hint is that the pigment is always K+ green, even if it looks brown in water. According to our study, the K+ green reaction mostly disappears in 30 minutes.

Occasionally, *M. nigella* also has a third pigment, the Melaenida-red (K+ purple). This pigment was not found in the Finnish specimens but is sometimes seen in the Central European specimens included in this study and mentioned also by Coppins (1983) and Czarnota (2007). The Melaena-red and Melaenida-red pigments can be intermixed and appear in varying concentrations.

Additional specimens studied. Czech Republic, Central Bohemia, Brdy Protected Landscape Area, Míšov, Na Skalách Nature Reserve, old-growth beech forest, small scree with rock outcrops and sparse spruce forest in NW part of the protected area, 49°36'20"N, 13°45'56"E, 715–740 m, on stump, 2023, Malíček 16287, hb Malíček. **Western Bohemia**, Domažlice, Český les Protected Landscape Area, Pec, Bystřice Nature Reserve, natural mixed forest up to 150 years old, 49°22'56"N, 12°48'39"E, 650–750 m, on lying decaying trunk, 2015, Malíček 8029 (hb Malíček); ibid., Tachov Lesná: managed spruce forest 1 km NE of Knížecí strom Hill (829 m), 49°46'13.0"N, 12°29'28.3"E, 750 m, on stump of *Picea abies*, 2019, Malíček 13161 & Rydlo, hb Malíček. **Southern Bohemia,** Prachatice, Šumava National Park, Nová Pec old-growth beech-spruce forest on N-facing slope of Mt Hraničník (1281 m), 48°45'13"N, 13°54'17"E, 1170 m, on decaying wood, 2017, Malíček 11296, hb Malíček. **Eastern Bohemia**, Žďár nad Sázavou, Žďárské vrchy Protected Landscape Area, Svratka managed beech-spruce forest on NW-facing slope of Bubnovaný kopec Hill (780 m), 49°42'41.6"N, 16°05'13.7"E, 775 m, on stump of *Picea abies*, 2020, Malíček 13865 & Sejfová, hb Malíček. Svratka forest mosaic 0.2 km SSE of Spálený kopec Hill (766 m), 49°43'28.0"N, 16°06'23.3"E, 755 m, on stump of *Picea abies*, 2020, Malíček 13868 & Sejfová, hb Malíček. Svitavy, Česká Třebová, Psí kuchyně Nature Reserve, old-growth beech forest 0.1 km NW of Psí kuchyně Hill (526 m), 49°50'38.3"N, 16°26'47.5"E, 505 m, on lying wood of *Fagus sylvatica*, 2020, Malíček 13975 & Rydlo, hb Malíček. **Silesia**, Beskydy Protected Landscape Area, Horní Lomná, Velký Polom Nature Reserve, valley of a brook

with old-growth, beech predominated forest in the E part of the protected area, 49°30'36"N, 18°41'00"E, 860–910 m, on stump of *Picea abies*, 2021, Malíček 14664 & Sejfová, hb. Malíček; ibid., gorge on NW-facing slope of Mt Velký polom (1067 m), c. 49°30'25"N, 18°40'04"E, 950–1000 m, on stump, 2021, Malíček 14649, Hlisnikovský & Sejfová, hb Malíček; ibid., Karolinka, Malý Javorník Nature Reserve, old-growth spruce-beech forest, 49°18'20.9"N, 18°17'18.5"E, 880–970 m, on wood of stump, 2023, Malíček 16392, hb Malíček; ibid., Valašská Bystřice, Kutaný Nature Reserve, old-growth beech-silver fir forest, 49°22'15.6"N, 18°6'0.4"E, 610–770 m, on fallen wood, 2020, Malíček 14246 & Konečná, hb Malíček. Jeseníky Protected Landscape Area, Karlova Studánka, old-growth spruce forest on SE-facing slope in valley of Bílá Opava Brook, along tourist path 1.1 km NE of Ovčárna, 50°04'37"N, 17°15'06"E, 1170–1200 m, on roots of *Picea abies*, 2015, Malíček 8547, hb. Malíček.

Finland, Pohjois-Karjala, Lieksa, Koli National Park (plot 9), East side, old-growth forest, on wood of fallen *Picea abies* (decay stage 2), 63.1033°N, 29.8140°E, 2013, Kantelinen 1971 (DNA A589), H; ibid., Kantelinen 1974 (DNA A588), H; ibid., Kantelinen 1921 (DNA A572), H. **Etelä-Häme**, Hämeenlinna, Evo (plot 8), protected old managed forest, on wood of a *Picea abies* stump (decay stage 5), 61.2088°N, 25.1363°E, 2013, Kantelinen 2851 (DNA A769), H; ibid., Kantelinen 2881 (decay stage 4, DNA A764), H.

Slovakia, Eastern Slovakia, Bukovské vrchy Mts., Nová Sedlica, protected area Stužica, NNE-facing slope of Temný vršok Mt. (838 m), old-growth beech forest, 49°04'11"N, 22°32'26"E, 750–820 m, on stump of *Abies alba*, 2013, Malíček 6511 & Vondrák, hb Malíček.

***Micarea osloensis* (Th. Fr.) Hedl.**
MycoBank No: 627666
Fig. 4A, E

Type. Bih. Kongl. Svenska Vetensk.Akad. Hand. III, 18: 97 (1892). *Lecidea osloensis* Th. Fr. Lich. Scand. 2: 524 (1874). Type: Norway, Oslo, In cacumine Ryenbjerget, 10 July 1874. N.G. Moe (UPS L-153276! – holotype).

Description. ***Thallus*** endoxylic or visible as a thin pale greenish-grey to dark green-grey layer on top of substrate. Photobiont micareoid, 4–7 µm in diam.

Apothecia infrequent or rare, absent or numerous, immarginate, convex to hemispherical, dark brown to black, matt, simple, 0.1–0.2(–0.3) mm in diam. ***Hymenium*** 30–50 µm tall (Coppins c. 30 µm tall), hyaline, sometimes olivaceaous, often with warm brown vertical streaks, K–, HNO_3– (Superba-brown). ***Epihymenium*** warm dark brown to blackish (Coppins: red-brown), rarely greenish, mostly K– but sometimes K+ green, HNO_3– or HNO_3+ purplish (Cinereorufa-green). ***Paraphyses*** of two type: 1.) hyaline or coated with a brown pigment, thick, 2–3 µm wide, simple or branched, sometimes wider from apices, often uneven in shape, abundant, sometimes concentrated into fascicles, 2.) thinner, c. 1–1.5 µm wide, rarely branched, rare. ***Asci*** cylindrical to cylindrical-clavate, 30–40 × 10–12 µm (Coppins: 26–30 × 11–13 µm). ***Ascospores*** 7–10 × (2.5–)3.0–3.5 (–4.0) µm (Coppins: 6–9.5 × 3–4 µm), ellipsoid, cylindrical or sometimes roughly shaped, 0(–1) sept. ***Hypothecium*** warm dark brown (Coppins: red-brown), composed of hyaline hyphae 1–2 µm wide surrounded by

brown pigment giving it an unevenly coloured/randomly spotted appearance, K–, HNO_3– (Superba-brown), c. 85 µm tall.

Mesopycnidia often numerous and crowded, sometimes absent, simple or branched from the base, emergent or shortly stalked ca. 50–180 µm tall, 40–70 µm in diam., dark brown to blackish, walls brown, greenish brown from the top with a warm brown lower part, K– (Superba-brown) or sometimes K+ green, HNO_3– or HNO_3+ purplish (Cinereorufa-green), usually extruding white mass of conidia that may merge with neighbouring conidia. Mesoconidia ellipsoid or short cylindrical 3.5–4.5(–5) × 1.2–1.5 (–1.8) µm. Micro- or macropycnidia not seen.

Chemistry no substances detected by TLC (Coppins 1983).

Crystalline granules not present in apothecia, pycnidia or thallus.

Habitat and distribution. The type of *M. osloensis* occurs on soil. Another morphologically identical specimen collected in 2007 occurs on bark of decaying trunk (Palice 11684). Our newer specimens occur on bark, dead wood and dead mosses. The type specimen was collected from Norway from a woodland clearing on the site of an old bonfire, and the newer specimens are from the Czech Republic, Finland, Sweden and Ukraine. In the Czech Republic, *M. osloensis* occurs commonly from middle to montane elevations. It appears to be toxitolerant and is known in areas with higher levels of air pollution in the past (i.e. acidification by acid rain). The typical habitats are bark on bases and roots of *Fagus sylvatica*, *Larix decidua*, *Picea abies*, *Pinus sylvestris*. It is abundant also on dead wood and dead bark on stumps, fallen trunks and snags. In Finland, *M. osloensis* is likely relatively common but overlooked in coniferous forests on bark, dead wood and dead mosses. In both countries, *M. osloensis* is known from managed and old-growth forests.

Notes. The two previously known *M. osloensis* specimens, including the type, have not been sequenced, although an unsuccessful sequencing attempt of a specimen collected by Palice (11684) was made by Kantelinen in 2011, and therefore we cannot compare our new specimens to the type of *M. osloensis* using DNA. Subtle morphological features differentiate the type from new specimens, i.e. taller hymenium and asci. Most of the new specimens are K– and have only the Superba-brown pigment, similar to the type. However, some specimens have a K+ greenish, HNO_3+ purple reaction in the epihymenium and pycnidial walls suggesting the presence of the Cinereorufa-green pigment which is not known from the type of *M. osloensis*. Specimens with the Cinereorufa-green pigmentation appear to be more frequent in the Czech Republic. The Finnish specimens have sometimes olivaceous tones that are K– but slightly HNO_3+ purple.

Another difference between the type of *M. osloensis* and our newly sequenced specimens is reproduction. The type specimen has apothecia and no pycnidia. The new specimens, on the other hand, often have shortly stipitate pycnidia. Our specimens appear to be dimorphic, however, so that the specimens represent either sexual (rare) or asexual reproduction modes which are monophyletic in DNA level.

Because of overlapping variation in reproduction and pigmentation between the type of *M. osloensis* and our new specimens, we cannot exclude the possibility that they are conspecific. On the other hand, we also cannot exclude the possibility that the new specimens represent a yet undescribed taxon in the *M. melaeniza* group.

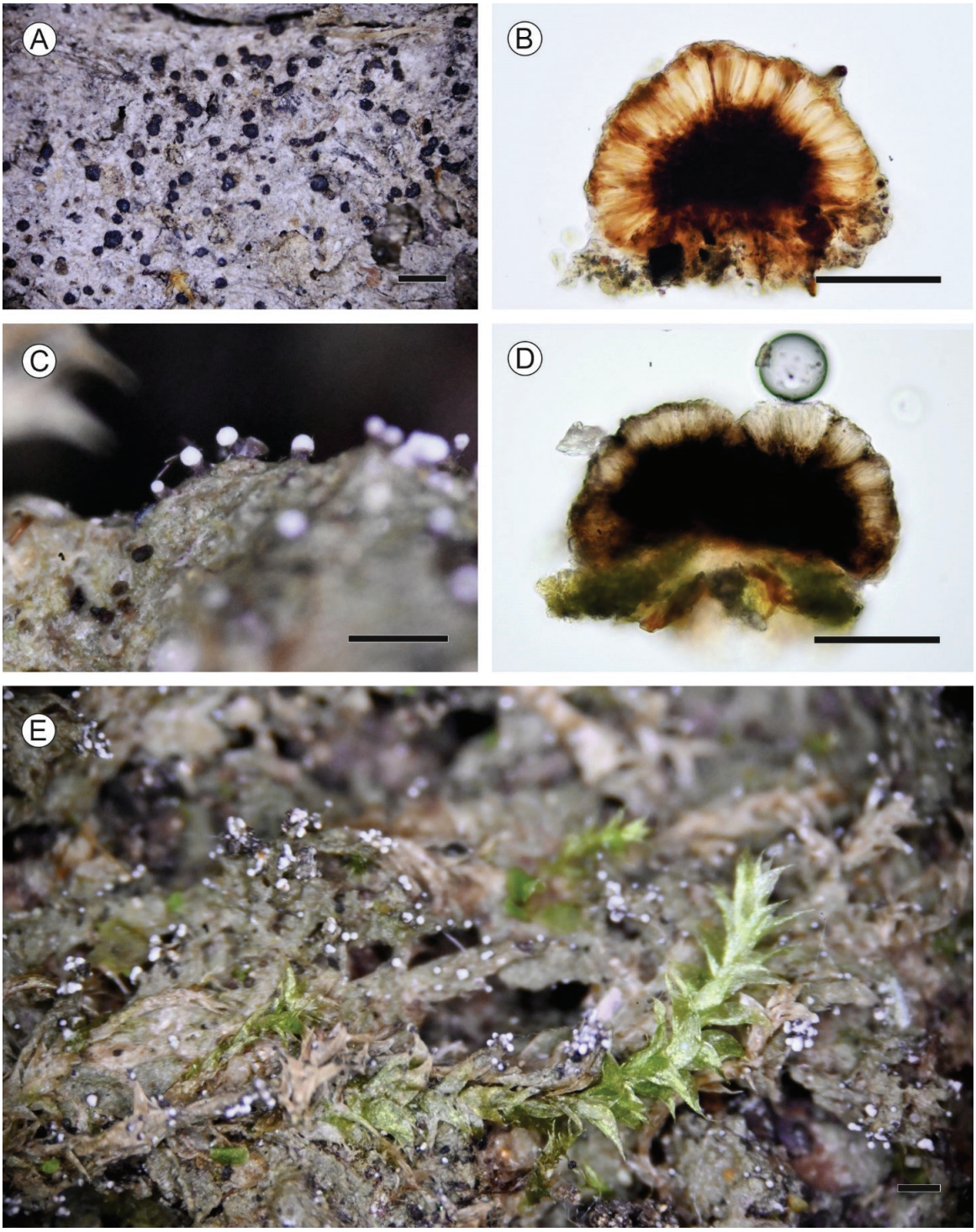

Figure 4. Morphological and anatomical features of old and new *Micarea osloensis* collections **A, B** old *Micarea osloensis* **A** habit, apothecia on soil (Holotype) **B** apothecial section in water (Palice 11684, H) **C–E** new *Micarea osloensis* (Kantelinen 2648, H) **C** mesopycnidia extruding mesoconidia as a white drop **D** apothecial section in water **E** mesopycnidia on dead wood and mosses. Scale bars: Habit 0.5 mm (**A, C, E**); Apothecial sections 100 µm (**B, D**).

M. osloensis resembles *M. eurasiatica*, *M. melaeniza*, *M. misella* and *M. nigella*. The most important characters of *M. osloensis* are the combination of sessile to shortly stalked pycnidia, mesoconidia of the size 3.5–4.5(–5) × 1.2–1.5 (–1.8) µm, warm-brown, sometimes olivaceous colouration in apothecia

and pycnidia (Coppins: red-brown), and often a K– reaction. *Micarea eurasiatica* sp. nov. has mostly sessile to emergent pycnidia and bigger mesoconidia ((4–)4.5–6.0 × 1.2–1.5(–1.8) µm). *Micarea misella*, on the other hand, has a K+ violet reaction in the epihymenium and pycnidia (Coppins 1983; Czarnota 2007). *Micarea nigella* has similar mesoconidia and spore size, but its pycnidia are usually taller and it has the brown/purple-brown Melaena-red pigment (K+ green) in hypothecium and pycnidia.

Based on our phylogenetic analyses, *M. osloensis* and *M. melaeniza* are sister species. They have morphological similarities including pigmentation and spore size. However, *M. osloensis* has slightly larger mesoconidia, shorter pycnidia and wider often roughly shaped paraphyses. The concentration of the Cinereorufa-green pigment (K+ green, HNO_3+ purple) appears to vary in both taxa, but especially in *M. osloensis*. *Micarea melaeniza* is mostly K+ green in epihymenium, hymenium, upper hypothecium and pycnidia. *Micarea osloensis*, on the other hand, is rarely K+ green and then from the epihymenium and pycnidia.

Additional specimens studied. Czech Republic, **Northern Bohemia**, Jizerské hory Mts, Josefův Důl: valley of Jedlový potok, protected zone of nature reserve Jedlový důl, fragment of fir-beech old-growth forest, 50°47'45"N, 15°14'47.5"E, on dry wood of old conifer stump, 780 m, 2020, Palice 30266, PRA (in GenBank as *M. nigella*: OQ646320); ibid., Hejnice, Jizerskohorské bučiny National Nature Reserve, valley of Velký Štolpich brook, S of Ořešník Mt. (800 m), ca 50°51'13"N, 15°11'13"E, 660 m, on base of *Fagus sylvatica*, 2013, Malíček 6020, hb Malíček. Lužické hory Protected Landscape Area, Mařenice, Horní Světlá: managed spruce-beech forest on E-facing slope, 0.3 km NNW of Kopřivnice Hill (638 m), 50°50'13.6"N, 14°37'56.6"E, 600 m, at base of *Picea abies*, on stump of *Picea*, 2020, Malíček 14019, 14020 & Rydlo, hb Malíček. **Central Bohemia**, Brdy Protected Landscape Area, Míšov, Na Skalách Nature Reserve, old-growth beech forest, small scree with rock outcrops and sparse spruce forest in NW part of the protected area, 49°36'20"N, 13°45'56"E, 715–740 m, at base of *Fagus sylvatica*, 2023, Malíček 16281, hb Malíček. Brdy Hills, Rožmitál pod Třemšínem, Nepomuk: managed forest 0.4 km N of Praha Hill (862 m), 49°39'48"N, 13°49'06"E, 825 m, at base of *Larix decidua*, 2018, Malíček 12007 & Vondrák, hb Malíček; ibid., Strašice, managed mixed forest 3 km E of village, 49°43'34"N, 13°47'56"E, 610 m, at base of *Larix decidua*, 2018, Malíček 12000 & Vondrák, hb. Malíček. Příbram, Brdy Hills, Jince managed coniferous forest 0.5 km SSE of Velcí pond, 49°45'17"N, 13°56'34"E, 600 m, at base of *Larix decidua*, 2018, Malíček 12016 & Vondrák, hb Malíček. **Eastern Bohemia**, Rychnov n. Kněžnou, Orlické hory Protect. Lands. Area, Rokytnice v Orlických horách, Černý důl Nature Reserve, fragment of old-growth beech-spruce-silver fir forest, along brook, 50°12'01.4"N, 16°31'18.2"E, 800–810 m, on bark of stump of *Picea abies*, 2012, Malíček 4536 et al., hb Malíček. Žďár nad Sázavou, Žďárské vrchy Protected Landscape Area, Svratka fragment of old beech predominated forest 0.6 km SW of Spálený kopec Hill (766 m), 49°43'18.2"N, 16°06'11.4"E, 750 m, on stump of *Picea abies*, 2020, Malíček 13864 & Sejfová, hb Malíček; ibid., Svratka, Pustá Rybná: spruce-beech forest on S-facing slope of Kaštánkův kopec (753 m), 49°43'03.9"N, 16°06'46.4"E, 740 m, on stump of *Picea abies*, 2020, Malíček 13953, hb Malíček. Svitavy, Česká Třebová managed spruce forest 3 km W of Opatov, 49°49'47.6"N, 16°27'40.0"E, 445 m, on stump of *Picea abies*, 2020, Malíček 13970 & Šámalová, hb Malíček. **Western Bohemia**, Český les Protected

Landscape Area, Tachov, Lesná: young beech forest 0.8 km E of Knížecí strom Hill (829 m), 49°45'54.2"N, 12°29'18.5"E, 780 m, on stump of *Picea abies*, 2020, Malíček 13784 & Rydlo, hb Malíček; ibid., spruce-beech forest 1 km NE of Knížecí strom Hill (829 m), 49°46'17.3"N, 12°29'18.1"E, 770 m., at base of *Picea abies*, 2019, Malíček 13167 & Rydlo,hb Malíček; ibid., Pec, Bystřice Nature Reserve, natural mixed forest up to 150 years old, 49°22'56"N, 12°48'39"E, 650 m, at base of *Picea abies*, 2015, Malíček 8028, hb Malíček. Kdyně, Mezholesy: managed mixed forest 0.3 km SE of Koráb Hill (773 m), 49°23'37.7"N, 13°04'44.1"E, 750 m, at base of *Picea abies*, 2019, Malíček 13371 & Rydlo, hb Malíček. **Southern Bohemia**, Novohradské hory Mts, Horní Stropnice, NPP Hojná Voda, fragment of primeval forest predominated by beech, 48°42'20"N, 14°45'08"E, 840–870 m, on snag, 15 October 2019, Malíček 13500, herb. Malíček. Šumava Mts., Volary, Nová Pec, 740 m, 48°49'11.2"N, 13°56'12.151"E, on bark of *Pinus sylvestris* at base of trunk, 2017, Vondrák 19007, PRA. Prachatice, Šumava Protected Landscape Area, Kubova Huť, Boubínský prales National Nature Reserve, managed spruce forest c. 120 years old, 0.4 km NNE of top of Mt Boubín (1362 m), 48°59'42.2"N, 13°49'05.7"E, 1275 m, on decaying stump 2015, Malíček 8349 & Palice, hb Malíček. Jindřichův Hradec, Javořická vrchovina Hills, Stráž nad Nežárkou, Sedlo: managed coniferous forest SSE of Otínský kopec Hill (538 m), 49°02'44.0"N, 14°59'45.7"E, 530 m, on stump, 2020, Malíček 13817, hb Malíček; ibid., Lásenice: mixed forest S of Šemburský rybník, 49°03'34.6"N, 14°59'55.2"E, 520 m, on stump, 2020, Malíček 13821, hb. Malíček; ibid., managed coniferous forest between Nová Ves and Sedlo, 49°03'36.1"N, 15°00'55.3"E, 560 m, at base of *Pinus sylvestris*, 2020, Malíček 13824, hb Malíček. Tábor Chýnov, young beech forest SSE of Blanička, 49°28'00.6"N, 14°50'34.9"E, 690 m, on fallen wood, 2020, Malíček 13834 & Rydlo, hb Malíček; ibid., mixed forest SE of Batkovy Hill (724 m), 49°27'43.3"N, 14°50'00.9"E, 700 m, at base of *Larix decidua*, 2020, Malíček 13838 & Rydlo, hb Malíček. **Northern Moravia**, Jeseník, Jeseníky Protected Landscape Area, Bělá pod Pradědem, Vysoký vodopád, Nature Reserve, valley of Studený p. brook, ca. 50°06'57"N, 17°12'10"E, 900–1000 m, on base of *Picea abies*, 2012, Malíček 5102, hb Malíček. Šumperk, Králický Sněžník Mts, Staré Město: Mt. Králický Sněžník, c. 100 years old spruce forest on S-facing slope 0.1 km SE of Františkova chata, 50°12'05.2"N, 16°51'28.3"E, 1210 m, at base of *Picea abies*, 2015, Malíček 8381, Kocourková & Vondrák, hb Malíček. **Eastern Moravia**, Beskydy Protected Landscape Area, Bílá, Salajka: beech dominated forest 0.6 km SE of gamekeeper's house, 49°24'37.9"N, 18°25'39.5"E, 730 m, on decaying stump, 2019, Malíček 13344 & Rydlo, hb Malíček; ibid., Frenštát pod Radhoštěm, Kněhyně-Čertův mlýn National Nature Reserve, W-facing slope of Kněhyně Mt. (1257 m), old-growth spruce forest above red-marked tourist path, 49°29'57"N, 18°18'38"E, 1080–1100 m, on stump of *Picea abies*, 2013, Malíček 6090 & Vondrák, hb Malíček. **Western Moravia**, Žďár nad Sázavou, Žďárské vrchy Protect. Landsc. Area, Cikháj, Žákova hora National Nature Reserve, beech virgin forest, 49°39'18"N, 15°59'35"E, 750–800 m, on stump of *Fagus*, 2012, Malíček 5110 & Syrovátková, hb Malíček. **Silesia,** Bruntál, Jeseníky Protected Landscape Area, Karlova Studánka, managed spruce forest (c. 100 years old) on N-facing slope in valley of Bílá Opava Brook, 1.8 km ENE of Ovčárna, 50°04'35"N, 17°15'53"E, 1170–1180 m, on bark of *Picea abies*, 2015, Malíček 8490, Kocourková, Vondrák & Zemanová, hb Malíček; ibid., Praděd National Nature Reserve, old-growth spruce forest c. 200 years old on E-facing slope of Mt

Vysoká hole (1464 m), 0.2 km WNW of Eustaška hut, 50°03'35"N, 17°15'12"E, 1220 m, at base of *Picea abies*, 2015, Malíček 8563, Kocourková, Palice & Vondrák, hb Malíček. Frýdek-Místek, Beskydy Protected Landscape Area, Ostravice, Mazák National Nature Reserve, old-growth spruce forest with intermixed sycamores on W-facing slope of Mt Lysá hora (1323 m), 49°32'41"N, 18°26'43"E, 1200 m, on bark of *Picea abies*, 2016, Malíček 9743 & Palice, hb Malíček.

Finland, Pohjois-Karjala, Lieksa, Koli National Park (plot 9), East side, old-growth forest, on bark of fallen *Picea abies* (decay stage 3), 63.1033°N, 29.8140°E, 2013, Kantelinen 1865 (DNA A575, apothecia and pycnidia), H. Ibid., on wood of fallen *Picea abies* (decay stage 4), 2013, Kantelinen 1909 (DNA A583), H. Ibid., on wood of dead standing *Picea abies* (decay stage 3), Kantelinen 1685 (DNA A574), H. Ibid., on wood of fallen *Picea abies* (decay stage 5), 2013, Kantelinen 2003 (DNA A594), H. Ibid., on wood of fallen *Picea abies* (decay stage 3), 2013, Kantelinen 1923 (DNA A573), H. **Etelä-Häme,** Hämeenlinna, Evo (plot 8), protected old managed forest, on wood/mosses of a *Picea abies* stump (decay stage 5), 61.2088°N, 25.1363°E, 2013, Kantelinen 2899 (DNA A736). Ibid., on wood of *Picea abies*, 2013, Kantelinen 1686 (DNA A768), H. Ibid., Rajakallio, boreal forest on a bouldery slope, forest of *Picea*, *Pinus* and *Betula*, 61°15.27'N, 025°06.43'E, on bark of rotten wood among boulders, 2007, Palice 11684, conf. Coppins, H. **Uusimaa**, Tuusula, west of Korso, shaded and dense *Picea abies* dominated managed forest (plot 2), on wood of a *Picea abies* stump (decay stage 5), 60.3544°N, 25.0322°E, 2013, Kantelinen 2643 (DNA A484), H.

Sweden, Jämtland, Kall par., about 850 m NW of the northwestern tip of Lake Spjuttjärnen, S side of stream Konäsån, on stump of *Betula pubescens* in old-growth *Picea abies* forest, 63°34'30"N, 13°04'05"E, elev. 440 m, 2022, Svensson 4335, UPS L-1091180.

Ukraine. Eastern Carpathians, Nadvirna, Bysrytsia, N of hill Skali verkhni, 48°27'48.492"N, 24°18'35.46"E, 1233 m, on bark of *Picea abies*, 2019, Vondrák 22217, PRA.

Discussion

Our aim was to clarify systematics and species boundaries among *Micarea melaeniza* and similar-looking species. We propose the new species *Micarea eurasiatica*, characterized by the combination of cylindrically shaped, sessile to emergent pycnidia with greenish-black walls, long mesoconidia (up to 6 µm in length), a K+ olive green reaction and by mostly occurring in the anamorphic stage. The species is known from Japan and Finland. We also discovered another, putatively new species, marked *Micarea* sp. in the phylogeny that we refrain from describing because of insufficient morphological data and few available collections. This putative new species has sessile to emergent, brownish black pycnidia with a purple tinge and a K+ green reaction, but apothecia are few (see Table 2). Despite our efforts, we did not find or sequence *M. olivacea*, a species that could be related to the *M. melaeniza* group.

Generally, the species in the *M. melaeniza* group are challenging to identify because they are small, have relatively few morphological characters and because the current literature is not up to date particularly in relation to pigmentation (Coppins 1983; Czarnota 2007). The challenges while identifying

our fresh specimens underline this issue, and are discussed in the notes under *M. melaeniza*, *M. nigella* and *M. osloensis*. According to our study, the species in the *M. melaeniza* group are characterized by having a thin or endosubstratal thallus and dark, sessile to stipitate mesopycnidia that often extrude a white mass of conidia at their top. Apothecia are often absent, but when present, they are 0.1–0.3 mm wide and brown to black in colour. They have hyaline or slightly coloured hymenium, dimorphic paraphyses, simple spores and dark hypothecium where hyphae are surrounded by brown pigment giving them an unevenly coloured appearance, also noted by Coppins (1983). Based on results of this study, the size of pycnidia and mesoconidia, and to some extent also the general pigmentation in K and HNO_3 are the most useful morphological characters in separating the species, however in some cases DNA sequencing is the only reliable way for identification. *Micarea eurasiatica*, and *M. olivacea* develop sessile to emergent pycnidia, *M. osloensis* emergent to shortly stipitate pycnidia, and *M. melaeniza* and *M. nigella* develop stipitate pycnidia. *Micarea deminuta* does not develop distinctive stalked pycnidia, at least according to current knowledge. The Cinereorufa-green pigment (K+ green, HNO_3+ purple) is present in pycnidia and apothecia of *M. eurasiatica*, *M. deminuta*, *M. melaeniza*, *M. nigella*, *M. olivacea* (according to Coppins 1983) and occasionally in *M. osloensis* in varying concentration, accompanied by the Superba-brown pigment (K–). The brown or purple-brown Melaena-red pigment (K+ dull sordid green) is present in *M. nigella* (and possibly in one specimen of *M. melaeniza*) and is sometimes intermixed with the Melaenida-red pigment (K+ purplish-red) (Table 3).

Our study indicates that the pigmentation of some species may correlate with geography. In the central European specimens some pigments are encountered more often or higher concentrations than in Fennoscandia. For example, in the Fennoscandian specimens of *M. osloensis*, the Cinereorufa-green pigment is barely visible even when using HNO_3, and the Melaenida-red pigment in *M. nigella* was not found at all. In the central European specimens, however, both pigments were found, and sometimes in relatively high concentrations. The central European material also includes samples that appear to be morphologically "intermediate" between species, for example *M. melaeniza* (ZP32013) may have Melaena-red pigment like *M. nigella*, although its mesoconidia size and DNA profile is similar to *M. melaeniza*. Some of the "intermediate" specimens have not been sequenced and therefore we do not know their identity or whether they are undescribed species. Obviously, more work is needed to understand the pigments and species in this group.

Because of these morphological challenges, we even considered that the species in the *M. melaeniza* group are conspecific, i.e. variation of just one species. However, we excluded this possibility because of several reasons 1) molecular differences, 2) existing morphological differences, even though they may be hard to interpret, 3) the type specimens studied are not morphologically conspecific, 4) the types correspond in morphology to most of our specimens. Based on morphology, one might suggest that *M. melaeniza*, *M. nigella* and *M. osloensis* are variation of one species, but according to our phylogenies, they are not monophyletic without *M. deminuta*, *M. eurasiatica* and *Micarea* sp. Even between *M. melaeniza* and *M. nigella*, the pigmentation is mostly different (Superba brown vs. Melaena-red), and although these pigments may look quite similar to the human eye, they may have different ontologies and evolutionary paths.

According to morphological studies by Coppins (1983), *M. botryoides* and *M. melaeniza* are relatives (group G) and possibly close to *M. contexta*, *M. eximia*, *M. nigella* and *M. olivacea* (group H). Our Bayesian and ML phylogenies conclude that groups G and H are intermixed, however, based on DNA sequencing *M. eximia* is likely not a close relative of the *M. melaeniza* group (unpublished data) and molecular relationships of *M. olivacea* are still unknown. Our phylogenetic analyses also show that *M*. *melaeniza* and *M*. *osloensis* are sisters, a relationship that has not been noted in previous publications, but the latter clade is not supported (0.68 / 74). A closer look at the sequences and alignment shows that there are nucleotide differences in the mtSSU region between *M*. *melaeniza* and *M*. *osloensis* (ca. 1–2% between specimens Kantelinen 2430 and 1923), but the ITS regions are nearly identical with only two nucleotide differences. At least three conclusions could be drawn from these results. 1) The two clades are, in fact, two species as we suggest in our study. This conclusion is supported by molecular and morphological data, to some extent at least, 2) The two clades are conspecific and represent morphological and molecular variation of *M*. *melaeniza*, 3) Our new specimens of *M*. *osloensis* are not conspecific to the type of *M*. *osloensis* or *M*. *melaeniza*, but instead a scientifically undescribed species. Any conclusion we make suffers from the uncertainty caused by the *M*. *melaeniza* and *M*. *osloensis* type specimens not having sequenced, which means that we cannot compare our sequences to the types and the connections between fresh and old specimens are based solely on morphology. This is also the reason why we refrain from describing our new specimens of *M*. *osloensis* as a new species to science. The type specimens are over 100 years old and hence likely beyond successful DNA sequencing – based on our experience, sequences are usually difficult to get from *Micarea* specimens just over 3 years old, and nearly impossible when over 6 years old.

All species in the *M*. *melaeniza* group are either obligate or facultative lignicoles. According to a previous study, the wood-inhabiting lifestyle of *Micarea* species influences their reproductive biology: obligate lignicoles primarily reproduce asexually, likely due to the transient nature of decaying wood, which imposes a time constraint on the species occupying it (Kantelinen et al. 2022a). Asexual reproduction via mesoconidia is likely a more rapid and efficient strategy than sexual reproduction. In the here studied *M*. *melaeniza* group and relatives, several species are found mostly asexual, viz. *M*. *melaeniza*, *M*. *nigella*, *M*. *osloensis*, *M*. *eurasiatica*, *M*. *anterior* and *M*. *substipitata*.

Based on our field experience as well as previous works by Coppins (1983) and Czarnota (2007), the species in the *M*. *melaeniza* group are probably common in boreal and hemiboreal forests, both in natural and managed forests. In spite of this, their small size and often anamorphic lifestyle make them easily overlooked, resulting in rare mentions in ecological studies or species inventories. We hope that the morphological and molecular features presented in this study will pave the way for future research endeavors.

Acknowledgements

We warmly thank prof. Teuvo Ahti, emeritus curator Arto Kurtto and Dr. Juha Pykälä for their valuable help with this manuscript. Laura Häkkinen, Emilia Piki and Emelie Winquist are thanked for the DNA lab work. Permission for collection of

lichens on Mt. Oku-Shirane (Mt. Nikko-Shirane), Nikko National Park to GT in 2019 was kindly granted by the Nikko National Park office, the Ministry of Environment (no. 1908283, 400), the Nikko District Forest Office of the Forest Agency and The Nikko District Forest Office of Nihon Paper Company in Gunma Prefecture. ZP, JM and JV acknowledge the long-term research development project RVO 67985939.

Additional information

Conflict of interest

The authors have declared that no competing interests exist.

Ethical statement

No ethical statement was reported.

Funding

This research was financially supported by the Finnish Ministry of Environment as a part of the research programme on data deficient and threatened forest species (grant YTB067 to LM), a postdoctoral fellowship of the Finnish Museum of Natural History and Societas pro Fauna et Flo-ra Fennica (personal grants for AK), and the Research Council of Finland (Grant 323711 to LM). Research by MS was financially supported by the Swedish Taxonomy Initiative (grant no. 2016-206 4.3). Open access is funded by Helsinki University Library.

Author contributions

Conceptualization: AK, Data curation/collection: AK, JV, JM, SS, MS, ZP, GT, Formal Analysis: AK, Funding acquisition: AK, LM, Investigation: AK, MS, JM, JV, ZP, Project administration: AK, LM, Visualization: AK, Writing – original draft: AK, MS, Writing – review & editing: AK, MS, ZP, JM, JV, GT, LM.

Author ORCIDs

Annina Kantelinen https://orcid.org/0000-0001-8664-7662
Måns Svensson https://orcid.org/0000-0003-1664-8226
Jiří Malíček https://orcid.org/0000-0002-3119-8967
Jan Vondrak https://orcid.org/0000-0001-7568-6711
Göran Thor https://orcid.org/0000-0003-1166-6898
Zdeněk Palice https://orcid.org/0000-0003-4984-8654
Stanislav Svoboda https://orcid.org/0000-0001-9797-4984
Leena Myllys https://orcid.org/0000-0002-9566-9473

Data availability

All of the data that support the findings of this study are available in the main text.

References

Andersen HL, Ekman S (2005) Disintegration of the Micareaceae (lichenized Ascomycota): A molecular phylogeny based on mitochondrial rDNA sequences. Mycological Research 109(1): 21–30. https://doi.org/10.1017/S0953756204001625

Aras S, Cansaran D (2006) Isolation of DNA for sequence analysis from herbarium material of some lichen specimens. Turkish Journal of Botany 30: 449–453.

Berger F, Türk R (1991) Zur Kenntnis der Flechten und flechtenbewohnenden Pilze von Oberösterreich und Salzburg III. Linzer Biologische Beitrage 23: 425–453.

Coppins BJ (1983) A taxonomic study of the lichen genus *Micarea* in Europe. Bulletin of the British Museum (Natural History), Botany Series 11: 17–214.

Czarnota P (2007) The lichen genus *Micarea* (Lecanorales, Ascomycota) in Poland. Polish Botanical Studies 23: 1–190.

Czarnota P, Guzow-Krzemińska B (2010) A phylogenetic study of the *Micarea prasina* group shows that *Micarea micrococca* includes three distinct lineages. Lichenologist 42(1): 7–21. https://doi.org/10.1017/S0024282909990211

Edgar RC (2004) MUSCLE: Multiple sequence alignment with high accuracy and high throughput. Nucleic Acids Research 32(5): 1792–1797. https://doi.org/10.1093/nar/gkh340

Gardes M, Bruns TD (1993) ITS primers with enhanced specificity for Basidiomycetes – application to the identification of mycorrhizae and rusts. Molecular Ecology 2(2): 113–118. https://doi.org/10.1111/j.1365-294X.1993.tb00005.x

Guzow-Krzemińska B, Czarnota P, Łubek A, Kukwa M (2016) *Micarea soralifera* sp. nov., a new sorediate species in the *M. prasina* group. Lichenologist 48(3): 161–169. https://doi.org/10.1017/S0024282916000050

Guzow-Krzemińska B, Sérusiaux E, van den Boom PPG, Brand AM, Launis A, Łubek A, Kukwa M (2019) Understanding the evolution of phenotypical characters in the *Micarea prasina* group (Pilocarpaceae) and descriptions of six new species within the group. MycoKeys 57: 1–30. https://doi.org/10.3897/mycokeys.57.33267

Hedlund JT (1892) Kritische Bemerkungen über einige Arten der Flechtengattungen *Lecanora* (Ach.), *Lecidea* (Ach.) und *Micarea* (Fr.). Bihang till Kungliga Svenska Vetenskapsakademiens Handlingar III, 18: 1–104.

Huelsenbeck JP, Larget B, Alfaro ME (2004) Bayesian phylogenetic model selection using reversible jump markov chain Monte Carlo. Molecular Biology and Evolution 21(6): 1123–1133. https://doi.org/10.1093/molbev/msh123

Index Fungorum (2023) Partnership Index Fungorum [WWW resource]. http://www.indexfungorum.org [Accessed 2023]

Kantelinen A, Printzen C, Poczai P, Myllys L (2022a) Lichen speciation is sparked by a substrate requirement shift and reproduction mode differentiation. Scientific Reports 12(1): 11048. https://doi.org/10.1038/s41598-022-14970-9

Kantelinen A, Purhonen J, Halme P, Myllys L (2022b) Growth form matters - Crustose lichens on dead wood are sensitive to forest management. Forest Ecology and Management 524: 120529. https://doi.org/10.1016/j.foreco.2022.120529

Kantvilas G, Coppins BJ (2019) Studies on *Micarea* in Australasia II. A synopsis of the genus in Tasmania, with the description of ten new species. Lichenologist 51(5): 431–481. https://doi.org/10.1017/S0024282919000343

Launis A, Myllys L (2019) *Micarea fennica*, a new lignicolous lichen species from Finland. Phytotaxa 409(3): 179–188. https://doi.org/10.11646/phytotaxa.409.3.6

Launis A, Pykälä J, van den Boom P, Sérusiaux E, Myllys L (2019a) Four new epiphytic species in the *Micarea prasina* group from Europe. Lichenologist 51(1): 7–25. https://doi.org/10.1017/S0024282918000555

Launis A, Malíček J, Svensson M, Tsurykau A, Sérusiaux E, Myllys L (2019b) Sharpening species boundaries in the *Micarea prasina* group, with a new circumscription of the type species *M. prasina*. Mycologia 111(4): 574–592. https://doi.org/10.1080/00275514.2019.1603044

Maddison WP, Maddison DR (2023) Mesquite: a modular system for evolutionary analysis. Version 3.61. http://www.mesquiteproject.org

Malíček J, Coppins B, Palice Z, Vančurová L, Vondrák J, Sanderson N (2023) *Coenogonium nimisii* – a new isidiate epiphytic lichen similar to *Porina rosei*. Lichenologist 55(5): 305–313. https://doi.org/10.1017/S0024282923000257

Meyer B, Printzen C (2000) Proposal for a standardized nomenclature and characterization of insoluble lichen pigments. Lichenologist 32(6): 571–583. https://doi.org/10.1006/lich.2000.0294

Myllys L, Lohtander K, Källersjö M, Tehler A (1999) Sequence insertion and ITS data provide congruent information in *Roccella canariensis* and *R. tuberculata* (Arthoniales, Euascomycetes) phylogeny. Molecular Phylogenetics and Evolution 12(3): 295–309. https://doi.org/10.1006/mpev.1999.0620

Orange A, James PW, White FJ (2010) Microchemical Methods for the Identification of Lichens. British Lichen Society, London.

Palka K, Śliwa L (2006) Lichens of Oran Dosh protected area in the Lake Khubsugul National Park (Mongolia). Part 1: Corticolous and lignicolous species. Nova Hedwigia 82(1–2): 51–68. https://doi.org/10.1127/0029-5035/2006/0082-0051

Rambaut A, Drummond AJ, Xie D, Baele G, Suchard MA (2018) Posterior Summarization in 444 Bayesian Phylogenetics Using Tracer 1.7. Systematic Biology 67(5): 901–904. https://doi.org/10.1093/sysbio/syy032

Renvall P (1995) Community structure and dynamics of wood-rotting Basidiomycetes on decomposing conifer trunks in northern Finland. Karstenia 35(1): 1–51. https://doi.org/10.29203/ka.1995.309

Ronquist F, Huelsenbeck JP (2003) MrBayes 3: Bayesian phylogenetic inference under mixed 451 models. Bioinformatics 19(12): 1572–1574. https://doi.org/10.1093/bioinformatics/btg180

Sérusiaux E, Brand AM, Motiejūnaitė J, Orange A, Coppins BJ (2010) *Lecidea doliiformis* belongs to *Micarea*, *Catillaria alba* to *Biatora* and *Biatora lignimollis* occurs in Western Europe. The Bryologist 113(2): 333–344. https://doi.org/10.1639/0007-2745-113.2.333

Spribille T, Fryday AM, Pérez-Ortega S, Svensson M, Tønsberg T, Ekman S, Holien H, Resl P, Schneider K, Stabentheiner E, Thüs H, Vondrák J, Sharman L (2020) Lichens and associated fungi from Glacier Bay National Park, Alaska. Lichenologist 52(2): 61–181. https://doi.org/10.1017/S0024282920000079

Trifinopoulos J, Nguyen LT, von Haeseler A, Minh BQ (2016) W-IQ-TREE: A fast online phylogenetic tool for maximum likelihood analysis. Nucleic Acids Research 44(W1): W232–W235. https://doi.org/10.1093/nar/gkw256

van den Boom PPG, Brand AM, Coppins BJ, Sérusiaux E (2017) Two new species in the *Micarea prasina* group from Western Europe. Lichenologist 49(1): 13–25. https://doi.org/10.1017/S0024282916000633

van den Boom PPG, Guzow-Krzemińska B, Kukwa M (2020) Two new *Micarea* species (Pilocarpaceae) from Western Europe. Plant and Fungal Systematics 65(1): 189–199. https://doi.org/10.35535/pfsyst-2020-0014

Vondrák J, Svoboda S, Malíček J, Palice Z, Kocourková J, Knudsen K, Mayrhofer H, Thüs H, Schultz M, Košnar J, Hofmeister J (2022) From Cinderella to Princess: An exceptional hotspot of lichen diversity in a long-inhabited central-European landscape. Preslia 94(1): 143–181. https://doi.org/10.23855/preslia.2022.143

White TJ, Bruns T, Lee S, Taylor J (1990) Amplification and direct sequencing of fungal ribosomal RNA genes for phylogenetics. In: Innis MA, Gelfand DH, Sninsky JJ, White

TJ (Eds) PCR protocols: a guide to methods and applications. Academic Press, San Diego, 315–322. https://doi.org/10.1016/B978-0-12-372180-8.50042-1

Zhou S, Stanosz GR (2001) Primers for amplification of the mtSSU rDNA, and a phylogenetic study of *Botryosphaerina* and associated anamorphic fungi. Mycological Research 105(9): 1033–1044. https://doi.org/10.1016/S0953-7562(08)61965-6

Zoller S, Scheidegger C, Sperisen C (1999) PCR primers for the amplification of mitochondrial small subunit ribosomal DNA of lichen-forming ascomycetes. Lichenologist 31(5): 511–516. https://doi.org/10.1006/lich.1999.0220